Biosystems & Biorobotics

Juan C. Moreno · Jawad Masood · Urs Schneider · Christophe Maufroy · Jose L. Pons *Editors*

Wearable Robotics: Challenges and Trends

Proceedings of the 5th International Symposium on Wearable Robotics, WeRob2020, and of WearRAcon Europe 2020, October 13–16, 2020

Springer

Biosystems & Biorobotics

Volume 27

The BIOSYSTEMS & BIOROBOTICS (BioSysRob) series publishes the latest research developments in three main areas: 1) understanding biological systems from a bioengineering point of view, i.e. the study of biosystems by exploiting engineering methods and tools to unveil their functioning principles and unrivalled performance; 2) design and development of biologically inspired machines and systems to be used for different purposes and in a variety of application contexts. In particular, the series welcomes contributions on novel design approaches, methods and tools as well as case studies on specific bio-inspired systems; 3) design and developments of nano-, micro-, macro- devices and systems for biomedical applications, i.e. technologies that can improve modern healthcare and welfare by enabling novel solutions for prevention, diagnosis, surgery, prosthetics, rehabilitation and independent living. On one side, the series focuses on recent methods and technologies which allow multi-scale, multi-physics, high-resolution analysis and modeling of biological systems. A special emphasis on this side is given to the use of mechatronic and robotic systems as a tool for basic research in biology. On the other side, the series authoritatively reports on current theoretical and experimental challenges and developments related to the "biomechatronic" design of novel biorobotic machines. A special emphasis on this side is given to human-machine interaction and interfacing, and also to the ethical and social implications of this emerging research area, as key challenges for the acceptability and sustainability of biorobotics technology. The main target of the series are engineers interested in biology and medicine, and specifically bioengineers and bioroboticists. Volume published in the series comprise monographs, edited volumes, lecture notes, as well as selected conference proceedings and PhD theses. The series also publishes books purposely devoted to support education in bioengineering, biomedical engineering, biomechatronics and biorobotics at graduate and post-graduate levels.

Indexed by SCOPUS, WTI Frankfurt eG, SCImago

More information about this series at http://www.springer.com/series/10421

Juan C. Moreno · Jawad Masood · Urs Schneider ·
Christophe Maufroy · Jose L. Pons
Editors

Wearable Robotics: Challenges and Trends

Proceedings of the 5th International Symposium on Wearable Robotics, WeRob2020, and of WearRAcon Europe 2020, October 13–16, 2020

Springer

Editors
Juan C. Moreno
Cajal Institute, Madrid, Spain

Urs Schneider
Fraunhofer Institute for Manufacturing Engineering and Automation
Stuttgart, Germany

Jose L. Pons
Shirley Ryan AbilityLab (formerly Rehabilitation Institute of Chicago)
Chicago, IL, USA

Jawad Masood
Processes and Factories of the Future
Centro Tecnológico de Automoción de Galicia
Porriño, Spain

Christophe Maufroy
Fraunhofer Institute for Manufacturing Engineering and Automation
Stuttgart, Germany

ISSN 2195-3562 ISSN 2195-3570 (electronic)
Biosystems & Biorobotics
ISBN 978-3-030-69546-0 ISBN 978-3-030-69547-7 (eBook)
https://doi.org/10.1007/978-3-030-69547-7

This Springer imprint is published by the registered company Springer Nature Switzerland AG
The registered company address is: Gewerbestrasse 11, 6330 Cham, Switzerland

Contents

What Should We Expect from Passive Exoskeletons?

The Hidden Potential of Energetically Passive Exoskeletons

Amanda Sutrisno and David J. Braun

Abstract Bicycles have successfully augmented top human movement speed despite supplying no external power or increasing human limb force. This raises the question on what are the fundamental requirements for moving faster, when increasing force or supplying external power are not necessary to moving faster. This presentation will communicate our recent efforts to develop analytical models to study the fundamental physics of human locomotion, and the development of energetically passive devices that maximize top running speed given the limited force and power of human limbs. We take inspiration from the bicycle, which uses pedals to allow the legs to supply energy continuously instead of intermittently in running.

1 Introduction

How can bicycles and ice-skates increase human running speed compared to shoes, despite supplying no external energy? Understanding the disparity between cycling, ice-skating, and running shoes could lead to lightweight passive exoskeletons for faster running [1].

We have investigated the fundamental physics of energetically passive human augmentation devices, and found that the top speed of human running is mainly limited by the *time available for human to supply energy*. In running, the legs only supply energy on the ground, 20% of the step time, as opposed to the 100% in cycling. We proposed a method of increasing running speed by allowing the legs to supply

A. Sutrisno · D. J. Braun (✉)
Center for Rehabilitation Engineering and Assistive Technology, Advanced Robotics and Control Laboratory, Vanderbilt University, 2031 Vanderbilt Place, Nashville, TN 37235, USA
e-mail: david.braun@vanderbilt.edu

A. Sutrisno
e-mail: amanda.s.sutrisno@vanderbilt.edu

Department of Mechanical Engineering, Vanderbilt University, 2031 Vanderbilt Place, Nashville, TN 37235, USA

J. C. Moreno et al. (eds.), *Wearable Robotics: Challenges and Trends*,
Biosystems & Biorobotics 27, https://doi.org/10.1007/978-3-030-69547-7_1

energy during swing instead of during stance [2]. This can be done using a variable stiffness spring compressed by the leg during swing which releases the stored energy on the ground to accelerate the body.

2 Materials and Methods

We use the simple spring mass model in [3] to theoretically compute the benefit of supplying energy during swing. We assumed that the spring stiffness can vary between steps while it is constant during ground contact, and the spring is preloaded with energy at touchdown $E_{\mathrm{spr,td}} = p_{\mathrm{leg}} \Delta t_{\mathrm{sw}}$, where p_{leg} is the energy supply rate of each leg [4] and Δt_{sw} is the swing time. The spring stiffness is adjusted without changing the energy stored inside the spring, to exert sufficient force to redirect the vertical motion of the body.

3 Results

Figure 1 shows the top speed of various passive devices and the theoretical prediction of the energetically passive variable stiffness running exoskeleton, using parameters from the world's fastest runner. The upper limit of the top running speed approaches

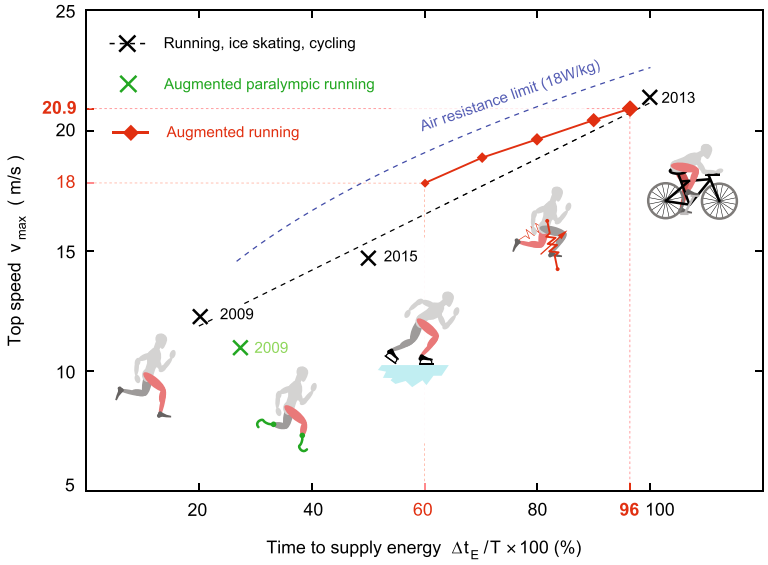

Fig. 1 Top speeds of human-powered locomotion. World records in running, ice-skating, cycling, and the top speed predicted for augmented running (18–20.9 m/s). There is a linear empirical relation between the world record speeds and the time available for each leg to supply energy

the top speed of cycling. We found that, even if the human only supplies energy 60% of the step time, they could still theoretically run at 18 m/s speed.

4 Discussion

Developing a variable stiffness spring exoskeleton for running requires a spring with energy density of 600 J/kg; significantly higher compared to paralympic running blades 150 J/kg. Therefore, fundamental advances in materials are still required to develop the envisioned energetically passive running exoskeleton.

5 Conclusion

Running could theoretically reach the top cycling speed provided the legs could supply energy in the air instead of on the ground.

References

1. A.M. Dollar, H. Herr, Lower extremity exoskeletons and active orthoses: challenges and state-of-the-art. IEEE T. Robot. **24**, 144–158 (2008)
2. A. Sutrisno, D.J. Braun, How to run 50% faster without external energy. Sci. Adv. **6**(13), eaay1950 (2020)
3. R. Blickhan, The spring-mass model for running and hopping. J. Biomech. **22**, 1217–1227 (1989)
4. J.-B. Morin, M. Bourdin, P. Edouard, N. Peyrot, P. Samozino, J.-R. Lacour, Mechanical determinants of 100-m sprint running performance. Eur. J. Appl. Physiol. **112**, 3921–3930 (2012)

Effect of a Back-Assist Exosuit on Logistics Worker Perceptions, Acceptance, and Muscle Activity

Matthew B. Yandell, Anna E. Wolfe, Matthew C. Marino, Mark P. Harris, and Karl E. Zelik

Abstract A workplace study was conducted to evaluate user perceptions, acceptance, and muscle activity amongst logistics workers wearing an unmotorized, dual-mode, back-assist exosuit prototype. Eleven workers performed a lifting/lowering task with versus without the exosuit, while back muscle activity was recorded. They then used the exosuit while performing their actual work tasks in a distribution center before completing a questionnaire about their user experience. Worker perceptions of the exosuit were overwhelmingly positive: 100% felt the exosuit could be useful and fit into their daily job without interfering, >90% felt assisted and that the exosuit made lifting easier, and >80% felt it was comfortable and that they were free to move naturally while wearing the exosuit. Finally, the majority of workers showed reduced back muscle activity while wearing the exosuit during lifting/lowering, consistent with results from prior lab studies. Worker feedback on this prototype was then used to inform design of the HeroWear Apex exosuit.

Funding support was provided by NSF SBIR Award 1913763.

M. B. Yandell · M. C. Marino · M. P. Harris · K. E. Zelik (✉)
HeroWear, Nashville, TN, USA
e-mail: karl.zelik@vanderbilt.edu

M. B. Yandell
e-mail: myandell@herowearexo.com

M. C. Marino
e-mail: mmarino@herowearexo.com

M. P. Harris
e-mail: mharris@herowearexo.com

A. E. Wolfe · K. E. Zelik
Center for Rehabilitation Engineering & Assistive Technology, Vanderbilt University, Nashville, TN, USA
e-mail: anna.e.wolfe@vanderbilt.edu

J. C. Moreno et al. (eds.), *Wearable Robotics: Challenges and Trends*,
Biosystems & Biorobotics 27, https://doi.org/10.1007/978-3-030-69547-7_2

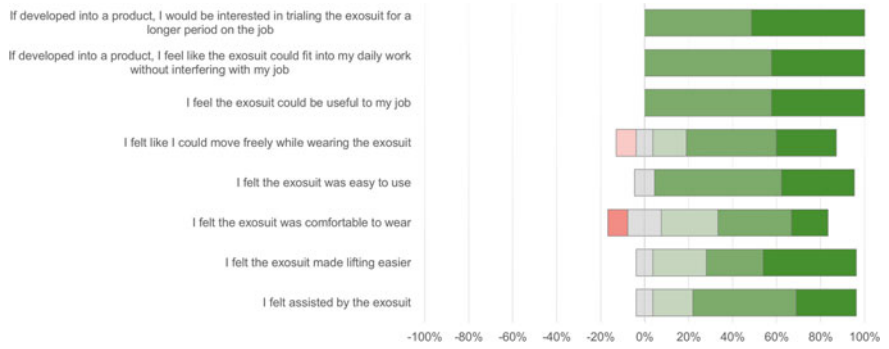

Fig. 1 Results from worker questionnaire after using exosuit on the job

1 Introduction

Work-related musculoskeletal disorders from overexertion due to lifting and handling objects are the leading cause of disabling injuries in the US [1], accounting for 23.5% of claims, and costing $14 billion annually. Back-assist exoskeletons are designed to reduce strain, fatigue, and injury risk for workers who bend, reach, and lift. A large body of evidence indicates that back-assist exoskeletons (both rigid devices and soft exosuits) can reduce back extensor muscle activity, muscle fatigue, spine compression, and/or metabolic cost for bending and lifting across various occupations, tasks, and postures (e.g. [2–4]).

The potential for back-assist exoskeletons to impact safety, performance, health, and quality of life across a spectrum of occupations is promising; however, key adoption barriers have been related to practical factors such as comfort, fit, integration with typical workflow, and not interfering. Here we evaluated an unmotorized back-assist exosuit prototype on logistics workers in distribution centers. The exosuit is comprised of textiles and elastomers to achieve a lightweight, low-profile, flexible, and unobstructive design. It uses elastic bands along the back to provide assistive torque about the spine, and was previously found to reduce back strain and fatigue in lab studies [3, 4]. It also includes a proprietary dual-mode feature (patent-pending on/off switch) that enables users to quickly engage/disengage assistance. The goals of this field test were to evaluate worker perceptions of exosuit assistance, comfort, ease of use, and integration into daily work, and to confirm reductions in back muscle activity with the exosuit as observed in lab studies.

2 Methods

Eleven distribution center workers from an international logistics firm and national retailer participated in the study. All participants in this field study were male because

the prototype available at the time of testing had a male-specific fit. Though it is noted that both prior lab studies involved males and females, and the subsequent version of this exosuit (HeroWear Apex) includes both male- and female-specific fits. This study was approved by the Vanderbilt University Institutional Review Board and the workers gave informed written consent prior to participation.

2.1 Training

Workers were introduced to the exosuit over a 45-min period. This introduction included an overview of the exosuit and the testing protocol. Then each worker was fit with the exosuit and allowed a limited amount of time to acclimate by performing a series of general bending and lifting tasks to get a feel for how the device functioned.

2.2 Simulated Lifting and Lowering Tasks

Workers were instrumented with electromyographical (EMG) sensors (Delsys Trigno Mini) on six back muscles: left and right Multifidus, Longissimus Thoracis, and Iliocostalis Lumborum. Workers then completed lifting cycles with and without wearing the exosuit. A full cycle of the task involved beginning in an upright standing posture, lifting a 22-lb box from a pallet (5.5 in. in height), turning 90°, and setting the box down on a table (36 in. in height), then lifting, turning 90°, and lowering the box down to the starting location, and returning to upright standing. Each cycle was repeated 15 times. Workers were allowed to lift/lower using any technique they would normally use at work (i.e., technique was not controlled). EMG data were analyzed to extract total and peak values, and averaged to obtain an EMG summary metric for comparison purposes.

2.3 Real Work Environment Evaluation

After completion of the simulated tasks, individuals returned to work (Fig. 2) and wore the exosuit during their actual distribution center job for an average of 20–30 min. Workers did picking or auditing work (i.e., de-palletizing and re-palletizing product). User feedback and experiences were recorded through audio/video recordings and a 7-point Likert-scale questionnaire (Fig. 1).

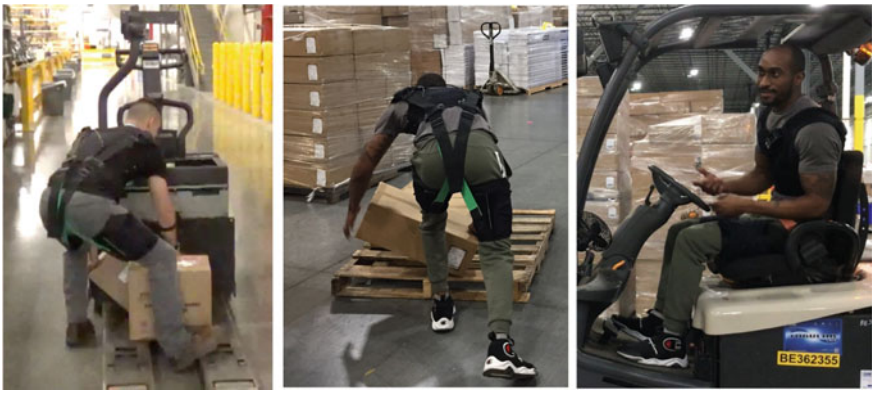

Fig. 2 Distribution center workers using an exosuit prototype on the job for a variety of logistics tasks: picking, palletizing, forklift driving

3 Results

The questionnaire results (Fig. 1) indicate that the vast majority of the workers reported feeling assisted, comfortable, and free to move naturally while wearing the exosuit. They also felt the exosuit was easy to use, useful for their job, that it could fit into their daily work without interfering, and that they would be interested in using the exosuit to do their job for an extended period of time. The majority of workers showed reduced back muscle activity while wearing the exosuit during both lifting and lowering tasks (e.g., Fig. 3), consistent with results observed in prior lab studies (e.g. [3]). Average reductions in peak and total back muscle activity were ~10% across the full lifting/lowering task, and about two-thirds of workers exhibited reductions >15% during lifting or lowering.

Worker testimonials corroborated the questionnaire results and reductions in back muscle activity. Example excerpts: (1) "I get tired quicker without the exosuit." (2) "The suit slingshots you back up. Once you start it pushes you the rest of the way." (3) "It didn't hinder the movements at all, I could still do everything I needed to do; boxes that I pick up all the time felt lighter and easier to pick up." (4) "Can already tell a big difference, feel that it's really helping. My back hurts 75% of the time, but I can already feel a difference."

4 Discussion and Conclusion

User feedback, perceptions, and acceptance of the exosuit prototype were all positive. The workers reported feeling assisted, comfortable, and unrestricted while wearing the exosuit. The workers also felt the exosuit could be useful and fit into their daily work without interfering. Because user acceptance plays such a critical

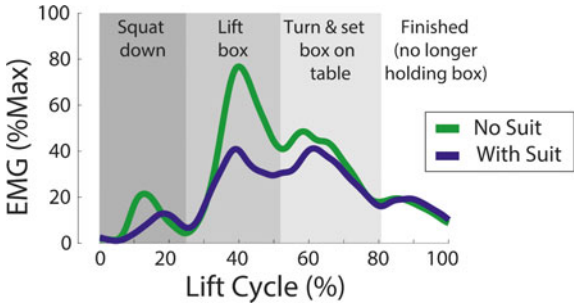

Fig. 3 Results from representative worker showing reduced back muscle activity (EMG) when wearing the exosuit prototype

role in sustained use and successful long-term outcomes from using any new technology, these results suggest that the exosuit has excellent potential for adoption by logistics workers. EMG testing in this logistics field study also confirmed and supported results observed in previous lab studies, indicating that the exosuit reduces peak back muscle activity (which may be associated with injury risk) and total back muscle activity (which may be associated with fatigue) during lifting, lowering and bending. Collectively these results demonstrate that this type of low-profile, unmotorized, dual-mode exosuit can reduce back strain and make lifting objects easier, without restricting posture or movement. Muscle activity findings and user feedback from this logistics field test on the prototype were used to inform and finalize design of the HeroWear Apex exosuit, which was commercially released in March 2020.

Acknowledgement The authors thank: Shimra Fine for help with prototype development, Emily Matijevich for help with data collection.

References

1. Liberty Mutual Insurance Company, Liberty Mutual Workplace Safety Index (2020)
2. M.M. Alemi et al., Effects of two passive back-support exoskeletons on muscle activity, energy expenditure, and subjective assessments during repetitive lifting. Human Factors (2020)
3. E.P. Lamers et al., Feasibility of a biomechanically-assistive garment to reduce low back loading during leaning and lifting. IEEE Trans. Biomed. Eng. (2018)
4. E.P. Lamers et al., Low-profile elastic exosuit reduces back muscle fatigue. Nat. Sci. Rep. (2020)

A Design Tool for Passive Wrist Support

Ali Amoozandeh Nobaveh, Giuseppe Radaelli, and Just L. Herder

Abstract A design tool for passive wrist support using compliant spatial beams as gravity balancer is presented. The aim of this assistive device is to reduce required effort for pronation-supination and flexion-extension by 70% to help patients with muscular weakness keeping their hand's posture and doing daily tasks, while the forearm is rested. To reach this goal, a setup with three connection points to the user's hand, and two optimized spatial beams as elastic gravity compensators, are developed. The overall shape and cross-sectional dimensions of the compliant beams are attained using an optimization technique. The objective is reaching a desired endpoint kinetostatic behaviour which is determined based on the hand's weight and available muscular forces. A design case is presented to show the ability of the method, and the final errors from the desired behaviour are clarified. In the end, possible further applications of the design tool are discussed.

1 Introduction

A plain wrist support can help people who are suffering from muscular weakness [1] by keeping their hand in a normal posture and avoid further damages to the body tissues due to hanging of the hand. The majority of mentioned people have control on their muscles, but are not able to provide sufficient muscular power to keep the desired postures, e.g., patients with Duchenne muscular dystrophy (DMD). Previously there were only fixed orthoses available for those people. However, with recent developments, there exist active and passive assistive devices to help them control their hand's posture to some extent [2]. Among those, passive devices which mainly work based on reducing required effort by static balancing of the hand's weight are more widespread as they are lighter and cheaper. In the case of using compliant

Supported by NWO (P16-05: Shell Skeletons).

A. Amoozandeh Nobaveh (✉) · G. Radaelli · J. L. Herder
Precision and Microsystems Engineering Department, Delft University of Technology, Delft, The Netherlands
e-mail: A.AmoozandehNobaveh@tudelft.nl

J. C. Moreno et al. (eds.), *Wearable Robotics: Challenges and Trends*,
Biosystems & Biorobotics 27, https://doi.org/10.1007/978-3-030-69547-7_3

mechanism instead of conventional linkages in the mentioned passive devices, they could be even more flexible and slender.

The goal of this paper is to present a design tool for a flexible passive wrist support using spatial compliant beams which work as elastic elements for gravity balancing to keep the normal posture of hand and facilitate movement of the wrist in a limited range of motion while the forearm is rested horizontally. This design tool can provide tunable sizing and kinetostatic characterization for gravity balancing based on different user requirements, by using the elastic deformation of optimized spatial compliant beams [3].

The paper is structured as follows. In Sect. 2, the design of the wrist support and its functional requirements are described together with the details of the spatial beam optimizer. In Sect. 3 the results are shown for a case, and discussion is given on them. In the end, the conclusion and possible future applications are discussed in Sect. 4.

2 Methods

2.1 Proposed Design

The wrist support is designed to have three interfaces with the hand, two on the upper and lower forearm and one under the palmar side of the hand. These three points are connected from the outer side of the hand with two slender compliant beams which are shaped by the optimization process based on defined requirements. The hand and lower forearm supination, while they are rested horizontally, are balanced by the first beam connecting the upper and lower forearm interfaces to provide the required moment by elastic deformation. The required wrist extension balancing force is provided by the elastic bending of the second beam between the lower forearm and palmar side of the hand. The requirements for passive balancing beams are set to reach $30° \pm 25°$ for the wrist pronation-supination and $0° \pm 40°$ for the hand flexion-extension with 70% less muscular effort. The resulted beams could have different shapes in restricted design area and base on dissimilar requirements of users.

Figure 1 shows the resulted beams and the wrist support interfaces. The hand interfaces are made based on the parallelogram mechanism, which leads to easier wearing and size adaptability of the device, as well as keeping the beams aligned with the user's hand.

2.2 Beam Shape Optimization

The developed optimization process uses the general shape of the beams and their cross-sectional properties to reach the design requirements. Concerning the general shape of the beam, the coordinates of six control points along the beam together with

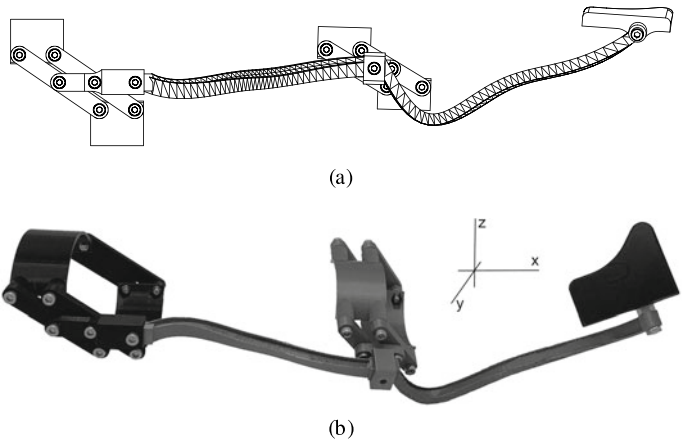

(a)

(b)

Fig. 1 **a** Designed wrist support, **b** 3D printed prototype

the cross-sectional orientations on those points are subjected to the optimization to form the B-spline of the beam spine shape. Regarding cross-sectional optimization, an I-shaped cross-section is selected for the beam, since it is a commercial section and changing its parameters enables a large variety of section properties for the optimizer. All dimensional parameters of the mentioned section are subjected to the optimization. The endpoint stiffnesses in this process are derived from a self-developed finite element solver using geometrically non-linear co-rotational beam elements introduced by Battini [4] with Euler-Bernoulli beam model. Concerning the optimization process the *Multi Start*, using the *fmincon* from the Matlab® *optimization toolbox* is used and subjected to the bounds to form the beam inside the required design space.

3 Results and Discussion

The resulted connection beams could have varying shapes and cross-sections based on different user requirements. Here we present results based on requirements of an average human size [5]. Figure 2 shows the wrist beam (top) and forearm beam (bottom) deflections from undeformed shape (transparent) to deformed shape, under three different loadings. The middle beams shows shapes loaded by the users hand's weight when wearing the device for keeping the hand in a normal posture without any muscular effort. The right beams shows shapes when users provide 30% of the hand's weight in order to do wrist extension (top) and supination (bottom). Finally, the left beams show wrist flexion (top) and pronation (bottom) again with 30% effort in opposite direction. The resulted deflection angles for pronation-supination and flexion-extension are showed in Table 1. It is important to note that those angels are measured from the rest posture without any muscular effort while wearing the

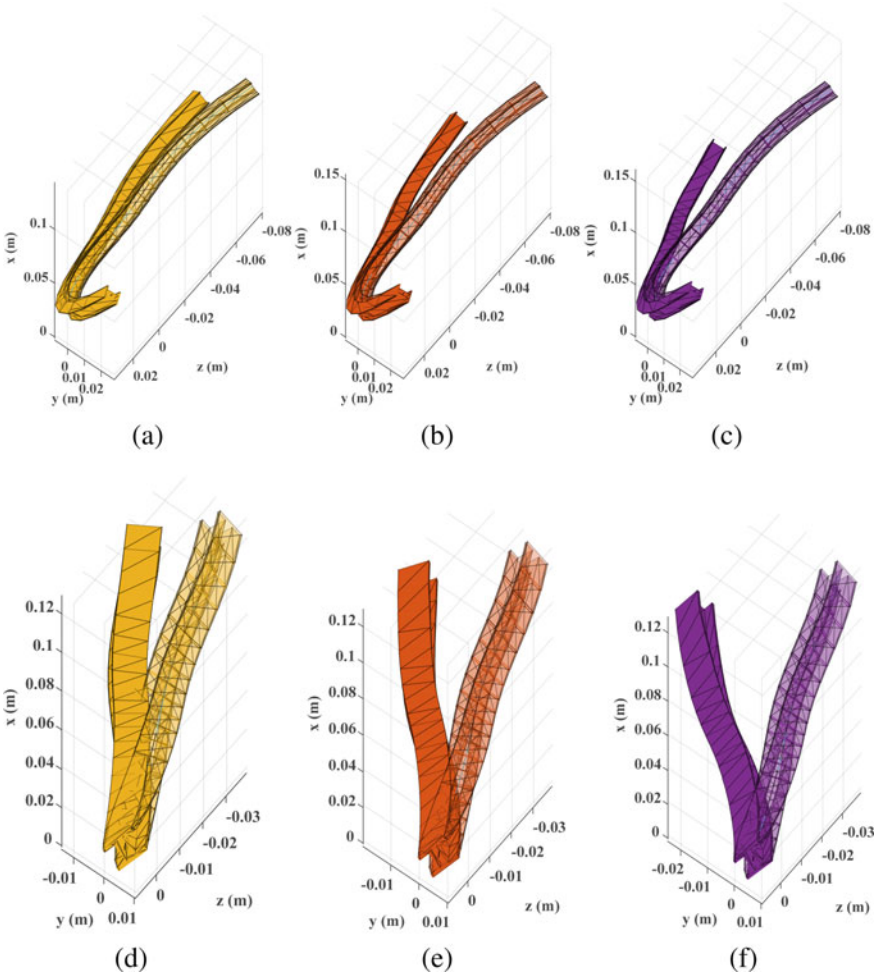

Fig. 2 Deflection of the beams from initial form (transparent) to final form, **a** wrist beam under −30% force, **b** wrist beam in neutral position under hand's weight, **c** wrist beam under +30% force, **d** forearm beam under −30% force, **e** forearm beam in neutral position under hand's weight, **f** forearm beam under +30% force

device. The device keeps the hand in 32.4° (supination) and 3.1° (extension) as normal posture. Comparing the resulting angles from Table 1 with the desired angles mentioned in Sect. 2, the average of all errors is 5.9%. Reaching this error from these slender compliant beams in the such extensive range of motion, shows the ability of the method to replace the conventional passive assistive wrist supports with this flexible and light design. Also it shows the potential of the method to handle more complicated requirements of other assistive devices.

Table 1 determined angles

Force	Supination (+) Pronation (−)	Extension (+) Flexion (−)
+30%	+24.2°	+42.5°
−30%	−23.1°	−39.0°
Avg. error	5.57%	4.29%

4 Conclusion

This paper presents a design tool for a passive wrist support using optimized compliant beams as weight compensator to keep the normal hand's posture and enable the wrist movement in an extensive working range with 30% of required muscular forces. The effectiveness of this method has been shown by exploring resulting angles in pronation-supination and flexion-extension. Such design requirements and flexibility are not easily achievable with passive conventional mechanisms and existing compliant mechanisms design methods, which shows the capacity of this approach to handle more complex demands for passive assistive devices.

References

1. A.E.H. Emery, Population frequencies of inherited neuromuscular diseases–a world survey. Neuromuscul. Disord **1**(1), 19–29 (1991)
2. R.A.R.C. Gopura, K. Kiguchi, D.S.V. Bandara, A brief review on upper extremity robotic exoskeleton systems, in *6th International Conference on Industrial and Information Systems* (IEEE, New York, 2011)
3. A.A. Nobaveh, G. Radaelli, J.L. Herder, Asymmetric spatial beams with symmetric kinetostatic behaviour, in *Symposium on Robot Design, Dynamics and Control* (Springer, Cham, 2020)
4. J.-M. Battini, C. Pacoste, On the choice of local element frame for corotational triangular shell elements. Commun. Numer. Methods Eng. **20**(10), 819–825 (2004)
5. S. Plagenhoef, F. Gaynor Evans, T. Abdelnour, Anatomical data for analyzing human motion. Res. Q. Exercise Sport **54**(2), 169-178 (1983)

The Key Elements in the Design of Passive Assistive Devices

Maziar A. Sharbafi

Abstract Nowadays, enhancing the physical abilities of able-bodied humans attracted the researchers' attention besides the development of assistive devices for people with mobility disorders. As a result, the interest in designing of cheap and soft wearable exoskeletons called exosuits is distinctly growing. Careful investigation of the biological musculoskeletal systems reveals three essential features simplifying gait control. The first property is the embedded compliance in the muscle-tendon-complex (MTC). Force-velocity or damper-like muscle behavior is the second feature. The last useful feature is in the biological morphological design of multi-articular muscles. These properties can be implemented in passive, assistive devices in isolation or combination. In this paper, we summarize a few studies on passive lower limb assistive devices that benefit from these two design concepts. We elaborate more on the outcomes of a recent study on a lower limb exosuit design with two biarticular elastic elements that combine the two aforementioned mechanisms in a single device.

1 Introduction

Biomechanical models with different levels of complexity are of advantage to understand the underlying principles of legged locomotion. This is an essential step to develop machines that aim at assisting human locomotion, namely assistive devices. Nowadays, these devices assist not only impaired people, but also healthy humans by reducing metabolic cost, fatigue, or increasing comfort. Among different types

This article is partially supported by the German Research Foundation (DFG) under the Grant No. AH307/2-1.

M. A. Sharbafi (✉)
Lauflabor Locomotion Lab, Center of Cognitive Science, TU Darmstadt, Darmstadt, Germany
e-mail: sharbafi@sport.tu-darmstadt.de

J. C. Moreno et al. (eds.), *Wearable Robotics: Challenges and Trends*,
Biosystems & Biorobotics 27, https://doi.org/10.1007/978-3-030-69547-7_4

of assistive technologies, passive devices became more popular due to their simple, cheap, light, and user-friendly designs. Removing electronics, including motors, sensors, and batteries from the exo design and development reduces the required effort and cost for maintenance. In short, people can wear passive wearable devices like clothes or shoes needless to charge the batteries and carry heavy backpacks. The cost for achieving this level of comfort is the lacking of energy resources, which lower the potential performance of passive devices compared to active ones, regarding metabolic consumption or supporting patients with severe disabilities (e.g., paraplegic patients). In other words, passive gait assistance devices can support energy management without energy injection.

Since passive devices can not inject energy, how can they improve energy management? The only possibilities are energy shuffling or dissipation; both are supported by biological evidence. Energy shuffling can be performed regarding time or position. In that respect, elastic elements can store energy at a specific time domain (gait phase) and return it at another time. For this, springs are essential elements in different types of passive assistive devices, from carbon foot prostheses to exoskeletons [3]. More advanced techniques of using nonlinear springs or their combinations with clutches can provide more significant advantages regarding energy management by defining more complex force-length behaviors [6]. However, this is not the only method for energy shuffling. Biarticular muscles are smart biological solutions for transferring energy between two joints. For example, using cables [4] or springs [5] in a biarticular arrangement can easily implement energy shuffling between two positions (joints) in a robot as well as in an assistive device [6]. Regarding energy dissipation, biomechanical studies demonstrated damper-like behavior in legged locomotion (e.g., knee joint in downhill walking). This energy dissipation will be costly in the human body or active assistive devices. Instead, passive dampers (e.g., hydraulics) can provide this property, which could surprisingly yield improvement in gait performance by dissipating energy [7].

In this paper, we first present a brief overview of the state-of-the-art of passive assistive devices, which are designed based on these three basic elements. Then, a recent study [2] on gait assistance with a passive exosuit having biarticular thigh elastic elements will be briefly described. These compliant elements are in parallel to the hamstring and rectus femoris muscles of the leg, which combine energy transferring within time and location.

2 Methods

Passive assistive devices can be roughly categorized as: (1) Passive prostheses [8], (2) Exoskeletons supporting upper body (e.g., for load carrying [10]), and (3) exoskeletons for supporting lower limb in locomotion [3, 9]. The focus of this article is on the third category and also the compliance and biarticular design from the three aforementioned key features.

2.1 Compliance and Multi Articular Engagement

Employing passive devices for enabling amputees to locomote is not new [11]. The documented schematic drawing from previous centuries demonstrates the interest of researchers to facilitate locomotion for healthy subjects using assistive devices. In [1], a multiarticular bow spring with a limited range of motion exerted by cords or chains was introduced to support humans for different gaits (see Fig. 1(left). The idea of storing and returning energy with elastic elements and transferring energy between different joints provides the core concept of this invention in late 19 century. In 2003, van den Bogert introduced the exotendons as poly-articular elastic mechanisms with a significant contribution to the economy of legged locomotion [4]. This passive assistive technology is based on long elastic cords attached to an exoskeleton and guided by pulleys, which are placed at the joints. With human experiment-based simulations, he demonstrated the ability of a complex exotendon system to reduce the joint moments required for normal walking by 71% and joint power by 74% [6]. However, this amount of metabolic reduction could never be approached in reality. In [12], van Dijk et al. tested an exoskeleton with exotendons, which could reduce human mechanical work up to 40% in simulations. Contrarily, the developed device could never reduce the metabolic in human experiments [6]. In 2015, Collins et al. developed an ankle exoskeleton that could reduce the metabolic cost of healthy human walking by more than 7%. This lightweight elastic device acts parallel with the user's calf muscles, off-loading muscle force in contractions. Using a mechanical clutch to tune engagement of the spring supports the function of the calf muscles and Achilles tendon. In another recent study, Nasiri et al. developed a passive compliant exoskeleton which benefits from energy transfer between the right and left hip joints [13]. The simple spring can generate about 8% metaboic rate reduction by shuffling the energy between the two hip joins during running at 2.5 ms^{-1}. Using biarticular thigh springs, the significant advantages of biarticular springs in a new passive exosuit was demonstrated in [2]. A summary of the methods and achievements in this latter study will be presented in the following.

2.2 Case Study

(A) Design concept

Investigating joint power consumption in human locomotion (e.g., walking) shows reciprocal behavior between hip and knee joints during swing phase. This means that instead of generating and dissipating energy in two adjacent joints, shuffling energy between them using biarticular coupling is a much more efficient solution. In [2], this concept was utilized to develop a biarticular thigh exosuit, shown in Fig. 1(right). Instead of multi articular leaf springs of [1], we employed biarticular elastic rubber bands. In this bioinspired design, the passive artificial muscles (rubber bands) are utilized to mimic human rectus femoris and hamstring muscles. With these passive

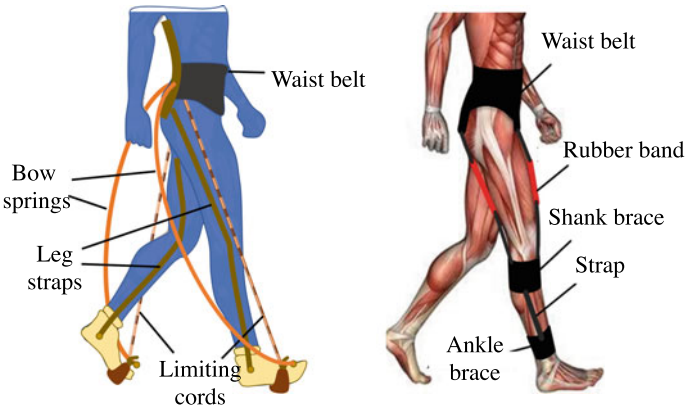

Fig. 1 Examples of Passive exos with multiarticular compliant mechanisms. (left) A schematic drawing, adopted from the *apparatus for facilitating for walking running and jumping* from Yagn in 19th century [1]. (right) The passive biarticular thigh exosuit from [2]

elements we can nicely predict human swing leg movement [14]. In [15], we showed that active control of these biarticular spring stiffness using the ground reaction force withing the FMCH (force modulated compliant hip) framework [16] can acceptably support human balancing. The FMCH method was developed to generate the VPP (virtual pivot point) as a biological posture control strategy in humans and animals [17]. Our previous studies on using constant stiffness for balance control showed that without GRF (ground reaction force) feedback in the FMCH, the VPP can still be predicted [18], but the gait will not be as robust as with the FMCH [19]. However, the passive mechanism (without feedback) could be useful to assist human gait as stability is guaranteed by human subject [20].

(B) Experiments

Eight non-impaired male subjects (age, 23–26 years; mass, 60–87 kg; height, 170–185 cm) participated in the experiments. They had no previous experience of walking with the exosuit. They voluntarily signed an informed consent form approved by the Sport Science Research Institute of Iran. The experimental setup and the developed exosuit are shown in Fig. 2.

We measured the metabolic rate to investigate the effect of the assistive device and the corresponding stiffness of the artificial muscles on energy expenditure in human walking. All participants walked on a treadmill at 1.3 ms^{-1} under different conditions: normal walking without the exoskeleton (NE for No-Exosuit); walking with the exosuit but no spring connected (NS for No-Spring); and walking with three different stiffness (low, medium and high) for each of the biarticular artificial muscles (in total 8 combinations). The measured data is from five minutes experiments for each walking condition. These conditions were randomized to prevent fatigue, learning and order effects on experimental results. Switching between NE and other cases needed wearing or taking off the exosuit preceded by two minutes warm-up

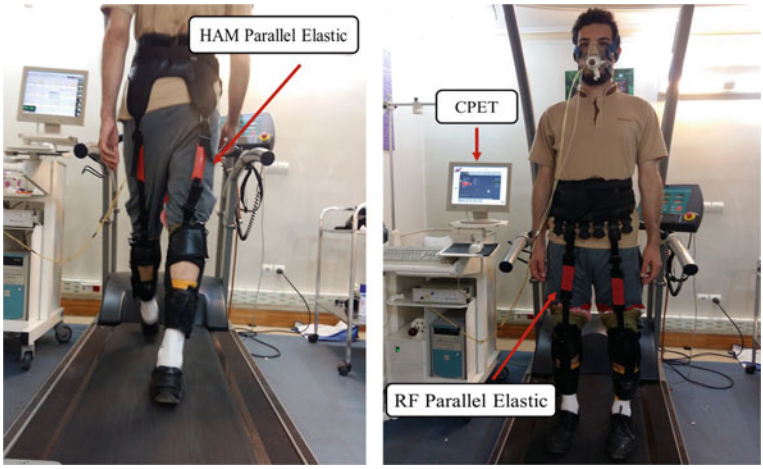

Fig. 2 Soft passive exosuit: (Left) back side view in the experimental trial of treadmill walking with metabolic cost measurement. (Right) the frontal view of exosuit

walking. In addition, for measuring bias metabolic cost with and without exosuit, we consider data collection during three minutes standing still for each of the two conditions.

3 Results

We first compare the metabolic cost of the assisted test with no-Spring (NS), to realize the effect of adding the biarticular springs. Then, the results are compared to normal (unassisted) walking (NE). For each subject, we select the data of the assisted experiment (when the springs are contributing) with the lowest metabolic rate, and the "Assisted" data is the average of these trials for different subjects. This way, we demonstrate the results of the optimal stiffness arrangement (among the tested combinations) for each subject. The optimal arrangements are different for different subjects.

We present the experimental results of the average metabolic rate for the last two minutes of walking trial subtracted by standing metabolic rate. Just by wearing the exosuit without springs contributions, the metabolic rate will increase by 12.9 $\pm$ 6.5%. This could be due to the non-optimal design of the wearable parts and additional mass. Asbeck et al. showed that additional mass at different places in the legs could already increase the metabolic cost up to 8%/kg [21]. Surprisingly, comparison between assisted and NS (paired t-test with $P = 0.0035$) cases shows that just by adding compliance (with optimal stiffness) 14.7 $\pm$ 4.27% reduction in metabolic cost can be achieved. Compared to the normal walking without assistance

(NE), the proposed passive exosuit can reduce the average metabolic rate by 4.68 ± 4.24%. More details can be found in [2].

4 Conclusion and Future Work

In this article, we summarized the key elements of designing passive assistive devices in (1) elasticity, (2) multi-articular arrangements, and (3) damping. We focused on the first two elements and, more specifically, on lower limb assistive devices. After presenting a brief overview of the developed devices and state-of-the-art, we detailed more about our passive exosuit with biarticular thigh springs.

In this device, we benefit from both elasticity and biarticular design. We showed that transferring energy from hip to knee and vice versa could result in metabolic cost reduction. In spite of about 13% increase in metabolic cost just by wearing the suit without compliant elements, involving the artificial biarticular thigh muscles (elastic bands) could reduce energy consumption even compared to normal walking (about 5%). These passive elements not only compensate for the effect of the imperfect design but also provide additional benefit for walking efficiency. We improved the design and manufacturing to minimize the effects of additional mass and other non-optimized mechanical parts of the wearable parts (without springs). The recent version was successfully tested in pilot experiments (not reported). Doing experiments with more subjects will be the next step.

In the here presented experiments, we only tested three stiffness values for each of the biarticular springs. Recently, Human-in-the-loop-Optimization (HILO) was introduced as a practical tool to optimize control parameters in the assistive devices [22]. This method can be used in the future to find the optimal stiffness with here presented exosuit.

References

1. Apparatus for facilitating walking, running, and jumping
2. H. Barazesh, M.A. Sharbafi, A biarticular passive exosuit to support balance control can reduce metabolic cost of walking. Bioinspiration & Biomimetics **15**(3), 036009 (2020)
3. S.H. Collins, M. Bruce Wiggin, G.S. Sawicki, Reducing the energy cost of human walking using an unpowered exoskeleton. Nature **522**(7555), 212 (2015)
4. A.J. Van Soest, A.L. Schwab, M.F. Bobbert, G.J. van Ingen Schenau, The influence of the biarticularity of the gastrocnemius muscle on vertical-jumping achievement. J. Biomech. **26**(1), 1–8 (1993)
5. M.A. Sharbafi, C. Rode, S. Kurowski, D. Scholz, R. Möckel, K. Radkhah, G. Zhao, A.M. Rashty, Oskar von Stryk, A. Seyfarth, A new biarticular actuator design facilitates control of leg function in biobiped3. Bioinspiration & biomimetics **11**(4), 046003 (2016)
6. A.J. Van den Bogert, Exotendons for assistance of human locomotion. Biomed. Eng. Online **2**(1), 17 (2003)

7. S. Portnoy, A. Kristal, A. Gefen, I. Siev-Ner, Outdoor dynamic subject-specific evaluation of internal stresses in the residual limb: hydraulic energy-stored prosthetic foot compared to conventional energy-stored prosthetic feet. Gait & Posture **35**(1), 121–125 (2012)
8. A. Naseri, M.M. Moghaddam, M. Gharini, M.A. Sharbafi, A novel adjustable damper design for hybrid passive ankle prosthesis. Actuators (2020)
9. M.C. Faustini, R.R. Neptune, R.H. Crawford, S.J. Stanhope, Manufacture of passive dynamic ankle-foot orthoses using selective laser sintering. IEEE Trans. Biomed. Eng. **55**(2), 784–790 (2008)
10. M.M. Alemi, S. Madinei, S. Kim, D. Srinivasan, M.A. Nussbaum, Effects of two passive back-support exoskeletons on muscle activity, energy expenditure, and subjective assessments during repetitive lifting. Hum. Factors **62**(3), 458–474 (2020)
11. B.F. Palmer, Artificial leg. US Patent (1846)
12. W. Van Dijk, H. Van der Kooij, E. Hekman, A passive exoskeleton with artificial tendons: design and experimental evaluation, in *2011 IEEE International Conference on Rehabilitation Robotics* (IEEE, New York, 2011), pp. 1–6
13. R. Nasiri, A. Ahmadi, M.N. Ahmadabadi, Reducing the energy cost of human running using an unpowered exoskeleton. IEEE Trans. Neural Syst. Rehab. Eng. **26**(10), 2026–2032 (2018)
14. M.A. Sharbafi, A.M.N. Rashty, C. Rode, A. Seyfarth, Reconstruction of human swing leg motion with passive biarticular muscle models. Hum. Movement Sci. **52**, 96–107 (2017)
15. M.A. Sharbafi, H. Barazesh, M. Iranikhah, A. Seyfarth, Leg force control through biarticular muscles for human walking assistance. Front. Neurorobot. **12**, 39 (2018)
16. M.A. Sharbafi, A. Seyfarth, FMCH: a new model for human-like postural control in walking, in *2015 IEEE/RSJ International Conference on Intelligent Robots and Systems (IROS)* (IEEE, New York, 2015), pp. 5742–5747
17. H.-M. Maus, S.W. Lipfert, M. Gross, J. Rummel, A. Seyfarth, Upright human gait did not provide a major mechanical challenge for our ancestors. Nat. Commun. **1**, 70 (2010)
18. M.A. Sharbafi, M.N. Ahmadabadi, M.J. Yazdanpanah, A.M. Nejad, A. Seyfarth, Compliant hip function simplifies control for hopping and running, in *2013 IEEE/RSJ International Conference on Intelligent Robots and Systems* (IEEE, New York, 2013), pp. 5127–5133
19. M.A. Sharbafi, A. Seyfarth, Stable running by leg force-modulated hip stiffness, in *5th IEEE RAS/EMBS International Conference on Biomedical Robotics and Biomechatronics* (IEEE, New York, 2014), pp. 204–210
20. G. Zhao, M.A. Sharbafi, M. Vlutters, E. van Asseldonk, A. Seyfarth, Bio-inspired balance control assistance can reduce metabolic energy consumption in human walking. IEEE Trans. Neural Syst. Rehab. Eng. (2019)
21. A.T. Asbeck, S.M.M. De Rossi, I. Galiana, Y. Ding, C.J. Walsh, Stronger, smarter, softer: next-generation wearable robots. IEEE Rob. Autom. Maga. **21**(4), 22–33 (2014)
22. J. Zhang, P. Fiers, K.A. Witte, R.W. Jackson, K.L. Poggensee, C.G. Atkeson, S.H. Collins, Human-in-the-loop optimization of exoskeleton assistance during walking. Science **356**(6344), 1280–1284 (2017)

Novel Designs for Passive Elastic Lower Limb Exoskeletons

Daniel P. Ferris and W. Sebastian Barrutia

Abstract Engineers and scientists have long tried to build powered robotic lower limb exoskeletons without success (at least commercially). A major limitation has been the need for large amounts of mechanical power from the actuators. Simply put, human muscles are amazing motors. The size and mass of robotic actuators that can match human muscle limit exoskeleton hardware designs. An alternative to heavy motors that engineers have relied on throughout history has been power amplification from passive elastic mechanisms. We review examples of successful passive elastic systems that have been previously used by humans and discuss how elastic mechanisms can be incorporated into lower limb exoskeletons for assisting human locomotion.

1 Introduction

Fifty years of building powered robotic lower limb exoskeletons have not yielded a commercially successful device [1]. There are many companies currently developing robotic exoskeletons around the world, but none of them have gained enough profit from their sales to balance out past research and development investments into the technology. The large bulk and mass of actuators and frames are major obstacles to successful human performance augmentation [1]. Another limitation has been an inability to develop controllers that truly move the exoskeleton synergistically with the human [1]. Agile and smooth motion is necessary for the human user to choose to use the exoskeleton.

One of the offshoots of exoskeleton research has been to turn to soft exosuits that deliver less mechanical power than rigid exoskeleton devices, but are fairly lightweight and more comfortable to wear [2]. They can be targeted to specific joints

D. P. Ferris · W. Sebastian Barrutia (✉)
J. Crayton Pruitt Family Department of Biomedical Engineering, University of Florida, Gainesville, FL, USA
e-mail: wbarrutia@ufl.edu

D. P. Ferris
e-mail: dferris@bme.ufl.edu

J. C. Moreno et al. (eds.), *Wearable Robotics: Challenges and Trends*,
Biosystems & Biorobotics 27, https://doi.org/10.1007/978-3-030-69547-7_5

or specific activities, providing a smaller boost in mechanical power at the right moment to assist human locomotion [3]. However, even exosuits as they are currently designed rely on external energy sources (i.e. batteries) to deliver mechanical energy to the human.

Another alternative would be to rely on passive elastic mechanisms for storage and return of energy during human movement. Inventors have long relied on elastic mechanisms for human power amplification. Sometimes the designs have been incredibly innovative and fundamentally changed the advancement of human society. Other times the designs have been small tweaks to existing devices, but still have had positive effects that have benefitted humans.

We will briefly review some of examples of passive elastic mechanisms that have benefitted humankind. These can serve as examples covering some of the design space for passive elastic devices. Next, we consider a few specific device designs that were able to provide storage and return of elastic energy during human movement.

2 Historical Devices

Prior to the creation of motorized robotic devices, human have looked to elastic mechanisms for amplifying human power output or assisting human movement. Both the traditional bow and the compound bow can greatly enhance mechanical power output of a human in launching projectiles [4]. In sports, humans have repeatedly used elastic energy storage and return to increase mechanical power output. The use of fiberglass poles in the pole vault and elastic strings in a tennis racquet are just two examples. McMahon originally proposed elastic running surfaces for enhancing a runner's speed [5, 6]. Although his theory was later invalidated due to the nature of damping in the runner's leg mechanics, a compliant running surface can indeed improve running performance [7, 8]. Building on McMahon's ideas, Van Phillips created his elastic lower limb prosthesis for running, which has fundamentally changed the way that individuals with lower limb amputations approach athletic mobility [9]. Herr and Langman showed that tuning of elastic elements can indeed be very important for maximizing human performance in an early exosuit [10]. This history doesn't even include novelties such as pogo sticks, kangaroo shoes, or bungee jumping tethers. The take home message, however, is that there is a rich collection of previous elastic devices intended to assist with human movement.

3 Lower Limb Exoskeleton Devices

Michael Cherry set out to build a unique elastic lower limb exoskeleton for human running. He joined the Human Neuromechanics Laboratory at the University of Michigan in 2005. After multiple attempts at building elastic energy mechanisms into a leg assist device, he settled on a design using both energy storing springs in a

backpack that delivered the energy by Bowden cables to the knee, and an elastic leaf spring parallel to the ankle that provided additional storage and return [11]. Biomechanical measurements showed that the exoskeleton could reduce quadriceps muscle activation and the net muscle moment at the knee during the stance phase of running [12]. However, due to the added inertia of the leg during swing and the loss of elastic energy to tissue compression during stance that reduced the biomechanical assist, metabolic energy costs increased when comparing running with the exoskeleton to running without the exoskeleton. Although the device was not successful in reducing the energy cost of running, the lessons learned from the design and testing provide important insight for future exoskeletons.

A new passive elastic exoskeleton design in the Human Neuromechanics Laboratory at the University of Florida hopes to avoid some of the drawbacks of the previous design. By using 3D printing of carbon fiber, frame strength can be achieved while keeping overall mass of the exoskeleton low. Rather than focusing on running initially, which has high ground reaction forces and net muscle moments, the new exoskeleton design is targeting walking. Forces and moments are much lower for walking compared to running.

The initial design (Fig. 1) is a prototype that will be scaled down for children with walking disabilities. Scaling laws benefit engineers creating lower limb exoskeletons for humans with body masses of 10–30 kg in comparison to creating lower limb exoskeletons for humans with body masses of 50–200 kg. Materials generally increase their strength to weight ratio as geometric size decreases. This is because strengths of materials increase proportionally with cross sectional areas, but weight

Fig. 1 Lightweight, 3D printed lower limb exoskeleton relying on elastic energy storage to assist knee extension

increases proportionally with volumes. There are many different neurological and developmental disabilities that cause muscle weakness in the knee extensors of children (e.g. cerebral palsy, spina bifida). A common approach to facilitate walking exercise in these individuals is to use bodyweight support harnesses for walking on a treadmill. A passive lower limb exoskeleton that could allow walking exercise over ground would enable more cognitively stimulating and physically diverse environments (e.g. surface changes, obstacles, outdoor exercise). If the majority of the parts are 3D printed, it becomes easier to fabricate new parts for the exoskeleton as the child grows [13].

4 Conclusion

The coming years will see more advances in passive elastic lower limb exoskeletons due to their advantages in minimizing exoskeleton mass and bulk. Additive manufacturing technology allows 3D printers to generate carbon fiber and Kevlar frames that can be quickly customized for individual users. By taking advantage of the insight provided by past elastic mechanisms designed to assist human movement, it may be possible to design future exoskeletons to provide novel ways to recycle and amplify energy for walking and running, both in health and disability.

Acknowledgements Funded by NSF CBET-0347479, Lockheed Martin Corp., and the Leo Claire & Robert Adenbaum Foundation.

References

1. A.J. Young, D.P. Ferris, State of the art and future directions for lower limb robotic exoskeletons. IEEE Trans. Neural Syst. Rehabil. Eng. **25**(2), 171–182 (2017)
2. J. Kim et al., Reducing the metabolic rate of walking and running with a versatile, portable exosuit. Science **365**(6454), 668 (2019)
3. A. Asbeck, S. De Rossi, I. Galiana, Y. Ding, C. Walsh, Stronger, smarter, softer: next-generation wearable robots. Robot. Autom. Maga. **21**(4), 22–33 (2014)
4. A.E. Minetti, Passive tools for enhancing muscle-driven motion and locomotion. J. Exp. Biol. **207**(8), 1265–1272 (2004)
5. T.A. Mcmahon, P.R. Greene, Fast running tracks. Sci. Am. **239**(6), 148 (1978)
6. T.A. Mcmahon, P.R. Greene, Influence of track compliance on running. J. Biomech. **12**(12), 893–904 (1979)
7. D.P. Ferris, M. Louie, C.T. Farley, Running in the real world: adjusting leg stiffness for different surfaces. Proc. R. Soc. B-Biol. Sci. **265**(1400), 989–994 (1998)
8. A.E. Kerdok, A.A. Biewener, T.A. McMahon, P.G. Weyand, H.M. Herr, Energetics and mechanics of human running on surfaces of different stiffnesses. J. Appl. Physiol. **92**(2), 469–478 (2002)
9. J. Poskett, The fastest man on no legs. Phys. World **25**(7), 22–25 (2012)
10. H. Herr, N. Langman, Optimization of human-powered elastic mechanisms for endurance amplification. Struct. Optim. **13**(1), 65–67 (1997)

11. M.S. Cherry, S. Kota, D.P. Ferris, An elastic exoskeleton for assisting human running, in *ASME 2009 International Design Engineering Technical Conferences and Computers and Information in Engineering Conference* (American Society of Mechanical Engineers, 2009), pp. 727–738
12. M.S. Cherry, S. Kota, A. Young, D.P. Ferris, Running with an elastic lower limb exoskeleton. J. Appl. Biomech. **32**(3), 269–277 (2016)
13. T. Rahman et al., Passive exoskeletons for assisting limb movement. J. Rehab. Res. Dev. **43**(5), 583–589 (2006)

Passive Compliance in Legged Systems and Assistive Devices

Andre Seyfarth

1 Summary

At the Cybathlon 2016 the performance of active and passive assistive devices for legged locomotion was compared. In the category of legged prostheses, surprisingly passive devices outperformed active ones regarding their performance in challenging tasks. Also the performance of active exoskeletons clearly demonstrated the still limited mobility performance in assisting the users. Why are passive systems are still so powerful compared to active systems? What can be learned form the design and function of the human locomotor system regarding assisting legged locomotion by passive mechanisms?

In this paper selected design and movement strategies of human legged locomotion are reflected with the aim to provide insights for the transfer into robotic and assistive systems, such as prosthetic or orthotic devices for supporting human gait.

2 The Upright Human Body Posture

During human standing and walking, the body segments are aligned in a close to vertical arrangement. This can be compared to a tower with vertically arranged segments of increasing mass with height. This has several advantages such as (1) a low mechanical work required to move a given distance (cost of transport), (2) the low effort to initiate gait, and (3) the ability to rapidly change the direction of movement (e.g. for manoeuvrability). At the same time this particular arrangement of body segments also poses some challenges regarding body design and movement control. For instance, the almost straight knee configuration in midstance during human walking requires a delicate mechanical interplay between knee joint mechanics and neuromuscular control in the leg.

A. Seyfarth (✉)
Lauflabor Locomotion Laboratory, Institute of Sport Science and Centre for Cognitive Science, TU Darmstadt, Darmstadt, Germany
e-mail: seyfarth@sport.tu-darmstadt.de

J. C. Moreno et al. (eds.), *Wearable Robotics: Challenges and Trends*,
Biosystems & Biorobotics 27, https://doi.org/10.1007/978-3-030-69547-7_6

3 Mechanical Design of Human Legged Locomotion

Human locomotion is a cyclic movement. It is characterized by a continuous exchange between kinetic and potential energy as reflected in a vertical excursion of the center of mass. This exchange of energies is moderated by muscle work which benefits from compliant structures in the muscle fibers and the tendons. Elastic elements help to reduce the energetic costs of legged locomotion. With this, the leg function becomes spring-like which can be described by characteristic parameters like leg stiffness and joint stiffness. This poses the question of how to distribute the compliance in a segmented leg. Here, the human leg has a quite remarkable design with about equal shank and thigh length and a shorter foot, which is about perpendicular to the leg axis [1].

The foot provides a clever mechanisms to control the interaction with the ground. In walking, the heel contacts first, enabling the foot to cushion the impact of landing with knee flexion and ankle plantarflexion. Once the foot is flat on the ground, the leg pivots around the ankle joint with a shift of the centre for pressure from heel to toe. Finally, at the end of contact, the heel leaves the ground and the foot pivots around the metatarsal joints by loading the toes. In this phase, the ankle joint already starts to accelerate forwards while the tip of the foot is still on the ground. The foot is thus an accelerator for the swing phase by quickly releasing energy stored around the ankle joint. This catapult-like mechanisms is characteristic for human walking [2]. Interestingly, this power-amplification mechanism based on elastic energy storage in calf muscles is more pronounced in walking than in jumping or running tasks.

4 Assistance by Compliant Mechanisms

The advantages of elastic structures attached to be body become visible in sports. Here the performance of Markus Rehm in long jump clearly shows that with an compliant prosthetic foot similar and even larger jumping distance can be achieved compared to non-amputee jumpers [3]. Still, the advantages of more efficient energy storage and release are counteracted by other challenges, e.g. in achieving a high running speed during approach with asymmetric leg function, which may required an increased control effort of the athlete.

By adding parallel (e.g. soft exoskeleton) or serial compliance to the human body (e.g. by a compliant foot prosthesis) the operation point of the human musculature is shifted. In long jump, serial compliance can increase muscle work by extending the duration of eccentric muscle operation during the support phase [4]. So far, it is however not yet clear how the optimal tuning of the serial stiffness (e.g. muscle tendon stiffness in the human body) is achieved in the biological system. This challenge will be discussed below.

Fig. 1 Soft passive exosuit from Lauflabor. Parallel elastic elements: RF = rectus femoris, HAM = hamstrings

5 Tuned Mechanics by Control

Surprisingly, until recently the metabolic advantages achieved by passive compliant assistive systems have been only minor. The work of Collins and coworkers [5] clearly shows that energetic benefits can be achieved by a purely passive elastic mechanisms supporting the ankle joint using a clutch. Here reductions in the metabolic cost of about 7% could be achieved. One of the key challenges is to find the individually optimal stiffness of assisting the ankle joint. Similar reduction were also found with an passive exosuit (Fig. 1) from the Lauflabor Locomotion Laboratory [6]. Here the focus in on assisting the function of the bi-articular muscles in the thigh. These muscles play an important role in the tuning of the swing leg and in supporting the upright posture during human gait [7, 8].

6 Tuned Mechanics by Control

The compliant leg function found in human locomotion is a result of muscle activity. Thus, neural control is important to tune joint stiffness and leg stiffness, both in steady-state behavior (effective of quasi stiffness [9] and in response to perturbations.

With this, stiffness will change during the gait cycle and may depend on sensory conditions. For instance, leg force was found to be a possible tuning mechanism to control hip stiffness [10]. With this, hip torques are small at the beginning and the end of ground contact. With the help of a specific mechanical design, this stiffness adjustment strategy could be implemented in an assistive device.

7 Conclusion and Future Work

In this paper some passive mechanisms in human locomotion are reflected from a biomechanics perspective. The most promising passive assistive systems so far are using elastic structures arranged in parallel to biological muscles (e.g. ankle muscles, bi-articular thigh muscles). One of the open challenges is the effective tuning of the passive structures assisting human movements. Here compliant and damping properties could be tuned depending on the gait and the phase of the gait cycle [11]. Similar to neuronal control of muscle properties there could be complementing (long-term) control loops to adjust the properties of passive compliant structures in (or assisting the) human body. Finding such control laws would allow to design future prosthetic or orthotic systems which could adapt the morphological properties to the individual body and movement conditions (morphological learning, see review [12]).

Acknowledgements This work was partially supported by the German Research Foundation (DFG) under grants No. SE1042/29-1.

References

1. A. Seyfarth, M. Günther, R. Blickhan, Stable operation of an elastic three-segment leg. Biol. Cybern. **84**(5), 365–382 (2001)
2. S.W. Lipfert, M. Günther, D. Renjewski, A. Seyfarth, Impulsive ankle push-off powers leg swing in human walking. J. Exp. Biol. **217**(8), 1218–1228 (2014)
3. V. Wank, V. Keppler, Vor-und nachteile von sportlern mit hochleistungsprothesen im vergleich zu nichtbehinderten athleten. German J. Sports Med./Deutsche Zeitschrift fur Sportmedizin **66**(11) (2015)
4. A. Seyfarth, R. Blickhan, J.L. Van Leeuwen, Optimum take-off techniques and muscle design for long jump. J. Exp. Biol. **203**(4), 741–750 (2000)
5. S.H. Collins, M. Bruce Wiggin, G.S. Sawicki, Reducing the energy cost of human walking using an unpowered exoskeleton. Nature **522**(7555), 212 (2015)
6. H. Barazesh, M.A. Sharbafi, A biarticular passive exosuit to support balance control can reduce metabolic cost of walking. Bioinspiration & Biomimetics **15**(3), 036009 (2020)
7. C. Schumacher, M. Sharbafi, A. Seyfarth, C. Rode, Biarticular muscles in light of template models, experiments and robotics: a review. J. R. Soc. Interface **17**(163), 20180413 (2020)
8. C. Schumacher, A. Berry, D. Lemus, C. Rode, A. Seyfarth, H. Vallery, Biarticular muscles are most responsive to upper-body pitch perturbations in human standing. Sci. Rep. **9**(1), 1–14 (2019)

9. Y. Blum, S.W. Lipfert, A. Seyfarth, Effective leg stiffness in running. J. Biomech. **42**(14), 2400–2405 (2009)
10. A. Davoodi, O. Mohseni, A. Seyfarth, M.A. Sharbafi, From template to anchors: transfer of virtual pendulum posture control balance template to adaptive neuromuscular gait model increases walking stability. R. Soc. Open Sci. **6**(3), 181911 (2019)
11. S. Peter, S. Grimmer, S.W. Lipfert, A. Seyfarth, Variable joint elasticities in running, in *Autonome Mobile Systems 2009* (Springer, Berlin, 2009), pp. 129–136
12. R. Pfeifer, M. Lungarella, F. Iida, Self-organization, embodiment, and biologically inspired robotics. Science **318**(5853), 1088–1093 (2007)

Spring Like Passive Elastic Exoskeletons May Improve Stability and Safety of Locomotion in Uneven Terrain

Laksh Kumar Punith, James Williamson, Taylor J. M. Dick, and Gregory S. Sawicki

Abstract Passive elastic exoskeletons have been shown to reduce the energetic costs of steady-state locomotion. However, it is unclear how they affect the stability of unsteady movements, such as locomoting in uneven terrain. To answer this question, we developed a mathematic model of a human hopping with an ankle exoskeleton on a platform that can arbitrarily change its height. Although passive elastic exoskeletons cannot generate or dissipate energy, we found that hopping with a passive elastic exoskeleton results in faster and safer recovery from unexpected changes in ground height. Our results suggest that lightweight passive ankle exoskeletons have potential to move beyond the lab and improve locomotor stability in real-world natural terrain environments.

1 Introduction

Exoskeletons are wearable robotic devices that externally support people's limbs and aim to augment human movement. To date, lower limb exoskeletons have reduced the energetic efforts required during hopping, walking, and running [1]. In fact, even spring-like passive elastic exoskeletons—that cannot impart net energy to a person—have reduced the energetic effort associated with walking and running [1]. However, these exoskeletons were tested on subjects walking and running on level ground at

L. K. Punith (✉) · G. S. Sawicki
Physiology of Wearable Robotics Lab, Georgia Institute of Technology, Atlanta, GA, USA
e-mail: lpunith@gatech.edu

G. S. Sawicki
e-mail: gsawicki3@gatech.edu

J. Williamson · T. J. M. Dick
Neuromuscular Biomechanics Laboratory, University of Queensland, St. Lucia, QLD, Australia
e-mail: james.williamson@uq.net.au

T. J. M. Dick
e-mail: t.dick@uq.edu.au

J. C. Moreno et al. (eds.), *Wearable Robotics: Challenges and Trends*,
Biosystems & Biorobotics 27, https://doi.org/10.1007/978-3-030-69547-7_7

steady movement speeds and it is unclear how passive elastic exoskeletons affect locomotion in natural, more variable and unpredictable, environments.

In natural terrain, humans need to generate and dissipate net energy to navigate unexpected changes in ground height and maintain steady movement. Since spring-like passive elastic exoskeletons can neither generate nor dissipate net energy, they cannot directly aid in navigating variable terrain. However, since these devices change the activation, length, and velocity of the human's muscle fascicles during movement [2–4], they inherently alter the capacity of the human to generate and dissipate energy. Thus, the main question of our research is: how do passive elastic exoskeletons affect the stability of human movement in the context of unexpected discrete changes in ground height associated with real world environments?

We study this question in a simple task that isolates the perturbation in the vertical plane from the unperturbed movement in the horizontal—hopping on a platform that can change its height arbitrarily. Hopping is an ankle dominated task, where the mechanics and energetics of the triceps-surae complex and the passive exoskeleton are directly coupled to the mechanics and energetics of the entire body. This enables us to observe how passive exoskeletons affect the muscle's mechanics and energetics—and thereby the whole body's mechanics and energetics during unsteady hopping.

Since calf muscles are less active when people hop using passive ankle exoskeletons [2]—thus reducing the capacity of the muscle to generate and dissipate energy—we hypothesize that passive exoskeletons will increase the number of hops taken to return to steady-state hopping. In addition, since passive exoskeletons increase the operating lengths of the ankle plantarflexor muscle fascicle's during steady-state hopping [3], we hypothesize that passive exoskeletons increase muscle fascicle strain when faced with unexpected changes in height of the ground during hopping.

2 Material and Methods

2.1 Mathematical Model

We use a mathematical modeling approach to answer this question. We developed a model of human hopping on a surface that can change its height arbitrarily. The model consists of a mass that is acted upon by gravity in the aerial phase and the sum of gravity and ground reaction forces in stance phase. The ground reaction forces are generated by the summation of the forces generated by the triceps-surae complex (modeled as a single Hill-type muscle-tendon unit) and a passive exoskeleton (modeled as an extension spring). The model parameters are chosen to match physiological parameters from literature [4].

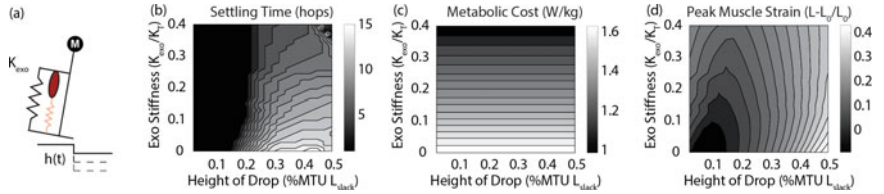

Fig. 1 **a** Diagrammatic representation of the model. Contour plots showing **b** Settling Time, **c** Metabolic cost of steady-state hopping and **d** Muscle fascicle strain as a function of exoskeleton stiffness and drop in ground height

2.2 Experimental Protocol

The muscle was cyclically stimulated by a square wave at 2.5 Hz and 10% duty factor to generate hopping. The amplitude of the square wave is chosen as a function of the exoskeleton stiffness to maintain the same total stance average positive power in each case. Once the system reaches steady hopping, we suddenly change the height of the ground and analyze the whole body and muscle-level behavior of the system until it regains steady-state behavior. We repeated these simulations for a range of exoskeleton stiffnesses (0–0.5 times tendon stiffness) and drop heights (0–0.5 times MTU length).

2.3 Outcome Measures

1. Settling Time: Number of hops taken to return to steady-state hopping after drop.
2. Metabolic Cost: The average metabolic power consumed in steady state hopping.
3. Muscle Fascicle Strain: The maximum difference between muscle fascicle length and optimal fascicle length (L_0) during the first recovery hop after the change in ground height divided by L_0.

3 Results

Figure 1b shows how settling time trends with exoskeleton stiffness and the magnitude of the drop in ground height. For small drop heights (less than 0.2 MTU lengths), the settling time is similar regardless of exoskeleton stiffness (<3 hops). For larger drop heights, increasing exoskeleton stiffness decreases the settling time.

Figure 1c shows how metabolic cost of steady-state hopping trends with exoskeleton stiffness and the magnitude of the drop in ground height. Since the

metabolic cost of steady-state hopping is unaffected by drop height, we find that metabolic cost is only affected by exoskeleton stiffness and that increasing exoskeleton stiffness reduces metabolic cost.

Figure 1d shows how muscle fascicle strain changes with changes in exoskeleton stiffness and the magnitude of the drop in ground height. For small drop heights (<0.2 MTU lengths), muscle strain increases with increasing exoskeleton stiffness—however the strain remains below $0.3L_0$. For larger drops (>0.2 MTU lengths), muscle strains exceed $0.3L_0$ without an exoskeleton and increasing exoskeleton stiffness decreases muscle strain to below $0.3L_0$.

4 Discussion

Although spring-like passive elastic exoskeletons cannot generate or dissipate net energy, our results indicate that they may enable faster and safer recovery from unexpected changes in ground height—contrary to our hypotheses.

At low drop heights, exoskeletons do not change the person's ability to recover from the perturbation and regain stable hopping. In addition, although the muscle strain increases with increasing exoskeleton stiffness, these strains stay below $0.3L_0$—thus staying within the limits of muscle injury. At increasingly larger drop heights, exoskeletons decrease the number of hops required to recover from the perturbation and regain stable hopping. They also decrease muscle strain to below $0.3\ L_0$—thus enabling lower injury risk when compared to not using exoskeletons.

Preliminary experiments (single trial data) with a single human subject hopping with bilateral passive ankle exoskeletons on a moveable platform support these simulation results, displaying that recovery from a drop of 20cm in ground height is faster with an exoskeleton (2 hops) than without (3 hops). In addition, soleus fascicle strains, measured using dynamic ultrasound imaging, were ~9% larger during the perturbed hop with an exoskeleton compared to without an exoskeleton. However, the absolute peak fascicle length (44.1 mm) was lower than L_0 as reported in the literature for the soleus muscle used in our model [4]—potentially resembling the results for small drop heights in our simulations. Ongoing human experimental studies will be combined with these simulation results to provide a comprehensive understanding of how passive elastic exoskeletons affect movement in uneven terrain.

5 Conclusion

This study took a first step towards understanding how spring-like passive elastic exoskeletons affect movement in uneven terrain. We show that exoskeletons may in fact enable faster and safer recovery from uneven terrain perturbations, which is intriguing given that passive devices cannot generate or dissipate energy. This is an exciting result as it potentially indicates that lightweight portable passive elastic

exoskeletons not only augment steady-state locomotion energetics but also have the ability to improve stability in uneven terrain. These devices have strong potential to move beyond the research environment and into the real world.

References

1. G.S. Sawicki, O.N. Beck, I. Kang, A.J. Young, The exoskeleton expansion: improving walking and running economy. J. Neuroeng. Rehabil. **17**(1), 1–9 (2020)
2. D.J. Farris, G.S. Sawicki, Linking the mechanics and energetics of hopping with elastic ankle exoskeletons. J. Appl. Physiol. **113**(12), 1862–1872 (2012)
3. D.J. Farris, B.D. Robertson, G.S. Sawicki, Elastic ankle exoskeletons reduce soleus muscle force but not work in human hopping. J. Appl. Physiol. **115**(5), 579–585 (2013)
4. B.D. Robertson, D.J. Farris, G.S. Sawicki, More is not always better: Modeling the effects of elastic exoskeleton compliance on underlying ankle muscle–tendon dynamics. Bioinspir. Biomim. **9**(4), 046018 (2014)

Balance Recovery Support Using Wearable Robotic Devices

Ankle-Exoskeleton Control for Assisting in Balance Recovery After Unexpected Disturbances During Walking

C. Bayón, W. F. Rampeltshammer, A. Q. L. Keemink, H. van der Kooij, and E. H. F. van Asseldonk

Abstract In the last two decades, lower-limb exoskeletons have been developed to assist human standing and locomotion. One of the ongoing challenges is still balance support. Here we present a control strategy for an ankle-exoskeleton to assist balance recovery after unexpected disturbances during walking. We evaluated the controller in two healthy participants wearing the ankles of the Symbitron exoskeleton while receiving forward pushes at the pelvis during walking. Providing low and medium assistance resulted in improvement of balance recovery (decreased center of mass movement in the direction of the perturbation) and reduction of muscle activity, respect to trials with no assistance. These effects saturated with high levels of assistance. The results are promising, but the controller should be improved to use human's real-time response as a feedback to trigger the support.

1 Introduction

Balance is a fundamental skill to ensure upright standing and locomotion. An often-heard wish of exoskeletons users is to receive support with balance and decrease the reliance on crutches [1]. Current studies involving the "assist-when-needed" approach for balance support with exoskeletons are mainly focused on hip control. However, the ankle is a crucial joint to maintain balance [2] and should be considered for recovery strategies.

In this work we present a controller intended to assist the ankles in balance recovery after perturbations in the sagittal plane during walking. It is a first step for the support of balance with exoskeletons in challenging environments.

C. Bayón (✉) · W. F. Rampeltshammer · A. Q. L. Keemink · H. van der Kooij · E. H. F. van Asseldonk
Department of Biomechanical Engineering, University of Twente, Enschede, The Netherlands
e-mail: c.bayoncalderon@utwente.nl

J. C. Moreno et al. (eds.), *Wearable Robotics: Challenges and Trends*,
Biosystems & Biorobotics 27, https://doi.org/10.1007/978-3-030-69547-7_8

2 Material and Methods

2.1 Robotic Exoskeleton

The Symbitron is a force-controlled modular lower-limb exoskeleton with bilateral actuation on hip, knee and ankle. For this experiment, only the ankle modules of the exoskeleton were used. These modules have 4 degrees of freedom, of which 2 are active (plantar-dorsi flexion) and 2 are passive (inversion-eversion).

2.2 Controller

The developed controller was focused on providing ankle plantar-dorsi flexion assistance to counteract perturbations in the sagittal plane. The objective was assisting balance recovery by accelerating the center of mass (COM) of the subject in the opposite direction of the provided perturbation. Immediately after an unexpected perturbation, the controller triggered the robotic assistance, which was delivered to the foot or feet in contact with the ground, i.e. to both feet during double support phase and to the stance foot during single support phase (see Table 1). For example, with a forward perturbation in double support phase, the leading foot received ankle plantar-flexion assistance, while the trailing foot received ankle dorsi-flexion assistance. In single support, if the stance foot was in front of the COM, it received ankle plantar-flexion assistance to counteract a forward perturbation.

Table 1 Ankle torque-based assistances for forward perturbations. Positive torque refers to plantar-flexion

Normal walking	Forward pert
$\tau = 0$ (transparent mode)	**Double support**
	$\tau_{lead} = \overline{\tau} \cdot \frac{GRF_{lead}}{GRF_{Total}}$ $\tau_{trail} = -\overline{\tau} \cdot \frac{GRF_{trail}}{GRF_{Total}}$
	Single support
	$\tau_{stance} = \overline{\tau}$ (if foot in front of COM) $\tau_{stance} = -\overline{\tau}$ (if foot behind COM)

Table 2 Trials performed in the pilot tests

	Fam	No Assist	Med. Assist	High Assist	Low Assist
Time	3’	4.5’	4.5’	4.5’	4.5’
Perturbations	Off	On	On	On	On
Max. robotic assistance	Off	Off	25 Nm	40 Nm	10 Nm

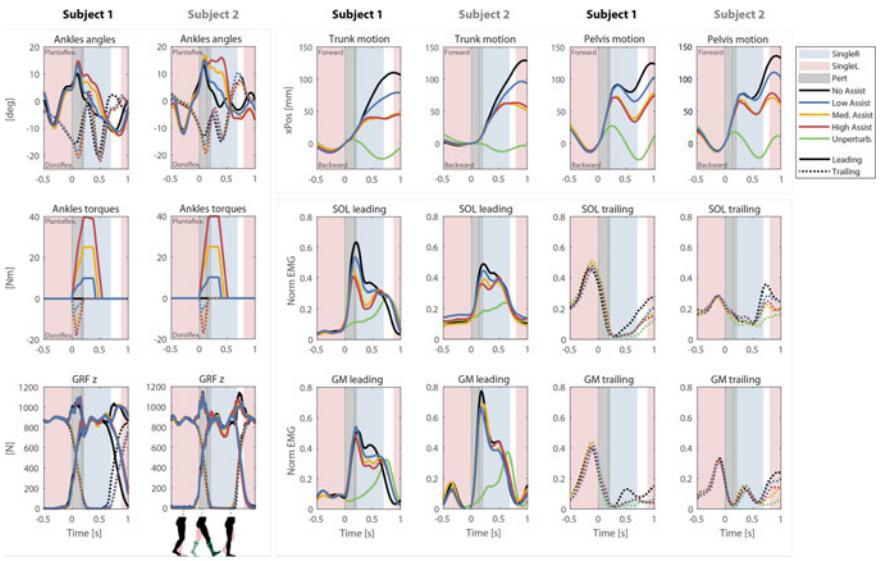

Fig. 1 Mean of individual responses within each trial. Perturbation duration is in grey. Leading limb is with continuous lines and trailing limb with dotted

The torque assistances were based on a constant torque magnitude (τ) that scaled with the corresponding vertical ground reaction forces measured below each foot (Table 1). The changes in torque were rate limited to prevent abrupt responses. Finally, the torques changed in sign depending on the direction of the perturbation (forward or backward pushes). Here only forward perturbations were applied.

For unperturbed walking the robotic assistance was set to zero, and the exoskeleton imposed minimal impedance.

2.3 Experiment

As a proof of concept, a pilot test with two healthy male participants (78 kg and 80 kg respectively) was performed. The subjects wore the ankle modules of the Symbitron exoskeleton while walking on a split-belt treadmill (Y-mill, Motek Medical, Amsterdam) at a constant speed of 2 km/h. The test with each subject consisted in a familiarization trial of 3 min (unperturbed walking), followed by four different perturbed walking trials of 4.5 min each (ordered as showed in Table 2). Medium, High and Low assistance levels were included to assess up to which level of assistance the controller showed diminishing returns.

The perturbations (square force of approx. 17% subject's weight, forward direction) were applied at the pelvis level, and timed with the gait phase with an onset coinciding with the start of the double support phase (right leg leading, left leg

trailing). Each perturbation lasted 0.2 s, so they ended during the start of right single support (left swing). After a perturbation, we ensured a minimum of 6 s of unperturbed walking before the next perturbation appeared.

Motion capture data was recorded with 8 Oqus cameras (Qualisys, Sweden). Markers located on the pelvis and on the center of the torso at the level of the clavicle, were used to estimate the movement of the pelvis and trunk after a perturbation. Muscle activities (EMG) of tibialis anterior (TA), soleus (SOL), gastrocnemius medialis (GM) and gastrocnemius lateralis (GL) of each leg were recorded with 8 bipolar electrodes (Bagnoli, Delsys, USA).

3 Results

An average of 27 perturbations for each trial were analyzed. The mean of the individual responses within each trial were processed to compare the results between trials (Fig. 1), taken 0.5 s before and 1 s after the perturbation onset.

The motion of the pelvis and trunk in forward direction decreased for all trials with robotic assistance comparing to No Assist. On average for both subjects, the improvements at the point of maximum motion for the pelvis were: Med.—36%, High—38%, Low—17%. For the trunk they were even larger: Med—49%, High—49%, Low—25%.

The EMG for SOL and GM improved in all trials with assistance, with respect to No Assist. (e.g. averaged improvement for High Assist., leading limb: SOL—12.6%, GM—6.6%). For TA and GL the differences between trials were not that clear.

4 Discussion and Conclusion

We developed a controller that was effective in improving balance recovery. A saturation effect was detected between medium or high assistances profiles. The main reduction of EMG in the leading limb was produced immediately after the perturbation, while for the trailing limb, the bigger differences appeared at the next heel strike (reduced ground impact). In the present study, no algorithm was used to detect the occurrence of the perturbation, therefore, the robotic assistance was prescribed simultaneously with the perturbation signal. For future experiments, locally measured information of the COM will be used in the controller to trigger and scale the provided assistance.

Acknowledgements This work is part of the research program Wearable Robotics with project number P16-05, (partly) financed by the Dutch Research Council (NWO).

References

1. A.W. Heinemann et al., Experience of robotic exoskeleton use at four spinal cord injury model systems centers. J. Neurol. Phys. Ther. **42**(4), 256–267 (2018)
2. M. Vlutters, E.H.F. Van Asseldonk, H. Van Der Kooij, Lower extremity joint-level responses to pelvis perturbation during human walking. Sci. Rep. p. 12 (2018)

Coupling an Active Pelvis Orthosis with Different Prosthetic Knees While Transfemoral Amputees Manage a Slippage: A Pilot Study

Monaco Vito, Aprigliano Federica, Arnetoli Gabriele, Doronzio Stefano, Giffone Antonella, Vitiello Nicola, and Micera Silvestro

Abstract This pilot study aimed at testing the hypothesis that the effectiveness of an Active Pelvis Orthosis (APO)—mediated strategy to counteract the fall risk in transfemoral amputees (TFAs) can depend on the adopted prosthetic knee. Two TFAs with good and similar functional capabilities (k-level = 3) were asked to manage unexpected slipping like perturbations: the first used a hydraulic knee; the second a microprocessor-controlled knee. Results revealed that the APO-mediated strategy against the fall risk was more effective in the second participant. Accordingly, the adopted prosthetic knee seems to significantly condition the overall balance response despite the balance recovery is supposed to be mainly driven by the APO assistance. Therefore, the prosthetic knee should be considered a confounding factor for these types of experiments and its relevance deserves further investigations.

1 Introduction

The fall risk is widely described as one of the most disabling conditions that can affect fragile persons since it compromises both physical capabilities (e.g., it reduces people's overall autonomy) and physiological status (e.g., it restricts social activities and community participation). Lower limb amputation is known to further impair

A. Gabriele, D. Stefano, G. Antonella are equally contributed.
V. Nicola and M. Silvestro are equally contributed.

M. Vito (✉) · A. Federica · V. Nicola · M. Silvestro
Department of Excellence in Robotics & AI, The BioRobotics Institute, Scuola Superiore Sant'Anna, Pisa, Italy
e-mail: vito.monaco@santannapisa.it

M. Vito · A. Gabriele · D. Stefano · G. Antonella
IRCCS Fondazione Don Carlo Gnocchi, 20148 Milan, Italy

M. Silvestro
Bertarelli Foundation Chair in Translational Neuroengineering, Center for Neuroprosthetics and Institute of Bioengineering, School of Engineering, Ecole Polytechnique Federale de Lausanne, Lausanne, Switzerland

J. C. Moreno et al. (eds.), *Wearable Robotics: Challenges and Trends*,
Biosystems & Biorobotics 27, https://doi.org/10.1007/978-3-030-69547-7_9

walking capabilities and balance control, thus increasing the fall risk and exacerbating its consequences [1, 2].

Current research in the field of wearable robotics (e.g., powered exoskeleton, robotic prostheses) is exploring novel strategies to effectively support users while recovering their balance [3–6]. In this respect, subjects with lower limb amputation, especially transfemoral amputees (TFAs), can take advantage of such platforms to counteract the inherent consequences of their disease [3].

Based on our previous research, an active pelvis orthosis (APO) can effectively promote balance control in TFA after a slippage [3]. However, amputees can show different behavior in terms of balance recovery capabilities especially when they don the APO. This result is in part due to the typical inter-subjects variability (e.g., age, functional capabilities, etiology and level of the amputation). However, little is known about if and how the used prosthesis can affect the balance recovery while TFAs were assisted by the APO. In this respect, this pilot study aims at testing the hypothesis that our APO can be more effective against the fall risk when coupled with a microprocessor-controlled knee.

2 Materials and Methods

2.1 Subjects, Experimental Setup, Protocol and Data Analysis

For this study, we collected data from two male amputees who were experienced and successful prosthesis wearers. A summary of their main features and the outcomes of some clinical tests (i.e., timed up and go, TUG; six minute walking test at ax speed, 6 MWT) are reported in Table 1.

Participants were asked to manage antero-posterior (AP) slipping like perturbations unexpectedly delivered at the heel strike of the prosthetic foot while steadily walking at their self selected speed (see [3, 6] and Fig. 1 for further details). During the experimental sessions, subjects donned an APO designed to assist balance recovery in case of slippages [3, 6]. In particular, the APO could work either in transparent (Z-mode) or in assistive (A-mode) mode.

The 3D kinematics of 44 markers was collected by means of a 8-cameras system (Vicon) and used to assess the following variables at the heel strikes just after the onset of the perturbation: (i) the Margin of Stability along the AP direction (i.e., MoS_{AP}; [7]); (ii) the limb support quotient (i.e., $S_{Hip;}$ [8]); (iii) the stability index (i.e., s; [8]).

Noticeably:

- negative [positive] values of s suggest that the dynamical status of the subjects involve a backward fall risk [more stable condition];

Table 1 Participants' features

	A01	A02
Age [year]	52	71
Height [m]	1.70	1.80
Weight [kg]	71	70
Prosthetic side	L	R
K-level	3	3
Etiology	Traumatic	Traumatic
TUG [s]	1.70	1.80
Covered distance during the 6 MWT [m]	312	320
Self-selected treadmill walking speed [m/s]	0.63	0.55
Time from amputation [year]	38	16
Prosthetic knee	Ottobock 3R45	Ottobock C-Leg III

Table 2 Outcomes of the stability analysis

	A01		A02	
	Z-Mode	A-Mode	Z-Mode	A-Mode
s [adim]	0.30	0.53	0.54	0.01
S_{hip} [s^{-1}]	−0.02	−0.33	−0.01	0.08
MoS_{AP} [mm]	37	55	22	−72

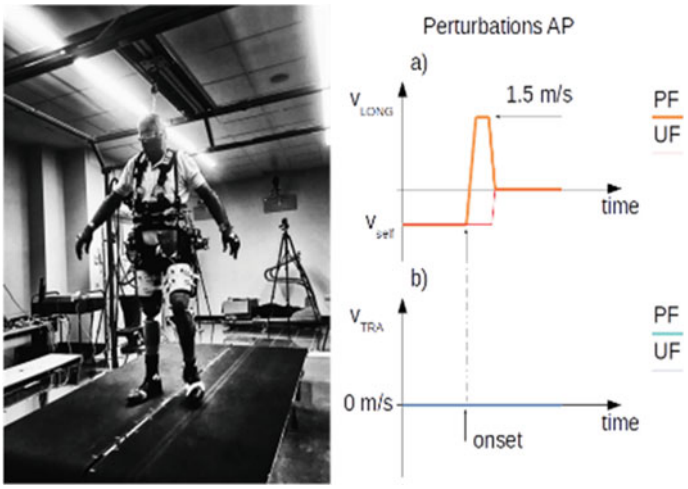

Fig. 1 The left panel shows an amputee during a typical experimental session. On the right panel, speed profiles related to the longitudinal (v_{LONG}) and transversal (v_{TRA}) belts movements, for both perturbed and unperturbed limbs (namely, PL and UL, respectively) are reported

- negative [positive] values of S_{Hip} involve downward [upward] movement of the body center of mass;
- positive [negative] values of the MoS_{AP} refer to a posterior [anterior] shift of the velocity adjusted center of mass position, namely extrapolated center of mass, with respect to the base of support.

3 Results

Enrolled subjects showed good and comparable functional capabilities (Table 1) albeit they were mainly different in terms of age.

Table 2 reports the main outcomes of our analysis, referring to both transparent and assisted modes. Results revealed that the subject A1 did not take advantage of the assistive APO: its dynamical status (see s) was always in the feasible stability region even if, when assisted by the APO, his center of mass was more directed backward (see MoS_{AP}) and downward (see S_{Hip}) than in Z-mode. The subject A2 did benefit from the assistive APO: its dynamical status (see s and MoS_{AP}) shifted from the risk of backward balance loss to the feasible stability region while his center of mass was upward directed (see S_{Hip}) thanks to the assistive support of the APO.

4 Discussion and Conclusion

This study aimed at investigating the hypothesis that the outcome of the proposed APO-mediated assistive strategy, in terms of balance recovery against slippages, can be affected by the used prosthetic knee. To test this hypothesis, we enrolled two TFAs with comparable functional capabilities but different age thus the older one (i.e., A2) was supposed to show worsen performance compared to the younger one. Noticeably, A1 and A2 donned their regular prosthetic knee, that is, the hydraulic Ottobock 3R45 and the microprocessor-controlled knee C-Leg III knee, respectively.

Surprisingly, results revealed that A2 took greater advantage while being assisted by the APO. In particular, all variables describing his dynamical status after a slippage improved when the APO was in A-mode (Table 1). Conversely, A1′s dynamical status did not show relevant improvements due to the assistive contribution of the APO.

Actually, we acknowledge that several factors could have led these results. In addition, the small number of enrolled subjects does not have any statistical power. However, we believe that one of the key aspects underlying the different behaviors between subjects was the adopted prosthesis. In particular, results suggest that the efficacy of the proposed APO-mediated strategy can be further improved if this device is coupled with smart prosthetic components, especially the knee. This insight paves the way to two parallel conclusions: from the methodological viewpoint, the adopted prosthetic knee is expected to be a confounding factor which may affect the assessment the efficacy of the proposed robot-mediated strategy against the fall risk;

on the other hand, wearable robotic platforms purposely coupling exoskeletons and prosthesis can potentially be more effective to counteract the fall risk than the APO alone. In both cases, further investigations are required to confirm these conclusions.

5 Conclusion

The purpose of this pilot study was to provide initial, hypothesis-generating findings for the assessment of the effectiveness of an APO-mediated strategy against the fall risk in TFAs. Results suggest that the adopted prosthetic knee can significantly condition the overall balance response despite the balance recovery is supposed to be mainly driven by the APO assistance. Accordingly, the prosthetic knee is a confounding factor for these types of experiments and its relevance deserves further investigations.

Acknowledgements This work was supported by EU Grant CYBERLEGs++ (The CYBERneticLowEr-Limb CoGnitive Ortho-prosthesis Plus, H2020-ICT-2015 731931).

References

1. J. Kulkarni et al., Falls in patients with lower limb amputations: prevalence and contributing factors. Physiotherapy **82**(2), 130–136 (1996)
2. J.M. Stepien et al., Activity levels among lower-limb amputees: self-report versus step activity monitor. Arch. Phys. Med. Rehab. **88**(7), 896–900 (2007)
3. V. Monaco et al., An ecologically-controlled exoskeleton can improve balance recovery after slippage. Sci. Rep. **7** (2017)
4. N. Thatte et al., Toward balance recovery with leg prostheses using neuromuscular model control. IEEE Trans. Biomed. Eng. (2015)
5. T. Zhang et al., Design and experimental verification of hip exoskeleton with balance capacities for walking assistance. IEEE-ASME Trans. Mechatron. **23**(1), 274–285 (2018)
6. F. Aprigliano et al., Effectiveness of a robot-mediated strategy while counteracting multidirectional slippages. Robotica (2019)
7. A.F. Hof et al., The condition for dynamic stability. J. Biomech. **38**, 1–8 (2005)
8. F. Yang et al., Limits of recovery against slip-induced falls while walking. J. Biomech. **44**(15), 2607–2613 (2011)

Self-induced Gyroscopic Torques in Lower Extremities During Gait: A Pilot Study

Saher Jabeen, Bram Sterke, Heike Vallery, and Daniel Lemus

Abstract To affect functional relevant task-space gait parameters such as foot placement or progression angle, conventional lower-limb robotic gait rehabilitation devices require active control and synchronization of their actuators. As an alternative, we propose the use of gyroscopic actuators, portable actuators that have the ability to generate torques that are caused by and therefore intrinsically synchronized with the swing motion of the legs. Here we investigate the kinematic and kinetic effects at hip-joint level of self-induced gyroscopic torques of a shank-worn gyroscopic actuator. Preliminary results show the wearer's swing leg motion can induce gyroscopic effects that significantly alter the kinematics of the hip-joint ($p < 0.05$) for both tested conditions in hip-joint endo/exo rotation and ab/ad-duction.

1 Introduction

Wearable gait rehabilitation devices face large challenges in hardware and control. Conventional lower-limb wearable gait rehabilitation devices require actuators and transmission structures that span multiple joints to affect functionally relevant task-space gait parameters such as foot placement or progression angle. Here gyroscopic actuators can affect such parameters in a more direct fashion, via free couple moments applied at the shank. We have already demonstrated the higher effectiveness of such an approach for step length [2]. Moreover, to affect these parameters, conventional wearable gait rehabilitation devices require complex methods to generate references for the control of assistive torques which must be synchronized to a user's individual gait, for example using gait event detection methods and physiological reference

S. Jabeen · B. Sterke · H. Vallery · D. Lemus
Biomechanics Department, Delft University of Technology, Delft, The Netherlands

B. Sterke · H. Vallery (✉) · D. Lemus
Department of Rehabilitation Medicine, Erasmus MC, Rotterdam, The Netherlands
e-mail: h.vallery@tudelft.nl

J. C. Moreno et al. (eds.), *Wearable Robotics: Challenges and Trends*,
Biosystems & Biorobotics 27, https://doi.org/10.1007/978-3-030-69547-7_10

patterns. Also in this context, passive gyroscopic actuators can offer a solution: a drastically different principle that does not require any explicit control, namely self-induced gyroscopic torques (SIGTs). By mounting fast spinning wheels on a user's legs, the swing of the leg acts as the control input of the gyroscope and thereby inducing gait-synchronized gyroscopic torques that can affect other degrees of freedom (Figs. 1b, c). Here, we investigate how the swing motion of the leg can directly affect hip-joint kinematics and kinetics in endo/exo rotations (EXR) and ab/ad-duction (ABD) and thus step width and progression angle [1].

We hypothesized that these torques would result in significant changes in gait kinematics, most specifically in hip-joint EXR and ABD, and kinetics, showing significant changes in muscle activity. We assessed these hypothesis using a set of passive toy gyroscopes attached to the shank of the non-dominant leg of healthy subjects, instrumented motion capture and surface EMG sensors.

2 Materials and Methods

To evaluate the effect of SIGTs in hip kinematics during gait, we attached six motorized toy gyroscopes in two predefined directions (Self-induced ABD Fig. 1b and EXR Fig. 1c) to the shank of the non-dominant leg (perturbed leg) via a rigid shinguard (Fig. 2c). Dead weight was also attached to the dominant leg (sound leg) to compensate for the effect of the added mass in the perturbed leg. The 6 gyroscope's spinning wheels were aligned in parallel to increase the overall gyroscopic effect.

The protocol consisted of a simple walking task. Participants walked back and forth at a comfortable walking speed on a 4 m-long straight path with and without the

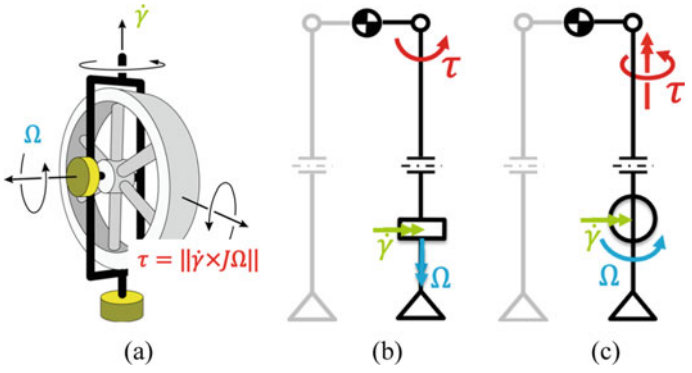

Fig. 1 **a** Schematic of a gyroscopic actuator. Once the wheel spinning at a fast angular speed $\boldsymbol{\Omega}$ is 'gimbaled' by an angular velocity $\dot{\boldsymbol{\gamma}}$, a gyroscopic torque $\boldsymbol{\tau}$ is generated about a mutually perpendicular axis. **b**, **c** show the placement and orientation of the gyroscope in the shank to self-induce ab/ad-duction and endo/exo rotation respectively. The self-induced gyroscopic torque is generated by the regular swing of the leg ($\dot{\boldsymbol{\gamma}}$) acting as a gimbal

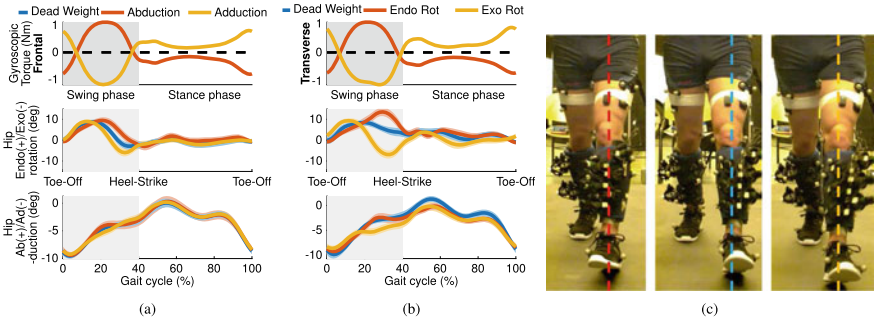

Fig. 2 Left hip-joint kinematics (bottom) and gyroscopic torques (top) of self-induced **a** ab/adduction (Frontal plane) and **b** endo/exo rotation (Transversal plane) for representative participant S3. Solid lines represent the mean and shaded areas the standard deviation of the recorded 78 gait cycles for S3. **c** Visual comparison of self-induced endo/exo rotation at heel strike. Conditions dead-weight (middle) and self-induced exo- (right) and endo- (left) rotations at heel strike of a representative stride

device. While donned, we tested the device in 5 configurations based on the direction of the SIGTs on the leg; 1- Dead-weight 'DW' (No torque), 2a,2b- Frontal plane torque resulting adduction and abduction respectively (Fig. 1b), 3a,3b- Transverse plane torque resulting in endo/exo rotations respectively (Fig. 1c). In conditions 2a and 3a the spinning direction of the flywheel was reversed with respect to that of 2b and 3b respectively.

Three healthy subjects, one female and two males (Id: S1, S2, S3, age: (29.7 $\pm$ 2.5 years); height: (1.7 $\pm$ 0.07 m); mass: (65.6 $\pm$ 8.7 kg) were recruited with approval from the Human Research Ethics Committee of TU Delft. We conducted the experiment in accordance with the recommendations of the review board. All subjects were volunteers and gave their written informed consent prior to participation and for use of their data.

We measured gait kinematics using a marker-based motion capture (Qualisys). In addition, we used 6 EMG wireless sensors (Delsys) to record muscle activity of the perturbed leg *tensor faciae latae*, *adductor longus*, *gluteus medius*, *semitendinosus*, *biceps femoris* and *rectus femoris*.

Motion capture data was processed using QTM (Qualisys) and 'Visual 3D (C-Motion)'. Gait analysis, EMG filtering and statistical analysis of the data was performed in MATLAB 2018b (MathWorks).

One-dimensional statistical parametric mapping was used to check for significant differences of time-series hip joint EXR and ABD angles and filtered EMG using the swing phase as 'Region Of Interest'.

3 Results and Discussion

Preliminary results showed that the SIGTs significantly affected hip-joint kinematics during swing phase. Transverse plane SIGTs affected significantly hip EXR ($p < 0.001$, Fig. 1c middle) opposed to the weaker effect, yet significant, of frontal plane SIGTs in hip ABD ($p < 0.05$, Fig. 1b bottom). This can be explained by the difference in magnitude of the rotational inertia between both EXR and ABD conditions. Interestingly both transverse and frontal plane SIGTs also significantly affected ($p < 0.001$) hip ABD and EXR (Fig. 1b middle and Fig. 1c bottom). This could be explained by the musculoskeletal motion coupling between ABD and EXR.

Opposed to what we hypothesized, muscle activity of any of the 6 instrumented muscles did not show any significant differences during swing phase of both EXR and ABD conditions of the SIGTs respect to the baseline DW. Three main reasons could explain the lack of significant differences in muscle activation. (i) Limited access to endo/exo dominant rotators due to limitation of surface EMG. (ii) Weak SIGTs effect in ABD due to high inertia of the leg and low angular momentum of the gyros, and (iii) Lack of strong corrective strategies against the SIGTs, presumably due to the lack of challenge in balance caused by the weak SIGTs of the device despite the strong kinematic effects in some conditions.

4 Conclusion

We showed that self-induced gyroscopic torques in lower extremities are suitable to significantly alter hip endo/exo rotation or ab/ad-duction. This passive effect can be beneficial in therapy training to reinforce balance compensatory strategies or suppress undesired non-compensatory ones. In this sense passive gyroscopic actuators might be alternative to conventional wearable gait rehabilitation devices given that their intrinsically gait-synchronized torques do not require the implementation of any controller.

Acknowledgements This research was supported by the Innovational Research Incentives Scheme Vidi with Project No. 14865, which is (partly) financed by The Netherlands Organization for Scientific Research (NWO).

References

1. K.A. Bowsher, C.L. Vaughan, Effect of foot-progression angle on hip joint moments during gait. J. Biomech. **28**(6), 759–762 (1995)
2. S. Jabeen et al., Assisting gait with free moments or joint moments on the swing leg, in *2019 IEEE 16th International Conference on Rehabilitation Robotics (ICORR)*, pp. 1079–1084 (2019)

Comparison of Balance Recovery Among Current Control Strategies for Robotic Leg Prostheses

Nitish Thatte and Hartmut Geyer

Abstract Over the past two decades, a number of control strategies have been developed for powered transfemoral prostheses. These strategies have in common that they help restore gait in amputee locomotion. However, it remains unclear how well they support balance recovery after disturbances. Here, we first present a comparison of balance recovery performance among current controls for powered transfemoral when their users are subjected to unexpected ground slips. While some controls perform better than others in this comparison, they all suffer from a limited awareness of both the environment and the user's intent, which inevitably leads to catastrophic failures and eventual falls. We then introduce our current efforts toward more interactive prosthesis controls that continuously adapt to changes in the environment and user intent. In initial work, we find that such continuous adaptations substantially improve gait robustness, encouraging a more aggressive research agenda toward real-time reactive leg prosthesis controls.

1 Introduction

A number of control strategies have been proposed for powered leg prostheses, ranging from time based strategies such as echo control [1] and minimum jerk control [2] to state based strategies such as impedance control [3], complementary limb motion control [4], virtual neuromuscular control [5, 6], and phase variable control [7]. Many of these strategies help to restore gait in amputee locomotion. But their relative merit for helping amputees recover balance after a gait disturbance remains unclear.

N. Thatte · H. Geyer (✉)
Robotics Institute, Carnegie Mellon University, Pittsburgh, PA, USA
e-mail: hartmut.geyer@uni-jena.de

J. C. Moreno et al. (eds.), *Wearable Robotics: Challenges and Trends*,
Biosystems & Biorobotics 27, https://doi.org/10.1007/978-3-030-69547-7_11

2 Comparison of Balance Recovery

We were interested in understanding this merit for two particular strategies, the widely-used impedance control (IMP) [3] and a virtual neuromuscular control (NM) developed in our group [5]. To objectively compare the two strategies, we designed and built a powered transfemoral prosthesis [8] with active knee and ankle joints that can output the high torques and speeds observed in, and required for, human balance recovery [9] (Fig. 1a). In addition, we developed new methods and algorithms that objectively and sample-efficiently tune parameters of prosthesis controllers with high-dimensional parameter spaces [6, 10]. Equipped with these tools, we then performed experiments with non-amputee subjects who used the transfemoral prosthesis via an adapter and walked on a split belt treadmill that introduced sudden velocity changes modeling slips of either stance leg (Fig. 1a). If such a random slip caused the subject to hold on to the safety rails of the treadmill, we considered it a controller failure and counted it as a 'fall'. Comparing the IMP and NM strategies subjected to these slip disturbances, we found that NM evoked significantly fewer falls than IMP control [8] (Fig. 1b). However, it still caused falls.

3 Continuously Reactive Prosthesis

The results were somewhat disappointing. Current prosthesis controllers do not seem well equipped to handle even the small slip disturbances we investigated. To better understand the underlying issues, we analyzed the types of falls that occurred in the experiments (Fig. 1c) and two clearly stood out: missed transitions in the state machines of the controllers and tripping of the leg due to foot scuffing in swing. We addressed the first issue in [11]. The second issue led us to engage in research on reactive control of powered leg prostheses that continuously adapts to changes in user intent and in the environment.

Figures 2 and 3 summarize two experiments that showcase the potential of such a more integrated control approach. In preliminary work, we have identified a prosthesis control that learns in real time from sensor data of a powered prosthetic limb to detect an amputee's intent to avoid an obstacle before it is encountered and, in response, to alter the prosthesis behavior in swing and seamlessly clear the obstacle [12] (Fig. 2). In another preliminary work, we have integrated environment awareness in the real-time planning and control of the same powered prosthesis, leading to a control that (i) continuously estimates the pose of the prosthetic limb relative to the ground fusing sensor data from a laser range finder and an inertial measurement unit mounted on the prosthesis, (ii) predicts future hip angles and heights of the user with sparse Gaussian processes, and (iii) plans updated ankle and knee trajectories with a fast quadratic program solver to avoid foot scuffing and premature landing with a flexed knee [13] (Fig. 3). In both experiments, the interactive controllers more than halved the rate of tripping compared to state of the art controllers.

(a)

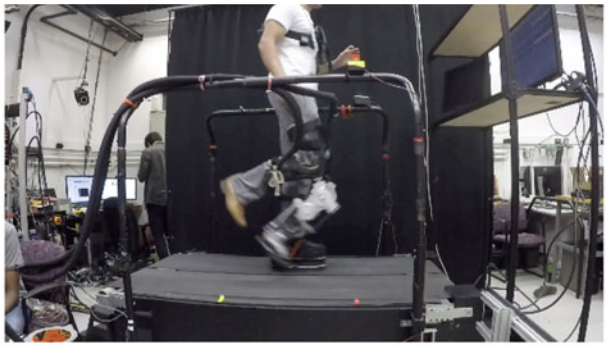

(b)

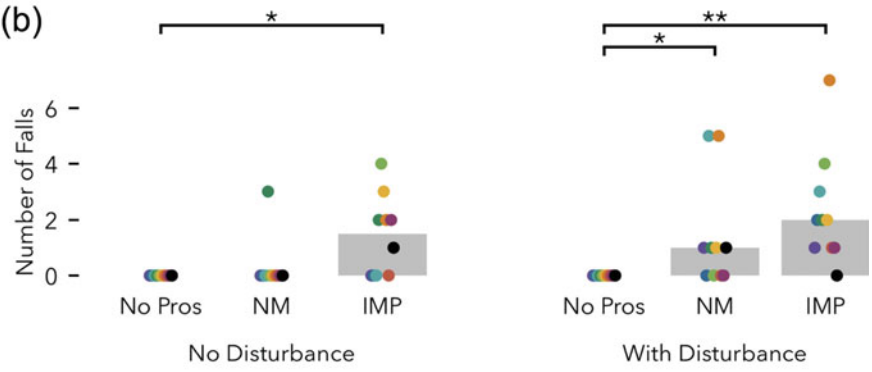

(c)

Fall Types	Neuromuscular	Impedance
Fall Forward	1	0
Fall Backward	6	4
Fall Left	1	0
Fall Right	0	3
Missed Stance / Swing Transition	3	0
Missed Stance 2 / Stance 3 Transition	0	7
Knee Collapse	0	15
Swing Trip	4	12

Fig. 1 Objective comparison of balance recovery among prosthesis control strategies. **a** Walking experiments with CMU powered transfemoral prosthesis and belt velocity changes mimicking slipping during gait. **b** Prevalence of falls in walking experiments without disturbances (left) and with disturbances (right) using either no prosthesis, or the prosthesis with IMP control or NM control. Dot colors indicate individual subjects. **c** Fall types in either control

Fig. 2 User intent recognition for interactive control of obstacle avoidance. (Top) Amputee walking on the CMU powered knee-ankle prosthesis with state of art control and tripping over obstacle. (Bottom) Prosthesis control learns in real time to predict the intent of an amputee to step over an obstacle before it is encountered and helps to clear it

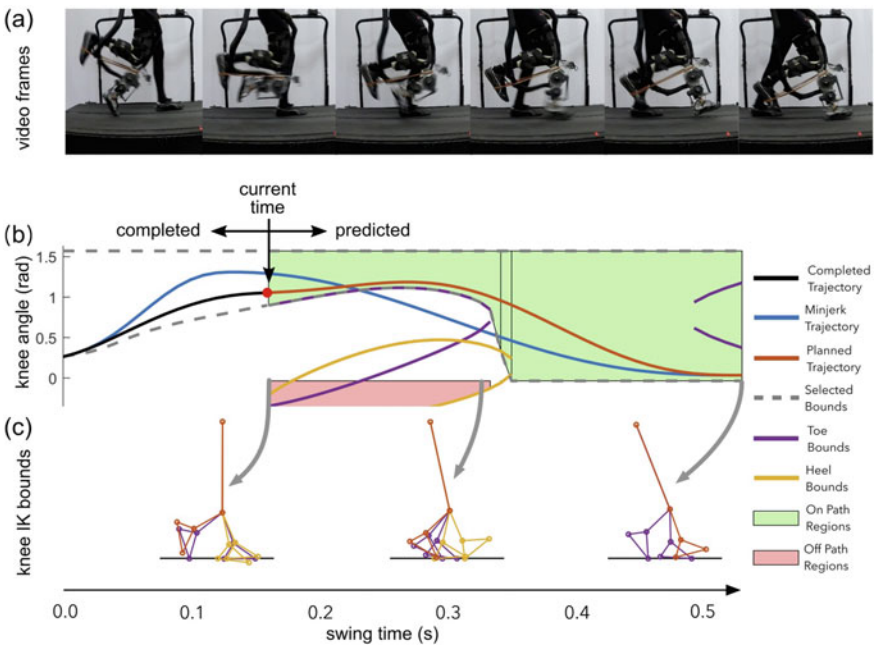

Fig. 3 Environment integration for interactive planning and control of artificial limb motion. **a** User purposefully lowering the hip of prosthesis side in swing to elicit foot scuffing. **b** State of art swing controls (blue) violate ground contact bounds on leg motion (dashed gray lines), increasing tripping hazard. By contrast, our environment-aware trajectory plan (red, prediction horizon in green) and execution (black) lie within the bounds. **c** Inverse kinematics solutions for toe (purple) and heel contact (yellow) define the bounds on the knee (panel b) and ankle trajectories (not shown) in swing

4 Conclusion

Current prosthesis (and exoskeleton) controllers focus mainly on steady gait, which even for small disturbances can lead to catastrophic failures. To substantially improve performance including balance recovery, a shift toward real-time interactive controllers will be needed. These controllers should integrate more awareness about their human user's intent as well as about the environment condition. Additionally, these controllers should be capable of learning to accommodate drift in user behavior.

Acknowledgements This work was supported by NSF (grants #1527140 and #1734559) and is currently supported by NIH (grant #R01-EB029765).

References

1. D.L. Grimes, W.C. Flowers, M. Donath, Feasibility of an active control scheme for above knee prostheses. J. Biomech. Eng. **99**(4), 215–221 (1977)
2. T. Lenzi, L. Hargrove, J. Sensinger, Minimum jerk swing control allows variable cadence in powered transfemoral prostheses, in *Conference Proceedings IEEE Engineering in Medicine and Biology Society*, pp. 2492–2495 (2014)
3. F. Sup, H.A. Varol, J. Mitchell, T.J. Withrow, M. Goldfarb, Preliminary evaluations of a self-contained anthropomorphic transfemoral prosthesis. IEEE/ASME Trans. Mech. **14**(6), 667–676 (2009)
4. H. Vallery, R. Burgkart, C. Hartmann, J. Mitternacht, R. Riener, M. Buss, Complementary limb motion estimation for the control of active knee prostheses. Biomedizinische Technik/Biomed. Eng. **56**(1), 45–51 (2011)
5. N. Thatte, H. Geyer, Toward balance recovery with leg prostheses using neuromuscular model control. IEEE Trans. Biomed. Eng. **63**(5), 904–913 (2016)
6. N. Thatte, H. Duan, H. Geyer, A sample-efficient black-box optimizer to train policies for human-in-the-loop systems with user preferences. IEEE Robot. Autom. Lett. (2017)
7. S. Rezazadeh, D. Quintero, N. Divekar, R.D. Gregg, A phase variable approach to volitional control of powered knee-ankle prostheses, in *IEEE/RSJ International Conference on Intelligent Robots and Systems (IROS)* (IEEE, New York, 2018), pp. 2292–2298
8. N. Thatte, Design and Evaluation of Robust Control Methods for Robotic Transfemoral Prostheses. Doctoral Thesis, CMU-RI-TR-19-20 (2019)
9. M.D. Grabiner, T.J. Koh, T.M. Lundin, D.W. Jahnigen, Kinematics of recovery from a stumble. J. Gerontol. **48**(3), M97–M102 (1993)
10. N. Thatte, H. Duan, H. Geyer, A method for online optimization of lower limb assistive devices with high dimensional parameter spaces, in *Proceedings of the 2018 IEEE International Conference on Robotics and Automation (ICRA)* (IEEE, New York, 2018)
11. N. Thatte, T. Shah, H. Geyer, Robust and adaptive lower limb prosthesis control via extended Kalman filter-based gait phase estimation, in *Proceedings of the IEEE/RSJ International Conference on Intelligent Robots and Systems (IROS 2019)* (2019)
12. M. Gordon, N. Thatte, H. Geyer, Online learning for proactive obstacle avoidance with powered transfemoral prostheses, in *2019 IEEE International Conference on Robotics and Automation (ICRA)* (IEEE, New York, 2019)
13. N. Thatte, N. Srinivasan, H. Geyer, Real-time reactive trip avoidance for powered transfemoral prostheses, in *Proceedings of Robotics: Science and Systems (2019)* (2019)

Reflex-Model with Additional COM Feedback Describes the Ankle Strategy in Perturbed Walking

Maarten Afschrift and Friedl De Groote

Abstract Here we evaluate if a neuromechanical model, controlled by reflexes, can describe the reactive control of balance in response to anterior-posterior directed perturbations during walking. We optimized the parameters of the reflex model to track the measured joint moments in unperturbed and perturbed walking. We showed that an additional feedback loop, based on COM feedback, is needed to describe the response of the ankle muscles during perturbed walking.

1 Introduction

Neuromechanical models are currently being used to control wearable robotic devices, such as exoskeletons and prostheses [1]. Reflex-driven models of the musculskeletal dynamics can describe human walking in forward simulations [2]. Despite the success of this approach in the control of wearable robotic devices [1], it is currently unclear if these models can also assist in the control of walking balance.

In most neuromechanical models, balance is controlled by the adjustment of foot placement [3]. Human perturbation experiments during walking showed that adjustment of foot placement is indeed the main strategy in response to medio-lateral directed perturbations [4], but not in response to anterior-posterior directed perturbations. Following anterior-posterior perturbations, balance is mainly controlled by adjusting the location of the center of pressure in the stance foot [5]. This is mainly achieved through modulating the ankle moment and is therefore referred to as ankle strategy.

M. Afschrift (✉)
Department of Mechanical Engineering, KU, Leuven, Belgium
e-mail: maarten.afschrift@kuleuven.be

F. De Groote
Department of Movement Sciences, KU, Leuven, Belgium

J. C. Moreno et al. (eds.), *Wearable Robotics: Challenges and Trends*,
Biosystems & Biorobotics 27, https://doi.org/10.1007/978-3-030-69547-7_12

Here we will evaluate if a neuromechanical model [2], controlled by reflexes, can describe the ankle strategy in perturbed walking. We hypothesize that an additional feedback loop is needed to describe the ankle strategy. Similar as in standing balance control [6], we expect that the ankle strategy can be described by delayed feedback of COM position and velocity.

2 Methods

We used a dataset with normal treadmill walking to identify the parameters of a reflex-based model. We also identified reflex-parameters in perturbed walking and evaluated if an additional feedback loop is needed to describe the ankle strategy.

2.1 Experiments

Steady-state walking was perturbed by means of a sudden increase or decrease in speed of the treadmill belts. Integrated motion capture data was collected in 18 young (age 21 $\pm$ 2 std years) subjects to describe the human response to the perturbation. All subjects walked at 1.1 m/s on a split-belt treadmill. Whole body motion was recorded using 3D motion capture with an extended plug in gait marker set (Vicon). Ground reaction forces were collected on a split-belt treadmill (Motek-ForceLink).

2.2 Inverse Kinematic and Dynamic Analysis

Joint kinematics and kinetics were computed using a scaled generic musculoskeletal model (gait 2392) in OpenSim. This model was scaled to the anthropometry and mass of the subject based on the marker positions and ground reaction forces in the static trials. Joint kinematics of the scaled model were computed using a Kalman smoothing algorithm. Joint kinetics were computed with OpenSim's inverse dynamics tool. Whole body COM position and velocity was computed from the joint kinematics and the model of the skeleton, and was expressed relative to the position and velocity of the base of support.

2.3 Reflex Parameter Estimation

We used as data-driven approach to estimate the parameters of a reflex-based model with 7 hill-type muscles per leg [2, 7]. Similar a similar approach as in [7], with the inverse kinematics and inverse dynamics as input the model, but optimized the

feedback gains with a different numerical method and on beltspeed perturbations. The feedback gains (K) of the reflex-model were optimized to track inverse dynamic joint moments, which involves a forward simulation of the muscle dynamics. We optimized the parameters of the default reflex model to (1) track unperturbed walking and (2) track the response to a perturbation (Eq. 1).

$$J(K) = \int_{t_o}^{t_{end}} \sum_{j=1}^{M} (T_{id,j} - T_{m,j})^2 dt \tag{1}$$

with t_0 and t_{end} the start and end time of in total three gait cycles, M the number of muscles T_{id} the inverse dynamic joint moments and T_m the joint moments generated by the hill-type muscles (driven by feedback).

We also evaluated if extending the neuromechanical model with an additional feedback loop based on COM kinematics improves the tracking of the ankle joint moments in response to a perturbation (Eq. 2). This feedback loop was added to the soleus, gastrocnemius and tibialis anterior.

$$e(t) = e_r(t) + k_p \Delta COM(t - \tau) + k_v \Delta C\dot{O}M(t - \tau) \tag{2}$$

with $e(t)$ the muscle excitation, $e_r(t)$ the standard reflex excitations, k_p and k_v the position and velocity feedback gains, ΔCOM and $\Delta C\dot{O}M$ the deviation in center of mass position and velocity from the unperturbed trajectory and τ a time-delay of 60 ms representing the time needed for signal transmission and sensory integration in the nervous system.

The parameter estimation was solved using a direct collocation approach with an Euler integration scheme. We formulated the muscle dynamics in casadi with implicit differential equations and solved the large sparse nonlinear program using IPOPT. The optimization takes 120–250 on a standard laptop. The 'goodness of fit' was evaluated using the coefficient of determination(R^2) and Root mean square error (RMSE) between the inverse dynamic joint moments and simulated joint moments in the perturbed gait cycle.

3 Results

We found that the reflex-model model can reconstruct the ankle, knee and hip joint moment during normal unperturbed walking (respectively R^2: 0.98 0.80 0.97, RMSE: 8.92 7.08 7.33 Nm). Despite re-optimization, the reflex-model was unable to track the ankle joint moment in response to a sudden decrease (R^2: 0.90, RMSE: 20.82 Nm) or increase in beltspeed (R^2: 0.93, RMSE: 14.87 Nm). Extending the neuromechanical model with an additional feedback loop based on COM kinematics improves the tracking of the ankle joint moment in response to a decrease in beltspeed (R^2: 0.94, RMSE: 6.75 Nm) and increase in beltspeed (R^2: 0.99, RMSE: 5.42 Nm) (Fig. 1).

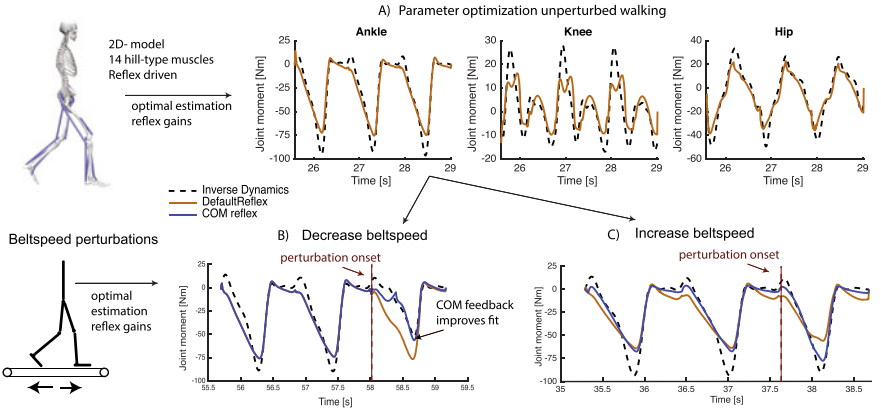

Fig. 1 Optimizing the parameters of a reflex-model [2] to track measured joint moment resulted in a good fit between inverse dynamics based joint moments (black dotted) and joint moments of the reflex model (orange) (**a**). We found that the addition of COM feedback improves the tracking of the ankle moment (blue) in response to a sudden decrease **b** or increase **c** in the speed of the treadmill belts

4 Discussion

We confirmed our hypothesis and showed that an additional feedback loop, based on feedback of COM kinematics, improved the tracking of the ankle moment in response to anterior-posterior directed perturbations during walking. Optimizing the reflexes of the default reflex-model [2] to track the ankle strategy in perturbed walking resulted in a poor fit. This suggests that the local reflexes at the ankle joint, modelled as delayed force-feedback, cannot describe the neural control involved in the ankle strategy in perturbed walking. Similar as in standing balance [6] and in pelvis-push perturbations during walking [7], we found that feedback of COM kinematic improved the fit of the ankle moment. This indicates that higher-level feedback, assumed to be the result of sensory integration in supra-spinal structures [6], is needed to describe human balance control. In the future we will cross-validate the model on multiple perturbation magnitudes and compare the COM-feedback model with and alternative model based on local feedback of muscle length and velocity.

5 Conclusion

Additional feedback of COM-kinematics is needed to describe the ankle strategy in response to anterior-posterior directed perturbations during walking. We believe that integrating this additional feedback loop in the control of wearable robotics will improve balance of the user.

Funding FWO 12ZP120N.

References

1. A.R. Wu et al., Front. Neurorobot. **11**, 1–14 (2017)
2. H. Geyer, H. Herr, IEEE Trans. Neural Syst. Rehabil. Eng. **18**(3), 263–73 (2010)
3. S. Song, H. Geyer, J. Physiol. **593**(16), 3493–3511 (2015)
4. Y. Wang, M. Srinivasan, Biol. Lett. **10**(9), 1–5 (2014)
5. M. Vlutters, E.H.F. van Asseldonk, H. van der Kooij, J. Biomech. **68**, 93–98 (2018)
6. D.B. Lockhart, L.H. Ting, Nat. Neurosci. **10**(10), 1329–36 (2007)
7. T.J.H. Brug, A.Q.L. Keemink, E.H.F. van Asseldonk, H. van der Kooij, *Abstract from Dynamic Walking* (Mariehamn, Finland, 2017)

Optimising Balance Margin in Lower Limb Exoskeleton to Assist User-Driven Gait Stability

Xiruo Cheng, Justin Fong, Ying Tan, and Denny Oetomo

Abstract When exoskeletons are driven in open loop with predetermined trajectories, the onus is placed on the user to maintain balance through their crutches. This work uses simulation of a human-exoskeleton model to explore the idea that such trajectories could be optimised to give the user the 'best chance' to maintain their balance in the presence of perturbations. The method evaluates a reward function under different gait trajectories and initial poses. It is concluded that such an optimisation method could increase the set of perturbations which a user can counter without adding significant complexity or expense to the exoskeleton.

1 Introduction

In order to reduce device complexity and cost, many lower limb exoskeletons do not have sufficient actuated degrees of freedom to actively balance—instead, they rely on the user to maintain balance with crutches. The control of these exoskeletons generally combines an offline-generated reference trajectory and online balance adjustment [1, 2]. Such strategies are viable when gait with low variability is feasible, such as in the clinic and other well-controlled environments. Outside of these circumstances, however, these techniques become less effective due to 'perturbations' to these nominal conditions. Perturbations may include physical interactions caused by collision with the exoskeleton-human system, variations to the ground level, or stationary or moving obstacles. Typically, able-bodied individuals adapt their gait to handle such perturbations—for example, when navigating a bumpy road, shorter steps are used [3]—but the ability of the user to adapt is not considered whilst designing trajectories for exoskeletons.

The present work investigated the idea of using a step-specific optimisation of the gait trajectory to give the user the 'best chance' to deal with perturbations. To do this, a reward function related to the balance margin near (nominal) heel strike was defined. The balance margin is correlated with the size of perturbation that can successfully

X. Cheng (✉) · J. Fong · Y. Tan · D. Oetomo
Fourier Intelligence Joint Laboratory, University of Melbourne, Parkville, VIC, Australia
e-mail: xiruoc@student.unimelb.edu.au

J. C. Moreno et al. (eds.), *Wearable Robotics: Challenges and Trends*,
Biosystems & Biorobotics 27, https://doi.org/10.1007/978-3-030-69547-7_13

be countered by the user, and the time near heel strike is when perturbations due to uneven ground are likely to occur. Using a model-based simulation, the reward function was evaluated across different crutch placements (accounting for different crutch placements at each step) and different gait trajectories. The results indicate that no single trajectory is optimal across all crutch positions, suggesting that a user could maintain balance against a larger set of perturbations, if the gait trajectory is optimised for this.

2 Materials and Method

This study aimed to evaluate whether changes in gait trajectory affect the ability of an exoskeleton user to maintain balance, through model-based simulations of a balance-related reward function across different parameterised gait trajectories.

2.1 Human-Exoskeleton Model

The human-exoskeleton system was modelled as ten rigid links and ten degrees of freedom (Fig. 1). The modelled lower-limb exoskeleton has three actuated degrees of freedom on each leg—hip and knee flexion/extension and ankle dorsi-/plantar flexion. The inertial parameters of the body segments were based on average values [4], with additional exoskeleton masses. The pose of the system is thus described by $\mathbf{x} = [\mathbf{q}, \mathbf{x}_{c,L}, \mathbf{x}_{c,R}] \in \mathbb{R}^{10}$, where $\mathbf{q} \in \mathbb{R}^6$ are the joint angles of the ankles, knees and hips, and $\mathbf{x}_{c,L}, \mathbf{x}_{c,R} \in \mathbb{R}^2$ are the positions of the left and right crutch in the horizontal plane.

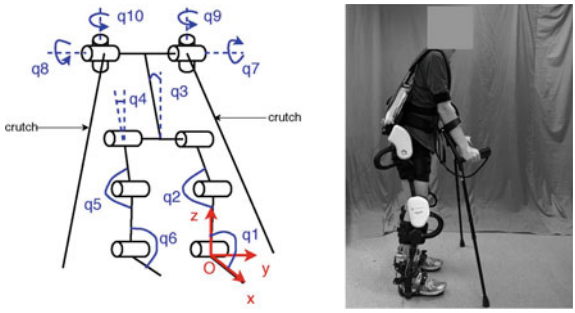

(a) Kinematic model (b) Real system

Fig. 1 The human-exoskeleton system

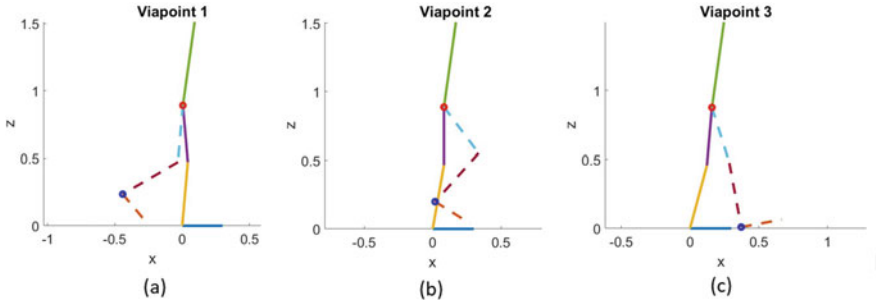

Fig. 2 Via points of joint trajectory (dashed line representing the swing leg): **a** heel lift at $t_1 = 0.4t_f$, **b** maximum toe clearance at $t_2 = 0.6t_f$, **c** heel strike at $t_3 = 0.9t_f$

2.2 Gait Parameterisation

For purposes of illustration, the joint trajectory for each step is parameterised by step length only. The hip and ankle positions ($\mathbf{x}_{hip}$, $\mathbf{x}_{ankle}$) are specified at three via points (see Fig. 2). Trajectories are then constructed as a series of polynomials, ensuring continuity in position, velocity and acceleration for whole gait. Inverse kinematics are then used to compute the joint trajectories $\mathbf{q}(t)$.

2.3 Reward Function

The reward function is defined as a measure of how large a perturbation can be rejected by the user particularly near heel strike, when perturbations related to uneven ground are most likely to be encountered. For a given joint trajectory $\mathbf{q}(t)$, $t \in [0, t_f]$ (where t_f is step duration), this is defined as:

$$J(\mathbf{q}(t), t, t_f) = \int_{0.8t_f}^{t_f} d(\mathbf{q}(\tau), \tau) d\tau$$

where $d(\mathbf{q}(\tau), \tau)$ is the distance between the location of the Zero Moment Point (ZMP) [5] and the nearest edge of the support polygon, on the assumption that the ZMP remains within the support polygon (i.e. $d(\mathbf{q}(\tau), \tau) > 0$). This reward function considers the margin of stability in the last 20% of the gait period, assuming that nominal heel strike occurs at $0.9t_f$. A larger value indicates that a larger perturbation is required to turn over the human exoskeleton system [6], translating to the user having a 'better chance' of maintaining balance when a perturbation is encountered.

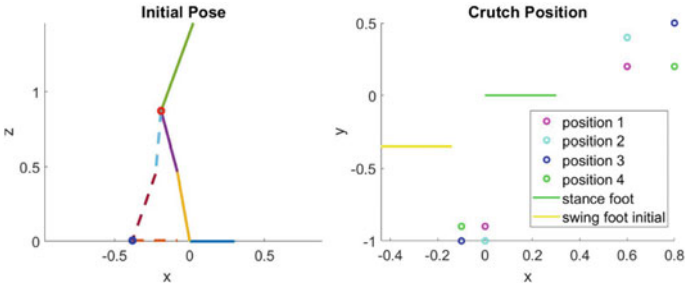

(a) The initial pose (b) Crutch positions

Fig. 3 Initial conditions

2.4 Simulation and Evaluation

An illustrative example is presented representing situations in which crutches position must be varied (for example, due to obstacles on the ground). Specifically, the exoskeleton's initial posture is defined ($\mathbf{q}(t_0)$), but crutch positions are varied ($\mathbf{x}_{c,L,i}, \mathbf{x}_{c,R,i}$) (see Fig. 3). The positions of crutches were chosen to compare different sizes and shapes the of support polygon as follows:

$$\begin{aligned}
\mathbf{q}(t_0) &= [100^\circ, 175^\circ, 20^\circ, -5^\circ, 166^\circ, 71^\circ]^T \\
\mathbf{x}_{c,L,1} &= [0.6, 0.2]^T, \quad \mathbf{x}_{c,R,1} = [0, -0.9]^T \\
\mathbf{x}_{c,L,2} &= [0.6, 0.4]^T, \quad \mathbf{x}_{c,R,2} = [0, -1]^T \\
\mathbf{x}_{c,L,3} &= [0.8, 0.2]^T, \quad \mathbf{x}_{c,R,3} = [-0.1, -1]^T \\
\mathbf{x}_{c,L,4} &= [0.8, 0.2]^T, \quad \mathbf{x}_{c,R,4} = [-0.1, -0.9]^T
\end{aligned}$$

Trajectories were generated using the parameterisation defined in Sect. 2.2, with step lengths between 0 and 0.6 m, and trajectories resulting in constraint violation (ZMP outside the support polygon) were removed. The reward function was calculated for the remainder of the trajectories.

3 Results

Figure 4 illustrates the evaluation of the reward $J(\mathbf{q}(t), t, t_f)$ for various step lengths.

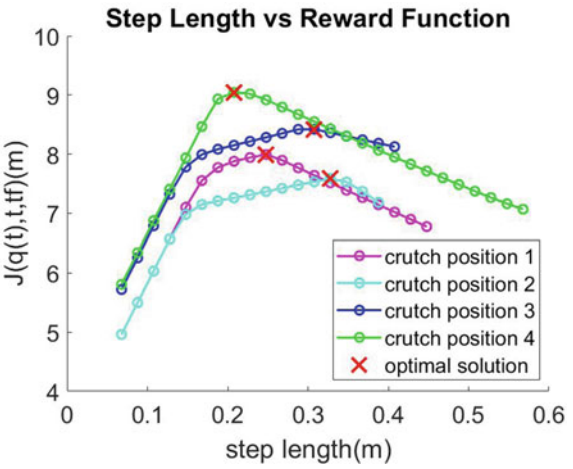

Fig. 4 The resulting evaluation of the reward function ($t_f = 1.5s$)

4 Discussion

The results show that under different crutch positions, the reward function is maximised by different step lengths. This suggests that an optimisation-based gait trajectory generation method can be used to give the user the 'best chance' of maintaining balance. For example, if the user places their crutches in crutch position 4, and the optimal step length from crutch position 1 is used to generate the gait trajectory, a smaller set of perturbations can be accounted for by the user (compared to if the optimal for position 4 is used).

Whilst the example presented here assumes that the height of the crutch position does not vary, this would be an obvious extension which could result in a better estimate of balance margin when steps are encountered. It is also noted that many other gait parameterisations are possible, such as varied toe clearance, final step height, and step duration, which could result in even larger differences between optimal and non-optimal solutions. However, implementation on a real system will require an optimisation to be run online, which may also present a challenge. This may require simplification of the problem statement, or pre-calculation of the solutions.

5 Conclusion

This work investigates the utility of a trajectory generation method which optimises an 'end of step' balance metric, corresponding to the idea that this gives the user the 'best chance' of maintaining balance. The results illustrate that the optimal step length varies with different crutch positions, indicating the potential benefits of using this approach.

References

1. T. Yan, M. Cempini, C.M. Oddo, N. Vitiello, Review of assistive strategies in powered lower-limb orthoses and exoskeletons. Robot. Autonom. Syst. **64**, 120–136 (2015)
2. M.F.B. Miskon, M.B.A.J. Yusof, Review of trajectory generation of exoskeleton robots, in *IEEE International Symposium on Robotics and Manufacturing Automation (ROMA)*, vol. 2014, pp. 12–17 (2014)
3. P.M. McAndrew, J.B. Dingwell, J.M. Wilken, Walking variability during continuous pseudo-random oscillations of the support surface and visual field. J. Biomech. **43**(8), 1470–1475 (2010)
4. R. Drillis, R. Contini, M. Bluestein, Body segment parameters. Artif. Limbs **8**(1), 44–66 (1964)
5. M. Vukobratović, B. Borovac, Zero-moment point thirty five years of its life. Int. J. Humanoid Robot. **1**(01), 157–173 (2004)
6. J.H. Kim, Y. Xiang, R. Bhatt, J. Yang, H.-J. Chung, J. Arora, K. Abdel-Malek, Generating effective whole-body motions of a human-like mechanism with efficient zmp formulation. Int. J. Robot. Autom. **24**(2), 125 (2009)

Active Life with Prosthesis

Control of Servomotor Rotation in a Myoelectric Upper-Limb Prosthesis Using a 16-Channel sEMG Sensor System

Elisa Romero Avila, Elmar Junker, and Catherine Disselhorst-Klug

Abstract The characteristics to consider during the development of myoelectric prostheses are the cultural, socio-economic and climatic conditions in which they are used. The weather condition affects in particular the recording of muscular activation for the prosthesis control. The aim of this study was the development of an easy to use myoelectric control system that can be used for the myoelectric control of opening and closing of the hand through electrodes that are not inside the prosthesis socket. Two time-domain features and Channel Selection were used to identify the specific channels corresponding to the biceps and triceps muscles. Eleven healthy subjects were tested. Channel selection was correct in 80% of all trials ensuring that the myoelectric sensor system can be used in any position outside of the prosthesis socket. This study provides an essential step towards the development of a mechanism for grip control in a myoelectric-controlled prosthetic hand.

1 Introduction

Despite technological advances in myoelectric upper-limb prostheses, they continue to attain low user acceptance [1]. This is particularly in developing countries were the main challenges are related to the cultural, socio-economic and climatic conditions. An additional challenge is the prosthesis control through muscular activation which is influenced by the contact between the electrode and the skin, the electrode´s position and the sEMG signal processing. The aim of this study is the development of an easy to use myoelectric control system for developing countries. This system should allow the control of the opening and closing of the hand via electrodes that are not inside the prosthesis socket. By this, the myoelectric sensor system can be used in any position.

E. Romero Avila (✉) · E. Junker · C. Disselhorst-Klug
Department of Rehabilitation and Prevention Engineering, Institute of Applied Medical Engineering - Helmholtz Institute, RWTH-Aachen University, Aachen, Germany
e-mail: romero@ame.rwth-aachen.de

J. C. Moreno et al. (eds.), *Wearable Robotics: Challenges and Trends*,
Biosystems & Biorobotics 27, https://doi.org/10.1007/978-3-030-69547-7_14

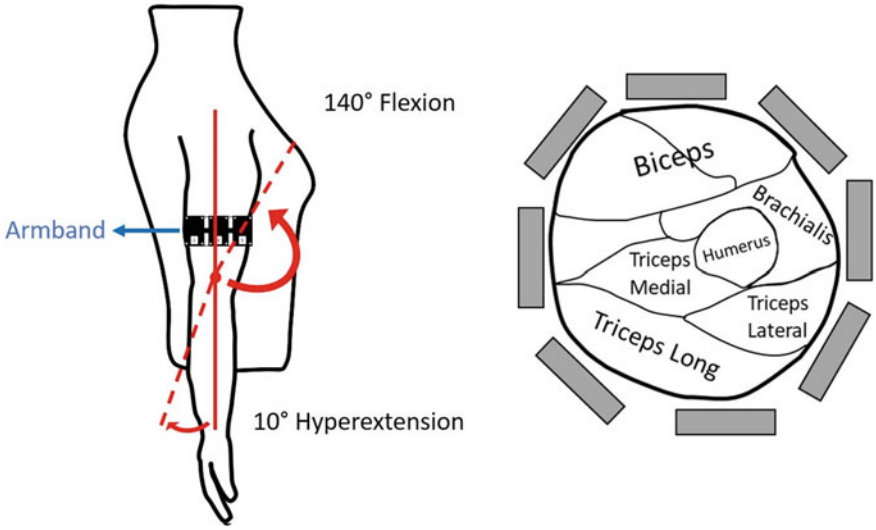

Fig. 1 Range of motion (ROM) of the elbow joint during the measurements. The figure also shows the approximate location of the armband in the arm of the subject and the position of each unit (eight units in grey). Adapted from [3]

2 Materials and Methods

2.1 Recording of the Measurements

In this study, a sensor system was used with 16 surface electromyography (sEMG) channels in form of an armband. This system is expandable to fit the size of the arm and has a rotational symmetry to avoid movement artifacts. The dry electrodes are distributed across 8 units (2 channels per unit) [2]. The movement for the calibration of the system consisted of elbow flexion and extension movements (140° of flexion to 10° of hyperextension, as shown in Fig. 1) while using external loads of either 2.5 or 3.5 kg at a velocity of 40 beats per minute (bpm). Each measurement included eight movement repetitions followed by a one-minute pause to avoid fatigue. Each measurement was repeated three times giving a total of 24 repetitions.

2.2 Channel Identification

A program was developed using MATLAB (version R2019a) to identify the armband's units that specifically correspond to biceps and triceps. For this purpose, the information obtained by the 16 channels of the armband was converted to millivolts (mV) based on (1) from [4]:

$$EMG_{data} = data \times \frac{Vref}{resolution} \quad (1)$$

where

data = armband output.

Vref = 3.3 V.

resolution = 65536 (16-Bits Resolution).

Subsequently, the data obtained from the 16 channels were filtered according to the SENIAM recommendations (Butterworth, 9th order, 10–500 Hz) [5]. To reduce the complexity of the system, two time-domain features and Channel Selection (CS) was used [5]. The mean absolute values (MAV) and the root mean square values (RMS) were obtained in 80 ms sEMG-windows [6]. The mean value of the sEMG-windows in the three measurements was then calculated and sorted in ascending order. The channels corresponding to the first six positions (out of 16) in both RMS and MAV were considered as the main channels corresponding to either biceps or triceps. As six channels were identified, the mean values of three units were obtained. Given that the loads affected mainly the flexion movement, the highest value of the three units was assigned to biceps. The second value was considered to be possible crosstalk and since the movement was made with a hyperextension of ~10°, the third value was assigned to triceps.

2.3 Servomotor Control

A servomotor (Parallax Servo Motor) was used as an actuator for the prosthesis. The real time control of the rotational direction of the servomotor via the sEMG sensor system was made possible by an application designed in MATLAB using the "App Designer" function. The connection between MATLAB and the servomotor was implemented using an Arduino Nano.

2.4 Validation

Measurements were performed on eleven healthy subjects (5 female, 6 men, age 28.81 ± 9.04 years) while they wore the myoelectric sensor system. Each channel was labeled, and the armband was arbitrarily positioned by the subjects on their dominant arm (see Fig. 1).

The first component of the application described in Sect. 2.3 (Servomotor control) consisted of reading all the channels of the sensor system while performing the calibration measurements. After channel identification, the channels corresponding to biceps and triceps were stored in the application. Then, the program read the two

channels of the armband (those corresponding to biceps and triceps) in real-time and rotated the motor according to the movement performed by the subject (flexion or extension). The application was written so that every second, the mean value of the two channels is obtained and when the difference between the mean values of the two channels is greater than 10 mV, then it recognizes that either biceps or triceps is the primary muscle and the motor rotates in the corresponding direction.

3 Results and Discussion

None of the subjects experienced any discomfort during or after the measurements. The armband was cleaned before and after each measurement. The algorithm developed for the identification of the channels was visually verified and correct identification was achieved in 80% of all trials. Channels which could not be correctly identified were probably due to crosstalk by the brachialis muscle. Six positions where considered because two channels correspond to one unit and because of the size of the units, two units detect biceps and one unit detects the lateral head of the triceps (see Fig. 1). The servomotor rotated clockwise and counter-clockwise (visualized through the servomotor horn) and was tested on both arms of a subject, where the armband was placed in different positions. In both arms, it was possible to correctly identify the biceps and triceps and control the servomotor. Figure 2 shows the setup required for testing the servomotor control.

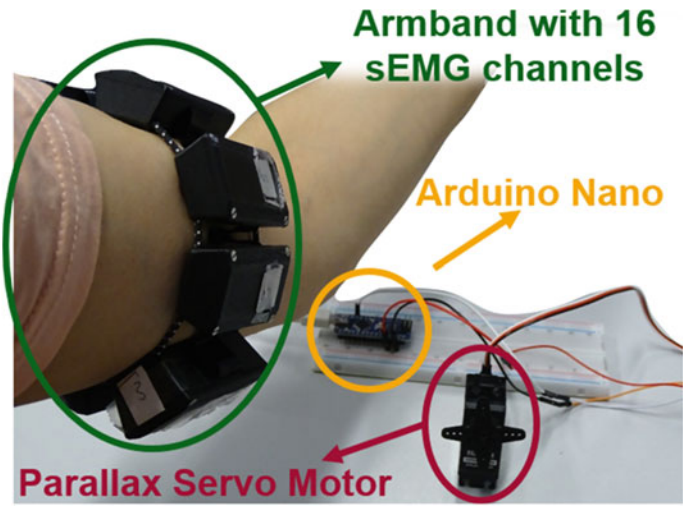

Fig. 2. Setup for the servomotor control. The MATLAB application reads the output from the armband and sends it to the Arduino for controlling the servomotor

4 Conclusion

Since the myoelectric sensor system can be positioned outside the prosthesis socket, it represents a solution for countries with humid weather conditions. Channel selection was correct in 80% of all trials ensuring that the myoelectric sensor system can be used in any position. Additionally, the calibration required for CS is quick and easy as well as the real-time control of a servomotor through the performance of elbow flexion or extension on either arm. This allows for the myoelectric sensor system to be used by even unexperienced users. More subjects are needed to ensure a larger reproducibility of the control system of the servomotor in real-time. This study represents an initial experiment towards the development of a potential mechanism for grip adjustment in a myoelectric-controlled upper-limb prosthesis.

References

1. B. Peerdeman et al., Myoelectric forearm prostheses: State of the art from a user-centered perspective. J. Rehabil. Res. Dev. **48**(6), 719–738 (2011)
2. E. Junker, C. Disselhorst-Klug, S. Becker, Design of a portable 32-channel sEMG-IMU sensor system for the assessment of upper limbs' movements in daily living, in *XXVII Congress of the International Society of Biomechanics (ISB2019)*, 2019, p. 2178
3. D.L. Menkes, R. Pierce, Needle EMG muscle identification: A systematic approach to needle EMG examination. Clin. Neurophysiol. Pract. **4**, 199–211 (2019)
4. T. Instruments, MSP430x55/MSP430x6xx Family User's Guide, (SLAU208Q) (2018)
5. D. Stegeman, H. Hermens, *Standards for Surface Electromyography: The European Project "Surface EMG for Non-invasive Assessment of Muscles (SENIAM)"* (1999)
6. U. Côté-Allard et al., Deep learning for electromyographic hand gesture signal classification using transfer learning. IEEE Trans. Neural Syst. Rehabil. Eng. (2018)

Compliant Control of a Transfemoral Prosthesis Combining Predictive Learning and Primitive-Based Reference Trajectories

Sophie Heins and Renaud Ronsse

Abstract This paper reports the development of a novel compliant controller for a transfemoral prosthesis that combines a feed-forward prediction torque component with a feedback error correction. The controller architecture aims to track primitive-based reference trajectories by the prosthetic joints. It relies on Locally Weighted Projection Regression, a function approximator that acts as an inverse internal model of the prosthesis. The proposed strategy is validated in a simulation environment.

1 Introduction

Despite the recent progress achieved in research on active lower-limb prostheses, developing efficient control strategies for these devices remains challenging. Given the dynamic nature of human locomotion and the periodic interactions with the environment, it is essential to design compliant control laws to ensure robustness to perturbations [1]. Numerous control methods are being investigated in different devices [1], the most popular combining a finite state machine with impedance control, like in [2]. Other controllers are based on time- or phase-dependent trajectories to be tracked by the prosthetic joints. A recent trend consists in adapting these trajectories to the user in real-time, such as in [3].

In this paper, we outline an adaptive control architecture aiming at tracking continuous, primitive-based reference trajectories. The controller combines predictive learning mechanisms in real-time with feedback error correction. The controller is validated in a simulation environment for normal walking.

S. Heins (✉) · R. Ronsse
Institute of Mechanics, Materials, and Civil Engineering, Université catholique de Louvain, Louvain, Belgium
e-mail: sophie.heins@uclouvain.be

Institute of Neuroscience, Université catholique de Louvain, Louvain, Belgium

Louvain Bionics, Université catholique de Louvain, Louvain, Belgium

J. C. Moreno et al. (eds.), *Wearable Robotics: Challenges and Trends*,
Biosystems & Biorobotics 27, https://doi.org/10.1007/978-3-030-69547-7_15

2 Control Architecture

Our control framework combines predictive learning and primitives-based reference trajectories (see Fig. 1). For each joint of the prosthesis (i.e. the ankle and the knee), compliant position tracking is achieved by combining feedback and feed-forward torque commands (τ_{FB} and τ_{predict} respectively):

$$\tau_{\text{des}} = \tau_{\text{predict}} + \tau_{\text{FB}} \tag{1}$$

This control architecture is bio-inspired, i.e. it mimics the function of the cerebellum in human locomotion. Indeed, the putative role of the cerebellum is twofold: (1) it provides a feed-forward predictive action based on continuous learning of the task, and (2) it provides an error correction action to ensure robustness to perturbations [4, 5].

2.1 Generation of Reference Trajectories

For each joint, the reference trajectory θ_{ref} is obtained from a weighted combination of pre-computed Gaussian primitives, similarly as in [6]. These primitives are synchronised with the gait phase, and their weights are modulated as a function of the gait cadence. The gait phase and cadence are estimated in real-time from the hip angle (θ_h) and the ground reaction force (GRF), by means of an adaptive oscillator [7].

2.2 Feed-Forward Contribution: Prediction Torque

The feed-forward torque component is a prediction torque computed by the inverse internal model of the joint, which is incrementally learned by Locally Weighted Projection Regression (LWPR), an algorithm that uses local linear models to achieve non-linear function approximation. It has been successfully used as inverse model in different simulation studies including [8]. In our approach, the LWPR computes τ_{predict} from the inputs $\mathbf{x} = (\text{GRF}, \theta, \dot{\theta}, \theta_{\text{ref}}, \dot{\theta}_{\text{ref}}, \ddot{\theta}_{\text{ref}})$, where θ and $\dot{\theta}$ are the joint position and velocity, and θ_{ref}, $\dot{\theta}_{\text{ref}}$ and $\ddot{\theta}_{\text{ref}}$ are the joint reference position, velocity and acceleration. The prediction torque is a weighted mean of k local linear models $\psi_k(\mathbf{x})$, and the weights $w_k(\mathbf{x})$ are Gaussian functions called receptive fields (RFs):

$$\tau_{\text{predict}}(\mathbf{x}) = \sum_k w_k(\mathbf{x})\psi_k(\mathbf{x}) \tag{2}$$

$$w_k(\mathbf{x}) = \exp\left((\mathbf{x} - c_k)^T D_k(\mathbf{x} - c_k)/2\right) \tag{3}$$

where D_k is the distance metric and c_k is the center of each RF (see [9] for more details about LWPR).

Table 1 Controller gains

Joint	K_p (Nm/rad)		K_d (Nms/rad)	
	Stance	Swing	Stance	Swing
Knee	6000	1000	200	25
Ankle	5000	150	15	1.3

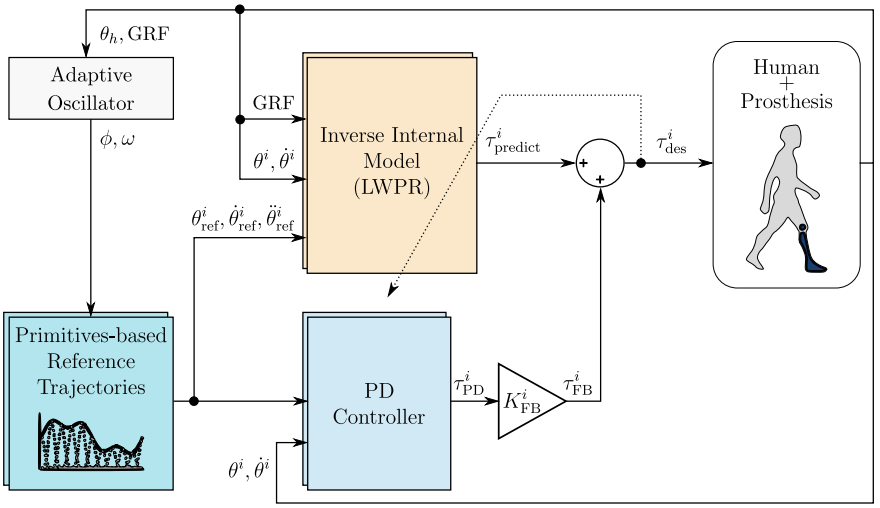

Fig. 1 The control architecture combines adaptive feed-forward (orange) and feedback (blue) torque components for the ankle and the knee joints

2.3 Feedback Contribution: Error Correction

The feedback controller provides error correction following the reference trajectory. It is a proportional-derivative (PD) controller, whose gains K_p and K_d take independent values for the swing phase and for the stance phase (see Table 1). The global feedback gain K_{FB} (see Fig. 1) decreases the feedback contribution once the inverse model is learned, in order to increase the controller compliance.

3 Simulation Results

We evaluated the performance of the incrementally learned dynamic model in increasing the controller compliance on a simulated biped model. This biped model was developed in the Robotran multibody software [10]. It is composed of 7 rigid bodies (a trunk and 2 segmented leg with foot, shank and thigh), 6 revolute joints that only move in the sagittal plane (ankle, knee and hip of both legs), and 1 prismatic joint

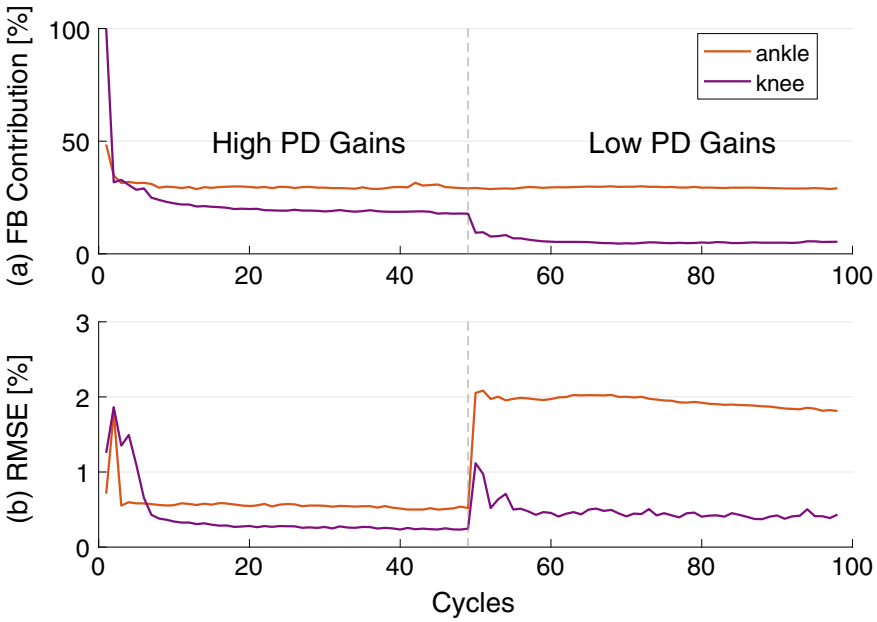

Fig. 2 The feedback torque contribution to the total joint torque per cycle rapidly decreases while the inverse internal model is learned, for both joints

that only moves in the vertical direction (the center of mass). In the ground contact model, only the vertical component of the GRF is modelled, and its computation is based on [11]. The hip, knee and ankle joints of the left leg and the hip joint of the right leg are forced to follow Winter angle trajectories for normal walking, corresponding to a cadence of 0.83 stride/s [12]. The control architecture presented in Sect. 2 is implemented on the knee and ankle joints of the right leg.

Results of the simulation showed that the LWPR was able to rapidly learn the inverse model of both joints and provided an accurate torque prediction after a few cycles only. The evolution of the contribution of the feedback torque component to the total joint torque per cycle is provided in Fig. 2, for both joints. It quickly converges to 30% for the ankle joint and 18% for the knee joint. Then, after 50 gait cycles, the controller compliance was increased by reducing the gains of the PD controller, i.e. K_{FB} was set to 25% for the ankle joint and to 5% for the knee joint, which are the lowest values associated with a tracking accuracy similar than with high PD gains. This further decreased the feedback contribution to the total torque to 29% and 5% for the ankle and the knee respectively, while the RMSE of the ankle and knee angles remained under 2.1% and 1% of the maximum angular amplitude respectively (see Fig. 2). This lead to compliant position tracking.

4 Discussion and Conclusion

We developed a bio-inspired controller for a transfemoral prosthesis that mimics the role of the cerebellum in human locomotion. The controller combines a feed-forward prediction torque command with a feedback error correction mechanism. The feed-forward action uses the LWPR algorithm, acting as an inverse internal model of the system. We validated the proposed approach on a simple biped model. Results showed that the LWPR is able to quickly learn the inverse model of each joint and provides accurate torque commands in real-time. This allows to decrease the PD gains of the feedback action, leading to a more compliant position tracking. Future work includes the validation of this control architecture on a real transfemoral prosthesis.

Acknowledgements This work was supported by the European Community's H2020 Research and Innovation Programme under grant number 731931 (the CYBERLEGsPlusPlus collaborative project).

References

1. M.R. Tucker, J. Olivier, A. Pagel, H. Bleuler, M. Bouri, O. Lambercy, J.d.R. Milln, R. Riener, H. Vallery, R. Gassert, Control strategies for active lower extremity prosthetics and orthotics: a review. J. NeuroEng. Rehab. **12**(1) (2015)
2. F. Sup, A. Bohara, M. Goldfarb, Design and control of a powered transfemoral prosthesis. Int. J. Robot. Res. (2008)
3. R.W. Jackson, S.H. Collins, Heuristic-based ankle exoskeleton control for co-adaptive assistance of human locomotion. IEEE Trans. Neural Syst. Rehabil. Eng. **27**(10), 2059–2069 (2019)
4. I. Saunders, S. Vijayakumar, The role of feed-forward and feedback processes for closed-loop prosthesis control. J. NeuroEng. Rehab. **8**, 60 (2011)
5. I. Pisotta, M. Molinari, Cerebellar contribution to feedforward control of locomotion. Front. Hum. Neurosci. **8** (2014)
6. S. Heins, L. Flynn, H. Laloyaux, J. Geeroms, D. Lefeber, R. Ronsse, Compliant control of a transfemoral prosthesis by combining feed-forward and feedback, in *2020 8th IEEE RAS & EMBS International Conference on Biomedical Robotics and Biomechatronics (BioRob)* Accepted for publication (2020)
7. T. Yan, A. Parri, V. Ruiz Garate, M. Cempini, R. Ronsse, N. Vitiello, An oscillator-based smooth real-time estimate of gait phase for wearable robotics. Autonom. Robot. **41**, 759–774 (2017)
8. S. Tolu, M. Vanegas, N.R. Luque, J.A. Garrido, E. Ros, Bio-inspired adaptive feedback error learning architecture for motor control. Biol. Cybern. **106**, 507–522 (2012)
9. S. Vijayakumar, A. D'Souza, S. Schaal, Incremental online learning in high dimensions. Neural Comput. **17**, 2602–34 (2006)
10. N. Docquier, A. Poncelet, P. Fisette, ROBOTRAN: a powerful symbolic generator of multibody models. Mech. Sci. **4**(1), 199–219 (2013)
11. N. Van der Noot, A.J. Ijspeert, R. Ronsse, Bio-inspired controller achieving forward speed modulation with a 3D bipedal walker. Int. J. Robot. Res. (2018)
12. D.A. Winter, *The Biomechanics and Motor Control of Human Gait* (University of Waterloo Press, 1987)

Design and Testing of a Fully-Integrated Electro-Hydrostatic Actuator for Powered Knee Prostheses

Federico Tessari, Renato Galluzzi, Nicola Amati, Andrea Tonoli, Matteo Laffranchi, and Lorenzo De Michieli

Abstract Electro-hydrostatic actuation represents a well-suited alternative in prosthetic and robotic applications to electro-mechanical actuation. In this regard, its favorable controllability and intrinsic back-drivability are key enabling features. This work offers a specific design methodology to obtain a highly-integrated and back-drivable electro-hydrostatic unit for a powered knee prosthesis to be used both in active and regenerative modes. The designed actuator was manufactured, assembled and tested in position tracking and admittance control, where promising performance was attained.

1 Introduction

The last decade has foreseen a strong academic and industrial interest on powered knee prostheses. This is due to the need of outperforming semi-active prostheses, which now represent the main solution for trans-femoral amputees.

According to Pieringer et al. and El-Sayed et al., most of the existing powered knee prostheses are based on electro-mechanical actuation [1]: an electrical motor coupled to a mechanical transmission mechanism, such as a harmonic drive or a ball screw. In contrast, Electro-Hydrostatic Actuation (EHA) is based on the coupling of an electric motor to a bi-direction hydraulic pump, that in turn is connected to a linear or rotary hydraulic actuator.

Several works have already investigated EHA in different fields. Favorable controllability and back-drivability are two common attributes of EHA in literature, both representing key features in prosthetic devices [2, 3].

F. Tessari (✉) · M. Laffranchi · L. De Michieli
Italian Institute of Technology, Genoa, Italy
e-mail: federico.tessari@iit.it

R. Galluzzi · N. Amati · A. Tonoli
Department of Mechanical and Aerospace Engineering (DIMEAS),
Politecnico di Torino, Turin, Italy

J. C. Moreno et al. (eds.), *Wearable Robotics: Challenges and Trends*,
Biosystems & Biorobotics 27, https://doi.org/10.1007/978-3-030-69547-7_16

Nevertheless, many of the EHA devices in literature are based on commercial-off-the-shelf components, thus leading to non-optimized and poorly integrated actuators of difficult implementation in real-life applications.

In this work, the authors offer a specific design methodology for a custom EHA with a high level of integration for a powered prosthetic knee, while also maintaining the required performance based on the knee biomechanics.

2 Materials and Methods

2.1 Biomechanical Requirements

A proper sizing of EHA subsystems requires the definition of geometrical constraints for the actuation, as well as torque-speed-power requirements. These specifications are obtained from a biomechanical analysis of the human gait. Bovi et al. provided a wide database of biomechanical requirements for different gaits [4]. In this application, the actuator is designed for a level walking condition.

2.2 Kinematics of Actuation

In this application, a linear EHA unit is preferred over a rotary one. This choice is based on two main advantages:

1. Advantageous mass distribution of the actuator: In contrast to rotary solutions constrained around the knee joint axis, linear actuators can be distributed along the prosthetic leg, hence mimicking the bulk of the calf muscle.
2. Variable transmission ratio: With proper mounting of the hydraulic cylinder, non-linear kinematics can be exploited to vary the effective length of the lever arm.

The kinematics of the actuator (Fig. 1) were defined by combining these observations with geometrical constraints of the lower limb physiology [5].

2.3 EHA Unit

For the output actuator, a through-rod cylinder was selected due to its symmetry during motion and the lack of an additional accumulator. Its cross section A_p was sized by considering the ratio among maximum required force and maximum allowable pressure. The hydraulic cylinder was equipped with low-friction spring-energized PTFE seals.

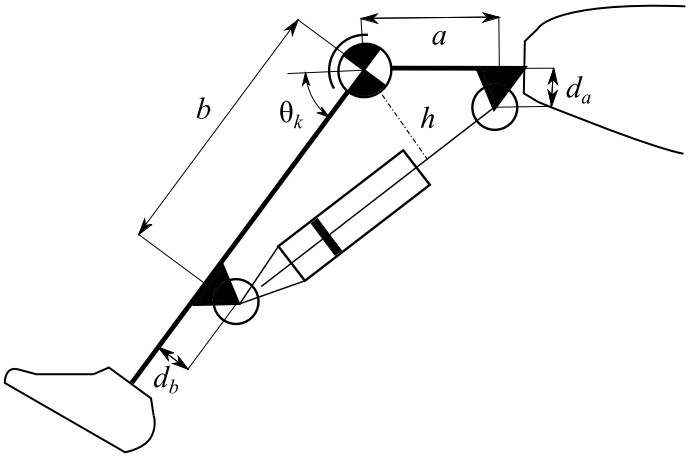

Fig. 1 Linear actuation designed kinematics: $a = 30$ mm, $d_a = 20$ mm, $b = 179.5$ mm, $d_b = 20$ mm

The pump is a fixed-displacement gerotor architecture, which guarantees low-noise, simple and compact layout and extended service life. The tooth profile generation was based on previous design experiences [6, 7], whereas the pump displacement was selected by bounding the hydraulic port flow rate and angular speed of the input shaft. To reduce mechanical losses, the pump outer gear was supported mechanically by a ball bearing. For optimal torque transmission, the inner gear is fitted into the shaft by means of a spline profile. The pump ports are symmetrically shaped to guarantee proper filling and bi-directional operation. Moreover, mirrored shadow ports are added to balance axial pressure and reduce drag.

As electric machine, a brushless permanent magnet motor was selected. Its design aimed at finding the best pole-slot combination to maximize the output torque while minimizing its ripple. The stator was wound using concentrated windings to minimize end-turn impedance. To favor compactness, the motor is installed within the same oil medium as the pump, thus avoiding the use of gasket seals on the pump shaft.

The EHA unit was designed to guarantee up to 45 Nm of torque and 60 rpm of angular speed at the knee joint level. The final assembly (Fig. 2) is $123.5 \times 91 \times 60$ mm^3 and has a mass of 1.2 kg. It is equipped with two analog Hall sensors for motor position feedback, two strain gauge pressure sensors to estimate actuation force and an absolute encoder to measure the knee angle.

3 Results

Tests were performed on a dedicated rig to validate the operation of the designed EHA unit. This setup consisted in coupling the EHA knee axis to a controllable variable load—a 2-kW PM motor with a 1:30 reduction stage—to reach all the

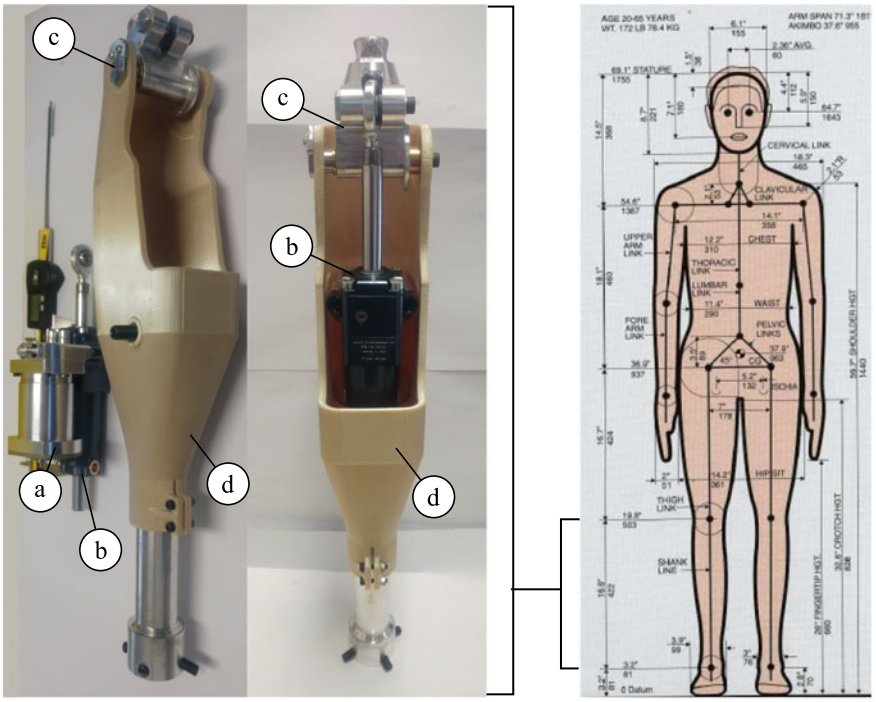

Fig. 2 Knee prosthesis EHA disassembled (left) and assembled (center). **a** motor-pump group, **b** hydraulic actuator, **c** knee joint, **d** body

desired working points. Two strategies were implemented on the EHA: a position control for the tracking of relevant biomechanical knee trajectories and an admittance control. The commands of these loops were fed to the electric machine current loop. Results are shown in Fig. 3.

4 Discussion

The designed EHA unit shows a higher level of integration when compared to off-the-shelf-based solutions. The obtained actuator size is within the geometric constraints of a physiological lower limb, thus guaranteeing its integration in a real prosthesis. Moreover, the mass of the actuator is comparable to standard electro-mechanical solutions. Tests show a satisfactory position tracking capability on three gaits: normal walking, step ascending and step descending. Also, the system is able to provide a reliable stiffness behavior through admittance control.

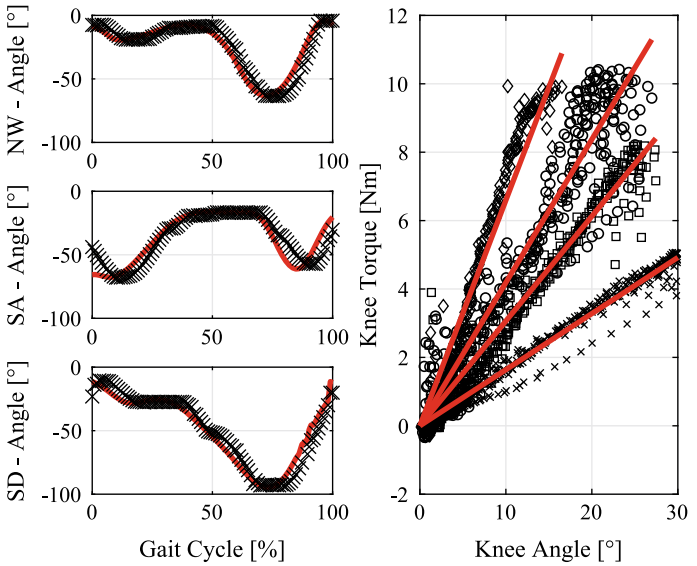

Fig. 3 On the left plots: position tracking control. Reference signals (solid) versus measure (cross). From top to bottom: normal walking (NW), step ascending (SA) and step descending (SD) trajectory profiles. On the right plot: admittance control at different stiffness (0.16 Nm/deg crosses, 0.30 Nm/deg squares, 0.42 Nm/deg circles, 0.66 Nm/deg diamonds)

5 Conclusions

The paper analyzed the design of a fully-custom and highly-integrated electro-hydrostatic unit for active knee prostheses. A top-down design strategy was presented to define the electro-hydrostatic unit from biomechanical requirements. Design choices were assumed to maximize integration and efficiency. A prototype was validated through position tracking and admittance control tasks. The device showed favorable performance in both cases.

Acknowledgements This work has been funded by INAIL/Rehab Technologies Laboratory in the Italian Institute of Technology. Support was also provided by Politecnico di Torino.

References

1. D.S. Pieringer, M. Grimmer, M.F. Russold, R. Riener, Review of the actuators of active knee prostheses and their target design outputs for activities of daily living, in *Proceedings of the International Conference on Rehabilitation Robotics (ICORR)*, London, UK, QEII Centre, 2017, pp. 1246–1253
2. T. Yu, A. Plummer, P. Iravani, J. Bhatti, S. Zahedi, D. Moser, Testing and electrohydrostatic powered ankle prosthesis with transtibial and transfemoral amputees, in *Proceedings of the IFAC*

Symposium on Mechatronic Systems, Loughborough University, Leicestershire, UK, 2016, pp. 185–191
3. J. Fang, X. Wang, R. Li, S. Wang, W. Wang, Active ankle prosthesis powered by electrohydrostatic actuation technology: design and implementation, in *CSAA/IET International Conference on Aircraft Utility System (AUS 2018)*, Guiyang, China, IET, 2018, pp. 1170–1175
4. G. Bovi, M. Rabuffetti, P. Mazzoleni, M. Ferrarin, A multiple-task gait analysis approach: kinematic, kinetic and EMG reference data for healthy young and adult subjects. Gait & Posture **33**(1), 6–13 (2011)
5. H.D. Associates, A.R. Tilley, *The Measure of Man and Woman: Human Factors in Design* (Wiley, Hoboken, NJ, 2001)
6. R. Galluzzi, Y. Xu, N. Amati, A. Tonoli, Optimized design and characterization of motor-pump unit for energy-regenerative shock absorbers. Appl. Energy **210**(1), 16–27 (2018)
7. F. Tessari, R. Galluzzi, N. Amati, Efficiency-driven design methodology of gerotor hydraulic units. J. Mech. Des. **142**(6), 063 501 (1–12) (2020)

Controlling Upper-Limb Prostheses with Body Compensations

Mathilde Legrand, Nathanaël Jarrassé, Charlotte Marchand, Florian Richer, Amélie Touillet, Noël Martinet, Jean Paysant, and Guillaume Morel

Abstract With their advanced mechatronics, myoelectric upper-limb prostheses now have many motion possibilities. Yet, the latter are not fully employed because of the inconvenient control and prostheses wearers often use their device as a rigid tool while achieving hand positioning and orientation with compensatory movements. In this paper, we propose to take advantage of this natural human behaviour to control prosthesis motions: the user is in charge of the end-effector while the device's role is to correct the human posture when necessary. We here apply this concept to control a prosthetic wrist pronosupination. A Rolyan clothespin test performed by two transradial amputees shows that the proposed control is as efficient as myoelectric control while requiring no learning.

M. Legrand (✉) · N. Jarrassé · C. Marchand · F. Richer · G. Morel
Institute of Intelligent Systems and Robotics, Sorbonne University, CNRS UMR7222, INSERM U1150, Paris, France
e-mail: mathilde.legrand@sorbonne-universite.fr

N. Jarrassé
e-mail: nathanael.jarrasse@sorbonne-universite.fr

C. Marchand
e-mail: charlotte.marchande@sorbonne-universite.fr

F. Richer
e-mail: florian.richere@sorbonne-universite.fr

G. Morel
e-mail: guillaume.morel@sorbonne-universite.fr

A. Touillet · N. Martinet · J. Paysant
Institut Régional de Réhabilitation, IRR UGECAM Nord-Est, Nancy, France
e-mail: amelie.touillet@ugecam.assurance-maladie.fr

N. Martinet
e-mail: noel.martinet@ugecam.assurance-maladie.fr

J. Paysant
e-mail: jean.paysant@ugecam.assurance-maladie.fr

J. C. Moreno et al. (eds.), *Wearable Robotics: Challenges and Trends*,
Biosystems & Biorobotics 27, https://doi.org/10.1007/978-3-030-69547-7_17

1 Introduction

With the latest advances of mechatronics, the motion possibilities of upper-limb (UL) prostheses have increased a lot [1, 2] but they are not fully exploited because the control of these devices remains highly challenging.

The most widespread approach directly connects electromyographic signals generated by the user to the movement of the prosthesis. It includes conventional myoelectric control (on/off or proportional), integrated into most of the commercially available devices, and pattern-recognition based myoelectric control. Performant enough when controlling one degree of freedom (DOF), these two schemes become limited with an increasing number of DOF [3]. The muscular fatigue and the mental burden induced by theses control approaches often lead prostheses users to employ their device as a rigid tool and move their end-effector with compensatory movements (see e.g. [4]). Body compensations are indeed efficient to achieve many tasks, but they are to be avoided since they cause musculoskeletal disorders [5].

In this paper, we propose to take advantage of this natural reaction of prostheses users to control the device: the end-effector task (placing and orientating the hand) will be achieved by the human subject while prosthesis motions will correct the human posture. This will be performed by servoing prosthetic joint motions to the user's compensatory movements. Note that this scheme is valid to control intermediate joints like wrist, elbow and shoulder, but not for hand since no body compensation substitutes grasping functions.

This paradigm has already been explored and validated for the control of wrist pronosupination with able-bodied subjects [6]. In the work presented here, we extend this study to transradial amputated people, on a different task.

2 Materials and Methods

2.1 Control Law

The control law implemented to servo the prosthetic wrist pronosupination to the user's compensatory motions is the same as the one presented in [6]; we briefly recall it below. To supplant wrist pronosupination, amputated subjects tend to use trunk and arm compensatory motions to change the hand orientation [4]. To avoid an artificial mapping between these motions and prosthesis' motions, we directly measured the forearm rotation around its longitudinal axis (elbow-hand axis) and servoed the wrist motion to it.

First, the rotation between θ_{fa}, the current posture of the lower-arm, and θ_0, an objective posture for the subject to go back to, is computed:

$$\epsilon(t) = \theta_{fa}(t) - \theta_0 \tag{1}$$

θ_0 is set here as the initial forearm posture but can change if necessary, depending on the task. ϵ is then used as the input of the control law, which pilots the prosthetic wrist angular velocity, $\dot{\theta}$:

$$\dot{\theta}(t) = \begin{cases} 0 \text{ if } |\epsilon(t)| < \epsilon_0 \\ \lambda(\epsilon(t) - sign(\epsilon(t) - \epsilon_0)\epsilon_0) \text{ otherwise,} \end{cases} \tag{2}$$

where ϵ_0 is a deadzone threshold (here set to 5 deg) and λ is a scalar gain (set to $2\,s^{-1}$) that tunes the rate of correction. These values were chosen experimentally to ensure stability.

2.2 Experimental Set-Up

Two transradial amputees, regular myoelectric-prosthesis users, participated to this experiment. They were asked to perform the refined Rolyan Clothespin test [7], both with their usual myoelectric control (MYO) and with the proposed control scheme, later called Compensations Cancellation Control (CCC). There were no specific training session and the Rolyan was achieved 5 times with each control mode. For the latter, the participants' wrist rotator was replaced with one from the laboratory, including an encoder, and controlled with an external Raspberry Pi 3©. As CCC cannot be implemented for the hand, the usual myoelectric control of each participant was conserved for the grasping function. For this experiment, θ_{fa} was obtained with an Inertial Measurement Unit located on the prosthetic forearm (see Fig. 1). The protocol of this experiment was approved by the Université Paris Descartes ethic committee CERES. All participants gave their written informed consent in accordance with the Declaration of Helsinki.

3 Results

3.1 Task Performance

Figure 2a shows the time, averaged over trials, obtained with the two control modes, for both subjects. The times are clearly similar between the direction of the motion (upwards –horizontal-to-vertical– or downwards –vertical-to-horizontal–) and the control modes. We can also notice that the standard deviation is small, for both MYO and CCC.

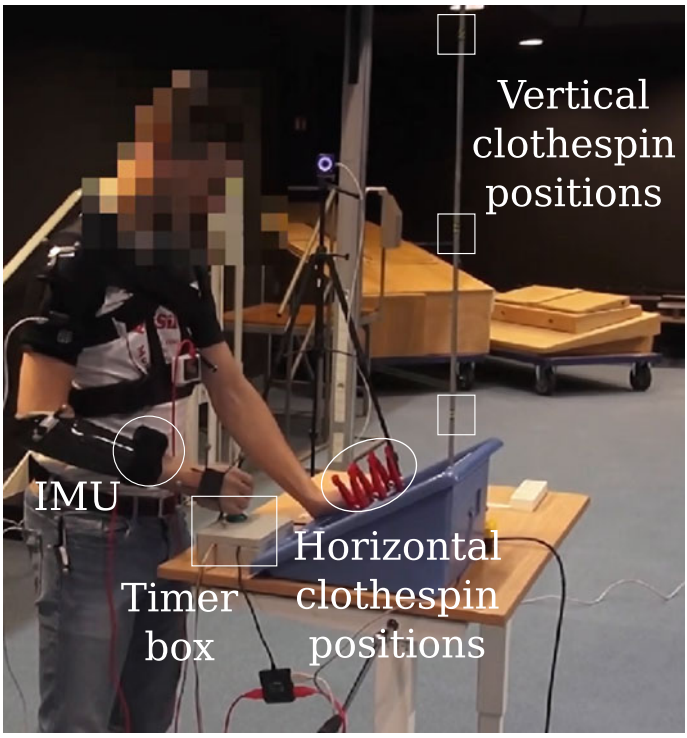

Fig. 1 Set-up of the refined Rolyan Clothespin test with transradial amputees

3.2 Joint Motions

The example of wrist angular trajectories of Fig. 2b illustrates that CCC gives trajectories very close to the ones given by MYO. Considering shoulder and trunk, it has to be checked that, with CCC, the use of compensatory motions as input of the controller does not enhance them. The maximum Ranges of Motion (over trials and pins location) of shoulder abduction (Abd.) and trunk angles (flexion, rotation and lateral bending—T.Flex., T.Rot., T.Lat.Bend.–) with CCC are thus compared to the ones with MYO. Yet, as prosthesis users may employ undesirable compensatory motions to achieve the task with MYO, it was also verified that compensations of these participants were not troublesome (angles values and holding time) [8]. In Fig. 2, we see that compensatory joint motions are not higher with CCC than with MYO and stay in acceptable ranges.

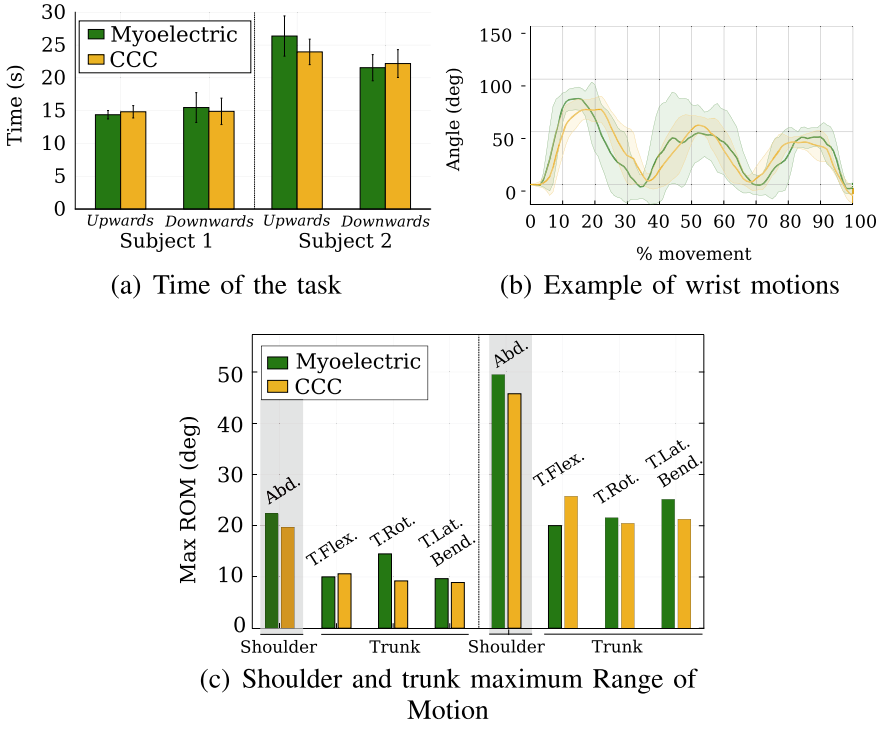

(a) Time of the task

(b) Example of wrist motions

(c) Shoulder and trunk maximum Range of Motion

Fig. 2 Rolyan assessment (mean and standard deviation over the 5 trials for each mode and subject). **a** Task performance; **b** wrist motion (wrist pronosupination for downwards pins relocation, by one subject) and **c** body compensations

4 Discussion

The different metrics assessing Rolyan test all show that CCC was quickly mastered and was as good as MYO, while it was totally unknown from the participants, who discovered it during the experiment: the time of the task is similar, with a small standard deviation, wrist angular trajectories are close and body compensations are not heightened. Both participants also appreciated the absence of co-contraction with CCC and reported that this control mode induces less muscle fatigue than MYO. These results confirm what has been obtained with able-bodied subjects, on a different task.

Yet, as seen Fig. 2, the subjects called different shoulder and trunk strategies (Subject 2 moved them much more than Subject 1). We are thus intending to perform an extensive study with more amputated participants to have a larger overview of users' strategies. The definition of the objective posture also merits further attention, to confirm that a same objective can be used for multiple arm movements.

5 Conclusion

The new control scheme for UL prostheses presented in this paper proposes to use the device to control the user's posture, while letting him/her in charge of the end-effector positioning and orientation. Tested with two transradial amputees, it was as good as conventional myoelectric control without any specific learning, while potentially reducing the muscle fatigue. Following these promising results, the concept developed here could be extended to the control of more than one DOF. We think that it could also be adapted to other rehabilitation devices like UL exoskeletons.

Acknowledgements This work was supported by the ANR-BYCEPS, ANR-18-CE19-0004.

References

1. F. Cordella et al., Literature review on needs of upper limb prosthesis users. Front. Neurosci. **3** (2016)
2. N.M. Bajaj, A.J. Spiers, A.M. Dollar, State of the art in prosthetic wrists: commercial and research devices, in *IEEE ICORR* (2015)
3. G. Li, *Advances in Applied Electromyography* (IntechOpen, 2011)
4. S.L. Carey, M.J. Highsmith, M.E. Maitland, R.V. Dubey, Compensatory movements of transradial prosthesis users during common tasks. Clin. Biomech. **23**(9), 1128–1135 (2008)
5. K. Østlie, R.J. Franklin, O.H. Skjeldal, A. Skrondal, P. Magnus, Musculoskeletal pain and overuse syndromes in adult acquired major upper-limb amputees. Arch. Phys. Med. Rehab. **92**(12), 1967–1973 (2011)
6. M. Legrand, N. Jarrassé, F. Richer, G. Morel, A closed-loop and ergonomic control for prosthetic wrist rotation, in *IEEE ICRA* (2020)
7. A. Hussaini, W. Hill, P. Kyberd, Clinical evaluation of the refined clothespin relocation test: a pilot study. Prosthet. Orthot. Int. **43**(5), 485–491 (2019)
8. D. Kee, W. Karwowski, Luba: an assessment technique for postural loading on the upper body based on joint motion discomfort and maximum holding time. Appl. Ergon. **32**, 357–366 (2001)

HandMECH—Mechanical Hand Prosthesis: Conceptual Design of a Two Degrees-of-Freedom Compliant Wrist

Ahmed A. I. Elsayed and Ramazan Unal

Abstract A compliant wrist joint is important for positioning the hand in different positions to perform various daily tasks. It is also important that the wrist is able to achieve sufficient range of motion (RoM). The RoM is determined by classifying the daily activities and the most critical applications. This study presents kinematical, structural and kinetic analyses of the conceptual design of a wrist joint in mechanical hand prosthesis: HandMECH. Kinematic and kinetic analyses are carried out to determine the design parameters of the wrist to handle daily activities. Structural analyses is performed to evaluate the stress distributed over the critical part of the wrist and show that the design with a mass of 50 g satisfies the applied boundary condition.

1 Introduction

The human wrist is a complex structure that regulates the stiffness in accordance with the task the person is about to do. It achieves that by contracting muscles that cause the bones in the wrist to compress and becomes stiff [1, 2]. Currently, many prosthetic hands lack the functionality of a wrist which causes the user to move his upper body too much and put too much effort while performing simple tasks that do not require a lot of body motion, e.g. using a computer mouse, picking up small objects. On the other hand, a light-weight wrist is always more beneficial as it provides a low inertia. In this paper we attempt to achieve the RoM in ulnar/radial deviations like the human hand and flexion/extension to ensure a natural transition of the wrist while performing tasks. Even though it is critical to have the 3rd DoF, i.e. rotation along the elbow axis [3], we decided not to implement this DoF and leave it to be compensated by the elbow rotation. This reduces the complexity and # of parts in design and allows achieving simpler, lightweight and compact wrist structure.

One study has approached to design a light-weight wrist by using a wire-based joint that is elliptical in shape as an attempt to mimic the human wrist [4]. In another

A. A. I. Elsayed · R. Unal (✉)
Department of Mechanical Engineering, Ozyegin University, Istanbul, Turkey
e-mail: ramazan.unal@ozyegin.edu.tr

J. C. Moreno et al. (eds.), *Wearable Robotics: Challenges and Trends*,
Biosystems & Biorobotics 27, https://doi.org/10.1007/978-3-030-69547-7_18

studies the stiffness of the wrist is controlled by using actuators and a system of springs but the disadvantage of such a system is that it is too heavy to be combined with a prosthetic hand [5]. After analyzing different designs, we propose a design that provides an advantage in terms of weight and performance by including a ball and socket joint approach [6] with tendon routing. This gives the flexibility that is required for achieving desired DoF. Then combine it with a body powered mechanism [7] which is attached to the upper arm and actuates the socket to stiffen the wrist. We also implement a manual lock to be able to perform tasks that require rigid wrist. In addition to the tendon routing the wrist is accompanied by a flexible material connecting the base and top part together to provide a controlled stiffness for radial/ulnar deviation in a dynamic activity like hammering.

2 Design

2.1 Design of the Wrist

Here, the kinematics of the base joint (connecting the wrist to the hand) have been studied [1] to come up with a surface that can provide enough RoM. As a result, the design can operate with a similar RoM of the human wrist. The proposed design is shown in Fig. 1. The design consists of three parts; a wrist base, socket and joint lock.

The parts are connected via tendons running from the wrist base into the socket and joint lock to provide joint stiffness. Tasks that require a high stiffness can be achieved by locked mode and compliant wrist can be achieved by unlocking the wrist. This design allows for moving in flexion/extension and ulnar/radial deviation directions.

Fig. 1 The wrist design—locked (left) and unlocked mode (right)

2.2 Locking Mechanism

The aim of the locking mechanism in the wrist is to provide enough stiffness to carry out tasks that require a stiff wrist such as picking up heavy objects and performing a dynamic task such as hammering. Activation of the locking mechanism is performed by a body powered mechanism connected to the elbow. When the arm is fully extended the mechanism pulls the base of the wrist and the locking part together via tendons running through the ball joint and the wrist becomes fully rigid, behave as a single part.

In other studies [8], kinematics of the joint structure is used to lock the wrist, but the only disadvantage is that the geometries provide a RoM restriction and DoF restriction which allows the wrist only to move on one axis.

We decided to implement a tendon based locking mechanism. Pathways are added to the design to achieve an actuation in a smooth manner. The wrist base part enters to a place that allows the locking mechanism to sit and fit into the socket. After that it does not move unless it is manually unlocked. Tendons are routed inside the geometrical structure in order to ensure the safety and proper functionality the mechanism. These also ensure the desired RoM while the wrist is in unlocked mode. Fig. 2 shows the positioning of the locking mechanism in section view.

3 Analyses and Results

3.1 Kinematics and Kinetics

Kinematic analysis is carried out to determine the required RoM in our design. The defined tasks and objects that require radial/ulnar deviation are set and according to the largest diameter we determine the suitable geometry that can provide similar RoM w.r.t. to the human wrist. The simple kinematic model is employed to identify elbow flexion-extension and elbow pronation-supination to determine the position and length of the body powered mechanism for actuating the wrist. The aim is to provide wrist control by making use of body power without the discomfort of the user. This system starts from the elbow. After performing the analyses, we achieved the results that cover the two modes; locked mode of the wrist and unlocked mode.

- Locked mode: From elbow to reach an object that is located at 20 cm distance requires a 250 N/m spring constant, since the wrist requires to sustain a maximum force of 50N. The upper limit is considered for locking the wrist and since this is a linear motion, the elbow pronations are not considered in this case.
- Unlocked mode: Wrist can perform flexion/ extension and ulnar/radial deviations. The results are obtained considering the upper limit of the force which is 50 N.

Some of the results of these analyses are summarized in Tables 1, 2, and 3 for different object handling.

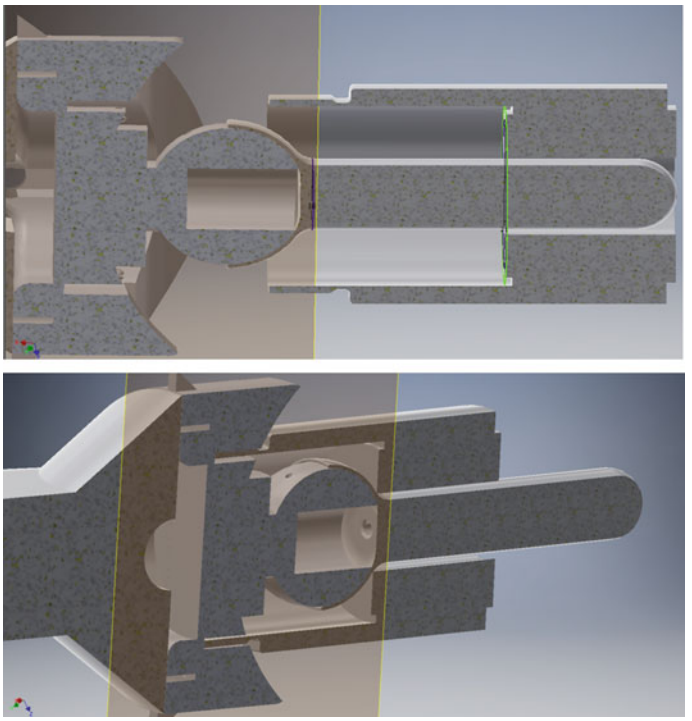

Fig. 2 Unlocked mode (top) and locked mode (bottom)

Table 1 Flexion

Desired angle	75°	Calculated angle from elbow (q_4)	29°
Considered object	Pencil	Spring deflection	40 mm
Location of object from elbow	160 mm below	Force to achieve angle at elbow (q_4)	4.4 N

Table 2 Extension

Desired angle	75°	Calculated angle from elbow (q_4)	79.5°
Considered object	Ball	Spring deflection	132.5 mm
Location of object from elbow	320 mm above	Force to achieve angle at elbow (q_4)	9.11 N

Table 3 Ulnar/radial deviation

Desired angle	35°	Calculated angle from elbow (q_4)	18°
Considered object	Mouse	Spring deflection	7.96 mm
Location of object from elbow	70 mm to right/left	Force to achieve angle at elbow (q_4)	15.3 N

3.2 Structural analysis

Here, we employed structural analysis to define design parameters of critical parts, such as the base of the wrist that is connected to a prosthetic hand. In this case we set the heaviest mass as 5 kg as the heaviest object that hand carries during daily activities. According to this analysis max stress is 14.5 MPa and maximum deformation is 0.128 mm.

4 Conclusion

This study presents a 2 DoF wrist joint for prosthetic hands. Kinematic and kinetic analyses are conducted to define the design parameters. Structural analyses are carried out to check the critical parts under loading conditions. After the design and analyses, 50g wrist that has a RoM of flexion/extension and ulnar/radial deviation in various tasks is obtained.

References

1. S. Casini, et al., Design of an under-actuated wrist based on adaptive synergies, in *IEEE International Conference on Robotics and Automation (ICRA)* (2017)
2. A. Zonnino, F. Sergi, Model-based analysis of the stiffness of the wrist joint in active and passive conditions. J. Biomech. Eng. **141**(4) (2019)
3. S. Oyama, et al., Biomechanical reconstruction using the tacit learning system: intuitive control of prosthetic hand rotation. Frontiers Neurorobot (2016)
4. N. Kim, W.H. Choi, D. Shin, Design optimization of a wire-based ellipsoid joint for bionic wrists, in *14th International Conference on Ubiquitous Robots and Ambient Intelligence* (2017)
5. F. Montagnani, G. Smit, M. Controzzi, C. Cipriani, D.H. Plettenburg, A passive wrist with switchable stiffness for a bodypowered hydraulically actuated hand prosthesis, in *International Conference on Rehabilitation Robotics* (London, UK, 2017)
6. N. M. Bajaj, A.J. Spiers, A.M. Dollar, State of the art in prosthetic wrists: commercial and research devices, in *IEEE International Conference on Rehabilitation Robotics* (2015).
7. T. Kulkarni, R. Uddanwadiker, Overview: mechanism and control of a prosthetic arm. Molecular Cellular Biomech (2015)
8. O.A. van Nierop, A. van der Helm, K.J. Overbeeke, T.J.P. Djajadiningrat, A natural hand model. Visual Comput. **24**, 31–44 (2008)

HandMECH—Mechanical Hand Prosthesis: Conceptual Design of the Hand Compartment

Baris Baysal and Ramazan Unal

Abstract In this study, conceptual design of the hand compartment of a body-powered hand prosthesis, HandMECH, is presented. HandMECH is a body-powered prosthesis and the hand compartment is designed according to human finger size and range of motion (RoM). Moreover, the design is governed by the daily activities performed by hand. In this regard, three types of grasp that are mostly used are identified. The thumb is designed with three degrees of freedom (DoF), i.e., translation and rotation, the index finger with three rotational DoF, and the other three fingers that generally move together are designed as combined and having one rotational DoF. In order to give the human finger flexibility, the fingers are designed to be made of flexible material and the other parts are of ABS material with the consideration of 3D printer for prototyping. CAD model is presented as an outcome of this study.

1 Introduction

The prosthetic hand is a basic solution resource for people with disabilities to meet their daily needs. In general, there are two types of prosthetic hands in the prosthetic market; body-powered hand prosthesis and robotic hand prosthesis. Body-powered prosthetic hands generally do not have much grasping modes and they need constant body strength. Besides being more useful, robotic hand prostheses are more complex, heavy and expensive.

The prosthetic hand should be able to grasp different materials, perform different gestures, and reaching objects in narrow spaces. For instance, in [1], it is shown that the prosthetic hand can perform 144 different grasping postures. To achieve defined grip postures, there is a lock mechanism located on each finger. When functionality is taken into consideration, the prosthetic hands need to perform pinch grip (55%), hook grip (50%), sensitive grip (30%) and lateral grip (20%) movements [2]. However, the study in [3] states that daily activities are at the rate of power grip (35%), pinch

B. Baysal · R. Unal (✉)
Department of Mechanical Engineering, Ozyegin University, Istanbul, Turkey
e-mail: ramazan.unal@ozyegin.edu.tr

J. C. Moreno et al. (eds.), *Wearable Robotics: Challenges and Trends*,
Biosystems & Biorobotics 27, https://doi.org/10.1007/978-3-030-69547-7_19

grip (30%) and lateral grip (20%). Considering these results, 3 basic types of grasp were identified for the design; pinch grip, lateral grip and power grip.

Tendon-driven mechanisms are generally used as prosthetic hand activation mechanisms. In [1], tendons were passed through low friction tubes and a motor was used to activate the fingers. Cables are generally preferred since they are simpler systems that reduce the number of parts used. In another study, finger joints are activated by a single motor drive via Smart Memory Alloy (SMA) cables [4].

In [2], the general problems of disabled users regarding prosthetic hand are given as follows; aesthetics (62%), discomfort (52%), overweight (58%), lack of functional abilities (50%), technical assistance and maintenance problems (31%), and disturbing noise (27%). For these reasons, the design should be aesthetically beautiful and human-like, functional as well as lightweight. Regarding the weight problem, it has shown that the ABS material is suitable for prosthetic hand [4]. In another study, ABS was used, and the length of the prosthesis was 165mm and the mass with the belt and silicone parts was 200 g [5].

In this study, we present the design of a low cost, functional, and light hand prosthesis. Since the prosthesis is desired to be light and low-cost, passive body-powered system is adopted. The presented design can realize different types of grip with different objects. The transition between these grip types is possible with the thumb being able to slide. The prosthetic hand is mainly designed to perform power grip, pinch grip and lateral grip movements.

2 Design

In this section, a body powered hand prosthesis with 7 DoF is described. 1 DoF of the index, middle, ring and little finger is designed to perform common movements of the hand. These generally include grasping and grabbing movements. The thumb has a swinging head with two DoF for greater grasping range. In this way, the prosthetic hand can perform movements such as holding relatively large objects or lateral grasping like holding a paper. 3D CAD model of the hand is shown in Fig. 1.

Fig. 1 3D CAD model of the HandMECH (wrist is included)

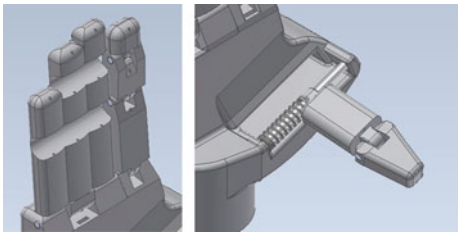

Fig. 2. Design of index and combined middle, ring and little fingers (left)—design of thumb (right)

2.1 Design of the Index Finger

The index finger has a completely different design and features from the other fingers, the middle, ring and little fingers, since it is the most used finger and functions in all kinds of movements. It has three rotational DoF and three joints as shown in Fig. 2. These play a role in opening and closing the finger. Voluntary Closing (VC) approach is adopted in the overall design so the fingers are opening via body-power and opening by itself with the use of spring. The stored energy on the spring is used to hold objects and bring back to fingers to the anatomical (neutral) position. This mechanism also functions as a pressure control, preventing the user from applying excessive force to the object.

2.2 Design of the Middle, Ring and Little Fingers

In most cases, these three fingers act as if they are a single finger, so these fingers are designed as combined, shown in Fig. 2. Two options stand out to produce these fingers, one is articulated like the index finger with joint design, the other is a solid production flexible jointed production. The latter approach is chosen to achieve lighter and simpler design.

2.3 Thumb Design

Generally, prosthetic thumbs have 1 DoF and can reach a limited RoM. In our design, the thumb has three DoF, 2 rotations and 1 translation as shown in Fig. 2. The 3rd DoF allows prosthesis to realize different grasp types in a simple, effective and light-weight manner This DoF is controlled with a spring to bring back the thumb to its neutral position.

With these design considerations, the HandMECH can realize three different types of grasp as shown in Fig. 3. The first of these is the mode that enables the movement of gripping objects such as glasses. The second is the pencil-style mode that combines

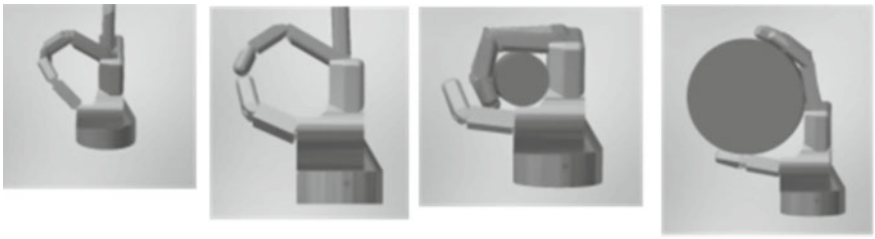

Fig. 3. Lateral (1st), pinching (2nd) and power grasp—small (3rd) and big (4th) objects—grip types

the thumb and index finger to hold relatively smaller objects. The third one allows holding the paper-style mode horizontal objects.

2.4 Body-Powered Mechanism

Body-powered hand prostheses generally use a specific activation mechanism. In this mechanism, the sling worn on the patient's shoulder is attached to the opposite shoulder where the hand is attached. In this way, the pushing and pulling movements of the shoulder move the device. Tendon connection between this mechanism and fingers provides the closing of the hand and tendons are connected to a spring to bring the hand to its anatomical position. Spring placed into the thumb sliding trajectory functions in the same way and thanks to this spring thumb moves smoothly when the tendon is pulled in order to handle fragile objects as well. It must be noted that when tendons pulled, hand is closing and thumb joint slides with the same action. When handling bigger objects hand opens passively and comes back to the original position as well. Since thumb motion requires further motion of the shoulder, if there is no further movement index finger and thumb is aligned in the neutral position so pinching and lateral grasp can be achieved.

3 Analyses and Results

The design variables for the analyses are given in Fig. 4. Finger dimensions are defined according to the study in [6].

It is crucial to determine the spring to be used in the drive of the system. The kinematic analysis is employed for determining the change in length. As a result, the length change in springs is 22.35 mm for index finger and 1.91 mm for thumb RoM. The weight of the HandMECH according to these parameters and with the use of ABS material is 80 g.

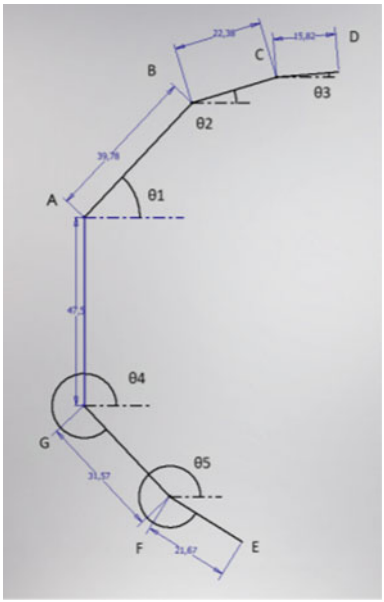

Fig. 4. Design parameters

4 Conclusion

In this study, a light, functional, and low-cost hand prosthesis is presented. For a low cost and light prosthesis, body-powered type is chosen and VC approach is employed. Tendons to move the fingers are connected via spring to the body-power mechanism. The HandMECH can realize different types of grip with different objects. The transition between these grip types is possible with the 3 DoF thumb that can translate. The prosthetic hand is mainly designed to perform power grip, pinch grip and lateral grip movements.

References

1. G.P. Kontoudis, M.V. Liarokapis, A.G. Zisimatos, C.I. Mavrogiannis, K.J. Kyriakopoulos, Open-source, anthropomorphic, underactuated robot hands with a selectively lockable differential mechanism: towards affordable prostheses, in *IEEE/RSJ International Conference on Intelligent Robots and Systems (IROS)* (2015)
2. J. Pons et al., The MANUS-HAND dextrous robotics upper limb prosthesis: mechanical and manipulation aspects. Auton. Robot. **16**(2), 143–163 (2004)
3. C. Cipriani, M. Controzzi, M.C. Carrozza, Objectives, criteria and methods for the design of the SmartHand transradial prosthesis. Robotica **28**(06), 919–927 (2009)
4. G. Roznowski, M. Drzewiecki, A new approach to the prosthetic finger design, in *TCSET*'2004, Lviv-Slavsko, Ukraine.
5. M. Bustamante, R. Vega-Centeno, M. Sanchez, R. Mio, A parametric 3D-printed body-powered hand prosthesis based on the four-bar linkage mechanism, in *IEEE 18th International Conference on Bioinformatics and Bioengineering (BIBE)* (2018)
6. A. Buryanov, V. Kotiuk, Proportions of hand segments. Int. J. Morphol. **28**(3) (2010)

Legislation, Safety and Performance: Regulatory Aspects in Wearable Robots

CO-GUIDING: Ergonomic Analysis of a Hand Guidance System for Car Door Assembly

Erika Triviño-Tonato, Jawad Masood, Ruben P. Cibeira, and Angel Dacal-Nieto

Abstract Hand Guidance is a type of Human-Robot Collaboration with high interest in the manufacturing industry. In this paper, we present an ergonomic analysis of an assisted hand guidance operation of car door assembly that can also be applied to the wearable robots. A simulated scenario and an experimental specific safety protocol are created. Two subjects perform a work cycle. Biomechanical data from the subjects and mechanical data from the robots are collected. We follow guidelines of UNE-EN 1005–3:2002, UNE-EN 1005–5:2007 and UNE-EN ISO 8996:2005 to execute risk assessment procedures. We consider the cycle time, applied force (push/pull), external load, muscle load, and workstation adaptability as key risk analysis measures. The results show the external load is acceptable by the subjects; the applied forces on the subjects do not exceed the followed norms; arm muscles activities (load) remains within acceptable ranges, and subject one shows better task adaptability.

1 Introduction

Ergonomics studies the relationship between the working environment and those who do the work. It aims to reduce ailments and injuries arising from over-efforts at work [1]. In the automotive sector, assembly processes like collaborative door assembly system (CDAS) are usually exposed to ergonomic risks like over-effort.

CO-GUIDING is a subproject of the European initiative COVR, which provides a common approach to safety assessment across robotics fields and applications. The CO-GUIDING project aims to improve safety of the assisted hand guidance CDAS. The system helps to mount side doors in the body in white (BIW) such that the operator handles the complex trajectories and finished quality, while a robot takes care of door weight and accuracy. At CTAG, the CDAS is simulated according to automotive standards.

E. Triviño-Tonato (✉) · J. Masood · R. P. Cibeira · A. Dacal-Nieto
Department of CTAG, Centro Tecnológico de Automoción de Galicia, O Porriño, Spain
e-mail: erika.trivino@ctag.com

J. C. Moreno et al. (eds.), *Wearable Robotics: Challenges and Trends*,
Biosystems & Biorobotics 27, https://doi.org/10.1007/978-3-030-69547-7_20

We focus on the ergonomic analysis of the workstation, for which an experimental protocol is developed to assess if there is a risk from forces exerted (Push/Pull), over-effort, muscle activity and adaptability to the workstation.

The paper is organised as follows: Section 2 deals with the development of the testing process, Section 3 presents the results. Section 4 show discussion and conclusions.

2 Development

In order to perform the risk assessment of the CDAS, a simulated workstation was set-up at CTAG facilities, a testing protocol was developed and controlled tests were performed.

2.1 Workstation Description

The CDAS operation consists of four sub-tasks: (1) the human hand guides the robot with the gripper to collect the door, (2) he/she can pick the door from the hanger with the help of a robot with a gripper, (3) he/she can place the door on the BIW with the help of the robot with gripper, and (4) he/she can hand guide the robot with the gripper back to the home position. A simulated workstation scenario has been deployed at CTAG facilities to perform the evaluation (Fig. 1).

The system consists of a robot (Fanuc 2000*ic* 165 F), a force sensor (Fanuc FS-15*ia*), a gripper (designed by CTAG), a manual guidance unit (purchased from Fanuc), conveyor belt, car body and door.

2.2 Experimental Protocol

The cycle time of the work is defined in 120 s, in which the operator provides 26 s for grabbing the door, 35 s for assembling, and 19 s for returning to its initial position. The total time of the assembly process is 80 s, adding 40 s for the return of the conveyor belt to its initial position ($V = 6$ m/min), and for the subject to rest.

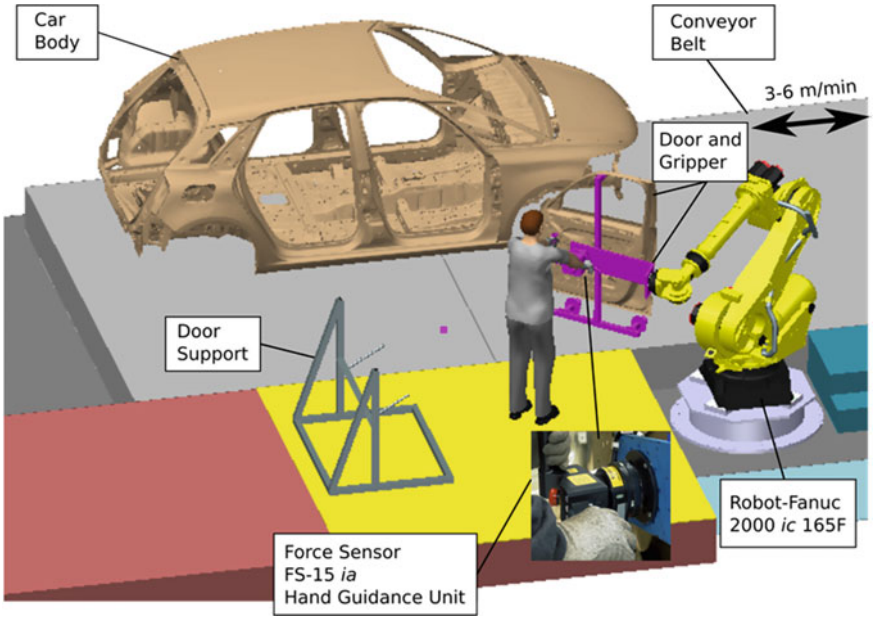

Fig. 1. Scheme of the CDAS operation

2.3 Simulated Test

The tests are performed by two male subjects with similar physical constitution from CTAG. The subjects have no prior task experience, so they underwent a familiarization session of the CDAS. After 14hrs of practice, a 10-cycle test is performed on each subject to verify its protocol compliance.

Afterwards, the test started, consisting 15 cycles of work for each subject, using different speeds of the conveyor belt (3, 4, 5, 6 m/min) and the maximum speed of the robot (250 mm/s).

The following information is collected during the execution of the tests: cycle time, heart rate (HR), heart rate variability (HRV), electromyography (EMG) signals of muscle groups (right and left: forearm, biceps, deltoids, trapezoid), and force applied for each Push/Pull cycle. The HR/HRV data was collected with the Elite HRV application and for the EMG data the Muscle Monitor version 3.0 software was used, which provides the data at a frequency of 25Hz, from where the data was exported for further processing. Rest periods are not included in the analysis.

For the compilation of the data the following devices are used: video camera, Polar H10 monitor, Fitbit Charge 3 monitor, and Myontech Mbody 3® sensorized clothing. The robot mounted a hand guidance tool and a force sensor.

2.4 Evaluation Method

The Physical workload was analyzed by studying HR by applying the Frimat criterion [2]. The HRV was evaluated using the time domain method considering the normal ranges of the parameters in [3] (R-R, interval, RMSSD, SDNN, PNN50%).

EMG: The risk of over-effort injuries for which the maximum voluntary contraction (MVC) of all muscle groups is analyzed and assessed using European standards [4, 5].

Subjective Analysis: We conducted a subjective questionnaire interview with both subjects, based on the 10 questions questionnaire which is developed by CTAG for CDAS and similar operations, to evaluate posture.

3 Results

Physical load of work: cardiac demand of the workstation is considered acceptable. The average HR of the subjects at the maximum speed of the conveyor belt does not exceed the limits established by the Frimat's criterion [2]. It is maintained between 83 and 85 bpm in the collected data.

Adaptability: Subject one has a better ability to adapt in this workstation because he maintains a good balance of the HRV when performing the task. The intensity of the mental load in this workstation is high for subject two.

EMG: The results show that the deltoid and trapezius muscles of the left and right arm do not reach a muscle activity above 2% and the forearm and bicep muscles (right and left) do not exceed 50% of MVC of both subjects. The standards [5, 4] indicate that there is a presence of risk when the internal force value is equal to or greater than 50% MVC for at least 10% of the time.

Forces exerted (Push/Pull): The force values (shown in Table 1) do not exceed the maximum values set by [6] $F_{PUSH} = 40$ N, $F_{PULL} = 29$ N (Recommended maximum force calculated for push/pull action of this workstation).

Subjective Analysis: Subject 1 finds that the CDAS system can allow adopting comfortable postures while subject 2 finds that the CDAS system cannot allow adopting comfortable postures. The results of the mean force applied at each velocity show that there is no risk for exercised forces.

Table 1 Mean forces exerted at automotive assembly line speeds

Mean forces	3 (m/min)	4 (m/min)	5 (m/min)	6 (m/min)
Push	24 (SD = 2.9)	25 (SD = 2.1)	20 (SD = 1.7)	28 (SD = 1.5)
Pull	17 (SD = 4)	19 (SD = 5)	19 (SD = 4)	20 (SD = 4)

4 Conclusions and Discussion

This study facilitates the validation of the developed protocol (according to the ISO–12100 regulations, and the UNE-EN Safety of machinery—Ergonomics regulations) that can help the community of collaborative robots to ensure safety and evaluating wearable robots.

HR and HRV signals show that the physical workload is acceptable regarding cardiac demand for the subjects. Subject one is better adapted to the workstation than subject two.

From the EMG records, medium-low activation values have been obtained for all muscles analysed; the RMS value is in ranges less than 2 μV for subject one and for subject two are found in values less than 7 μV, except in the left forearm (9.55 μV) and left biceps (8.85 μV). None of the upper limb muscles is found fatigued. The distribution of muscle activity in the forearm and right biceps at all velocity levels of the conveyor belt is found at an average of 14% and the rest of the muscles on mean not exceeding 13%. Applied force (Push/Pull) results exhibit a small increase in force, observed as the speed of the conveyor increases.

From the subjective questionnaire analysis, we conclude that both subjects rate the CDAS and the use-case as low physical demanding. The tests of this study are performed for 2 h with less than 120 s cycle time, which does not guarantee the results of a full day of work. In addition, we perform tests on only two subjects that is a low number for conclusive evidence. We recommend larger pilot trials based on the presented protocol to improve the fidelity of such systems.

Acknowledgement The authors want to thank the project COVR (Being safe around collaborative and versatile robots in shared spaces), which has received funding from the European Union's Horizon 2020 research and innovation programme under grant agreement No 779966, and supports this work.

References

1. H. Hendrick, Determining the cost-benefits of ergonomics projects and factors that lead to their success. Appl. Ergon. **34**(5), 419–427 (2003)
2. GÓMEZ, Mª Dolores Solé. NTP 295: Assessment of physical load by monitoring heart rate. INSST. **1**, 1–6 (1991)
3. D. Nunan, et al., A quantitative systematic review of normal values for short-term heart rate variability in healthy adults. Pacing Clinical Electrophysiol **33**(11), 1407–1417 (2010)
4. ISO, ISO 11228-3. Ergonomics—manual handling—Part 3: handling of low loads at high frequency (AENOR, Madrid, 2007)
5. UNE-EN 1005-5, Safety of machinery—Human physical performance—Part 5: Risk assessment for repetitive handling at high frequency (AENOR, Madrid)
6. UNE-EN 1005–3, + A1, 2009 Safety of machinery—Human physical performance—Part 3: recommended force limits for machinery operation. (AENOR, Madrid, 2002)

ATEX Certification for ALDAK Exoskeleton in Petrochemical Industry

Ane Intxaurburu, Iñaki Díaz, Juan Martín, and Xabier Justo

Abstract Most certification processes require the complex and tedious analysis of multiple normative and references to understand and apply the appropriate methods to get the desired mark. This work intends to ease the way for ATEX certification of exoskeletons, especially relevant for mining and petrochemical industries. GOGOA's ALDAK exoskeleton aims to become the first ATEX certified exoskeleton and this work reviews the process and steps to follow.

1 Introduction

Musculoskeletal disorders (MSDs) were the leading cause of disability in four of the six WHO regions in 2017. While the prevalence of musculoskeletal conditions increases with age, younger people are also affected, often during their peak income-earning years [1].

Industrial and service companies are involved in the challenge of improving the occupational safety and health of their employees, facilitating their work and reducing musculoskeletal injuries, but they have difficulties in finding the ideal solution that rationally inclines them to its implementation. Technological solutions based on exoskeletons can help reinforce these ergonomic aspects for the benefit of the worker, the company and society.

A. Intxaurburu (✉) · J. Martín
GOGOA Mobility Robots S.L, Abadiano, Spain
e-mail: aintxaurburu@gogoa.eu

J. Martín
e-mail: jmartin@gogoa.eu

I. Díaz · X. Justo
Smart Systems for Industry 4.0 Group of CEIT-Basque Research and Technology Alliance (BRTA) and Universidad de Navarra, San Sebastián, Spain
e-mail: idiaz@ceit.es

X. Justo
e-mail: xjusto@ceit.es

J. C. Moreno et al. (eds.), *Wearable Robotics: Challenges and Trends*,
Biosystems & Biorobotics 27, https://doi.org/10.1007/978-3-030-69547-7_21

Exoskeletons can assist workers in repetitive lifting of heavy objects that is one of the most common risk factors for MSDs [2]. Several exoskeletons-based solutions are currently appearing in the market for different types of tasks. Nevertheless, there is a lack of active exoskeleton for helping in activities to be performed in atmospheres with risk of explosion (due to inflammable gas or powder), which require ATEX ("ATmosphères EXplosibles") certification.

This work intends to review and showcase the ATEX certification process we are carrying out for GOGOA's ALDAK exoskeleton to become the first ATEX certified exoskeleton in the world. ALDAK is an active exoskeleton developed by GOGOA, at the present at TRL6 level (Fig. 1). It provides lower back assisted movement using assist-as-needed algorithms, helping workers to lift heavy weights (until 35 kg) protecting the lumbar zone and decreasing back pain. One of the target market for this system is the petrochemical industry where ATEX certification would be necessary in many workplaces to operate. This paper intends to clarify the process and guide other works in this certification.

Fig. 1. Active ALDAK exoskeleton from GOGOA

2 Material and Methods

2.1 Normative References

The following directives have to be taken into account for ATEX certification of exoskeletons in petrochemical (and similar) workplaces:

The Directive 89/391/EEC on Prevention of Occupational Risks, determines the responsibilities and guarantees to ensure health protection of workers against the risks of working conditions. The Article 16 (1) lays down the minimum requirements for the safety and health protection of workers in potentially risky explosive atmospheres.

ATEX is the name commonly given to the two EU directives aiming to control the risks caused by explosive atmospheres [3]: Directive 1999/92/EC (ATEX Workplace Directive) and Directive 2014/34/EU (ATEX Equipment Directive).

Directive 1999/92/EC is a directive laying down minimum requirements (employer obligations) for protecting health and safety at work, especially through zone classification of hazardous areas, i.e. areas where explosive atmospheres may occur, and through explosion risk assessments and appropriate ATEX equipment selection. The petrochemical sector is considered as ATEX, taking into this Directive.

Directive 2014/34/EU is a product directive harmonizing the Essential Health and Safety Requirements (EHSR) to be complied with by the manufacturers of ATEX equipment, including instructions for equipment categorization, conformity assessment procedures and CE- and Ex-marking obligations.

Besides the ATEX Equipment Directive 2014/34/EU, compliance with other product directives, as for instance the Machinery Directive 2006/42/EC and the Electromagnetic Compatibility Directive 2014/30/EU, may be relevant for the manufacturer.

Four international standards are also relevant:

- EN 1127–1: Explosive atmospheres: Explosion prevention and protection. Basic concepts and methodology.
- EN 60079–10-1: Explosive atmospheres: Classification of areas. Explosive gas atmospheres.
- EN 60079–10-2: Explosive atmospheres—Classification of areas—Combustible dust atmospheres.
- ISO/IEC 80079–34:2012: Application of quality systems for equipment manufacture.

2.2 Risk Assessment

Fig. 2 show the main steps for a complete ignition hazard risk assessment necessary for ATEX certification. Two main methods for developing risk assessments are used: FTA (Fault Tree Analysis) and FMEA (Failure Mode and Effect Analysis). With the

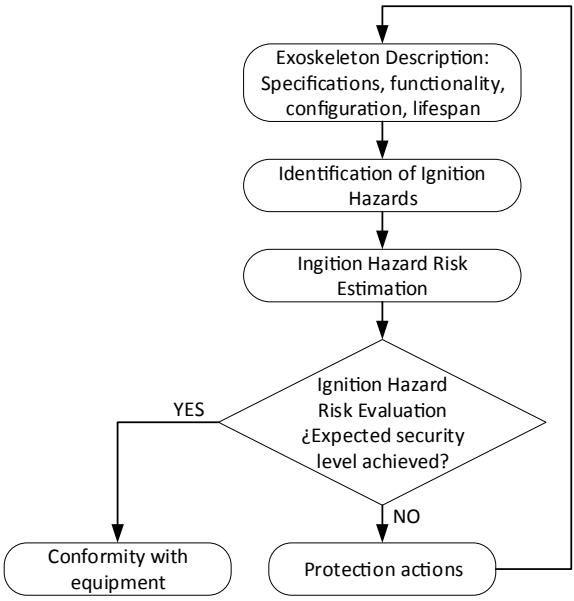

Fig. 2. Ignition hazard risk assessment

aim of classifying and evaluating the risks, HAZOP method (Hazard and Operability) is used.

First step is the complete description of the exoskeleton (specifications, functionality, intended use, configuration, life span) and the specific workplace considered (in our case the transport of liquid petroleum gas containers in the petrochemical industry). Then, with the workplace description and the intended use of the exoskeleton, all possible ignition hazards are identified.

Third step is the estimation of ignition hazard risks. For this step, the presence of explosive atmospheres and the identification of relevant possible ignition sources (e.g. hot surface, mechanical sparks) and their likelihood (normal operation, foreseeable malfunction and rare malfunction) are considered.

Next step is the evaluation of the ignition hazard risks. For each equipment related ignition source identified, it is specified the preventive measure applied, and the eventual assessment with the results and final categorization of the equipment. If results are as expected in terms of safety, equipment conformity is reached: otherwise, protective actions are taken and the process starts again.

The resulting equipment category is finally determined by the ignition source linked to the lowest categorized group (least protection). ATEX divides equipment into categories according to how well the equipment is protected against becoming an active ignition source.

2.3 Technical Documentation and Marking

This certification process must be undertaken by an ATEX Notified Body. Technical documentation requirements are:

- A general description of the equipment.
- The design and manufacturing drawings and layouts/schemes, and description of operation.
- List of harmonized standards applied (or solutions adopted where standards have not been applied).
- Results of calculations, examinations and test reports.
- The ignition hazard assessment report.
- Certificates and other documents issued by a Notified Body (including relevant documentation enabling the conformity of the product with the requirements of the directive to be assessed).

The certification process includes testing and assessment of the product, with an ATEX certificate and report being issued for conforming product. Equipment, protective systems and devices must be accompanied by an EU Declaration of Conformity (and bearing the CE-marking affixed) with reference to the ATEX Equipment Directive 2014/34/EU.

3 Conclusion

This works reviews main steps for carrying out an ignition hazard risk assessment for ATEX certification of exoskeletons, as well as main directives and standards to follow and technical documentation and marking description. Future work will detail the risk assessment and evaluation carried out for ALDAK exoskeleton to get the ATEX certification to operate in the petrochemical industry.

Acknowlegments This work has been supported by the European Union's Horizon 2020 research and innovation programme under COVR project, gran agreement No. 779966.

References

1. S.L. James et al., Global, regional, and national incidence, prevalence, and years lived with disability for 354 diseases and injuries for 195 countries and territories, 1990–2017: a systematic analysis for the global burden of disease study 2017. Lancet **392**(10159), 1789–1858 (2018)
2. Eurofund, Sixth European working conditions survey, overview report, *Publications Office of the European Union* (Technical Report, 2016)
3. T. Jespen, ATEX—explosive atmospheres, risk assessment, control and compliance (Springer Series in Reliability Engineering, 2016)

Acceptance of Exoskeletons: Questionnaire Survey

Liên Wioland, J. Jean-Jacques, Atain-Kouadio, Latifa Debay, and Hugo Bréard

Abstract The introduction of exoskeletons in companies, like any new technology, is a major change. In this context the specific question of the acceptance of these devices by workers is addressed. To this end, a questionnaire was specifically developed and administered to current and former exoskeleton users. The results presented provide information on the quality of the operator-exoskeleton interaction, and identify blocking and/or facilitating points for the use of these devices.

1 Introduction

Exoskelettons are presented as systems that reduce physical demands, assist the operator [1] or improve physical performance [2]. Companies consider them as devices that could limit musculoskeletal disorders. Thus, they test them with workers who have very contrasting reactions. Some refuse to test them, others use them and then reject them, while some integrate them into regular use. Therefore, even if an exoskeleton may appear simple to use and have potential, users will not necessarily accept it. The issue of acceptance is a challenge for both, designers and companies. The objective of this study is to identify the determinants of acceptance and rejection of exoskeletons by users. The best known model to explain user intent is the Davis Technology Acceptance Model (TAM) [3]. He posits that intention to use is partly preceded by the "social normative factor" (normative beliefs and the judgment of others). Then he incorporates two major concepts into his model: "perceived usefulness" (the degree to which an individual believes that using a system improves work performance) and "perceived ease of use" (the degree to which an individual believes that using the system requires no effort). Venkatesh [4] merges

L. Wioland (✉) · Atain-Kouadio · L. Debay
Department of Working Life, French National Research and Safety Institute for the Prevention of Occupational Accidents and Diseases (INRS), Paris, France
e-mail: lien.wioland@inrs.fr

J. Jean-Jacques · H. Bréard
Paris-Nanterre University, Master Workplace Psychology, Ergonomics and Orientation, Paris, France

J. C. Moreno et al. (eds.), *Wearable Robotics: Challenges and Trends*,
Biosystems & Biorobotics 27, https://doi.org/10.1007/978-3-030-69547-7_22

several models, including the TAM, to propose the Unified Theory of Acceptance and Use of Technology (UTAUT) model, which he validates empirically on many occasions. Thus, he takes the three dimensions proposed by Davies and adds a dimension relating to "enabling conditions" which refers to the degree to which a worker believes that an organizational and technical infrastructure exists to support the use of the system. Acceptance can also be considered from the point of view of the user's emotional reactions related to the use of exoskeleton [5, 6]. The last type of model presented concerns the "situated acceptance which concerns the real use of the technology in a work situation [7]. The principle is based on the idea whereby the exoskeleton transforms user activity and thus affects acceptance. He adds 3 variables to those already identified. The "individual dimension" (cognitive demands, emotional load (anxiety, satisfaction…), the "relational dimension" which concerns the way in which technology affects collective activities in work and the "identity dimension" which concerns the consequences of the use of technology on the construction and recognition of identity. Exoskeletons are supposed to provide physical assistance by limiting effort and helping to preserve the health and safety of users. To date, none of the acceptance models incorporate this aspect. In this work it is added to the "performance expectations" dimension. Acceptance would also be determined from the users' feelings in terms of reduced fatigue and pain or improved working conditions.

2 Material and Method

INRS has developed a questionnaire survey to analyse the acceptance of exoskeletons. It integrates the dimensions described by the different models presented. It is therefore built around six dimensions: facilitating conditions, ease of use, performance expectations (production and health and safety), social influence, professional identity, and user emotional reaction. For each of tem, specific questions to the use of exoskeletons were developed. The survey contains about 40 questions and takes about 20 min to fill it out. The response modalities follow a Likert scale with 5 levels, from "strongly disagree" to "strongly agree".

3 Results

The questionnaire was completed by 88 current or former users of exoskeletons (72 males and 16 females). The data was collected from 13 french companies from different sectors (logistics, food processing, transport, automotive industry…). 97% of the exoskeletons used by the surveyed operators were passive. 76% of them were dedicated to back support, the others were dedicated to upper or lower limbs and other parts of the body (e.g. cervicals). The respondents were mainly engaged in handling. They were divided into two groups according to whether they accepted (n

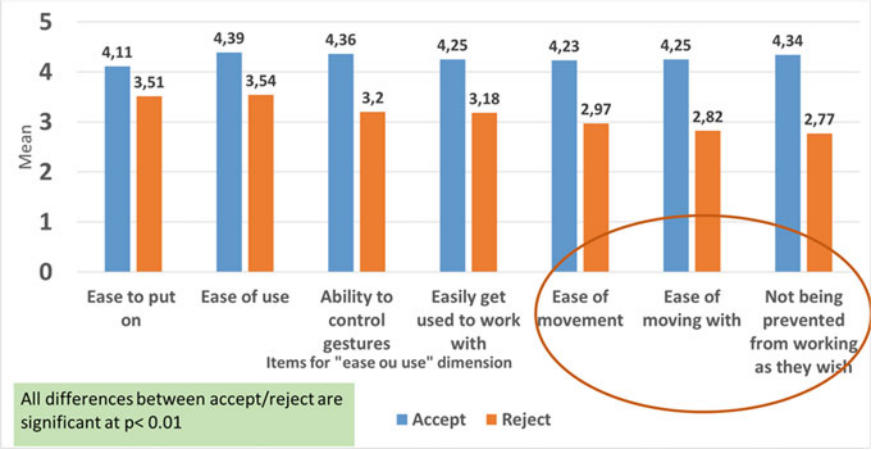

Fig. 1. Accept/reject results for the dimension "ease of use"

= 44 noted *Accept* in the text) or rejected (n = 39 noted *Reject* in the text). This information was accessible through a specific question asking to the respondent if he accepts or rejects the exoskeleton. We have compared the results of the "*Accept"* and the "*Reject"* for each of the 6 dimensions to identify blocking and facilitating points for acceptance. We have assigned numerical values to the response modalities (5 for strongly agree) and calculated the mean value and the T of student to compare the both groups. Only a few results are presented.

3.1 Ease of Use

Respondents were generally positive for some of the items related to the ease of use of the exoskeleton. So, the "*Accept"* are nevertheless more positive than the "*Reject*" for the items on the left of the Fig. 1. For the items circled in red the opinions of the "*Accept"* are positive unlike those of the "*Reject"*.

3.2 Performance Expectations

From a productivity point of view, the majority of the "*Accept*" or the "*Reject*" say that their performance is identical with or without an exoskeleton. The "*Reject*" (40%) stress that it is less with the exoskeleton in terms of speed, productivity, efficiency and quality, while the "*Accept*" agree with this statement only moderately. For example for speed (Maccept = 3.09, Mreject = 2.38, t = 5.38, $P < 0.01$) or efficiency (Maccept = 3.29, Mreject = 2.56, t = 4.69, $P < 0.01$).

From a health and safety perspective, both "*Accept*" and "*Reject*" perceive physical exertion with the exoskeleton to be less. The "*Accept*" are more positive on this item than the "*Reject*" (Maccept = 3.57, Mrejec[2] = 3.18, t = 2.19, $P < 0.05$). On the other hand, concerning fatigue, the "*Reject*" evaluated it as "identical" (51%) with or without exoskeleton, whereas 53% of the "*Accept*" were more positive, and perceived it as "less occuring" when using the exoskeleton (Maccept = 3.59, Mreject = 2.95, t = 3.70, $P < 0.01$). A majority of the "*Accept*" (69%) express that back pain is "less occuring" with the exoskeleton as opposed to the "*Reject*" (Maccept = 1.05, Mreject = 0.37, t = 2.81, $P < 0.01$). In fact, 46% of the "*Reject*" expressed that they see no change in their back with the exoskeleton. Operators, mostly the "*Reject*", report the appearance of new discomfort or pain for example in the back (12%), or shoulders (20% of the "*Reject*" and 11% of the "*Accept*").

3.3 Social Influence

The managers are perceived as being favourable to the use of the exoskeleton by 93% of the "*Accept*" and 73% "*Reject*". When it comes to colleagues, the "*Reject*" expressed significantly more negatively than the "*Accept*" (Mfavo = 4, Mdefavo = 2.79, t = 5.31, $P < 0.01$).

3.4 User's Emotional Reactions

On the Fig. 2. We can see that the "*Accept*" significantly qualify the wearing of the exoskeleton as relatively pleasant and like to work with it unlike the "*Reject*". The exoskeleton does not cause anxiety nor nervousness. On the other hand, the "*Reject*" have less confidence in the system, and are not enthusiasm to use it.

4 Discussion and Conclusion

The acceptance process is complex because several dimensions are involved and interact. Accepting the technology does not mean that all items of the dimensions must receive a favourable opinion from users. Accepting an exoskeleton requires finding the right balance between these different dimensions which do not have the same weight in the final decision. This balance is not easy to define, especially since the acceptance process is complex, fragile and dynamic. Nevertheless, it is crucial to take it into account because, in terms of occupational risks, imposing an unaccepted exoskeleton may constitute a psycho-social, physical or even accidental risk factor.

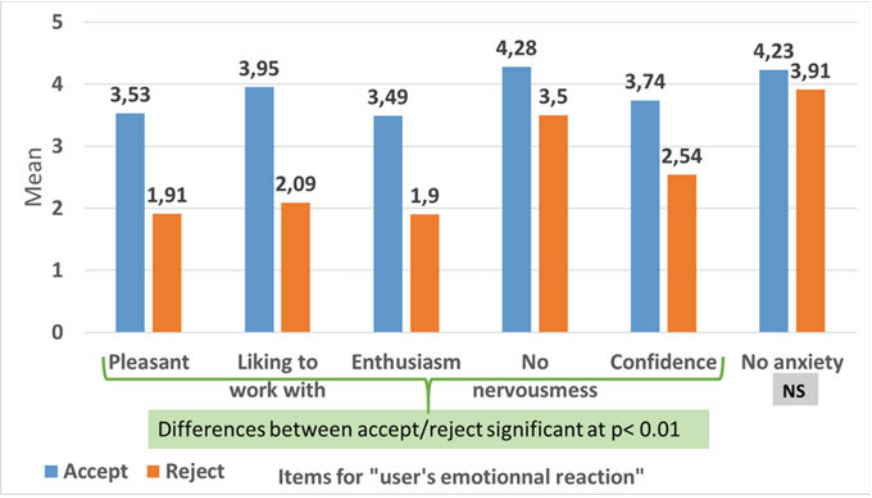

Fig. 2. Accept/reject results for the dimension "user' emotional reactions"

References

1. J. Theurel, K. Desbrosses, T. Roux, A. Savescu, Physiological consequences of using an upper limb exoskeleton during manual handling tasks. Appl. Ergon **67**, 211–217 (2018)
2. M.P. De Looze, T. Bosch, F. Krause, K.S. Stadler, L.W. O'Sullivan, Exoskeletons for industrial application and their potential effects on physical work load. Ergonomics **59**(5), 671–681 (2016)
3. F.D. Davis, Perceived usefulness, perceived ease of use, and user acceptance of information technology. MIS Q. 319–340 (1981)
4. V. Venkatesh, M.G. Morris, G.B. Davis, F.D. Davis, User acceptance of information technology: Toward a unified view. MIS Q. 425–478 (2003)
5. S. Mahlke, User experience of interaction with technical systems, in *Theories, Methods, Empirical Results and Their Application to the Development of Interactive System*. Thèse pour legrade d'ingénieur. (Université technique de Berlin, faculté V, 2008), 194 pp
6. W.H. Delone, E.R. Mclean, Information systems success: the quest for the dependant variable. Inf. Syst. RES **3**(1), 60–95 (1992)
7. M.E. Bobillier Chaumon, L'acceptation située des technologies dans et par l'activité: premiers étayages pour une clinique de l'usage. Psychologie du Travail et des Organisations **22**(1), 4–21 (2016)

Perceived Exertion During Robot-Assisted Gait After Stroke

Nina Lefeber, Emma De Keersmaecker, Eric Kerckhofs, and Eva Swinnen

Abstract The present study investigated the level of perceived exertion during robot-assisted walking in non-ambulatory stroke survivors. In addition, we studied the relationship between the user's subjective level of perceived exertion and objective measures of exertion (i.e. oxygen consumption and heart rate). Our results suggest that stroke survivors perceive fully assisted Lokomat walking as extremely light to very light and fully assisted Ekso GT walking as very light to somewhat hard. Weak positive correlations were found between subjective and objective measures of exertion.

1 Introduction

Worldwide, stroke is a prevalent health issue. Each year, roughly 15 million people experience a stroke. Initially after stroke, half of the stroke survivors is unable to walk and around 12% needs assistance of a person to walk [1]. As a result, stroke survivors spend the majority of their rehabilitation time on practicing walking (25–45%) [2].

To induce neuroplasticity, gait rehabilitation requires sufficient training intensity. To increase the intensity and volume of gait rehabilitation, two types of lower limb robotic exoskeletons have been introduced: (1) static (or treadmill-based) exoskeletons, such as the Lokomat (Hocoma), and (2) dynamic (or wearable) exoskeletons, such as the Ekso GT (Ekso Bionics) [3]. However, few studies have evaluated the training intensity of robot-assisted gait rehabilitation after stroke [4].

The aims of this study were: (1) to investigate how physically exerting stroke survivors perceive static and dynamic exoskeleton training and (2) to investigate if the user's subjective level of exertion correlates with objective physiological measures of exertion.

N. Lefeber (✉) · E. De Keersmaecker · E. Kerckhofs · E. Swinnen
Rehabilitation Research Group, Vrije Universiteit Brussel, Brussels, Belgium
e-mail: nina.lefeber@vub.be

J. C. Moreno et al. (eds.), *Wearable Robotics: Challenges and Trends*,
Biosystems & Biorobotics 27, https://doi.org/10.1007/978-3-030-69547-7_23

2 Methods

2.1 Study Protocol

In this manuscript, we present a secondary analysis of the data collected as part of two clinical trials investigating the physiological responses during robot-assisted gait after stroke. Detailed descriptions of the protocols can be found elsewhere [5, 6]. The studies were approved by the medical ethics committees of the University Hospital Brussels (B.U.N. 143201526040 and 143201734424), the Jessa Hospital Hasselt (16.124/reva16.15), the IRCCS Fondazione Santa Lucia Rome (CE/PROG.630) and the GasthuisZusters Antwerp Hospitals (HD/vv/2018/07.19). All participants signed consent prior to participation in this trial.

2.2 Participants

We included 20 adult non-ambulatory stroke survivors (functional ambulation category ≤ 2) in the subacute stage after stroke (1 week to 6 months) and excluded persons with unstable cardiovascular conditions, lower limb musculoskeletal problems (unrelated to stroke), concurrent pulmonary diseases, concurrent neurological diseases, communicative or cognitive problems constraining the ability to comprehend and follow instructions, and other contra-indications for exoskeleton training (Table 1).

Table 1 Participant characteristics

Outcome	Lokomat group (n = 10)	EksoGT group (n = 10)
Age (years)	66 (11)	71 (9)
Sex (male/female)	6/4	5/5
BMI (km/m^2)	25 (3)	23 (3)
Time since stroke (days)	89 (40)	50 (42)
FAC (0/1/2)	1/2/7	0/7/3
β-blockers (yes/no)	4/6	4/6
Bodyweight support (%)	44 (7)	–
Walking speed (m/s)	0.61 (0.03)	0.21 (0.02)

Continuous variables are reported as mean (standard deviation) and categorical variables as numbers
BMI body mass index; *FAC* functional ambulation category

2.3 Experimental Procedure

One group (n = 10) walked 20 minutes on a treadmill wearing a static lower limb exoskeleton (Lokomat, Hocoma; Fig. 1). Robotic assistance was set to the maximum (100%). The level of bodyweight was decreased as much as tolerable and the walking speed was increased as much as tolerable (Table 1).

A second group (n = 10) walked 20 minutes overground wearing a mobile lower limb exoskeleton (Ekso GT™, Ekso Bionics; Fig. 1). Robotic assistance was set to the maximum (100%). Participants walked at a self-selected walking speed and did not use any walking aid. A certified and experienced physiotherapist guided the exoskeleton in the back.

At the start of each session, a flexible mouth mask, portable respiratory gas analysis system (MetaMax3B, Cortex, Germany) and heart rate belt (Polar H7, Polar, Finland) were fitted. Participants rested in their wheelchair for 5 minutes wearing the equipment. Thereafter, participants were accommodated in the exoskeleton. Gas exchange and heart rate were monitored from the beginning of rest to the end of walking. At the end of seated rest and every 3 or 5 minutes during walking (resp. Lokomat and EksoGT group), participants were asked to rate their rating of perceived exertion (RPE) by pointing on a 6–20 Borg Scale (6 meaning "no exertion at all" and 20 meaning "maximum exertion"). Gas and volume calibrations were performed in accordance with manufacturer's instructions. Participants were asked not to consume food, alcohol, caffeine, or nicotine at least 3 h prior to the sessions, nor to perform additional strenuous activities (apart from their regular therapy) at least 12 h prior to the sessions.

Fig. 1 Illustration of a person in the static Lokomat (left) and dynamic Ekso GT™ (right) exoskeleton. (© Johan Swinnen)

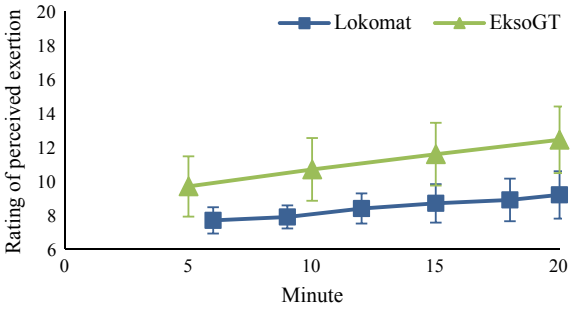

Fig. 2 Mean (95% CI) rating of perceived exertion during 20-minutes Lokomat and EksoGT walking

2.4 Outcomes

Outcomes of interest were RPE (6–20 Borg scale), heart rate (beats/min) and oxygen consumption (mL/kg/min). The first 4 minutes (EksoGT group) and 5 minutes (Lokomat group) of walking were used to reach a steady-state condition and were omitted from the analyses.

2.5 Statistical Analysis

Repeated measures ANOVAs were conducted to investigate changes in RPE over time. Pearson correlation coefficients were calculated to measure the relationship between RPE, oxygen consumption and heart rate (SPSS version 25).

3 Results

In both groups, RPE significantly increased over time (Lokomat: $F(4.906, 1.236)$, $p = 0.043$; Ekso GT: $F(8.791, 3)$, $p = 0.0004$; Fig. 2) and RPE was weakly correlated with objective measures of exercise intensity (Table 2).

4 Discussion and Conclusion

Our results suggest that non-ambulatory stroke survivors perceive fully assisted Lokomat walking as extremely light to very light and fully assisted Ekso GT walking as very light to somewhat hard. However, since patient characteristics were not matched between both groups, no between-group comparisons could be made. Weak correlations between the subjective and objective measures of exercise intensity in both groups suggest that subjective measures alone may be insufficient to monitor

Table 2 Pearson correlation coefficients between subjective and objective measures of exertion

	Group	Minute	VO_2	HR
RPE	Lokomat	6	0.30	0.50
		9	0.08	0.45
		12	0.26	0.18
		15	0.01	0.52
		18	0.08	0.43
		20	0.06	0.44
	Ekso GT	5	0.21	0.11
		10	0.01	0.05
		15	0.03	0.15
		20	0.42	0.45

$^{*}p < 0.05$; *HR* heart rate; *VO_2* oxygen consumption; *RPE* rating of perceived exertion

exercise intensity during robot-assisted gait rehabilitation. A more extensive set of subjective and objective measures (including e.g. motivation and discomfort) should be studied in future large-scale trials.

Acknowledgment The work of N. Lefeber and E. De Keersmaecker was supported by the Research Foundation Flanders (FWO).

The authors would like to thank the patients and therapists of the neurorehabilitation units of the IRCCS Fondazione Santa Lucia, the Jessa Hospital campus St-Ursula and the Rehabilitation Hospital RevArte for participating in this trial.

References

1. H.S. Jorgensen, H. Nakayama, H.O. Raaschou, T.S. Olsen, Recovery of walking function in stroke patients: the Copenhagen Stroke Study, (in eng). Arch. Phys. Med. Rehabil. **76**(1), 27–32 (1995)
2. N.K. Latham et al., Physical therapy during stroke rehabilitation for people with different walking abilities, (in eng). Arch. Phys. Med. Rehabil. **86**(12 Suppl 2), s41–s50 (2005)
3. G. Morone et al., Robot-assisted gait training for stroke patients: current state of the art and perspectives of robotics, (in eng). Neuropsychiatr. Dis. Treat **13**, 1303–1311 (2017)
4. N. Lefeber, S. De Buyzer, N. Dassen, E. De Keersmaecker, E. Kerckhofs, E. Swinnen, Energy consumption and cost during walking with different modalities of assistance after stroke: a systematic review and meta-analysis, (in eng), Disabil. Rehabil. 17 (2019)
5. N. Lefeber et al., Physiological responses and perceived exertion during robot-assisted treadmill walking in non-ambulatory stroke survivors, (in eng), Disabil. Rehabil. 1–9 (2019)
6. N. Lefeber et al., Robot-assisted overground walking: physiological responses and perceived exertion in nonambulatory stroke survivors. IEEE Robot Automat Magz. 0 (2019)

Testing Safety of Lower Limbs Exoskeletons: Current Regulatory Gaps

Stefano Massardi, David Pinto-Fernandez, Jan F.Veneman, and Diego Torricelli

Abstract Exoskeletons are a growing technology that is increasingly being studied and researched in various application domains. However, new technologies must fit into current regulations, which update more slowly than market needs. This paper analyses the main regulations and standards in which exoskeletons can fit, underlining the gaps and barriers that still exist and may hinder the smooth introduction of exoskeleton technology in the market.

1 Introduction

Exoskeletons may be used in a wide range of applications, spanning from military to industrial use, personal care, and medical applications. Exoskeletons' range of applicability is expanding with an increasing number of devices present on the market [1]. Aging is associated with increasing mobility impairments, making the demand for rehabilitation and assistive devices growing every year [2]. An important challenge remains to have a clear unambiguous procedure for certification (CE-mark) of such products. Both development and certification require the assessment of device performance and safety. Nevertheless, the literature on this topic is scarce [3]; protocols or standards to validate exoskeletons are still limited. In recent years, several clinical studies into exoskeletons and their use have been performed, but researchers usually use own protocols to evaluate the benefits and assess performances, often without taking into account the adverse events the user might experience. This paper aims

S. Massardi (✉) · D. Pinto-Fernandez
Neural Rehabilitation Group of the Spanish National Research Council (CSIC), Madrid, Spain

D. Pinto-Fernandez
e-mail: david.pinto@cajal.csic.es

J. F.Veneman
Hocoma AG, Volketswil, Switzerland

D. Torricelli
Bioengineering Group of the Spanish National Research Council (CSIC), Madrid, Spain
e-mail: diego.torricelli@csic.es

J. C. Moreno et al. (eds.), *Wearable Robotics: Challenges and Trends*,
Biosystems & Biorobotics 27, https://doi.org/10.1007/978-3-030-69547-7_24

to clarify the current state of the art regarding applicable standards and standards development.

2 Legislations

2.1 EU Directives and Regulations

European legislation consists of directives and regulations. Some of them apply to exoskeletons such as the Electromagnetic Compatibility Directive 2014/30/EU [4], the Low Voltage Directive 2014/35/EU [5] and the Machinery Directive 2006/42/EC [6]. Additionally, in 2017 the new Medical Device Regulation (MDR) 2017/745 [7] came into force, whose final implementation in May 2021 will replace the Medical Device directive (MDD) 93/42/EC. Article 1.3 in MDR states "devices with both a medical and a non-medical intended purpose shall fulfill the requirements applicable to devices cumulatively with an intended medical purpose and those applicable to devices without an intended medical purpose" arising questions regarding the boundaries between different fields where new exoskeleton technologies may apply. From this statement, an exoskeleton shall apply the MDR independently from its medical or non-medical purpose, if it reasonably can be expected to be used for medical purposes, making the intended purpose declared by the manufacturer playing a key role in the classification. Due to this, a lack of proper terminology and specific regulation may cause uncertainty about the practical application of the current legislation [8]. Annex I of MDR describes the general safety and performance requirements a device shall meet, while Annex XIV defines the clinical evaluation and investigation that shall be performed. Being a law act, it cannot provide any guidance on how to achieve the requirements. Proving compliance with regulations constitutes a complex task, in which manufacturers and other parties rely on additional technical harmonized standards. However, specific standards related to exoskeletons in different domains are still scarce.

2.2 American Food and Drugs Administration (FDA)

For the US market, US food, and drug administration (FDA) is the federal agency controlling and supervising several products, including medical devices. FDA explicitly mentions exoskeletons, describing them as "a prescription device that is composed of an external, powered, motorized orthosis that is placed over a person's paralyzed or weakened limbs for medical purposes" (Regulation 21 CFR 890.3480) [9]. In the Federal register vol.80 n.36 [10] FDA identified 9 risks associated with exoskeleton use, each of them combined with related special controls to mitigate the risk and provide assurance of safety and effectiveness. The document doesn't

specify technical parameters or how to implement the tests mentioned, however, FDA guidelines successfully streamlined the approval of three exoskeleton devices [9].

2.3 ISO/IEC Standards

Compliance with European directives and regulations can be achieved through harmonized standards. The consolidated standard ISO 10218-1 have evolved but lacks in addressing possible industrial use of wearable devices [11]. The needs following the growing field of service robots led to the publication of the ISO 13482 for personal care robots [12], where exoskeletons can fit in service robot category: 'Restrain type—Physical assistant robots'. ISO 13482 provides the guidelines to achieve the safety requirements starting from the well-accepted risk assessment and risk reduction steps contained in ISO 12100. Attempting to help the user, Annex A of ISO 13482 presents general requirements and risk reduction measures that can be applied to control the risks associated with these hazards. Although ISO 13482 is a specific standard for personal care robots, it cannot contain specific or practical sections on how to achieve compliance with the stated requirements. An effort in this direction has lately been taken by technical reports. Technical reports (TR) are not International Standards (IS) and do not have the authority of an IS, but are rather collections of data coming from surveys, informative reports, tests, or state of the art. They can be anyway useful in providing examples of how the standard can be used for a specific technology. Recently, ISO TR 23482-1 [13] and ISO TR 23482-2 [14] have been published; the latter intended as a guide for users not familiar with the risk assessment procedure. ISO TR 23482-2 presents risk assessment examples while TR 23482-1 aims to guide manufacturers in proving compliance with ISO 13482. Proposed test methods are either universal, e.g. applicable to all the personal care robot families, or specific to one subfamily (mobile robots, physical assistance robots). Work needs to be done to present more supportive procedures that still appear generic and sometimes without clear test pass/fail criteria. For medical applications, ISO 14971 [16] provides the general risk management approach to be applied to medical exoskeletons and ISO TR 24971 [17] supports users normally not familiar with risk assessment, focusing on the method rather than the technical content. Under the IEC 60601-1, the general standard for medical electrical devices, a particular specification has been published: IEC 80601-2-78 [15]. These standards need to find the balance between description and clarity taking into account the necessity of being unambiguous and the impossibility of building a particular standard for each device. Further developments of IEC 80601-2-78 could be directed in a clearer and explicit inclusion of exoskeletons technologies, or they could be addressed in more detail as examples in its annexes.

2.4 ASTM

The American Society for Testing and Materials (ASTM), is an international standards organization that develops and publishes technical standards for a wide range of applications. ASTM International Committee F48 on Exoskeletons and Exosuits was first proposed in September 2017, to develop new standards and protocols directly applicable to exoskeletons in industrial use and especially in the lift supporting exoskeletons [18]. Conscious of the growing market, ASTM started a first attempt to fill the gap in standardization and information in exoskeleton applications. From August 2018 new subcommittees (Sc) were proposed, charged to produce new standards for safety, quality, and efficiency in different frameworks. F48 is then going in the needed direction to produce a harmonized literature in the field. The main topic ASTM subcommittees are currently covering regard labelling and information (Sc F48.01), practice for training (Sc F48.02), documenting environmental conditions (Sc F48.03), practice for wearing and maintenance (F48.014), and terminology (F48.91). Future efforts should be directed in experimental protocols to assess performance and safety requirements. However, ASTM also explicitly stays out of the medical and service robot domains, to not interfere with safety-related topics already covered by ISO and IEC.

3 Conclusion

Standards and guidelines should support and clarify how to implement and demonstrate safety. Exoskeletons are approaching a growing range of environments and applications, which pose several questions on their correct design and use according to current legislation and standards. Clear and validated testing procedures for safety and performance are still largely missing. One important challenge would be to adapt regulations and standards such that exoskeletons are addressed explicitly and unambiguously, distinguishing exoskeletons from traditional protective personal equipment and establishing supporting test methods that could guide manufacturers to comply with the requirements of the related legislation and standards.

Acknowledgments This research was supported by the 'Realistic Trial Award' EXOSAFE, funded by the European Union's Horizon 2020 research and innovation programme under grant agreement No 779966 (COVR Project).

References

1. M. Peters, S. Wischniewski, D*iscussion Paper—Impact of Using Exoskeletons on OSH* (2019), p. 10

2. J. Vaibhav, Z. Wenlong, Design of a knee exoskeleton for gait assistance. J. Chem. Inf. Model. **53**(9), 1689–1699 (2013). https://doi.org/10.1017/CBO9781107415324.004
3. N.N. Rukina, A.N. Kuznetsov, V.V. Borzikov, O.V. Komkova, A.N. Belova, Principles of efficiency and safety assessment in using exoskeletons for patients with lower limb paralyses. Sovrem. Tehnol. v Med. **8**(4), 231–240 (2016). https://doi.org/10.17691/stm2016.8.4.28
4. European Parliament and European Council, Directive 2014/30/EU Electromagnetic compatibility. Off. J. Eur. Union **29**(3) 79–106 (2014)
5. Low Voltage Directive 2014, pp. 357–374 (2014)
6. Machinery directive 2006. Manuf. Eng. **68**(8), 46–48 (1989) https://doi.org/10.1049/me:19890129
7. A.B. Weisse, Medical device regulation 2017. Hosp. Pract. (Off. Ed). **27**(4), 97–100, 103, 113 (1992). https://doi.org/10.1080/21548331.1992.11705401
8. P. Wenger, C. Chevallereau, D. Pisla, H. Bleuler, A. Rodić (eds.), *New Trends in Medical and Service Robots Human Centered Analysis, Control and Design Mechanisms and Machine Science MMS 39* (Springer, Cham, 2016) https://doi.org/10.1007/978-3-319-30674-2
9. Y. He, D. Eguren, T.P. Luu, J.L. Contreras-Vidal, Risk management and regulations for lower limb medical exoskeletons: a review. Med. Devices Evid. Res. **10**, 89–107 (2017). https://doi.org/10.2147/mder.s107134
10. A.C.M. Damian Farrow, J. Baker, Federal register **80**(36), *Nhk技研*, **151**(36), 10–17 (2015), https://doi.org/10.1145/3132847.3132886
11. B.S. Rupal, S. Rafique, A. Singla, E. Singla, M. Isaksson, G.S. Virk, Lower-limb exoskeletons: research trends and regulatory guidelines in medical and non-medical applications. Int. J. Adv. Robot. Syst. **14**(6), 1–27 (2017). https://doi.org/10.1177/1729881417743554
12. ISO 13482:2014 Robots and robotic devices—Safety requirements for personal care robots
13. ISO TR 23482–1:2020 Safety-related test methods for ISO 13482
14. ISO TR 23482–2:2019 Application guide to ISO 13482
15. IEC 80601-2-78:2019 Particular requirements for basic safety and essential performance of medical robots for rehabilitation, assessment, compensation, or alleviation (2008)
16. ISO 14971:2019 Medical devices—Application of risk management to medical devices
17. ISO 24971:2020 Medical devices—Guidance on the application of ISO 14971
18. B.D. Lowe, W.G. Billotte, D.R. Peterson, ASTM F48 Formation and standards for industrial exoskeletons and exosuits. IISE Trans. Occup. Ergon. Hum. Factors **7**(3–4), 230–236 (2019). https://doi.org/10.1080/24725838.2019.1579769

The Testing of Industrial Exoskeletons

Evaluation of Two Upper-Limb Exoskeletons for Ceiling Welding in the Naval Industry

Francisco Mouzo, Florian Michaud, Urbano Lugris, Jawad Masood, and Javier Cuadrado

Abstract Shipbuilding entails demanding operator tasks in several scenarios, like workshops, blocks or even ships under construction. This work focuses on ceiling welding, a usual task in the two latter scenarios, for which two commercial upper-limb exoskeletons were evaluated. Tests were conducted with two expert operators wearing the exoskeletons in a motion analysis lab equipped with an optical motion capture system, force plates and electromyographic sensors. Heart rate was also measured, videos were recorded and a questionnaire was filled by each operator. Muscular activity, kinematics, driving torques, metabolic cost, donning/doffing and execution times, were compared for both operators without and with the two exoskeletons in three assistance levels. It is concluded that improvement is achieved with both exos in most indicators although the total time to perform the task is not always reduced.

1 Introduction

Naval construction entails an intensive use of workforce characterized by high physical demand and wear along the workday. An investigation was carried out at Navantia shipyard in Ferrol, Spain, to identify tasks whose labor conditions could be improved

F. Mouzo · F. Michaud · U. Lugris · J. Cuadrado (✉)
Laboratory of Mechanical Engineering, University of La Coruña, Ferrol, Spain
e-mail: javier.cuadrado@udc.es

F. Mouzo
e-mail: francisco.mouzo@udc.es

F. Michaud
e-mail: florian.michaud@udc.es

U. Lugris
e-mail: urbano.lugris@udc.es

J. Masood
FoF Department, CTAG—Centro Tecnologico de Automocion de Galicia, Porriño, Spain
e-mail: jawad.masood@ctag.com

J. C. Moreno et al. (eds.), *Wearable Robotics: Challenges and Trends*,
Biosystems & Biorobotics 27, https://doi.org/10.1007/978-3-030-69547-7_25

by assistive devices in general and, more specifically, by exoskeletons, which are proposed nowadays to relieve pain and fatigue to workers in factories [1]. For each identified task, the objective was to find out which assistive device could fit better and to quantify the achievable improvement.

Several tasks were identified, among which ceiling welding, both in workshop or on board, was found to be the best candidate to begin with, as it implies long periods of time with arms in stretched-up position and can be assisted by commercial upper-limb exoskeletons.

2 Material and Methods

2.1 Instrumentation

Tests were carried out at the Laboratory of Mechanical Engineering of University of La Coruña in Ferrol, which features a motion analysis lab equipped with an optical motion capture system integrated by 12 infrared cameras to record the position of reflective markers, two force plates to measure foot-ground contact forces, a 16-channel EMG system to record muscular activity, and a software to generate a subject's model that, from the captured motion and the measured ground reactions, calculates the driving torques occurred during the motion [2] and can even estimate the exerted muscular forces [3].

2.2 Assistive Devices

The following two upper-limb exos were considered for the study: (i) ShoulderX, from suitX; (ii) Skelex, from the company of the same name. They were included in the subject's model alluded above by adding their inertias and applying the forces they generate to the corresponding human segments, in a similar way as that shown in [4].

2.3 Task Definition

Figure 1 shows the scenario prepared for the tests in the motion analysis lab. The task to be done was to follow, with a MIG welding gun (heavier than those used for other techniques), a 1-m horizontal line situated over the head of the worker. To provide a reference for the subjects, the line was materialized by means of an aluminium profile.

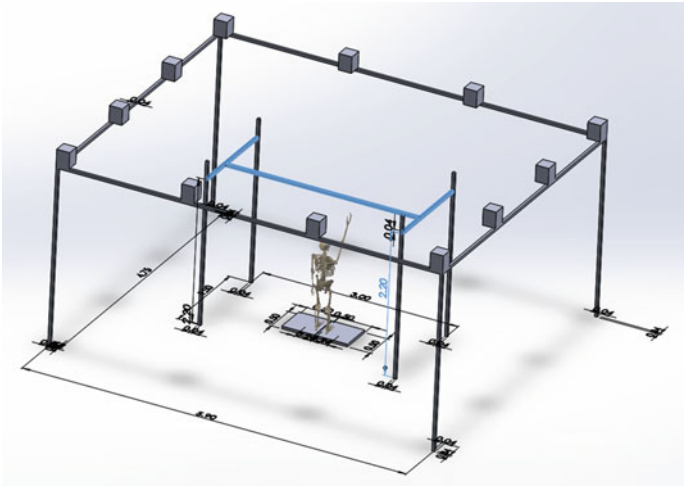

Fig. 1 Scenario prepared for the tests and task definition. The twelve infrared cameras are all around the motion analysis lab. The two force plates are in the ground, in parallel configuration. In blue, the aluminium profile that served as reference for the task

2.4 Subjects, Tests and Measurements

Two experienced welders from the shipyard took part in the tests. They are shown in Fig. 2. Each subject performed tests without assistance, wearing the ShoulderX device, and wearing the Skelex device. Moreover, when using the exos, they carried out tests in the low, medium and high assistance modes (the high mode was discarded for ShoulderX).

The measurements made for each test were: (i) optical motion capture with markers and foot-ground reactions in plates (MOCAP); (ii) EMG signals in eight muscles: biceps brachii long head, triceps brachii long head, anterior deltoid, medial deltoid, posterior deltoid, pectoralis major, infraspinatus and latissimus dorsi; (iii) heart rate; (iv) video recording. Furthermore, a questionnaire was completed by each subject after the tests.

3 Results

The MOCAP provided relevant kinematic information, as thorax, arms, neck and head rotations, and also dynamic information, as driving torques at shoulders and the lumbar region. Figure 3 shows the posture of the first subject when performing the task without assistance and when wearing the Skelex device in the low-assistance mode. Figure 4 presents the comparison, again for the first subject, between the

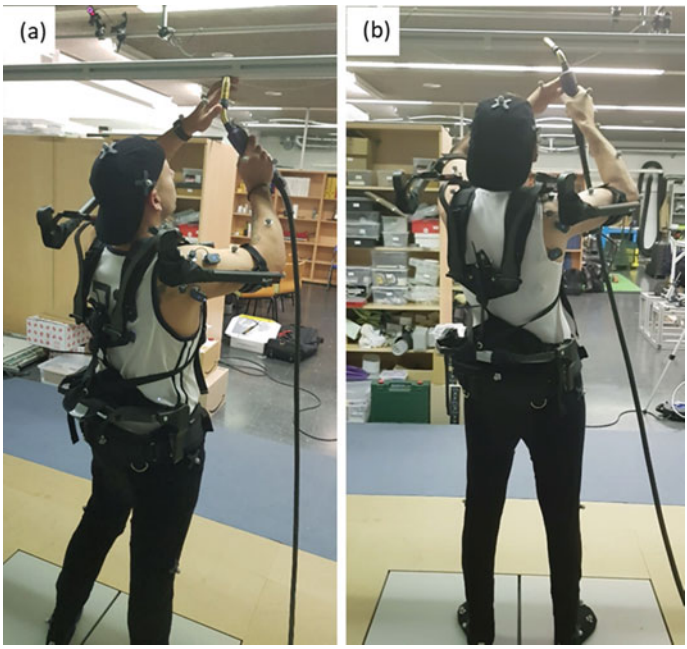

Fig. 2 The two experienced welders from the shipyard during the tests

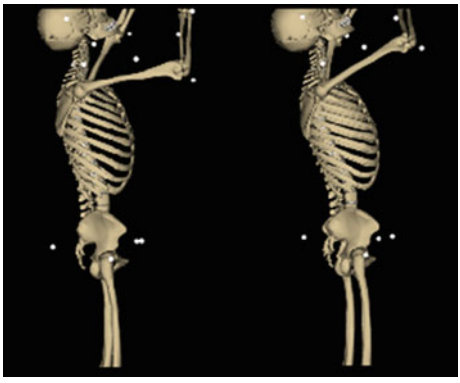

Fig. 3 Posture of the first subject during the task with no assistance (left) and wearing the Skelex device in low-assistance mode (right)

required average torque at the right shoulder in the non-assisted case and when using the exos in the various assistance modes.

Table 1 gathers the percent reduction in muscular activity of the first subject achieved with each exo in the various assistance modes with respect to the non-assisted case.

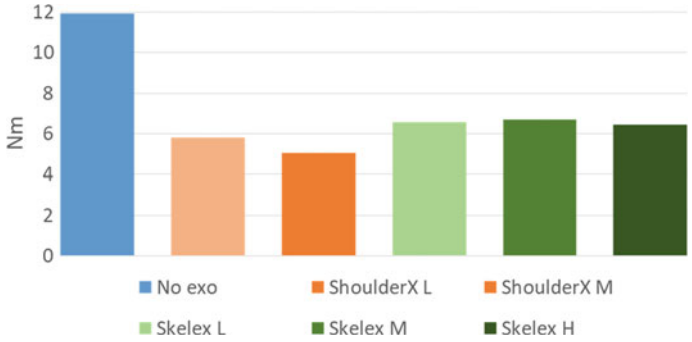

Fig. 4 Average torque at the right shoulder for the first subject in several operating conditions. Assistance modes are labeled as L (low), M (medium) and H (high)

Table 1 Reduction in muscular activity (%)

Test	Muscle							
	I	II	III	IV	V	VI	VII	VIII
ShoulderX L	40	44	10	36	15	70	11	33
ShoulderX M	49	55	24	53	16	83	7	47
Skelex L	20	−28	−6	44	21	28	4	−26
Skelex M	36	7	14	74	25	31	11	−16
Skelex H	36	13	32	30	10	12	9	−11

4 Discussion

From the MOCAP, it was found that lumbar postures improved with the exos, thus reducing the risk of injuries. Besides, driving torques were notably reduced in shoulders. Results from EMG showed a reduced activity for most muscles when using the exos, although the amount of reduction was observed to depend on the subject, the exo and the assistance mode. The heart rate was also reduced when wearing the exos, thus indicating a lower metabolic cost. The time to complete the task was reduced in most cases, but not in all of them. Use of Skelex required less training than use of ShoulderX. The preferred level of assistance depended on the subject.

Acknowledgements This work was funded and by the Galician Government under grants IN853B-2018/02 and ED431C-2019/29, and by the Spanish MICIU under project PGC2018–095145-B-100, cofinanced by the EU through the EFRD program.

References

1. K. Huysamen, T. Bosch, M. de Looze, K.S. Stadler, E. Graf, L.W. O'Sullivan, Evaluation of a passive exoskeleton for static upper limb activities. Appl. Ergon. **70**, 148–155 (2018)
2. U. Lugris, J. Carlin, A. Luaces, J. Cuadrado, Gait analysis system for spinal cord-injured subjects assisted by active orthoses and crutches. J. Multi-body Dyn. **227**(4), 363–374 (2013)
3. F. Michaud, F. Mouzo, U. Lugris, J. Cuadrado, Energy expenditure estimation during crutch-orthosis-assisted gait of a spinal-cord-injured subject. Frontiers Neurorobot. **13**(55), 11 (2019)
4. F. Mouzo, U. Lugris, R. Pamies-Vila, J. Cuadrado, Skeletal-level control-based forward dynamic analysis of acquired healthy and assisted gait motion. Multibody Sys.Dyn. **44**(1), 1–29 (2018). https://doi.org/10.1007/s11044-018-09634-4

Preliminary Study of an Exoskeleton Index for Ergonomic Assessment in the Workplace

Giorgia Chini, Christian Di Natali, Stefano Toxiri, Francesco Draicchio, Luigi Monica, Darwin G. Caldwell, and Jesús Ortiz

Abstract Work-related low-back disorders represent the most common and costly musculoskeletal problems, so, recently, industrial exoskeletons have been developed to prevent injury by reducing the load on the back. Their effects are described by a growing body of literature, but is not captured by any standard risk index used in ergonomic practice. This study aims to suggest a method to quantify how the effect of a back-support exoskeleton might be accounted in the NIOSH Lifting Index. Twelve subjects participated in the study and we recorded the surface electromyographic signals of the erector spinae longissimus. Subjects held four different loads in a static position for 10 s without the exoskeleton and wearing it. A substantial reduction in the median of the muscle activity when wearing the exoskeleton was observed. We suggest that this reduction could be reflected in a multiplicative factor that directly affects the NIOSH Lifting Index.

1 Introduction

Work-related low-back disorders (WLBDs) represent the most common and costly musculoskeletal problem [1, 2]. Reports in recent studies indicate that WLBDs account for between 26 and 50% of the total number of reported cases of occupational musculoskeletal disorders [3]. Prevalence of work-related musculoskeletal disorders (WMSDs) is associated with manual material handling (MMH), [2]. Hence, recently, industrial exoskeletons have been developed to prevent injury by reducing

G. Chini (✉) · C. Di Natali · S. Toxiri · D. G. Caldwell · J. Ortiz
Department of Advanced Robotics, Istituto Italiano Di Tecnologia, Genoa, Italy
e-mail: giorgia.chini@iit.it

F. Draicchio
Department of Occupational and Environmental Medicine, Epidemiology and Hygiene, INAIL, Monte Porzio Catone, Rome, Italy
e-mail: f.draicchio@inail.it

L. Monica
Department of Technological Innovation and Safety Equipment, INAIL, Rome, Italy
e-mail: l.monica@inail.it

J. C. Moreno et al. (eds.), *Wearable Robotics: Challenges and Trends*,
Biosystems & Biorobotics 27, https://doi.org/10.1007/978-3-030-69547-7_26

the load on the back by taking over part of the torques normally generated by back muscles to counteract moments due to gravity and inertia [4, 5]. All the methods commonly used to quantify the ergonomic risk in MMH activities from the biomechanical point of view (e.g. NIOSH Lifting Index, [2]) take into account different aspects of the task (e.g. posture, frequency, load), but none still consider the effect of the exoskeleton assistance.

This study tries to fill this gap: we identify a quantitative link between the load lifted without exoskeleton and that with the exoskeleton assistance and suggest a method to quantify how the effect of a back-support exoskeleton might affect a relevant index (i.e. NIOSH Lifting Index) for one of the manual material handling concerned configurations.

2 Materials and Methods

2.1 Experimental Design

Twelve subjects, six men (mean age 32.2 ± 3.7 years) and six women (mean age 42.0 ± 3.6 years), were recruited in the study. Subjects were asked to hold four different loads: no load (0); low (L), 4 kg for women and 5 kg for men; medium (M), 8 kg for women, and 10 kg for the men; and high (H), 12 kg for the women and 15 kg for the men. Each subject kept the different loads in a static position for 10 s once standing in a neutral position and once with in a forward bending position, with an angle between the back and the coronal plane of about 30°. In both postures, the subjects held the loads with the elbows flexed at 90°, (Fig. 1).

Each subject performed all these tasks twice without the exoskeleton and twice wearing it, conditions respectively denoted as noExo and ExoON. The exoskeleton used in this study was the XoTrunk, a revised version of the device presented in [6]. It was controlled to generate a constant torque (24 Nm for women and 30Nm for men) during the 10 s trials. We recorded the surface electromyographic signals (EMG) of the erector spinae longissimus (ESL) because of their role as trunk extensors.

2.2 Data Analysis

The raw EMG signals were processed as in [7]. To characterize differences in the amplitude of the EMG activity among the exoskeleton conditions (noExo vs ExoON) and the trunk bending conditions (0° vs. 30°) we computed the median of the EMG activity.

Fig. 1 Panel A: an example of the experiment with a subject holding the load with a trunk bending of about 30° in the no Exo condition. Panel B: the exoskeleton used for the experiments

3 Results

We found a substantial reduction in the median of the EMG activity between noExo and ExoOn conditions for all the weights hold both in the neutral position and with a trunk bending of 30° for the ESL (Fig. 2). Table 1 reports the values of the median of the EMG activity in the noExo condition for all the loads both at 0° and at 30° and the relative reduction in the median of the EMG activity in the ExoOn condition with respect to noExo condition. The average reduction among all the loads at 0° is approximately 50.1% and at 30° is about 36.8%.

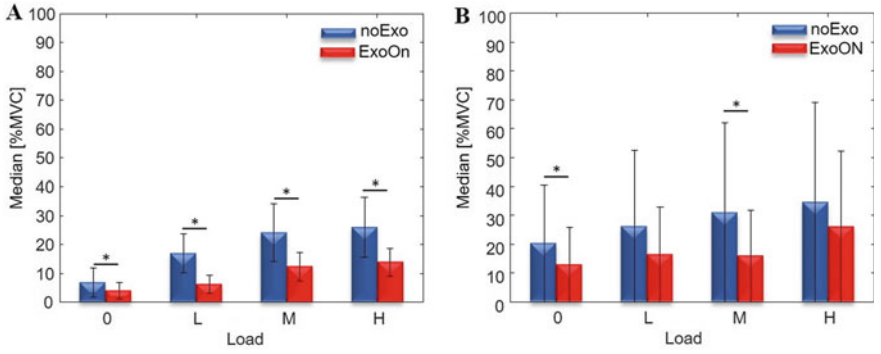

Fig. 2 A and B panels report the results for the ESL with the trunk in upright position and with a trunk bending of 30° respectively. The blue and red bars represents the mean among all the subjects of the median of the EMG activity with and without the exoskeleton

Table 1 Median of the ESL at each load without the exoskeleton and corresponding percentage reductions with the exoskeleton

	noExo		ExoON	
	0°	30°	0°	30°
Load	[MVC%]	[MVC%]	Red. %	Red. %
0	6.9	20.3	−41.7	−36.5
L	16.9	26.2	−63.3	−37.5
M	24.1	30.9	−48.8	−48.5
H	25.9	34.6	−46.5	−24.8

4 Discussion

The results of our study reveal, in accordance with what literature reports, that the use of a back-support exoskeleton reduces trunk muscles effort during lifting task from about 20–60% (with an average of 33%) [6].

Interestingly, our results indicate a corresponding similar increase in overall muscular activity, in fact, as can be seen in Table 1, the average median computed across all loads is about 18.5% at 0° and about 28.0% at 30° (average increase from 0° to 30° of 51.7%).

The same consideration might be extended to the effect of the exoskeleton in a given condition. As observed in our data, the device causes a reduction in the muscle effort (Fig. 2) by about 50.1% at 0° and by 36.8% at 30° (average of 43%) (Table 1).

Correspondingly, an equal reduction in the NIOSH Lifting Index, LI, [2], may be proposed, associated with reduced ergonomic risk in the two conditions. At 0°, all the multipliers needed to compute the NIOSH Recommended Weight Limit (RWL) are equal to one except for the Vertical Multiplier, which is $VM = 1 - 0.003|V - 75| \cong 0.93$ (vertical height of the hands above the floor is $V = 100 \pm 5$ cm), therefore the RWL is 0.93*LC (Load Constant). At 30°, VM increases to 0.96 ($V = 90 \pm 5$ cm), the Horizontal Multiplier is $HM = 25/H \cong 0.63$ (the horizontal distance of the load from the body is $H = 40 \pm 5$ cm), therefore the RWL becomes approximately equal to 0.96*0.63*LC = 0.60*LC. The LI is computed using the reciprocal of the RWL, so that the greater the RWL, the lower the LI, and the lower the ergonomic risk.

Moving from 0° to 30° the LI increases by about 54% (due to a decrease in RWL from 0.93 to 0.60, as detailed above).

This study considers static tasks and EMG activity, our next steps are; (i) to investigate in which conditions this approach can be extended to dynamic tasks; (ii) overcome the limits of the emg-based analysis (e.g. nonlinear relationship between stimulation frequency and muscle force, crosstalk) by considering mechanic properties of the exoskeleton (e.g. force, torque).

Additionally, the simplified control strategy adopted may have limited the exoskeleton's effectiveness, which could be improved with more sophisticated approaches.

5 Conclusion

The exoskeleton reduces muscle activity at the lower back while holding external objects. This reduction may be interpreted as if the subject is holding a lower load than the actual one. The exoskeleton could be accounted for by a factor that increases the NIOSH RWL and correspondingly decreases the Lifting Index.

Future works will focus on proposing a new multiplicative factor to add to the NIOSH Lifting Index to account for the assistance of the exoskeleton and expressing it in terms of equivalent weight.

Acknowlegments This work was supported by the Italian Workers' Compensation Authority (INAIL).

References

1. M.L. Lu, T.R. Waters, E. Krieg, D. Werren, Efficacy of the revised NIOSH lifting equation to predict risk of low-back pain associated with manual lifting: a one-year prospective study. Hum. Factors **56**(1), 73–85 (2014)
2. NIOSH, Work practices guide for manual lifting. NIOSH technical Report No. 81–122 (U.S. Dept. of Health and Human Services, National Institute for Occupational Safety and Health, Cincinnati, OH, 1981)
3. INAIL,*Italian Worker's Compensation Authority Annual Report. Part IV Statistics, Accidents and Occupational Diseases* (2011)
4. S. Toxiri, M.B. Näf, M. Lazzaroni, J. Fernández, M. Sposito, T. Poliero, L. Monica, S. Anastasi, D.G. Caldwell, J. Ortiz, Back-support exoskeletons for occupational use: an overview of technological advances and trends. IISE Trans. Occ. Erg. H. Fact. 1–13 (2019)
5. M.P. de Looze, T. Bosch, F. Krause, K.S. Stadler, L.W. O'Sullivan, Exoskeletons for industrial application and their potential effects on physical work load. Ergonomics **59**(5), 671–681 (2016)
6. S. Toxiri, A.S. Koopman, M. Lazzaroni, J. Ortiz, V. Power, M. P. de Looze et al., Rationale, implementation and evaluation of assistive strategies for an active back-support exoskeleton. Front. Robot. AI (2018)
7. A. Ranavolo, T. Varrecchia, S. Iavicoli, A. Marchesi, M. Rinaldi, M. Serrao et al., "Surface electromyography for risk assessment in work activities designed using the 'revised NIOSH lifting equation. Int. J. Ind. Ergonom. **68**, 34–45 (2018)

Effect of a New Passive Shoulder Exoskeleton on the Full Body Musculoskeletal Load During Overhead Work

A. van der Have, S. Van Rossom, M. Rossini, and I. Jonkers

Abstract Objective to investigate the effect of a passive shoulder exoskeleton on full body musculoskeletal loading during a wiring and lifting task above shoulder height. Methods: Three participants performed a wiring and lifting task with 10 kg above shoulder height with and without âssive shoulder exoskeleton. OpenSim was used to calculate kinematics, kinetics, muscle forces and joint contact forces at the shoulder and L5. Results: Kinematics did not change during the lifting task but kinematics did change for two out of the three participants during the wiring task while wearing the exoskeleton. Moreover, joint moments and muscle forces in the shoulder were decreased. In addition, compression forces at L5 were decreased but shear forces were increased while wearing the exoskeleton during both tasks. Conclusion: Considering that this is preliminary data, this exoskeleton could decrease the risk of developing work-related shoulder disorders in specific tasks.

1 Introduction

Repetitive movements are commonly reported by the European working population (61%) [1]. As a result, 30–56% of this population indicates to have suffered from an upper limb disorder in the past 12 months [1]. Ergonomic interventions do not significantly reduce the risk of developing upper limb disorders and the need for flexibility of the worker is high. As a result, the industry has high interest in exoskeletons in order to decrease the risk of developing work-related musculoskeletal disorders (WMSDs) [2]. Currently, main focus is on passive exoskeletons as they are cheaper and lighter to work with [2] and have been proven to be effective in decreasing muscle activations and compression forces of the lower back [3] and shoulder [4]. However, while wearing an exoskeleton, musculoskeletal load could shift from the assisted

A. van der Have (✉) · S. Van Rossom · I. Jonkers
Human Movement Biomechanics Research group of the KULeuven, Leuven, Belgium
e-mail: tuur.vanderhave@kuleuven.be

M. Rossini
Department of Mechanical Engineering, VUB, Brussels, Belgium

J. C. Moreno et al. (eds.), *Wearable Robotics: Challenges and Trends*,
Biosystems & Biorobotics 27, https://doi.org/10.1007/978-3-030-69547-7_27

joint to the non-assisted joints and lead to new and other WMSDs [2]. This shift in musculoskeletal load is not commonly analyzed by the lack of full-body analysis [2–4]. Therefore, this study analyzed the effects of a passive shoulder exoskeleton equipped with elastic elements to store and release energy when needed, developed within the Exo4Work project, on the full body musculoskeletal load using a detailed full-body musculoskeletal model in OpenSim [5].

2 Material and Methods

Three healthy participants (EXO01, EXO02, and EXO03) pulled laces through holes at 50 cm above shoulder height (overhead wiring task) and a lifting task during which the participant had to lift a 10 kg box from shoulder height to 50 cm above shoulder height. Both tasks were performed with and without a passive shoulder exoskeleton, developed for the Exo4Work project (FWO–grant nº S000118N) (exo and non-exo condition respectively) which cannot be described due to patents pending. Marker trajectories and ground reaction forces were measured synchronously in order to calculate full-body kinematics, kinetics, muscle forces and joint contact forces using the OpenSim workflow [5]. The full-body OpenSim model used, combined a lower limb model, an articulated spine model and a detailed shoulder model [6, 7]. In addition, the mass of the exoskeleton (3.8 kg) was taken into account by adding an extra body of 3.8 kg to the model at the location of the exoskeletons center of mass. The assistance given by the exoskeleton was applied in the model as a torque assistance, calculated at each time frame based on the measured elastic elements deformation and its stiffness. This assistance was applied to the humerus and the torso. In order to evaluate the exoskeleton's effect per participant on the muscle forces and joint contact forces, the mean of the integrated muscle forces and joint contact forces was calculated per participant and per condition. The kinematics and kinetics are visualized in Figs. 1a, b and 2a, b. The difference in muscle and contact forces at L5 between the two conditions is visualized in Figs. 1a, b, c, and d and 2a, b, c, and d, with positive values indicating a reduction in muscle or joint contact forces while wearing the exoskeleton. No statistical analyses were performed due to the limited number of participants but results were analyzed per participant.

3 Results

During the lifting task, kinematic differences between the exoskeleton (solid lines) and without exoskeleton condition (dashed lines) are rather small. But, shoulder flexion moments were reduced during the lifting phase while wearing the exoskeleton. This resulted in lower muscle efforts in the shoulder and compression forces on L5 during the exoskeleton condition as shown by the positive values in Fig. 1c, d. However, shear forces on L5 were increased while wearing the exoskeleton.

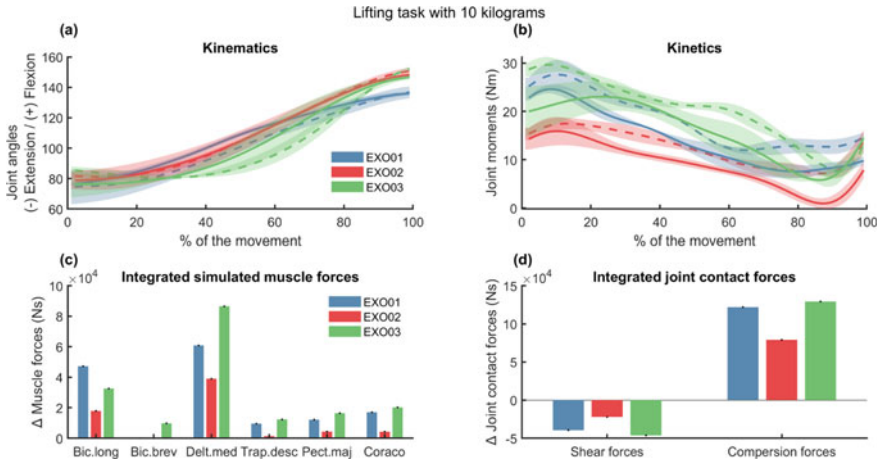

Fig. 1 **a** Shoulder flexion and extension angle, b Shoulder moments, c Difference in muscle forces during non-exo condition and exo condition of the m. bicpes longus, biceps brevis deltoideus medius, trapezius descendens, pectoralis major, coracobrachialis **d** shear and compression forces at L5 during the lifting task with 10kg. The blue, red and green colors are indicating the different particpants (in all 4 subplots) as the solid line (−) is indicating the exoskeleton condition as the dashed line (—) is indicating the non-exo condition

The magnitude of the exoskeleton effects was variable between participants but a decrease in musculoskeletal load was observed for all participants.

During the wiring task, a decreased flexion angle is observed for the participants EXO02 (red) and EXO03 (green) as seen in Fig. 2a. Shoulder flexion moments were decreased for all participants. This resulted in decreased muscle forces and compression forces as described for the lifting task. Again, muscle forces in the shoulder and compression forces on L5 were decreased but shear forces on L5 were increased while wearing the exoskeleton. In contrast to the lifting task, the first participant (EXO01, blue) experienced the highest positive effects while wearing the exoskeleton as during the lifting task the third participant (EXO03, green) experienced the largest effects.

4 Discussion

The developed passive shoulder exoskeleton is decreasing joint moments and muscle forces thereby decreasing musculoskeletal loading in the shoulder during the wiring and in the lifting task. In addition, compression forces at L5 were lowered but shear forces were increased during both tasks. As the exoskeleton is not limiting the kinematics of the shoulder and decreasing the musculoskeletal load, the exoskeleton can be considered a good ergonomic intervention in order to decrease the risk on developing WMSDs for the shoulder joint. Moreover, musculoskeletal load did not shift from the shoulder to the lower back as compression forces at L5 were not increased.

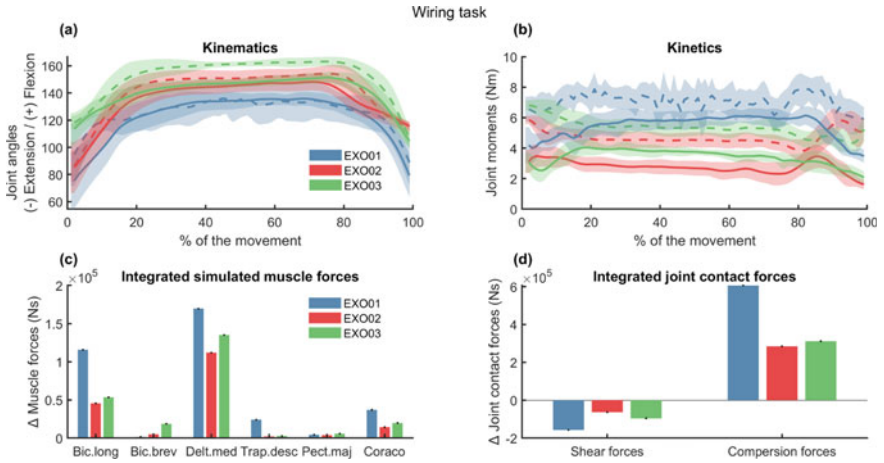

Fig. 2 **a** Shoulder flexion and extension angle, **b** Shoulder moments, **c** Difference in muscle forces during non-exo condition and exo condition of the m. bicpes longus, biceps brevis deltoideus medius, trapezius descendens, pectoralis major, coracobrachialis **d** shear and compression forces at L5 during the lifting task with 10kg. The blue, red and green colors are indicating the different particpants (in all 4 subplots) as the solid line (−) is indicating the exoskeleton condition as the dashed line (—) is indicating the non-exo condition

This could be due to the fact that the mass of the exoskeleton is located at the back, posterior of the L5 vertebrae. However, shear forces did increase while wearing the exoskeleton which is considered a negative effect but this negative effect is rather small. Further full body analyses will show the effects on the full body musculoskeletal load while wearing the exoskeleton. However, multiple joint analyses are performed for this study but are not presented in this abstract.

Moreover, all participants experienced a reduction in shoulder moments and muscle forces but the magnitude of the effects were variable between participants and even between the different tasks. This variability could be due to the time of adaption to the exoskeleton but no evidence could support this statement.

5 Conclusion

Considering that this is preliminary data, the developed passive shoulder exoskeleton is decreasing musculoskeletal load in the shoulder and did not transfer this musculoskeletal load to the lower back during a lifting and wiring task. The presented methods could be used to investigate the effects of any exoskeleton on full body musculoskeletal load.

Acknowledgments This research was funded by Exo4Work, SBO-E-S000118N.

References

1. EU-OSHA European Agency for Safety and Health at Work, in *Sixth European Working Conditions Survey—Overview Report* (2017 update), p. 164, https://doi.org/10.2806/422172.
2. M.P. de Looze, T. Bosch, F. Krause, K.S. Stadler, L.W. O'Sullivan, Exoskeletons for industrial application and their potential effects on physical work load. Ergonomics **59**(5), 671–681 (2016). https://doi.org/10.1080/00140139.2015.1081988
3. A.S. Koopman, I. Kingma, G.S. Faber, M.P. de Looze, J.H. van Dieën, Effects of a passive exoskeleton on the mechanical loading of the low back in static holding tasks. J. Biomech. (2018). https://doi.org/10.1016/j.jbiomech.2018.11.033
4. I. Pacifico et al., Experimental evaluation of the proto-MATE, a novel ergonomic upper-limb exoskeleton for reducing the worker' s physical strain (2019)
5. S.L. Delp et al., OpenSim: Open source to create and analyze dynamic simulations of movement. IEEE Trans. Biomed. Eng. **54**(11), 1940–1950 (2007). https://doi.org/10.1109/TBME.2007.901024
6. M. Christophy, N.A.F. Senan, J.C. Lotz, O.M. O'Reilly, A Musculoskeletal model for the lumbar spine. Biomech. Model. Mechanobiol. **11**(1–2), 19–34 (2012). https://doi.org/10.1007/s10237-011-0290-6
7. K.R.S. Holzbaur, W.M. Murray, S.L. Delp, A model of the upper extremity for simulating musculoskeletal surgery and analyzing neuromuscular control. Ann. Biomed. Eng. **33**(6), 829–840 (2005). https://doi.org/10.1007/s10439-005-3320-7

The Experience of Plasterers Towards Using an Arm Support Exoskeleton

Aijse W. de Vries, Michiel P. de Looze, and Frank Krause

Abstract Positive effects of arm support exoskeletons in reducing the shoulder load, have been reported mainly from laboratory studies. However, for exoskeletons to provide worker support in practice, they need to be accepted as well. Therefore, it is necessary to obtain insight into the user experience and attitude towards exoskeleton use, in relevant working fields. Eleven plasterers were recruited to perform their activities while wearing an arm support exoskeleton. Before the experiment, participants were asked for which activities they could use support, and which body regions they wished to be supported. After working with the exoskeleton, they reported their experience and will to use the exoskeleton during daily work. Overall, the user experience of the plasterers was positive, and all reported they would probably, or even definitely, use the exoskeleton for a selection of activities, mainly overhead work, but not during the whole day. Together with earlier findings on reduced muscle activity, exoskeleton use in certain tasks seems promising.

1 Introduction

Heavy manual labor is still prevalent in many working fields. Especially work involving exposure to tiring or painful positions, carrying or moving heavy loads, or repetitive movements can result in musculoskeletal diseases and sick leave [1]. One of the sectors in which workers are exposed to these conditions, is the construction area. 37% of the workers in this sector report that their work affects their health negatively [1]. Working with elevated arms, is one of the most important risk factors for the development of musculo-skeletal shoulder disorders [2, 3].

Arm support exoskeletons are a relatively new technology, that can support work with elevated arms, by providing part of the required shoulder moment. In passive exoskeletons this supportive moment is generated through spring like mechanisms,

A. W. de Vries (✉) · M. P. de Looze · F. Krause
Department of Sustainable Productivity and Employability of Healthy Living, TNO, Leiden, The Netherlands
e-mail: Aijse.devries@tno.nl

J. C. Moreno et al. (eds.), *Wearable Robotics: Challenges and Trends*,
Biosystems & Biorobotics 27, https://doi.org/10.1007/978-3-030-69547-7_28

that are particularly effective in static postures and movements in one direction, but might oppose movements in other directions.

Lab studies on the effectivity of arm support exoskeletons, mainly in static conditions, have shown a reduction of muscle activity in agonist muscles as well as reductions on subjective measures [4, 5]. However, these results were also dependent on the specific tasks tested. Moreover, in manual labour, activities are often more dynamic, requiring movements against the force provided by the springs.

One of the jobs in the construction sector involving highly dynamic work with elevated arms is plastering. A study was performed to test the effectivity of an arm support exoskeleton during plastering activities. Instead of looking at isolated movements or postures, we studied muscle activity over the total task duration of about two to seven minutes. Muscle activity was mainly reduced, of up to $\pm 33\%$ in agonists muscles during overhead work [6]. However, for exoskeletons to actually have an effect on reducing loads and eventually MSD development, it is important that they are accepted by the users. Therefore, we also studied the following questions: what are the expectations towards using the exoskeleton before the experiment, and what are the user's experiences and will to use the exoskeleton after working with it?

2 Methods

2.1 Subjects

Twelve participants were recruited via internet, social media and word of mouth. They were active plasterers, without musculoskeletal disorders that would prevent them from carrying out their normal plastering activities. One subject dropped out due to logistic reasons.

2.2 Procedures

The following is a short description of the procedures. An extended description has been reported previously [6]. Plasterers were asked to perform their work with and without an exoskeleton (Skelex 360, Rotterdam, The Netherlands). The studied tasks, were applying gypsum (apply), smoothing (smooth) and finishing with a spatula (finish). All tasks were performed on the ceiling (ceil) as well as on the wall.

Before the participants put on the exoskeletons they were asked about their expectations (q1) and desire for support. The latter included questions about body regions (q2) and specific tasks for which support was desired (q3). After the experiment, we asked the participants about their experiences. This involved a question about whether their work was experienced as heavier or lighter when working with the exoskeleton (q4) and whether they would want to use the exoskeleton for the entire

day or only for particular tasks (q5). Followingly, we asked them for which tasks they would use the exoskeleton (q6). The questions q1, q4, q5 were scored on a Likert scale, q2, q3 and q6 were scored binary.

3 Results

Before the experiment, plasterers indicated that support was desired for applying and smoothing the gypsum, especially when working on the ceiling (Fig. 1). The most mentioned body regions for which they desired support were shoulders (10), back (8) and neck (3).

The results for the Likert scale based questions can be seen in Fig. 2. The first question regards the expectations (before the experiment) of working with the exoskeleton. It is clear that there is a strong positive bias in the expected support provided by the exoskeleton.

The second graph shows that the actual work with the exoskeleton was experienced as lighter. This result was especially strong when working on the ceiling, as reflected by the higher percentages of participants that responded "much lighter". When asked whether they would wear the exoskeleton, during their work, all participants responded positively towards using it for particular tasks, but a high percentage responded negatively towards using the device for (almost) a whole work day.

Fig. 3 shows that seven plasterers indicated that they would want to use the exoskeleton for all of the tasks when working on the ceiling. When working on the wall, none of the plasterers wanted to use the exoskeleton for all tasks. However eight would use it during smoothing the gypsum on the wall (Fig. 3).

In answers to our open question about using the exoskeleton, some concerns, such as comfort of arm cuffs and size of the device in confined spaces were raised.

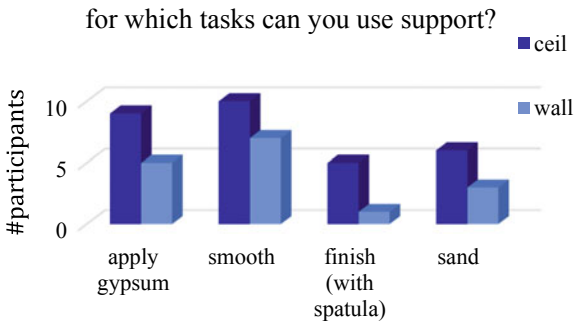

Fig. 1 The number of participants (11 max) which indicated that support was desired, for specific activities. Measured before the experiment

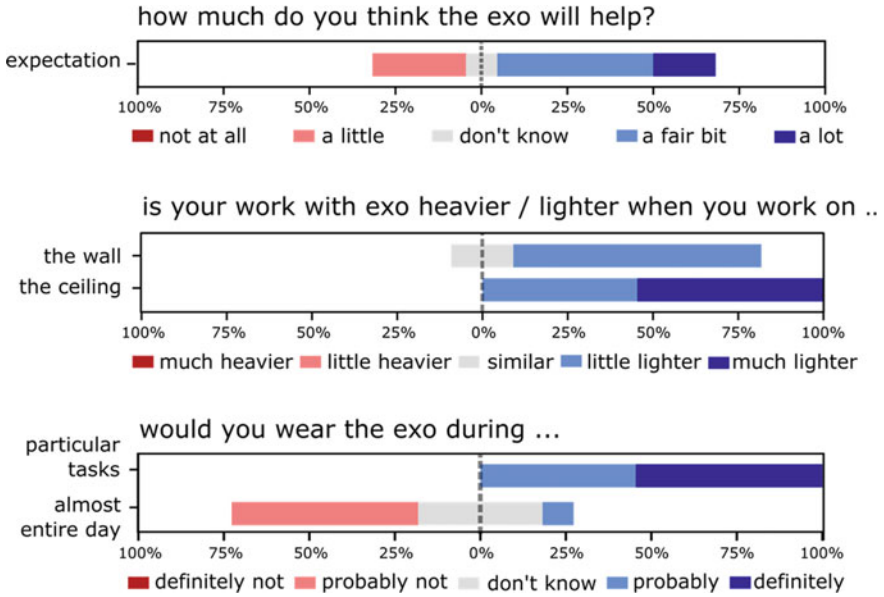

Fig. 2 These stacked bar plots compare the positive versus the negative responses. The neutral answers are balanced around the mid line

Fig. 3 The number of participants (11 max) which indicated that they would use the exoskeleton for these specific, or all activities. Measured after the experiment

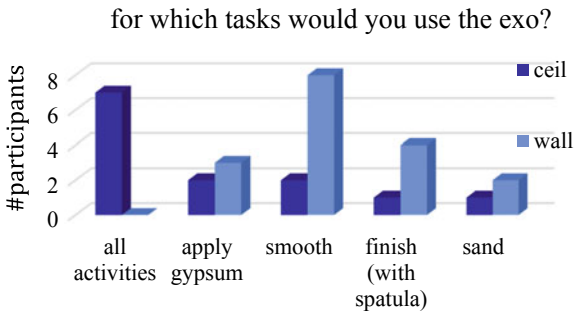

4 Conclusion

The user experience of exoskeletons is an important aspect to consider, since, exoskeletons can only make a real impact if they are worn during a substantial portion of the work. The results in this study emphasize that the user experience and will to use the exoskeleton is task dependent. It was shown that especially work on the ceiling, with arms raised above the head, yielded positive results. Studies, in which a larger group of workers is followed over a longer period of time, are required, to show acceptance, performance and behaviour in day to day work.

Acknowledgements This research was supported by Knauf (supplier of plasterers materials) and Dutch Topsector of Life Sciences and Health (TKI-LSH-VT2017). The exoskeleton was provided by Skelex and the test location by NOA.

We would like to thank KNAUF, Skelex and NOA, respectively for making this research possible, providing the exoskeleton and test location.

References

1. S.E. Eurofound, *Working Conditions Survey—Overview Report (2017 Update)* (Publications Office of the European Union, Luxembourg, 2017).
2. R.M. Van Rijn, B.M. Huisstede, B.W. Koes, A. Burdorf, Associations between work-related factors and specific disorders of the shoulder—A systematic review of the literature. Scand. J. Work. Environ. Heal. **36**(3), 189-201 (2010)
3. S.W. Svendsen, J.P. Bonde, S.E. Mathiassen, K. Stengaard-Pedersen, L.H. Frich, Work related shoulder disorders: quantitative exposure-response relations with reference to arm posture. Occup. Environ. Med. **61**(10), 844-853 (2004)
4. T. McFarland, S. Fischer, *Considerations for Industrial Use: A Systematic Review of the Impact of Active and Passive Upper Limb Exoskeletons on Physical Exposures*, IISE Trans. Occup. Ergon. Hum Factors (2019)
5. A. De Vries, M. De Looze, The effect of arm support exoskeletons in realistic work activities: a review study. J Ergon. **9**(4), 1–9 (2019)
6. A.W. de Vries, F. Krause, M.P. de Looze, The effectivity of a passive arm support exoskeleton in reducing muscle activation and perceived exertion during plastering activities. *Ergonomics* (2021)

Biomechanical Evaluation of the Effect of Three Trunk Support Exoskeletons on Spine Loading During Lifting

Idsart Kingma, Axel S. Koopman, Michiel P. de Looze, and Jaap H. van Dieën

Abstract To evaluate the biomechanical effect of exoskeletons during lifting, three studies were performed to compare spine compression during lifting without and with three exoskeletons (Laevo, Robo-Mate, SPEXOR). In these studies, participants (11, 10 and 10, respectively) lifted boxes (10, 15 and 10 kg, respectively) from ankle height. Spine compression reductions ranged from minor changes in the first exoskeleton to 17% and 14% reductions in the second and third exoskeleton, respectively. Lumbar flexion was increased by the first exoskeleton while it was reduced by the second and unaffected by the third. Effects of exoskeletons on spine compression were affected by support moments, reductions in lifting speed and subtle changes in lifting style. Modifications of design and control could help to improve the timing and magnitude of support of exoskeletons during lifting.

1 Introduction

Worldwide, low back pain (LBP) affects about 37% of the population each year [1] and the recurrence rate is about 33% within a year [2]. Additionally, effect sizes of treatments are moderate at best [2]. Consequently, more focus on prevention seems warranted. Cumulative occupational low back loading has been shown to be a risk factor for LBP [3]. This suggests that reduction of spine loading during activities such as manual lifting could be effective in reducing the risk of LBP. However, only small effects of interventions to reduce low back loading have been found [4], which might be attributable to interactions between lifting style and task conditions [5].

Trunk support exoskeletons might contribute to reduction of spine loading during manual work. While substantial effects of such devices have been reported for static work [6], a thorough evaluation of biomechanical effects during manual lifting was

I. Kingma (✉) · A. S. Koopman · J. H. van Dieën
Department of Human Movement Sciences, Amsterdam Movement Sciences, Vrije Universiteit, Amsterdam, The Netherlands
e-mail: i.kingma@vu.nl

M. P. de Looze
TNO, Leiden, The Netherlands

J. C. Moreno et al. (eds.), *Wearable Robotics: Challenges and Trends*,
Biosystems & Biorobotics 27, https://doi.org/10.1007/978-3-030-69547-7_29

lacking until recently. Therefore, we recently performed a biomechanical analysis of the effects of three trunk support exoskeletons during dynamic lifting [7–9]. In this paper we compare findings between those devices. We hypothesized that each of the devices reduces spine loading during dynamic lifting.

2 Material and Methods

2.1 Participants, Exoskeletons and Procedure

After approval of the local ethics committee, three studies were performed to evaluate the biomechanical effect of three trunk support exoskeletons, that represented a substantial range of support methods and magnitudes. Symmetrical dynamic lifts were performed without and with exoskeleton using a box with handles slightly above the ankle joint. In the first study, 11 male participants used two versions of a light weight passive (commercially available) device, the Laevo [7], while lifting a 10 kg box from a near and a far location. In the second study, 10 male participants lifted a 15 kg box with a prototype actuated exoskeleton (Robo-Mate [10]), using three lifting techniques (stoop, squat, free) [9] and three modes of controlling the EXO (mode 1: support based on trunk inclination; mode 2: support based on forearm EMG; mode 3: 50% of the support based on each of modes 1 and 2). In the third study, 10 male professional luggage handlers lifted a 10 kg box with a newly developed passive exoskeleton (SPEXOR [11]), using the same three lifting techniques [8]. This device is also still a prototype. It contains features such as two joints, misalignment compensation, and stronger support, but it is substantially heavier than the Laevo.

2.2 Measurements and Analyses

During lifting, 3D kinematics of the lower and upper legs, pelvis and trunk were recorded (50 samples/s; Optotrak opto-electronic motion analysis system). Ground reaction forces were recorded (200 samples/s) using a 1.0 by 1.0 m custom-made force plate. Surface EMG was recorded (1000 samples/s) bilaterally on five back and abdominal muscles.

Using inverse dynamics, 3D net moments of subject plus exoskeleton at the lumbo-sacral joint (L5-S1) were calculated [12]. Support moments of the two passive exoskeletons were calculated from measured bending angles, in combination with angle-moment relations measured prior to the lifting experiment. For the actuated exoskeleton, support moments were measured in the motors at the hip joints. Subject-moments were calculated by subtracting exoskeleton support moments from net moments.

Net moments, lumbar flexion and trunk muscle activity normalized to maximum voluntary contraction, were used as input to an EMG-driven trunk muscle model [13] to calculate compression forces at the L5-S1 joint. Exoskeleton support moments during peak loading, subject moments, compression forces and peak lumbar flexion and trunk velocity were tested for effects of exoskeletons using repeated measures ANOVAs for each experiment separately.

3 Results

In all three studies, average total net moments during ankle height lifts ranged between 200 and 300 Nm. The maximum support the devices could generate, was about 30, 40 and 50 Nm, for the lightweight, actuated, and new passive exoskeleton.

With the light weight passive exoskeleton (Laevo) support moments during peak loading were less than 20 Nm. As a result, for far lifts, peak spine compression slightly decreased, by 5% averaged over the two versions of the exoskeleton. For near lifts, support effects were counteracted by slight changes in lifting style, resulting in non-significant changes in compression forces.

The actuated exoskeleton (Robo-Mate) generated, at the instant of peak spine loading, support moments of on average 17 Nm. Nevertheless, spine compression, averaged over lifting techniques, decreased by 17%. This decrease only slightly varied over lifting techniques (stoop, squat or free) and did not depend on control mode.

The new passive exoskeleton (SPEXOR) generated a support moment of 33 Nm at the instant of peak spine loading. It resulted in a decrease of spine compression of 14%, and this did not depend on lifting technique.

In all studies, lifting with the exoskeleton resulted in a reduction of peak trunk angular velocity (by 17, 26 and 17%, respectively). Lumbar flexion increased (8%) with the light weight exoskeleton, decreased (28%) with the actuated exoskeleton and was unaffected by the new passive exoskeleton.

4 Discussion

In this study, we evaluated the biomechanical effects of three exoskeletons on low back loading during lifting. The actual support of the exoskeletons during peak spine loading was substantially lower than the maximum the devices could generate. The main reason is that peak spine loading during lifting occurs early during the upward phase of the movement, when the trunk accelerates upward. In this phase, passive exoskeletons do not generate their maximum support. Additionally, the lightweight exoskeleton suffered from hysteresis [7], and the motors in the actuated exoskeleton failed to generate the intended peak torque during upward acceleration.

Spine load reductions were not fully consistent with exoskeleton support. Specifically, for the lightweight exoskeleton subtle changes in lifting style counteracted the effect of the support. For the actuated exoskeleton, the reduction in spine compression (17%) was larger than expected, based on the support moment (17 Nm). This was mainly due to a substantial reduction in lifting speed when using the exoskeleton. For the new passive exoskeleton, only minor changes in lifting style were found, and the resultant reduction in compression force (14%) was consistent with the support moment (33 Nm). Based on our findings we would recommend for future design of exoskeletons to increase the magnitude of the support, and to better align the timing of peak support with peak spine loading. Evaluation of exoskeletons should not be based on EMG alone, as kinematics may change when wearing an exoskeleton, which requires correction of EMG. Furthermore, safety and versatility in tasks other than lifting should be evaluated.

5 Conclusion

Peak spine compression during lifting was reduced by each of the three exoskeletons tested for the present study. The new passive exoskeleton reduced spine compression more than the lightweight passive exoskeleton. Additionally, spine load reductions when wearing the exoskeletons were affected by changes in lifting style and lifting speed. Design changes (for passive exoskeletons) and control and motor changes (for actuated exoskeletons) should enhance the timing and magnitude of their support.

Acknowledgements This work was supported by the European Union's Horizon 2020 through the SPEXOR project, contract no. 687662, and by the Dutch Research Council (NWO), program 'perspectief' (project P16–05).

References

1. J. Hartvigsen, M.J. Hancock, A. Kongsted, Q. Louw, M.L. Ferreira, S. Genevay et al., What low back pain is and why we need to pay attention. Lancet **391**, 2356–2367 (2018)
2. C. Maher, M. Underwood, R. Buchbinder, Non-specific low back pain. Lancet **389**, 736–747 (2017)
3. P. Coenen, I. Kingma, C.R. Boot, P.M. Bongers, J.H. van Dieën, Cumulative mechanical low-back load at work is a determinant of low-back pain. Occupat. Envirmon. Med. **71**, 332–337 (2014)
4. N.E. Foster, J.R. Anema, D. Cherkin, R. Chou, S.P. Cohen, D.P. Gross et al., Prevention and treatment of low back pain: evidence, challenges, and promising directions. Lancet **391**, 2368–2383 (2018)
5. I. Kingma, G.S. Faber, A.J. Bakker, J.H. van Dieën, Can low back loading during lifting be reduced by placing one leg beside the object to be lifted? Phys. Ther. **86**, 1091–1105 (2006)
6. M.P. de Looze, T. Bosch, F. Krause, K.S. Stadler, L.W. O'Sullivan, Exoskeletons for industrial application and their potential effects on physical work load. Ergonomics **59**, 671–681 (2016)

7. A.S. Koopman, I. Kingma, M.P. de Looze, J.H. van Dieën, Effects of a passive back exoskeleton on the mechanical loading of the low-back during symmetric lifting. J. Biomech. **102**, 109486 (2020)
8. A.S. Koopman, M. Näf, S.J. Baltrusch, I. Kingma, C. Rodriguez-Guerrero, J. Babic et al., Biomechanical evaluation of a new passive back support exoskeleton. J. Biomech. **105**, 109795 (2020)
9. A.S. Koopman, S. Toxiri, V. Power, I. Kingma, J.H. van Dieën, J. Ortiz et al., The effect of control strategies for an active back-support exoskeleton on spine loading and kinematics during lifting. J. Biomech. **91**, 14–22 (2019)
10. S. Toxiri, A.S. Koopman, M. Lazzaroni, J. Ortiz, V. Power, M.P. de Looze et al., Rationale, implementation and evaluation of assistive strategies for an active back-support exoskeleton. Frontiers Robot AI **5**, 1–4 (2018)
11. M.B. Näf, A.S. Koopman, S. Baltrusch, C. Rodriguez-Guerrero, B. Vanderborght, D. Lefeber, Passive back support exoskeleton improves range of motion using flexible beams. Frontiers Robot AI **5**, 1–6 (2018)
12. I. Kingma, M.P. de Looze, H.M. Toussaint, J.G. Klijnsma, T.B.M. Bruijnen, Validation of a full body 3-D dynamic linked segment model. Hum. Mov. Sci. **15**, 833–860 (1996)
13. J.H. van Dieën, I. Kingma, Effects of antagonistic co-contraction on differences between electromyography based and optimization based estimates of spinal forces. Ergonomics **48**, 411–426 (2005)

Can HDEMG-Based Low Back Muscle Fatigue Estimates Be Used in Exoskeleton Control During Prolonged Trunk Bending? A Pilot Study

Niels P. Brouwer, Ali Tabasi, Alejandro Moya-Esteban, Massimo Sartori, Wietse van Dijk, Idsart Kingma, and Jaap H. van Dieën

Abstract The effectiveness of exoskeletons could be enhanced by incorporating low back muscle fatigue estimates in their control. The aim of the present study was to evaluate whether low back muscle fatigue can be estimated using the spectral content of trunk extensor muscle high-density EMG (HDEMG) by considering the motor unit action potential conduction velocity (MUAP CV) as a reference. The HDEMG-based MUAP CV was estimated for multiple sites on the lower back consistently throughout a 30 degrees lumbar flexion endurance trial. Significant linear relationships were observed between MUAP CV and spectral content. However, MUAP CV and spectral changes over time did not show the expected decrease, probably due to additional recruitment of motor units or alternating activity of synergistic muscles. The anatomical information about the sites that allow MUAP CV estimation can be valuable for future low back muscle fatigue estimations.

1 Introduction

Excessive cumulative low back load, for instance due to prolonged static bending, and a limited trunk extensor muscle endurance are considered important risk factors for low back pain [1, 2]. Hence, actuated trunk support exoskeletons would benefit from including low back muscle fatigue estimates in their control. Muscle fatigue has been estimated previously in the lower back using the shift in spectral content of the EMG [3], which has been associated with low back muscle endurance time [4]. In other

N. P. Brouwer (✉) · A. Tabasi · I. Kingma · J. H. van Dieën
Department of Human Movement Sciences, Vrije Universiteit Amsterdam, Amsterdam Movement Sciences, Amsterdam, The Netherlands
e-mail: n.p.brouwer@vu.nl

A. Moya-Esteban · M. Sartori
Department of Biomechanical Engineering, University of Twente, Enschede, The Netherlands

W. van Dijk
TNO, Leiden, The Netherlands

J. C. Moreno et al. (eds.), *Wearable Robotics: Challenges and Trends*,
Biosystems & Biorobotics 27, https://doi.org/10.1007/978-3-030-69547-7_30

muscles, such as the tibialis anterior muscle, these spectral changes have been associated with physiological manifestations of muscle fatigue, e.g. a decrease in motor unit action potential (MUAP) conduction velocity (CV) [5]. However, generalizing the latter well-established association to the low back muscles may be complicated [6]. The muscle fatigue analysis based on the spectral content of low back muscle EMG is likely affected by (1) cross-talk of other back muscles; (2) complex muscle architecture [6], e.g. varying distribution of motor-end plates and a large volume of tendinous tissue; and (3) potential local manifestations of muscle fatigue [7]**.** So, the relationship between the spectral content of low back muscle EMG and the MUAP CV may be questioned. The aim of the present study was to evaluate whether low back muscle fatigue can be estimated using the spectral content of high-density EMG (HDEMG) measurements obtained at the low back, by relating it to the estimated HDEMG-based MUAP CV as a muscle fatigue-related physiological reference [5].

2 Material and Methods

One male participant volunteered for the present study (age: 26 yr.; height: 1.75 m; body mass: 68.0 kg). At the time of the experiment, the participant did not have a history of low back pain. Four HDEMG 8x8 electrode grids with an 8.5mm inter-electrode distance were placed bilaterally 1cm from the spine (two grids per side), stacked with a 5mm inter-grid distance, starting from the height of the spinous process of L5. The low back muscle activity was recorded at 2048 Hz using the Refa system (TMSi, Oldenzaal, The Netherlands). One inertial measurement unit (Xsens, Enschede, The Netherlands) was attached to the spine at the height of the spinous process of T10 to record the lumbar flexion angle. The participant was instructed to perform one maximum endurance effort at 30 ± 5 degrees lumbar flexion, while the pelvis was fixed in a frame. The 256 monopolar HDEMG signals were synchronized and band-pass filtered using a zero-lag second order Butterworth filter with cut-off frequencies 30–500Hz. A total of 192 double differential channels (48 per grid) was constructed in cranial-caudal direction to reduce fibre-end potentials and other far-field potentials in the HDEMG signals [5]. These signals were interpolated to increase the sample rate with a factor 16.

Per pair of double differential channels, the MUAP CV was estimated in the cranial-caudal direction using an analysis on individual peaks [8]. For each signal, 2s standard deviations were computed and peaks exceeding this windowed threshold were selected. Selected peaks were matched between channels considering a delay range equal to infinite CV (i.e. no delay) down to 1 m s^{-1}, allowing cranial and caudal MUAP propagation. Pearson correlation coefficients were computed using 15.6 ms windows constructed around matched peaks. Matched peaks with a Pearson correlation (R) higher than 0.9 were selected for analysis [8]. Median CV, median frequency (MDF), mean frequency (MNF), and root-mean-square amplitude (RMS) were computed over 5s windows. MDF, MNF, and RMS time series were averaged per pair of double differential channels. A second order polynomial was fitted through

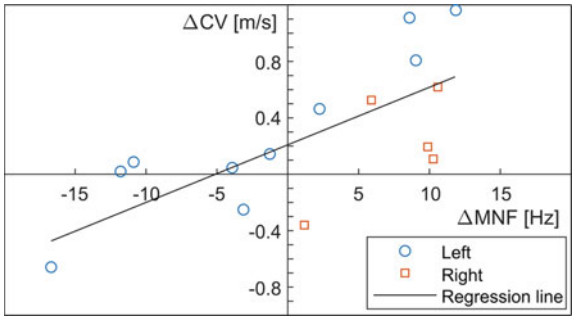

Fig. 1 Relationship between change in CV and change in MNF ($R^2 = 0.53$, $p = 0.002$). Red squares and blue circles depict a measurement from the right and left side of the spine, respectively

the median CV, spectral, and RMS time series. The root-mean-square error was used to evaluate the quality of the fit and CV estimations with a median CV fit exceeding a root-mean-square error of 0.2 were excluded. Linear regression was employed to evaluate the relationship between the change (i.e. difference between initial and final value of the fit) in CV and the change in MDF, MNF, and RMS across double differential channel locations.

3 Results

Endurance time was 785s. The peak velocity analysis on the bottom two grids did not reveal consistent travelling MUAPs. The analysis on the top two grids revealed travelling MUAPs in caudal direction consistently throughout the trial between fifteen (5 right, 10 left) pairs of double differential channels. However, unexpectedly, 8 out of the 15 showed an increase of MUAP CV, MDF and MNF. The initial values of the median CV fit ranged from 2.05 to 4.27 m s^{-1} (m ± sd: 3.14 ± 0.85 m s^{-1}). Linear regression revealed significant relationships between changes over time of CV and both spectral measures (MDF: $R^2 = 0.38$, $p = 0.015$; MNF: $R^2 = 0.53$, $p = 0.002$; see Fig. 1), but no significant relationship between the CV and RMS change over time. All averaged RMS signals increased throughout the trial (m ± std: 57.7 ± 17.2%).

4 Discussion

The aim of the present study was to evaluate whether trunk extensor muscle fatigue can be estimated using the spectral content of HDEMG, considering the estimated HDEMG-based MUAP CV as a reference. In contrast to previous work [6], we estimated the MUAP CV at a total of 15 sites. These sites were at the lateral end of both grids (approximately at the spinal level of T12-L2). Three of the CV time series showed a decrease over time, indicating the development of muscle fatigue.

However, the majority of the CV time series showed an increase, and this coincided with an increase in frequency content (Fig. 1). As might be supported by the observed increase in amplitude for all channels, this could be related to additional recruitment of larger, faster and more superficial motor units due to the reduced force capacity of the already recruited and fatigued motor units [6]. Additionally, this could also be related to alternating activity of synergistic trunk extensor muscles [7]. Both manifestations may have masked fatigue related spectral and CV changes.

The bottom two grids and medial side of the upper grids yielded no successful MUAP CV estimates, probably due to the complex low back muscle architecture. Placement of electrodes close to the innervation zones or fibre-ends of muscles can affect the CV estimates and result in additional high frequency content [9]. Nevertheless, the results of the present study indicate a potential anatomical location where the CV and low back muscle fatigue can be estimated using HDEMG. Future studies should evaluate the consistency of the present finding regarding the anatomical location of the CV estimates across subjects.

5 Conclusion

In the present pilot study, we estimated the trunk extensor MUAP CV using HDEMG for multiple sites consistently throughout a 30 degrees lumbar flexion endurance trial. Hence, the relationship between the CV and shift of the corresponding spectral content could be evaluated for the trunk extensor muscles. However, estimating trunk extensor muscle fatigue based on CV or surface EMG spectral content appears not feasible yet, possibly due to the additional recruitment of motor units or alternating activity of synergistic muscles.

Acknowledgements This work was supported by the Dutch Research Council (NWO), program 'perspectief' (project P16-05).

References

1. P. Coenen, I. Kingma et al., Cumulative low back load at work as a risk factor of low back pain: a prospective cohort study. J. Occup. Rehabil. **23**(1), 11–18 (2013)
2. W.E. Hoogendoorn, P.M. Bongers, et al., Flexion and rotation of the trunk and lifting at work are risk factors for low back pain. Spine (Phila. Pa. 1976), **25**(23), 3087–3092 (2000)
3. J.H. van Dieën, E.P. Westebring-van der Putten et al., Low-level activity of the trunk extensor muscles causes electromyographic manifestations of fatigue in absence of decreased oxygenation. J. Electromyogr. Kinesiol. **19**(3), 398–406 (2009)
4. J.H. van Dieën, H.H.E. Oude Vrielink, et al., Trunk extensor endurance and its relationship to electromyogram parameters. Eur. J. Appl. Physiol. **66**(5), 388–396 (1993)
5. R. Merletti, M. Knaflitz et al., Myoelectric manifestations of fatigue in voluntary and electrically elicited contractions. J. Appl. Physiol. **69**(5), 1810–1820 (1990)

6. D. Farina, M. Gazzoni et al., Assessment of low back muscle fatigue by surface EMG signal analysis: Methodological aspects. J. Electromyogr. Kinesiol. **13**(4), 319–332 (2003)
7. J.H. Van Dieën, H.H.E. Oude Vrielink, et al., An investigation into the relevance of the pattern of temporal activation with respect to erector spinae muscle endurance. Eur. J. Appl. Physiol. **66**(1), 70–75 (1993)
8. R.B.J. Beck, C.J. Houtman et al., A technique to track individual motor unit action potentials in surface EMG by monitoring their conduction velocities and amplitudes. IEEE Trans. Biomed. Eng. **52**(4), 622–629 (2005)
9. J.Y. Hogrel, J. Duchêne et al., Variability of some SEMG parameter estimates with electrode location. J. Electromyogr. Kinesiol. **8**(5), 305–315 (1998)

Back-Support Exoskeleton Control Using User's Torso Acceleration and Velocity to Assist Manual Material Handling

Maria Lazzaroni, Ali Tabasi, Stefano Toxiri, Darwin G. Caldwell, Idsart Kingma, Elena De Momi, and Jesús Ortiz

Abstract This work analyzes the use of users' dynamics to define the assistance of a back-support exoskeleton for assisting manual material handling. Exploiting the acceleration and velocity of the user's torso on the sagittal plane allows to distinguish between lifting and lowering phases and accordingly adapt the assistance. Theoretical and practical issues of strategy implementation are discussed.

1 Introduction

In many industrial sectors, workers perform manual material handling (MMH) activities, that overload and compress the spine causing injuries and musculoskeletal disorders (MSDs). Back-support exoskeletons are being introduced in industries, where full-automation is not feasible and human's flexibility is required [1]. Exoskeletons promise to reduce the MSDs risk, by reducing the compression of the spine [2].

Our group has developed a torque-controlled back-support exoskeleton for which we explore different possible control strategies to suit the need for assistance. For improving the effectiveness of the assistance provided in dynamic MMH tasks with respect to state-of-the-art methods, valuable information can be obtained from the user's dynamics during the execution of the task. In a previous work [3] we presented a new strategy that uses the user's torso angular acceleration for assisting symmetric lifting and lowering, while a similar device [4] employed the torso angular velocity for the same purpose.

Work funded by the Italian Workers' Compensation Authority (INAIL).

M. Lazzaroni (✉) · S. Toxiri · D. G. Caldwell · J. Ortiz
Department of Advanced Robotics, Istituto Italiano di Tecnologia, Genova, Italy
e-mail: maria.lazzaroni@iit.it

M. Lazzaroni · E. De Momi
Department of Electronics, Information and Bioengineering, Politecnico di Milano, Milan, Italy

A. Tabasi · I. Kingma
Department of Human Movement Sciences, Faculty of Behavioural and Movement Sciences, Vrije Universiteit Amsterdam, Amsterdam, The Netherlands

J. C. Moreno et al. (eds.), *Wearable Robotics: Challenges and Trends*,
Biosystems & Biorobotics 27, https://doi.org/10.1007/978-3-030-69547-7_31

This work analyzes the difference of designing a control strategy using the acceleration against using the velocity for assisting lifting and lowering tasks. The strategies were implemented on the XoTrunk back-support exoskeleton, an evolution of the prototype employed in [3].

2 Control Strategies

2.1 Rationale for Using User's Dynamics

Most current strategies for assisting lifting and lowering tasks act to compensate for the effect of gravity [1]. The assistance is based on the static characteristics of the user's movement (mainly torso inclination), and thus would not adapt to different task phases. An inclination-based strategy generates the peak assistance corresponding with the maximum torso flexion, as happens for a passive exoskeleton.

However, as clarified in [5], the lumbar moment reaches its peak at the beginning of lifting, i.e. when the user grasps the box and starts to lift it (after the maximum flexion occurred), because upper body mass and the mass of the load requires acceleration upwards. As a result, (1) an inclination-based strategy would not generate the peak assistance corresponding with the peak in torque need [5]. Moreover, providing the same assistive torque during the descent phase (lowering) and the ascent phase (lifting) (2) limits the maximum physical assistance, because increasing assistance in the latter corresponds to increasing hindrance in the former. Therefore, for inclination-based strategies, as for passive exoskeletons, the assistance provided for supporting the user during lifting must be scaled according to his acceptance of hindrance during lowering. because he has to accelerate upward his mass plus the mass of the box.

Measuring the dynamics of the user's torso allows to distinguish the lowering and the lifting phases, and thus assist them differently. If the angular acceleration of the user's torso is used to proportionally define the assistive torque, additional support is provided accordingly with the peak in the assistance need (1) i.e., when the user grasps the box and starts the lifting phase, accelerating his and the box's masses. On the other end, the reduction of the assistance due to the inclination-based torque during the lowering phase, achieved by employing the torso acceleration or velocity, reduces the hindrance for the flexion of the torso (2).

2.2 Implementation

Focusing on overcoming these two limitations (1) and (2), in a previous work [3] we presented a new strategy making use of the user's torso angular acceleration.

Additionally, we implemented a strategy based on user's torso angular velocity on the same exoskeleton for comparing the two strategies.

The angular velocity $\dot{\theta}_h$ is measured with an Xsens MTw IMU (Xsens Technology), attached to the user's torso (approximately at the sternum). The angular acceleration $\ddot{\theta}_h$ is obtained by differentiating and filtering the angular velocity on the sagittal plane (low-pass filter, cut-off frequency 1 Hz). Then, dynamic torques $\tau_{dynamic}$ are defined proportional to the torso angular velocity or acceleration, while the static torque τ_{static} is proportional to torso inclination. The assistive torque $\tau_{assistive}$ is finally computed as the sum of the static (inclination-based) and the dynamic (velocity or acceleration-based) torques, that can be scaled adjusting the respective control gains K:

$$\tau_{assistive} = \tau_{static} + \tau_{dynamic}$$

$$\tau_{static} = K_{incl}\, sin(\theta_h) \quad \text{inclination-based}$$

$$\tau_{dynamic} = \begin{cases} -K_{vel}\, \dot{\theta}_h & \text{velocity-based} \\ -K_{acc}\, \ddot{\theta}_h & \text{acceleration-based} \end{cases}$$

In the following, *acceleration* and *velocity* strategies indicates that the assistive torque is computed as the sum of the inclination-based with velocity or acceleration-based torques, respectively. The *inclination* strategy has $\tau_{dynamic} = 0$.

3 Experimental Results

Experiments were done with 9 subjects. The differences in lumbar compression peaks (estimated as in [2]) of *velocity* and *acceleration* strategy w.r.t the condition without the exoskeleton were statistically significant (ANOVA test, $p < 0.05$). The difference between *velocity* and *acceleration* strategy (compression force reductions w.r.t no exoskeleton equal to 11% and 15%, respectively) was not significant.

4 Discussion

A noticeable difference between velocity and acceleration signals emerges at the beginning of lifting (c), when the subject is accelerating upwards. As the acceleration increases, the *acceleration* strategy provides greater assistance which is in time

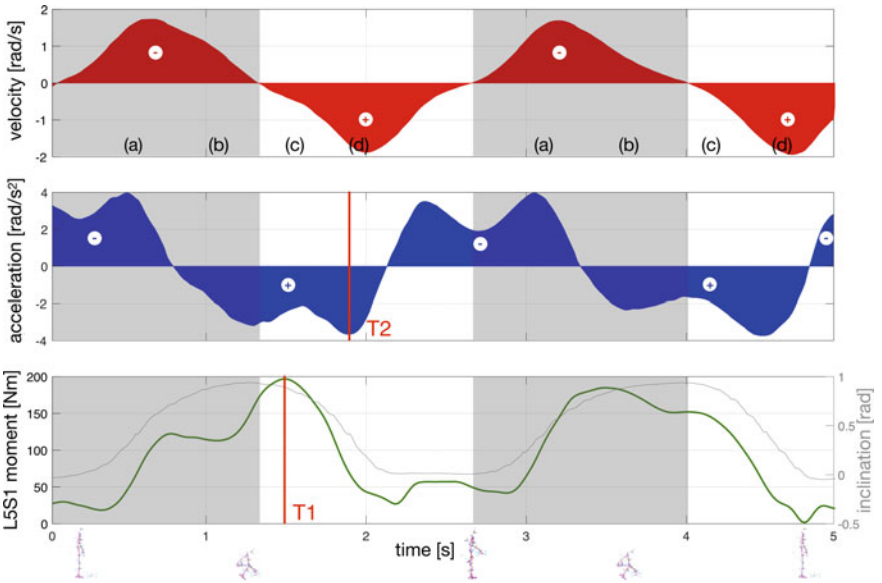

Fig. 1 The curves of a subject's torso angular velocity and acceleration are shown during box lifting and lowering. Their contribution to $\tau_{assistive}$ is indicated as: (+) the total torque is increased by $\tau_{dynamic}$, (−) if it is decreased. The lumbar moment generated at L5S1 disc (as estimated in [2]) is displayed at the bottom (green line). T1 is the instant of peak L5S1 moment, T2 is the instant of peak angular acceleration. To highlight task phases, trunk inclination and the human model position (at the bottom) are included; the phases are: beginning (a) and end (b) of lowering (grey background), beginning (c) and end (d) of lifting (white background)

with the subject need, as the lumbar moment (and hence the compression) reaches its maximum value (1). Conversely, the velocity starts to increase at the beginning of lifting and reaches its maximum after the lumbar moment peak, actually increasing the assistance at the end of lifting (d). Results show larger compression force reductions for the *acceleration* strategy, although not significant. Further analysis is needed to reveal the benefits of the two strategies, focusing on other aspects of the assistance, e.g., subjective perception of support and hindrance or changes in the execution speed.

With respect to an *inclination* strategy, another advantage of using the velocity and acceleration emerges during the lowering phase (indicated with grey background in Fig. 1). Indeed, at the beginning of lowering (a), the assistance provided by the *inclination* strategy may be perceived by the wearer as hindering the flexion of the trunk. This behavior is similar to the support of passive exoskeletons, for which the assistance during lifting cannot be incremented at will, as it results in a higher resistance during lowering. However, with the *velocity* and the *acceleration* strategies, the torque working against the subjects can be reduced, correspondingly reducing the resistance for trunk flexion (2). Moreover, it can be observed in Fig. 1 that the box's mass contributes to increase lumbar moment (phases (c) and (d) of lifting and

(a) and (b) of lowering). A solution to account for this need of additional assistance was evaluated in [2]: the assistance is increased when a load is detected on user's hands.

As regards the *acceleration* strategy, one limitation concerns the delay of the acceleration signal (T1-T2 in Fig. 1), as it results in the delay of the dynamic component of the assistance. Furthermore, stability may also be compromised, if the acceleration is overestimated. As this controller acts as compensating the inertia of the user's upper body, overcompensating may lead to feedback inversion and instability [6]. On the contrary, with the *velocity* strategy, force augmentation is achieved by positive feedback (i.e., the generated forces augment the movement initiated by the wearer) that was proved to decrease the user's stability [3]. A further limitation for both strategies, particularly related with real workplace use, is the need to add an IMU on the user's torso to acquire the angular velocity, instead of using the one embedded in the exoskeleton. The need for this sensor is due to the user-exoskeleton coupling, which allows for relative movement between the two, i.e., the motion of the exoskeleton is delayed respect to the user's torso motion.

References

1. S. Toxiri, M.B. Näf, M. Lazzaroni, J. Fernández, M. Sposito, T. Poliero, L. Monica, S. Anastasi, D.G. Caldwell, J. Ortiz, Back-support exoskeletons for occupational use: an overview of technological advances and trends. IISE Trans. Occup. Ergon. Human Factors, 1–13 (2019)
2. A.S. Koopman, S. Toxiri, V. Power, I. Kingma, J.H. van Dieën, J. Ortiz, M.P. de Looze, The effect of control strategies for an active back-support exoskeleton on spine loading and kinematics during lifting. J. Biomech. (2019)
3. M. Lazzaroni, S. Toxiri, D.G. Caldwell, S. Anastasi, L. Monica, E. De Momi, J. Ortiz, Acceleration-based assistive strategy to control a back-support exoskeleton for load handling: preliminary evaluation, in *2019 IEEE 16th International Conference on Rehabilitation Robotics (ICORR)* (2019)
4. H.K. Ko, S.W. Lee, D. Koo, I. Lee, D.J. Hyun, Waist-assistive exoskeleton powered by a singular actuation mechanism for prevention of back-injury. Robot. Auton. Syst. (2018)
5. A. S. Koopman, S. Toxiri, M.P. de Looze, I. Kingma, J.H. van Dieën, Effects of an inclination-controlled active spinal exoskeleton on spinal compression forces, in International Symposium on Wearable Robotics, pp. 505–509 (2018)
6. A. Calanca, R. Muradore, P. Fiorini, Impedance control of series elastic actuators: passivity and acceleration-based control. Mechatronics **47**, 37–48 (2017)

Subjective Assessment of Occupational Exoskeletons: Feasibility Study for a Custom Survey for Braces

M. Sposito, D. G. Caldwell, E. De Momi, and J. Ortiz

Abstract Occupational exoskeletons are emerging as a viable solution to mitigate the effect of poor ergonomic work tasks. However, there is still a lack of understanding of which are the key factors to improve the low acceptance rate, from a subjective point of view. Effectively translating users' feedback in requirements is of paramount importance to raise adoption of exoskeletons. To this end, we present and evaluate a tailored set of constructs and questions to collect subjective ratings of braces, that are the physical interface between users and exoskeletons and play a key role in acceptance rate.

1 Introduction

Occupational Exoskeletons (OEs) are showing their effectiveness to lower risk injuries in un-ergonomic working tasks [1]. Researchers and designers still lack a substantial acceptance assessment from users because OE's effectiveness is proved mostly in laboratory setups [2]. In particular, choosing a proper design to raise comfort is central to enhance OE's acceptance rates. Indeed, balancing mechanical requirements, human factors and users' requirements is difficult and requires intensive testing and effective data collection methods. In this paper we introduce a first attempt to collect data of subjective comfort of an OE physical interfaces. Braces can be composed of rigid shells (e.g. cuff) and compliant textiles (e.g. harness) and they have two key functions: secure the exoskeleton to the limbs and unload assistance to the users. However, standard collection forms, like SUS or Nasa TLX, are

M. Sposito (✉) · E. D. Momi
Department of Electronics, Information and Bioengineering (DEIB), Politecnico di Milano, Milan, Italy
e-mail: matteo.sposito@iit.it

M. Sposito · D. G. Caldwell · J. Ortiz
Advanced Robotic Department (ADVR), Istituto Italiano di Tecnologia, Genova, Italy

J. C. Moreno et al. (eds.), *Wearable Robotics: Challenges and Trends*,
Biosystems & Biorobotics 27, https://doi.org/10.1007/978-3-030-69547-7_32

not suitable to collect all the subjective perceptions regarding all of the OE's components. In fact, [3, 4] and [5] present custom-made survey to collect subjective data about distinct parts of exoskeletons. We present a feasibility study of our custom questionnaire on an active OE and two different braces version (Alpha and Beta). We will show the subjective scores of the two versions and perform a formative evaluation of the proposed custom constructs and items for the survey.

2 Methods

The feasability tests were conducted using the procotol described in this section. We first introduce the physical arrangement that allow subjects to complete the sequence of tasks. Work pattern reasonably resemble real activities to rate the comfort with custom survey.

2.1 Experimental Setup

The experiments were performed using the XoTrunk, an updated revision of the OE presented in [6]. XoTrunk assists the lumbar region in tasks that, due to muscle overload, could increase the risks of injuries; like carrying, lifting and lowering a load (i.e. Manual Material Handling (MMH)). The test is composed of a pattern, close to real-work scenarios, repeated for 10 mins at a self-determined pace. Repetitions are performed wearing always the same exoskeleton, varying braces' version. The load L is a 7 kg box, for all the subjects. The pattern is composed of lifting, lowering, squatting, walking and carrying, details are provided in Table 1 and Fig. 1.

The subjects move between two different boxes, B1 and B2, with distinct heights (50 and 70 cm). B1 and B2 allow the subjects to lower and lift L with different bending angles and distinct techniques. NIOSH score of the test is 0.9, resembling a low risk MMH activity. All the subjects were given 5 min familiarization with the activities, with and without the exoskeleton in one configuration. Assistance levels were chosen during familiarization, based on each personal preferences and were the same for the two trials. Assistance profiles are the same of the ones presented in [6]. XoTrunk was fitted with the right harness sizes (where possible) to fit the subjects' body sizes and shapes.

2.2 Experimental Design

We chose 6 healthy volunteers (age 28 ± 2.2 years, height 171 ± 7.1 cm) for the test. XoTrunk could be adjusted to fit every volunteer and be secured to the limbs, no subject was excluded. The population is equally divided between males and females

Table 1 Movements pattern

Movement Nr	Description
M1	Lift L from ground and place on B1
M2	Lift and carry L over B2
M3	Lower L to ground and lift to waist for three times
M4	Lift L on B2 and then walk to B1 and back to B2
M5	Carry L from B2 to B1 and place on the ground

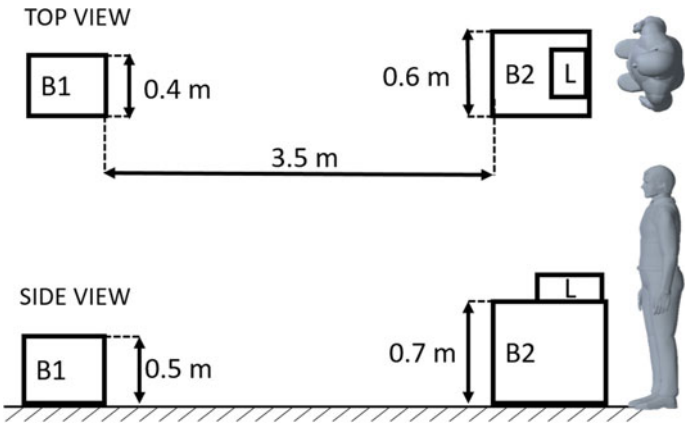

Fig. 1 Physical arrangement of the experimental setup. B1 and B2 are surfaces to lower and lift the load L at different heights. Distances, dimensions and mannequin are not in scale

and Expert of OE and Un-Expert (more than 5 h use or not). In this experimental design, *Independent variable* is garment version (Alpha or Beta) and *Dependent variables* are perceived physical comfort, usability, and general opinions. We used a Repeated Measurements experimental design, within the selected test group. To mitigate order effect, we split the test group to counterbalance the testing order. Half of the group tried Alpha first and Beta afterwards, the other tested Beta first. Questionnaire was administered after each one of the two trials.

2.3 Questionnaire Form

The questionnaire form is composed of three different constructs (the dependent variables). Each construct is composed of different of items (or questions):

(1) *Physical Comfort*: Breathability; Perceived Pressure; Perceived Pain; Fixation Stability and Friction.

(2) *Usability*: Ease to don and doff; Freedom of movement and Perceived assitance delivery.
(3) *General Opinions*: Fabric look and feel; Expectations and Appreciation.

The questionnaire's score is a 5 point Likert-like scale to rate each item from "Completely Disagree" to "Strongly Agree". There are no different weights for the constructs, all the questions are positive. Because of the formative evaluation nature of this tests, the subjects are given the opportunity to add any relevant suggestion to each construct (e.g. additional items).

3 Results

This feasibility test does not allow to have independent measures for the size of the test group, we will report results with a descriptive statistics analysis [7]. Data in Fig. 2 is presented as *Cumulative Score* and scores for *Constructs A, B and C*. *Cumulative Score* shows an overall preference of Beta version, 75.5 versus 68 for Alpha. The *Physical Comfort* construct is the one that scored less with respect to the maximum, 29.5 and 32.5 with a maximum of 45. In spite of this, it is not clear if it is caused by a real discomfort or due to a different number of questions with respect to others. Beta version scored best in Pressure, Stability and Look and Feel; while obtained same score in Breathability and Freedom of Movement. Although most of the items were answered without any assistance from the researchers, meaning that

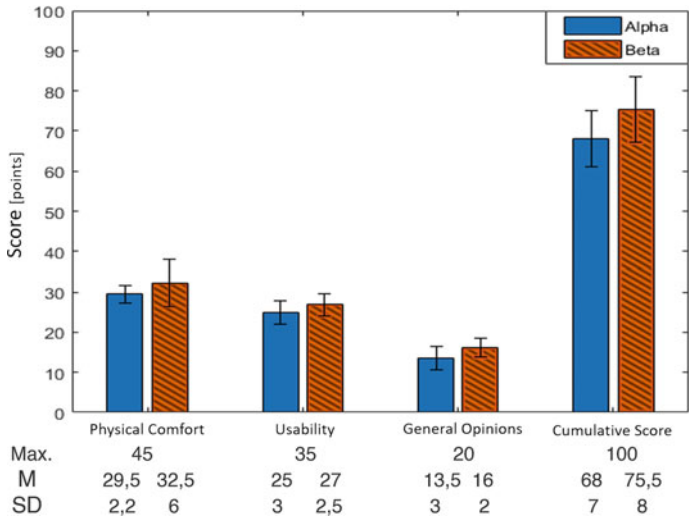

Fig. 2 Box plot reporting the average values and standard deviation computed from the scores of the six subjects. Blue bars refer to Alpha condition while orange bars refer to Beta condition. Numerical values are reported under the respective bars

the question meets the requirements of good wording, unambiguity and correct score system, we were asked to add: Not Applicable for items in *Usability* and *General Opinions*, increase the score to 7 points and add items for evaluation of single body area in contact with the braces, especially in *Physical Comfort*.

4 Conclusion

We were able to collect valuable information from this formative evaluation: experimental protocol and the custom made constructs can be improved implementing test subjects' suggestions to overcome the problems highlighted. Though, the custom questionnaire proved to be a good starting point. Indeed, data shows that Beta version is preferred for every construct over Alpha, though no advancements were confirmed in Breathability and Freedom of Movement. A new testing campaign involving more users will allow to apply a between group experimental design and obtain relevant data, informing on how different brace's version can affect user's comfort and OE's acceptance rate.

Acknowledgements This work has been co-founded by the Italian Workers' Compensation Authority (INAIL), The authors would like to thank Dr. G. Barresi for the helpful suggestions regarding the experimental setup and analysis methods.

References

1. M.A. Nussbaum, B.D. Lowe, M. de Looze, C. Harris-Adamson, M. Smets, An introduction to the special issue on occupational exoskeletons. IISE Trans. Occup. Ergon. Human Fact. **7**(3–4), 153–162 (2019)
2. L. Stirling, H.C. Siu, E. Jones, K. Duda, Human factors considerations for enabling functional use of exosystems in operational environments. IEEE Syst. J. **13**(1), 1072–1083 (2019)
3. L. Shore et al., Exoscore: a design tool to evaluate factors associated with technology acceptance of soft lower limb exosuits by older adults. Human Fact. (2019)
4. R. Hensel, M. Keil, Subjective evaluation of a passive industrial exoskeleton for lower-back support: a field study in the automotive sector. IISE Trans. Occup. Ergon. Human Fact. **7**(3–4), 213–221 (2019)
5. P. Maurice et al., Objective and subjective effects of a passive exoskeleton on overhead work. IEEE Trans. Neural Syst. Rehabil. Eng. **28**(1), 152–164 (2020)
6. S. Toxiri, A.S. Koopman, M. Lazzaroni, J. Ortiz, V. Power, M.P. de Looze, L. O'Sullivan, D.G. Caldwell, Rationale, implementation and evaluation of assistive strategies for an active back-support exoskeleton. Front. Robot. AI **5** (2018)
7. E.C. Lee, A.L. Whitehead, R.M. Jacques, S.A. Julious, The statistical interpretation of pilot trials: should significance thresholds be reconsidered? BMC Med. Res. Methodol. (2014)

Evidenced-Based Indications/Contraindications for and Potential Benefits of Exoskeletal-Assisted Walking in Persons with Spinal Cord Injury

Alteration of Push-Off Mechanics During Walking with Different Prototype Designs of a Soft Exoskeleton in People with Incomplete Spinal Cord Injury—A Case Series

Eveline S. Graf, Christoph M. Bauer, Carole Pauli, and Markus Wirz

Abstract The push-off is a key factor determining the walking capability. People with impaired function due to incomplete spinal cord injury (iSCI) have altered biomechanics and are, therefore, at a disadvantage during activities of daily living such as walking. XoSoft is a prototype soft exoskeleton designed to assist during walking. Different generations of XoSoft followed different strategies of tailoring the garment (custom-made vs. one-size fits all). This may result in altered effects on the mechanics of walking. In this study, we assessed two generations of XoSoft with three people with iSCI and focused on the push-off mechanics (ankle kinematics & kinetics) during level walking. The results showed that XoSoft was able to support the gait, but systematic differences between prototype generations were not found. Consequently, a more general approach for the garment design may be feasible.

1 Introduction

The ankle joint and its ability to produce power during push-off is highly relevant for gait [1, 2]. It has been shown that modulation of the peak ankle power has direct impact on the workload of the proximal leg muscles [2]. If people are unable to produce the necessary power at the ankle, due to impairments such as incomplete spinal cord injury (iSCI), the more proximal joint muscles, mainly at the hip, may need to compensate in order to allow for walking ability, which presents a mechanical disadvantage. It has been shown that people with iSCI have altered ankle kinematics and kinetics during different walking tasks [3, 4]. Also, it has been shown that the plantarflexor muscles have diminished ability to produce torque [5]. Consequently, they are at a disadvantage during everyday motion tasks such as walking.

Previous work using custom powered ankle-foot orthoses supporting the plantarflexion have shown that the ankle range of motion was increased with a powered

E. S. Graf (✉) · C. M. Bauer · C. Pauli · M. Wirz
School of Health Professions, Institute of Physiotherapy, Zurich University of Applied Sciences, Winterthur, Switzerland
e-mail: eveline.graf@zhaw.ch

J. C. Moreno et al. (eds.), *Wearable Robotics: Challenges and Trends*,
Biosystems & Biorobotics 27, https://doi.org/10.1007/978-3-030-69547-7_33

orthosis compared to no orthosis [6] and that the dynamics of the push-off could be improved [7].

In the XoSoft project, prototypes for a modular, soft, exoskeleton have been developed following a user-centered approach [8]. The goal is to provide assistance for people with impaired walking due to diagnoses such as iSCI. The aim of this study was to assess the effect of the ankle actuation of XoSoft on the ankle joint and dynamics of walking during the push-off in people with iSCI.

2 Methods

2.1 XoSoft

The detailed technical description of XoSoft has previously been published [9]. Participants were tested wearing both the Beta2 and the Gamma prototype. All had plantarflexion actuation, which stores energy using a textile based clutch in series with an elastic band during the stance phase and releases it during terminal stance and initial swing phase (Participant 1 and 3: bilateral, Participant 2: right side). The main difference between Beta2 and Gamma prototype was the garment: Beta2 had tight custom-tailored garments while for Gamma a loose design suitable for various participants was chosen.

2.2 Participants

Three male participants with iSCI and normal range of motion in the lower extremity joints (Table 1) performed gait analysis at two separate time points. In both sessions, they were tested first without XoSoft (None) and then with the prototype (XoSoft).

Table 1 Participant characteristics

	Participant 1	Participant 2	Participant 3
Age [years]	79	71	55
Height [m]	1.57	1.68	1.64
Mass [kg]	55.8	63.4	78.3
Diagnosis	Hereditary spastic paraplegia	Traumatic spinal cord injury	Hereditary spastic paraplegia
Walking impairment	Paraspastic gait with partial toe dragging. Able to walk without aid	Paraspastic gait combined with spinal ataxia. Uses two trekking poles for community walking	Paraspastic gait with partial toe dragging. Wears an ankle foot orthosis on left side for community walking

2.3 Data Collection

Gait kinematics were collected with markers and a 3D optoelectronic camera system (Vicon Vantage, Vicon Motion Systems) and calculation of joint angles followed a standardized approach [10]. Simultaneously, ground reaction forces were collected using in-ground force plates (AMTI Inc). Kinetic data was calculated using an inverse dynamics approach (Bodybuilder, Vicon Motion Systems). All subsequent analysis was done with Matlab (Matlab Inc.)

Each participant performed four walking trials with each condition at a self-selected speed. The self-selected speed was determined during the None condition and had to remain consistent for the XoSoft condition to ensure comparability of the kinematic and kinetic results.

3 Results

All participants had increased peak ankle plantarflexion angles during push-off with XoSoft (except participant 3, left, Gamma; Table 2). The maximal ankle angular joint power showed small increases of XoSoft compared to None for participant 1 and divergent results between prototypes for participants 2 and 3. The anterior ground reaction force impulse showed small changes: increasing impulse for Beta2 compared to None, while Gamma had reduced values compared to None (except participant 2 right ankle).

Table 2 Difference of discrete values of ankle biomechanics and kinetics: xosoft versus none (mean of 4 trials)

		Participant 1		Participant 2	Participant 3	
		L	R	R	L	R
Angle [°]	β2–θ	3.1	1.9	5.1	8.4	4.5
	γ–θ	0.5	1.5	9.7	−1.4	0.1
Power [W]	β2-θ	5.6	16.7	−35.3	7.8	0.0
	γ–θ	6.1	18.5	20.5	−24.8	−90.8
GRF Imp. [Ns]	β2–θ	0.8	0.4	0.7	0.7	3.5
	γ–θ	−0.3	−1.5	0.5	−1.7	−0.4

β2: Beta2 prototype, θ: None, γ: Gamma prototype; negative values represent smaller values for XoSoft compared to None

Angle: peak ankle plantarflexion angle during push-off; Power: maximum total ankle angular joint power; GRF Imp.: anterior ground reaction force impulse (Participant 2 did not have actuation at the left ankle)

4 Discussion

The increase of peak ankle plantarflexion angle during push-off of walking with XoSoft was a favorable result as it represents a movement pattern that supports a more dynamic push-off, which is necessary for a dynamic walking pattern [1, 6]. However, the increased movement does not directly translate into more total joint power. Participant 1 is able to generate more power with Beta2 and Gamma. The improvements were between 5 and 22%. Previous work has shown a decrease in joint moment generation of 26–38% in people with iSCI compared to healthy [5]. It can be assumed that XoSoft is able to compensate some of the lost function for participant 1. Participant 3 showed small to no effects with Beta2 and reduced power with Gamma, while participant 2 was able to benefit from Gamma but not Beta2.

The ground reaction force impulse is one determining factor during the push-off as it propels the body forward [2]. The increases in GRF impulse are between 4 and 43%. But, decreases (mainly for Gamma) in the range of 2–11% were also reported. Based on the combination of reported results, no clear trend on which prototype has more promising effects on the walking mechanics can be concluded. Generally, the actuation strategy of XoSoft can influence the push-off during gait positively, however, not for every person. The participants were only given a short amount of time to familiarize with XoSoft. Consequently, walking with XoSoft may have been more of a challenge than support leading to negative effects of XoSoft for some participants.

No clear trend emerged on which approach for garment design is favorable, as participant 2 seemed to benefit more from Gamma, for participant 3 it was Beta2 that resulted in better outcomes (participant 1 with comparable results for Beta2 and Gamma). The design of the garment is essential regarding the functionality of the actuation (anchor points need to be securely fastened to the leg in order to transfer the energy). It may be the individual's characteristics that determine which design results in a better fit and, therefore, a transfer of energy. Overall, the approach of Gamma with non-custom garments seems promising to follow up as it appears to be capable to serve the intended purpose.

5 Conclusion

Overall, it can be concluded that XoSoft has the potential to support the dynamics of gait during push-off. However, there are no consistent findings yet based on the case-series with three participants. A more systematic approach with larger sample size is needed now to determine the detailed effects of XoSoft on gait mechanics.

Acknowledgements This work has received funding from the European Union's Horizon 2020 research and innovation programme under grant agreement No. 688175 (XoSoft).

The authors would like to acknowledge the contribution of the whole XoSoft Consortium to the project and the development of the prototypes.

References

1. R.R. Neptune, S.A. Kautz, F.E. Zajac, Contributions of the individual ankle plantar flexors to support, forward progression and swing initiation during walking. J. Biomech. **34**, 1387–1398 (2001)
2. S.N. Fickey, M.G. Browne, J.R. Franz, Biomechanical effects of augmented ankle power output during human walking. J. Exp. Biol. **221**(22), (2018)
3. E. Desrosiers, C. Duclos, S. Nadeau, Gait adaptation during walking on an inclined pathway following spinal cord injury. Clin. Biomech. **29**(5), 500–505 (2014)
4. A. Pépin, K.E. Norman, H. Barbeau, Treadmill walking in incomplete spinal-cord-injured subjects: 1. adaptation to changes in speed. Spinal Cord **41**(5), 257–270 (2003)
5. A. Jayaraman et al., Lower extremity skeletal muscle function in persons with incomplete spinal cord injury. Spinal Cord **44**(11), 680–687 (2006)
6. G.S. Sawicki, A. Domingo, D.P. Ferris, The effects of powered ankle-foot orthoses on joint kinematics and muscle activation during walking in individuals with incomplete spinal cord injury. J. Neuroeng. Rehabil. **3**(3) (2006)
7. L.N. Awad et al., A soft robotic exosuit improves walking in patients after stroke. Sci. Transl. Med. **9**(400) (2017)
8. V. Power, A. de Eyto, B. Hartigan, J. Ortiz, L.W. O'Sullivan, Application of a user-centered design approach to the development of XoSoft—A lower body soft exoskeleton. Biosyst. Biorobot. **22**, 44–48 (2019), Springer International Publishing
9. J. Ortiz, C. Di Natali, D.G. Caldwell, XoSoft—Iterative design of a modular soft lower limb exoskeleton. Biosyst. Biorobot. **22**, 351–355 (2019), Springer International Publishing
10. G. Wu et al., ISB recommendation on definitions of joint coordinate system of various joints for the reporting of human joint motion—part I: ankle, hip, spine. J. Biomech. **35**, 543–548 (2002)

The Effect of Exoskeletal-Assisted Walking on Bowel and Bladder Function: Results from a Randomized Trial

Peter H. Gorman, Gail F. Forrest, Pierre K. Asselin, William Scott, Stephen Kornfeld, Eunkyoung Hong, and Ann M. Spungen

Abstract A three center randomized controlled crossover clinical trial of exoskeletal-assisted walking (EAW) compared to usual activity (UA) in people with chronic spinal cord injury (SCI) was performed. As secondary outcome measures, the effect of this intervention on bowel and bladder function was assessed using the 10Q Bowel function Survey, the Bristol Stool Form Scale (BFS) and the bowel and bladder components of the Spinal Cord Injury Quality of Life (SCI-QOL) instrument. Fifty subjects were completed the study, with bowel and bladder data available for 49. The amount of time needed for the bowel program on average was reduced in 24% of the participants after EAW. There was a trend toward normalization of stool form noted. There were no significant effects in patient reported outcomes for bowel or bladder function on the SCI-QOL components, although time since injury may have played a role.

P. H. Gorman (✉)
University of Maryland School of Medicine, Baltimore, Maryland, USA

University of Maryland Rehabilitation and Orthopaedic Institute, Baltimore, Maryland, USA

G. F. Forrest
Kessler Foundation, West Orange, NJ, USA

Rutgers New Jersey Medical School-Rutgers University, Newark, NJ, USA

P. K. Asselin · E. Hong · A. M. Spungen
Spinal Cord Damage Research Center, James J. Peters VA Medical Center, Bronx, NY, USA

P. K. Asselin · S. Kornfeld · E. Hong · A. M. Spungen
Icahn School of Medicine at Mount Sinai, New York, NY, USA

W. Scott
VA Maryland Healthcare System, Baltimore, MD, USA

S. Kornfeld
Spinal Cord Injury Service and the Spinal Cord Damage Research Center, James J. Peters VA Medical Center, Bronx, NY, USA

J. C. Moreno et al. (eds.), *Wearable Robotics: Challenges and Trends*,
Biosystems & Biorobotics 27, https://doi.org/10.1007/978-3-030-69547-7_34

1 Introduction

Spinal cord injury (SCI) is well known to adversely affect bowel [1–3] and bladder function [4, 5]. Constipation related to slowed transit time and a sedentary lifestyle is a major issue as is incomplete bladder emptying related to positioning in non-ambulatory individuals. There are some suggestions that frequent upright posture [6] and locomotor training [7] could help bowel function in SCI, but the data is inconclusive [8]. Exoskeletal-assisted walking may be another intervention that could potentially improve bowel and bladder function in this population [9]. We therefore proposed a randomized clinical trial of the effects of 36 sessions of exoskeletal-assisted walking on bowel and bladder function in individuals with chronic non-ambulatory SCI.

2 Materials and Methods

We designed and implemented a three-center randomized crossover controlled clinical trial of exoskeletal-assisted walking (EAW) in non-ambulatory individuals with chronic SCI (>6 months post injury). As secondary outcome measures, we investigated whether this intervention would improve bowel and bladder function as compared to usual activity (UA).

Individuals were screened using a complete history and physical examination incorporating the following: the International Standards for Neurological Classification of SCI (ISNCSCI) examination to determine level and completeness of injury, range of motion at the hips, knees and ankles bilaterally, Ashworth spasticity examination in the lower extremities, standing orthostatic tolerance test, and bone mineral density (BMD) scanning of bilateral knees (proximal tibia and distal femur) and hips (femoral neck and total hip) by Dual Energy X-ray Absorptiometry (DXA).

Eligible participants were randomized within site to one of two groups for 12 weeks (three months): Group 1 received EAW first, three times per week for 12 weeks then crossover (UA) for a second 12 weeks; Group 2 received UA first for 12 weeks then crossover to EAW for 12 weeks of training.

Two powered exoskeleton devices were used in this study, namely the ReWalk 6.0® (ReWalk Robotics, Marlborough, MA) [10] and the Ekso GT® (Ekso Bionics, Richmond, CA) [11]. These powered exoskeletons were chosen because they were the only devices commercially available and FDA approved for use within rehabilitation centers at the time of study development.

Within the first two sessions, standing balance skills were practiced and achieved prior to progression to walking skills. Walking skills were then initiated utilizing a weight shifting pattern. Continuous walking resulted from serial performance of weight shifting. Participants were advanced in their degree of activity and number of steps based on individual progress as determined by the instructing trainer. Missed

sessions were added to the end of the 12 weeks to achieve a 36-session total intervention.

The 10 Question Bowel Function Survey (10Q) and the Bristol Stool Form Scale (BFS) was administered before and after both interventions during the two arms of the study. The 10Q provided patient reported outcomes with regard to bowel program satisfaction including information about the time it took to perform a bowel program as well as the amount of assistance needed. The BFS provided information about stool firmness. The BFS rates stool consistency from 1 (hard to pass) to 7 (watery liquid), where 4 is the desired medium consistency [9]. The Bowel Management and the Bladder Management Difficulties item bank forms from the SCI-QOL instrument were performed three times: at baseline, at crossover, and after the second arm for both the EAW and UA arm interventions. The Bowel SCI-QOL instrument consisted of 26 questions (possible score range 25–130) and the Bladder SCI-QOL of 15 questions (possible score range 15–75). Lower scores indicated greater satisfaction with management.

3 Results

A total of 50 subjects completed the exoskeletal-assisted walking protocol including crossover. Of these, 49 individuals completed the bowel surveys and the BFS.

The 10Q Function survey results specifically related to external assistance needed and bowel evacuation times are presented in Table 1. In looking at the whole group (regardless of randomization order), a portion of patients reported a reduction by 12% in the need for external help and a reduction by 24% in evacuation time during each session and across a full week after the EAW three-month intervention.

Table 1 Selected patient reported outcomes from the 10Q Function Survey. External help included enemas, irrigations, suppositories, oral laxatives or stool softeners, and manual digital stimulation

Category	Frequency reported	Pre EAW (%)	Post EAW (%)	Percent of participants improved (%)
External help needed for each bowel evacuation in the past week	Never to a few times	57	63	12
	Most to every time	41	35	
Average bowel evacuation time needed per bowel day during the past week	5 to 60 min	80	92	24
	>1–3 h	18	6	
Average bowel evacuation time needed in the past week	1–6 h	80	92	24
	>6–8 h	16	6	

The BFS data suggested a slight qualitative improvement (i.e. trend to a medium consistency of 4) after EAW not seen in the UA group, although by chance the UA group tended to do better at baseline (Fig. 1).

Overall, for the whole group, there were no significant effects found for changes in patient-reported outcomes for the Bowel Management Difficulties SCI-QOL survey after EAW when compared to usual activity. This was also true of the Bladder Management Difficulties SCI-QOL survey.

We performed a post hoc sub-analyses based on time since injury, since it was noticed that the newer injured participants (< two years since injury) were often still learning to maximize their bowel management. Stratification by the duration of injury (DOI) sub-categories for outcomes of bowel function showed that those persons injured for more than two years demonstrated an improvement trend in the Bowel Management SCI-QOL survey after EAW (51.0 ± 9.5 pre versus 48.8 ± 10.2 post EAW, $p = 0.1439$). In contrast, the newer injured cohort (DOI <2 y) did not show improvement (48.3 ± 7.6 pre to 48.0 ± 8.3 post).

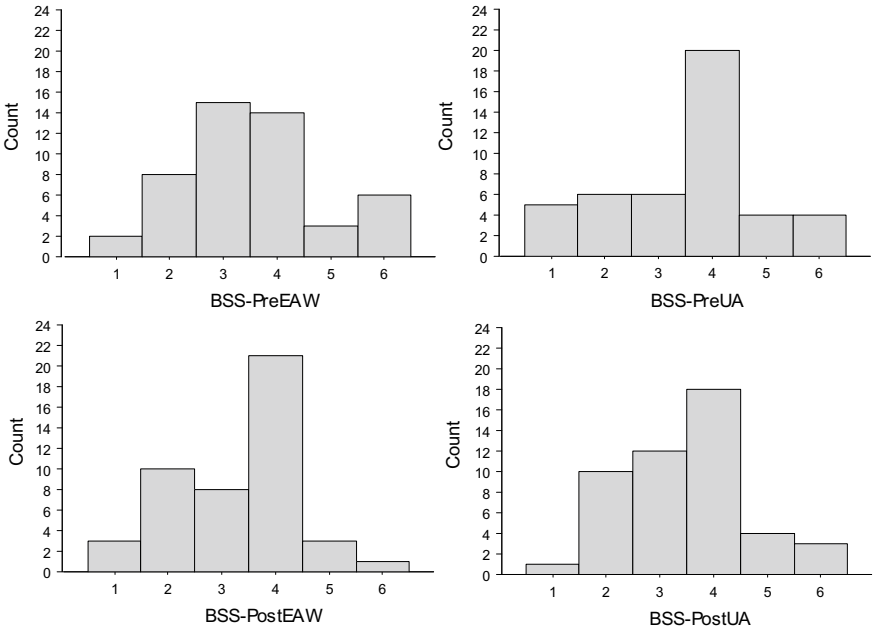

Fig. 1 Bristol Stool Form Scale Results. Frequency distribution of pre and post EAW and pre and Post UA. Top row represents pre and bottom row post data

4 Discussion

EAW training had a positive effect on about one quarter of the participants for the patient-reported outcomes for bowel function and management. There were also trends towards normalization of stool form in the EAW group not seen in the UA group. The Bowel and Bladder SCI-QOL batteries were unable however to detect a significant improvement in patient's perception of their evacuation management with the EAW intervention. Our time since injury sub-analysis suggested that those with newer SCI may still be adjusting and becoming competent with their bowel program, thus negating any potential positive effect from the EAW intervention.

5 Conclusion

A 36-session exoskeletal assisted walking program implemented over three months in non-ambulatory persons with spinal cord injury provided some, albeit limited improvement in several measures of bowel function when compared to a usual activity control group. Most notable improvement (i.e. reduction) was seen in average bowel evacuation time and in a trend to normalization of bowel form consistency. The degree of subjective improvement as determined by quality of life survey instruments may be in part related to the time since injury.

Acknowlegements Supported by the Department of Defense/CDMRP SC130234 Award: W81XWH-14-2-0170 and National Center for the Medical Consequences of SCI (B9212-C, B2020-C) at the James J. Peters VA Medical Center.

References

1. M.A. Korsten, N.R. Fajardo, A.S. Rosman, G.H. Creasey, A.M. Spungen, W.A. Bauman, Difficulty with evacuation after spinal cord injury: colonic motility during sleep and effects of abdominal wall stimulation. J. Rehabil. Res. Dev. **41**(1), 95–100 (2004)
2. J.J. Adriaansen, F.W. van Asbeck, D. van Kuppevelt, G.J. Snoek, M.W. Post, Outcomes of neurogenic bowel management in individuals living with a spinal cord injury for at least 10 years. Arch. Phys. Med. Rehabil. **96**(5), 905–912 (2015)
3. P.M. Faaborg, P. Christensen, N. Finnerup, S. Laurberg, K. Krogh, The pattern of colorectal dysfunction changes with time since spinal cord injury. Spinal Cord. **46**(3), 234–238 (2008)
4. G. Savic, H.L. Frankel, M.A. Jamous, B.M. Soni, S. Charlifue, Long-term bladder and bowel management after spinal cord injury: a 20-year longitudinal study. Spinal Cord. **56**(6), 575–581 (2018)
5. R. Hamid, M.A. Averbeck, H. Chiang, A. Garcia, R.T. Al Mousa, S.J. Oh et al., Epidemiology and pathophysiology of neurogenic bladder after spinal cord injury. World J. Urol. **36**(10), 1517–1527 (2018)
6. J.J. Eng, S.M. Levins, A.F. Townson, D. Mah-Jones, J. Bremner, G. Huston, Use of prolonged standing for individuals with spinal cord injuries. Phys. Ther. **81**(8), 1392–1399 (2001)

7. S.A. Morrison, D. Lorenz, C.P. Eskay, G.F. Forrest, D.M. Basso, Longitudinal recovery and reduced costs after 120 sessions of locomotor training for motor incomplete spinal cord injury. Arch. Phys. Med. Rehabil. **99**(3), 555–562 (2018)
8. J.J. Wyndaele, Does regular standing improve bowel function in people with spinal cord injury? Spinal Cord. **53**(1), 1 (2015)
9. D.B. Fineberg, M.A. Korsetn, P.K. Asselin, W.A. Bauman, N.Y. Harel, A. Spungen, Effect of robotic exoskeleton assisted ambulation on bowel function inpersons with paraplegia: one-month follow-up. J. Spinal Cord Med. **36**, 533–534 (2013)
10. ReWalk [Available from: https://rewalk.com/]
11. Ekso Bionics [Available from: https://eksobionics.com/eksohealth/]

Smartwear with Artificial Intelligence (AI) in Assessing Workload in View of Ergonomics

Pekka Tolvanen, Riitta Simonen, and Janne Pylväs

Abstract Myontec's wearable technology is designed to decrease work based musculoskeletal disorders (MSDs), reduce accidents and sick leaves. Smartwear with embedded muscle activation level (EMG), upper arm elevation and trunk bending, together with wrist watch measuring heart rate apps are used to execute the measurements wirelessly. This smartwear based solution takes biosignal measurements to workplaces and gives results fast and accurate, thus being a cost-effective method for assessing exoskeletons, product design and research.

1 Introduction—Smartwear and Ergo Analysis™ by Myontec Oy

Myontec's wearable technology consists of smart clothing with embedded measurement sensors and devices, synchronized video recording, Windows application ErgoLink and ErgoAnalysis™ Cloud Service, which together construct a platform for data storage, data analysis, reporting and results transfer to the client (Fig. 1).

The ErgoAnalysis™ includes algorithms taking into account validated, scientific recommendations for maximum work physical loading. The technology is patented and scientifically validated and it has been in routine use since 2017 in various industries in Europe [1–3].

2 System, Methods and Use Cases

The ErgoAnalysis™ system and methods are used e.g. for the following uses:

- Ergonomics projects as Service
- Assessing Exoskeletons
- Designing and Assessing Hand Tools

P. Tolvanen (✉) · R. Simonen · J. Pylväs
Myontec Oy, Kuopio, Finland

J. C. Moreno et al. (eds.), *Wearable Robotics: Challenges and Trends*,
Biosystems & Biorobotics 27, https://doi.org/10.1007/978-3-030-69547-7_35

Fig. 1 The ErgoAnalysis™ System comprising of Smart clothes with sensory and mobile app controlling the system and recording video during the work

In future development phase intelligence will be added to the method by utilizing Artificial Intelligence (AI) to the growing database (Fig. 2).

3 Results

3.1 Ergonomics Projects as Worksite Service

Properly designed work will result in better health, quality and cost savings. This should be done by gathering information on how to maximize work quality and optimize workload at worksite.

3.2 Assessing Exoskeletons

Industrial use cases have already been collected on several fields in order to get a view of the complexity in selecting suitable exoskeleton for specific work tasks and conditions [4]. The benefit of exoskeleton reducing work physical loading level can be assessed combing the loading level with and without exoskeleton. In scaffold assembly, physical loading using exoskeleton was 20 and 8% lower compared with the similar work without exoskeleton when lifting in horizontal plane and during the

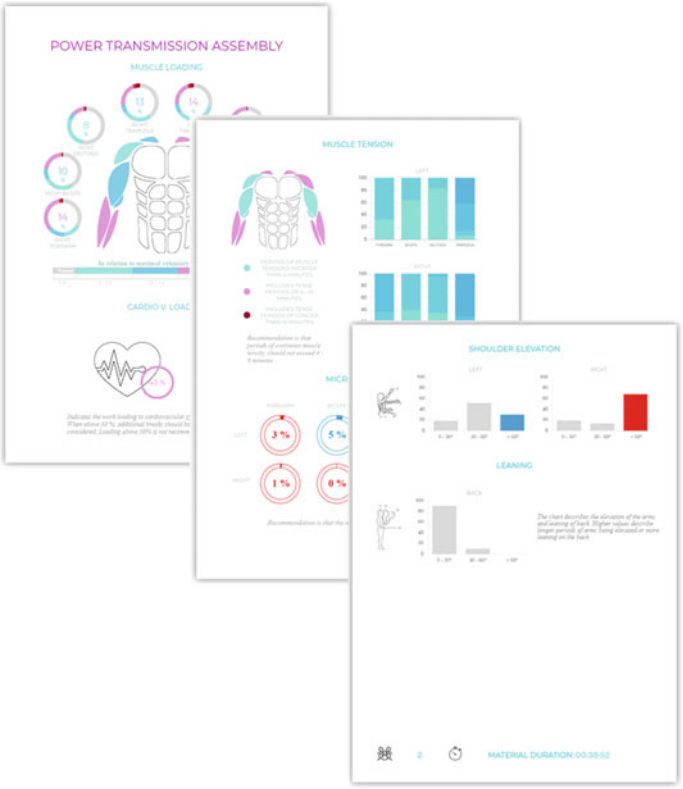

Fig. 2 The ErgoAnalysis™ Report indicating possible muscular and cardiovascular overload, microbreaks and excessive joint angles.

whole 2-h assembly work phase, respectively. Also static muscle loading level was 30% less with exoskeleton use, than without.

In electrician's installation work [5], compared with the work without exoskeleton, the benefit of exoskeleton use in shoulder deltoid muscle loading was considerable (56%) when using maximum exoskeleton support level, whereas with the mid-support level there was no benefit at all. In above shoulder level work the use of exoskeleton may even increase the loading level in forearm muscles (14 and 32% in middle and maximum support setting, respectively), compared to the same work without exoskeleton use (Fig. 3).

3.3 Designing and Assessing Hand Tools

Myontec's ErgoAnalysis™ provides objective data of the ergonomic design of hand-held tools and right end-user technique to use the tool. Comparing alternative product

Fig. 3 Assessing exoskeleton by smartwear system

models and finding out the one with least physical loading as well as positive used experience [6]. Furthermore, the supreme ergonomic feature is also an excellent instrument for marketing purposes.

4 Discussion

Results from ErgoAnalysis™ projects offer better decision making for example to the business owners and HR management. This onsite ergonomic assessment provides fast and accurate way to discover work phases which are predisposing to musculoskeletal disorders, or even reveal occupational safety hazards.

Exoskeleton feasibility studies and case reports will help in selecting suitable exoskeleton model and its adjustments for a given task.

Utilizing the method makes it easier for product developers to optimize the ergonomic features of new products. At best, the ErgoAnalysis™ enhances workers' health, performance, and furthermore, increase work fluency, efficiency and productivity.

4.1 Artificial Intelligence (AI)

Currently, there are ambiguous scientific recommendations for optimal workload thresholds, which are based on general ergonomic settings such as maximum lifting weight, grip force, mean heart rate level, shoulder elevation degree and duration of

static muscle loading. However, the practical application of the recommendations to different work environments requires additional workplace-specific assessment by experienced professionals.

ErgoCloud-database is an extensive digital storage of industry-specific reference data obtained from the ErgoAnalysis™ projects. Artificial Intelligence methods enable reference databases for most common occupations that provide customers with more accurate, comparable, and illustrative information about the workload quickly, easily, and cost-effectively.

5 Conclusion

The solution is made easy-to use so any health, work safety or quality professionals or product developers can do the recordings, run quick results and make beneficial conclusions for their industry and customers.

References

1. P. Tolvanen, Myontec ErgoAnalysis™ in assessing benefits of an Exoskeleton in reducing upper extremity workload, Presentation at ExoBerlin congress October 22–23 (2019)
2. P. Tolvanen, Smart Clothing For Ergonomics Assessment In real working conditions, Presentation at IDTechEx congress in Berlin April 10, (2019)
3. V. Louhevaara, Wearable EMG in the prevention of work-related Musculoskeletal disorders, Presentation at IEA International Ergonomics Association conference August 27. (Florence, Italy, 2018)
4. Article Interviewing Exoskeleton And Wearables Expert Matthew Marino. link https://www.myontec.com/post/interviewing-wearables-and-exoskeleton-expert-matthew-marino
5. R. Simonen, , Myontec ErgoanalysisTM workshop, Presentation at NES-The Nordic Ergonomics and Human Factors Society congress 25–28. August 2019 in (Elsinore, Denmark, 2019)
6. K. Kokkonen, Video presentation regarding tool design by Fiskars Group. link https://www.fiskars.eu/products/gardening/professional-selection Fit for human use–Optimal Ergonomics

Comparison of ReWalk® and Ekso® Powered Exoskeletons for Stepping and Speed During Training Sessions

Pierre K. Asselin, Gail F. Forrest, Stephen Kornfeld, Eunkyoung Hong, Peter H. Gorman, and Ann M. Spungen

Abstract Design attributes specific to the powered exoskeletons contribute to differences in walking performance. As part of a large multicenter trial that used two powered exoskeletons, the design attributes that contribute to the differences in average number of steps per session and walking speed were explored.

1 Introduction

The stepping performance of persons with spinal cord injury (SCI) using a powered exoskeleton to ambulate overground is dependent on many factors. Within-device performance relies on attributes of the individual user such as completeness and level of injury (LOI) [1]. However, performance measures such as walking speed, initial stepping ability and rate of progression also depend on the design of the specific system. The goal of this investigation was to identify differences in walking performance between participants who used two different powered exoskeletons during a

P. K. Asselin (✉) · S. Kornfeld · E. Hong · A. M. Spungen
Spinal Cord Damage Research Center, James J. Peters VA Medical Center, Bronx, NY, USA
e-mail: pierre.asselin@va.gov

Icahn School of Medicine at Mount Sinai (ISMMS), New York, NY, USA

G. F. Forrest
Kessler Foundation, West Orange, NJ, USA

Rutgers New Jersey Medical School-Rutgers University, Newark, NJ, USA

S. Kornfeld
Spinal Cord Injury Service, James J. Peters VA Medical Center, Bronx, NY, USA

P. K. Asselin
Center for the Medical Consequences of Spinal Cord Injury, James J. Peters VA Medical Center, Bronx, NY, USA

P. H. Gorman
University of Maryland School of Medicine, Baltimore, MD, USA

University of Maryland Rehabilitation and Orthopaedic Institute, Baltimore, MD, USA

J. C. Moreno et al. (eds.), *Wearable Robotics: Challenges and Trends*,
Biosystems & Biorobotics 27, https://doi.org/10.1007/978-3-030-69547-7_36

36-session training protocol. Discussion of the different design considerations that may contribute to the difference performance level is provided.

2 Materials and Methods

2.1 Participants

Fifty volunteers with SCI participated in a randomized crossover study with a control phase consisting of 12 weeks of observation and an intervention phase consisting of 12 weeks of exoskeletal assisted walking (EAW). Male and female volunteers were included if they were between the ages of 18–65, SCI $\geq$ 6 months, not community ambulators, height between 160 and 190 cm, weight under 100 kg, and able to hold crutches. They were excluded if they had another neurological condition, concurrent medical illness, fracture in the past two years, bone density by dual-energy x-ray absorptiometry (hip T-score < -3.5 and knee Bone Mineral Density (BMD) $<$ 0.60 g/cm^2), limited range of motion at hip and knee, pressure ulcers, and any other criteria that was felt to be a contraindication to using powered exoskeletons.

2.2 Exoskeleton Training

During the EAW training, two different exoskeletons (ReWalk 6.0® and EksoGT®) were used to train participants to walk for 36 sessions for up to one hour, three times a week. Participants with higher LOI were assigned to use the Ekso device as it provides support for the trunk and those with lower LOI were assigned the use of the ReWalk device. The initial training was focused on teaching the participants basic skills such as standing balance and the mechanism needed to walk using the powered exoskeleton. As the sessions progressed, the focus shifted to walking faster, more independently and over different terrain. The number of steps taken during the training session was recorded. In addition, walking speed was determined during sessions 12, 24 and 36 using a 10 m walk test (10MWT) [2, 3].

2.3 Statistical Analysis

Descriptive statistics were used to report the demographic characteristics of the participants. Total steps taken during training sessions were smoothed using a 5-session moving average. Differences in the smoothed total steps between devices from the sessions were determined using a t-test. Differences in walking speed was

Table 1 Participant demographics

	All	Ekso	ReWalk
Participants (n)	50	22	28
Age (year)	39 ± 14	43 ± 17	35 ± 11
Male/Female (n)	38/12	14/8	24/4
Tetra (n)	14	13	1
High para (n)	24	6	18
Low para (n)	12	3	9
DOI (year)	5 ± 5	3 ± 3	6 ± 6
Motor Complete/Incomplete (n)	31/19	11/11	20/8

assessed using a two-way repeated measure analysis of variance (ANOVA) between devices (Ekso and ReWalk) over three time points (12–, 24–, and 36-session).

3 Results

Participant demographics are presented in Table 1. Of the 50 participants that completed the study, 22 used the Ekso and 28 used the ReWalk. No differences in age or duration of injury (DOI) were found between the device groups. Because devices were assigned to participants according to their LOI, there were a disproportionate number of tetraplegic participants that used the Ekso and a disproportionate number of paraplegic participants that used the ReWalk device.

The Ekso group took significantly more steps during the initial sessions than the ReWalk group (Fig. 1). However, by session 17 the average total number of steps between devices was no longer statistically different.

Sub-group average walking speeds measured during sessions 12, 24 and 36 for each device are presented in Table 2.

4 Discussion

Differences in total steps taken during initial training and walking speed were identified between devices. During earlier sessions, those using the Ekso were able to take significantly more steps than those who used the ReWalk. The Ekso is designed to achieve independent stepping in tiers allowing the user to take a greater number of steps during the initial sessions. Learning to use the Ekso starts in a mode called "First Step" which relies on the trainer to trigger stepping. This enables the trainer to control the device while the user learns how to appropriately shift their weight and maintain their balance prior to taking the next step. The second purpose of "First Step" is to establish the forward and lateral targets for "Prostep" mode. The "Prostep" mode

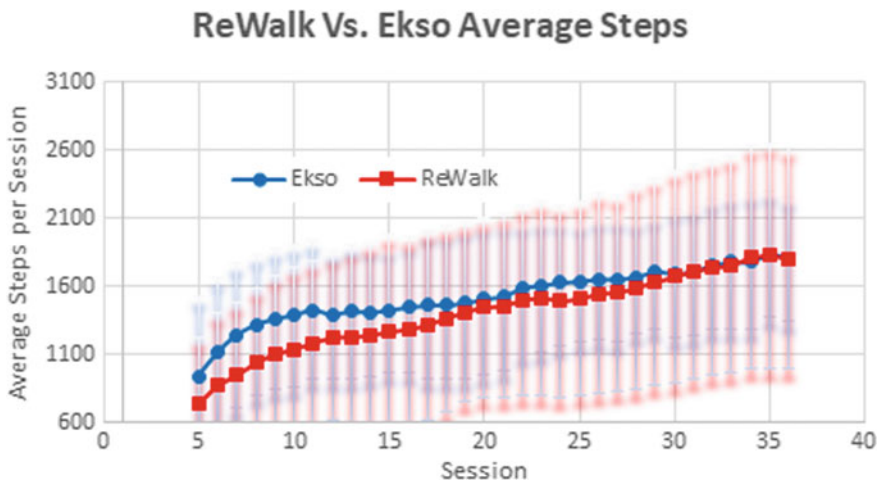

Fig. 1 Five-session moving average of steps taken during training sessions. The blue line and blue shading are the average and standard deviation of steps over 5 sessions for the Ekso. The red line and red shading are the average and standard deviation of steps over 5 sessions for the ReWalk

Table 2 10 MWT walking speeds

Device	Session 12	Session 24	Session 36
Ekso (m/s)	0.21±0.06	0.22±0.06	0.27±0.09
ReWalk (m/s)	0.36±0.09	0.40±0.10	0.42±0.11

automatically triggers the next step when the participant successfully shifts their weight to these predetermined targets.

The ReWalk device is more sensitive to trigger stepping and the trainer needs to add a delay between steps to delay the device from stepping. If the participant does not shift their weight appropriately to clear the foot, causing the device to sense resistance on the swing leg, it will stop walking. This approach requires the trainer to explain how far and how quickly to weight shift in between walking bouts. It is also challenging for some users to understand the mechanism of weight shifting because they do not have the proprioception of where their upper body position is relative to their legs. This leads to a large portion of time during the initial sessions for the trainer to to explain how the system works, how to perform weight shifts, and how to maintain balance using mirrors with verbal cueing. This training requirement ultimately reduces the number of steps achievable during a one-hour training session.

Faster walking speed was achieved with the ReWalk than the Ekso for all time points. Although this may be attributed to the disproportionate difference in the participant's LOI between devices, there is a significant design difference between the devices. The ReWalk forces the person to shift their weight forward onto the contralateral limb immediately after the step was completed. The Ekso's stepping trigger is less sensitive than the ReWalk, allowing the participant to take their time

and remain in double stance for longer periods of time while learning, ultimately reducing the walking speed.

The different device settings that control step length and speed of movement also contribute to walking velocity. Comparisons of device settings is confounded because the settings controlling these parameters are different. The Ekso uses step height, step length and step time parameters. The ReWalk uses hip range and a step speed setting. Further comparisons would be needed to explore how these settings affect the walking speed.

5 Conclusion

Both devices have their strengths and challenges. The Ekso design uses a tiered learning approach. This enabled the user to have an easier time to take steps during the initial sessions, maximizing the number of steps achievable. The ReWalk requires the user to consistently take steps which makes initial use more difficult for some, but ultimately leads to faster walking speeds.

Acknowledgements We would like to thank all the participants and the powered exoskeleton trainers.

Supported by the Department of Defense/CDMRP SC130234 Award: W81XWH-14-2-0170 and National Center for the Medical Consequences of SCI (B9212-C, B2020-C) at the James J. Peters VA Medical Center.

References

1. D.R. Louie, J.J. Eng, T. Lam, Gait speed using powered robotic exoskeletons after spinal cord injury: a systematic review and correlational study. J. NeuroEng. Rehab. **12**(1), 82 (2015)
2. H.J. van Hedel, M. Wirz, V. Dietz, Assessing walking ability in subjects with spinal cord injury: validity and reliability of 3 walking tests. Archiv. Phys. Med. Rehab. **86**(2), 190–196 (2005)
3. E. Hong et al., Mobility skills with exoskeletal-assisted walking in person with sci: results from a three center randomized clinical trial. Front. Robot. AI **7**, 93 (2020)

Indications and Contraindications for Exoskeletal-Assisted Walking in Persons with Spinal Cord Injury

Ann M. Spungen, Peter H. Gorman, Gail F. Forrest, Pierre K. Asselin, Stephen Kornfeld, Eunkyoung Hong, and William A. Bauman

Abstract Adopting appropriate eligibility criteria for research and clinical programs in which powered exoskeletal-assisted walking devices are used remains a challenge to avoid risk of injury and to encourage the successful use of these devices. Reducing the risk of fracture is a primary concern when establishing eligibility criteria. Evidence from a three-site clinical trial supports the use of screening criteria for bone mineral density at the knee to permit safe use of exoskeletal devices.

1 Introduction

Restoration of ambulatory function and the potential for improvement of health due to increased upright mobility has long been a goal of rehabilitation research for those with spinal cord injury (SCI). The use of powered exoskeletons may offer a partial solution to this problem. The establishment of appropriate eligibility criteria remains a challenge to provide the proper balance between inclusion and exclusion in order to avoid risk of injury while concurrently encouraging successful use of these devices. While exclusion criteria for pressure ulcers, limited range of motion at lower extremity (LE) joints, non-modifiable contractures, severe spasticity, and medical health problems were straightforward to implement, exclusion criteria to mitigate the risk of a fragility fracture, especially at the knee, were not so obvious. Existing literature available at time of planning used to develop exclusion criteria

A. M. Spungen (✉) · P. K. Asselin · S. Kornfeld · E. Hong · W. A. Bauman
Spinal Cord Damage Research Center, James J. Peters VA Medical Center, Bronx, NY, USA
e-mail: ann.spungen@va.gov

Icahn School of Medicine at Mount Sinai (ISMMS), New York, NY, USA

P. H. Gorman
University of Maryland School of Medicine, University of Maryland Rehabilitation and Orthopaedic Institute, Baltimore, MD, USA

G. F. Forrest
Kessler Foundation, West Orange, NJ, USA

Rutgers New Jersey Medical School-Rutgers University, Newark, NJ, USA

J. C. Moreno et al. (eds.), *Wearable Robotics: Challenges and Trends*,
Biosystems & Biorobotics 27, https://doi.org/10.1007/978-3-030-69547-7_37

was limited to work by Garland et al. that reported those at increased risk of fracture by knee bone mineral density (BMD) obtained by dual-energy x-ray absorptiometry (DXA) [1, 2]. We are proposing that the inclusion/exclusion criteria used for this study support the safe use of exoskeletons for hospital-based training.

2 Materials and Methods

A three-site, randomized (for order of intervention or control arm), crossover clinical trial was conducted with 12 weeks of exoskeletal-assisted walking (EAW) as the intervention arm and 12 weeks of usual activity (UA) as the control arm. Two exoskeletal devices were available for use by participants (ReWalk 6.0® and Ekso GT®). The criteria for the choice of device for each participant has been reported previously [3]. Participants with SCI were included who were non-community ambulators, duration of injury > 6 months, age 18–65 years, able to hold Loftstrand crutches or a walker, weight < 100 kg, and height between 160–190 cm. Medical and safety exclusion criteria were also applied; a complete list of the eligibility criteria can be found at clinicaltrials.gov NCT02314221. The risk of fragility fracture was a major consideration in study design. A fragility fracture was defined as "a low impact fracture that may occur under conditions such as, but not limited to, a fall from a seated position, during stretching or crossing one's legs, during a transfer, bumping the lower extremity, dropping a foot to the ground, a light object falling on a lower extremity body part, carrying someone or something in one's lap, or any fracture that occurred without the knowledge of its occurrence." To reduce the risk of fragility fracture during EAW, DXA scans were performed at the hip and knee. Participants were excluded who had a hip T-score < -3.5 or a knee BMD < 0.60 gm/cm^2. No criteria exist for BMD of the feet. An unhealed high impact LE fracture or any fragility or low impact fracture of the LE since SCI.

3 Results

Fifty participants completed the 36 EAW sessions. A full description of the participants demographic characteristics by exoskeleton used for training are previously reported [3].

Of the 104 consented participants to screening, 33 were screen failures: 16 for knee BMD, eight for schedule conflicts, four for contractures, three for weight or level of SCI, and two for medical complications. Seventy-one participants were randomized; 21 had an early withdrawal (11 for compliance, seven with medical problems (two related, two possibly, three unrelated to study participation), two for schedule conflicts, and one who lost interest. There were eight serious adverse events (SAE); four were possibly related and four were unrelated to study participation. Six of the eight SAEs were resolved with the participants returning to complete the study.

One participant was discontinued from the study because of an unrelated knee fracture due to a fall during vehicle transport and one for a possibly related medial malleolus fracture after the 2nd session. Most adverse events (AE) (41 of 75) were related to skin abrasion from contact with the devices; these occurred early in the course of the study and were minimized with the gain of experience to more properly fit the participants in the devices. There were 19 AEs for musculoskeletal/edema issues (four unrelated, seven possibly, eight related), six falls (four unrelated, two related, but no injuries), four urinary tract infections (unrelated) and four medical issues (unrelated); 70 of 75 AEs were satisfactorily resolved with the participants continuing in the study. Two participants were withdrawn due to shoulder or knee pain (both related), two were withdrawn due to medical problems (unrelated), and one was withdrawn due to a calcaneal fracture (possibly related) after the 4th EAW session without trauma or fall. Both fractures were reported to be of indeterminate age, possibly representing pre-existing conditions that were undiagnosed. Because of the occurrence of the medial malleolus and calcaneal fractures, bilateral foot x-rays were added to the screening procedures to rule out potentially undiagnosed foot fractures. More than 50% of the participants achieved successful mobility and walking skills by 12 sessions and more than 75% by 36 sessions [3]. Successful achievement of the EAW skills was not dependent on device or level/completeness of injury [3].

4 Discussion

Although two participants may have had foot fractures from weight bearing and stepping in an exoskeleton, the 50 participants who successfully completed the study without fracture lend to support the use of the exclusion criteria that were chosen for this study, which included knee BMD, hip T-score, bilateral foot x-rays, and fracture history. Subsequent to the development of these criteria, two studies have been reported that also support the use of a knee BMD of < 0.60 cm^2 [4, 5]. It is important to note that during the sit-to-stand maneuver in an exoskeleton the forces at the knee are greater than during weight bearing while walking and, thus, of greater concern for risk of fracture.

Excluding those with pre-existing, undiagnosed foot fractures from participation is critical for preventing additional fracture complications as a result of weight bearing during EAW. Several case reports have detailed fractures during EAW [6–9]. Bass et al. reported bilateral ankle swelling after the first EAW session; computed tomography (CT) scan revealed bilateral calcaneal fractures without their age reported [6]. In a report by Benson et al. a participant was found to have a swollen ankle after the fourth exoskeletal walking session with magnetic resonance imaging identifying a hairline fracture of the talus [7]. Two cases of fracture were reported by van Herpen et al. [9]; one exoskeleton user had a left tibia fracture "during standing from the ground after a graceful collapse" [9]; the other had a fracture reported after the fifth training session when ankle swelling was noted and "radiography revealed a fracture of the distal tibia at the tibial plateau with damage of the subchondral bone

[9]." Similar to our foot fractures, in all three reports, swelling was noted early during training and imaging revealed fractures in the feet. Neither of the two foot fractures observed in this investigation, and none of the four reported from the cited literature were the result of trauma but appeared to be caused by simply weight bearing during standing and stepping in the exoskeletal devices. It is quite possible that persons with SCI may have pre-existing and undiagnosed foot fractures. In the past, standard of care for bilateral ankle or foot swelling consisted of elevation of the affected leg or, if unilateral edema was present, a duplex venous ultrasound of the affected leg to rule out deep venous thrombosis, but a foot x-ray was not routinely obtained. As such, there may be an indeterminate prevalence of undiagnosed foot fractures in the SCI population. Because there are no DXA standards for measuring BMD of the feet, in addition to the screening criteria for the hip and knee BMD, we are recommending bilateral x-rays or CT scans of the feet prior to initiating EAW to identify any occult prior foot fractures that would predispose to recurrent fractures during normal weight bearing while using a powered exoskeleton.

5 Conclusion

Persons with non-ambulatory SCI, if screened appropriately for BMD at the knee and other select skeletal criteria, appear to be able to safely participate in EAW. However, additional work is required to develop more accurate criteria for preventing or reducing the risk of fracture, as well as to maximize participation in EAW to achieve greater mobility and improved health. Clinicians should be vigilant during hospital-based training programs for any AEs yet unappreciated that may result from participation in EAW.

Acknowledgements Supported by the Department of Defense/CDMRP SC130234 Award: W81XWH-14-2-0170 and National Center for the Medical Consequences of SCI (B9212-C, B2020-C) at the James J. Peters VA Medical Center.

References

1. D. Garland, R. Adkins, Bone loss at the knee in spinal cord injury. Topics Spinal Cord Injury Rehab. **6**(3), 37–46 (2001)
2. D. Garland, R. Adkins, V. Kushwaha, C. Stewart, Risk factors for osteoporosis at the knee in the spinal cord injury population. J. Spinal Cord Med. **27**(3), 202–206 (2003)
3. E. Hong et al., Mobility skills with exoskeletal-assisted walking in person with sci: results from a three center randomized clinical trial. Front. Robot. AI **7**, 93 (2020)
4. D. Lala et al., Exploring the determinants of fracture risk among individuals with spinal cord injury. Osteoporosis Int. **25**(1), 177–185 (2014)
5. C. Tan et al., Adiponectin is associated with bone strength and fracture history in paralyzed men with spinal cord injury. Osteoporosis Int. **25**(11), 2599–2607 (2014)

6. A. Bass, S. Morin, M. Vermette, M. Aubertin-Leheudre, D. Gagnon, Incidental bilateral calcaneal fractures following overground walking with a wearable robotic exoskeleton in a wheelchair user with a chronic spinal cord injury: is zero risk possible?, Osteoporosis Int.1–5 (2020)
7. I. Benson, K. Hart, D. Tussler, J.J. van Middendorp, Lower-limb exoskeletons for individuals with chronic spinal cord injury: findings from a feasibility study. Clinical Rehab. **30**(1), 73–84 (2016)
8. Y. He, D. Eguren, T. P. Luu, J. L. Contreras-Vidal, Risk management and regulations for lower limb medical exoskeletons: a review. Medical devices, vol. 10 (Auckland, NZ, 2017) pp. 89
9. F. van Herpen, R. van Dijsseldonk, H. Rijken, N. Keijsers, J. Louwerens, I. van Nes, Case Report: description of two fractures during the use of a powered exoskeleton. Spinal Cord Series and Cases **5**(1), 1–4 (2019)

The Impact of Exoskeletal-Assisted Walking on the Immune System of Individuals with Chronic Spinal Cord Injury (SCI)

Anthony A. Arcese, Ann M. Spungen, and Ona Bloom

Abstract Persons with chronic spinal cord injury (SCI) are at increased risk for stroke and cardiovascular disease (CVD). Systemic inflammation is commonly observed in persons with SCI and is inversely correlated with mobility. In the general population, light-moderate intensity exercise such as walking reduces risk of stroke, CVD and reduces systemic inflammation. Powered exoskeletons for persons with SCI offer a means to provide physical activity through overground ambulation. It is currently unclear if, and to what extent, exoskeletal-assisted walking (EAW) leads to health benefits associated with walking. A pilot case series was performed to determine if EAW impacts whole blood gene expression in persons with chronic SCI.

1 Introduction

Spinal cord injury (SCI) resulting in paralysis leads to drastically reduced mobility. Finding treatments to help lessen impacts of immobilization is important for the health of persons with SCI. Adults are advised by the American Heart Association to maintain general health by performing 2.5 h of moderate intensity aerobic exercise and at least 2 days of muscle-strengthening exercise per week.

Acute exercise triggers anti-inflammatory signals from muscles that help to improve strength. Consistent exercise leads to weight loss and fat is a strong source of inflammatory signals [1]. Physical activity also modifies relative proportions and

A. A. Arcese · O. Bloom (✉)
Feinstein Institutes for Medical Research, Feinstein Institutes for Medical Research, Manhasset, NY, USA

A. M. Spungen
Icahn School of Medicine at Mount Sinai, NY, USA

A. M. Spungen · O. Bloom
James J. Peters VA Medical Center, Bronx, NY, USA

O. Bloom
Zucker School of Medicine at Hofstra Northwell, Hempstead, NY, USA

J. C. Moreno et al. (eds.), *Wearable Robotics: Challenges and Trends*,
Biosystems & Biorobotics 27, https://doi.org/10.1007/978-3-030-69547-7_38

biological activities of circulating white blood cells, including reducing expression and signaling of Toll like Receptors [2]. In persons with SCI, mobility correlates inversely with inflammation [3]. Unfortunately, persons with SCI are often unable to do upright activity/exercise or walking and/or do not have regular access to adaptive sports or gym equipment. Powered exoskeletons are a relatively new type of technology to enable walking by persons with SCI. The US Centers for Medicare and Medicaid just approved a billing code for the ReWalk powered exoskeleton. Recent data suggests that for persons with SCI, walking with assistance from an exoskeleton is a light-to-moderate intensity physical activity [4–7]. Several groups are investigating if exoskeletal-assisted walking (EAW) provides health benefits similar to walking in able-bodied persons. The aim of this pilot case series was to determine if EAW (36 sessions) has an impact on whole blood gene expression in persons with chronic SCI.

2 Materials and Methods

Six adults (n = 3 males) in a phase III randomized controlled clinical trial (NCT02314221) were studied. The participant median age was 47.5 years (32.75 IQR, range 22-69 years). The median time after SCI was 3.2 years (10.37 IQR, range 0.5-27 years). Neurological levels of injury were: one each at C4, C5, T3, and T10 and two at T4. AIS grades were: two each for A and B, and one each for C and D. Three participants used the Ekso and three participants used the ReWalk exoskeletons.

Blood was obtained before and after 36 sessions of EAW. Blood samples were also obtained from uninjured (CTRL) participants (n = 2 males, 1 female; ages 63, 64, and 66, respectively, from a convenience sample). RNA was extracted, RNA Sequencing (RNA-Seq) libraries were created with KAPA RNA Hyperprep Kits (Roche), and 100 base pair paired-end reads were collected on the NextSeq Illumina platform (Cold Spring Harbor Laboratories Genome Center). Trimmed reads were aligned using STAR to the human genome (hg38) assembly, filtered for expression ≥ 50, normalized (TMM) and log2 transformed (Partek Genomics Flow, St. Louis, MO). Principal component analysis (PCA) was used to examine overall variation in gene expression profiles using default settings (9 components) for SCI pre-samples compared to CTRL individuals (Partek). Differentially expressed (DE) genes were identified with a fold change ≥ 2, using gene set enrichment analysis (GSA) between groups (SCI pre vs. CTRL) or within SCI participants (Post vs. Pre), using the step-up method of Benjamini-Hochberg to correct p-values with a false discovery rate (FDR) ≤ 0.05. For gene symbols present more than once (multiple transcripts), the transcript with the smallest P-value was used for functional analysis performed using *Enrichr*, a bioinformatics platform [8, 9].

3 Results

Participants who completed the parent RCT demonstrated improvements in the primary outcome measures of faster completion time in the Timed Up and Go and the six-minute walk tests test [10]. Total body mass changes ranged from-1.5 to + 7.4 kg after 12 weeks of EAW.

The first question examined was: How distinct are whole blood gene expression profiles in persons with SCI before EAW training compared to CTRLs? Major variations in gene expression determined by PCA were demonstrated, with > 50% of the total variation explained by the first 2 components (Fig. 1). Functions of the top 500 genes (component loadings) combined from PC1 and PC2 each were analyzed using the PANTHER bioinformatics platform. The 3 pathways enriched with smallest p-values were: mannose metabolism, p38 MAP kinase and Toll receptor signaling, reflecting previous studies [1, 11]. GSA identified 3,814 unique DE genes: 1,286 were down- and 2,528 were up-regulated in persons with SCI before EAW. Among upregulated DE genes, the PANTHER platform again identified the pro-inflammatory Toll receptor signaling pathway, which is essential for pathogen sensing and promotes inflammation, as enriched with the smallest p value ($p = 6.01E\text{-}05$). Among down-regulated DE genes, PANTHER identified epidermal growth factor receptor (EGFR) signaling, a protein tyrosine kinase with many cellular functions, as the pathway with the smallest p value.

The second question examined was: How does EAW influence whole blood gene expression? The number of DE genes varied widely among participants and was: 68, 783, 361, 1, 9, and 67 genes, respectively. Within participants, there was no significant correlation between number of DE genes and change in body mass (Spearman $r = -0.08$). Volcano plots (Fig. 2) show differential gene expression for participants 2 and 3, who had the most DE genes. There were 238 (211 up- and 27 down-regulated) DE genes common among them. Among the top 5 pathways identified by the PANTHER platform enriched in the upregulated common genes were angiotensin-II stimulated

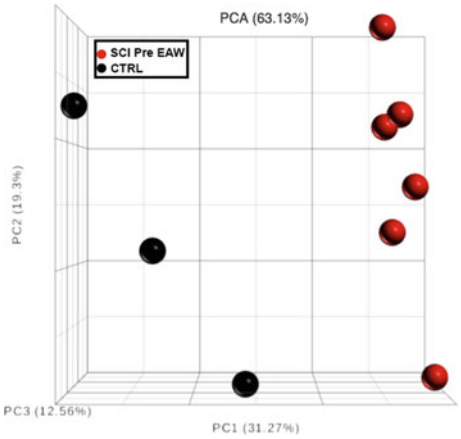

Fig. 1. Principal components analysis of whole blood gene expression profiles of individuals with SCI (n = 6, red) before EAW training and controls (able-bodied) individuals (n = 3, black). PCA shows that the first two components explain 50.6% of variation in gene expression among participants (n = 33,189 filtered transcripts)

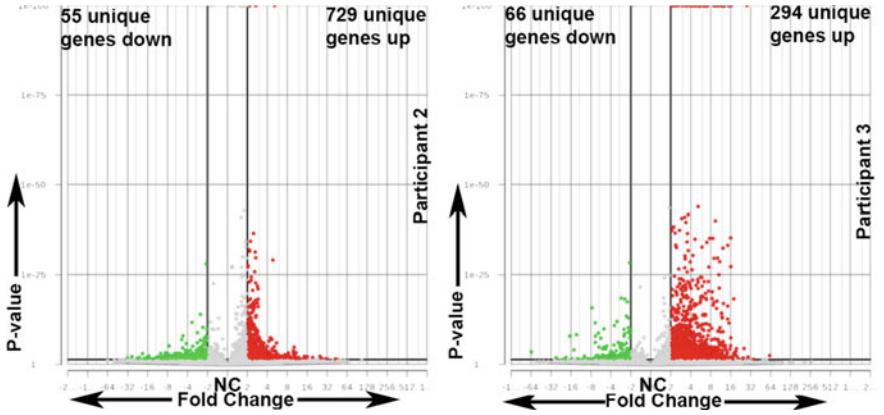

Fig. 2. Differential gene expression after EAW in the two most affected SCI participants. Dots represent gene transcripts: red (up-), green (down-) regulated after vs. before 36 sessions of EAW. Criteria for differential gene expression: FDR ≤ 0.05, fold change ≥ 2

signaling through G proteins ($P < 0.00002$), integrin signaling ($P < 0.0002$), and interleukin signaling ($P < 0.0003$). Common downregulated genes, REACTOME identified the histamine H2 receptor mediated signaling ($P < 0.01$) as the pathway with the smallest p-value.

4 Conclusions

This case series examined whole blood gene expression in persons with chronic SCI before and after 36 sessions of EAW. Compared to CTRLs, persons with SCI had increased inflammatory gene expression, in agreement with previous findings [1, 10]. Gene expression was highly variable among participants in response to EAW in this pilot case series. Larger studies are needed to determine if EAW can have consistent effects on gene expression.

Acknowledgements This work was supported by the DOD CDMRP (#11501823, SCI130234) to AS and the NY State Spinal Cord Injury Research Board (to OB and AS).

References

1. O. Bloom, P.E. Herman, A.M. Spungen, Systemic inflammation in traumatic spinal cord injury. Exp. Neurol. **325**, 1131–43 (2020). https://doi.org/10.1016/j.expneurol.2019.113143
2. M. Gleeson, B. McFarlin, M. Flynn, Exercise and toll-like receptors. Exerc. Immunol. Rev. **12**, 34–53 (2006). Available https://www.ncbi.nlm.nih.gov/pubmed/17201071

3. L.R. Morse et al., Association between mobility mode and C-reactive protein levels in men with chronic spinal cord injury. Arch. Phys. Med. Rehab. **89**(4), 726–731 (2008)
4. P. Asselin et al., Heart rate and oxygen demand of powered exoskeleton-assisted walking in persons with paraplegia. J. Rehab. Res. Dev. **52**(2), 147–158 (2015)
5. C.-Y. Tsai, P.K. Asselin, S. Knezevic, N.Y. Harel, S.D. Kornfeld, A.M. Spungen, The effect of exoskeletal-assisted walking training on seated balance—a pilot study. in *2017 International Symposium on Wearable Robotics and Rehabilitation (WeRob)*, November 2017, pp. 1–2. https://doi.org/10.1109/werob.2017.8383818
6. N. Evans, C. Hartigan, C. Kandilakis, E. Pharo, I. Clesson, Acute cardiorespiratory and metabolic responses during exoskeleton-assisted walking overground among persons with chronic spinal cord injury. Top Spinal Cord Inj. Rehab. **21**(2), 122–132 (2015)
7. A. Ramanujam et al., Mechanisms for improving walking speed after longitudinal powered robotic exoskeleton training for individuals with spinal cord injury. Conf. Proc. IEEE Eng. Med. Biol. Soc. **2018**, 2805–2808 (2018)
8. E.Y. Chen et al., Enrichr: interactive and collaborative HTML5 gene list enrichment analysis tool. BMC Bioinf. **14**, 128 (2013)
9. P. Herman, A. Stein, K. Gibbs, I. Korsunsky, P. Gregersen, O. Bloom, Persons with chronic spinal cord injury have decreased natural killer cell and increased toll-like receptor/inflammatory gene expression. J. Neurotrauma **35**(15), 1819–1829 (2018)
10. E. Hong et al., Mobility skills with exoskeletal-assisted walking in persons with SCI: results from a three center randomized clinical trial. Front. Robot. AI **7**, 93 (2020)
11. P.E. Herman, O. Bloom, Altered leukocyte gene expression after traumatic spinal cord injury: clinical implications. Neural Regen. Res. **13**(9), 1524–1529 (2018)

Exoskeleton Controller and Design Considerations: Effect on Training Response for Persons with Spinal Cord Injury

Gail F. Forrest, Peter H. Gorman, Arvind Ramanujam, Pierre K. Asselin, Steven Knezevic, Sandra Wojciehowski, and Ann M. Spungen

Abstract The objective of this research was to identify variables (demographic, device, neurological, clinical, and training session dose) that were associated with results of the ten-minute walk test (10MWT) for individuals with a spinal cord injury (SCI) who participated in a large randomized crossover clinical trial of exoskeletal walking. Fifty individuals were randomized into Group AB or BA (A = exoskeleton intervention arm, B = control arm). A generalized linear mixed model was applied to model 10MWT and found that a training dose of 36 sessions and gender were the most significant. These variables were more significant than neurological level of injury or completeness of injury. Understanding the effects of exoskeleton/human interface for different devices is crucial for identifying suitable candidates to use the device and developing effective/efficient clinical training protocols for community ambulation, rehabilitation, and recovery post-SCI.

1 Introduction

The determinants of the exoskeleton/human interface that influence gait speed are especially relevant when using powered robotic devices for rehabilitation of function and community ambulation [1]. The device interface and user interaction needs to

G. F. Forrest (✉) · A. Ramanujam
Kessler Foundation, West Orange, NJ, USA
e-mail: gforrest@kesslerfoundation.org

P. H. Gorman
University of Maryland School of Medicine, University of Maryland, Baltimore, MD, USA

University of Maryland Rehabilitation and Orthopaedic Institute, University of Maryland, Baltimore, MD, USA

S. Wojciehowski
PEAK Center at Craig Hospital, Englewood, CO, USA

P. K. Asselin · S. Knezevic · A. M. Spungen
James J. Peters Veterans Affairs Medical Center, Bronx, NY, USA

J. C. Moreno et al. (eds.), *Wearable Robotics: Challenges and Trends*,
Biosystems & Biorobotics 27, https://doi.org/10.1007/978-3-030-69547-7_39

accommodate individuals with different levels of a spinal cord injury (SCI), associated with different levels of impaired motor and sensory function [1]. Several studies have evaluated the biomechanical and neural effects of exoskeletal training on kinematic and biomechanical training variables among different devices and evaluated the gains in speeds and distance [2, 3]. However, there is minimal research evaluating the exoskeleton/human interface effect on exoskeleton ambulation. This study's main aim was to determine the most significant determinants (Table 2) associated with the exoskeleton assisted gait speed after exoskeleton training.

2 Materials and Methods

2.1 Participant Demographics and Training Protocol

Fifty individuals with SCI participated in a randomized crossover clinical trial consisting of an intervention phase (12 weeks, 36 sessions) of exoskeletal assisted walking and a within-group control phase (12 weeks of observation, usual activity) [4]. Randomization determined group assignment: Group AB (intervention phase followed by control phase) and Group BA (control phase followed by intervention phase). The ambulatory performance outcome collected after 12, 24, and 36 exoskeleton training sessions was ten-meter walk test (10MWT, secs). Participants were included if they were between ages 18-65, SCI $\geq$ 6 months, unable to ambulate, height between 160-190 cm, weight < 100 kg, and able to hold crutches. Individuals were excluded if there was another neurological condition, concurrent medical illness, lower extremity fracture in the past two years, bone density by dual-energy x-ray absorptiometry less than criteria (hip T-score < -3.5 and knee BMD < 0.60 g/cm^2), limited range of motion at hip and knee, pressure ulcers, and other criteria felt to be a contraindication to using powered exoskeletons.

2.2 Exoskeleton Training

During exoskeleton training, two different exoskeletons (ReWalk 6.0®, ReWalk Robotics, Inc., Marlborough, MA and EksoGT®, Ekso Bionics, Richmond, CA) were used to train participants to walk for 36 sessions (up to 1 h). Participants with higher level of injury (LOI) were assigned to the EksoGT device as it provides greater support for the trunk; those with lower LOI were assigned to the ReWalk device.

2.3 Variables of Interest—Statistical Analysis

Descriptive statistics were computed, i.e. mean and standard deviation (SD) for normally distributed continuous variables, median and inter-quartile (IQ) range for nonnormally distributed continuous variables, and number of participants and percentages for categorical variables. For group comparison, t-test was applied for normally distributed continuous variables, while Kruskal-Wallis rank sum test was used for continuous variables whose normality assumption were violated; chi-square tests were applied for categorical variables. Generalized linear mixed model (GLMM) was applied to model repeatedly measured 10MWT, considering potential correlation within subjects. Gamma distribution with random intercept was assumed for 10MWT. Covariates considered in the model included age, group, gender, race, device, LOI (paraplegia versus tetraplegia), and duration of injury.

3 Results

3.1 Descriptive Comparisons

Table 1 shows group-wise descriptive characteristics & statistics. No significant differences exist between groups.

3.2 Velocity Comparisons

Figure 1 shows the group-wise distribution of the 10MWT measurements at 12, 24, and 36 sessions. The GLMM applied to model repeatedly measured 10MWT, with covariates. Residual plots suggest no heterogeneity in variance. Table 2 shows parameter estimates from the model for 10MWT. Type of device is the most significant variable associated with 10MWT. EksoGT ambulation was slower than ReWalk at all time points. Number of sessions was the next variable to be significantly associated with 10MWT after adjusting covariates, but only after 36 sessions (Table 2). There was a significant increase in 10MWT velocity at 36 compared to 12 and 24 sessions, but not at 24 sessions compared to 12 (Table 3). Females had significantly lower 10MWT velocity than male subjects, and subjects with ReWalk had significantly greater 10MWT velocity than those with EksoGT. The effect of group was not significant.

Table 1 Descriptive Statistics

		Group AB	Group BA	p
n		26	24	
Male (%)		18 (69.2)	20 (83.3)	0.404
LOI% (3 cat)		High Para, Low Para, Tetra		0.331
LOI% (4 cat)		High Para/Tetra, Low Para/Tetra		0.192
ReWalk (%)		11 (42.3)	17 (70.8)	0.081
Neur Def (%)	C.Para	14 (53.8)	13 (54.2)	0.866
	C.Tetra	3 (11.5)	1 (4.2)	
	IC.Para	4 (15.4)	5 (20.8)	
	IC.Tetra	5 (19.2)	5 (20.8)	
AIS (%)	A	10 (38.5)	11 (45.8)	0.556
	B	7 (26.9)	3 (12.5)	
	C	5 (19.2)	4 (16.7)	
	D	4 (15.4)	6 (25.0)	
Mean (SD)				
Age (y)		38.27 (13.31)	39.12 (15.28)	0.833
HT baseline (in)		67.96 (4.41)	69.21 (3.64)	0.283
Total Steps		52369.4 (17649.7)	49651.7 (18306.7)	0.596
Avg. Steps		1454.71 (490.27)	1383.38 (499.28)	0.613
[Median, IQR]				
10MWT Velocity (m/s) 12		0.25 [0.20, 0.31]	0.31 [0.24, 0.40]	0.156
10MWT Velocity (m/s) 24		0.23 [0.19, 0.38]	0.34 [0.28, 0.45]	0.038
10MWT Velocity (m/s) 36		0.30 [0.25, 0.36]	0.39 [0.31, 0.48]	0.062
DOI:y		3.00 [1.12, 5.75]	2.50 [1.00, 6.00]	0.807
LOI: (3 Cat)		11.00 [7.25, 12.00]	11.50 [8.25, 17.25]	0.488

LOI: Level of Injury; 3 CAT = Cervical, Thoracic, lumbar; C: Complete; IC: Incomplete; AIS: ASIA Impairment Scale [4]; HT: Height; DOI: Duration of Injury; Neur Def, Neurological Deficit

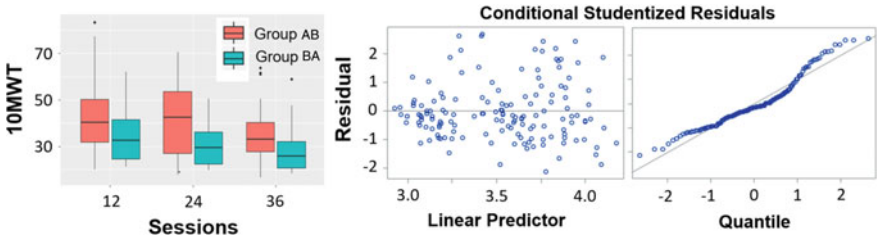

Fig. 1 Boxplot of measured 10MWT at different sessions (12, 24, 36) and Conditional residual plots

Table 2 Parameter Estimates From Model for 10MWT (secs)

Effect	Level	Est.	SE	t	Pr > |t|
Intercept		3.4901	0.112	31.19	<.0001
Age		0.0028	0.002	1.79	0.0755
DOI (y)		−0.0030	0.004	−0.77	0.4426
Group	Group AB versus BA	0.04429	0.041	1.09	0.2796
Gender	Female versus Male	0.1512	0.052	2.93	0.004
Device	Ekso versus ReWalk	0.572	0.059	9.77	<.0001
Sessions	24	−0.0904	0.089	−1.01	0.3137
	36	−0.3124	0.089	−3.5	0.0006
LOI	Para*Tetra	0.1490	0.097	1.54	0.1262
Sessions* LOI	Para*Tetra24	−0.0319	0.110	−0.29	0.7731
	Para*Tetra36	0.1546	0.110	1.40	0.1631
NeurDef	C*IC	0.1037	0.115	0.90	0.3705
Sessions* NeurDef	C*IC24	0.0640	0.102	0.63	0.5311
	C*IC36	0.0250	0.102	0.25	0.8065

C: Complete; IC: Incomplete; DF (Degrees of Freedom) = 131
LOI: Level of Injury; DOI: Duration of Injury; Neur Def: Neurological Deficit

Table 3 Pairwise difference in LS means of 10MWT(secs)

Session Pair	Est.	SE	t	Pr > |t|	Adj P
24*36	0.1483	0.0498	2.98	0.0035	0.0104
24*12	−0.0743	0.0498	−1.49	0.1383	0.4149
36*12	−0.2226	0.0498	−4.47	<.0001	<.0001

DF (Degrees of Freedom) = 131

4 Discussion

The research determined that the most significant variables influencing 10MWT were the device, number of sessions, and gender. Walking velocity during the session 24 assessment was not significantly faster. However, after 36 sessions, there was a significant increase in walking velocity compared to 12 and 24. Potentially, this significant increase in velocity was due to the ReWalk participants, as acquiring skill is prolonged for the ReWalk device. More sensitive analyses are required to identify the principal components or main independent variables that determine exoskeleton gait velocity. Surprisingly, neurological parameters including the LOI and level of completeness were not associated with walk velocity.

5 Conclusion

The method described in this report identifies the variables relevant to exoskeleton/user control for gait speed. Future work using this technique could be applied to other ambulation measures (six minute walk test, timed up and go) and examine dependent variables associated with recovery outside of the device.

Acknowlegements Research supported by Department of Defense/CDMRP SC130234 Award: W81XWH-14-2-0170.

References

1. J.R. Koller et al., Comparing neural control and mechanically intrinsic control of powered ankle exoskeletons. IEEE Int. Conf. Rehab. Robot. **2017**, 294–299 (2017). https://doi.org/10.1109/ICORR.2017.8009262
2. A. Ramanujam, et.al., Neuromechanical adaptations during a robotic powered exoskeleton assisted walking session. J. Spinal Cord Méd. **41**(5), 518–528 (2018)
3. G.F. Forrest et al., in *Muscle Changes After Exoskeleton Training*. ISCOS, (Dublin, Ireland, 2017)
4. E. Hong et'al., Results from a three center randomized clinical trial. Front. Robot. AI **7**(93) (2020)

Neuromechanical Modelling and Control for Wearable Robots: Enhancing Movement After Neuromuscular Injuries

Neuromusculoskeletal Model-Based Controller for Voluntary and Continuous Assistance in a Broad Range of Locomotion Tasks

Guillaume Durandau, Wolfgang Rampeltshammer, Herman van der Kooij, and Massimo Sartori

Abstract Neuromusculoskeletal modeling driven by electromyograms (EMG) has shown the ability to predict joint torque for a wide variety of movements. Taking advantage of this, we connected a real-time version of an EMG-driven model to a bilateral ankle exoskeleton to continuously assist during a wide repertory of locomotion tasks. The advantage is that the user controls the exoskeleton voluntarily, i.e. as a direct function of own muscle force. As a result, the developed framework can seamlessly assist in different tasks as well as transitions between tasks without having to change any parameters or using an additional algorithm to switch between states. Results on three participants show that an exoskeleton controlled via this framework reduces EMGs during locomotion tasks with various speeds and/or inclinations. This is the first step toward creating controller allowing to assist in tasks independent manner.

1 Introduction

Wearable exoskeletons have the potential to enhance patients mobility or protect them from musculoskeletal injuries. For wide adoption of these devices voluntary, continuous and task-independent assistance is needed. Currently, few wearable robotic exoskeletons have shown metabolic benefit during locomotion [1]. These methods rely on switching between states or using machine learning algorithms, which have various disadvantages such as misclassification or the inability to assist in the transition between tasks or in unknown conditions.

We previously showed that EMG-driven modelling after personalization offers extrapolation capabilities to unknown tasks and degree of freedom (DOF) [2]. In [3], we also showed that models calibrated via simple isometric movements could enable voluntary control of robotic exoskeletons in neurologically injured patients performing knee and ankle movements from seated positions or control a soft exosuit for the elbow [4]. Here, we extend our framework to control a bilateral

G. Durandau (✉) · W. Rampeltshammer · H. van der Kooij · M. Sartori
Department of Biomechanical Engineering, Technical Medical Centre, University of Twente, Enschede 7522, NB, The Netherlands

J. C. Moreno et al. (eds.), *Wearable Robotics: Challenges and Trends*,
Biosystems & Biorobotics 27, https://doi.org/10.1007/978-3-030-69547-7_40

ankle exoskeleton during complex tasks, i.e. a broad range of locomotion conditions including transitions between those conditions.

2 Methods

Our framework is based on a real-time EMG-driven model previously developed [2]. The framework is using a Hill-type muscle model with the following equation:

$$F^{MTU}(t) = F^{T} = F^{Max}\left(f\left(L^{M}\right)f\left(V^{M}\right)E(t) + f_{p}\left(L^{M}\right)\right)\cos\left(\alpha^{M}(t)\right) \quad (1)$$

With $F^{MTU}(t)$ the musculo-tendon unit (MTU) force at instant t, F^{T} the tendon force, F^{Max} the maximum isometric force, $f\left(L^{M}\right)$ the force length relationship, $f\left(V^{M}\right)$ the force velocity relationship, $E(t)$ the normalized muscle activation, $f_{p}\left(L^{M}\right)$ the passive force length relationship and $\alpha^{M}(t)$ the pennation angle. Muscle tendon length and moment arm are computed in real-time from joint angles via multi-dimensional Bsplines [5]. Joint torques were computed by projecting MTU forces via muscle moment arm. The model contains four DOFs: left and right plantar dorsi-flexion and knee flexion extension as well as eight muscles: left and right soleus, tibia anterior, gastrocnemius medialis and lateralis.

To obtain joint torque personalized to the user, the model parameters need to be calibrated to the user. For this, we first scaled the model using the scaling tool from OpenSim [6]. We then used a pre-tuning algorithm to personalize optimal fiber length and tendon slack length [2]. These parameters as well as maximal isometric muscle force and EMG shape factor are further calibrated using a simulated annealing optimization algorithm that reduces the error between predicted and experimental joint torque.

The exoskeleton used is a bilateral ankle exoskeleton with two DOFs for each module, active plantar dorsiflexion and passive subtalar. Each module is powered by a series elastic actuator with a peak torque of 100 N.m and a weight of 4.5 kg. A back-pack contains a battery pack and a processing unit (NUC, Intel USA). Each module communicates with the processing unit using real-time communication protocol (Ethercat, Berkhoff, Germany).

Predicted joint torques computed from EMG sensor after filtering and normalization and joint angle (Link, Xsens, the Netherlands for the knee and joint encoder for the ankle) are sent to the main controller where they are multiplied by a support ratio and send to the actuator to provide assistance.

3 Experiments and Results

Three healthy subjects (age: 28.4 ± 5, height: 177.6 ± 6 cm, weight: 72.6 ± 6.5 kg) were recruited for this experiment. The experiment was conducted in three steps.

The first step consisted of recording experimental data for scaling and calibrating the user's model. The data recorded were markers (Oqus, Qualisys, Sweden), ground reaction forces (M-Gait, MotekForce Link, The Netherlands) and EMGs (Axon-Master 13E500, Ottobock, Germany). For calibration, experimental joint angle and joint torque were computed using the inverse kinematics and inverse dynamics tool from OpenSim [6].

The second step consisted of testing the calibrated model of the user with the exoskeleton and finding the experimental parameters such as a comfortable support ratio for the user and comfortable step frequency for the tested speeds.

The last step consisted of the experimental recording. Two conditions were tested: assistance computed from the framework and minimal impedance (no assistance). Each condition was tested in one long trial consisting of six randomized locomotion tasks on treadmill (Thera-Treadpro, Sportplus) (1.8 km/h, 0%; 1.8 km/h, −5%; 1.8 km/h, 12%; 2.8 km/h 0%, 2.8 km/h, −5%; 2.8 km/h 12%). Each task had a duration of 3 min. When walking with the exoskeleton, a fall prevention system was used, which gave a 5 kg body weight support (ZeroG, Aretech LLC, USA).

Figure 1 presents the overall (i.e. all recorded muscles) reductions for each task, task transitions and the complete experiment between the two conditions. Figure 1 also presents spider plots with individual muscles. Reductions were observed for all tested tasks as well as during the transition between tasks with a reduction of 16% (significant, $p < 0.05$) and an overall reduction for the complete experiments of 12% (significant, $p < 0.05$).

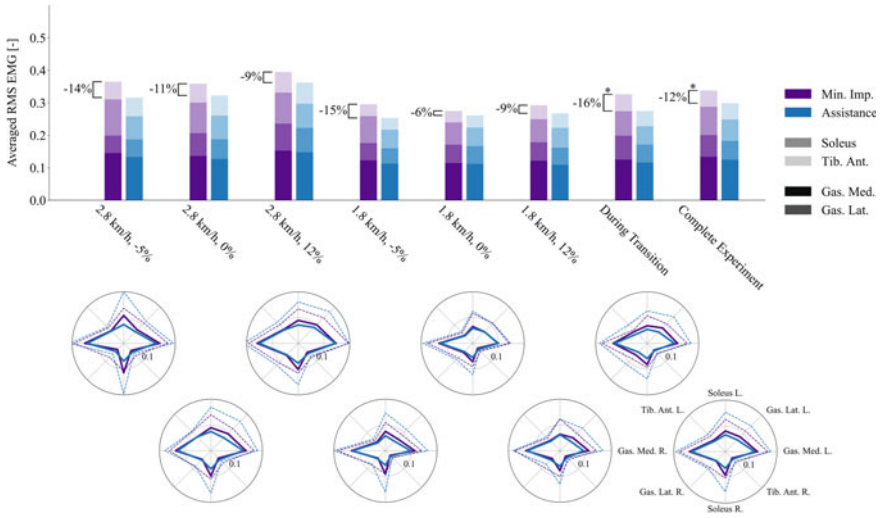

Fig. 1 EMG reduction for the tested locomotion tasks, transition between tasks and the complete experiment.* represents significance ($p < 0.05$)

Reduction in the predicted torque was also observed in all tasks (23% during transition (significant, $p < 0.05$) and 21% for the complete experiment (significant, $p < 0.05$)).

4 Discussion and Conclusion

These results demonstrated the possibility of using EMG-driven model for controlling an exoskeleton and offering positive assistance for a wide repertoire of locomotion tasks.

Furthermore, reduction in EMG was also observed during the transition during tasks, which is enabled by the continuous and voluntary type of assistance offered by the framework. All recorded muscles always underwent EMG reduction except for the tibia anterior, which displayed increased EMGs in a few cases during the swing phase. This is due to the fact that 100% of the gait cycle was assisted, which caused instability during the swing phase.

Future work will go towards incorporating estimation of muscle and joint stiffness which is extremely relevant for control, rehabilitation and musculoskeletal injury prevention.

Acknowlegements The study was supported by ERC Starting Grant INTERACT (803035) and H2020 Grant SOPHIA (871237).

References

1. G.S. Sawicki, O.N. Beck, I. Kang, A.J. Young, The exoskeleton expansion: Improving walking and running economy. J. Neuroeng. Rehabil. **17**(1), 1–9 (2020)
2. G. Durandau, D. Farina, M. Sartori, Robust real-time musculoskeletal modeling driven by electromyograms. IEEE Trans. Biomed. Eng. (2017)
3. G. Durandau et al., Voluntary control of wearable robotic exoskeletons by patients with paresis via neuromechanical modeling. J. Neuroeng. Rehab. **16**(1), 91 (2019)
4. N. Lotti et al., Adaptive model-based myoelectric control for a soft wearable arm exosuit: A new generation of wearable robot control. IEEE Robot. Autom. Mag. **0** (2020)
5. M. Sartori, M. Reggiani, A.J. van den Bogert, D.G. Lloyd, Estimation of musculotendon kinematics in large musculoskeletal models using multidimensional B-splines. J. Biomech. **45**(3), 595–601 (2012)
6. S.L. Delp et al., OpenSim: open-source software to create and analyze dynamic simulations of movement. Biomed. Eng. IEEE Trans. **54**(11), 1940–1950 (2007)

Energy Cost of Transport in Overground Walking of a Transfemoral Amputee Following One Month of Robot-Mediated Training

C. B. Sanz-Morère, E. Martini, G. Arnetoli, S. Doronzio, A. Giffone, B. Meoni, A. Parri, R. Conti, F. Giovacchini, Þ. Friðriksson, D. Romo, R. Molino-Lova, S. Crea, and N. Vitiello

Abstract Transfemoral amputees (TFAs) require higher energy expenditure than able-bodied individuals during walking. In this study we examined the effects on one TFA of training for a month with a portable bilateral hip exoskeleton on (i) energy cost of transport (CoT) and (ii) distance covered during a 6-minute walking test (6mWT), assessed without (NoExo) and with (Exo) the exoskeleton. Results showed that in NoExo the CoT was reduced by 13.4% after the training, while the 6mWT distance increased by 20.3%. However, the CoT increased in Exo compared to NoExo both before (24.8%) and after (11.8%) the training. These results provide initial evidence that robot-mediated training should deserve further exploration as a tool for improving walking efficiency of TFAs. Future research will investigate customized tuning procedures more in depth to maximize the beneficial effects of this approach.

Research supported by the European Commission under the CYBERLEGs Plus Plus project (grant n°731931), within the H2020 framework (H2020-ICT-25-2016-2017).

Part of the IP covering the technology presented in this paper has been exclusively licensed to IUVO for commercial exploitation.

C. B. Sanz-Morère (✉) · E. Martini · S. Crea · N. Vitiello
BioRobotics Institute, Scuola Superiore Sant'Anna, 56127 Pisa, Italy
e-mail: clarabeatriz.sanzmorere@santannapisa.it

G. Arnetoli · S. Doronzio · A. Giffone · B. Meoni · R. Molino-Lova · S. Crea · N. Vitiello
IRCCS Fondazione Don Carlo Gnocchi, 50143 Florence, Italy

S. Crea · N. Vitiello
Department of Excellence in Robotics & AI, Scuola Superiore Sant'Anna, 56127 Pisa, Italy

A. Parri · R. Conti · F. Giovacchini
IUVO S.R.L, Via Puglie, 9, 56025 Pontedera, PI, Italy

Þ. Friðriksson · D. Romo
Össur, Grjótháls 5, 110 Reykjavík, Iceland

J. C. Moreno et al. (eds.), *Wearable Robotics: Challenges and Trends*,
Biosystems & Biorobotics 27, https://doi.org/10.1007/978-3-030-69547-7_41

1 Introduction

Trans-femoral amputees (TFAs) exhibit lower walking self-selected speed and higher energy expenditure compared to able-bodied individuals, with subsequent secondary disorders [1, 2]. Gait training programs for TFAs have been developed to normalize kinematics, reduce compensatory strategies and increase energetic efficiency of walking [3].

In the last decade, the use of robotic exoskeletons has shown promising results in the recovery of motor deficits. Among them, bilateral hip orthoses have been tested for the rehabilitation of stroke survivors and other frail individuals, improving treadmill walking efficiency after several weeks of training [4, 5].

In this study we explore the use of a portable powered hip exoskeleton, the Active Pelvis Orthosis (APO), to improve the energetic efficiency of walking of TFAs following a one-month robot-mediated training program.

2 Materials and Methods

2.1 Active Pelvis Orthosis (APO)

The APO has been designed for gait support of frail individuals and provides flexion-extension assistance at the hip. The APO in this study is an advanced version of the prototype described in [5], with a similar weight (~ 6.5 kg) and a more conformant belt-like physical human-robot interface, purposively designed by the Össur R&D team (Reykjavík, Iceland).

The APO control strategy was based on a hierarchical architecture [6]: (i) the stride phase was computed in real-time by means of a pool of adaptive-frequency oscillators, and (ii) for each joint the assistive torque versus phase profile was a sum of two Gaussian functions, with tunable peak amplitude [N·m], peak occurrence [% of the stride phase], and duration [% of the stride phase].

2.2 Protocol

This study was included in the EU H2020 CYBERLEGs Plus Plus project approved by the local Ethics Committee "Comitato Area Vasta Centro Toscana" (approval number: 12739_spe) and carried out at the premises of Fondazione Don Gnocchi (Firenze, Italy). Here we report the results of a K2 right TFA amputated since 2017, aged 46 years old with a BMI of 37 kg/m^2.

The protocol included the following 12 sessions.

Enrolment session: To verify the participant's compliance with inclusion/exclusion criteria.

Tuning session: To set and tune the assistive profile provided by the APO. We initially set the Gaussian-based flexion-extension torque profile to maximize the net power transferred from the robot to the participant by synchronizing the Gaussian flexion-extension peaks with the respective hip joint velocity peaks estimated by means of the APO sensors. Fine-tuning was carried out on each Gaussian profile considering the subject's feedback to ensure a high transferred power in real-time while maintaining a comfortable interaction by (i) adjusting the phase and duration (<5% variations) and (ii) increasing the peak amplitude (up to 0.1 N · m/kg) of the torque versus phase profile.

Two *Assessment* sessions, namely *Pre-training* (*PreTA*) and *Post-training Assessment* (*PostTA*): To evaluate the energetic walking efficiency before and after the training program. In each *Assessment* session, the participant carried out two six-minute walking tests (6mWTs) at his self-selected speed both without (N*oExo*) and with (*Exo*) the exoskeleton.

Eight *Training* sessions: carried out between the *PreTA* and *PostTA* sessions, each consisting of a 20-minute overground training with the APO assistance. The *Training* sessions were carried out two or three times per week for three weeks and included stair negotiation and sit-to-stand activities that will be reported in future publications.

2.3 Analysis of Walking Efficiency

We computed the net oxygen uptake by measuring the instantaneous uptake through a portable gas analyser (Oxycon Mobile, CareFusion, Germany), averaging the values of the last 3 minutes of each 6mWT and subtracting a baseline calculated in the last 3 minutes of a 5-minutes resting period prior to each test. Energy Cost of Transport (CoT) was obtained by normalizing the net uptake by the weight of the participant and the average speed during the 6mWT.

Hip joint angles and assistive torque profiles were recorded through the APO onboard sensors. Delivered power was computed by multiplying the estimated hip velocity by the actual delivered torque. Recorded data were segmented and resampled between 0% and 100% of the stride phase (0% corresponding to the hip joint flexion peak of the sound limb).

3 Results

Figure 1 (left) presents the hip angle, torque and power delivered during the *PostTA* 6mWT in *Exo* condition. Torque and power were repeatable throughout the test with median peaks of: (i) flexion torque equal to 0.064 Nm/kg and 0.069 Nm/kg, (ii) extension torque equal to 0.055 Nm/kg and 0.057 Nm/kg, and (iii) flexion power equal to 0.27 W/kg and 0.17 W/kg, respectively on the prosthetic and sound sides.

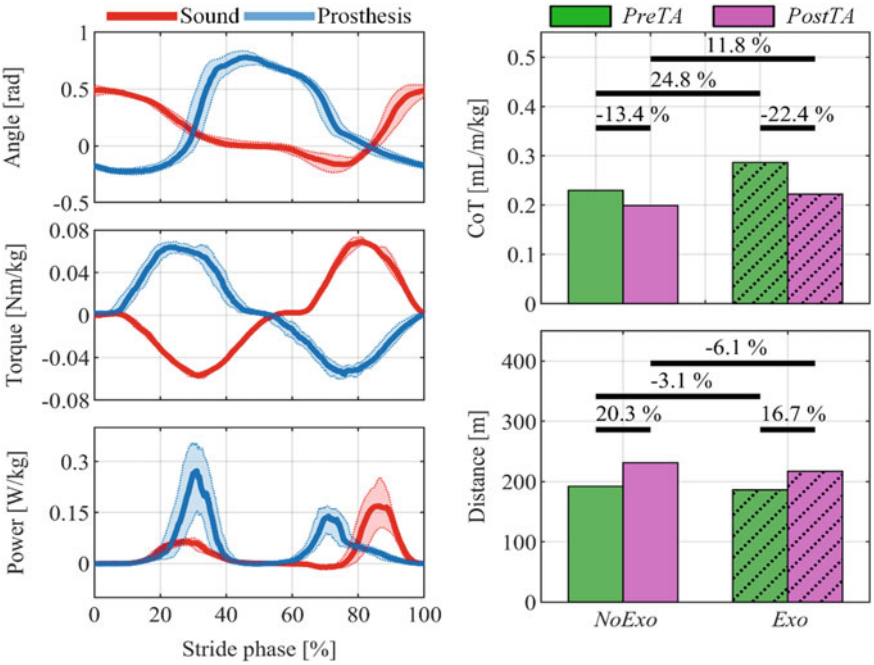

Fig. 1 (left) Data recorded from the APO during the *PostTA* session shown as Median (25–75 IQR); (right) Energy Cost of Transport (CoT) and distance walked during the 6mWTs.

Results from CoT and distance covered across all conditions are shown in Fig. 1(right). In the comparison *PreTA* versus *PostTA*, CoT was reduced by 13.4% and 22.4%, respectively in *NoExo* and *Exo* conditions. Similarly, the participant increased the distance covered by 20.3% and 16.7% in *NoExo* and *Exo* conditions respectively. In the *Exo* versus *NoExo* comparison, wearing the APO penalized the energetic efficiency: CoT in the *Exo* condition was higher than in the *NoExo* condition by 24.8% and 11.8% during *PreTA* and *PostTA* sessions respectively.

4 Discussion

This study presents an APO-mediated overground gait training program to improve the walking efficiency of TFAs. Preliminary results with one participant showed an improved walking capability at the end of the training, quantified by longer covered distance and reduced energy CoT compared to the participant's initial performance. The APO thus seems to be a suitable technology to train TFAs to improve walking efficiency, as results are in line with previous training protocols involving TFAs and frail individuals [3, 4]. Nevertheless, future efforts should focus on comparing the APO to an equivalent control training program.

The comparison between walking with and without the APO resulted in a lower CoT when walking without the APO differently from what was observed in [5, 7]. This result may be related to several factors such as the weight of the device or the different assistive parameters. Indeed, in [7], the assistance was tuned for metabolic cost efficiency whereas here the assistance was mainly grounded on kinematic considerations which could have led to suboptimal energetic efficiency. A more suitable set of parameters might have been selected by considering the real-time effect of the assistance on the metabolic cost [7, 8]. Applying human-in-the-loop optimization techniques with TFAs is still an open challenge and will require dedicated future studies.

References

1. L. van Schaik, J.H.B. Geertzen, P.U. Dijkstra, R. Dekker, Metabolic costs of activities of daily living in persons with a lower limb amputation: a systematic review and meta-analysis. PLoS ONE (2019). https://doi.org/10.1371/journal.pone.0213256
2. R. Gailey, K. Allen, J. Castles, J. Kucharik, M. Roeder, Review of secondary physical conditions associated with lower-limb amputation and long-term prosthesis use. J. Rehab. Res. Develop. (2008). https://doi.org/10.1682/JRRD.2006.11.0147
3. B.J. Darter, D.H. Nielsen, H.J. Yack, K.F. Janz, Home-based treadmill training to improve gait performance in persons with a chronic transfemoral amputation. Arch. Phys. Med. Rehabil. (2013). https://doi.org/10.1016/j.apmr.2013.08.001
4. H.J. Lee et al., Training for walking efficiency with a wearable hip-assist robot in patients with stroke a pilot randomized controlled trial. Stroke (2019) https://doi.org/10.1161/STROKEAHA.119.025950
5. E. Martini et al., Gait training using a robotic hip exoskeleton improves metabolic gait efficiency in the elderly. Sci. Rep. **9**(1), 1–12 (2019). https://doi.org/10.1038/s41598-019-43628-2
6. T. Yan, A. Parri, V. Ruiz Garate, M. Cempini, R. Ronsse, N. Vitiello, An oscillator-based smooth real-time estimate of gait phase for wearable robotics. Auton. Robot. **41**(3), 759–774 (2017). https://doi.org/10.1007/s10514-016-9566-0
7. E. Martini et al., Lower-limb amputees can reduce the energy cost of walking when assisted by an Active Pelvis Orthosis. in *IEEE International Conference on Biomedical Robotics and Biomechatronics (Biorob)* (2020)
8. M. Kim et al., Human-in-the-loop Bayesian optimization of wearable device parameters. PLoS One (2017). https://doi.org/10.1371/journal.pone.0184054

Physical Therapy and Outdoor Assistance with the Myosuit: Preliminary Results

Michele Xiloyannis, Florian L. Haufe, Jaime E. Duarte, Kai Schmidt, Peter Wolf, and Robert Riener

Abstract Soft robotic suits are good candidates both for supporting physical therapy in clinical environments and for improving mobility in outdoor settings. Here, we investigate both modes of use using the Myosuit, a lightweight robotic suit for the lower limbs: (1) we show that it can be safely used to support a supervised physical therapy program, and (2) present a single-case study on the immediate effects that Myosuit assistance can have in an outdoor setting. Eight participants with diverse walking impairments completed a five-sessions Myosuit-assisted training program, showing an average improvement in walking performance that is encouraging for the design of a future controlled study. When walking on a sloped mountain path, one participant with incomplete spinal cord injury showed a 30% increase in walking speed and 9% reduction in cost of transport when assisted by the Myosuit, compared to when not wearing the device.

1 Introduction

A plethora of neurological, muscular and traumatic disorders can significantly affect our ability to move. Conditions such as post-stroke hemiparesis, muscular dystrophy, multiple sclerosis or incomplete spinal cord injury (iSCI) can reduce one's ability to walk at normal speeds in a safe and efficient way. Even after targeted rehabilitation, most individuals retain deficits that prevent them from reaching walking speeds suitable for community ambulation, hindering social integration and ultimately affecting quality of life [1].

M. Xiloyannis (✉) · F. L. Haufe · P. Wolf · R. Riener
Sensory-Motor Systems (SMS) Lab, Institute of Robotics and Intelligent Systems (IRIS), ETH Zurich, Switzerland
e-mail: michele.xiloyannis@hest.ethz.ch

Spinal Cord Injury Center, University Hospital Balgrist, University of Zurich, Zurich, Switzerland

J. E. Duarte · K. Schmidt
MyoSwiss AG, Zurich, Switzerland

J. C. Moreno et al. (eds.), *Wearable Robotics: Challenges and Trends*,
Biosystems & Biorobotics 27, https://doi.org/10.1007/978-3-030-69547-7_42

Robotic technologies are an increasingly important part of the physical training process and have been shown to lead to outcomes at least as good as traditional manual therapy [2]. However, mostly due to high complexity and cost, their contribution is limited to hospitals and specialized clinics. When patients go back home, training stops and their conditions plateau or even deteriorate.

The recent development of soft wearable robots, using compliant actuators and textiles to transfer forces to the human body [3], may be a solution for some cases. The simplicity and portability of these devices allow them to be integrated in a supervised physical therapy program in a clinic and to deliver immediate mobility benefits at home and outdoors.

Here, we show the feasibility of using the Myosuit, a lightweight, portable, tendon-driven wearable robot [4], for providing support during physical therapy to people with a diverse range of neurological, muscular and traumatic conditions (Fig. 1a). In addition, we investigate the immediate benefits that the Myosuit could provide in outdoor settings (Fig. 1b), in a single-case study. Both of these scenarios are more thoroughly analysed in our recent works [5, 6].

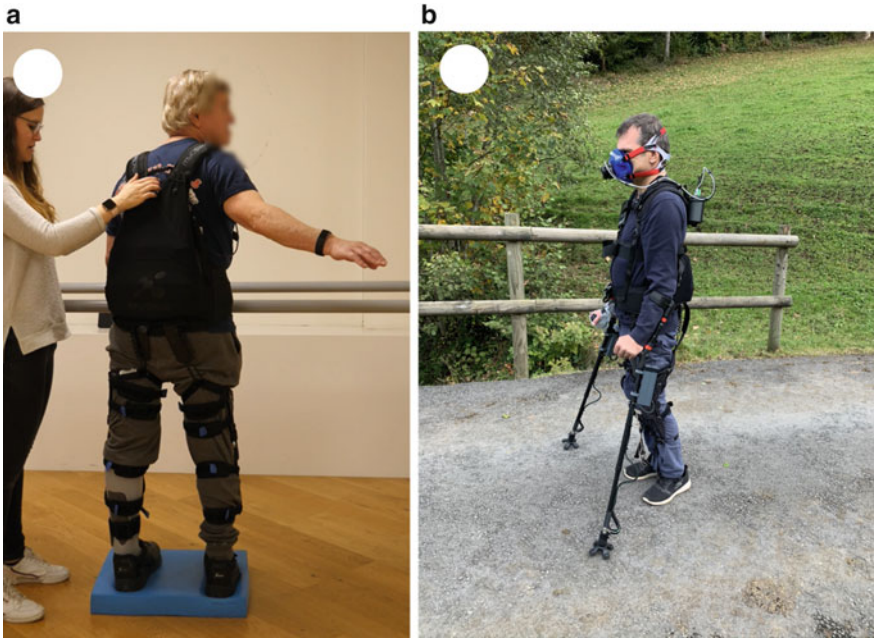

Fig. 1 The Myosuit is a lightweight tendon-driven robot suitable both for supporting its user during physical therapy (**a**) and to improve mobility in outdoor settings (**b**)

2 Methods

The Myosuit (MyoSwiss AG, Zurich, Switzerland) is an untethered wearable robot that actively supports knee and hip extension in the early to mid stance phase of the gait cycle and passively aids hip flexion during swing, using elastic rubber bands. Active support is provided with artificial tendons, routed along a biarticular path on each leg and tensioned by two electric motors. Forces are transmitted to the joints using a combination of fabric and plastic cuffs.

In a clinical setting, twelve participants with diverse mobility impairments (physical therapy group in Table 1) and naive to the use of the Myosuit, were enrolled to undergo five training sessions. Each training session consisted of 45 min of net training time and was scheduled on a weekly basis. All training sessions included overground and treadmill walking and exercises targeting strength, balance and functional tasks, performed while wearing the Myosuit and supervised by a physiotherapist.

The main outcome for physical therapy was feasibility. As a secondary outcome we evaluated walking speed of the participants using the 10-meter walk test (10 MWT). Baseline unassisted walking speed was assessed during the first session

Table 1 Participants demographics and pathologies

	Condition	Chronicity	Sex	Age	Height (cm)	Mass (kg)
	Physical therapy					
P_1	Charcot-Marie Tooth disease		F	43	164	48
–	Multiple sclerosis					
–	Grade II brain tumor					
–	Limb-girdle muscle dystrophy					
P_2	iSCI Th7		M	67	168	79
P_3	iSCI L4 Cauda equina syndrome		M	32	185	104
P_4	Syringomyelia at Th5		M	54	186	67
P_5	Post-stroke hemiparesis (L)		M	72	164	72
-	Muscle dystrophy					
P_6	Post-stroke hemiparesis (R)		M	63	177	73
P_7	Spinal tumor L1/2		F	67	160	65
P_8	Muscle sarcoma		F	49	181	91
	Outdoor					
P_9	iSCI C5		M	51	178	70

with two 10MWTs; sessions 2–5 included the same 10 MWTs but with assistance from the Myosuit.

In an outdoor setting, one participant with iSCI (P9 in Table 1, chronicity > 25 years), with previous experience in using the Myosuit, performed four trials of walking on a paved sloped mountain road in the municipality of Herisau, Switzerland (47° 22′ 06.8″ N 9° 14′ 42.8″ E). Each trial consisted of a time-bounded 4-minute test during which the participant was asked to cover as much distance as possible. Two of the trials were performed without wearing the Myosuit (A) and two with assistance from the Myosuit (B), in ABBA format, to account for potential order effects.

Outcome measures for outdoor mobility were cost of transport—estimated by dividing the expended metabolic energy by the weight of the participant and the distance covered during each trial—and walking speed. Energy expenditure was estimated via indirect calorimetry (K5, COSMED, Italy) and average walking speed by dividing the distance covered, acquired via GPS, by the trial duration. The study design and protocol were approved by the institutional review board of ETH Zurich (EK 2018-N-31).

3 Results and Discussion

Eight of the twelve participants enrolled in the physical therapy programme completed the study (Table 1), three dropped out for reasons unrelated to the study and one because of feeling unsafe when walking with the Myosuit. All others completed the study with no adverse events. Five of the eight participants, upon completion of the training program, showed an increase in assisted walking speed in the 10MWTs relative to baseline. On average, participants were 2% slower during the first 10MWTs with the Myosuit than at baseline. By training session 5, participants were on average 27% faster during the assisted 10MWTs than at baseline.

These results confirm the feasibility and safety of using the Myosuit as a training device for people suffering with mobility impairments deriving from diverse conditions. They provide encouraging evidence for the design of a controlled study to calrify the source of the observed positive trend in walking speed.

Figure 2 shows the path covered by the participant during the outdoor test, in all four trials, both when assisted by the Myosuit (blue) and when not wearing the Myosuit (red). Myosuit-assisted walking was 30% faster than walking without the Myosuit. Cost of transport was 9% lower during Myosuit-assisted walking than when not wearing the Myosuit.

This single-case study allows no generalizable conclusion but encourages a larger scale investigation on the impact of the Myosuit on walking capacity in unstructured environments. By allowing for faster and more efficient locomotion, we posit that lightweight and versatile devices such as the Myosuit could improve mobility, foster a more active and independent lifestyle and ultimately improve the quality of life of people with walking impairments.

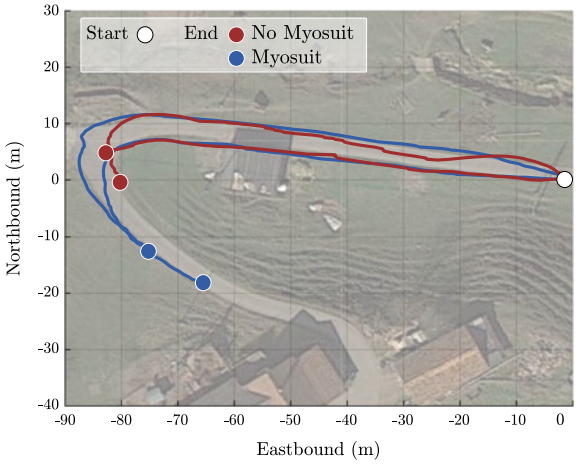

Fig. 2 Effects of Myosuit-assisted outdoor assistance. Path covered by one participant (P9 in Table 1), with assistance from the Myosuit (blue) and without wearing the Myosuit (red), in a time-bounded 4-minute walk test, outdoor on a sloped terrain

4 Conclusions

Our initial results provide encouraging evidence to further investigate the effects of portable and lightweight robots for walking assistance both on physical therapy and on outdoor mobility.

Acknowledgements This work was supported by the Swiss National Center of Competence in Research (NCCR) Robotics, by the Swiss Center for Clinical Movement Analysis (SCMA), Balgrist Campus AG and by MyoSwiss AG.

References

1. D. Rand, J.J. Eng, P.F. Tang, C. Hung, J.S. Jeng, Daily physical activity and its contribution to the health-related quality of life of ambulatory individuals with chronic stroke. Health and Quality of Life Outcomes (2010)
2. C.G. Burgar, P.S. Lum, P.C. Shor, H.F. Van Der Loos, Development of robots for rehabilitation therapy: the Palo Alto VA/Stanford experience. J. Rehabil. Res. Develop. **37**(6), 663–673 (2000)
3. A.T. Asbeck, S.M. De Rossi, I. Galiana, Y. Ding, C.J. Walsh, Stronger, smarter, softer: next-generation wearable robots. IEEE Robot. Autom. Mag. **21**(4), 22–33 (2014)
4. F.L., A.M. Haufe, K. Kober, A. Schmidt, J.E. Sancho-Puchades, J.E. Duarte, P. Wolf, and R. Riener, User-driven walking assistance: first experimental results using the MyoSuit, in *IEEE International Conference on Rehabilitation Robotics*, vol. 2019 (June, 2019), pp. 944–949
5. F.L. Haufe, P. Wolf, J.E. Duarte, R. Riener, M. Xiloyannis, Increasing exercise intensity during outside walking training with a wearable robot, in *IEEE RAS and EMBS International Conference on Biomedical Robotics and Biomechatronics* (New York, NY, USA, 2020). in press.
6. F.L. Haufe, K. Schmidt, J.E. Duarte, P. Wolf, R. Riener, M. Xiloyannnis, Training with the Myosuit: a feasibility study across diverse gait disorders. J. NeuroEng. Rehabil. (under review)

Predictive Simulation of Sit-to-Stand Movements

David Munoz, Leonardo Gizzi, Cristiano De Marchis, and Giacomo Severini

Abstract The development of technology that can assist people during movements such as sit to stand can benefit from simulations that can estimate the effect of different assistance patterns. These simulations need to be based on frameworks that can replicate the neuromechanical features of non-pathological sit-to-stand movements. In this study, we present a framework for predictive simulations of sit to stand that can be used to synthesize physiological data in the absence of experimental ones. Here we reproduce sit-to-stand movements on a model with 9 degrees of freedom and 52 actuators by optimizing the parameters of a feedback controller that accounts for the position, velocity and acceleration of the pelvis and torso, under the constraints dictated by a specifically designed cost function. We obtained a simulation that could replicate the kinematics and muscular activation observed in previous studies.

1 Introduction

Sit-to-stand (STS) is an essential activity of daily living. Consequently, impairments that affect mobility during the STS movement require training programmes that can benefit from the use of assistive devices such as exoskeletons. Having the possibility to estimate the effect of different assistance patterns during STS would greatly

This work was supported by the H2020 Project EUROBENCH under Grant 779963.

D. Munoz · G. Severini (✉)
School of Electrical and Electronic Engineering and the Insight Centre for Data Analytics, University College of Dublin, Dublin, Ireland
e-mail: giacomo.severini@ucd.ie

D. Munoz
e-mail: david.munoz@ucdconnect.ie

L. Gizzi
Institute for Modelling and Simulation of Biomechanical Systems, Continuum Biomechanics and Mechanobiology Group, University of Stuttgart, Stuttgart, Germany

C. De Marchis
Department of Engineering, Roma Tre University, Rome, Italy

J. C. Moreno et al. (eds.), *Wearable Robotics: Challenges and Trends*,
Biosystems & Biorobotics 27, https://doi.org/10.1007/978-3-030-69547-7_43

facilitate the design of assistive devices. Bearing this in mind, predictive modelling can be a useful tool for studying the neuromechanical characteristics of assisted movements in absence of experimental data. Controller-based environments such as SCONE [1], with the appropriate musculoskeletal model and controller, can be used to simulate several natural movements, including STS, and the potential effect of assistive devices. The aim of this work is to present a controller for STS predictive simulations and compare its performance with previous literature [2, 3]. The controller uses feedback information from position, velocity and acceleration of the Center of Mass (CoM) of the pelvis and the torso to calculate the activation of the different muscles.

2 Methods

2.1 Musculoskeletal Model

A gait model with 9 degrees of freedom was used in the simulations [4–6]. The model consists of the lower limbs, the torso and the head. The muscles included are *gluteus medius, gluteus maximus, erector spinae, iliacus, psoas, adductor magnus, rectus femoris, biceps femoris, semitendinosus, semimembranosus, gastrocnemius, soleus, tibialis posterior, tibialis anterior, vastus intermedius, vastus lateralis, flexor digitorum longus* and *flexor hallucis longus* [7]. Each muscle can have more than one actuator, for a total of 52 musculo-tendinous units between the two sides. The model represents a subject 1.8 m tall and with a mass of 80.17 kg. The pelvis and the torso were placed above a platform to simulate a sitting initial position. The ankle, knee and hip angles in the sagittal plane were 23°, −103° and 80°, respectively. The model was implemented using OpenSim [8].

2.2 Feedback Controller

According to previous literature [2, 3], the STS movement can be segmented in 4 consecutive phases (Fig. 1): (1) *leaning forward*; (2) *momentum transfer*; (3) *extension*; (4) *standing up/stabilization.* The transition between the different phases was implemented in the controller by using phase-specific *task-goals* to be reached for advancing to the following phase. Accordingly, the *leaning forward* phase was set to finish when the antero-posterior position of the CoM of the torso was closer than 0.21 m to the calcaneus bone. The *momentum transfer* phase was set to finish when the pelvis moved upward by 0.12 m and forward (torso at 0.1 m from the calcaneus), and the feet become the new base of support. The *extension* phase, consisted of the hips, knee and ankle extending together to lift the body, and terminated when the vertical speed of the torso was lower than 0. Finally, in the fourth phase, the model

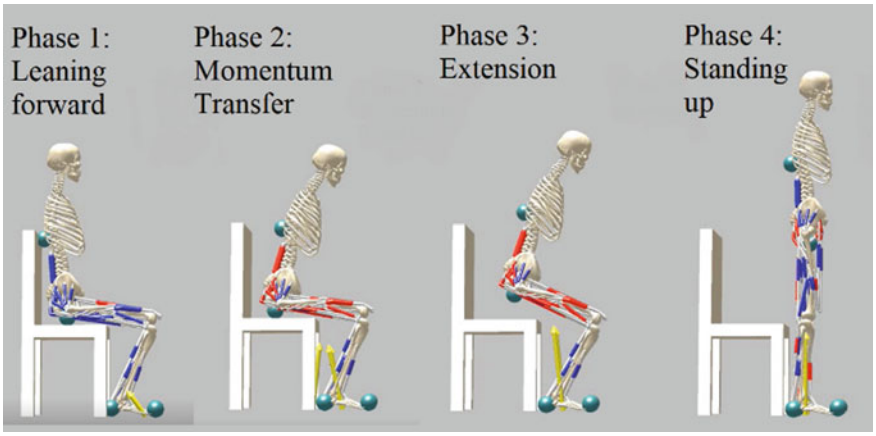

Fig. 1 The four phases of the STS movement

kept balance for the rest of the simulation. The controller calculates the activation of the actuators from the feedback information on position, velocity and acceleration of the pelvis and/or the torso. A gain is assigned to each feedback component. The relative control equation obtained is:

$$A_{[i]} = O_{[i]} + k_{p[t][i]}P + k_{v[t][i]}V + k_{acc[t][i]}Acc + k_{l[i]}Lx_{[i]} \quad (1)$$

In the equation, $A_{[i]}$ is the activation of the i-th musculo-tendinous unit, $O_{[i]}$ is the tonic activation of the i-th actuator, and P, V and Acc are the position, velocity and acceleration of the CoM (of the torso or pelvis), respectively. $Lx_{[i]}$ is the muscle length value of the i-th actuator used to model muscle length reflexes. The gains, $k_{p[t][i]}$, $k_{v[t][i]}$ and $k_{acc[t][i]}$ are feedback-specific gains for the phase t, for the i-th actuator. The $k_{l[i]}$ is the muscle reflex gain for the i-th actuator. During the simulations, a Covariance Matrix Approximation algorithm was used to optimize the values of the offset O and of all the gains k across the different iterations, with symmetry enforced between the left and right side actuators to minimize the number of variables to be optimized. In the first phase, the sensory gains depended on the position, velocity and acceleration of the CoM of the torso, while in the second and third phase they depended from the CoM of the pelvis. In the fourth phase, the sensory feedbacks of both pelvis and torso were used. This was done by adding to Eq. (1) the feedback components relative to the feedback of the additional body segment.

2.3 Cost Function

A composite cost function was implemented to drive the optimization process towards a realistic STS movement. The different components of the cost function were also phase- dependent. In the *leaning forward* phase, torso and pelvis backward or null movements were penalized to achieve a forward displacement. During the *momentum transfer* phase, the pelvis backward and downward movements together with the tibia backward movements were penalized in order to make the transfer of weight from the seat to the feet possible. Then, jumping-like movements were avoided by penalizing the raise of the talus during *extension.* Finally, during *standing up*, falling was prevented by penalizing a vertical torso position lower than 1.3 m. Other components of the cost function, common to all phases, were penalizations for knee hyperextension or excessive actuators activation as in [9]. The effort penalization minimized the average sum of joint torques squared in order to reduce muscle activations. Finally, we enforced a fixed position of the feet during the whole simulation by minimizing the talus and toes velocities.

3 Results

Each simulation was set to last 10 s. It took 24 h to finish the optimization with a 3 GHz Intel Core i7-9700 processor. The simulation was set to stop after 2000 iterations. As it can be observed in Figs. 1 and 2, the simulation was able to replicate the four phases and achieve a natural STS movement. The hips, knee and ankle angles observed from the simulations were substantially consistent with those observed experimentally in

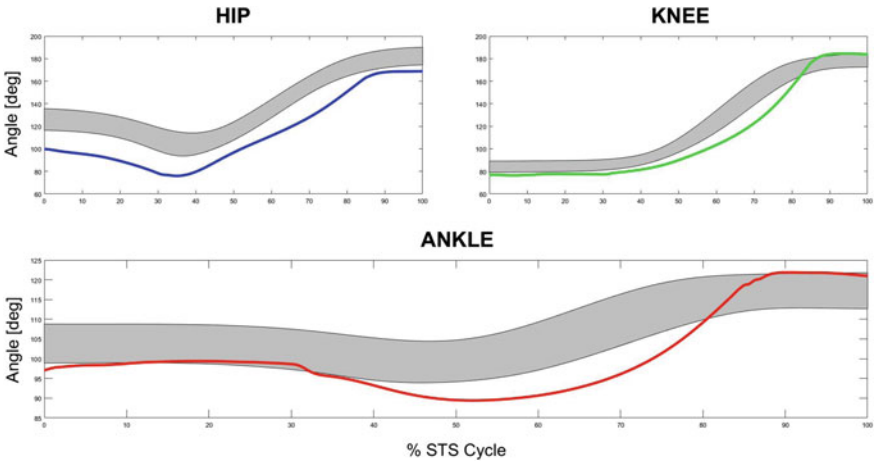

Fig. 2 Angles [deg] for hip, knee and ankle up to the beginning of the standing up phase. Grey: experimental data from [11] (average ± std), colour: data from the model.

healthy individuals [3–11] and like those obtained in another simulative work [10]. As can be observed in Fig. 2, knee and ankle angles changed physiologically during the STS movement.

4 Conclusion

Overall, our model can simulate a natural-like STS movement, with joints angles similar to the experimental ones. However, torso and pelvis position—together with the profile of the hip angle—can be improved in the *momentum transfer* phase. In future simulations, these problems will be solved by adjusting the weights of the different components of the cost function. Also, in further simulations, the height and weight of the model will be modified in order to test the robustness of the controller. Future works with the controller will aim at estimating the effect of different assistive devices and assistance patterns on the STS task.

References

1. T. Geijtenbeek, SCONE: open source software for predictive simulation of biological motion. JOSS 4(38), (2019)
2. E.J. Caruthers, J.A. Thompson, A.M.W. Chaudhari, L.C. Schmitt, T.M. Best, K.R. Saul, R.A. Siston, Muscles forces and their contributions to vertical and horizontal acceleration of the Center of Mass during Sit-to-Stand transfer in young, healthy adults. J. Appl. Biomech. **32**, 487–503 (2016)
3. M. Schenkman, R.A. Berger, P.O. Riley, R.W. Mann, W.A. Hodge, Whole-body movements during rising to standing from sitting. Phys. Ther. **70**(10), 638–648 (1990)
4. S.L. Delp, J.P. Loan, M.G. Hoy, F.E. Zajac, E.L. Topp, J.M. Rosen, An interactive graphics-based model of the lower extremity to study orthopaedic surgical procedures. IEEE Trans. Biomed. Eng. **37**, 757–767 (1990)
5. F.C. Anderson, M.G. Pandy, A dynamic optimization solution for vertical jumping in three dimensions. Comput. Method. Biomec. **2**, 201–231 (1999)
6. F.C. Anderson, M.G. Pandy, Dynamic optimization of human walking. J. Biomech. Eng. **123**, 381–390 (2001)
7. E.M. Arnold, S.R. Ward, R.L. Lieber, S.L. Delp, A model of the lower limb for analysis of human movement. Ann. Biomed. Eng. **38**(2), 269–279 (2010)
8. S.L. Delp, F.C. Anderson, A.S. Arnold, P. Loan, A. Habib, C.T. John, E. Guendelman, D.G. Thelen, OpenSim: open-source software to create and analyze dynamic simulations of movement. IEEE Trans. Biomed. Eng. **54**(11), (2007)
9. J. Wang, S. Hammer, S. Delp, V. Koltun, Optimizing locomotion controllers using biologically-based actuators and objectives. ACM Trans. Graph. **31**(4), Article 25 (2012)
10. H.R. Yamasaki, H. Kambara, Y. Koike, Dynamic optimization of the Sit-to-Stand movement. JAB **54**(11) (2007)
11. K. Kaneda, The features of muscle activity during chair standing and sitting motion in submerged condition. PLoS ONE **14**(8) (2019)

SimBionics: Neuromechanical Simulation and Sensory Feedback for the Control of Bionic Legs

Jose Gonzalez-Vargas, Massimo Sartori, Strahinja Dosen, Herman van der Kooij, and Johan Rietman

Abstract Lower limb prosthetic technology has greatly advanced in the last decade, but there are still many challenges that need to be tackled to allow amputees to walk efficiently and safely on many different terrain conditions. Neuro-mechanical modelling and online simulations combined with somatosensory feedback, has the potential to address this challenge. By virtually reconstructing the missing limb together with the associated somatosensory feedback, this approach could enable amputees to potentially perceive the bionic legs as extensions of their bodies. A prosthesis equipped with such biologically inspired closed-loop control could duplicate the mechanics of walking far more accurately than conventional solutions. The project SimBionics aims to explore these opportunities and advance the state-of-the-art in lower limb prosthesis control.

1 Introduction

The human musculoskeletal system is complex but optimized to provide safe and efficient locomotion [1]. The central mechanisms in the motor control of locomotion include neuromechanical synergies (i.e. at joint, muscle and neural levels) that establish coupling between different joints, segments and muscles [2, 3]. The neuromechanical synergies result in cyclical and automated movement patterns with rhythmic and coordinated motions of the trunk and lower extremities. However, after an amputation, the synergies are compromised, and the motions of the joints of a

J. Gonzalez-Vargas (✉)
Ottobock SE & KGaA, Duderstadt, Germany
e-mail: jose.gonzalez@ottobock.de

M. Sartori · H. van der Kooij · J. Rietman
Department of Biomechanical Engineering, Twente University, Enschede, The Netherlands

S. Dosen
Department of Health Science and Technology, Aalborg University, Aalborg, Denmark

J. Rietman
Roessingh Research and Development, Enschede, The Netherlands

J. C. Moreno et al. (eds.), *Wearable Robotics: Challenges and Trends*,
Biosystems & Biorobotics 27, https://doi.org/10.1007/978-3-030-69547-7_44

prosthetic device are not in synchrony with the movement of the rest of the body, which often results in non-natural compensatory movements. The compensatory movements have been considered as the leading cause for the lack of comfort, higher energy requirements during walking and standing, and cumulative trauma disorders [4].

In recent time, the mechatronic knee and ankle prostheses have improved substantially in terms of technology, and now a range of solutions from semi- to fully-actuated are available. However, robust and intuitive control of these devices is still a major challenge. Most commercial and research systems are controlled by using a hard-coded set of rules that trigger predefined changes in the damping and activation of the knee and ankle joints [5, 6]. This is in a sharp contrast to the activation of biological joints, which is based on continuous modulation of impedance (e.g. stiffness) and active forces (e.g. torque) in response to biomechanical demands of the task and the environment (e.g., terrain roughness and inclination).

Furthermore, none of the current commercial prostheses provides explicit somatosensory feedback to the user. Therefore, the user needs to rely on incidental cues (e.g., forces through the socket) or visual observation to assess the state of his/her lower limb [7] This leads to increased cognitive load as well as inefficient walking with asymmetric gait, slower cadence, and poor balance [8, 9]. The research on this topic is scarce, and the proposed non-invasive feedback systems are rather simple. Typically, the systems are based on a single stimulation point (a vibration motor) delivering simple information (e.g., heel strike). Also, due to delays in the embedded and biological system, the prosthesis user perceives and interprets the stimulation signal with a considerable delay, which makes it less effective in activities of daily living. This is far from the timely, continuous and spatially distributed feedback that able-bodied humans receive from their lower limbs.

2 Neuromechanical Simulation for Control of Prosthesis

Using neuromechanical modelling and online simulations of the musculoskeletal system to control assistive device is not a new concept and have been proposed by several research groups in the past. Eilenberg et al. [10] proposed a muscle reflex controller based on simulation studies that mimic the neuromechanics of the ankle plantar flexor. This type of controller allows adaptability of an ankle prosthesis to different conditions by emulating the spinal reflexes that are activated while walking. Although simple, the approach has proven to be effective in some activities of daily living. For examples, the Empower ankle prosthesis from Ottobock uses this control concept to generate the desire output power of the device while walking. However, due to the reactive nature of this approach, it can only provide support in certain activities. Also, this approach cannot be easily scaled for controlling a more complex system (e.g. knee-ankle prosthesis) or a semi-active prosthesis that does not provide positive torque but changes the joint characteristics (e.g. stiffness, dampening).

Neuromechanical simulations have also been proposed for the control of other assistive and rehabilitation devices. Pizzolato et al. [11] provide a general outlook on how neuromusculoskeletal modelling could be integrated with a variety of rehabilitation devices to improve the performance of the human-machine interface. Durandau et al. [12] successfully applied neuromechanical modelling to allow a neurologically impaired patient to achieve voluntary control of a lower limb exoskeleton. A similar approach was employed by Sartori et al. [13] for the continuous control of a prosthetic hand.

The results of these and other studies [14, 15] illustrate the potential of neuromechanical modelling and simulation for developing a biologically plausible control of wearable robotic systems. Specifically for lower limb amputees, this approach can be used to reproduce and approximate the missing limb by using its virtual substitute. The virtual limb will be simulated online to calculate the musculoskeletal dynamics and kinematics during balance and locomotion. This could be a game changer in the field of lower limb prostheses. A patient-specific simulation can be used to enhance the control of an assistive device by calculating the torque and impedance profiles that are optimal for that specific user during the whole gait cycle. Importantly, as demonstrated in [13], the neuromechanical simulation can enable continuous and voluntary control of multiple degrees of freedom in a myoelectric prosthetic hand by amputees.

2.1 Simbionics Project

SimBionics Project is funded by the EU—Marie Curie Skłodowska Action as a European Industrial Doctorate research network. The goal is to combine neuro-mechanical modelling and sensory feedback into a real-time, closed-loop and biomimetic control framework for bionic legs.

To achieve this goal, we will implement a control framework in which the feedforward control and somatosensory feedback signals are internally consistent (Fig. 1). To this aim, both components of the control loop will be developed in parallel throughout the project, with specific emphasis on their successful integration and interaction. Thus, the characteristics of the somatosensory feedback (e.g., resolution, range, and bandwidth) will complement the dynamics of the control commands and the system and vice versa. By doing so, we expect that the control performance and embodiment of the device will significantly increase. Importantly, the neuromechanical model will be able to estimate biomechanical parameters simultaneously within (e.g. joint stiffness and damping, together with torque) and across joints (e.g. knee and ankle). In addition, the feedback will be delivered using multichannel stimulation to increase the quantity of information that can be transmitted to the user. The tactile stimulation will be modulated in time and distributed spatially, mimicking the pressure patterns that are characteristic for the biological feedback. This approach will thereby yield a robust, safe and intuitive interface between transfemoral amputees and the bionic leg while walking and balancing during the activities of daily living.

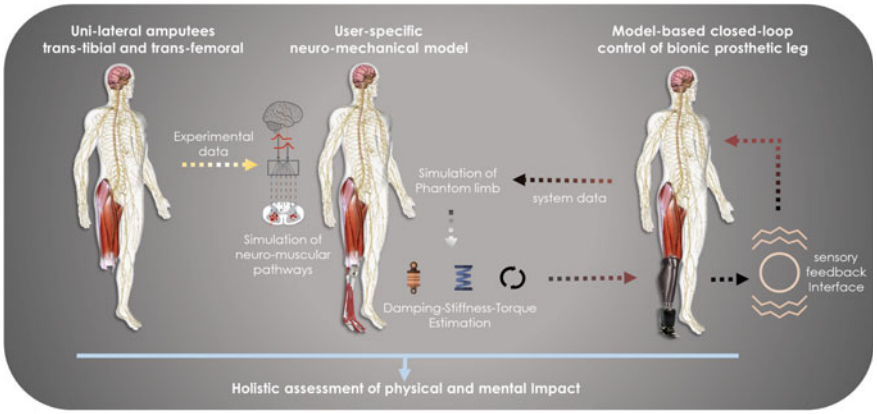

Fig. 1 The overview of the SimBionics concept. Neuromechanical modeling and online simulation will be combined with somatosensory feedback to provide a biologically plausible closed-loop control of an active lower limb prosthesis

Acknowledgements This work is supported by the Marie Skłodowska-Curie Actions (MSCA) Innovative Training Networks (ITN) H2020-MSCA-ITN-2019-860850-SimBionics (Neuromechanical Simulation and Sensory Feedback for the Control of Bionic Legs).

References

1. A. Esquenazi, Gait analysis in lower-limb amputation and prosthetic rehabilitation. Phys. Med. Rehabil. Clin. N. Am. **25**(1), 153–167 (2014)
2. J. Gonzalez-Vargas et al., A predictive model of muscle excitations based on muscle modularity for a large repertoire of human locomotion conditions. Front. Comput. Neurosci. **9**, (2015)
3. L.H. Ting et al., Review and perspective: neuromechanical considerations for predicting muscle activation patterns for movement. Int. J. Numer. Method. Biomed. Eng. **28**(10), 1003–1014 (2012)
4. R. Gailey et al., Unilateral lower-limb loss: Prosthetic device use and functional outcomes in servicemembers from Vietnam war and OIF/OEF conflicts. J. Rehabil. Res. Dev. **47**(4), 317 (2010)
5. M. Windrich et al., Active lower limb prosthetics: a systematic review of design issues and solutions. Biomed. Eng. Online **15**(S3), 5–19 (2016)
6. M.R. Tucker et al., Control strategies for active lower extremity prosthetics and orthotics: a review. J. Neuroeng. Rehabil. **12**(1), 1 (2015)
7. J. Martin, A. Pollock, J. Hettinger, Microprocessor lower limb prosthetics: review of current state of the art. JPO J. Prosthetics Orthot. **22**(3), 183–193 (2010)
8. S.B. Crea, et al., Time-discrete vibrotactile feedback contributes to improved gait symmetry in patients with lower limb amputations: case series. Phys. Ther. **97**(2), 198–207 (2017)
9. C. Dietrich et al., Leg prosthesis with somatosensory feedback reduces phantom limb pain and increases functionality. Front. Neurol. **9**, (2018)
10. M.F. Eilenberg, H. Geyer, H. Herr, Control of a powered ankle-foot prosthesis based on a neuromuscular model. IEEE Trans. Neural Syst. Rehabil. Eng. **18**(2), 164–73 (2010)

11. C. Pizzolato et al., Neuromusculoskeletal modeling-based prostheses for recovery after spinal cord injury. Front. Neurorobot. (2019)
12. G. Durandau et al, Voluntary control of wearable robotic exoskeletons by patients with paresis via neuromechanical modeling. J. Neuroeng. Rehabil. (2019)
13. M. Sreenivasa et al, (Ed).: Neuromechanics and control of physical behavior: From experimental and computational formulations to bio-inspired technologies. Front. Comput. Neurosci. (2019)
14. M. Sartori et al, Robust simultaneous myoelectric control of multiple degrees of freedom in wrist-hand prostheses by real-time neuromusculoskeletal modeling. J. Neural Eng. (2018)
15. M.A. Price, P. Beckerle, F.C. Sup, Design Optimization in Lower Limb Prostheses: a review. IEEE Trans. Neural Syst. Rehab. Eng. : a Publ. IEEE Eng. Med. Biol. Soc. (2019)

Pseudo-online Muscle Onset Detection Algorithm with Threshold Auto-Adjustment for Lower Limb Exoskeleton Control

J. Marvin Fernández García, Camila R. Carvalho, Filipe O. Barroso, and Juan C. Moreno

Abstract Spinal cord injury (SCI) is one of the main disabling injuries affecting people worldwide. The use of a wearable robot in rehabilitation reduces physical exhaustion during training. Moreover, developing novel control paradigms that allow the wearable system to move in a more intuitively way, resembling patients' intention, may enhance rehabilitation outcomes. In this paper, we present an algorithm that automatically detects users' onset and offset of lower limb muscle's contraction using electromyography (EMG) signals. The users' intention was detected through a single threshold algorithm. The algorithm auto-adjusts the threshold according to individual EMG characteristics. The algorithm was tested with EMG data from seven healthy subjects performing ankle and knee flexion/extension movements and correctly detected the intention of movement in approximately 96% of cases in an average time of 147.15 ms. To conclude, this algorithm can potentially be explored in future approaches to enable real-time triggering and control of a wearable exoskeleton to be used in the rehabilitation setting.

1 Introduction

Spinal cord injury (SCI) is one of the main disabling injuries and affects around 250,000 to 500,000 people worldwide every year [1]. The use of wearable robots in SCI rehabilitation can bring benefits and new outcomes for both patients and therapists, namely by assisting patients to achieve more precise and repetitive movements, and by reducing the physical burden to therapists [2].

The interaction between the wearable robot and the user is a critical factor to guarantee fluid and efficient control strategies. Systems based on biological signals such as electroencephalography (EEG) and electromyography (EMG) can be used to infer human movement intention in a quasi-instantaneous way, with very short time

J. M. Fernández García (✉) · C. R. Carvalho · F. O. Barroso · J. C. Moreno
Neural Rehabilitation Group of the Spanish National Research Council, Madrid, Spain

J. M. Fernández García
CEU San Pablo University, Madrid, Spain

J. C. Moreno et al. (eds.), *Wearable Robotics: Challenges and Trends*,
Biosystems & Biorobotics 27, https://doi.org/10.1007/978-3-030-69547-7_45

delays [3]. In this sense, constantly monitoring the patient's intention to move is a key task in systems that allow intuitive control of movement assistance in rehabilitation [4].

EMG signals are the most used biological signals in robotic rehabilitation [5] and can be acquired through surface or intramuscular electrodes. Surface EMG (sEMG) is the most used modality [6]. Nonetheless, sEMG is more prone to muscle crosstalk, motion artefacts, and environmental conditions. On the other hand, most of the signal processing models are oriented to sEMG recordings and are not optimized to intramuscular EMG (iEMG) signals, which in turn can overcome most of the drawbacks presented by sEMG. In this paper, we present an algorithm that automatically detects users' onset and offset of muscle's contraction using iEMG signals, which will be incorporated in a future application to control a lower limb exoskeleton.

2 Materials and Methods

EMG data from Vastus Lateralis (VL) and Tibialis Anterior (TA) of seven healthy participants (4 females and 3 males) was recorded with intramuscular thin wire electrodes (Fi-Wi2, Spes Medica). The participant is in a sitting position, without visual feedback, and performs 10 cycles of knee flexion/extension and 10 cycles of ankle flexion/extension, in a randomly assigned order. All procedures were approved by a local ethical committee ("Ethical Committee of Clinical Research with Medicines of the Hospital Complex of Toledo, Spain").

To detect the muscle onset, we used a Single Threshold (ST) method, first proposed by Cavanagh et al. in 1979 [7] that sets muscle onset timing when EMG amplitude surpasses a previously defined threshold. The algorithm created is divided into a pre-processing, training (performed offline) and detecting phase (performed pseudo-online), as shown in Fig. 1.

In the pre-processing block, EMG envelope is calculated through the application of the Hilbert-Huang transform followed by a second-order Butterworth low pass filter with cut-off frequency 480 Hz [8]. The training phase calculates the threshold value for each subject by multiplying the standard deviation (STD) of the envelope signal by an amplitude factor, calculated through visual inspection. The algorithm can automatically adjust the threshold according to each subject's characteristics.

The calculated threshold values were used during the detection phase to determine the onset and offset of the experimental data using iEMG data from TA and VL from 5 and 6 subjects respectively.

3 Results

The training phase used data recorded from up to three flexo-extension cycles to correctly determine the threshold values. The movement onset detection in tasks

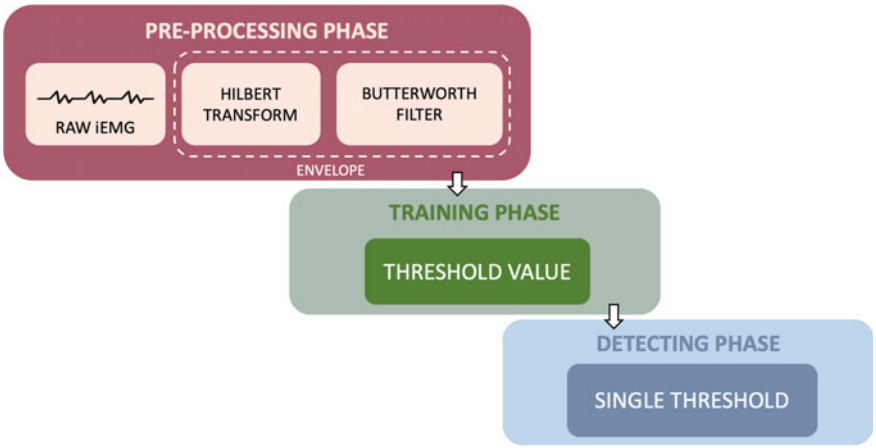

Fig. 1 Pseudo-online algorithm scheme

involving knee flexo-extension was correctly detected in 98.33% of all cycles. For the ankle tasks, the algorithm obtained a 94% success rate. For all 130 cycles of ankle and knee movements in all subjects, one false positive detection (0.77%) and three false negative detections (2.3%) were obtained. Evenly with the low number of incorrect detections, it is possible to apply a failure recognition to the code to avoid the occurrence of false and positive detections. Figure 2 shows an example of the onset and offset output of the algorithm.

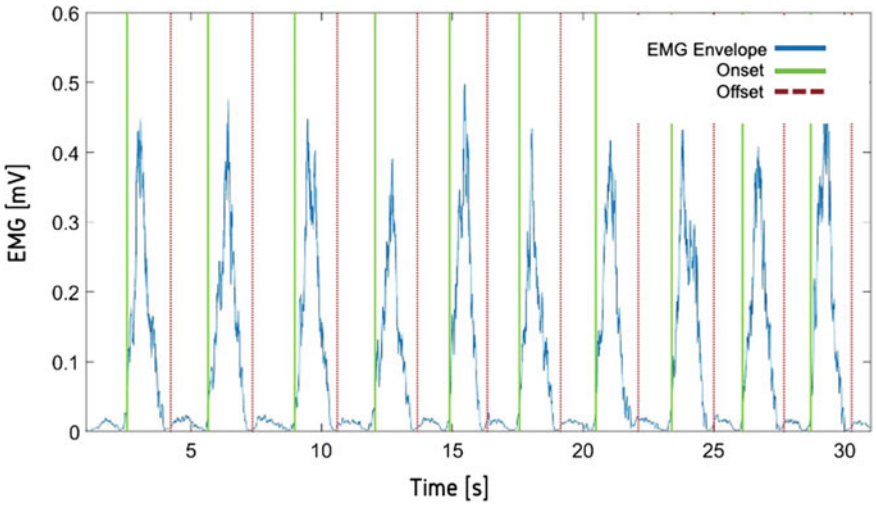

Fig. 2 EMG detection example

Table 1 Average differences between times of automatic and visual detection

Subject	Knee Mov. [ms]	Ankle Mov. [ms]
Subj.01	−5.38	–
Subj.02	−568.36	−53.12
Subj.03	−147.63	−188.25
Subj.04	+26.50	−211.75
Subj.05	−290.25	–
Subj.06	−249.50	−4.75
Subj.07	–	+15.25
Average	−205.77 ±218, 18	−88.25 ± 105,08

The accuracy of the algorithm was performed by measuring the difference in the detection times of the beginning of the contraction made by the algorithm concerning the detection times established visually by an expert. The results for all subjects are shown in Table 1. Negative values indicate a delay in the algorithm onset detection with respect to the time defined visually by the expert. The average difference among subjects was 205.769 ms for VL and 88.525 ms for TA.

4 Discussion

The training phase was able to properly detect the threshold value for each iEMG of each subject using no more than 3 cycles of ankle or knee movement. The algorithm needs a reduced amount of training time to function properly.

The algorithm also achieved a high rate of successful detections: it was higher than 90% in both knee and ankle tasks. This result suggests adequate adaptability of the algorithm to different healthy subjects and also to different types of muscle activity. This successful onset detection rate and the auto-adaptability characteristics of the algorithm are key in future applications with exoskeletons for the rehabilitation of neural impaired subjects. Taking into account that the average time it takes for the muscle to contract once it has received the electrical impulse (muscle reaction time) is set around 100 ms and the range of onset delays reported in the literature ($\approx$ 2–200 ms) [9], the average detection time of the muscle onset by the program is close to the value of the muscle reaction time, being even smaller in the TA muscle. This indicates that the program has a processing time small enough to be used in real-time applications. These results establish the algorithm as a viable solution for its implantation as a control system in real-time.

5 Conclusion

The algorithm has shown its capability of correctly detecting the intention of movement in 96.36% of cases in an average time of 147.15 ms, making it possible to apply it to the control of a robotic exoskeleton for rehabilitation in real-time. The system was able to achieve the objectives of detecting the users' onset and offset detection through intramuscular EMG signals. A reduction in the algorithm processing time will improve algorithm performance in future real-time code applications with exoskeletons.

Acknowlegements This work was funded by the European Union's Horizon 2020 research an innovation project (project EXTEND–Bidirectional Hyper-Connected Neural System) under grant agreement No. 779982.

References

1. ISCOS, "International Perspectives onSpinal Cord Injury. World Heal. Organ. (2013). https://doi.org/10.1007/978-1-4939-7880-9_11
2. W.H. Chang, Y.-H. Kim, Robot-assisted therapy in stroke rehabilitation. J. Stroke **15**(3), 174 (2013). https://doi.org/10.5853/jos.2013.15.3.174
3. W. Huo, S. Mohammed, J.C. Moreno, Y. Amirat, Lower limb wearable robots for assistance and rehabilitation: a state of the art. IEEE Syst. J. **10**(3), 1068–1081 (2016). https://doi.org/10.1109/JSYST.2014.2351491
4. D.J. Mcfarland, J.R. Wolpaw, in *Brain–Computer Interfaces for the Operation of Robotic and Prosthetic Devices* (2010), 169–187
5. R.A.R.C. Gopura, K. Kiguchi, Y. Li, SUEFUL-7: A 7DOF upper-limb exoskeleton robot with muscle-model-oriented EMG-based control. in *2009 IEEE/RSJ International Conference on Intelligent Robots and Systems*, Oct. (2009), pp. 1126–1131. https://doi.org/10.1109/iros.2009.5353935
6. J. Perry, C.S. Easterday, D.J. Antonelli, surface versus intramuscular electrodes for electromyography of superficial and deep muscles. Phys. Ther. **61**(1), 7–15 (1981). https://doi.org/10.1093/ptj/61.1.7
7. P.R. Cavanagh, P.V. Komi, Electromechanical delay in human skeletal muscle under concentric and eccentric contractions. Eur. J. Appl. Physiol. Occup. Physiol. **42**(3), 159–163 (1979). https://doi.org/10.1007/BF00431022
8. P. Hodges, A comparison of computer-based methods for the determination of onset of muscle contraction using electromyography. Electroencephalogr. Clin. Neurophysiol. **101**(6), (Dec, 1996). https://doi.org/10.1016/S0013-4694(96)95190-5
9. S.J. Currie, C.A. Myers, A. Krishnamurthy, B.A. Enebo, B.S. Davidson, Methods of muscle activation onset timing recorded during spinal manipulation. J. Manipulative Physiol. Therap. **39**(4), 279–287 (2016)

Benefits and Potential of a Neuromuscular Controller for Exoskeleton-Assisted Walking

N. L. Tagliamonte, A. R. Wu, I. Pisotta, F. Tamburella, M. Masciullo, M. Arquilla, E. H. F. van Asseldonk, H. van der Kooij, F. Dzeladini, A. J. Ijspeert, and M. Molinari

Abstract Controlling wearable exoskeletons to interact with people suffering from locomotion disabilities due to lesions of the central nervous system is a complex challenge since it entails fulfillment of many concurrent objectives: versatility in different applications (assistance and rehabilitation), user-specific adaptation to residual motor functions, compliance with different gait features (e.g. personal walking patterns and especially speed changes), smoothness of human-robot interaction, natural and intuitive exoskeleton control, acceptability and usability of the worn system. A novel bio-inspired modular controller for lower limb exoskeletons was developed by the Authors, which delivers assistive joint torques by using a reflex-based neuromuscular model. This paper presents an overview of previous and ongoing findings in testing this controller with the aim to highlight its benefits and potential in complying with user needs and with different applications.

Partial financial support was provided by: (i) the FP7 EU project SYMBITRON (ICT-2013-10-611626); (ii) the sub-project EXPERIENCE, funded by the FSTP-1 cascade funding program of the H2020 EU project EUROBENCH (ICT-2017-1-779963); (iii) the Italian Ministry of Health under *Ricerca Corrente* program.

N. L. Tagliamonte (✉)
Unit of Advanced Robotics and Human-Centred Technologies (CREO Lab), Universitá Campus Bio-Medico di Roma, Rome, Italy
e-mail: n.tagliamonte@unicampus.it

A. R. Wu
Department of Mechanical and Materials Engineering, Queen's University, Kingston, Canada

I. Pisotta · F. Tamburella · M. Masciullo · M. Arquilla · M. Molinari
Spinal Rehabilitation Laboratory (SPIRE Lab) and Laboratory of Robotic Neurorehabilitation (NeuroRobot Lab), Neurorehabilitation 1 Department, Fondazione Santa Lucia, Rome, Italy

E. H. F. van Asseldonk · H. van der Kooij
Department of Biomechanical Engineering, University of Twente, Enschede, The Netherlands

F. Dzeladini · A. J. Ijspeert
BioRobotics Laboratory, School of Engineering, Institute of Bioengineering, Ecole Polytechnique Federale de Lausanne, Lausanne, Switzerland

J. C. Moreno et al. (eds.), *Wearable Robotics: Challenges and Trends*,
Biosystems & Biorobotics 27, https://doi.org/10.1007/978-3-030-69547-7_46

1 Introduction

People with walking disabilities due to neurological impairments exhibit heterogeneous residual motor functions, specific locomotion performance and peculiar functional compensation strategies. Exoskeletons designed for gait assistance and rehabilitation should ideally properly fit the personal needs and clinical condition of individual subjects in terms of biomechanical and anthropometric parameters, functional behavior, clinical prescriptions, and personal expectations. Moreover, as wearable devices, the robots have to synchronously adapt to the intended motion of the impaired user, who in turn should be allowed to exploit robotic physical support to improve their motor function. This shared control is very crucial to obtain an effective human-machine interaction with the highest benefits for the user.

Multiple approaches have been explored to assist human movements with compliance and adaptability. Interaction control schemes use model-based or model-free approaches based on electromyographic (EMG) measurements to adjust joint torques. Kinematic-based approaches include nonlinear models that intrinsically synchronize with human movements and can use impedance controllers (i.e. haptically delivering viscoelastic torques) to impart a reference motion trajectory.

We developed a novel bio-inspired modular controller for lower limb exoskeletons that delivers assistive joint torques by using a reflex-based neuromuscular model that activates simulated muscle reflex loops based on ground contact detection and joint angles. This paper presents an overview of previous and ongoing findings in applying this controller to different case studies to highlight the benefits of this bio-inspired approach and its promising potential in complying with user needs and different applications.

2 Exoskeleton-Assisted Walking with a Neuromuscular Controller

2.1 Neuromuscular Controller

The NeuroMuscular Controller (NMC) we developed is based on a reflex-based neuro-mechanical simulation of walking reported in [1]. The full sagittal plane controller consists of seven Hill-type muscle units per leg (Fig. 1). Joint angles, which determine virtual muscle length and velocity information, activate the virtual muscles through reflex loops. The forces generated by these muscles are then combined to yield joint torques. The reflex loops employed depend on the gait phases detected by foot contact. Stance reflexes support body weight while swing reflexes allow for leg swing. The nominal torque output of the controller corresponds to the contribution of the muscles required for a simulated human (mass: 80 kg; height: 1.8 m) to walk at 1.3 m/s. A gain multiplying the nominal torque can be used to scale the level of

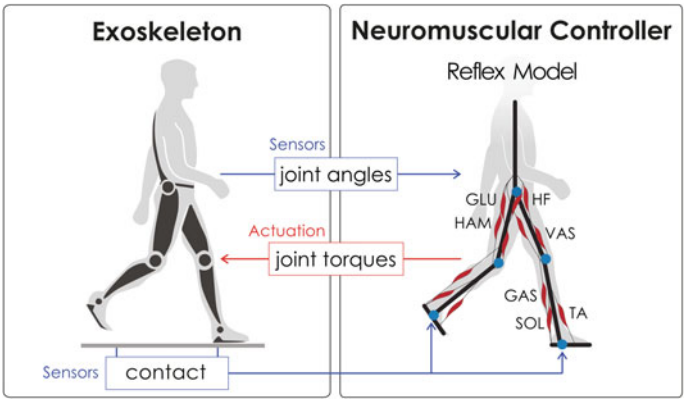

Fig. 1 Lower limb exoskeleton controlled by the NMC. The reflex model uses joint angles and foot contact information (blue) to derive assistive joint torques (red). To generate gait in the sagittal plane, the modeled muscles include the tibialis anterior (TA), soleus (SOL), gastrocnemius (GAS), vasti (VAS), hamstring (HAM), gluteus maximus (GLU), and hip flexors (HF)

assistance. The contribution of each single virtual muscle can also be regulated to fine-tune the model to deliver further user-specific assistance.

2.2 Case Studies

This section overviews Authors' studies applying the NMC to wearable lower-limb exoskeletons to be used as assistive devices. The modularity of the controller enabled its use on nearly any combination of actuated joints.

(1) *Ankle Exoskeleton*: The NMC-controlled Achilles ankle exoskeleton was tested during treadmill walking in 2 healthy subjects in [2] and during overground walking in 4 subjects with incomplete Spinal Cord Injury (iSCI) in [3]. For iSCI users, results suggested a possible unexpected rehabilitation effect (improvement of free walking) that was further investigated in [4] by comparing Achilles-aided training with conventional gait rehabilitation.
(2) *Hip/knee Exoskeleton*: The hip and knee NMC modules were tested with 6 SCI subjects (2 iSCI) during treadmill walking on LOPES III, a stationary gait trainer [5].
(3) *Knee/ankle Exoskeleton*: The NMC-controlled SYMBITRON knee-ankle exoskeleton was tested during overground walking in 2 iSCI subjects in [6].

3 Results and Discussions

The main findings from our studies show that the NMC:

- preserved ankle-assisted treadmill walking dynamics (e.g. ground reaction forces, joint kinematics), reduced metabolic cost, and lowered SOL and TA EMG activity for healthy subjects [2];
- improved the walking speed of iSCI subjects during ankle-assisted overground walking after a 5-session training, avoided altering walking stability (step width and stance duration were not perturbed) and personal walking style (ankle joint motion was not forced towards predefined stereotyped trajectories), and improved endurance [3];
- improved free overground walking of iSCI subjects on long and short distances thus providing an unexpected rehabilitation effect [3, 4];
- promoted motivation, engagement and satisfaction in the use of exoskeletons by inducing a feeling of autonomy and higher control on gait [3, 4];
- enabled SCI subjects to walk at various speeds, faster than typical for ambulatory SCI subjects, with natural increases in step length and close to physiological joint angle trajectories, with meaningful rhythmic EMG activation patterns in distal muscles of complete SCI subjects (medial GAS and TA) and with EMG activation timing more consistent among subjects for distal muscles [5];
- supported knee/ankle-assisted overground walking for a large range of speeds and generated healthy-like gait in iSCI subjects with various levels of mobility [6].

From these results, the NMC central benefits include:

- Versatility: changes in speed, whether as a result of the treadmill or the subjects' own initiative in overground walking, are easily facilitated;
- Robustness: appropriate gait behavior are successfully generated for both overground and treadmill walking for subjects with different anthropometric dimensions and residual functions;
- Modularity: sub-modules can be reconfigured to be applied to a range of lower-limb devices from one- to multi- joint combinations;
- Adaptability: subject-specific needs can be supported by assistive torque adjustments at the joint (coarse) or at virtual muscle (fine) levels;
- Intuitiveness: speed changes can simply be enacted by smoothly modifying footfall patterns;
- Simplicity: very few sensors (joint angles, foot contact events) are required;
- Usability: user experience during exoskeleton-assisted walking is perceived as comfortable, effective and interesting.

There are some limitations to the controller: it cannot generate gait initiation on its own and is better suited for walking speeds above 0.6 m/s [5].

Based on the promising results and benefits, the considerable potential of the NMC for future applications include the possibility to: (i) comply with complex and heterogeneous user needs in terms of different gait features and residual motor

functions; (ii) be applied in both daily life assistive scenario and in clinical rehabilitation environments; (iii) be used for both healthy (augmentation and energetic cost reduction) and impaired subjects (assistance and rehabilitation).

4 Conclusion

A bio-inspired controller for lower limb exoskeletons was developed, which delivers assistive joint torques by using a reflex-based neuromuscular model. Tests with SCI subjects with different impairments on various NMC-controlled devices demonstrated the NMC unique benefits and potential for gait assistance and rehabilitation.

References

1. H. Geyer, H. Herr, A muscle-reflex model that encodes principles of legged mechanics produces human walking dynamics and muscle activities. IEEE TNSRE **18**(3), 263–273 (2010)
2. F. Dzeladini, et al., Effects of a neuromuscular controller on a powered ankle exoskeleton during human walking, in *IEEE BioRob* (2016)
3. F. Tamburella, et al., Neuromuscular controller embedded in a powered ankle exoskeleton: effects on gait, clinical features and subjective perspective of incomplete spinal cord injured subjects. IEEE TNSRE **28**(5), 1157–1167 (2020)
4. F. Tamburella, et al., Gait training with achilles ankle exoskeleton in chronic incomplete spinal cord injury subjects. J. Biol. Regul. Homeostatic Agents **34**(5 Suppl. 3), 147–164 (2020)
5. A.R. Wu et al., An adaptive neuromuscular controller for assistive lower-limb exoskeletons: a preliminary study on subjects with spinal cord injury. Front. Neurorob. **11**, 30 (2017)
6. C. Meijneke, et al., Design, control and evaluation of a modular exoskeleton for incomplete and complete spinal cord injured subjects. IEEE TNSRE **29**, 330–339 (2021)

CANopen Robot Controller (CORC): An Open Software Stack for Human Robot Interaction Development

Justin Fong, Emek Barış Küçüktabak, Vincent Crocher, Ying Tan, Kevin M. Lynch, Jose L. Pons, and Denny Oetomo

Abstract Interest in the investigation of novel software and control algorithms for wearable robotics is growing. However, entry into this field requires a significant investment in a testing platform. This work introduces CANopen Robot Controller (CORC)—an open source software stack designed to accelerate the development of robot software and control algorithms—justifying its choice of platform, describing its overall structure, and demonstrating its viability on two distinct platforms.

J. Fong (✉) · V. Crocher · Y. Tan · D. Oetomo
University of Melbourne and Fourier Intelligence Joint Laboratory, the University of Melbourne, Melbourne, Australia
e-mail: fong.j@unimelb.edu.au

V. Crocher
e-mail: vincent.crocher@unimelb.edu.au

Y. Tan
e-mail: yingt@unimelb.edu.au

D. Oetomo
e-mail: doetomo@unimelb.edu.au

E. B. Küçüktabak · K. M. Lynch · J. L. Pons
McCormick School of Engineering, Northwestern University,Evanston, USA
e-mail: baris.kucuktabak@u.northwestern.edu

K. M. Lynch
e-mail: kmlynch@northwestern.edu

J. L. Pons
e-mail: jpons@sralab.org

E. B. Küçüktabak · J. L. Pons
Legs + Walking Lab, Shirley Ryan Ability Lab, Chicago, USA

J. C. Moreno et al. (eds.), *Wearable Robotics: Challenges and Trends*,
Biosystems & Biorobotics 27, https://doi.org/10.1007/978-3-030-69547-7_47

1 Introduction

The rapid progression of actuation, power and processing technologies has significantly improved the capabilities and possible applications of exoskeleton and wearable robotic devices. With these developments, interest in developing controllers and control algorithms for gait trajectory planning and human-robot interactions strategies has risen, with this field being recently identified as a key developmental opportunity for improving exoskeleton performance [1]. However, a key challenge in the pursuit of this field is the development of tools for testing said algorithms. This is particularly true for wearable devices, which see large variations in actuator and sensor configurations and designs.

The present work introduces the CANopen Robot Controller (CORC)—an open source software stack designed to accelerate the development of robotic devices based on CANopen hardware. CORC allows modular hardware use by leveraging the CANopen standardisation while providing a real-time system meeting the safety requirements of wearable devices. Within this work, the design and architecture of CORC is introduced, and the viability of the the stack is dermonstrated through measurement of control loop period jitter on two CORC implementations running respectively on the Fourier Intelligence X2 exoskeleton [2] and the EMU upper-limb manipulandum [3].

2 Materials and Methods

2.1 Goals and Objectives

CORC was developed as a common development platform for robots which primarily use CANopen devices. CANopen has a 25+ year history as a communications protocol in industrial automation, and is commonly used in robotic devices. Therefore, the objectives of CORC are to provide a flexible, modular architecture for different applications and devices, with a loop rate of 200 Hz with low jitter.

2.2 Platform

Two major decision points were made for the platform of the CORC software stack—the operating system and the programming language.

(1) *Operating System—Linux-Based*: Linux-based operating systems presented themselves as the obvious choice, primarily due to their open and stable nature, as well as their ability to be run with a real time kernel—which can be critical

in human-robot interactions. Furthermore, Linux is well-supported on a large range of hardware platforms.

(2) *Programming Language—C/C++*: For efficiency reasons, C is used for the critical sections of the software and C++ at the higher level to take advantage of the Object Oriented Programming design without sacrificing performance.

2.3 Software Architecture

The CORC software stack is divided into three distinct layers to enable flexible implementations on different platforms.

(1) *CANopen Layer*: The CANopen layer handles the application layer transfer of CAN messages, including poll-response (Service Data Object, SDO) and streamed (Process Data Object, PDO) protocols. This layer is based on CANopenSocket [4], and licensed under the Apache License, Version 2.0. Limited changes are required to this layer to develop using CORC.

(2) *Robot Layer*: The robot layer describes the robotic structure, and links it with the input (*e.g.* sensors) and output devices (*e.g.* motor drives). It acts as an abstraction between the control algorithms and the hardware, allowing implementation of kinematic and/or dynamic models. CORC also contains base classes according to CAN in Automation (CiA) standards. This layer is designed to be modified only when new hardware is added to the robotic device.

(3) *Application Layer*: The application layer implements overall program logic and control algorithms. In CORC, each application is a dedicated state machine, derived from a common class. This architecture encourages safe execution while leaving complete freedom for logic implementation. Specific ad hoc libraries can be used at this level to extend capabilities such as providing Robot Operating System (ROS) node capabilities to the application. Given an existing robot implementation, only application layer modification is required to perform research into novel control strategies. With this approach, a CORC application can also be used as a robot firmware for a specific application with routine execution, or for communication with a third-party software.

2.4 Viability Test

The viability test sought to demonstrate two key goals of the toolbox: flexibility for different hardware platforms, and consistency in control loop execution rate. Therefore, simple programs were implemented on two hardware platforms (Fig. 1), and executed at different control frequencies. The hardware platforms were:

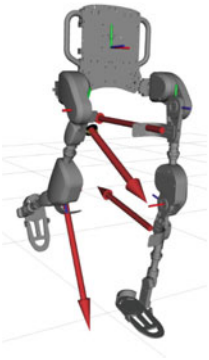

(a) RViz Visualisation of Fourier Intelligence X2 Exoskeleton showing forces at force sensors

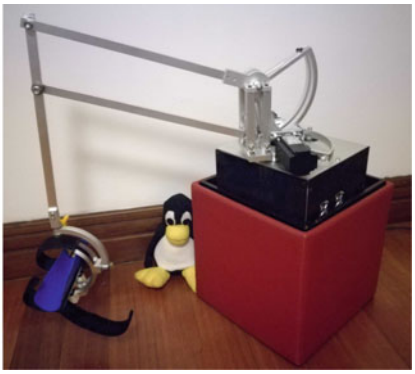

(b) EMU Upper Limb Manipulandum

Fig. 1 Hardware platforms tested

(1) A Fourier Intelligence X2 Exoskeleton including 4 Copley Accelnet ACK-055-06 motor drives and 4 custom force sensors, driven by a laptop computer (Intel Core i7-9750H CPU, 16.0 GB RAM, Ubuntu 18.04, ROS Melodic) with a PCAN-USB adapter [5].
(2) The EMU Upper Limb Manipulandum including 3 Kinco FD123-CA motor drives and driven by a Beaglebone AI singleboard computer (Dual Arm® Cortex®-A15, 1.0 GB RAM, Debian, Linux Kernel v4.14 with a PREEMPT-RT patch).

Three tests cases were run: *X2-P:* The X2 moving continually between sitting and standing with calculation of joint angles through inverse kinematics based on a hip position trajectory, and with the application set up as a ROS node broadcasting joint state and force sensor readings to be visualised using Rviz (Fig. 1a); *EMU-I*: the EMU operated in impedance control with a feedforward position-dependent gravity compensation term; and *EMU-P*: in position control following a minimum jerk task space trajectory.

Each test case was run with different nominal control loop periods for a minimum of 60 s, and the actual loop period recorded whilst the control was operational—with 'system configuration' periods removed. Loop periods were normalised against nominal for comparison.

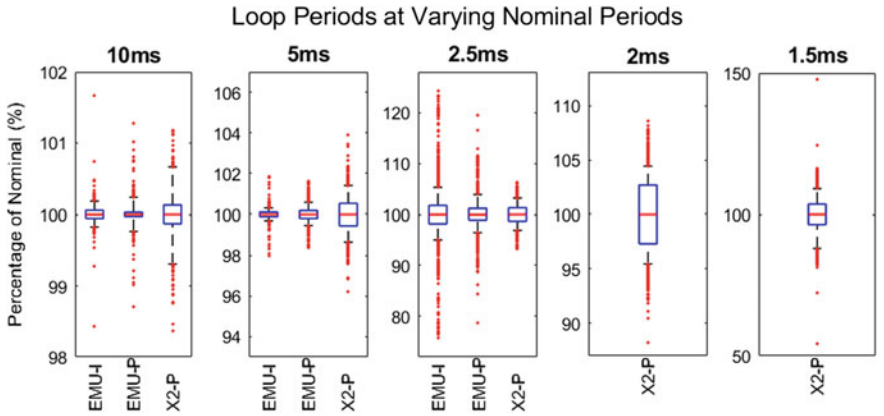

Fig. 2 Loop Periods (normalised to nominal). The extents of the box capture exactly 80% of datapoints, and the extents of the whiskers capture exactly 99%

3 Results

Figure 2 illustrates the control loop times. Note that it was not possible to run the EMU platform with a period of less than 2.5 ms. However, all cases produced a mean loop period within 0.001% of the nominal period.

It is to note that no changes were required at the CANopen layer between the applications on the two platforms, and only at the application layer for the two EMU cases.

4 Discussion

The results demonstrate the capability of the CORC software stack to be used on two entirely different platforms which share no common hardware. As such, CORC achieved its primary goal of portability and flexibility.

Increasing variation was observed with decreasing nominal period. It is noted that the effect of this variation is extremely dependent on the sensitivity of the implemented control, and as such, these results are presented only as an indication of performance. Interestingly, at lower frequencies and despite having less processing power, the EMU platform demonstrated less variation—likely due to the real time kernel running on the Beaglebone AI.

CORC's primary limitation is that it is designed primarily to run robots which have CAN devices. Whilst the choice of CANopen provides a number of advantages, its serial nature results in bandwidth limitations. Thus, as additional CAN devices are added to the bus, less bandwidth is available for each, reducing the possible motor update speeds.

5 Conclusions

The present work introduces the CORC toolbox—a software stack designed for robotic devices—to accelerate the development of control algorithms and trajectories. This first evaluation demonstrates its implementation flexibility and performance stability across different hardware platforms. This open software stack is available[1] to the wearable robotics community for use and development. Future work includes the development of a robust logging module and further integration with ROS, beyond the currently-implemented broadcast functionality.

References

1. G.S. Sawicki, et al., The exoskeleton expansion: improving walking and running economy. J. Neuroeng. Rehabil. **17**(1), 1–9 (2020)
2. Fourier Intelligence, X2 http://www.fftai-global.com/lower-extremity/
3. J. Fong, et al. EMU: a transparent 3D robotic manipulandum for upper-limb rehabilitation, in 2017 IEEE International Conference on Rehabilitation Robotics (ICORR) (2017), pp. 771–776
4. CANopenSocket https://github.com/CANopenNode/CANopenSocket
5. PEAK-System, PCAN-USB https://www.peak-system.com

[1] https://github.com/UniMelbHumanRoboticsLab/CANOpenRobotController.

Toward Efficient Human-Exoskeleton Symbiosis

Direct Collocation-Based Optimal Controller for Multi-modal Assistance: Simulation Study

Anh T. Nguyen, Vincent Bonnet, and Samer Mohammed

Abstract Multi-modal assistive system is a hybrid system that aims to provide assistance-as-needed for paretic subjects. The hybrid system combines human muscle efforts, stimulated by a Functional Electric Stimulator (FES) and an lower-limb active exoskeleton. With optimal sharing of the two activation inputs, a hybrid system could overcome several challenges, such as human force due to FES-induced muscular fatigue. In this paper, a novel optimal controller, based on an efficient (3.9 ms to predict a time windows of 40 ms) closed-loop direct collocation approach is proposed to predict the control allocation between FES and exoskeleton. Simulation results, performed with dynamically varying desired trajectory, show that the proposed controller adapts the control input with respect to muscular fatigue.

1 Introduction

Multi-modal assistive systems, combining FES and active exoskeleton, aim to provide assistance-as-needed to support paretic patients recovering normal walking gait patterns. However, to take into account the nonlinear muscular fatigue due to functional electrical stimulation, an adaptation of the level of support provided by each assistive device is required. To address this challenge, researchers have explored control allocation methods to automatically adjust the control tuning between FES and exoskeleton. In the literature, recent approaches based on high-bandwidth feedback control methods or non linear model predictive controller-based direct control allocation method developed by Kirsh et al. [1, 2] were proposed. These studies shows satisfactory results with patients. However, the investigated desired trajectories were limited to a step-wise. Thus, this paper proposes a novel approach based on popular and computationally efficient direct collocation optimisation method to solve the control allocation between FES and exoskeleton support during flexion/extension movements of the knee joint.

A. T. Nguyen · V. Bonnet (✉) · S. Mohammed
Univ Paris Est Creteil, LISSI, 94400 Vitry, France
e-mail: vincent.bonnet@u-pec.fr

J. C. Moreno et al. (eds.), *Wearable Robotics: Challenges and Trends*,
Biosystems & Biorobotics 27, https://doi.org/10.1007/978-3-030-69547-7_48

2 Methods

2.1 *Biomechanical Model of the Multi-modal Assistive System*

The multi-modal knee joint assistive system for flexion-extension movements is illustrated in Fig. 1 where control vector $\boldsymbol{u} = [u_{ke} \quad M_m]^T$ is composed of the FES current amplitude (u_{ke}, acting on quadriceps muscle) and the exoskeleton assistive torque (M_m). The system state vector is $\boldsymbol{x} = [q \quad \dot{q} \quad a_{ke} \quad \mu]^T$ which consists of the knee joint angle q and velocity $\dot{q}$, the muscle activation a_{ke}, and the quadriceps muscular fatigue μ. The control inputs are linked to the human-exoskeleton system dynamics thanks to the following models:

$$J\ddot{q} = -G\sin q - M_p + M_m + M_{ke} \tag{1}$$

where $\ddot{q}$ is the knee joint acceleration. J is the shank-exoskeleton inertia, and G represents the gravitational force. M_p is the passive joint torque modeled using six subject-specific parameters and exponential functions as proposed in [3].

When FES is applied, the resultant knee extension torque can be estimated as [3]:

$$M_{ke} = (c_2 q^2 + c_1 q + c_0)(1 + c_3\dot{q})a_{ke}\mu, \tag{2}$$

where $c_j \in \mathbb{R}\,\forall j = \{0-3\}$ are subject specific parameters.

$a_{ke} \in [0, 1]$ is the muscle activation which variation is based on a first-order differential equation [4]. μ is the muscle fatigue and is a function of the muscle activation as $\dot{\mu} = \frac{(\mu_{\min}-\mu)a_{ke}}{T_f} + \frac{(1-\mu)(1-a_{ke})}{T_r}$. $\mu_{\min} \in [0, 1]$ is the minimum fatigue level of muscle, T_r, T_f are the recovery and fatigue time constant, respectively.

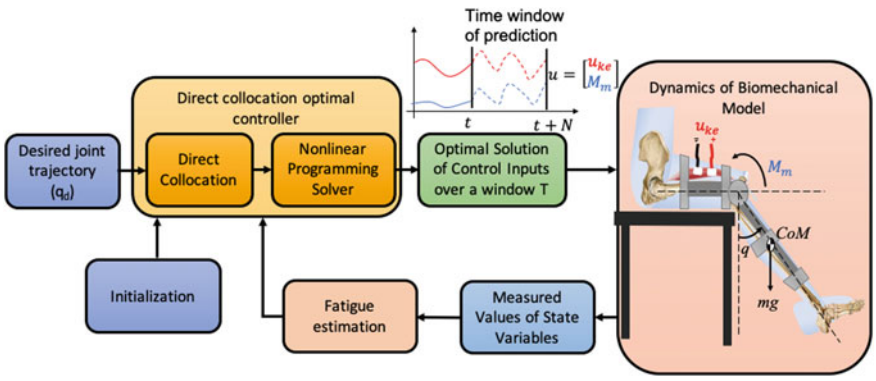

Fig. 1 Overview of the proposed optimal control scheme

Following the above formulation, the system dynamics can be expressed as a state-space model:

$$\dot{\boldsymbol{x}} = \boldsymbol{f}(u) = \begin{bmatrix} \dot{q} \\ \frac{1}{J}(M_m + M_{ke} - M_p - G) \\ \frac{u_{ke} - a_{ke}}{T_a} \\ \frac{(\mu_{\min} - \mu)a_{ke}}{T_f} + \frac{(1-\mu)(1-a_{ke})}{T_r} \end{bmatrix} \tag{3}$$

2.2 Direct Collocation-Based Optimal Controller

The control objective is to predict **u** over a time window, of length T and N samples, to be able to track the desired knee joint trajectory, while minimizing the control effort. The allocation between exoskeleton assistance and FES assistance will be modulated automatically while taking into account fatigue evolution. The problem can be summarized as follow.

Direct collocation is a trajectory optimization method [5] that converts the continuous-time trajectories problem into a Nonlinear Programming (NLP) problem. A trapezoidal approach is used due to its efficiency in discretizing the evaluation of the cost function and of the state-space dynamics (3). The continuous optimal control problem is then transformed into discrete-time formulations of NLP with collocation constraints [5]. Note that, in this optimization problem, the decision variables are the state and control variables which are unknowns in the system dynamics. The NLP problem is expressed as:

$$\min_{\boldsymbol{x}_k, \boldsymbol{u}_k} \sum_{k=0}^{N-1} \frac{h_k}{2} \left(\left(\frac{u_{ke(k)}}{u_{ke}^+} \right)^2 + \left(\frac{M_m(k)}{M_m^+} \right)^2 + \left(\frac{(q_d(k))_k - q(k)}{q^+} \right)^2 \right)$$

s.t.

$$\begin{aligned} &\boldsymbol{C}_{eq} = \boldsymbol{x}_{k+1} - \boldsymbol{x}_k - \tfrac{h_k}{2}(\boldsymbol{f}_{k+1} + \boldsymbol{f}_k) \; \forall k \in [0, ..., N-1] \\ &\boldsymbol{x}_k^- \leq \boldsymbol{x}_k \leq \boldsymbol{x}_k^+ \quad \forall k \in [0, \ldots, N] \\ &\boldsymbol{u}_k^- \leq \boldsymbol{u}_k \leq \boldsymbol{u}_k^+ \quad \forall k \in [0, \ldots, N] \end{aligned}$$

where q_d is the desired trajectory of angular position of knee joint, u_{ke}^+, M_m^+, q^+ show the upper bound of the associated variables. This problem was solved using C++ and IPOPT solver.

3 Simulation Results

For the validation of the proposed approach three types of trajectories were assessed in simulation with a large induced muscle fatigue: a stepwise, a sinusoidal and a trajectory of the knee corresponding to a normal walking gait pattern. The model parameters (see Sect. 2.1) were identified on a healthy male (stature:1.75 m, weight: 70 kg, age: 26 years) as proposed in [2]. Figure 2 shows results obtained with a step-wise trajectory. One can see that the proposed controller was able to adaptively allocate the control inputs while keeping high tracking performance of the desired trajectory. As the quadriceps fatigue increases, the knee extension torque due to FES automatically decreases to recover from fatigue. As shown in Fig. 3 and in Table 1, the controller showed its high accuracy and versatility even during dynamics motion of the desired input. Furthermore, controller performed well by adapting the knee join to various types of angular trajectories with an RMSE lower than 0.2 deg in any case. The calculation time, obtained in C++, required to determine the control input over the entire windows of 40 ms was of 4.9 ms (including the dynamical system simulation).

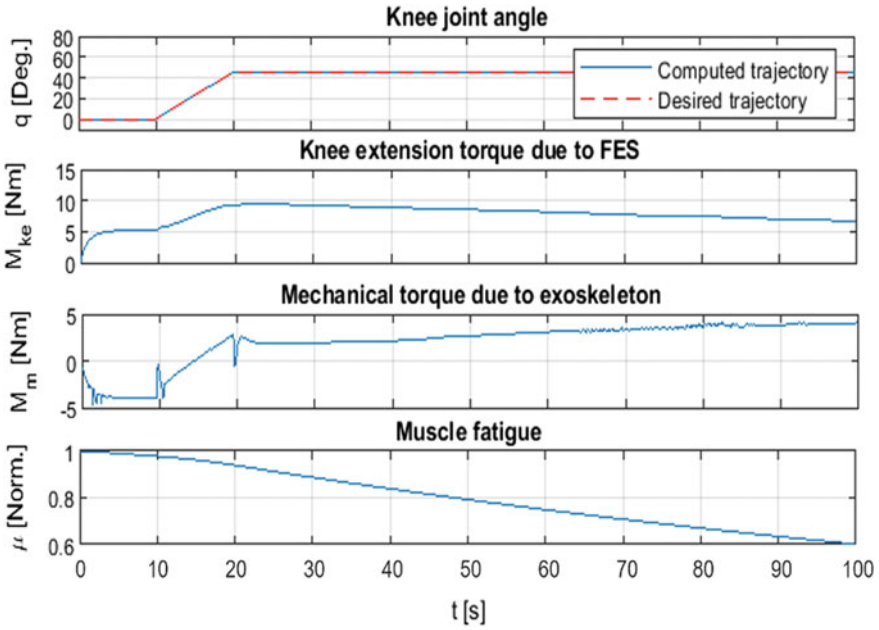

Fig. 2 Simulation results of regulation performance with a stepwise trajectory. Muscle fatigue is induced and the system complementarily increases torque from the actuator

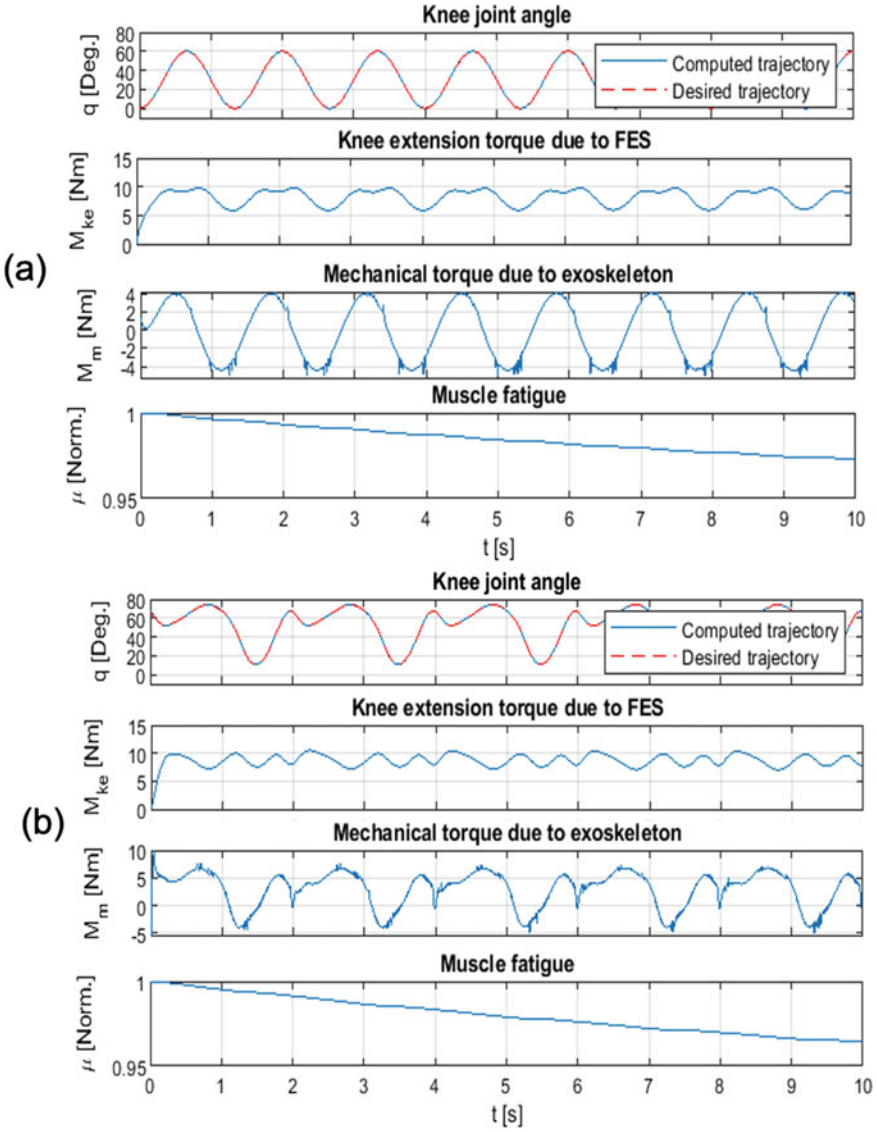

Fig. 3 Simulation results of regulation performance with **a** a sinusoidal trajectory and **b** a walking gait pattern

Table 1 Root mean square error (RMSE) between computed values and desired trajectory of knee joint angle

Desired trajectory	RMSE [deg]
Sinusoidal	0.0434
Normal walking	0.1267
Step-wise	0.0238

4 Conclusion

When compared to the technique used in the literature [1], the proposed direct collocation-based controller might be more efficient for its use in dynamic motions such as walking, or stair ascent/descent. Kirsch et al. reported an RMSE of 3.9 deg when tracking a constant desired knee joint angle but with a real patient. The present results, even if promising, are only obtained in simulation and further investigation are required with real-pathological subjects.

References

1. N.A. Kirsch, X. Bao, N.A. Alibeji, B.E. Dicianno, N. Sharma, Model-based dynamic control allocation in a hybrid neuroprosthesis. IEEE Trans. Neural Syst. Rehabil. Eng. 224–232 (2017)
2. N.A. Kirsch, N.A. Alibeji, N. Sharma, Nonlinear model predictive control of functional electrical stimulation. Control Eng. Practice 319–331 (2017)
3. D. Popovic, R.B. Stein, M.N. Oguztoreli, M. Lebiedowska, S. Jonic, Optimal control of walking with functional electrical stimulation: a computer simulation study. IEEE Trans. Rehabil. Eng. 69–79 (1999)
4. R. Riener, J. Quintern, G. Schmidt, Biomechanical model of the human knee evaluated by neuromuscular stimulation. J. Biomech. 1157–1167 (1996)
5. M. Kelly, An introduction to trajectory optimization: how to do your own direct collocation. SIAM Rev. 849–904 (2017)

A Semi-active Upper-Body Exoskeleton for Motion Assistance

Shaoping Bai, Muhammad R. Islam, Karl Hansen, Jacob Nørgaard, Chin-Yin Chen, and Guilin Yang

Abstract This paper describes a semi-active assistive exoskeleton for upper-body motion assistance. The exoskeleton combines a passive shoulder exoskeleton and an active elbow joint unit, which can achieve both passive gravity compensation and also active assistance to carrying and sit-to-stand motion. The design, sensing and control are introduced, with preliminary test results performed.

1 Introduction

Exoskeleton technology has been used in many applications, including medical care/rehabilitation, industrial workplace assistance, military applications, and also welfare service for the elderly [1–4]. While many systems have been developed and some of them were commercialized, design of powered upper-body systems which are lightweight yet powerful poses challenges to exoskeleton development. This is evidenced by the fact that commercial wearable exoskeletons for industrial markets are mainly passive exoskeletons [5]. In this paper, a novel exoskeleton designed in a hybrid approach is introduced. By combining both passive joints with gravity compensation and also powered joints, a lightweight exoskeleton able to support motions such as sit-to-stand and load carrying tasks is developed.

S. Bai (✉) · M. R. Islam
Department of Material and Production, Aalborg University, Aalborg, Denmark
e-mail: shb@mp.aau.dk

K. Hansen · J. Nørgaard
Department of Electronics Systems, Aalborg University, Aalborg, Denmark

C.-Y. Chen · G. Yang
Ningbo Institute of Industrial Technology, CAS, Ningbo, China

J. C. Moreno et al. (eds.), *Wearable Robotics: Challenges and Trends*,
Biosystems & Biorobotics 27, https://doi.org/10.1007/978-3-030-69547-7_49

2 Exoskeleton Design

Figure 1 shows the exoskeleton, called EXO-AIDER, developed at the exoskeleton lab, Aalborg University, Denmark. It integrates a passive exoskeleton from Skelex (www.skelex.com) and an elbow joint unit. The model Skelex-360 exoskeleton is used for this design. The passive exoskeleton is able to compensate gravity force by embedded springs. For the EXO-AIDER, this means that both the arm weight and also elbow joint weight can be compensated by the spring forces.

In the EXO-AIDER, an integrated driving unit is designed and fabricated to provide sufficient powered assistance for elbow joints, in particular, supporting body from sit to stand. Electrical motors were customized with selected gears. According to the design requirements, the motor has to provide assistive torque for 50 Nm, while the dimension needs to be minimum. A permanent magnet torque motor was thus designed on the basis of extensive simulations, shown in Fig. 2, to improve torque density of the permanent magnet torque motor. High-performance materials and design methods such as permanent magnet, soft magnetic and magnetic circuit

Fig. 1 A semi-active exoskeleton EXO-AIDER for upper-body motion assistance

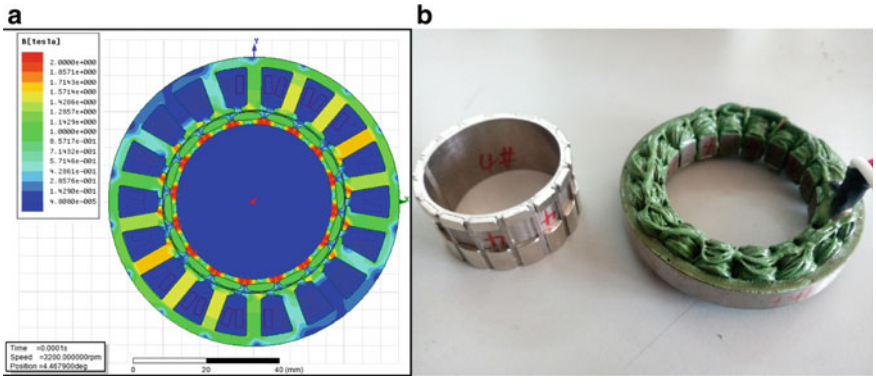

Fig. 2 Torque motor simulation and prototype. **a** magnetic cloud diagram for motor, **b** rotor and stator

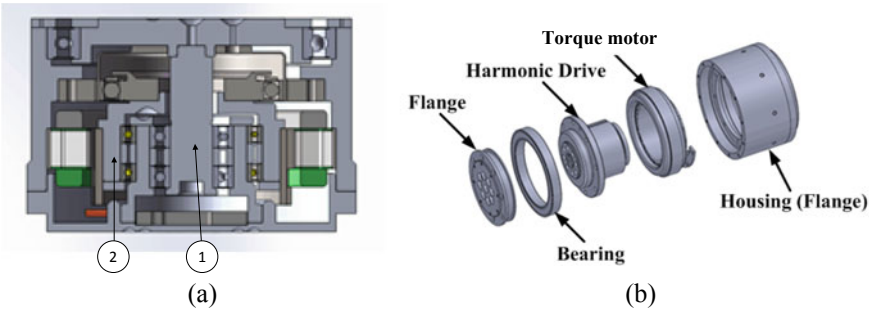

Fig. 3 Overall structure of elbow joint driving unit, **a** assembly, where: 1—inner shaft and 2—outer shaft, **b** an exploded view

topology were employed. Moreover, to reduce the cogging torque, parameters such as polar arc coefficient of permanent magnet, shape of permanent magnet, size of slot and skew angle of slot, are carefully examined.

Figure 3 shows the design of the driving unit for the elbow joint. In this unit, the customized high-performance permanent magnet torque motor was combined with a harmonic drive of high gear ratio (1:100) as the transmission system. As shown in Fig. 3a, there are two shafts in the joint unit, the "inner shaft" and the "outer shaft". The outer shaft, transmits torque and rotation from the rotor to the wave generator of the harmonic drive. The inner shaft is connected to an encoder to record the rotational angle. A magnet for the absolute rotary magnetic encoder is mounted on the tip of inner shaft. The angular rotation data is measured through an AS5145B 12bit encoder. Additionally, two angular contact bearings create a compact, high-moment-capacity support. The final design of the driving unit has a dimension of ∅ 72 mm × 48 mm and weighs 600g. The motor has a maximum torque 55 Nm, in other words, a torque density of 91.6 Nm/kg.

3 Sensing and Control

In motion assistance, it is essential to detect user motion intention for control purpose [6]. The EXO-AIDER uses a sensor armband with a sensor module dedicated to the both the biceps and the triceps. The armband is made of a stretchable material to make sure the modules are located on the muscles and stay in place. The sensors used in the armband consists of both surface electromyography (sEMG) and force sensitive resistor (FSR) sensors (Fig. 4). The sEMG sensors are used to measure muscle activity, while the FSR sensors measure the contraction of the muscles. The idea is to use a combination of the two types of sensors to observe a correlation determining the intention of the user to give a transparent experience while using the exoskeleton.

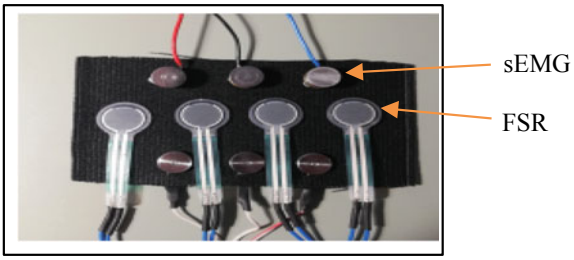

Fig. 4 A module of FRS and sEMG sensors

The sampling frequency of sEMG sensors is up to 500 Hz which is the spectrum of sEMG signals. Since the amplitude of sEMG signal is in the millivolt level, they are very sensitive to noise. To eliminate this noise, the signal is sampled through a differential amplifier to omit noise that exists on both inputs of the amplifier. FSR is sampled at 1000 Hz. The sEMG and the FSR signals are sampled through analog-to-digital converters and the signal data is transmitted through Bluetooth to a computer for further signal processing, analysis or control using the acquired signals. In addition, a load cell is mounted to the cuff in forearm to detect interaction force between human user and exoskeleton.

With these sensors, task based control technique is implemented to provide motion assistance. Block diagram of the control scheme is shown in Fig. 5. The exoskeleton adopts two modes for different assistance, one admittance control and the other the carrying assistance control. In admittance control, the control law is defined by:

$$\frac{\omega_d}{\tau_{int}} = \frac{1}{Ms + D + \frac{K}{s}}$$

here M, D and K are the desired inertia, damping and stiffness of the forearm link, whereas τ_{int} and ω_d represent the interaction torque and desired velocity. The computed angular velocity is then further controlled through PI velocity control.

In sit-to-stand assistance, the elbow joint follows a predefined trajectory. In this mode, motor is controlled by

$$u = k_p\theta_e + k_i \int \theta_e + k_d\dot{\theta}_e$$

4 Preliminary Testing

The exoskeleton has been developed. The system is about 5.0 kg with two arms, exclude battery. The exoskeleton is able to provide maximum 55 Nm assistive torque, which meets the design requirements in motion assistance.

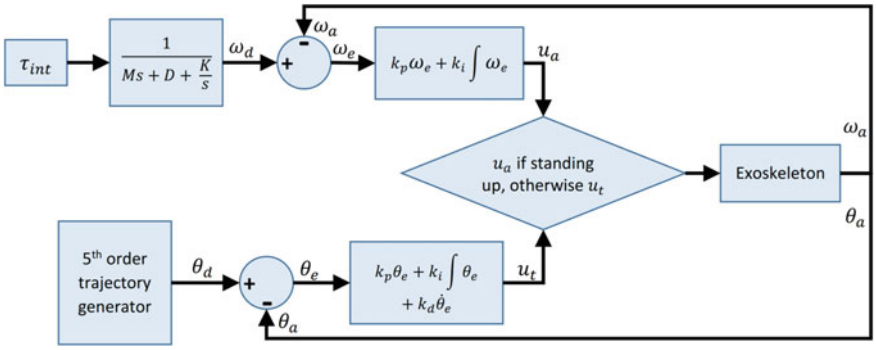

Fig. 5 Control diagram of EXO-AIDER

Preliminary tests were performed. The tests cover the functionalities of the exoskeleton, including the maximum torque, ranges of motions, and also performance assessment in motion assistance.

5 Conclusion

A novel lightweight hybrid exoskeleton was developed and tested preliminarily. Further on-site tests with the elderly and weak persons are planned. The exoskeleton, due to its compactness, lightweight and capacity of motion assistance, is applicable not only for the elderly, but also for workplace assistance.

Acknowledgements The reported work is supported by Innovation Funds Denmark.

References

1. B.A. Pearce, et al., Robotics to enable older adults to remain living at home. J. Aging Res. **2012**, 538169 (2012)
2. T. Proietti, V. Crocher et al., Upper-limb robotic exoskeletons for neurorehabilitation: a review on control strategies. IEEE Rev. Biomed. Eng. **9**, 4–14 (2016)
3. M.A. Gull, S. Bai, T. Bak, A review on design of upper limb exoskeletons. Robotics **9**(1), 16 (2020)
4. S. Christensen, S. Bai, Kinematic analysis and design of a novel shoulder exoskeleton using a double parallelogram linkage. ASME J. Mech. Robot. **10**(4), 041008 (2018)
5. T. Bosch et al., The effects of a passive exoskeleton on muscle activity, discomfort and endurance time in forward bending work. Appl. Ergon. **54**, 212–217 (2016)
6. M.R.U. Islam, S. Bai, Payload estimation using forcemyography sensors for control of upper-body exoskeleton in load carrying assistance. Model. Identification Control **40**(4), 189–198 (2019)

Ultrasound-Based Sensing and Control of Functional Electrical Stimulation for Ankle Joint Dorsiflexion: Preliminary Study

Qiang Zhang, Ashwin Iyer, and Nitin Sharma

Abstract Functional electrical stimulation (FES) is a potential technique for reanimating paralyzed muscles post neurological injury/disease. Several technical challenges, including the difficulty in measuring FES-induced muscle activation and muscle fatigue, and compensating for the electromechanical delay (EMD) during muscle force generation, inhibit its satisfactory control performance. In this paper, an ultrasound (US) imaging approach is proposed to observe muscle activation and fatigue levels during FES-elicited ankle dorsiflexors. Due to the low sampling rate of the US imaging-derived signal, a sampled-data observer (SDO) is designed to continuously estimate the muscle activation and fatigue based on their continuous dynamics. The SDO is combined with a delay compensation term to address the ankle dorsiflexion trajectory tracking problem with a known input delay. Experimental results on an able-bodied participant show the effectiveness of the proposed control method, and the superior tracking performance compared to a traditional control method, where the muscle activation and fatigue are computed from an off-line identified model.

1 Introduction

Drop foot is a typical symptom of weakened dorsiflexion function and is a common gait abnormality due to cerebral vascular accidents and neurological disorders such as multiple sclerosis [1]. Functional Electrical Stimulation (FES) has been acknowledged as a technique to correct drop foot by artificially stimulating the tibialis anterior (TA) muscle with externally applied electrical currents. Closed-loop control of a human joint using FES has been shown to provide robust performance and recreate precise and accurate functional movements, e.g., walking [2]. Current sensing approaches in FES control use angle encoders or inertial measurement units for limb kinematics as feedback. These control approaches miss real-time measurements of

Q. Zhang · A. Iyer · N. Sharma (✉)
UNC & NC State Joint Department of Biomedical Engineering, NC State University, Raleigh, NC, USA
e-mail: nsharm23@ncsu.edu

J. C. Moreno et al. (eds.), *Wearable Robotics: Challenges and Trends*,
Biosystems & Biorobotics 27, https://doi.org/10.1007/978-3-030-69547-7_50

muscle state variables, including FES-induced muscle activation and muscle fatigue. Using muscle activation and muscle fatigue as biofeedback can improve control performance as well as the design of new fatigue-resistant FES control approaches.

One solution to access muscle activation and fatigue levels during FES is evoked electromyography (eEMG) [3, 4]. However, this methodology required accurate timing differentiation of the artifacts between FES input signal and eEMG output signal. Poor differentiation will introduce high FES interference to eEMG, which will significantly deteriorate the muscle state detection. Also, the capability of using eEMG to measure muscle activation and fatigue levels during high-frequency FES is relatively limited.

We propose to use ultrasound (US) imaging-derived measures of muscle activation and muscle fatigue in FES control. With the advent of wearable US technology [5, 6], US imaging-based closed-loop FES control of neuromuscular system has become feasible. In this paper, the control scheme uses a sampled-data observer (SDO) to observe tibialis anterior (TA) muscle activation and FES-induced fatigue levels based on low-rate sampled echogenicity measurements from US imaging. The SDO is combined with a PID-type dynamic surface controller plus a delay compensation term to guarantee trajectory tracking performance for the nonlinear ankle neuromusculoskeletal system with a known input delay.

2 Methods

The study was approved by the Institutional Review Board (IRB) at the North Carolina State University (IRB approval number: 20602). The proposed closed-loop control methodology was tested on one male participant without any neuromuscular disorders. The participant signed an informed consent form before participating in the experiments.

The experimental setup is shown in Fig. 1a. The participant was seated on a chair with adjustable height and the right foot was kept suspended in the air to guarantee

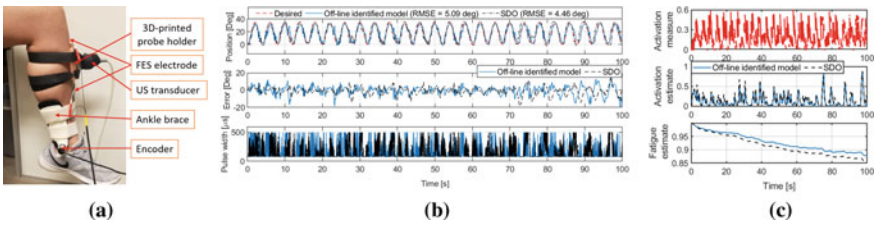

Fig. 1 **a** Experimental setup of the ankle neuromusculoskeletal system by applying FES for closed-loop control. Both the FES electrodes and US transducer are placed on the TA muscle belly. **b** Experimental results of trajectory tracking obtained from an able-bodied participant for each muscle activation and fatigue estimation method. **c** US imaging-derived muscle activation measurement, muscle activation and fatigue estimation from SDO and pure off-line identified model

the ground clearance within the ankle motion range. The participant's thigh was kept horizontal while the shank was kept almost perpendicular to the thigh. The participant was asked to relax both thigh and shank, and avoid voluntary TA muscle contraction during the FES closed-loop control experiment. A clinical linear US transducer (L7.5SC Prodigy Probe, S-Sharp, Taiwan) was attached to the TA muscle belly perpendicularly by a customized 3-D printed holder to image the targeted region in a longitudinal direction. A pair of electrodes were attached to the proximal and distal sides of the TA muscle, and the stimulation was generated by commercial stimulator (Rehastim 2, HASOMED GmbH, Germany). An incremental encoder (TRD-MX1024BD, AutomationDirect, GA, USA) installed on the ankle brace was used to measure the angular position and velocity. The US-derived echogenicity was passed through SDO to obtain continuous estimates of muscle activation and muscle fatigue. These estimates were combined with a proportional-integral derivative (PID)-type dynamic surface control (PID-DSC) method [7] with delay compensation (DC) to obtain FES control inputs. The new control method used a third-order musculoskeletal system that contains muscle activation and muscle fatigue dynamics [8]. Besides, the new controller also compensated for the electromechanical delay, modeled as an input delay, which is another technical challenge during closed-loop FES control. The new US-based control was compared to the PID-DSC-DC, where the muscle activation and fatigue feedback were calculated purely from the off-line identified activation and fatigue dynamical model.

3 Experimental Results and Discussion

Before the tracking experiment, the threshold (60 μs) and saturation (500 μs) of the FES pulse width were determined, where the echogenicity range was also determined. In the tracking experiment, the FES current amplitude was set as 25 mA, frequency was set as 35 Hz, and the pulse width was modulated automatically between the range from threshold to saturation by the proposed SDO-DSC-DC approach. The SDO sampling frequency, control frequency, and encoder measure frequency were all set as 1000 Hz. The measure time period of muscle activation by normalizing the echogenicity between the threshold and saturation was around 0.6 s. The control gains were tuned off-line by using the identified model through multiple simulation trials to minimize the trajectory tracking error, and then the optimal gains were implemented to the experiments. Fig. 1b presents the experimental results for the participant during one typical trial within 100 s. The relaxed ankle angular position as shown in Fig. 1b, is defined as 0°, while the desired ankle dorsiflexion trajectory was designed with amplitude between 0° and 35°, and with a frequency of 0.25 Hz. The root mean square error (RMSE) values of the PZD-DSC-DC control method with those two muscle activation and fatigue estimation methods are 5.09° and 4.46°, respectively. The results show the tracking error is reduced by using the proposed SDO-DSC-DC compared to the traditional DSC-DC with muscle activation and fatigue computed from pure off-line identified model. As shown in Fig. 1c, the average value of muscle

activation level observed by the SDO is higher than that calculated from the off-line identified model. This observation by using US measurements could represent a more realistic muscle physiological state than an idealization from the off-line model. Also, the muscle fatigue calculated from the off-line identified model under-estimates the actual fatigue level, which would deteriorate the trajectory tracking performance when implementing DSC-DC control method.

4 Conclusion

An SDO method was designed to continuously estimate the muscle activation and fatigue levels based on the discrete US imaging-derived echogenicity measurement, while a DSC method combined with a DC technique was used to deal with the EMD during FES control. Experimental results on a participant without neurological disorders validated the proposed SDO-DSC-DC method, and also showed a better trajectory tracking performance compared to the traditional DSC-DC method with pure muscle activation and fatigue calculation from the off-line identified model. This study indicates that US-derived measurements can be used to accurately reflect skeletal muscle activation and fatigue levels, which will potentially improve the FES control performance with the measurable the muscle's physiological state.

Acknowledgements This work was funded by NSF CAREER Award # 1750748.

References

1. M.H. Granat, D.J. Maxwell, A.C. Ferguson, K.R. Lees, J.C. Barbenet, Peroneal stimulator: evaluation for the correction of spastic drop foot in hemiplegia. Arch. Phys. Med. Rehabil. **77**(1), 19–24 (1996)
2. N.A. Alibeji, V. Molazadeh, F. Moore-Clingenpeel, N. Sharma, A muscle synergy-inspired control design to coordinate functional electrical stimulation and a powered exoskeleton: artificial generation of synergies to reduce input dimensionality. IEEE Cont. Syst. Mag. **38**(6), 35–60 (2018)
3. Q. Zhang, M. Hayashibe, C. Azevedo-Coste, Evoked electromyography-based closed-loop torque control in functional electrical stimulation. IEEE Trans. Biomed. Eng. **60**(8), 2299–2307 (2013)
4. Q. Zhang, M. Hayashibe, P. Fraisse, D. Guiraud, FES-induced torque prediction with evoked EMG sensing for muscle fatigue tracking. IEEE/ASME Trans. Mechatron. **16**(5), 816–826 (2011)
5. M.H. Jahanandish, N.P. Fey, K. Hoyt, Lower-limb motion estimation using ultrasound imaging: a framework for assistive device control. IEEE J. Biomed. Health Inform. 23(6), 2505–2514 (2019)
6. Q. Zhang, K. Kim, N. Sharma, Prediction of ankle dorsiflexion moment by combined ultrasound sonography and electromyography. IEEE Trans. Neural Syst. Rehabil. Eng. **28**(1), 318–327 (2020)

7. N. Alibeji, N. Kirsch, B.E. Dicianno, N. Sharma, A modified dynamic surface controller for delayed neuromuscular electrical stimulation. IEEE/ASME Trans. Mechatron. **22**(4), 1755–1764 (2017)
8. N. Sharma, N.A. Kirsch, N.A. Alibeji, W.E. Dixon, A non-linear control method to compensate for muscle fatigue during neuromuscular electrical stimulation. Front. Robot. AI **4**, 68 (2017)

Towards Crutch-Free 3-D Walking Support with the Lower Body Exoskeleton Co-Ex: Self-balancing Squatting Experiments

Sinan Coruk, Ahmed Fahmy Soliman, Oguzhan Dalgic, Mehmet C. Yildirim, Deniz Ugur, and Barkan Ugurlu

Abstract In this paper, we succinctly present the hardware properties and capabilities of the lower body exoskeleton Co-Ex, which was developed to attain self-balancing and crutch-free walking support for those experiencing ambulatory difficulties in general. To provide full 3-D walking support while containing the number of required actuators, it includes 4 active joints per leg. Custom-built series elastic actuators enable the torque sensing and controllability at each joint, enhancing the robot's physical interaction capabilities. While limiting the number of active joints minimizes the weight and energy requirements, the underactuated leg configuration increased the computational load. The preliminary squatting experiments revealed that Co-Ex may provide crutch-free 3-D movement support.

1 Introduction

Robot-aided walking support and rehabilitation enabled various patients with gait disorders to regain ambulatory functionality. The recent advances in lower body exoskeleton technology allowed a significant leap to ensure safe and dependable walking support, particularly for SCI patients. A great majority of SCI walking support exoskeletons have 2 active joints per leg to support hip and knee joints through the F/E (Flexion/Extension) axis [1]. While such a configuration significantly simplifies the hardware, users must engage their upper bodies via crutches to achieve static balancing.

An active ankle D/PF (Dorsi/Plantar Flexion) joint is definitely required for balancing in the sagittal plane. With this addition, Morimoto et al. developed the lower-body exoskeleton XoR, which can provide *crutch-free* sit down & stand up rehabilita-

S. Coruk and A. F. Soliman equally contributed to this works as primary authors.

S. Coruk · A. F. Soliman · O. Dalgic · D. Ugur · B. Ugurlu (✉)
Biomechatronics Laboratory, Faculty of Engineering, Ozyegin University, 34794 Istanbul, Turkey
e-mail: barkanu@ieee.org

M. C. Yildirim
Chair of Robotics Science and Systems Intelligence, Technical University of Munich (TUM), 80333 Munich, Germany

J. C. Moreno et al. (eds.), *Wearable Robotics: Challenges and Trends*,
Biosystems & Biorobotics 27, https://doi.org/10.1007/978-3-030-69547-7_51

tion and can actively reject disturbances in the sagittal plane [2]. In a recent example, Harib et al. developed a fully-actuated lower-body exoskeleton named Atalante, which possesses 6 active joints per leg [3]. This impressive *wearable humanoid* is a great achievement as it was able to fully support SCI patients with no need for crutches.

Although the solution provided by Harib et al. [3] solves the issues related to upper body engagement, the equipment of 12 active joints causes hardware complexity problems. Unlike the case of humanoids, the placement of motors and sensors are quite challenging. Another major concern appears to be power requirement and energy autonomy. All these issues raise several questions: Do we really need to place 6 active joints per leg? What is the minimum number of active joints to achieve crutch-free 3D walking support?

In addition to knee and hip F/E joints, which are included in conventional exoskeletons, an active ankle joint along the D/PF axis is necessary for balancing [2]. Furthermore, the study in [4] suggested that a hip joint along the A/A (Adduction/Abduction) axis is essential in 3D walking to achieve lateral swaying. Combining these pieces of information, we built an exoskeleton with 4 active joints per leg to see to what extent 3-D walking support can be provided [5, 6]. The rest of the paper is organized as follows: In Sect. 2, our methodology is succinctly explained. The paper is concluded in Sect. 3 with further discussion.

2 Methods

2.1 Hardware of Co-Ex

The lower body exoskeleton Co-Ex is a torque-controllable system, actuated via custom-built series elastic actuators with a high torque-to-weight ratio (94/2.45 Nm/kg). Each leg contains 4 DoF (Degrees of Freedom), namely, a 2 DoF hip joint that can rotate along with the A/A and F/E axes, a 1 DoF F/E knee joint, and a 1 DoF D/PF ankle joint. To improve usability and to reduce leg inertia, all actuators are gathered around the waist. A series of 4-bar mechanisms are used to transmit torque. Figure 1 illustrates the actual robot and its joint configuration.

The robot is equipped with an IMU (Lord 3DM-GX5-15 VRU) at the pelvis. A group of distributed force sensing elements (Interlink FSR UX 406) is placed at each foot sole to provide vertical force and center of pressure information. Furthermore, SEA units at each joint can provide real-time torque measurement with a torque resolution of 3.93 mNm. The main controller comprises an Intel Coffee Lake i5 9600K 3.7GHz CPU including an 8 GB DDR4 RAM, and a Samsung 250 GB 860 Evo SSD storage device. It runs on a 64-bit GNU/Linux operating system with an RT_Preempt patch enabled Linux kernel. Data communication is performed via a custom-built real-time Ethernet protocol.

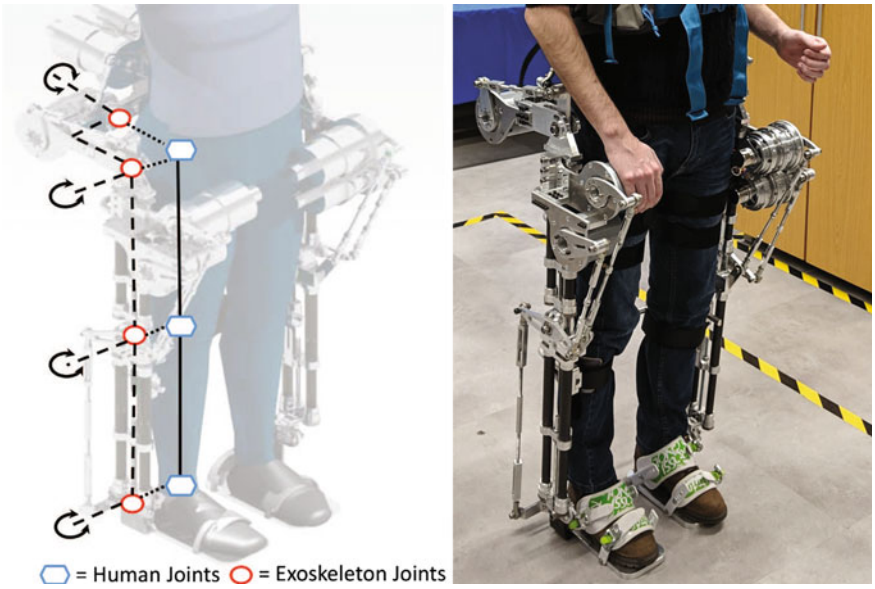

Fig. 1 Left: The joint configuration of a leg. Each leg contains 4 DoF: a 2 DoF hip joint, a knee joint, and an ankle joint. Right: the actual exoskeleton with an able-bodied user

2.2 Control of Co-Ex

(1) *Torque Control*: SEA units in each joint are torque-controlled for improved performance, allowing transparency (zero torque mode + gravity compensation) and high fidelity force/impedance control. The sliding mode observer method was employed and as a result, torque control bandwidth was measured to 19 Hz implying that high frequency inputs may be tracked well.
(2) *Locomotion Control*: Due to the underactuated leg configuration, the locomotion control has to include an optimization algorithm that sorts the tasks depending upon their priority levels. For instance, the CoM (Center of Mass) trajectory is given a higher priority compared to torso orientation, as it has a pivotal role in maintaining the balance. The algorithm ensures that the tasks with lower priority do not tamper with the tasks with higher priority.

Walking can be achieved based on centroidal momentum control or ZMP (Zero Moment Point) feedback control. The ZMP feedback was achieved using the ZMP impedance method that minimizes ZMP error by means of virtual spring dampers that reside at the feet sole. The centroidal angular momentum was attained via measured contact forces and the dynamic model of the robot. Compared to the classical trajectory-based approach, we could obtain more robust locomotion performance through the use of centroidal momentum or ZMP feedback controllers [6].

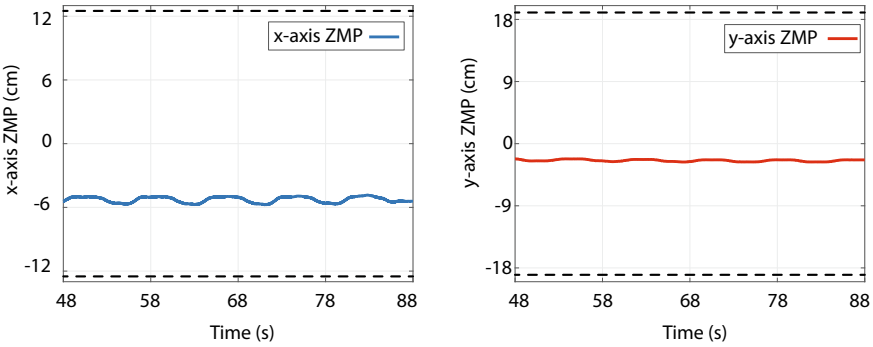

Fig. 2 Self-balancing squatting experiment, actual ZMP

In our preliminary experiments, the Co-Ex exoskeleton performed self-balancing squatting motion where it moves vertically 15 cm and horizontally 6 cm. The movement frequency was approximately 0.15 Hz. The actual ZMP is displayed in Fig. 2. As observed in this figure, ZMP is always within the support polygon, indicating dynamic balance.

3 Discussion

Walking simulation results indicate that crutch-free 3D walking is technically possible with a lower-body exoskeleton with 4 active joints per leg [6]. We argue that the proposed exoskeleton may enable SCI patients to receive hands-free walking support while containing the overall weight, cost, and complexity with relatively improved energy autonomy.

The same initial results also suggest certain problems to be addressed. As each robot leg has only 1 active joint along the A/A axis, the lateral CoM swaying can be achieved with certain contributions from the torso. While our locomotion controller outputs the optimal joint trajectories given the stack of prioritized tasks, the torso oscillation was observed to be $\pm$ 10 degrees. Therefore, the robot could walk in a similar fashion to that of Trendelenburg gait. Thus, particular research questions emerge: Could this problem be solved via a passive joint at the waist area? Could it affect user acceptance?

Another issue is that the underactuated nature of the robot requires an optimization algorithm to prioritize multiple tasks that cannot be collectively achieved. Combining with other full-body controllers, e.g., centroidal momentum, the computational load increases significantly. In our case, the whole computation was completed within 0.7 ms. Although the main controller frequency could go as high as 2 kHz, we had to set it to 1 kHz, thus comprising the controller performance.

In this paper, we reported balanced squatting & swaying experiments where the actual ZMP was within the support polygon. Currently, the walking experiments with dummy load are being conducted and initial tests will be finalized soon. We will report crutch-free 3D walking experiments in our next paper.

Acknowledgements This work is supported by the Scientific and Technological Research Council of Turkey (TÜBİTAK), with the project 215E138.

References

1. A. J. Young, D.P. Ferris, State of the art and future directions for lower limb robotic exoskeletons. IEEE Trans. Neural Syst. Rehabil. Eng. **25**(1), 171–182 (2017)
2. B. Ugurlu, C. Doppmann, M. Hamaya, P. Forni, T. Teramae, T. Noda, J. Morimoto, Variable Ankle Stiffness Improves Balance Control: experiments on a Bipedal Exoskeleton. IEEE/ASME Trans. Mechatronics **21**(1), 79–87 (2016)
3. O. Harib, A. Hereid, A. Agrawal, T. Gurriet, S. Finet, G. Boeris, A. Duburcq, M.E. Mungai, M. Masselin, A.D. Ames, K. Sreenath, J.W. Grizzle, Feedback control of an exoskeleton for paraplegics: toward robustly stable, hands-free dynamic walking. IEEE Control Syst. Mag. **38**(6), 61–87 (2018)
4. M.M. van der Krogt, S.L. Delp, M.H. Schwartz, How robust is human gait to muscle weakness? Gait Posture **36**(1), 113–119 (2012)
5. M.C. Yildirim, A.T. Kansizoglu, S. Emre, M. Derman, S. Coruk, A.F. Soliman, P. Sendur, B. Ugurlu, Co-Ex: a torque-controllable lower body exoskeleton for dependable human-robot co-existence, in *IEEE International Conference on Rehabilitation Robotics*, Toronto, Canada (2019), pp. 605–610
6. A.F. Soliman, B. Ugurlu, Robust locomotion control of a self-balancing and underactuated bipedal exoskeleton: task prioritization and feedback control, *IEEE Robotics and Automation Letters* (in print). https://doi.org/10.1109/LRA.2021.3082016

Ankle Dorsiflexion Assistance Using Adaptive Functional Electrical Stimulation and Actuated Ankle Foot Orthosis

Carlos Canchola-Hernandez, Hala Rifai, Yacine Amirat, and Samer Mohammed

Abstract This work presents the development of a hybrid control strategy to assist ankle joint dorsiflexion movements during walking. An actuated ankle foot orthosis (AAFO) is used in conjunction with Adaptive Functional Electrical Stimulation (AFES) of the peroneal nerve at the Tibialis Anterior (TA) muscle level. The purpose is to provide sufficient ankle dorsiflexion during the swing phase to compensate for foot-drop in paretic patients. The degree of ankle dorsiflexion is indexed with respect to the knee flexion through an adaptive FES paradigm.

1 Introduction

The merging of robotic technology and neuroprosthesis was originally conceived to compensate the individual drawbacks of the use of either Functional Electrical Stimulation (FES) or actuated orthosis separately [1]. The limitations of using FES-based techniques for rehabilitation purposes have been extensively reported in the literature. They include mainly the use of open-loop FES control strategies, inducing premature fatigue and uncertainties in human torque estimation and system modeling [2, 3].

One of the objectives of this research is to study the combination of an adaptive knee-joint based Functional Electrical Stimulation (AFES) system based on a previous work [4] along with an actuated ankle foot orthosis (AAFO). The goal is to reduce the stimulation intensity, compensate muscular induced fatigue and improve

C. Canchola-Hernandez (✉) · H. Rifai · Y. Amirat · S. Mohammed
Univ Paris Est Creteil, LISSI, 94400 Vitry, France
e-mail: carlos.canchola-hernandez@u-pec.fr

H. Rifai
e-mail: hala.rifai@u-pec.fr

Y. Amirat
e-mail: amirat@u-pec.fr

S. Mohammed
e-mail: samer.mohammed@u-pec.fr

J. C. Moreno et al. (eds.), *Wearable Robotics: Challenges and Trends*,
Biosystems & Biorobotics 27, https://doi.org/10.1007/978-3-030-69547-7_52

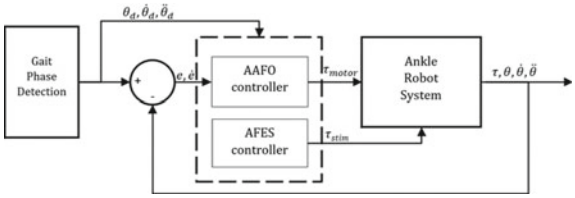

Fig. 1 Proposed hybrid controller. A Finite State Machine detects the beginning of the swing phase and enables the AFES and AAFO compensation accordingly. A variable speed reference trajectory is generated for position tracking based on [7]

the repeatably of each gait cycle. The proposed method is validated and compared with respect to the use of only Adaptive Functional Electrical Stimulation. The proposed hybrid control system is conceptually depicted in Fig. 1.

2 Method

2.1 Adaptive Functional Electrical Stimulation

AFES is applied to the peroneal nerve at the TA muscle using transcutaneous electrodes. Clinical tests have shown an increase of the ankle joint dorsiflexion angle during mid and late swing subphases [4]. Regarding the early swing phase, the stimulation of the peroneal nerve has shown minimal effect on the ankle joint dorsiflexion since the knee joint is already flexed during this subphase. A comparison of an ankle joint profile with and without AFES is provided in Fig. 2a. Based on these previous results and with the objective of increasing the range of motion (ROM) of the ankle joint while decreasing the duration of the stimulation during the swing phase, the stimulation has been delayed by 20% of the whole swing phase duration (Fig. 2b). This is an average delay value obtained during several tests performed by healthy subjects.

Additionally, to compensate for the lack of assistance at the beginning of the swing phase, a torque profile is provided by actuating the AAFO to ensure a sufficient foot clearance where no stimulation is provided.

2.2 AAFO Controller

Previous studies have focused on identifying the ankle foot model during walking [5]. The ankle orthosis system model has been defined as [8]:

$$J\ddot{\theta} + B\dot{\theta} + K\theta = \tau + d \tag{1}$$

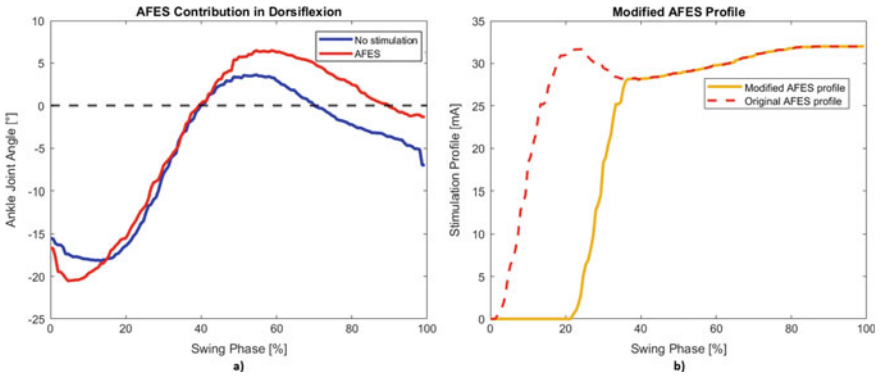

Fig. 2 **a** Comparison of the average profile of an ankle with and without AFES. An increase in the ankle joint dorsiflexion during the mid and late swing subphases is obtained as a result of the stimulation. **b** Proposed AFES profile. The current stimulation value changes reaching a maximum value ($I_{\max}$) at the last part of the swing phase

where J is the moment of inertia, θ is the angle between the foot and the shank, B represents the viscous friction coefficient and K the system's stiffness coefficient. Additionally, τ denotes the torque developed by the actuator and d represents all the non linear disturbances.

According to [6], the error dynamics of the system correspond to:

$$\ddot{e} + K_v\dot{e} + K_p e = 0 \tag{2}$$

where the position error (e) is defined as $e = \theta_d - \theta$, θ_d represents the desired ankle joint angle, K_p and K_v denote the positive design parameters of the desired error dynamics.

From (2), it is possible to obtain $\ddot{\theta}$ and substitute it in (1), resulting in:

$$\tau = J(\ddot{\theta}_d + K_v\dot{e} + K_p e) + d \tag{3}$$

3 Results

The proposed hybrid controller was validated in simulation. The ankle robot system model was identified based on the analysis of previous experimental data obtained from one healthy subject. For the AAFO controller, the positive design parameters were tuned by trial and error. Furthermore, the AFES maximum current intensity ($I_{\max}$) was determined based on the subject sensitivity threshold identified during the tests (Table 1).

Table 1 AAFO controller and AFES parameters

J (N ms^2/deg)	K_v (s^{-1})	K_p (s^{-2})	$I_{\max}$ (mA)
0.000025	0.01	200	20

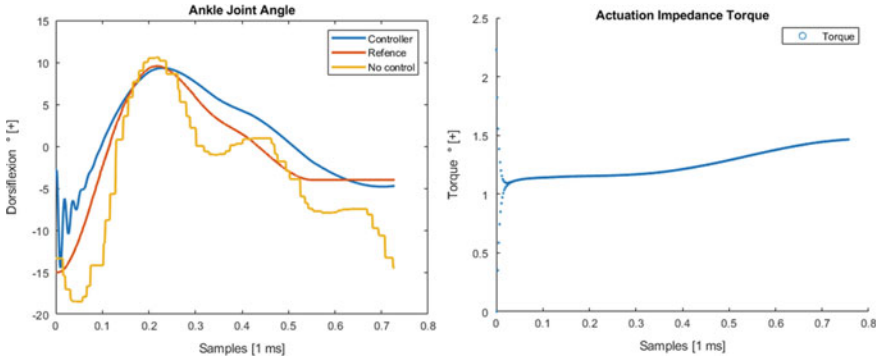

Fig. 3 Ankle joint angular position comparison (left) and torque profile (right). The initial disturbance in the ankle joint angle is caused by the AAFO controller that is enabled only during the swing phase

Table 2 Mean dorsiflexion values

No stimulation	AFES	Hybrid
1.74° ± 1.44°	6.34° ± 1.74°	11.04°± 2.37°

The AAFO controller showed an angular rms error of 0.0526 [rad] and a maximum torque of 1.5 [Nm]. An example of the performance for one swing phase if provided in Fig. 3.

To validate the hybrid control scheme, the motor actuation was applied to ensure a dorsiflexion of the ankle joint for the first 20% of the swing phase, whereas the modified AFES stimulation profile was applied during the swing phase. A total of 15 gait cycles were analyzed. The results were compared with AFES and no stimulation and are reported in Fig. 4 and Table 2. The hybrid approach obtains an increase of 4° compared to AFES stimulation.

4 Conclusion

The hybrid approach proved to enhance the ankle dorsiflexion compared to the conventional AFES stimulation. A future extension of this work is the consideration of a closed-loop AFES control and the development of a collaborative strategy to provide assistance as needed.

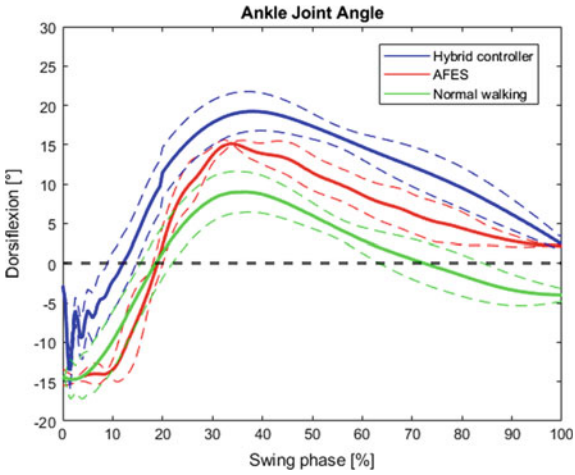

Fig. 4 Normalized mean ankle joint profiles. The ankle joint dorsiflexion angle resulting from the hybrid controller is depicted in blue, from the AFES stimulation in red and from the normal gait in green. The dotted lines correspond to the standard deviation

Acknowledgements This work was not supported by any organization.

References

1. A. del-Ama, A. Gil-Agudo, J. Pons, et al. Hybrid FES-robot cooperative control of ambulatory gait rehabilitation exoskeleton. J. NeuroEngineering Rehabil. **11**, 27 (2014)
2. A. del-Ama, A. Koutsou, J. Moreno, A. de-los-Reyes, A. Gil-Agudo, J. Pons, Review of hybrid exoskeletons to restore gait following spinal cord injury. J. Rehabil. Res. Dev. **49**(4), 497–514 (2012)
3. K. Ha, S. Murray, M. Goldfarb, An approach for the cooperative control of FES with a powered exoskeleton during level walking for persons with paraplegia. IEEE Trans. Neural Syst. Rehabil. Eng. **24**(4), 455–466
4. W. Huo, V. Arnez-Paniagua, M. Ghedira, Y. Amirat, J. Gracies, S. Mohammed, Adaptive FES assistance using a novel gait phase detection approach, in *2018 IEEE/RSJ International Conference on Intelligent Robots and Systems (IROS)*, Madrid (2018), pp. 1–9
5. H. Lee, N. Hogan, Time-varying ankle mechanical impedance during human locomotion. IEEE Trans. Neural Syst. Rehabil. Eng. **23**(5), 755–764 (2015)
6. J. Kim, J. Kim, An impedance control of human ankle joint using functional electrical stimulation, *2018 7th IEEE International Conference on Biomedical Robotics and Biomechatronics (Biorob), Enschede* (2018), pp. 1230–1235
7. V. Arnez-Paniagua, H. Rifaï, Y. Amirat, S. Mohammed, M. Ghedira, J.M. Gracies, Modified adaptive control of an actuated ankle foot orthosis to assist paretic patients, *2018 IEEE/RSJ International Conference on Intelligent Robots and Systems (IROS)*, Madrid (2018), pp. 2311–2317. https://doi.org/10.1109/IROS.2018.8594046
8. W. Huo, V. Arnez-Paniagua, G. Ding, Y. Amirat, S. Mohammed, Adaptive proxy-based controller of an active ankle foot orthosis to assist lower limb movements of paretic patients. Robotica **37**(12), 2147–2164 (2019)

Soft Wearable Robots for Health and Industry

Feasibility and Effectiveness of a Soft Exoskeleton for Pediatric Rehabilitation

Michele A. Lobo and Bai Li

Abstract Exoskeletons have the potential to improve outcomes for rehabilitation clients. For these devices to be effective, rehabilitation professionals and end users must be involved throughout the design process, so the devices meet the broad needs of users. In this article, we present a model to guide the design of rehabilitation devices. This model is user-centered and focuses on users' functional, expressive, aesthetic, and accessibility needs (FEA2) for devices. We then summarize the results of the first studies evaluating the feasibility and effectiveness of the Playskin Lift™ soft exoskeleton for pediatric populations utilized for intervention in the natural environment. The exoskeleton was feasible for daily use by families in the natural environment. For infants and toddlers with physical disabilities, the exoskeleton assisted reaching and play performance within a single session when it was worn and improved independent reaching function and play activity after months of daily intervention with the exoskeleton.

1 Introduction

Children with diagnoses such as arthrogryposis and muscular dystrophy have weakness that can impair their arm function for critical daily tasks [1, 2]. Young children born preterm or with a brain injury also demonstrate arm movement impairments that restrict interaction with objects, limiting children's ability to gather information and learn [3, 4]. Therefore, there are a number of pediatric populations that may benefit from rehabilitation devices aimed at supporting and assisting arm function.

Exoskeletons have been increasingly investigated with adult and adolescent rehabilitation populations [5, 6]. However, until recently, these devices had not been

M. A. Lobo (✉)
Move To Learn Innovation Lab, Super Suits FUNctional Fashion & Wearable Technology Program, Department of Physical Therapy and Biomechanics and Movement Science Program, University of Delaware, Newark, DE, USA
e-mail: malobo@udel.edu

B. Li
Biomechanics and Movement Science Program, University of Delaware, Newark, DE, USA

J. C. Moreno et al. (eds.), *Wearable Robotics: Challenges and Trends*,
Biosystems & Biorobotics 27, https://doi.org/10.1007/978-3-030-69547-7_53

studied with very young populations [1, 3, 7]. Furthermore, most of the existing research has been conducted in laboratories or clinics rather than in the natural settings in which clients reside and participate [5, 6]. The purpose of this article is to summarize the results of the first studies evaluating the feasibility and effectiveness of a soft exoskeleton for young pediatric populations utilized in the natural environment. Implementation in the natural environment is especially critical for young children as this is where early interventions are expected to be administered.

2 Material and Methods

2.1 The Exoskeleton

The Playskin Lift™ exoskeletal garment was designed by the author's team using the FEA2 user-centered design model that considers the functional, expressive, aesthetic, and accessibility needs of end users [8]. Parents of young children with arm movement impairments reported the need for a device to help children lift their arms for daily activities while also meeting other key needs, including ease of donning/doffing, aesthetics, affordability, and comfort. It was also important that the device not restrict other activities such as rolling and transitioning among positions [8].

The Playskin Lift™ is a passive exoskeletal garment [8]. It is a onesie or shirt that zips in the front and has vinyl tunnels under each arm to hold springs, bundles of steel wire, that provide antigravity assistance at the shoulders (Fig. 1). Level of assistance can be adjusted by selecting a greater number and/or larger diameter of wires. The exoskeleton can be fabricated for less than 30 US dollars in materials following instructions posted at the author's website.

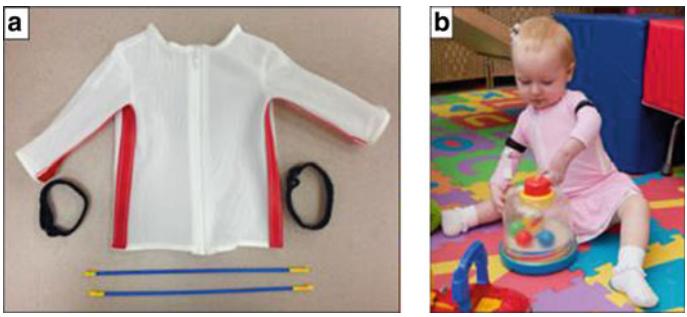

Fig. 1 The Playskin Lift™ exoskeletal garment **a** with vinyl tunnels under each arm for the springs (bottom of the image) and **b** on a child; hook and loop cuffs to be used as needed to maintain spring alignment

2.2 Methods

Feasibility and effectiveness of the Playskin Lift™ were evaluated in two groups of young children. The first group was of 10 infants born preterm and/or with a significant brain injury (PT/BI) [3]. They began the study at about 2 months of age, adjusted for prematurity. The second group was of 17 infants and toddlers with significant arm weakness due to arthrogryposis [1, 7]. They began the study between 6 and 35 months of age. Both groups were evaluated biweekly throughout a 1–2-month baseline (control), a 4-month intervention (with daily, parent-provided home intervention activities with the exoskeleton donned), and a 1-month post-intervention phase. Daily wearing logs and parent perception questionnaires assessed feasibility. A standardized reaching assessment was performed biweekly with and without the device to assess effectiveness for both groups. The arthrogryposis group was also assessed for active range of motion (AROM) and play ability as this group demonstrated limited AROM and play was developmentally appropriate for this older group. Experimenters blind to visit timing and participant details scored all assessments. Hierarchical linear modeling analyzed assistive effects (changes within a session with the exoskeleton donned) and rehabilitative effects (changes in independent performance across time) with $p \leq 0.05$ representing significance.

3 Results

3.1 Feasibility

The Playskin Lift™ exoskeletal garment was feasible for use by parents for daily intervention with infants and toddlers in the natural environment [1, 3]. Parents were asked to use the exoskeleton for intervention 45 min/day each day, skipping days as needed. Parents in the PT/BI group reported wearing times of 44.4 ± 9.3 min/day 3.9 ± 1.7 days/week; parents in the arthrogryposis group 96.8 ± 81.4 min/day 5.8 ± 1.2 days/week. Likert ratings on a scale from 1 to 5 with 5 being the best were positive for all outcomes, including ease of donning (PT/BI: 4.5 ± 0.5; arthrogryposis: 4.4 ± 0.4) and doffing (PT/BI: 4.5 ± 0.5; arthrogryposis: 4.6 ± 0.4), comfort (PT/BI: 4.3 ± 0.9; arthrogryposis: 4.7 ± 0.4), aesthetics (PT/BI: 3.7 ± 1.2; arthrogryposis: 3.9 ± 0.7), and restriction of other activities (PT/BI: 3.9 ± 1.2; arthrogryposis: 4.2 ± 0.7).

3.2 Assistive Effects

Infants and toddlers showed better reaching performance within sessions with the Playskin Lift™ donned [1, 3]. Infants with PT/BI showed significantly more

bimanual reaching, open-handed grasping, and multimodal (visual-manual) behavior when wearing the exoskeleton [3]. Toddlers with arthrogryposis showed significantly more unimanual and bimanual reaching, open-handed grasping with the palm, visual attention to objects, and multimodal behavior along with increased intensity of activity [1]. Toddlers with arthrogryposis showed better play performance, with significantly more object contacts, lifting of objects, bimanual object manipulation, and multimodal behavior along with increased intensity and variability of the behaviors performed [7].

3.3 Rehabilitative Effects

Infants and toddlers showed improved independent reaching performance across time after intervention with the Playskin Lift™ [1, 3]. Infants with PT/BI showed significantly more unimanual and bimanual reaching, open-handed grasping with the palm, attention to objects, and multimodal behavior along with increased intensity of activity [3]. Toddlers with arthrogryposis showed significantly improved AROM for both upper extremities, more unimanual reaching, open-handed grasping with the palm, visual attention to objects, and multimodal behavior along with increased intensity of activity [1]. Toddlers with arthrogryposis had better play performance, with significantly more object contacts, lifting of objects, unimanual object manipulation, and multimodal behavior along with increased intensity and variability of the behaviors performed [7].

4 Conclusion

This work suggests that upper extremity exoskeletons, such as the Playskin Lift™, designed to meet the broad needs of users are feasible for use in intervention programs implemented by parents for very young pediatric populations in the natural environment [1, 3, 7, 8]. Exoskeletons like the Playskin Lift™ can provide more immediate effects on reaching and play abilities (assistive effects when donned) for young children with upper extremity disability [1, 3, 7]. When coupled with effective intervention activities, they can also improve independent AROM, reaching, and play abilities across time [1, 3, 7]. Exoskeletons that improve motor performance for young children may lead to cascading benefits in cognition, language, and social abilities [3, 4]. Key limitations of the Playskin Lift™ for populations over 3 years of age are that it cannot support the weight of longer, heavier arms and it does not allow users to adjust the level of support in real time. Future research should apply the FEA2 design model to develop soft exoskeletons that address these limitations and the needs of older pediatric and adult populations.

Acknowledgements This work was supported by the Eunice Kennedy Shriver National Institute of Child Development (NICHD; 1R21HD076092-01A1) and National Science Foundation (1722596). Thanks to the participating families & M2L members.

References

1. I. Babik, A.B. Cunha, M.A. Lobo, Assistive and rehabilitative effects of the Playskin Lift^{TM} exoskeletal garment on reaching and object exploration in children with arm weakness. Am. J. Occup. Therapy (in press)
2. R. Suthar, N. Sankhyan, Duchenne muscular dystrophy: a practice update. Indian J. Pediatr. **85**(4), 276–281 (2018)
3. I. Babik, A.B. Cunha, M. Moeyaert, M.L. Hall, D.A. Paul, A. Mackley, M.A. Lobo, Feasibility and effectiveness of intervention with the Playskin Lift^{TM} exoskeletal garment for infants at risk. Phys. Therapy **99**(6), 666–676 (2019)
4. M.A. Lobo, R.T. Harbourne, S.C. Dusing, S.W. McCoy, Grounding early intervention: physical therapy cannot just be about motor skills anymore. Phys. Ther. **93**(1), 94–103 (2013)
5. N. Rehmat, J. Zuo, W. Meng, Q. Liu, S.Q. Xie, H. Liang, Upper limb rehabilitation using robotic exoskeleton systems: a systematic review. Int. J. Intell. Robot. Appl. **3**(3), 283–295 (2018)
6. T. Estilow et al., Use of the Wilmington Robotic Exoskeleton to improve upper extremity function in patients with Duchenne muscular dystrophy. Am. J. Occup. Ther. **72**(2), 1–5 (2018)
7. I. Babik, A.B. Cunha, M.A. Lobo, Play with objects in children with arthrogryposis: assistive and rehabilitative effects of the Playskin Lift^{TM} exoskeletal garment. Am. J. Med. Genetics, Part C **181**(3), 393–403 (2019)
8. M.L. Hall, M.A. Lobo, Design and development of the first exoskeletal garment to enhance arm mobility for children with movement impairments. Assist. Technol. **30**(5), 251–258 (2017)

FleXo—Modular Flexible Back-Support Passive Exoskeleton

Jesús Ortiz, Jorge Fernández, Tommaso Poliero, Luigi Monica, Sara Anastasi, Francesco Draicchio, and Darwin G. Caldwell

Abstract This paper presents a back-support exoskeleton concept, which mimics the biological structure of the human back. The design is based on a novel modular flexible mechanism, that allows a complete freedom of movement and a good level of comfort. The assistive forces are transmitted perpendicularly to the body, improving the benefits of the system, and distributed efficiently through the body thanks to a smart routing system. The current implementation, called FleXo, uses passive actuation based on an elastic band.

1 Introduction

Industrial exoskeletons are emerging as a promising solution to reduce the incidence of musculoskeletal disorders (MSD). In Italy during 2019, approximately 66% of the work-related injuries were associated to MSD.[1] While current industrial exoskeletons are showing a promising level of support and performance [1], most of them are based on rigid structures. This aspect limits the acceptability due to weight, complexity, reduced freedom of movement and wearability. The introduction of soft exoskeletons could improve significantly all these aspects, however the way they transmit the forces to the wearer affects significantly the level of assistance. For this reason, examples of soft industrial exoskeletons are scarce and limited to tasks that do not require a high level of assistance, such as the Bioservo Ironhand (Bioservo Technologies AB, Sweden). In the other hand, in the rehabilitation field, soft exoskeletons have been

[1] INAIL Open Data, https://dati.inail.it.

J. Ortiz (✉) · J. Fernández · T. Poliero · D. G. Caldwell
Advanced Robotics, Istituto Italiano di Tecnologia, Via Morego, 30, 16163 Genova, Italy
e-mail: jesus.ortiz@iit.it

L. Monica · S. Anastasi
Department of Technological Innovation and Safety Equipment, INAIL, Rome, Italy

F. Draicchio
Department of Occupational and Environmental Medicine, Epidemiology and Hygiene, INAIL, Monte Porzio Catone, Rome, Italy

J. C. Moreno et al. (eds.), *Wearable Robotics: Challenges and Trends*,
Biosystems & Biorobotics 27, https://doi.org/10.1007/978-3-030-69547-7_54

explored more widely. While these systems do not provide full body weight support, the benefits for the users are revealing to be very relevant [2, 3].

As already mentioned, it is important to consider how the forces are transmitted to the human body. Particularly, in the case of industrial back support devices, the exoskeleton might transmit forces (i) perpendicularly to the spine, thanks to rigid frames, like in RoboMate [4], Laevo V2 (Laevo B.V., The Netherlands), BackX (US Bionics, Inc., USA), Cray-X (GBS German Bionic Systems GmbH, Germany), Atoun Model Y (Atoun Inc., Japan), Hyundai H-WEX [5], or (ii) along the spine of the wearer, as in the case of passive exoskeletons with no rigid frame like in PLAD [6], SSL [7], and B.A. Garment [8]. The main advantage of the former examples is that they do not introduce additional compression forces on the vertebrae [9]. However, reaction forces are applied on a restricted number of application points, mainly thighs and pelvis, producing significantly high pressures of the body. On the contrary, soft exoskeletons are able to distribute the assistive forces over a larger body surface, consequently improving the comfort. A further problem that has emerged with the involvement of a rigid frames is that this solution reduces the user's Range of Motion (RoM) [10]. Recently, new solutions explore the possibility of introducing lighter flexible carbon fiber frames, like in Spexor [11], in order to increase the user's RoM.

Under these considerations, this paper presents a novel design for a back support exoskeleton, based on a modular mechanism which adapts to the natural movement of the human body, and at the same time is able to transmit the forces perpendicularly to the spine without adding any extra compression forces. The current implementation, called FleXo, uses only passive actuation based on a elastic band.

2 System Description

The proposed back support exoskeleton design is based on the concept of Modular Assistive Vertebra (MAV, patent pending), following a biomimetic architecture. The exoskeleton frame is made of multiple MAVs connected in series through a flexible material, allowing the adaptation to the movements of the human torso.

The key element that allows an effective force transmission is the routing of a cable or elastic band. Each MAV has two pulleys, which route the transmission cable following a 'S' shape, as shown in Fig. 1. Following this geometry, the tension on the cable T produces a force (F_x and F_y) and torque (τ) at the center of the MAV, expressed as force transmission ratio and equivalent lever arm:

$$\beta = a \sin\left(\frac{r_1 + r_2}{\sqrt{\Delta x^2 + \Delta y^2}}\right) + a \tan\left(\frac{\Delta y}{\Delta x}\right) \tag{1}$$

$$\begin{aligned} F_x/T &= \cos(\alpha_1) - \cos(\alpha_2) \\ F_y/T &= \sin(\alpha_1) - \sin(\alpha_2) \end{aligned} \tag{2}$$

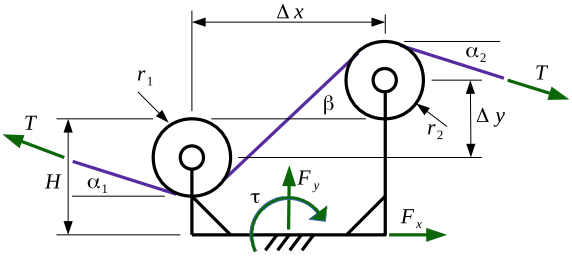

Fig. 1 Diagram of the transmission system of the MAV

$$\begin{aligned}\tau/T = {} & (\sin(\alpha_1) + \sin(\alpha_2) + 2\sin(\beta))\frac{\Delta x}{2} \\ & + (\cos(\alpha_1) - \cos(\beta))\left(H - \frac{\Delta y}{2}\right) \\ & - (\cos(\alpha_2) - \cos(\beta))\left(H + \frac{\Delta y}{2}\right)\end{aligned} \tag{3}$$

The friction, not accounted in these equations, would reduce the effectiveness of the tension transmitted through the cable. The residuar forces F_x and F_y tend to zero

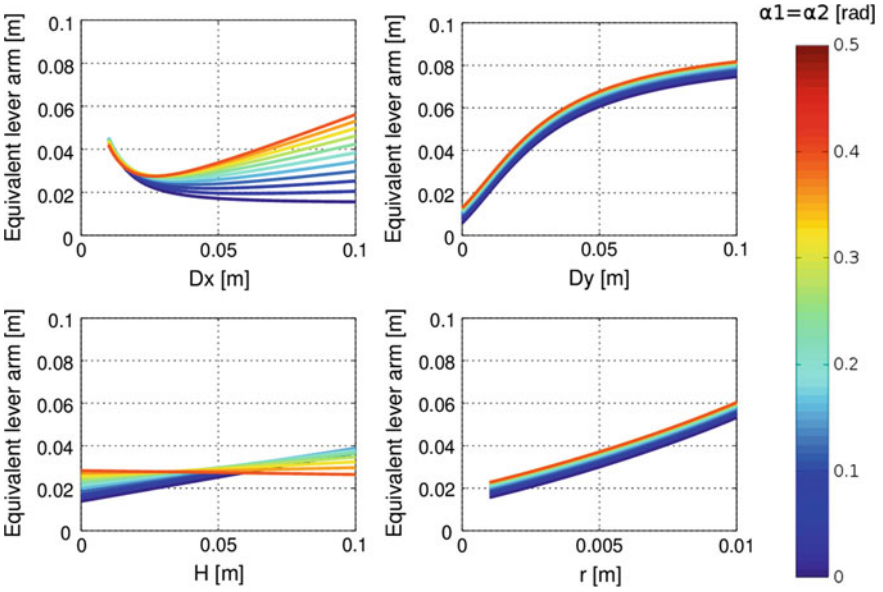

Fig. 2 Influence of the geometric parameters and the cable angle on the equivalent lever arm, with $\alpha_1 = \alpha_2 = [0.0, 0.5]$, $\Delta x = 30$ mm [10 mm, 100 mm], $\Delta y = 10$ mm [0 mm, 100 mm], $H = 30$ mm [0 mm, 100 mm] and $r_1 = r_2 = 2.5$ mm [1 mm, 10 mm] (these values refer to the base system, while the values between brackets indicate the range)

in a symmetric configuration where $\alpha_1 = \alpha_2$. The conversion from the cable tension to the force and torque at each MAV is conditioned by its geometry (Δx, Δy, H, r_1 and r_2), and by the cable angles (α_1 and α_2), which vary with the relative orientation between each pair of MAVs. Figure 2 shows the influence of the geometric parameters on the equivalent lever arm (τ/T). Note that the effect of the parameters Δy and r is barely affected by the cable angle, while Δx and H are strongly affected. This allows the optimization of the torque profile at different cable angles.

A first prototype of back support exoskeleton using the presented flexible mechanism, called FleXo, has been developed. The MAV mechanism is attached to the back of a full body textile garment, and it is connected to each of the legs in order to allow the transmission of the assistance. This prototype provides only passive assistance using an elastic band. Figure 3 shows the current implementation of the prototype, with a total weight of less than 1.5 kg. The garment is an essential part of the design of FleXo since the force distribution on the body surface depends on it.

Fig. 3 FleXo prototype using the MAV mechanism. On the left, the details of the current implementation. On the top right, a user wearing the prototype. On the bottom right, a side view of the elastic band routing

3 Conclusion and Discussion

In this paper we presented a passive back support exoskeleton based on a modular flexible mechanism. The current prototype is a proof of concept to demonstrate the feasibility of the mechanism. Preliminary testing showed that FleXo is able to transmit assistive forces to the wearer without limiting significantly the range of motion in the sagittal plane. Extensive laboratory testing will be carried out to validate this preliminary assessment, focused on the measurement of the effective assistance that FleXo provides to the wearer, and the efficiency and stability of the garment.

Acknowledgements This work has been co-funded by the Italian Workers' Compensation Authority (INAIL).

References

1. M.P. de Looze, T. Bosch, F. Krause, K.S. Stadler, L.W. O'Sullivan, Exoskeletons for industrial application and their potential effects on physical work load. Ergonomics **59**(5), 671–681 (2016)
2. J. Ortiz, C. Di Natali, D.G. Caldwell, Xosoft-iterative design of a modular soft lower limb exoskeleton, in *International Symposium on Wearable Robotics* (Springer, Berlin, 2018), pp. 351–355
3. L.N. Awad, P. Kudzia, D.A. Revi, T.D. Ellis, C.J. Walsh, Walking faster and farther with a soft robotic exosuit: implications for post-stroke gait assistance and rehabilitation. IEEE Open J. Eng. Med. Biol. **1**, 108–115 (2020)
4. S. Toxiri, A.S. Koopman, M. Lazzaroni, J. Ortiz, V. Power, M.P. de Looze, L. O'Sullivan, D.G. Caldwell, Rationale, implementation and evaluation of assistive strategies for an active back-support exoskeleton. Front. Robot. AI **5**, 53 (2018)
5. H.K. Ko, S.W. Lee, D.H. Koo, I. Lee, D.J. Hyun, Waist-assistive exoskeleton powered by a singular actuation mechanism for prevention of back-injury. Robot. Autonom. Syst. **107**, 1–9 (2018)
6. M. Abdoli-e, M.J. Agnew, J.M. Stevenson, An on-body personal lift augmentation device (PLAD) reduces EMG amplitude of erector spinae during lifting tasks. Clin. Biomech. **21**(5), 456–465 (2006)
7. Y. Imamura, T. Tanaka, Y. Suzuki, K. Takizawa, M. Yamanaka, Motion-based design of elastic belts for passive assistive device using musculoskeletal model, in *2011 IEEE International Conference on Robotics and Biomimetics* (IEEE, 2011), pp. 1343–1348
8. E.P. Lamers, A.J. Yang, K.E. Zelik, Feasibility of a biomechanically-assistive garment to reduce low back loading during leaning and lifting. IEEE Trans. Biomed. Eng. **65**(8), 1674–1680 (2018)
9. S. Toxiri, J. Ortiz, J. Masood, J. Fernández, L.A. Mateos, D.G. Caldwell, A wearable device for reducing spinal loads during lifting tasks: biomechanics and design concepts, in *ROBIO* (IEEE, 2015), pp. 2295–2300
10. S. Baltrusch, J. Van Dieën, C. Van Bennekom, H. Houdijk, The effect of a passive trunk exoskeleton on functional performance in healthy individuals. Appl. Ergon. **72**, 94–106 (2018)
11. M.B. Näf, A.S. Koopman, S. Baltrusch, C. Rodriguez-Guerrero, B. Vanderborght, D. Lefeber, Passive back support exoskeleton improves range of motion using flexible beams. Front. Robot. AI **5**, 72 (2018)

A Model-Based Control Strategy for Upper Limb Exosuits

N. Lotti, F. Missiroli, M. Xiloyannis, and L. Masia

Abstract Increase the symbiosis between the human and the machine, is the major open challenge in wearable robotics research. Limitations are not only in hardware but also on the control side which is often limited in its bandwidth lacking to match frequency ranges of biomechanics, but also in detecting and interpreting human intention. In this work we propose a control framework for an upper limb exosuit which works using an EMG model based *myoprocessor* module. Results suggest that using biosignal in the control loop for wearable robotics improves reliability and interaction between the device and its pilot.

1 Introduction

Exosuits represent one of the novel frontiers of robotics, embracing the two complementary realms of clinical rehabilitation and human augmentation. These kind of device has been conceived to improve the human-machine symbiosis, by partly solving the drawbacks arising from their predecessors: rigid exoskeletons. Yet, even the light exosuits without using biosignals in the loop, may reach their limits in inferring the intention of the user action therefore jeopardizing the acceptance and efficiency of such technology. The paradigms [1], relying on mechanical manifestations of movements, detected by sensors embedded in the robot, being triggered by the outcomes of human intention will inevitably suffer from a time lag between the device and its pilot, with a consequent degradation of the haptic rendering and sense of authority. A solution to these drawbacks can solely come if one considers an interface directly perceiving the signals arising from the brain and generating muscular activation. Proportional myoelectric controllers, for example, provide assistive forces proportional to the user's muscle recruitment [2]. Moreover, since electromyographic (EMG) signals are precursors of motion [3], the robot is more likely able

N. Lotti · F. Missiroli · L. Masia (✉)
Institut für Technische Informatik (ZITI), Heidelberg University, 69120 Heidelberg, Germany
e-mail: lorenzo.masia@ziti.uni-heidelberg.de

M. Xiloyannis
Institute of Robotics and Intelligent Systems, ETH Zürich, Zürich 8092, Switzerland

J. C. Moreno et al. (eds.), *Wearable Robotics: Challenges and Trends*,
Biosystems & Biorobotics 27, https://doi.org/10.1007/978-3-030-69547-7_55

to match the movement timing of its user. In our recent work [4], we showed that the combination of EMG detection with an accurate modelling of musculoskeletal geometry and activation dynamics, can be a powerful tool to control exosuits [5]. In the present paper we repropose the application of a reshaped and improved model-based EMG approach (*myoprocessor*) for the control of an elbow exosuit to simulate daily gestures typical of daily activities. Our aim was to assert how the controller can enhance the dualism between human and machine in terms of promptness, responsiveness and stability. To achieve this goal, we evaluated the controller performance by simulating a functional daily task that involves elbow movements.

2 Materials and Methods

2.1 Myoprocessor Module

The *myoprocessor* is a layer of the controller which computes the biological torque at the elbow joint from the EMG activities and successively feedbacks the value to the actuation stage for assistance delivery. The module comprises of four components:

- The *Activation dynamics* component converting the two recorded EMG signals into muscle fibers recruitment via second-order muscle twitch model and a non-linear transfer function [6].
- The *Muscle tendon kinematics* synthesizes the three-dimensional musculoskeletal geometry of the human arm into a set of multidimensional cubic B-splines.
- The *Muscle tendon dynamics* solves for muscle and tendon force using a Hill-type muscle model.
- The *Torque computation* projects forces onto the elbow joint using and estimation of the moment arms of the muscles.

The resulting elbow torque was scaled based on the desired level of assistance and then tracked by an indirect torque controller which send input to an actuation stage.

2.2 Experimental Setup

The exosuit shown in Fig. 1 comprises a tendon driven off board actuation mobilizing an elbow harness as described in [4]. A multi-channel EMG system (Trigno wireless, Delsys, Natick MA, USA) was used to record the two agonist and antagonist elbow muscles: biceps brachii (BIC) and triceps brachii (TRI). A DAQ board (Quanser QPIDe, Markham, Ontario, Canada) acquired all signals, with a sampling frequency of 1 kHz. The exosuit actuation was driven by a dedicated motor controller (EPOS2

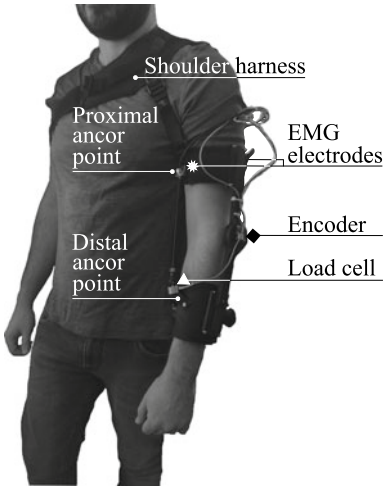

Fig. 1 Upper limb exosuit. The tested device is a soft wearable arm exosuit that assists during elbow flexion/extension movements through a Bowden cable attached to the front of the arm strap. During flexion movements an electric motor recovers the cable. During extension movements the cable is released

50/5, Maxon, Sachseln, Switzerland) closing a feedforward + feedback velocity loop at 1 KHz. The real-time control and data logging was implemented in a MATLAB/Simulink environment.

2.3 Experimental Protocol

Eight healthy subjects (three females, age 27.1 ± 3.3 years, mean ± sd, body weight 75.6 ± 13.8 kg and height 1.77 ± 0.09 m), with no history of neurological diseases, and exhibiting normal joint range of motion and muscle strength, participated in the study. All experimental procedures were carried out in accordance with the Declaration of Helsinki and approved by the ethical committee of Heidelberg University (Nr. S-311/2020). Subjects provided explicit written consent to participate in the study. During the experiment participants were requested to perform a pick and place task with different weights to test the adaptation of the controllers to different load conditions. We used three different precision weights for the experiment: 200, 500 and 1000 g: Each weight was placed on an initial position, then the subjects, after an external audio trigger, moved it to the corresponding target location. The sequence was repeated four times for each weight (back and forth between the target positions) for a total of 12 movements. Before starting the experiment, a calibration was necessary to tune the musculoskeletal model on individual anthropometrics. A 3D motion capture system (Krypton k600, Nikon Metrology, Brighton MI, USA) was used to record 50 Hz the trajectories of six markers, placed on anatomical landmarks: third metacarpus, lateral wrist, medial wrist, lateral elbow, medial elbow and acromion. As described in [4], the calibration procedure consisted of two different phases: a static pose acquisition and a dynamic calibration.

3 Results

We analized the Biceps activity reduction with a repeated-measures ANOVA (rANOVA) within-subject factors. All the parameters in this study resulted normally distributed ($p < 0.005$).For the biceps reduction we proceed with a post-hoc analysis applying the Tukey method. Exosuit assistance reduced the biceps activity (Fig. 2b, top) of $35.5 \pm 8.9\%$ (mean $\pm$ SE) by lifting the lowest weight (200 g), $32.5 \pm 9.2\%$ under the middle load condition (500 g) and $29.9 \pm 6.4\%$ in the maximum load setup (1000 g). The ANOVA test showed a significant difference between the no assistance and the myoprocessor conditions ($F(1, 7) = 56, 0.09$, $p < 0.0001$).

We did not find statistical difference ($F(1, 7) = 0.10$, $p = 0.749$) between the elbow torque estimated by using an inverse dynamics model in no assistance condition and the exosuit assistive torque (Fig. 2b. bottom) meaning that the the *myoprocessor* accurately estimates the torque needed to perform the task and provided to the joint: by lifting the lowest weight (200 g) the myoprocessor torque was 0.41 ± 0.08 N m (inverse dynamics 0.47 ± 0.05 N m), 0.58 ± 0.08 N m (inverse dynamics 0.57 ± 0.06 N m) for 500 g and 0.74 ± 0.07 N m (inverse dynamics 0.75 ± 0.08 N m) for 1000 g.

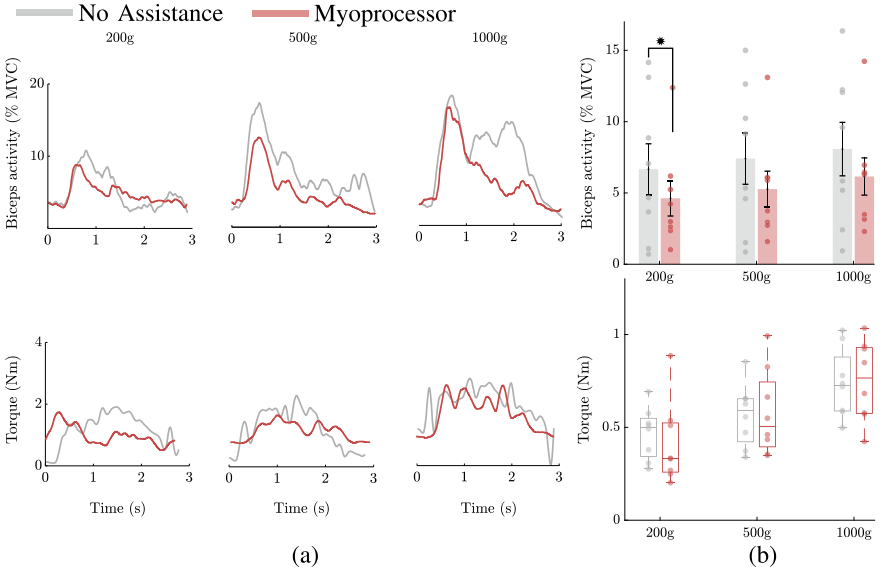

Fig. 2 Biceps activity reduction and joint torque estimation. Panel **a** shows the biceps activity (top) and the elbow torque estimated by the myoprocessor (bottom, red line) compared to the torque estimated by using and inverse dynamics model (bottom, grey line) during the task. Panel **b** displays the overall trend for all subjects

4 Conclusion

The *myoprocessor* module can control a soft exosuit and smoothly adapt the assistance by online estimating elbow torque during task. It represents a reliable strategy to detect movement intention and acting in concert with the human wearer. The proposed approach has advantage in human robot interaction robustness respect to controller not using biolsignals in the assistance loop, but requires additional work during the set up which needs extensive calibration procedure to be tuned on the user antropometry.

References

1. J.R. Koller, D.A. Jacobs, D.P. Ferris, C.D. Remy, Learning to walk with an adaptive gain proportional myoelectric controller for a robotic ankle exoskeleton. J. NeuroEng. Rehabil. **12**(1), 1–14 (2015). https://doi.org/10.1186/s12984-015-0086-5
2. A. Fougner, O. Stavdahl, P.J. Kyberd, Y.G. Losier, P.A. Parker, Control of upper limb prostheses: terminology and proportional myoelectric control—a review. IEEE Trans. Neural Syst. Rehabil. Eng. (2012)
3. R. Merletti, P. Parker, Electromyography: Physiology, Engineering, and Noninvasive Applications, 11th ed. (Wiley, IEEE Press, 2004)
4. N. Lotti, M. Xiloyannis, G. Durandau, E. Galofaro, V. Sanguineti, L. Masia, M. Sartori, Adaptive model-based myoelectric control for a soft wearable arm exosuit: a new generation of wearable robot control. IEEE Robot. Autom. Mag. (2020)
5. D. Chiaradia, M. Xiloyannis, C.W. Antuvan, A. Frisoli, L. Masia, Design and embedded control of a soft elbow exosuit, in *IEEE International Conference on Soft Robotics (RoboSoft)* (2018), pp. 565–571
6. D.G. Lloyd, T.F. Besier, An EMG-driven musculoskeletal model to estimate muscle forces and knee joint moments in vivo. J. Biomech. **36**(6), 765–776 (2003)

Pneumatic Control System for Exoskeleton Joint Actuation

Pavel Venev, Ivanka Veneva, and Dimitar Chakarov

Abstract The aim of the work is to present the design and construction of a pneumatic system for actuation of an exoskeleton for upper limbs, suitable for rehabilitation and training. Testing and adjustment of control system of the prototype as well as experimentation of the functionality of the exoskeleton and evaluation of joint actuation have been performed.

1 Introduction

One of the known approaches for exoskeleton actuation is the use of pneumatic artificial muscles (PAMs) [1]. Compared to other actuation systems PAMs are seen as an effective solution to safety problems [2] and light design with high power/weight ratio [3]. Due to the low inertia and inherent compliance of the compressed air, the impedance of the pneumatic muscle is low in a wide frequency range, reducing the influence of uncontrolled external forces to potentially safe levels. Pneumatic actuator produces torque as a result of the difference in the applied antagonistic forces and allows to adjust the stiffness of the joint by simultaneously contracting the antagonistic muscles [4].

The work presents a new appropriate solution for the construction and pneumatic actuation of an exoskeleton for upper limbs, suitable for rehabilitation and training, providing transparency and natural safety, as well as force and mobility. A new prototype control unit has been created. The control system is based on information from position, pressure and force sensors. The presented exoskeleton can be used as

P. Venev · I. Veneva (✉) · D. Chakarov
Mechatronics Department, Institute of Mechanics, Bulgarian Academy of Sciences, Sofia, Bulgaria
e-mail: veneva@imbm.bas.bg

P. Venev
e-mail: pavelvenev@abv.bg

D. Chakarov
e-mail: mit@imbm.bas.bg

J. C. Moreno et al. (eds.), *Wearable Robotics: Challenges and Trends*,
Biosystems & Biorobotics 27, https://doi.org/10.1007/978-3-030-69547-7_56

a haptic device to provide physical interaction in the virtual environment. It creates a force on the operator according to the interactions in the virtual scene.

2 Material and Methods

We have developed an active exoskeleton for haptic perception and assistive movement of the upper limbs [5]. The exoskeleton is with anthropomorphic range of motion and low mass/inertia characteristics fabricated with light materials through 3D printing. The exoskeleton segments are designed to be easily adjusted for one "typical adult". The CAD model of the exoskeleton and the real prototype made of plastic and carbon is presented in Fig. 1. The exoskeleton includes left and right upper limb with 4 degrees of freedom (DOF) for the shoulder and elbow. The main feature here is the third DOF of the shoulder which is transferred and performed by internal/ external rotation in the elbow.

The actuation system of the exoskeleton is based on pneumatic artificial muscles working in antagonistic scheme [6]. For each of the four joints, antagonistic driving muscles are attached to the segments of the exoskeleton, following the principle of the human arm muscles placement. Inflating the pipes with compressed air causes the muscle to expand radially and shorten axially. In this way, the muscle generates a one-way traction along the longitudinal axis (Fig. 2). A bundle of parallel PAMs is used to drive each joint. Two sheaves PAM, A1 and A2, work together in an antagonistic scheme, simulating a biceps-triceps system to provide the bidirectional motion/force. Through a rotating pulley, the torque is transmitted to the actuated

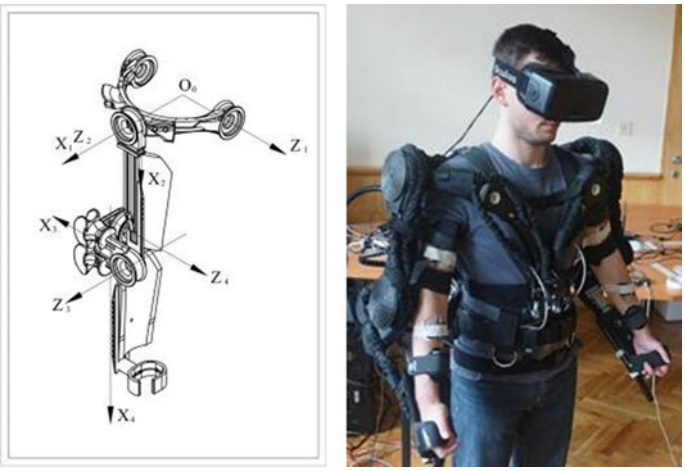

Fig. 1 Upper Limb Exoskeleton. **a** CAD model; **b** real prototype

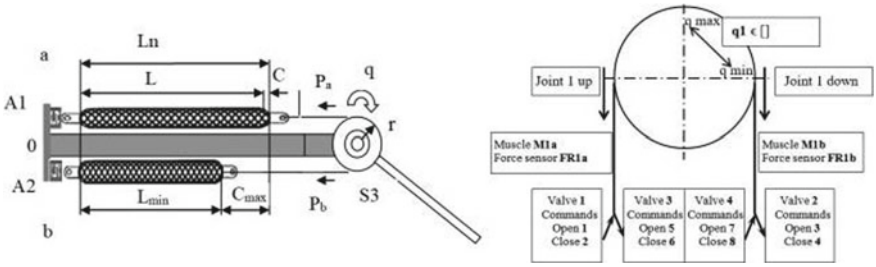

Fig. 2 Joint actuation with pneumatic muscles in antagonistic scheme

joints. Joint control required the integration of several sensors to measure pressure, angle and force signals.

The Control algorithm is built as impedance controller with gravity compensation (Fig. 3) based on a mechanical model of exoskeleton as active reflecting device during interaction with a virtual environment [7]. Pneumatic muscles that work antagonistically actuate the exoskeleton joint. Agonist muscle is active in one direction, when antagonist is passive and vice versa. At zero pressure the muscles show elastic properties ($\boldsymbol{P_a}$ and $\boldsymbol{P_b}$) determined of inner rubber liner.

The stiffness of the muscle bundle can be determined as a derivative of the muscle force about muscle contraction:

$$K = \frac{\partial P}{\partial C} = -(K_0 + tp)(2C - (L_n + C_{\max})), \tag{1}$$

where $\boldsymbol{P}$ is the pooling force of the muscles, $\boldsymbol{p}$ is the operating pressure, $\boldsymbol{L}$ and $\boldsymbol{L_{min}}$ are the muscle lengths according Fig. 2a, $\boldsymbol{K_0}$ and $\boldsymbol{t}$ are empiric derived coefficients that depend on the muscle number. The stiffness is a linear function of pressure and contraction of pneumatic muscles in the bundle, as well as of the number of muscles in the bundle.

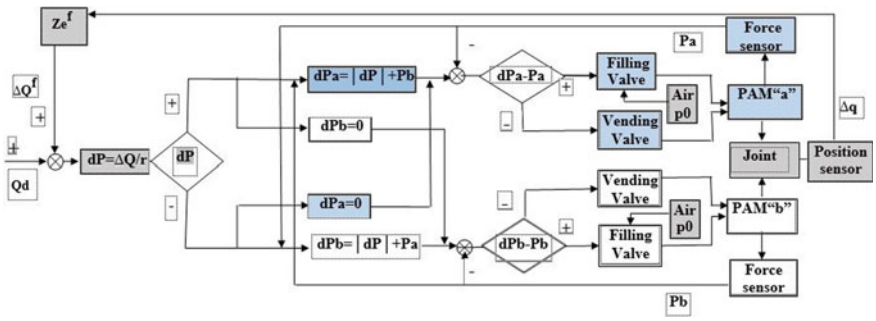

Fig. 3 Impedance controller for joint torque control

3 Results

Special pneumatic muscles are designed to actuate the exoskeleton system. Pneumatic muscles are light and produce high output powers. They are made of latex hoses covered with polyester braid. Two factors determine the length and diameter of the muscles that drive each joint. The first is the torque required in this joint, and the second is the range of motion of the joint. An additional factor is the radius, $\boldsymbol{r}$ of the pulley. For design reasons, the radius is $r = 0.0315$ m. The range of movements, effective muscle contractions, number of muscles and achieved torques are experimentally obtained (at 400 kPa pressure) and shown in Table 1. Muscle contraction, $\boldsymbol{C}$ is represented as a percentage of the nominal muscle length $\boldsymbol{L_n}$ determined by the outer braided layer c= $100\ C/L_n$. The maximum contraction of each muscle bundle is $c_{\max} = 40\%\ L_n$ *or* $C_{\max} = 0.156$ m.

Pneumatic control unit prototype (Fig. 4.) consists of pressure sensors, solenoid valves, microcontroller board and a plate with channels for airflow distribution. The bundle muscles are supplied in parallel with air through two parallel on/off valves, one

Table 1 Range of movements, number of muscles and achieved torques

Joint	Movement	Antagonist bundles	ROM (deg)	Muscle contraction (c%)	Muscles in the bundle	Joint torque (Nm)
Shoulder joint J1	Abduction	b	110	15.5	7	38.5–19.2
	Adduction	a		15.5	3	4.7–13.9
Shoulder joint J2	Flexion	b	120	16.9	6	32.9–16.2
	Extension	a		16.9	3	5.2–14.8
Elbow joint J3	Flexion	b	150	21.1	4	21.9–7.8
	Extension	a		21.1	2	2.0–9.8
Elbow joint J4	Int. Rotation	b	135	19.0	4	21.7–7.2
	Lat. Rotation	a		19.0	3	4.3–15.8

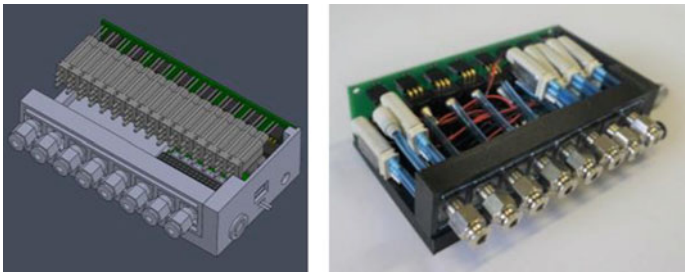

Fig. 4 Pneumatic control unit prototype

of which is used to supply pressure and the other to discharge into the atmosphere. 4 Port Solenoid Valve Series S070s (SMC Pneumatics) were used to actuate the joint, which are controlled by the ULN2803 driver. These valves supply muscles with compressed air up to 5 bar through a pneumatic plate with channels for air flow distribution. The Atmega 32U4 microcontroller is used to perform analog-to-digital conversions and digital filtering. The microcontroller uses angle and pressure sensors to monitor the position and valve control. For pressure measurement, 2 piezoresistive pressure sensors Honeywell 40PC100G with 0.2% accuracy were used. These sensors operate in the range between 0 and 100psi (6 bar) with 40.0mV/psi output signal. The Bourns Inc. Magnetic encoder AMS22B5 was used to measure the angle which has 12 bit resolution and can rotate up to 360°. This magnetic encoder converts the angular rotation into an analog signal.

3.1 Experiments with the Active Exoskeleton with Volunteers

Weight Lifting experiments with 15 middle aged male volunteers wearing the exoskeleton has been completed in virtual GYM (from a first person perspective). An evaluation of pneumatically compliable joint actuation have been performed. Questionnaires were completed to determine the comfort and degree of freedom of the exoskeleton. The analysis of the results for validation of the exoskeleton functionality showed that over 80% of the participants in the experiment gave a positive assessment.

4 Discussion

The experiments prove that the approach with pneumatic actuation of the active orthosis allows natural, safe and comfortable physical interaction and support of the human operator. The overall assessment of the system shows that participants feel comfortable with the exoskeleton and have not noticed a sharp or painful part of the exoskeleton and the weight of the device. Participants said they could perform the movements correctly and did not feel strange during the test.

5 Conclusion

An appropriate solution for the construction and pneumatic actuation of an exoskeleton for upper limbs, suitable for rehabilitation and training, providing transparency and natural safety, as well as force and mobility was presented. Tests and adjustments of all systems of the prototype were performed, as well as experimentation of the functionality of the orthosis with adjustable compliable joints.

Acknowledgments This research was supported by the EC (FP7 Project VERE-257695); Bulgarian Science Found (Project AWERON, DN 07/9) and Ministry of Education and Science in Bulgaria (National Scientific Program ICTinSES, contract No DO1–205/23.11.2018).

References

1. D.G. Caldwell et al., "Soft" exoskeletons for upper and lower body rehabilitation—design, control and testing. Int. J. Humanoid Robot. **4**(3), 549–573 (2007)
2. P. Chou, B. Hannaford, Measurement and modeling of McKibben pneumatic artificial muscles. IEEE Trans. Robot. Autom. **12**(1) (1996)
3. B. Vanderborght, et al., Variable impedance actuators: a review. Robot. Autonomous Syst. **61**, 1601–1614 (2013)
4. N. Tsagarakis, D.G. Caldwell, Improved modelling and assessment of pneumatic muscle actuators, in *ICRA 2000*, San Francisco (2000)
5. I. Veneva, D. Chakarov, M. Tsveov, D. Trifonov, E. Zlatanov, P. Venev, Active orthotic system for assistance and rehabilitation, in *20th International Conference on CLAWAR 2017*, Porto, Spain (2017), pp. 597–604
6. I. Veneva, D. Chakarov, M. Tsveov, D. Trifonov, E. Zlatanov, P. Venev, Active assistive orthotic system: (exoskeleton) enhancing movement, in *Handbook of Research on Biomimetics and Biomedical Robotics* (IGI Global eEditorial Discovery, 2017), pp. 48–75
7. D. Chakarov, I. Veneva, M. Tsveov, P. Venev, Powered upper limb orthosis actuation system based on pneumatic artificial muscles. J. Theor. App. Mech. **48**(1), 23–36 (2018)

PowerGrasp: Development Aspects for Arm Support Systems

Jean-Paul Goppold, Jan Kuschan, Henning Schmidt, and Jörg Krüger

Abstract Exoskeletons can support workers on physically demanding tasks, but in industry they lack of acceptance. This contribution gives an insight into design aspects for upper body exoskeletons, especially how active exoskeletons for industrial applications differ from military and medical use-cases. To overcome typical rigid exoskeleton problems, we suggest the use of modular soft-exosuit support systems and therefore checked different types of soft actuation principles for their eligibility for the use on upper body joints. Most promising approach is using two-layered actuators sting of robust fabric with embedded rubber tubes as pressure chambers. By inflating the tubes, it is possible to vary the stiffness of the chambers, which can be effectively used to generate assisting forces and moments at human joints (shoulder, elbow, wrist, finger).

1 Introduction

Physically demanding manual tasks in manufacturing, logistics, handcraft and service are major contributors to early damage of the musculoskeletal system (approx. 19% of all work disabilities) and especially the spine (approx. 47% of muscoskeletal disabilities) [1] and are responsible for a loss of the gross domestic product of approximately 1% [2]. For military and rehabilitation use-cases, exoskeletons already showed that wearable systems support the muscle activity of the wearer. Nevertheless, the criteria differ largely from industrial applications (requirements for plug&play behaviour and longtime wear) and first rigid exoskeletons in assembly lines often suffer on the wearers acceptance [3]. As a result, the exoskeleton-market nowadays is mainly restricted to passive exoskeletons [4], which are practical, individually adaptive, not power restricted and much cheaper than their active counterparts. But, active exoskeletons suit the flexibility required by industrial environments more, which opens a wider industrial acceptance if the focus of the classical design-principles of exoskeletons will shift to more medically dominated topics like effects of long-term wear and ergonomics.

J.-P. Goppold (✉) · J. Kuschan · H. Schmidt · J. Krüger
Fraunhofer Institute for Production Systems and Design Technology (IPK), Berlin, Germany
e-mail: jean-paul.goppold@ipk.fraunhofer.de

J. C. Moreno et al. (eds.), *Wearable Robotics: Challenges and Trends*,
Biosystems & Biorobotics 27, https://doi.org/10.1007/978-3-030-69547-7_57

2 Development Aspects

From [5, 6] and discussions with medical officers, works council, end users and management from our project partner from the automotive industry, we found the main barriers for integrating exoskeletons in industrial environments in an often not considered variety of restrictions. Those are mainly driven by economical aspects, medical concerns as well as issues concerning the level of comforts. Table 1 gives a comprehensive overview of the factors identified together with a qualitative evaluation on existing basic exoskeleton types. Rigid active exoskeleton, which are well

Table 1 Limiting factors for exoskeletons in industrial environments recorded from medical doctors, essence and [5, 6]

	Rigid-exoskeleton	Soft-exosuit
Economical factors		
Acquisition and maintenance costs	High	**Low**
Lack of generalization from specialized Use-Case	Specific to passive exos	
Adjustment to personal preferences & body type	Difficult	**Easy**
Medical factors		
Joint Misalignment between Exo and Wearer	Often	**Rare**
Degradation of muscle activity (due to exo)	Solvable with smart control on active exos	
Unpredictable effects of empowerment of non-ergonomic movements	Solvable with smart control on active exos	
Effects of restrictions of DoF due to compensation of movements/postures	Difficult to predict	**Easier to predict**
Effects of unnatural additional loading to joints and sinews	**Easier to predict**	Difficult to predict
Comfort factors		
Psychological impacts of interacting with robotic systems (safety concerns)	Higher	**Lower**
Joint misalignment between exoskeleton and wearer	Often	**Rare**
Restriction of movement	More frequent	**Less frequent**
Bulky exoskeleton dimension impractical in narrow industrial environments	Yes	**No**
Hygiene (shared use)	**Higher (rare direct skin contact)**	Lower (textiles)

suited for rehabilitation and military applications, would be mostly in contrast with these factors, while soft-robotic seems a suitable approach, especially when dealing with long-term medical considerations, while on the other hand still being robust, safe and also less costly.

In [7] we already proposed a rough concept for the PowerGrasp soft-exosuit system, which is primarily intended for the active support of overhead car assembly and whose key development factors are based on Table 1. Due to its modular, highly flexible setup and by supporting up to four different joints on one limb (shoulder, elbow, wrist and fingers), it can be easily adapted to changing requirements within various applications. Additional insights into the design process of the PowerGrasp soft-exosuit system from a more design and therapist perspective can be found in [6].

To figure out what type(s) of actuation units might serve the requirements of our soft-actuated system best we realised and tested different approaches. This includes 3D-printed Thermoplastic Polyurethane(TPU) based actuators, silicone-casted actuators, fabric encapsulated rubber tube actuators as well as tendon driven actuators, shown in Fig. 1.

The tendon-based is well known concerning design in robots and exoskeletons. The Application in exosuits can become troublesome though, since all of the tendon-forces will have to be redirected locally at the joints—most likely this will result in unacceptably high loads to the wearers' bone-joint structure, especially when higher assisting loads are required. In the context of modularization, this problem gets intensified, because of the intersection problem between the separate modules. To lower the effects of friction and to allow reasonable control the integration of rigid redirecting units would be advisable—the opposite of being soft.

For inflatable actuators the production methods of monolith casting and 3D-printing show high potential for unrestricted soft actuator design as well as supporting direct inclusion of sensors and electronics. But in real-world scenarios, achievable assisting loads are limited due to the material characteristics. The permeability of the TPU-based actuator was growing with time and in case of damage, these actuators are hard to repair. As profound knowledge on long-term characteristics for these types

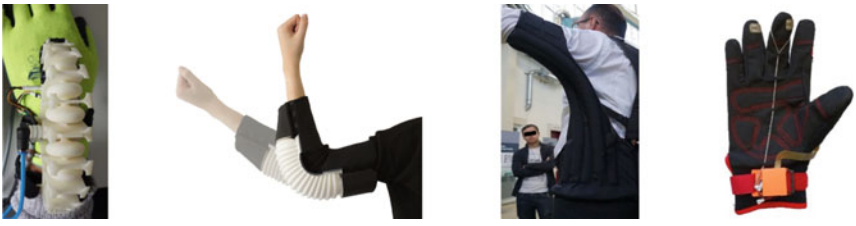

(a) Wrist: TPU 3D-printed (b) Elbow: Silicone-casted [6] (c) Shoulder: two-layered textile (d) Fingers: Tendon-driven

Fig. 1 Samples of tested manufacturing methods for actuator-design on different joints

of actuators is not available, we consider this fact as critical to a potential application in an industrial environment.

Alternative ways to create inflatable actuators is by using two-layer material setups. One approach uses an-isotropic structural behaviour of the outer layer (e.g. "bionic muscles"). Another uses predefined textile-patterns on the outer layer to achieve the (use-case specific) intended force vector and is mainly driven by varying the stiffness of the structure through pressure variation. Even though the design flexibility of this approach is lower compared to the generative approaches, one can still generate a large variety of actuation schemes. A major advantage, especially in the stiffness variation approach, is the high robustness of the setup due to the functional separation of inner and outer layer. The pattern of the outer layer indicates the resulting force vector as well as defines the overall flexibility and robustness against potential physical damage. The inner layer can be specifically designed to encapsulating high pressure. The functional separation also allows for easy maintenance and repair. Additionally, the actuators are flexible as textiles when depressurized - thus allowing a maximum of comfort. Because of the many advantages the actuation modules of the PowerGrasp system were finally designed according to the approach based on stiffness-control of a two-layered textile actuator—utilizing nylon polyamide fabric as outer layer and butyl tubes as inner layer—a sample can be seen in Fig. 1c. The use of Stratos–Cordura® 3-layer laminate (highly stressable) as outer layer allows the application of high pressuring states by far surpassing the other actuation methods (pressure of up to 3 bar repeatably applicable).

3 Conclusion and Discussion

To not only show technical feasibility but also to achieve high acceptance-rates for applications in industrial environment we made a revision of requirements for the design of exoskeletons and extended the scope from technical and economical aspects (classically references) by also considering medical concerns, medical long-term concerns and comfort (Table 1). We believe that considering these aspects in the design of future exoskeletons will play an essential role in the integration process of exoskeletons into the industrial environment. Next, we want to focus on identifying the control characteristics of the actuation units and include smart control schemes on the soft-exosuit to bring the benefits of the system to a maximum.

Acknowledgements PowerGrasp was funded by the German Federal Ministry of Education and Research (BMBF).

References

1. D. Hoy, P. Brooks, F. Blyth, R. Buchbinder, The epidemiology of low back pain. Best Practice Res. Clin. Rheumatol. **24**, 769–781 (2010)
2. C. Maar, R. Fricker, Vorteil Vorsorge Die Rolle der betrieblichen Gesundheitsvorsorge für die Zukunftsfähigkeit des Wirtschaftsstandortes Deutschland (*Booz & Company*, 2009)
3. M.P. De Looze, T. Bosch, F. Krause, K.S. Stadler, L.W. O'Sullivan, Exoskeletons for industrial application and their potential effects on physical work load. Ergonomics **59**(5), 671–681 (2016)
4. T. Butler, J.C. Gillette, Exoskeletons: used as PPE for injury prevention, in *Professional Safety* (2019), p. 33
5. R. Gopura, K. Kiguchi, Mechanical designs of active upper-limb exoskeleton robots: state-of-the-art and design difficulties, in *2009 IEEE International Conference on Rehabilitation Robotics* (IEEE, 2009), pp. 178–187
6. R. Flechtner, K. Lorenz, G. Joost, Designing a wearable soft-robotic orthosis: a body-centered approach, in *Proceedings of the Fourteenth International Conference on Tangible, Embedded, and Embodied Interaction (TEI-2020), Future Bodies, Future Technologies* (ACM, 2020), pp. 863–875
7. J. Kuschan, J. Goppold, H. Schmidt, J. Krueger, Powergrasp: concept for a novel soft-robotic arm support system, in *ISR 2018; 50th International Symposium on Robotics* (2018), pp. 1–6

Mobile Unilateral Hip Flexion Exosuit Assistance for Overground Walking in Individuals Post-Stroke: A Case Series

Richard W. Nuckols, Franchino Porciuncula, Chih-Kang Chang, Teresa C. Baker, Dorothy Orzel, Asa Eckert-Erdheim, David Perry, Terry Ellis, Louis Awad, and Conor J. Walsh

Abstract Stroke is a leading medical issue that can impact the person's ability to walk effectively. There is limited research into the design and biomechanical response for exosuits that assist more proximal joints such as the hip. For this case series, three subjects with chronic stroke participated in a single-session study to evaluate hip flexion exosuit assistance in overground walking. We iteratively tuned the unilateral hip flexion assistance profiles in overground gait. Compared to the initial unpowered baseline, walking speed at the end of tuning and with the device powered increased for 2 of 3 individuals and on average by 0.16 m s^{-1}. We then compared powered versus unpowered overground walking during a 5 min evaluation period. Circumduction was reduced by 9 $\pm$1 mm and cost of transport was reduced by 8.6 $\pm$1.7% for the 3 participants.

1 Introduction

Gait deficits following stroke can have varied effects on the joints of the paretic limb [1]. While much effort has focused on improving ankle function [2], the hip also provides important contributions to gait particularly in swing. In fact, for ground clearance during swing, hip flexion contribution to limb shortening is potentially more important than the contribution from ankle dorsiflexion [3]. Recently, there have been efforts to assist more proximal joints such as the hip during walking [4–6], but how exosuits can affect the mechanics of the hip and how best to apply assistance at the hip for individuals after stroke needs further understanding.

This study was supported by NIH BRG R01HD088619, NSF CNS-1446464, Wyss Institute for Biologically Inspired Engineering and the Harvard School of Engineering and Applied Sciences.

R. W. Nuckols · F. Porciuncula · C.-K. Chang · D. Orzel · A. Eckert-Erdheim · D. Perry · C. J. Walsh (✉)
School of Engineering and Applied Sciences, Harvard University, Cambridge, MA, USA
e-mail: walsh@seas.harvard.edu

T. C. Baker · T. Ellis · L. Awad
Department of Physical Therapy and Athletic Training, Sargent College, Boston University, Boston, MA, USA

J. C. Moreno et al. (eds.), *Wearable Robotics: Challenges and Trends*,
Biosystems & Biorobotics 27, https://doi.org/10.1007/978-3-030-69547-7_58

Our aim was to develop an initial prototype of a mobile soft hip flexion exosuit for individuals post-stroke. We started by first examining which biomechanical deficits may be addressed with a hip flexion system. Next, given the heterogeneity of post-stroke gait, we systematically tuned a hip flexion system to offset specific deficits and examined the exosuit-induced effects of the assistance on three individuals.

2 Methods and Materials

Three subjects with chronic stroke (Table 1) participated in this single-session study that included a familiarization/tuning phase followed by an evaluation phase. The hip exosuit used for preliminary investigation was adapted for unilateral hip flexion assistance from a device similar to what was shown in [7]. A hip mounted mobile actuator (2.6 kg) delivered an assistive force ranging from 60–100 N through a Bowden cable-driven transmission to anterior textile anchors on the waist and thigh. This force across the paretic hip textile components produced a flexion torque about the hip.

2.1 Familiarization and Tuning

To gain familiarization with the hip exosuit, subjects were asked to walk at comfortable speeds in a 36.3 m oval indoor gait lab track with the exosuit providing assistance for a series (3–5) of 2 min bouts. Each participant started with a baseline assistance profile. Following each bout, the assistance profile was modified based on user and device performance. This iterative tuning process was based on:

(1) Visual gait analysis [8] performed by a physical therapist to assess the individual's needs and understand how the hip flexion exosuit might augment the participant's gait.
(2) Quantitative gait metrics generated from body-mounted IMUs complemented visual gait analysis, with summary reports after each bout that provided insights on hip exosuit-induced changes on gait [9].

Table 1 Participant baseline characteristics and gait performance

Subject	Age	Sex	Stroke onset (months)	Paretic Side	Height (cm)	Weight (kg)	Device	Baseline speed (m/s)
1	45	M	90	Left	179	100.5	AFO	1.05
2	60	M	92	Right	178	72.5	None	0.97
3	50	F	91	Right	166	60	None	1.35

(3) Walking speeds during the 2-min walk to assess whole-body response to exosuit assistance measured by a researcher following with a measuring wheel.

The "optimized" assistance profile was identified based on settings that provided fastest walking speed without clinical gait decline per quantified metrics and physical therapist observations.

2.2 Evaluation of Assistance: Five Minute Walk Tests

To evaluate hip exosuit-induced effects, we asked participants to walk for 5 min around the indoor gait lab track at comfortable walking speed under the following conditions: (a) hip exosuit powered on (Active), and (b) unpowered (Slack). We collected data on energy consumption of walking using a mobile metabolic system (Cosmed K5, Italy), and kinematic data using motion capture (Qualysis, Sweden). To examine within-subject changes between Active vs Slack, we used the Wilcoxon Exact test.

3 Results

Relative to the initial unpowered baseline, walking speeds at the end of tuning with the device powered increased for 2 of 3 individuals and on average by 0.16 m s^{-1} (Subjects 1–3: 0.0, 0.33, 0.15 m s^{-1}, respectively). For the evaluation phase, Subjects 1, 2 and 3 were provided peak applied forces of 83.7, 90.7, 63.5 N, with timing onsets at 40%, 23%, and 40% of the gait cycle, respectively (Fig. 1). For the Active condition, circumduction was reduced on average by 9 ± 1 mm (Subjects 1–3: 11, 7, 7 mm) compared to Slack. Only modest changes to walking speeds were observed in response to Active assistance (Subjects 1–3: 1.22 (+0.02), 1.24 (−0.04), 1.51 (+0.04) m s^{-1}). Reductions in cost of transport (walking efficiency) were observed in Active relative to Slack, with average reduction of 8.6 ± 1.7% (Subjects 1–3: 6.4, 7.7, 10.4%).

Subject 1 responded with significant changes in various kinematic measures: increased ground clearance (2.2 ± 0.02 mm, $p < 0.0001$), increased peak knee flexion angle (12.2 ± 1 deg, $p < 0.0001$), and decreased circumduction (11 ± 5 mm, $p = 0.0196$). Subject 2 demonstrated small reduction in circumduction ($p > 0.05$), and Subject 3 had slight decrease in knee hyperextension during mid/late stance (4 deg, $p > 0.05$), however these were not statistically significant.

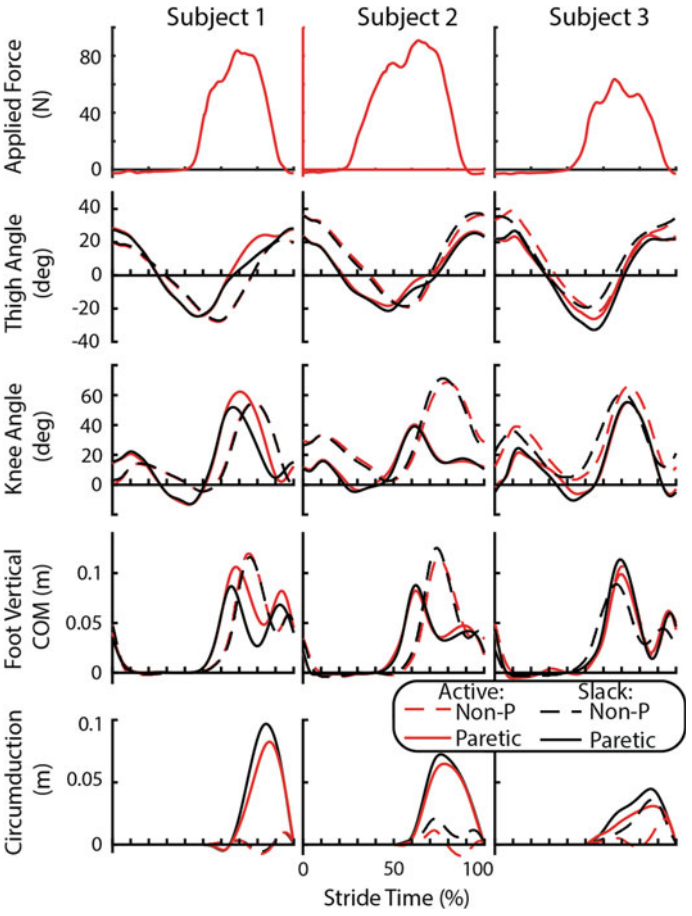

Fig. 1 Average stride biomechanical changes resulting from tuned hip flexion exosuit assistance

4 Discussion

These results support the idea that users may respond to hip flexion assistance differently based on their specific gait deficits. Despite similar baseline kinematic deficits between subject 1 and 2, the effect of the assistance on the kinematics was different. While subject 1 seemed to use the assistance to correct gait kinematics, subject 2 kinematics did not change despite the large applied assistance force.

Although our approach of tuning did not result in faster walking speed in the evaluation phase, our limited data suggest that the tuning process resulted in a 0.16 m s^{-1} improvement in walking speed with the device powered compared to initial unpowered baseline. We were also able to elicit improvement in walking efficiency

for each participant when walking with device powered versus unpowered, but we did not compare to a condition where the participant walked without a device.

5 Conclusions

This initial work suggests that individuals use unilateral hip flexion to improve walking efficiency through different biomechanical mechanisms. Additional work will need to dig deeper into these findings to understand how individuals effectively use the assistance and address additional metrics such as spatiotemporal parameters. Future work will also focus on developing a smaller and more lightweight system designed for the requirements of unilateral hip flexion support.

References

1. I. Jonkers, S. Delp, C. Patten, Capacity to increase walking speed is limited by impaired hip and ankle power generation in lower functioning persons post-stroke. Gait Posture **29**(1), 129–137 (2009)
2. L.N. Awad, et al., A soft robotic exosuit improves walking in patients after stroke. Sci. Transl. Med. **9**(400) (2017)
3. V.L. Little, T.E. McGuirk, C. Patten, Impaired limb shortening following stroke: what's in a name? PloS One **9**(10), e110140 (2014)
4. C. Buesing et al., Effects of a wearable exoskeleton stride management assist system (SMA®) on spatiotemporal gait characteristics in individuals after stroke: a randomized controlled trial. J. Neuroeng. Rehabil. **12**(1), 69 (2015)
5. C. Di Natali et al., Design and evaluation of a soft assistive lower limb exoskeleton. Robotica **37**(12), 2014–34 (2019)
6. M. Sposito, et al., Evaluation of XoSoft Beta-1 lower limb exoskeleton on a post stroke patient, in *Sixth National Congress of Bioengineering*, Milan, Italy, June 25–27, 2018
7. J. Kim et al., Reducing the metabolic rate of walking and running with a versatile, portable exosuit. Science **365**(6454), 668–72 (2019)
8. F. Ferrarello et al., Tools for observational gait analysis: a systematic review. Phys. Ther. **93**(12), 1673–1685 (2013)
9. P. Arens, et al., Real-time gait metric estimation for everyday gait training with wearable devices in people poststroke. Wearable Technol. (submitted for publication (accepted))

The SoftPro Wearable System for Grasp Compensation in Stroke Patients

L. Franco, M. Tschiersky, G. Wolterink, F. Barontini, M. Poggiani, M. Catalano, G. Grioli, M. Bianchi, A. Bicchi, S. Rossi, D. Prattichizzo, and G. Salvietti

Abstract This extended abstract presents a wearable system for assistance that is a combination of different technologies including sensing, haptics, orthotics and robotics. The result is a device that, by compensating for force deficiencies, helps lifting the forearm and thanks to a robotic supernumerary finger improves the grasping ability of an impaired hand. A pilot study involving three post-stroke patients was conducted to test the effectiveness of the device to assist in performing activities of daily living (ADLs), confirming its usefulness.

1 Introduction

Robotic devices have been developed to give supervised assistance to patients with mild to extreme motor disabilities after neurologic injury [1]. In the context of the EU project SoftPro (https://www.softpro.eu), a consortium of universities and companies has investigated novel solutions for assistive robotic tools to be used at home by chronic stroke patients. In addition to classical exoskeleton approaches [2], we have introduced the concept of using wearable robots as assistive tools for restoring grasping capabilities in people with paretic arms. We have also designed an sEMG interface embedded in a cap called e-CAP for the system control and a wearable haptic interface called CUFF which provides force feedback from a wearable robotic finger. We attached all devices to the Assistive Elbow Orthosis, a light passive exoskeleton that assists elbow flexion, to enlarge the number of potential final users.

L. Franco (✉) · S. Rossi · D. Prattichizzo · G. Salvietti
University of Siena, Siena, Italy
e-mail: leonardo.franco@student.unisi.it

M. Tschiersky · G. Wolterink
University of Twente, Enschede, The Netherlands

F. Barontini · M. Poggiani · M. Catalano · G. Grioli · A. Bicchi · D. Prattichizzo · G. Salvietti
Istituto Italiano di Tecnologia, Genova, Italy

M. Bianchi · A. Bicchi
University of Pisa, Pisa, Italy

J. C. Moreno et al. (eds.), *Wearable Robotics: Challenges and Trends*,
Biosystems & Biorobotics 27, https://doi.org/10.1007/978-3-030-69547-7_59

2 System Components

The Robotoic Sixth Finger is a wearable supernumerary robotic finger created by the University of Siena (US). It is an extra finger that acts as a functional replacement of the thumb, and has been demonstrated to compensate missing grasping capabilities of stroke subjects [3]. In the integrated device, the Sixth Finger has the end-effector function. It is the device of the system that enables the stroke patient to grasp objects in combination with the impaired limb. The e-Cap is a human-robot interface embedded in a regular cap which is easy to wear and can recognize the movement of the eyebrows through real-time sEMG measurement of the frontalis muscle [4, 5]. The e-Cap consists of an sEMG acquisition chain composed of dry electrodes, a commercial instrumentation amplifier and a Teensy 3.2 microcontroller to sample the analog signal. For the dry electrodes, we proposed a solution which combines a reusable sticky plastic tape and non-gelled 3D-printed flexible TPU-based sEMG electrodes developed by University of Twente (UT) [6].

The e-Cap electronic board is equipped with a Bluetooth antenna with which it can communicate with the Sixth Finger. Finally, at the back of the cap there is a 3D-printed box for the battery. Being an sEMG-based interface, it requires a calibration before operational use. The trigger for the calibration was upgraded in comparison to previous versions [4, 5]. The physical switch was replaced by a copper touch button. The described system maps the Sixth Finger's current load, an estimate of the force exerted onto the grasped object, to the CUFF [7]—a device developed by University of Pisa (UP) in collaboration with Istituto Italiano di Tecnologia (IIT), which renders a real-time force feedback by squeezing the arm. The device is composed of the structural frame, two mechanical actuation units and the feedback interface. A fabric band is attached to both motors, in such a way that when actuated in a counter-rotating motion the length of the band is reduced, squeezing the arm. Each added device increases the overall weight that the stroke patient has to lift when grasping something. To address this issue, we consider the use of the Assistive Elbow Orthosis [8], a passive gravity balancing device developed by the University of Twente, featuring a 3D-printed spring which is designed to provide weight compensation to the forearm of the affected limb. The device consists of a modified Wilmer elbow orthosis (Ambroise, Enschede, The Netherlands) which acts as the mechanical interface to the wearer, and a stack of nested springs that is mounted laterally onto the orthosis. The spring shape has been optimized to provide an angle-dependent moment at the elbow, which counteracts the moment caused by gravity acting on the forearm. The final prototype is shown in Fig. 1.

3 System Integration

When the patient raises the eyebrows, the e-Cap recognizes the gesture by sEMG real-time processing and triggers the Sixth Finger to close, in order to perform a grasp. This trigger signal is sent via Bluetooth antenna to the Robotic Sixth Finger,

Fig. 1 The Robotic Sixth Finger (**a**) and its power supply and control system (**b**) developed by US has been integrated with the Assistive Elbow Orthosis (**c**) developed by UT and the CUFF (**d**) from UP. The CUFF has been modified to be completely wearable. Motion of the finger is controlled by a new e-Cap version (**e**) developed by US with novel 3D-printed electrodes by UT

that starts closing itself until it reaches contact with an object. Once the Sixth Finger is in contact with the object, the patient can decide to increase the strength of the grasp by keeping the eyebrows raised. The amount of force is proportional to the time the patient keeps the eyebrows raised, and the value of the Sixth Finger load is sent to the CUFF device. The current that flows to maintain the motor torque level, was used as an estimate of the force that the Sixth Finger is exerting on the grasped object. The CUFF renders the force feedback in real-time by squeezing the arm in a way that is proportional to the estimated force. Finally, to open the finger, the patient has to raise the eyebrows upward twice consecutively. This movement is acknowledged by the system by vibrating twice. The act of integration required modifications to all components. The e-Cap was upgraded by using non-gelled 3D-Printed flexible TPU-based sEMG electrodes. The connection between the Assistive Elbow Orthosis, the Sixth Finger and the CUFF was improved to increase the wearing comfort. The CUFF control library was modified to use an UART port instead of a USB com port. To use the UART port, additional hardware was necessary to allow communication via the RS-485 protocol used by the CUFF device. The CUFF was modified to increase wearability in the integrated system. It was difficult to wear the CUFF for this specific application, because the fabric strip of the device got stuck on the arm of patients while donning the system. Thus, we cut the fabric strip in the middle and sewed velcro pads to the ends of the fabric. In addition, a button was added to be used as a redundant means of control since some users reported problems using the e-Cap interface.

4 Pilot Studies

We have conducted a pilot study on the usability of the integrated system involving three patients. Two subjects taking part in the experiment have been affected by stroke no more than three months before and one subject was in a chronic state. The device can be used by subjects showing a residual mobility of the arm. Patients received

the system on their paretic arm, the left hand for two subjects and the right one for the other. Patients were asked to wear the system, familiarise with the controls and then use the system to execute a series of bimanual tasks common of ADLs: opening a bottle, removing the cap from a jar, and peeling an apple. The paretic arm and the wearable system were used to stabilize the objects. We perform a qualitative evaluation of the system asking the participants to answer the ten questions of the System Usability Scale (SUS) [9] after 30 min of use. A quantitative analysis using adapted evaluation scales starting from the ARAT and the Frenchay Arm test will be performed as future work. The patients scored 70, 95 and 90, respectively. This means that the integration was deemed useful and the resulting device easy to use. We also collected suggestions for further improvements of the system. One patient suggested to provide the ability of adapting finger length depending on the task. Two patients suggested to further reduce the encumbrance of the feedback device. Finally one patient suggested to add the ability of regulating closing velocity and applied force through knobs embedded in the control box at the forearm.

5 Conclusion

In this work, different technologies such as a supernumerary robotic finger, an sEMG input device using 3D-printed electrodes, a wearable force feedback device, and a gravity balancing arm orthosis were combined to generate a new device that can assist an impaired arm. The positive response of the subjects that participated in the pilot study indicates the need for robotic assistive devices. The collected first impressions of the users will provide the starting point for further development.

References

1. A.C. Lo, P.D. Guarino, L.G. Richards, J.K. Haselkorn, G.F. Wittenberg, D.G. Federman, R.J. Ringer, T.H. Wagner, H.I. Krebs, B.T. Volpe et al., Robot-assisted therapy for long-term upper-limb impairment after stroke. N. Engl. J. Med. **362**(19), 1772–1783 (2010)
2. G. Kwakkel, B.J. Kollen, H.I. Krebs, Effects of robot-assisted therapy on upper limb recovery after stroke: a systematic review. Neurorehabil. Neural Repair (2007)
3. G. Salvietti, I. Hussain, D. Cioncoloni, S. Taddei, S. Rossi, D. Prattichizzo, Compensating hand function in chronic stroke patients through the robotic sixth finger. Trans. Neural Syst. Rehabil. Eng. **25**(2), 142–150 (2017)
4. I. Hussain, G. Salvietti, G. Spagnoletti, D. Prattichizzo, The soft-sixthfinger: a wearable EMG controlled robotic extra-finger for grasp compensation in chronic stroke patients. IEEE Robot. Autom. Lett. **1**(2), 1000–1006 (2016)
5. L. Franco, G. Salvietti, D. Prattichizzo, Command acknowledge through tactile feedback improves the usability of an emg-based interface for the frontalis muscle, in *IEEE World Haptics Conference (WHC)* (2019), pp. 574–579
6. G. Wolterink, P. Dias, R.G. Sanders, F. Muijzer, B.-J. van Beijnum, P. Veltink, G. Krijnen, Development of soft sEMG sensing structures using 3d-printing technologies. Sensors **20**(15), 4292 (2020)

7. S. Casini, M. Morvidoni, M. Bianchi, M. Catalano, G. Grioli, A. Bicchi, Design and realization of the cuff - clenching upper-limb force feedback wearable device for distributed mechano-tactile stimulation of normal and tangential skin forces, in *IEEE/RSJ IROS* (2015), pp. 1186–1193
8. M. Tschiersky, E.E.G. Hekman, D.M. Brouwer, J.L. Herder, Gravity balancing flexure springs for an assistive elbow orthosis. IEEE Trans. Med. Robot. Bionics **1**(3), 177–188 (2019)
9. J. Brooke, SUS: a 'quick and dirty' usability scale, in *Usability Evaluation in Industry* (1996), p. 189

Towards a Fabric-Based Soft Hand Exoskeleton for Various Grasp Taxonomies

Andrea Peñas, Juan C. Maldonado-Mejía, Orion Ramos, Marcela Múnera, Patricio Barria, Mehran Moazen, Helge Wurdemann, and Carlos A. Cifuentes

Abstract This paper describes a functional evaluation test of a fabric-based hand exoskeleton for various grasp taxonomies. We conducted an adapted version of the Jebsen Taylor Hand Function Test (JTHFT) with a healthy subject. The evaluation investigates a comparison of the times it takes the user to perform the task with and without the device, establishing a range of actions with a delay of 2.0–6.0 s maximum. This preliminary study aims to understand the implications of future clinical studies with post-stroke patients for rehabilitation.

Keywords Soft-robotics · Fabric-based exoskeleton · Rehabilitation robotics · Hand rehabilitation

A. Peñas · J. C. Maldonado-Mejía · O. Ramos · M. Múnera · C. A. Cifuentes (✉)
Department of Biomedical Engineering, Colombian School of Engineering Julio Garavito, Bogotá, Colombia
e-mail: carlos.cifuentes@escuelaing.edu.co

A. Peñas
e-mail: monica.penas@mail.escuelaing.edu.co

J. C. Maldonado-Mejía
e-mail: juan.maldonado-me@mail.escuelaing.edu.co

O. Ramos
e-mail: orion.ramos@mail.escuelaing.edu.co

M. Múnera
e-mail: marcela.munera@escuelaing.edu.co

M. Moazen · H. Wurdemann
Department of Mechanical Engineering, University College London, London, UK
e-mail: m.moazen@ucl.ac.uk

H. Wurdemann
e-mail: h.wurdemann@ucl.ac.uk

P. Barria
Research and Development Unit, Club de Leones Cruz del Sur Rehabilitation Center, Punta Arenas, Chile
e-mail: pbarria@rehabilitamos.org

Department of Electrical Engineering, University of Magallanes, Punta Arenas, Chile

J. C. Moreno et al. (eds.), *Wearable Robotics: Challenges and Trends*,
Biosystems & Biorobotics 27, https://doi.org/10.1007/978-3-030-69547-7_60

1 Introduction

Hand rehabilitation can improve people's quality of life after suffering a neurological impairment. Soft robotics presents an innovative and inherently safe solution for hand assistance and rehabilitation. These robotic devices are characterised by unconventional materials such as polymers, elastomers, fabrics or a combination of those materials [1].

Various actuation methodologies for soft robotics like fluidic actuation systems are very well researched and commonly applied [2]. These systems can generate complex movements using pressurised gas or fluids. Actuators are made from polymers such as silicone and fabric materials. In particular, fabric-based actuators offer advantages including high tensile strength and low weight [3]. Fabric-based actuators comprise a textile sleeve and a fluid-impermeable balloon inside. The textile sleeve prevents undesirable elongations or ballooning effects. In this paper, we present the design, manufacturing and preliminary evaluation of a hand exoskeleton made of soft fabric structures that are pneumatically actuated for grasping rehabilitation.

2 Design of the Fabric-Based Soft Hand Exoskeleton

The hand exoskeleton actuators' design was based on the design presented in [4]—a fabric-based actuator composed of three layers of fabric and two balloons of thermoplastic elastomer contained between each textile sleeves (see Fig. 1a). The flexion and extension of each finger were achieved by selective pressurisation of the inner balloons. Pleats were embedded across the textile sleeve to increase the material layer anisotropy. The textile actuators were placed easily with the combination of fixed fasteners and glued on the thumb and index finger of a polyurethane-coated nylon glove to achieve grasping. Figure 1c–e shows the final implementation of the based-fabric actuator hand exoskeleton and the fingers' flexion while the balloons are pressurised with air.

3 Validation Methodology

A well-established way to validate the functioning of exoskeletons is the Jebsen Taylor Hand Function Test (JTHFT) [5], consisting of a series of 7 subtests that allow the evaluation of various hand functions related to activities of daily living (ADL). The subtests include tasks such as writing, card turning and picking up small everyday objects. This study was carried out based on an adaptation of the JTHFT to validate the response times in the grasp compared with the results obtained in the study carried out in [6].

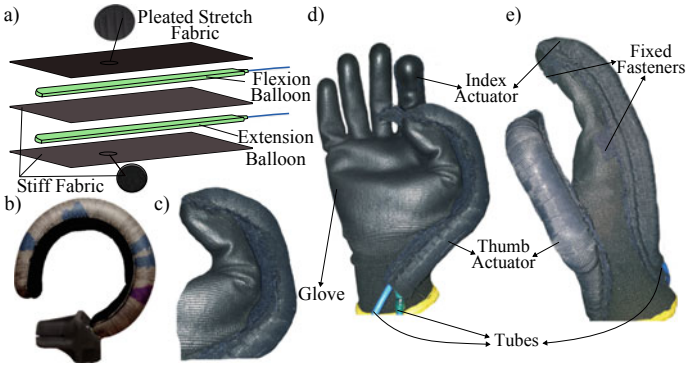

Fig. 1 Created prototype based on fabric-based actuation for hand exoskeleton for grasping. **a** Layers of based-fabric hand exoskeleton. **b** Bending of the fabric-based actuator. **c** Implementation of fabric-based actuator on a glove. **d** Palmar and e lateral views

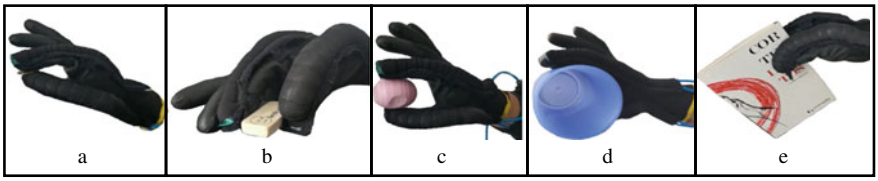

Fig. 2 ADL tasks performed by the participant while using the fabric-based exoskeleton: **a** grasping a coin, **b** grasping an eraser, **c** grasping a sphere, **d** grasping a plastic cup, and **e** grasping a book

Five objects were selected for the grasping task: a coin, an eraser, a sphere, a plastic cup and a book (see Fig. 2). A control board is used to operate an air pump that delivers up to 32 psi, mini solenoid valves that allow airflow to each actuator, pressure sensors ASDXACX100PAAA5 (Honeywell, USA), an Arduino UNO, a 12 V power source and switches to manual activation of the actuators. A static camera was used to record each task and once the results were obtained, the completion times for grasping different object with and without exoskeleton are compared.

The exoskeleton's ability to support grasping was evaluated practically with a healthy 23-years-old subject, implementing the mechanism of assistance in each of the experimental tests. The corresponding data for two scenarios, i.e. the time used for each grasp of the five objects, performing the grasp with and without the soft robotic exoskeleton was collected and analysed. The time was measured from the time the subject grasps the object, to the time of a stable grasp (i,e.,when the system is capable of maintaining a particular object without falling).

Table 1 Completion times for different objects in the adapted Jebsen Taylor hand function test

Object	Time with exo (s)	Time without exo (s)
Coin	6.0	2.0
Eraser	4.0	1.0
Sphere	5.0	2.0
Plastic cup	2.0	2.0
Book	2.0	3.0

4 Results

The results shown in Table 1 demonstrate that the subject required more time using the device than without it. Although there was a difference in response times, the results show that the time required to conduct a grasp wearing the exoskeleton is reasonable small considering that it is being done with a partial support assistance device [6].

5 Discussion

It was found that the hand succeeds in grasping all five different objects. However, different times in each case to complete the grasp were obtained. In particular, we concluded that the exoskeleton developed here has a better performance in grasping larger objects rather than the smaller one, based on the times reported in the Table 1.

The fact that overall the time that took to grasp the larger (and heavier) items were very similar with and without the exoskeleton is promising. However, further work is required to improve the manipulation and handling of small objects. Furthermore, we conclude that the time to grasp small objects has a small variation.

6 Conclusions and Future Works

Here we presented the development of a new hand-exoskeleton with a preliminary evaluation on its grasp functionality. The work has several limitations. The way that the grasp time was measured can be improved using contact sensors that determine when the grip is successful. We also observed a lack of friction at the fingertips of the exoskeleton and different objects, that makes the gripping process difficult. Therefore, further work is required perhaps to increase the surface roughness of the whole exoskeleton. A challenge in the operation of the fabric-based soft hand exoskeleton has to be addressed as the thumb and the index finger is pressurised

through the same airline. This leads to different timing in closure of thumb and index finger (see Fig. 1d). Thus, an unstable grip movement is generated.

Results show that the device will be able to provide the gripping ability to users with hand movement disabilities, the future work will focus on (1) implementing a pressure control mechanism for the balloon arrangement to contribute in a decrease of response time in the grip and (2) testing the exoskeleton in pathological users.

Additionally, although this test was evaluated by a healthy subject, in the future we will work on the evaluation with a group of stroke survivors in the rehabilitation centre "Corporación de Rehabilitación Club de Leones Cruz del Sur" in Chile.

Acknowledgements This work was supported by The Royal Academy of Engineering-Industry-Academia Partnership Programme Colombia/UK (IAPP18-1964), PrExHand Project.

References

1. S. Bagchi, M. Bishay, Soft robotics. IEEE Robot. Autom. Mag. **20**(3), 2011–2013 (2013)
2. T. Shahid, D. Gouwanda, S.G. Nurzaman, A.A. Gopalai, Moving toward soft robotics: a decade review of the design of hand exoskeletons, Biomimetics **3**(3) (2018)
3. L. Cappello, J.T. Meyer, K.C. Galloway, J.D. Peisner, R. Granberry, D.A. Wagner, S. Engelhardt, S. Paganoni, C.J. Walsh, Assisting hand function after spinal cord injury with a fabric-based soft robotic glove. J. NeuroEng. Rehabil. **15**(1), 1–10 (2018)
4. L. Cappello, K.C. Galloway, S. Sanan, D.A. Wagner, R. Granberry, S. Engelhardt, F.L. Haufe, J.D. Peisner, C.J. Walsh, Exploiting textile mechanical anisotropy for fabric-based pneumatic actuators. Soft Robot. **5**(5), 662–674 (2018)
5. E.D. Sears, K.C. Chung, Validity and responsiveness of the Jebsen-Taylor hand function test. J. Hand Surg. **35**(1), 30–37 (2010)
6. P. Tran, S. Jeong, S.L. Wolf, J.P. Desai, Patient-specific, voice-controlled, robotic FLEXotendon Glove-II system for spinal cord injury. IEEE Robot. Autom. Lett. **5**(2), 898–905 (2020)

Musculoskeletal Modelling to Evaluate and Optimize Performance of Wearable Robotic Devices

Predictive Gait Simulations of Human Energy Optimization

Anne D. Koelewijn and Jessica C. Selinger

Abstract We previously demonstrated that humans can continuously adapt their gait to optimize energetic cost in real-time when wearing a lower-limb exoskeleton. Here, we aim to recreate this paradigm using predictive gait simulations to further investigate how the nervous system performs this optimization and how energy costs change locally. To match the real-world experiment, we modeled a knee-worn exoskeleton that applied resistive torques that were either proportional or inversely proportional to step frequency—decreasing or increasing the energy optimal step frequency, respectively. We solved simulations with and without the knee exoskeleton and with fixed and free step frequency. We were able to replicate the experiment, finding higher and lower optimal step frequencies than in the natural walking under each respective condition. Our simulated resistive torques and optimized objective function resembled the measured experimental resistive torque and metabolic energy landscape. Muscle metabolic power changed for individual muscles spanning all three joints and revealed distinct coordination strategies consistent with each exoskeleton controller condition.

1 Introduction

Humans can adapt their gait to continuously optimize energetic cost in real-time. We have previously demonstrated this using robotic exoskeletons to shift people's energetically optimal step frequency to frequencies higher and lower than normally preferred [1]. In response, we found that subjects adapted their step frequency to converge on the new energetic optima within minutes and in response to relatively

A. D. Koelewijn (✉)
Machine Learning and Data Analytics (MaD) Lab, Faculty of Engineering, Friedrich-Alexander-Universität Erlangen-Nürnberg, Erlangen, Germany
e-mail: anne.koelewijn@fau.de

J. C. Selinger
Neuromechanics Lab, School of Kinesiology and Health, Queen's University, Kingston, Canada
e-mail: j.selinger@queensu.ca

J. C. Moreno et al. (eds.), *Wearable Robotics: Challenges and Trends*,
Biosystems & Biorobotics 27, https://doi.org/10.1007/978-3-030-69547-7_61

small savings in cost. However, how the nervous system actually performs this optimization in real-time—navigating an expanse of possible movements to arrive at the optimal coordination—is largely unknown. Here, we aim to re-create our experimental paradigm, where added torques at the knee alter the preferred and energy optimal gait, using predictive gait simulations. This modeling testbed will allow us to probe mechanisms underlying the energy optimization of gait—generating predictions of human behaviour and insight into aspects of optimization that are inherently difficult to investigate experimentally.

2 Methods

A. Musculoskeletal and Exoskeleton Models

We used a sagittal plane nine-degree of freedom musculoskeletal model of the lower limb [2]. We then added an ideal, massless, exoskeleton to our simulations by applying torques at the knee joints that resist both knee flexion and extension, and thereby added an energetic penalty. To replicate the control of the real-world exoskeleton, we made the average resistive torque throughout the stride proportional or inversely proportional to step frequency (penalize-high and penalize-low controller conditions, respectively), the within stride torque proportional to knee angular velocity, and the maximum allowable torque 12 Nm.

B. Energy-optimal Gait Simulations

We generated muscle-driven simulations of walking at 1.3 m/s by optimizing an objective that highly weighted effort minimization (cubed muscle activation) over error minimization (tracking of joint angles and ground reaction forces [3]) with an effort/error weighting ratio of 1000:1. Removing error from the objective function led to kinematically unrealistic gaits, but the effort weight was two orders of magnitudes higher than previous work [2]. Details of the optimization procedure are given in [2]. We generated walking simulations for all three exoskeleton controller conditions, where step frequency was free and optimized. Next, we generated simulations at a range of fixed step frequencies (-20 to $+20\%$ of natural preferred step frequency, at increments of 1%) for three conditions: exoskeleton controller on penalize-high, exoskeleton controller on penalize-low, and exoskeleton controller off, natural walking.

3 Results

Our simulated exoskeleton torques, both throughout the stride and averaged over the stride, resembled that from human experiments (Fig. 1a, b). These torques

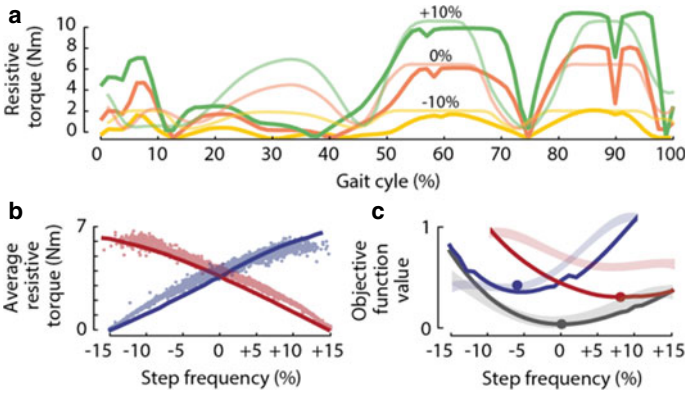

Fig. 1 **a** Torques throughout the gait cycle for the penalize-high condition at −10%, 0% and + 10% of natural step frequency. **b** Average torques across the gait cycle for the penalize-high (blue) and penalize-low (red) conditions. **c** Objective function landscapes for the penalize-high (blue), penalize-low (red), and natural (grey) conditions. Circles indicate optimal gaits for each condition. In all plots, solid lines are simulated data and faded are experimental data [1]

produced changes in simulated effort that were consistent with our experimental energy landscapes; the optimal step frequency shifted to lower and higher frequencies for the penalize-high and penalize-low conditions, respectively (Fig. 1c). When step frequency was included in the optimization, we found distinct gaits for each condition with changes in step frequency toward the optima.

An examination of simulated metabolic expenditures at the individual muscle level reveals distinct coordination strategies consistent with each exoskeleton controller condition (Fig. 2). Our simulated optimal gaits show changes in muscle expenditure not only for muscles spanning the knee, but also muscles crossing the hip or ankle. This indicates that exoskeleton torques are not simply counteracted or offset, but rather the predictive simulations solve for complex and adaptive lower limb coordination strategies. In the penalize-low condition, muscle metabolic power increased across nearly all muscles during swing, but showed decreases for muscles crossing the ankle during stance (i.e. gluteals, swing: +37%; tibialis anterior, stance: −32%). This is consistent with an adaptation toward higher step frequencies, requiring more work at the hip during swing and relatively less work during a shorter stance phase. In the penalize-high condition, the opposite was the case; muscle metabolic power decreased across many swing muscles, but showed large increases for muscles crossing the ankle during stance (i.e. gluteals, swing: −27%; tibialis anterior, stance: +29%). This is consistent with an adaptation toward lower step frequencies, requiring more work during push off at the ankle to lengthen steps and relatively less work to swing the limb.

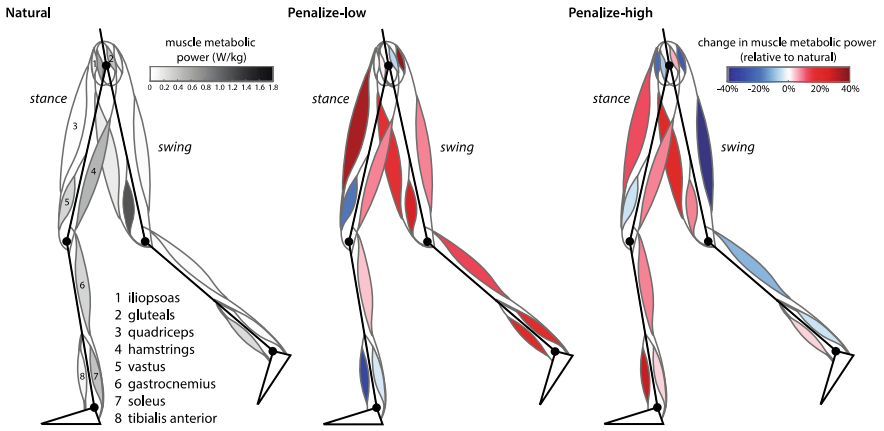

Fig. 2 Average muscle metabolic power, during stance (left, standing leg) and swing phase (right, swinging leg), in W/kg for the natural condition (left graph), and relative to natural for the penalize-low (middle) and penalize-high (right) conditions

4 Discussion

Using predictive gait simulations, we re-created our experimental paradigm where exoskeletons are used to alter preferred and energy optimal gaits. We were able to replicate the exoskeleton torque applied at the knee joint during gait in simulation, produce effort landscapes with optima at high and low step frequencies, and solve for optimal gaits through adaptations in step frequency, using the same tracking data for each optimization. Moreover, we show that the underlying local changes in predicted muscle metabolic power are consistent with adaptive coordination strategies specific to each distinct controller.

This modeling testbed has a number of fundamental and applied uses. For one, it can be used to further investigate aspects of human optimization that are inherently difficult to test experimentally. For example, we can systematically alter the weighting of objectives to predict and potentially understand the effect on gait adaptation. We can also implement physiologically realistic optimization algorithms to understand how people may adapt and learn gaits over time. In a more applied sense, it can be used to explore strategies for improved exoskeleton design and control. While here we used experimental results to validate our predictive simulations, in future we can do the opposite—designing and iterating controllers in advance of human testing to help identify reasonable solution spaces. We can also probe what individual muscles may be driving whole body changes in cost, potentially allowing us to tailor controller design based on user's abilities or disabilities.

Acknowledgements This work is funded by Adidas AG (faculty endowment to A.D.K.) and an NSERC Discovery Grant (RGPIN-2019-05677 to J.C.S.).

References

1. J.C. Selinger, S.M. O'Connor, J.D. Wong, J.M. Donelan, Humans can continuously optimize energetic cost during walking. Curr. Biol. **25**, 2452–2456 (2015)
2. A.D. Koelewijn, A.J. van den Bogert, Joint contact forces can be reduced by improving joint moment symmetry in below-knee amputee gait simulations. Gait Posture **49**, 219–225 (2016)
3. D.A. Winter, *Biomechanics and Motor Control of Human Movement*, 3rd edn. (Wiley, Hoboken, NJ, 2005)

Reconstruction of Hip Moments Through Constrained Shape Primitives

Henri Laloyaux and Renaud Ronsse

Abstract Among the various control laws developed for lower-limb wearable robotics, several intend to replicate leg joint moments observed in healthy humans. While this can be achieved by different means, inspiration can be gained from the so-called motor primitives, i.e. a small set of fundamental signals used by the nervous system to recruit numerous motor pools in a task-specific way. Here we report a methodology for the extraction of constrained-shape primitives. Stimulations of two antagonist hip muscles are initially retrieved from a database composed of different locomotion tasks. A first guess of the primitives parameters is then performed in order to reconstitute these stimulations. Finally these parameters are optimized with the aim of retrieving the original database moments. Our findings suggest that a small number of symmetric Gaussian-like periodic primitives may reconstruct these hip moments with a level of fidelity that would be sufficient for providing a task-specific user support.

1 Introduction

In the recent years several hip exoskeletons have been developed [1–3] with the prospect of assisting different profiles of disabled users, such as post-stroke patients [1], the elderly [3] and lower-limb amputees [4].

While there exist many different control strategies for these devices, few of them take into account the natural impedance of the human body. In order to incorporate a direct model of the body impedance in an assistive strategy, we previously designed and validated a control framework for lower-limb orthoses that models the human musculoskeletal system and uses arbitrary-shaped primitives [5]. Motor primitives

H. Laloyaux (✉)
PhD Student, Institute of Mechanics, Materials, and Civil Engineering (iMMC), Louvain Bionics, Université catholique de Louvain, Louvain-la-Neuve, Belgium
e-mail: henri.laloyaux@uclouvain.be

R. Ronsse
Institute of Mechanics, Materials, and Civil Engineering (iMMC), Institute of NeuroScience (IoNS), Louvain Bionics, Université catholique de Louvain, Louvain-la-Neuve, Belgium

J. C. Moreno et al. (eds.), *Wearable Robotics: Challenges and Trends*,
Biosystems & Biorobotics 27, https://doi.org/10.1007/978-3-030-69547-7_62

are low-dimensional signals that can be combined to reconstruct a large set of muscle stimulations, corresponding to different locomotion tasks.

Here, we extend the methodology presented in [6] by extracting simple constrained-shape primitives focusing on the reconstruction of hip moments, with the objective to test this approach with a wearable device in the near future.

2 Materials and Methods

2.1 Computation of Muscular Stimulations

A database of hip moments and their associated kinematics has been assembled from healthy gait data reported by three papers. This includes some of the most frequent locomotion tasks, namely ground level walking at different cadences [7], walking on slopes with various inclinations [8], and ascending/descending three different types of stairs [9].

These hip moments and kinematics were periodicized and low-pass filtered so as to guarantee their continuity at the end/start of the gait cycle.

Virtual muscular stimulations were then computed from these biomechanical signals by injecting them into an inverse musculoskeletal model. This model is based on the well-known Hill-type muscle model. We followed the same implementation as the one reported in [10], keeping only the hip mono-articular muscles in the sagittal plane, i.e. the lumped hip flexors (HFL) and the glutei (GLU). In the model parameters, the maximal isometric force of these muscles was furthermore increased so that the maximum hip flexion and extension torques while standing up are the same as the ones produced by the original model. The corresponding muscle forces thus generate net hip torques equal to those reported in the literature for every locomotion condition.

2.2 Extraction of the Motor Primitives

The primitives that we consider are periodic Gaussian-like functions with a potential asymmetry. They are combined through weights that follow quadratic evolution laws according to (a) the gait cadence and the slope inclination, or to (b) the stairs inclination, see details in [6]. This framework brings a sharp dimensionality reduction since only 2–3 parameters are needed to characterize each primitive (i.e. peak location, width, and possible level of asymmetry) and 3 or 5 parameters for each weight characterizing the weight modulation for a given locomotion task.

(i) Stimulations-Oriented Primitives

As we previously did in [6], primitives were first extracted by searching the parameters producing the best reconstruction of the virtual muscle stimulations. Since a convex method for extracting constrained-shape primitives from a given signal does not exist to our knowledge, a heuristic optimization was performed with the mean Variance Accounted For (VAF) of the reconstructed stimulations as fitness function.

(ii) Moments-Oriented Primitives

A second optimization was then performed on the retrieved primitive parameters and their associated weight coefficients. The objective here is to maximize the goodness of reconstruction of the hip moments when the primitives are combined and injected as muscular stimulations into the musculoskeletal model in a direct way.

Since the VAF of two signals does not account for their mean values, we used a slightly modified version of this metric as fitness function for the moments reconstruction, i.e. the so-called Mean-Square Accounted For (MSAF) that is defined as:

$$MSAF(y, \hat{y}) \triangleq \left(1 - \Sigma_i (y_i - \hat{y}_i)^2 / \Sigma_i \, y_i^2\right) \cdot 100\,\%.$$

Optimizations were performed by the `fminunc` function of MATLAB (R2016b, The MathWorks Inc., Natick, MA). We did not use a heuristic method for this second optimization stage because a starting point already existed, i.e. the symmetric primitives extracted after step (i).

3 Results and Discussion

We have found that 4 symmetric primitives already accounted for 74.5% of the variance of the extracted stimulations. In [6], we had to use 5 asymmetric primitives to account for 66% of the variance of the stimulations extracted for the 3 main leg joints. This likely comes from the fact that 9 muscles were used in the model of [6] instead of 2 here, and one more task was considered, i.e. running. We thus selected these 4 primitives for the second optimization step.

The averaged MSAF of the reconstructed moments increased from 87.1 to 93.1% by improving these 4 (i) stimulations-oriented primitives into (ii) moments-oriented ones. This increase in MSAF was observed for every locomotion condition, except for 2 conditions of flat ground walking which decreased by less than 5% of the mean-square values of the original moments. Figure 1 shows the worst and best reconstructions of the (ii) moments-oriented primitives, with an MSAF respectively of 72.7 and 99.2%.

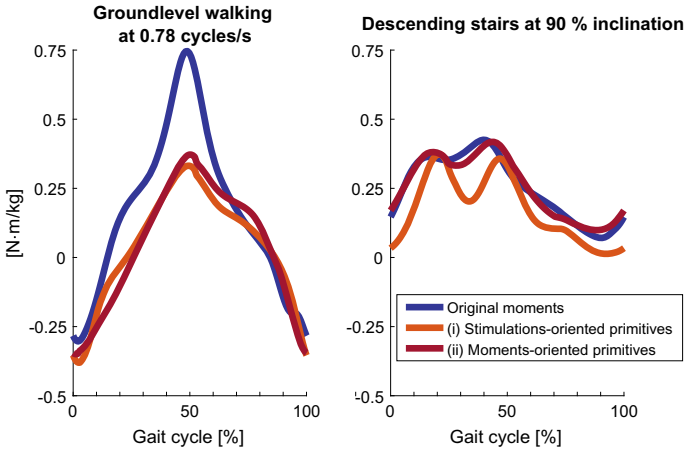

Fig. 1 Original normalized hip flexion moments and their reconstructions with 4 symmetric (i) stimulations-oriented and (ii) moments-oriented primitives for ground level walking at 0.78 cycles/s (references from [7]) and stairs descending at 90% inclination (Ref. [9])

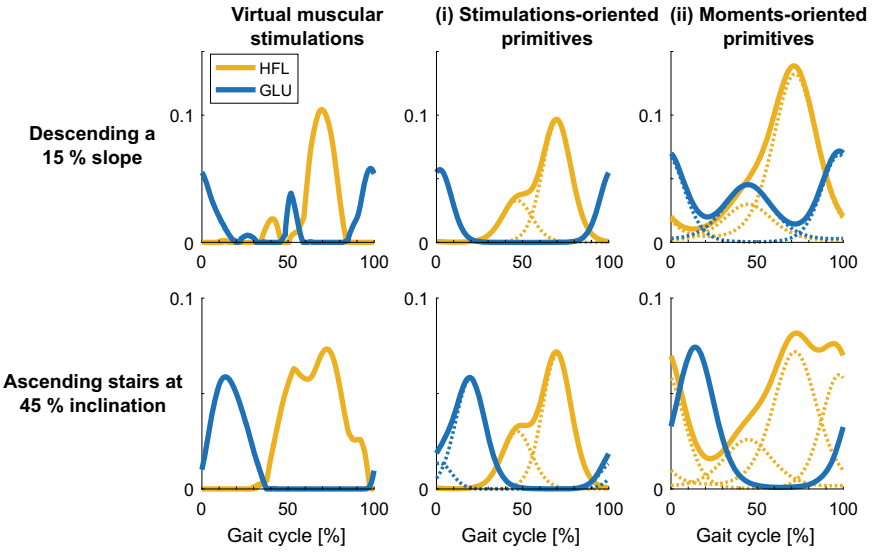

Fig. 2 Left panels: retrieved muscular stimulations for descending a slope with an inclination of 15% [8] and ascending stairs with a 45% inclination [9]. Middle panels: reconstructed stimulations with 4 symmetric stimulations-oriented primitives. Right panels: reconstructed stimulations obtained with the moments-oriented primitives. When relevant, the underlying Gaussian-like primitives are depicted in dotted lines

Noticeably, allowing the primitives to be asymmetric (see [6] for mathematical details) had a marginal effect since the averaged MSAF increased only up to 94%.

Although we followed an approach aiming at minimizing the muscular activation levels when the virtual stimulations were extracted, the second optimization step – i.e. the moments-oriented one – led to mild co-activations of both antagonist muscles in most tasks. Indeed, this was observed for all tasks – as illustrated for two conditions in Fig. 2—, except for ground level walking at a cadence below 0.8 cycles/s, descending a slope with an inclination of 39%, and stairs descending.

4 Conclusion

This paper has reported a method for extracting primitives from hip biomechanics data. These primitives relied on a very limited number of parameters, that were optimized to achieve the best possible reconstruction of the dynamics data.

It has appeared that adding a potential asymmetry in these primitives induced only a marginal improvement in the reconstruction. We have also noticed that our hypothesis that muscular activations tend to be minimized would not always be valid, since slight co-activations of antagonist muscles were observed in most of the considered locomotion tasks.

Future work will study the effectiveness of controlling a wearable hip orthosis with a strategy based on such primitives for providing task-specific locomotion assistance.

Acknowledgements This work was supported by the European Community's H2020 Research and Innovation Programme under grant number 731931 (the CYBERLEGs Plus Plus collaborative project. Computational resources have been provided by the supercomputing facilities of the Université catholique de Louvain (CISM/UCL) and the Consortium des Équipements de Calcul Intensif (CÉCI), funded by the Fonds de la Recherche Scientifique de Belgique (F.R.S.-FNRS) under Grant No. 2.5020.11 and by the Walloon Region.

References

1. C. Buesing et al., Effects of a wearable exoskeleton stride management assist system (SMA®) on spatiotemporal gait characteristics in individuals after stroke: a randomized controlled trial. J. NeuroEng. Rehabil. **12**(1) (2015)
2. F. Giovacchini et al., A light-weight active orthosis for hip movement assistance. Robot. Auton. Syst. **73**, 123–134 (2015)
3. H. Lee et al., A wearable hip assist robot can improve gait function and cardiopulmonary metabolic efficiency in elderly adults. IEEE Trans. Neural Syst. Rehab. Eng. **25**(9), 1549–1557 (2017)
4. M.K. Ishmael, M. Tran, T. Lenzi, ExoProsthetics: assisting above-knee amputees with a lightweight powered hip exoskeleton, in *2019 IEEE 16th International Conference Rehabilation Robotics*, pp. 925–930 (2019)
5. V. Ruiz Garate et al., Experimental validation of motor primitive-based control for leg exoskeletons during continuous multi-locomotion task. Front. Neurorobot. **11** (2017)

6. H. Laloyaux, R. Ronsse, Extraction of simple monophasic motor primitives towards bio-inspired locomotion assistance, in *2019 IEEE International Conference on Cyborg and Bionic Systems*, pp. 253–260 (2019)
7. B. Koopman, W. van Dijk, Basic Gait Kinematics: Reference Data of Normal Subjects (Univ. of Twente, Experimental data, 2010)
8. A.N. Lay, C.J. Hass, R.J. Gregor, The effects of sloped surfaces on locomotion: a kinematic and kinetic analysis. J. Biomech. **39**(9), 1621–1628 (2006)
9. R. Riener, M. Rabuffetti, C. Frigo, Stair ascent and descent at different inclinations. Gait Posture **15**(1), 32–44 (2002)
10. S. Song, H. Geyer, A neural circuitry that emphasizes spinal feedback generates diverse behaviours of human locomotion. J. Physiol. **593**(16), 3493–3511 (2015)

Simulated Exoskeletons with Coupled Degrees-of-Freedom Reduce the Metabolic Cost of Walking

Nicholas A. Bianco, Patrick W. Franks, Jennifer L. Hicks, and Scott L. Delp

Abstract Exoskeletons that assist multiple joints could reduce the metabolic cost of walking beyond reductions achieved with single-joint devices. However, assisting many degrees-of-freedom can require multiple actuators with complicated controllers and long experiment times to tune these controllers. Coupled assistance, where the same control signal is applied to multiple joints, may help simplify exoskeleton design but has not been tested extensively. In this study, we used direct collocation optimal control and a lower-limb musculoskeletal model to simulate five different exoskeleton control strategies to assist multiple joints during walking. We simulated strategies where the torque provided at each joint was controlled independently or coupled between joints. We found that coupled assistance was able to provide similar savings in whole-body metabolic power consumption compared to independent assistance. Our results may help device designers create exoskeletons that achieve good metabolic savings while requiring fewer actuators and less experimental testing to create effective assistance strategies.

N. A. Bianco (✉) · P. W. Franks
Department of Mechanical Engineering, Stanford University,
Building 530, 440 Escondido Mall, Stanford, CA 94305, USA
e-mail: nbianco@stanford.edu

P. W. Franks
e-mail: pfranks@stanford.edu

J. L. Hicks
Department of Bioengineering, Stanford University, 443 Via Ortega, Stanford, CA 94305, USA
e-mail: jenhicks@stanford.edu

S. L. Delp
Department of Mechanical Engineering, Department of Bioengineering, and Department of Orthopaedic Surgery, Stanford University, Building 530, 440 Escondido Mall, Stanford, CA 94305, USA
e-mail: delp@stanford.edu

J. C. Moreno et al. (eds.), *Wearable Robotics: Challenges and Trends*,
Biosystems & Biorobotics 27, https://doi.org/10.1007/978-3-030-69547-7_63

1 Introduction

Wearable robotic exoskeletons have the potential to improve human mobility. One common goal of exoskeleton devices is to reduce the metabolic cost of walking [1]. Many recent exoskeleton designs have successfully reduced metabolic cost, but most focus assistance at one lower-limb degree-of-freedom [1]. Exoskeleton devices that assist multiple joints at once, or "multi-joint" exoskeletons, have potential for improved metabolic savings compared to single degree-of-freedom devices [2]. However, the large number of assistance strategies possible with multi-joint exoskeletons can make controller design challenging, often leading to long experiment times. Assistance applied to multiple joints based on the same controller, or "coupled" assistance, could be a potential approach to simplify multi-joint exoskeleton designs. Recent experiments have achieved metabolic reductions by assisting multiple joints at once using a single actuator, demonstrating that coupled assistance strategies are feasible [3, 4]. However, it is unclear if exoskeleton designers should use coupled assistance as a design approach or if coupling would reduce the efficacy of assistance compared to controlling joints independently.

Musculoskeletal simulation has emerged as a promising approach for optimizing exoskeleton designs for a variety of motion tasks [5]. Simulations could test a wide range of multi-joint exoskeleton designs that would be prohibitively time consuming to evaluate with experiments; however, no study has used simulation to analyze multi-joint assistance for walking or to evaluate the efficacy of coupled control strategies. In this study, we evaluated ideal, massless multi-joint assistive devices added to lower-limb simulations of walking. Devices assisted joints using independent controls and using controls that were coupled across joints. Our aim was to determine if multi-joint devices with coupled assistance could achieve similar metabolic savings compared to devices with independent assistance.

2 Methods

We used direct collocation optimal control and a musculoskeletal model to optimize assistance for five different simulated multi-joint exoskeleton devices. Our musculoskeletal model had one leg with three sagittal plane degrees-of-freedom (hip flexion-extension, knee flexion-extension, and ankle plantarflexion-dorsiflexion) and 9 lower-limb muscles based on a previous study that could produce the major functions of normal gait [6]. We used 3 previously collected gait cycles of motion capture data from 5 healthy adult subjects during treadmill walking at 1.25 m/s [7]. The generic model was scaled to match subjects' static marker trials; joint and muscle kinematic and kinetic information was computed using OpenSim [8].

We used an existing direct collocation optimal control framework [9] to simulate walking. In each problem, muscle activation and tendon compliance dynamics were enforced and muscle-generated moments were constrained to match net joint moments computed from inverse dynamics. We minimized metabolic cost computed from a model with a continuous first derivative designed for gradient-based optimization [10]. Muscle metabolic cost was computed by summing metabolic rates across muscles, integrating over the gait cycle, and dividing by the gait cycle duration. Total metabolic cost was estimated by multiplying the muscles' metabolic cost by two (assuming mediolateral symmetry) and adding a constant basal rate of 1.2 W/kg.

In the assisted simulations, massless torque actuators with no power limits were added to the model to help enforce the net joint moment constraints while reducing muscle effort. We simulated five different multi-joint exoskeleton devices that provided assistance at the following five joint motion combinations: (1) hip extension and knee extension; (2) hip flexion and knee flexion; (3) knee flexion and ankle plantarflexion; (4) hip flexion and ankle plantarflexion; and (5) hip flexion, knee flexion, and ankle plantarflexion. The maximum possible torque assistance was 1.0 N m/kg for the hip and knee, and 2.0 N m/kg for the ankle. We simulated two different control strategies for each device: independent and coupled assistance. Independent assistance used separate torques for each joint motion. Coupled assistance used a single control signal and individual scale factors at each joint to determine device torques. Percent changes in metabolic cost between unassisted and assisted simulations were computed for all coupled and independent assistance conditions.

3 Results

All simulated multi-joint assistive devices reduced metabolic cost compared to unassisted walking (Fig. 1). The largest metabolic reduction, 39.4% relative to unassisted walking, was observed in the hip flexion, knee flexion, ankle plantarflexion device with independent assistance (Fig. 1, rightmost blue bar). However, coupled assistance with this device provided a 34.2% metabolic reduction (Fig. 1, rightmost orange bar), which was close to the 39.4% savings observed with independent assistance. Coupled assistance performed similarly well compared to independent assistance in the four remaining devices: hip extension, knee extension (coupled: 11.9%, independent: 13.6%); hip flexion, knee flexion (coupled: 25.3%, independent: 29.5%); knee flexion, ankle plantarflexion (coupled: 29.7%, independent: 31.7%); hip flexion, ankle plantarflexion (coupled: 29.2%, independent: 33.6%).

4 Discussion

We found that coupled assistance in simulated multi-joint exoskeletons produced metabolic savings similar to independent assistance. Our results suggest that exoskeleton designers should consider coupling torque actuators when building multi-joint

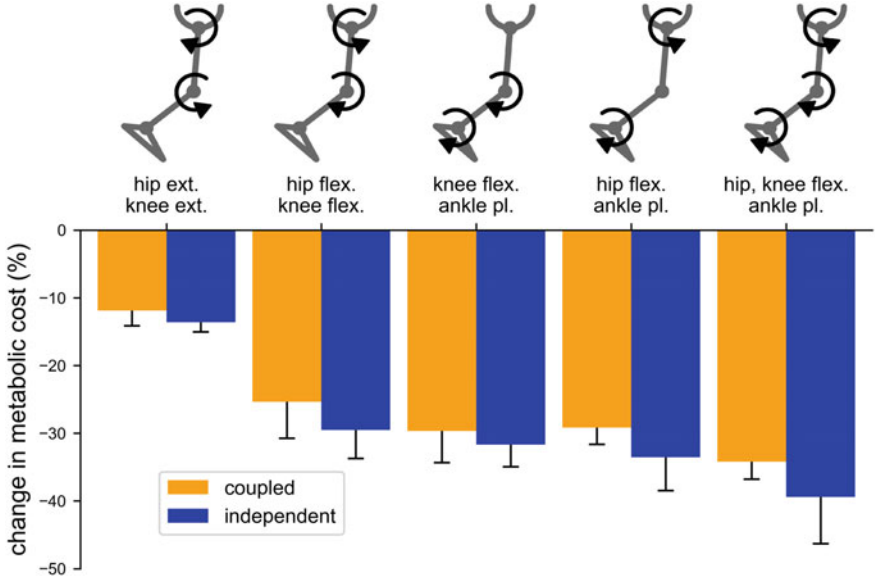

Fig. 1 Metabolic savings for multi-joint assistance strategies. Percent changes in metabolic cost relative to unassisted walking for coupled (orange) and independent (blue) multi-joint assistance strategies. Each bar represents the mean (solid bars) and one standard deviation (whiskers) across subjects

exoskeletons. In addition, the largest metabolic reduction with coupled assisted occurred when assisting hip flexion, knee flexion, and ankle plantarflexion simultaneously, suggesting that assisting more than two joints with one actuator can be beneficial.

We focused on comparing the relative efficacy of coupled and independent devices in reducing metabolic cost, since we have greater confidence in relative metabolic cost changes between simulation conditions than in absolute percent reductions [2]. To better estimate absolute percent metabolic changes, future work could model frontal plane muscles (e.g., hip adductors-abductors) to improve absolute metabolic cost predictions. In addition, future simulations could allow changes in walking kinematics due to assistance, which could impact predicted metabolic reductions.

5 Conclusion

Our simulation results showed that coupled assistance did not incur a large metabolic penalty in multi-joint exoskeletons. Exoskeleton designers should consider coupled assistance to simplify wearable devices, increase metabolic reductions when actuation is limited, and help keep experiment times tractable.

Acknowledgements N.A.B. received funding from the National Science Foundation Graduate Research Fellowship Program and the Stanford Graduate Fellowship Program. P.W.F. received funding from the U.S. Army Natick Soldier Research, Development and Engineering Center (W911QY18C0140). J.L.H. and S.L.D. received funding from the National Institutes of Health (P2C HD065690).

References

1. A.J. Young, D.P. Ferris, State of the art and future directions for lower limb robotic exoskeletons. IEEE Trans. Neural. Syst. Rehabil. Eng. **25**, 171–182 (2017)
2. P.W. Franks, N.A. Bianco, G.M. Bryan, J.L. Hicks, S.L. Delp, S.H. Collins,Testing simulated assistance strategies on a hip-knee-ankle exoskeleton: a case study, in *Proceedings IEEE International Conference on Biomedical Robotics Biomechatronics* (2020)
3. B.T. Quinlivan , L. Sangjun, P. Malcolm, D.M. Rossi, M. Grimmer, C. Siviy, et al., Assistance magnitude versus metabolic cost reductions for a tethered multiarticular soft exosuit. Sci. Robot. **2**, eaah4416 (2017)
4. P. Malcolm, S. Galle, W. Derave, D. de Clercq, Bi-articular knee-ankle-foot exoskeleton produces higher metabolic cost reduction than weight-matched mono-articular exoskeleton. Front. Neurosci. **12**(69) (2018)
5. E.P. Grabke, K. Masani, J. Andrysek, Lower limb assistive device design optimization using musculoskeletal modeling: a review. J. Med. Devices **13**(4) (2019). https://doi.org/10.1115/1.4044739
6. C.F. Ong, T. Geijtenbeek, J.L. Hicks, S.L. Delp, Predicting gait adaptations due to ankle plantarflexor muscle weakness and contracture using physics-based musculoskeletal simulations. PLOS Comp. Bio. **15**(10), e1006993 (2019)
7. E.M. Arnold, S.R. Hamner, A. Seth, M. Millard, S. Delp, How muscle fiber lengths and velocities affect muscle force generation as humans walk and run at different speeds. J. Exp. Biol. **216**(11), 2150–2160 (2013)
8. A. Seth, J.L. Hicks, T.K. Uchida, A. Habib, C.L. Dembia, et al., OpenSim: simulating musculoskeletal dynamics and neuromuscular control to study human and animal movement. PLOS Comp. Bio. **14**(7), e1006223 (2018)
9. F. De Groote, A.L. Kinney, A.V. Rao, B.J. Fregly, Evaluation of direct collocation optimal control problem formulations for solving the muscle redundancy problem. Ann. Biomech. Eng. (2016). https://doi.org/10.1007/s10439-016-1591-9
10. A.D. Koelewijn, E. Dorschky, A.J. van den Bogert, A metabolic energy expenditure model with a continuous first derivative and its application to predictive simulations of gait. Comput. Methods Biomech. Biomed. Eng. **21**, 521–531 (2018)

Model-Based Biomechanics for Conceptual Exoskeleton Support Estimation Applied for a Lifting Task

Elena Gneiting, Jonas Schiebl, Mark Tröster, Verena Kopp, Christophe Maufroy, and Urs Schneider

Abstract The aim of this study was to analyse biomechanics in lifting tasks and evaluate an exoskeleton concept using musculoskeletal model-based analysis. Three male participants lifted a box of 21 kg from waist level to 1.46 m height. Movement was recorded with motion capture and simulated with individual musculoskeletal models. The effect of an exoskeleton concept supporting the upper arm and/or forearm with external torque around the shoulder was examined for one subject. Muscle activity was reduced for arm flexors and shoulder muscles. Glenohumeral and elbow joint forces were also decreased by the support concept.

1 Introduction

DESPITE the ongoing automatization in the industry, musculoskeletal disorders (MSD) are ranked the most common occupational diseases (38.1 %) in the EU due to exposure to high physical stress of many workers [1].

Exoskeletons have the potential to reduce the risk of work-related MSDs by reducing physical stress at exposure limits. However, they may also increase the

E. Gneiting · J. Schiebl (✉) · M. Tröster · V. Kopp · C. Maufroy · U. Schneider
Department of Biomechatronic Systems of the Fraunhofer Institute for Manufacturing Engineering and Automation IPA, Stuttgart, Germany
e-mail: jonas.schiebl@ipa.fraunhofer.de

E. Gneiting
e-mail: elena.gneiting@ipa.fraunhofer.de

M. Tröster
e-mail: mark.troester@ipa.fraunhofer.de

V. Kopp
e-mail: verena.kopp@ipa.fraunhofer.de

C. Maufroy
e-mail: christophe.maufroy@ipa.fraunhofer.de

U. Schneider
e-mail: urs.schneider@ipa.fraunhofer.de

J. C. Moreno et al. (eds.), *Wearable Robotics: Challenges and Trends*,
Biosystems & Biorobotics 27, https://doi.org/10.1007/978-3-030-69547-7_64

load on other body parts. Therefore, a biomechanical understanding of the motion assisted by an exoskeleton and the effects of an exoskeleton on the musculoskeletal system are highly important. Thus, biomechanical model-based analysis was used in this study to investigate biomechanics in a lifting task and examine the effects of an external supporting torque around the shoulder, which is commonly found in exoskeleton support concepts.

2 Material and Methods

A. Experimental setup

Three male subjects (mean ± SD: age: 35 ± 7 years, height: 1.81 ± 0.09 m, weight: 74 ± 5 kg) participated in the experiments. For kinematic measurements, the subjects performed a symmetric lifting task by raising a 21 kg heavy box from waist level to a shelf at 1.46 m height.

Motion analysis was performed using an optical marker-based motion capture system (Qualisys AB, Gothenburg, Sweden) with a marker setup of 43 markers on the subject and 6 additional markers on the box. Data was recorded by 15 cameras (Oqus 400 and 700+, Qualisys AB, Gothenburg, Sweden) sampling at 100 Hz and Qualisys Track Manager (QTM, version 2019.2, Qualisys AB, Gothenburg, Sweden).

B. Model-based analysis

For each subject, a subject-specific musculoskeletal model was set up in the AnyBody Modeling System (AMS, v. 7.2, AnyBody Technology A/S, Aalborg, Denmark) using the AnyBody Managed Model Repository (AMMR) version 2.2. A modified shoulder model including three element Hill type muscles and allowing for translation of the glenohumeral (GH) joint, amongst others, was used in accordance with [2]. Ground reaction forces (GRF) were calculated using the GRF prediction included in the AMMR. The box was designed in SolidWorks (v. 2018, Dassault Systèmes, Vélizy-Villacoublay, France) and inserted into AMS using the AnyExp4SOLIDWORKS plugin.

For one subject (age: 45 years, height: 1.74 m, weight: 70.4 kg), three versions of an exoskeleton support concept were simulated and compared as a basis for further developments. The concept included an optimized external torque (AnyReacForce) acting around the transverse axis through the GH joint, inflicting forces on nodes either on the upper arm (UA), on the forearm (FA) or on both (UA + FA) simultaneously (Fig. 1). For simplification, the torques were grounded on the virtual environment.

C. Data analysis

The output data obtained from the simulations was further analysed with Matlab (version R2019b, The MathWorks Inc., Natick, USA). Data is presented over the

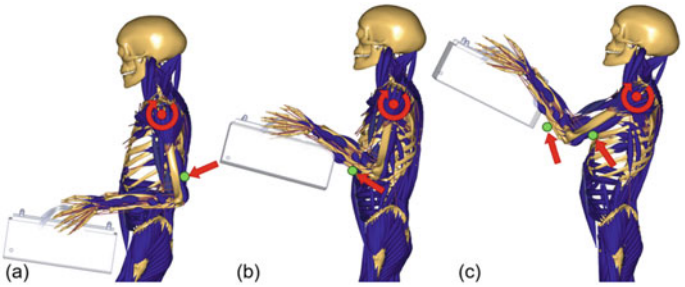

Fig. 1 Exoskeleton support concept. Torque (red) acting on nodes (green) on the **a** upper arm, **b** forearm and **c** upper arm and forearm. **a–c** Motion is depicted at 0, 50 and 100 % of lifting cycle.

lifting cycle, starting at holding the box at waist level (0 %) and ending 0.04 s before the box touches the shelf (100 %).

To evaluate the lifting task, the muscle activity (MA) envelopes integrated over time (%s) of several body regions were computed. Those areas include the arm flexors (biceps, brachialis), the shoulders (deltoideus, supraspinatus, infraspinatus, teres major and minor, subscapularis, coracobrachialis), the abdomen (transversus, rectus abdominis, obliquus internus and externus), the spine (multifidi, erector spinae, quadratus lumborum, semispinalis, spinalis) and all muscles of the lower extremities. Additionally, the maximum resulting joint force (JF) in the GH, elbow, hip and knee joint was examined. The JF was calculated as mean of both right and left side of the body. For the L4L5 joint, the maximum compression force was obtained instead. Data is presented as mean ± standard deviation (SD) of the three subjects.

In order to examine the support concept, only the MA of the arm flexors and shoulder muscles and the JF of the GH and elbow joint were analysed as described above. The plain simulation of the lifting task served as reference (Ref, see Table 2). Exerted torques on the right and left arm were averaged.

3 Results

A. Lifting task

The lifting task showed high resulting MAs in the upper body for the subject-specific models, especially in the arm flexors (86.2 ± 8 %s) and shoulder muscles (56.2 ± 16 %s), as can be seen in Table 1. Muscles in the abdomen (35.7 ± 3 %s) and spine (35.5 ± 3 %s) indicated activities lower than 50 %s. The area with the lowest MA was the lower extremities (22.1 ± 2 %s). The highest resulting JF was detected in the knee (3521.2 ± 1195 N), followed by the GH (3288.7 ± 1313 N) and hip joint (3288.4 ± 818 N). The maximum compression force in the L4L5 joint resulted in 3155.1 ± 671 N. The elbow joint showed the smallest peak force of 1084.7 ± 331 N.

Table 1 Lifting test

Integral of muscle activity (%s)		Maximum joint force (N)	
Arm flexors	86.2 ± 8	GH	3288.7 ± 1313
Shoulder	56.2 ± 16	Elbow	1084.7 ± 331
Abdomen	35.7 ± 3	L4L5	3155.1 ± 671
Spine	35.5 ± 3	Hip	3288.4 ± 818
Lower extremities	22.1 ± 2	Knee	3521.2 ± 1195

Table 2 Exoskeleton support concept

Variable	Unit	Ref	Exoskeleton support concept		
			UA	FA	UA + FA
Integral of MA arm flexors	(%s)	83.5	80.3	60.8	52.0
Integral of MA shoulder	(%s)	57.7	18.7	31.8	17.2
Max. JF GH	(N)	1981.5	794.9	1381.3	721.0
Max. JF elbow	(N)	1053.0	1043.9	625.2	643.4

B. Exoskeleton support concept

Table 2 depicts the outcomes of the exoskeleton support concept compared to the reference simulation of the lifting task. All three variations of the concept resulted in a decrease in MA and JF. MAs of the arm flexors were reduced from 83.5 %s (Ref) to 80.3 %s by supporting only the UA, to 60.8 %s by supporting the FA and to 52 %s by supporting both. Compared to reference (57.7 %s), UA support (18.7 %s) decreased the MA of shoulder muscles more than FA support (31.8 %s). However, supporting both UA and FA resulted in a decrease of 17.2 %s.

The JF in the GH joint was reduced from 1981.5 N to more than half 794.9 N with the UA support and 721 N supporting UA and FA, but only to 1381.3 N supporting the FA. On the other hand, the elbow JF decreased from 1053 N to 625.2 N with FA support and 643.4 N with UA and FA support, but only to 1043.9 N when supporting the UA.

During lifting, the exerted shoulder torques show a roughly constant support of 25 Nm for the UA and a decreasing support (30–5 Nm) for the FA. When both are supported, the torque on the FA decreases (30–10 Nm), whereas the torque on the UA increases (−10 to 30 Nm).

4 Discussion

The main objective of this study was to investigate a lifting task and examine the effect of a common exoskeleton concept for supporting the upper extremity. Since available exoskeleton designs often use a torque around the shoulder, this concept was selected to test its suitability for lifting.

The analysis of the lifting task showed that especially the upper extremities need assistance due to a high MA of arm flexors and shoulder muscles of over 50 %s. Also, during the lifting task, the GH joint force reached twice the magnitude of in vivo measurements detected during forward flexion over 90° holding 2 kg weight [3].

The exoskeleton support concept showed reduced musculoskeletal outcomes in all three conditions. Supporting the upper arm mainly assists the shoulder, whereas supporting the forearm assists the arm flexors and elbow. A combination of both would result in the best outcome, assuming it is technically feasible. However, in the preliminary analysis directions of resulting forces and their possible effects on tissue deformation and comfort (e.g. inflicted by shear forces) were not yet considered.

Another limitation of simulating the support concept is that it only affected the upper limb, since the torque around the shoulder was not redirected back onto the musculoskeletal system. Hence, no conclusions can be drawn upon how the concept affects the rest of the body.

5 Conclusion and Future Work

An exoskeleton concept that induces a torque around the shoulder seems biomechanically efficient in supporting the upper extremities during lifting. In a next step, fully constructed exoskeleton designs will be simulated to evaluate the impact on the entire body. Also, biomechanical side effects as well as interaction force directions causing potential tissue deformations should be considered.

Acknowledgements This work was supported by the Exolog Project funded by the German Armed Forces (Bundeswehr) under Grant No E/U2Ci/KA225/JF080.

References

1. E. Schneider, S. Copsey, X. Irastorza, Osh in figures: Work-related musculoskeletal disorders in the EU—facts and figures. Office for Official Publications of the European Communities (2010)
2. M. Aurbach, J. Spicka, F. Süß, S. Dendorfer, Evaluation of musculoskeletal modelling parameters of the shoulder complex during humeral abduction above 90°. J. Biomech. 109817 (2020)
3. G. Bergmann et al., In vivo gleno-humeral joint loads during forward flexion and abduction. J. Biomech. **44**(8), 1543–1552 (2011)

Calibrating an EMG-Driven Muscle Model and a Regression Model to Estimate Moments Generated Actively by Back Muscles for Controlling an Actuated Exoskeleton with Limited Data

Ali Tabasi, Maria Lazzaroni, Niels P. Brouwer, Idsart Kingma, Wietse van Dijk, Michiel P. de Looze, Stefano Toxiri, Jesús Ortiz, and Jaap H. van Dieën

Abstract Estimation of low-back load can be used to determine the assistance to be provided by an actuated back-support exoskeleton. To this end, an EMG-driven muscle model and a regression model can be implemented. The goal of the regression model is to reduce the number of required sensors for load estimation. Both models need to be calibrated. This study aims to find the impacts of limiting calibration data on low-back loading estimation through these models.

1 Introduction

Using a back-support exoskeleton helps to reduce the low-back load during manual load handling, which may decrease the risk of low back pain. In actuated exoskeletons, the assistive moments are generated by active components, e.g., motors. These active components are operated by a control system that utilizes a reference signal to regulate the assistive moment [1]. A logical solution to reduce the low-back loading is to derive the reference signal from a real-time estimation of low-back load measures, such as moments around the L5/S1 joint.

A. Tabasi (✉) · N. P. Brouwer · I. Kingma · J. H. van Dieën
Department of Human Movement Sciences, Vrije Universiteit Amsterdam, Amsterdam, The Netherlands
e-mail: ali.tabasi@vu.nl

M. Lazzaroni · S. Toxiri · J. Ortiz
Department of Advanced Robotics, Istituto Italiano di Tecnologia, Genova, Italy

M. Lazzaroni
Department of Electronics, Information and Bioengineering, Politecnico di Milano, Milan, Italy

W. van Dijk · M. P. de Looze
TNO, Leiden, The Netherlands

J. C. Moreno et al. (eds.), *Wearable Robotics: Challenges and Trends*,
Biosystems & Biorobotics 27, https://doi.org/10.1007/978-3-030-69547-7_65

Using body kinematics and external forces/moments, the net moment around the L5/S1 joint (M_{Net}^{ID}) can be estimated through inverse dynamics (ID) [2]. The superscript here and below denotes the primary model used to determine the variable. M_{Net}^{ID} is counterbalanced by a combination of the moment generated by the human (M_{Human}) and any assistive device. M_{Human} consists of the moments generated by trunk muscles active forces (M_{Active}) and moments produced by trunk tissue passive forces ($M_{Passive}$). $M_{Passive}$ is coupled to lumbar flexion and cannot be compensated by any assistive moment by the exoskeleton. Moreover, it reaches substantial magnitudes at extreme flexion angles [3]. Thus, ignoring it leads to overestimating the required assistive moment. To avoid this overestimation, the reference signal should be determined based on M_{Active}.

M_{Active} and $M_{Passive}$ can be estimated separately through an EMG-driven muscle model (EMGMod) using 12 EMG channels from trunk muscles and the lumbar flexion angle [4, 5]. In order to circumvent the need for many sensors on the human body, a regression model (RegMod) can be fitted between signals recorded by two of the EMG sensors and built-in exoskeleton kinematic sensors as the input variables and M_{Active} as the output variable [6]. The advantage of RegMod over EMGMod is that RegMod requires fewer EMG sensors attached to the body to estimate M_{Active} for exoskeleton control. With fewer sensors, real-time M_{Active} estimation in the workplace becomes more feasible.

EMGMod and RegMod need to be calibrated for each individual through several lifting trials. The number and type of calibration trials might affect the practical feasibility of using the models for exoskeleton control. Therefore, limiting calibration trials might be beneficial. This study aims to determine the impacts of using limited data for calibration on the estimation accuracy of EMGMod and RegMod.

2 Material and Methods

Ten healthy male participants lifted and lowered 7.5 and 15 kg boxes from ankle height to upright posture without and with wearing an active back-support exoskeleton [7]. Lifting trials were performed with three different techniques and at three speeds. Ground reaction forces and moments, and body kinematics were recorded. In addition, back and abdominal muscle EMG activities were recorded, filtered and normalized to MVC.

Post-processing steps are as follows. First, M_{Net}^{ID} was calculated using a bottom-up ID model. Then, for trials with an exoskeleton, M_{Human}^{ID} was determined by subtracting the assistive moment generated by the exoskeleton from M_{Net}^{ID}. In trials without an exoskeleton, M_{Human}^{ID} equals M_{Net}^{ID}. Next, a combination of a limited number of trials without exoskeleton was selected and used as calibration trials to calibrate EMGMod, i.e., optimize parameters reflecting mechanical properties of trunk muscles and tissues for each participant. Employing calibrated EMGMod, M_{Active}^{EMGMod} was estimated, combined with corresponding EMG and kinematic signals, and used to calibrate RegMod.

Data of trials with exoskeleton were used to evaluate the calibration quality. First, M_{Active}^{EMGMod} and $M_{Passive}^{EMGMod}$ were calculated and summed to create M_{Human}^{EMGMod}. Then, root mean square error (RMSE) between M_{Human}^{EMGMod} and M_{Human}^{ID} was calculated to assess the calibration quality of EMGMod. Subsequently, M_{Active}^{RegMod} was calculated, summed up with $M_{Passive}^{EMGMod}$ to create M_{Human}^{RegMod}. Then, RMSE between M_{Human}^{RegMod} and M_{Human}^{ID} was calculated as a measure of RegMod calibration quality.

This procedure was repeated for different sets of calibration trials. Three sets were selected and the corresponding RMSE of EMGMod and RegMod were compared. The first set (QUASI) was a combination of trials that were performed with free lifting technique at a very slow speed. During these trials, dynamically-induced loads are limited; therefore, calibration can be conducted with a limited motion capture system. The second set (BESTOF6) was a combination that resulted in the lowest RMSEs in both models among all tested combinations of six trials. The third set (FULL) consisted of all 14 calibration trials available.

A series of paired T-tests were conducted on RMSEs to determine the impact of calibration sets on calibration quality. A significance level of $p = 0.05$ was used.

3 Results

RMSEs depended on the number and type of calibration trials. Figure 1 shows the RMSEs of EMGMod and RegMod for selected calibration sets.

Regarding EMGMod, the lowest RMSE was obtained by implementing the FULL set (RMSE = 20.29). RMSEs of QUASI (RMSE = 22.83, $p = 0.02$) and BESTOF6 (RMSE = 20.83, $p = 0.03$) sets were significantly larger. The difference between RMSE of QUASI and BESTOF6 was not statistically significant ($p = 0.05$).

For RegMod, the RMSE of QUASI (RMSE = 32.53) set was significantly larger than that of BESTOF6 (RMSE = 26.51, $p = 0.03$) and FULL (RMSE = 25.04, $p < 0.01$) sets. The difference between RMSE of BESTOF6 and FULL was not statistically significant ($p = 0.07$).

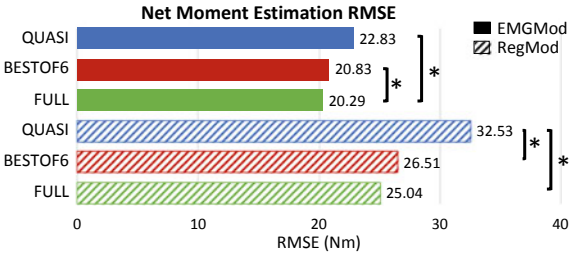

Fig. 1 Net moment estimation RMSE. QUASI, BESTOF6 and FULL represent the calibration sets that were used to calibrate the models. RMSEs of EMGMod depicted in full bars and RMSEs of RegMod depicted in hatched bars

4 Discussion

The resultant RMSEs show that EMGMod calibration was enhanced by implementing the FULL set. However, RMSEs of BESTOF6 and QUASI sets were only slightly higher. This suggests that EMGMod can be calibrated relatively accurately with just a few quasi-static calibration trials.

Resultant RMSEs of RegMod showed that the QUASI set resulted in considerably larger RMSE compared to BESTOF6 and FULL set. This can be a consequence of neglecting the effects of dynamically-induced loads when calibrating using the QUASI set. On the other hand, the lack of difference between RMSEs of BESTOF6 and FULL sets suggests that limited calibration of RegMod can result in similar calibration quality as a fully calibrated model.

It should be considered that some of the examined calibration sets result in considerably higher RMSEs than the BESTOF6 set, while the number of included trials was the same. This shows that not only the number of calibration trials is important, but also the selected lifting conditions is a factor to consider. The BESTOF6 set included trials with two choices for each lifting task characteristic, i.e., both weights lifted, two of the three speeds and two of the three lifting techniques.

Another issue that should be noted is that the RMSE of RegMod was always higher than that of EMGMod. One reason can be that RegMod was calibrated using an outcome of EMGMod, i.e., M_{Active}^{EMGMod}. Thus, estimation errors of EMGMod have adverse effects on the performance of RegMod. Another reason might be that RegMod employs a limited number of variables. This means that some relevant information might be neglected. Hence, additional minor errors in estimation are expected.

One limitation of this study is that both models were calibrated and examined over limited manual lifting conditions. However, in the workplace, manual liftings in other conditions and other tasks such as pulling and pushing are being done, which can be assisted with an exoskeleton. Thus, the estimation quality of the proposed models should be evaluated for other work-related tasks and conditions.

5 Conclusion

The current study shows that an EMG-driven muscle model can be calibrated relatively accurately with a few number of lifting trials. In contrast, a regression model requires more but still a limited number of trials for proper calibration. The present study showed that an appropriate set of calibration trials for a regression model should contain lifts with different loads, speeds and lifting techniques.

Acknowledgements This research was funded by the i-Botics Early Research Program of TNO (the Netherlands Organization for Applied Scientific Research). Additionally, this work was supported by the Dutch Research Council (NWO), program ‘perspectief’ (project P16-05).

References

1. M.P. De Looze, T. Bosch, F. Krause, K.S. Stadler, W.O. Sullivan, Exoskeletons for industrial application and their potential effects on physical work load. Ergonomics **0139**, 1–1 (2016)
2. I. Kingma, M.P. De Looze, H.M. Toussaint, H.G. Klijnsma, T.B.M. Bruijnen, Validation of a full body 3-D dynamic linked segment model. Hum. Mov. Sci. **15**(6), 833–860 (1996)
3. H.M. Toussaint, A.F. de Winter, Y. de Haas, M.P. de Looze, J.H. Van Dieën, I. Kingma, Flexion relaxation during lifting: Implications for torque production by muscle activity and tissue strain at the lumbo-sacral joint. J. Biomech. **28**(2), 199–210 (1995)
4. J.H. Van Dieën, Are recruitment patterns of the trunk musculature compatible with a synergy based on the maximization of endurance? J. Biomech. **30**(11–12), 1095–1100 (1997)
5. J.H. van Dieen, I. Kingma, Effects of antagonistic co-contraction on differences between electromyography based and optimization based estimates of spinal forces. Ergonomics **48**(4), 411–426 (2005)
6. A. Tabasi, I. Kingma, M. P. de Looze, W. van Dijk, A. S. Koopman, J.H. van Dieën, Selecting the appropriate input variables in a regression approach to estimate actively generated muscle moments around L5/S1 for exoskeleton control. J. Biomech. **102** (2020)
7. M. Lazzaroni, et al., Evaluation of an acceleration-based assistive strategy to control a back-support exoskeleton for manual material handling. Wearable Technol. (submitted for publication)

Effect of Mono- Versus Bi-Articular Ankle Foot Orthosis on Muscular Performance of the Lower Leg

Mahdy Eslamy, Florian Mackes, and Arndt F. Schilling

Abstract Ankle foot orthoses (AFOs) are used to assist impaired gait. In this study, we investigated the effects of a mono- and a bi-articular AFO with different stiffness on the muscles' performance in the lower extremities. The effects of both AFOs on the activation level and power of gastrocnemius, soleus and tibialis anterior muscles together with knee extensors and flexors were simulated in Opensim. The muscular performances were compared between the case without orthosis and the case with mono- and bi-articular AFO with different stiffness values (5, 10, 15, 20 and 25 kN/m). The simulations showed that increasing the stiffness of both AFOs led to reductions (up to 70%) of the activation levels of soleus and gastrocnemius in comparison to the case without orthosis. The overall stronger effects caused by the bi-articular configuration led us to investigate its effects on the knee extensors and flexors. Indeed, bi-articular AFO led to strong activation of the knee extensor muscles, suggesting a power interaction between upper and lower leg. Therefore, an intelligent design of mono- and bi-articular AFO with soft springs (<10 kN/m) may potentially allow to balance muscle activation and power consumption of the respective muscles of the leg. Experiments with customized patient-specific AFOs and with different human subjects walking at different speeds will be required to validate these conclusions.

1 Introduction

The collaboration of the ankle plantar flexors (soleus and gastrocnemius together with the Achilles tendon) has a key role in human propulsion during push-off phase through providing about half of the required muscle work [1]. Adaptation of the

M. Eslamy (✉) · F. Mackes · A. F. Schilling
Applied Rehabilitation Technology ART Lab, Department for Trauma Surgery, Orthopaedics and Plastic Surgery, Universitätsmedizin Göttingen (UMG), 37075 Göttingen, Germany
e-mail: mahdy.eslamy@med.uni-goettingen.de

A. F. Schilling
e-mail: arndt.schilling@med.uni-goettingen.de

J. C. Moreno et al. (eds.), *Wearable Robotics: Challenges and Trends*,
Biosystems & Biorobotics 27, https://doi.org/10.1007/978-3-030-69547-7_66

muscles in human lower extremities to walking, has led to very efficient gait, keeping metabolic costs at a minimum level [2].

To augment the ankle joint power or assist individuals with impaired ankle functionality, ankle foot orthoses (AFOs) are commonly used. Different active or passive AFOs have been developed [3–7]. Active devices are equipped with motor actuators and the required electronics. This added mass can however hinder the effectiveness of active AFOs in reducing the metabolic costs of walking. On the other side, passive devices are lighter, but they have less flexibility to provide the required power for different gaits and speeds. Different studies have concluded that one reason of low metabolic costs in walking can be attributed to the Achilles tendon [8]. The elasticity of the Achilles tendon allows storing and releasing energy and thus reduces necessary muscle work. Furthermore, it allows the ankle plantar-flexors to remain approximately in isometric condition during walking, thus reducing the mechanical work of the soleus and gastrocnemius muscles [8]. To emulate the functionality of this ankle plantar-flexors complex (soleus-gastrocnemius-Achilles-tendon), AFOs are usually equipped with a spring [4, 6, 9, 10].

The hypothesis behind using an AFO is that because of its similarity to the ankle plantar-flexor complex, it can take up the role of the ankle extensors and therefore reduce their workload and eventually reduce the walking metabolic costs. For long, bringing the walking metabolic costs further down through assistive devices seemed difficult [3, 11]. This was mainly attributed to mass issues and appropriate timing of the external assistance. Recent studies have now shown some promising first results for reducing the walking metabolic costs through passive [10] or active [4, 12] AFOs.

The main concentration of research in AFOs has been devoted to mono-articular structures, where the upper end of AFO is connected to the shank and the lower end to the heel-foot complex. The human ankle plantar-flexors however consist of two types; the mono-articular soleus, and the bi-articular gastrocnemius in which the upper end is connected to the lower section of the femur. Different studies have shown benefits of the bi-articular gastrocnemius, especially for power transfer from knee to ankle during explosive activities such as upward jumping or running [13–15]. The possibility to transfer power allows to reduce the mass and workload of the distal muscles [16]. Nevertheless, less attention has been paid to the development of bi-articular AFOs.

In this paper, we aimed to study possible effects of the mono- and bi-articular AFOs on the muscular performance of human lower extremities when a user wears them. To do so, we simulated and compared the effects of mono- and bi-articular AFOs with different stiffness values.

2 Methods

We used the Opensim simulation environment [17] to investigate the biomechancs of normal walking on a level ground. The Gait2392 model [18, 19] which includes 92 musculotendon actuators and 23-degree-of-freedom, was used for this purpose.

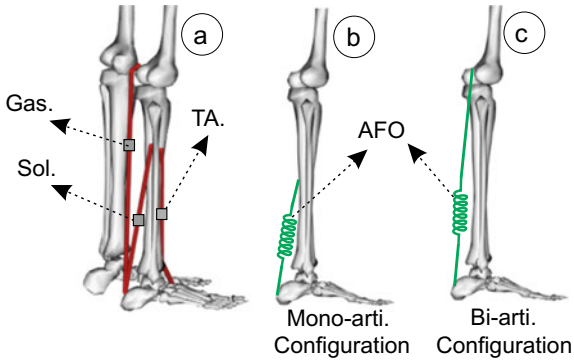

Fig. 1 Schematic view of the: **a** studied muscles gastrocnemius (Gas), soleus (Sol) and tibialis anterior (TA). **b** mono-articular AFO and **c** bi-articular AFO (**b** and **c** represented by uni-directional passive springs)

The above model was extended by adding spring-equipped AFOs (Fig. 1). Two different configurations of the AFO were considered (two models) as shown in Fig. 1. In mono-articular AFO (Fig. 1b), the first connection point was on the calcaneus and the second point was on the shank, whereas in the bi-articular configuration (Fig. 1c), the second connection point was placed on the thigh. In each model, a uni-directional spring was used to represent the AFOs. Five stiffness values (5, 10, 15, 20 and 25 kN/m) were considered for each case of AFO. The CMC (computed muscle control) module embedded in the software was used to extract muscle activation and power patterns.

Muscles' activation levels and powers were compared during complete gait cycles between the case without orthosis (w/o), mono-articular AFO and bi-articular AFO. A gait cycle started with the heel contact until the next heel contact of the same foot. The performance of gastrocnemius (Gas) and soleus (Sol) (ankle extensors) and the tibialis anterior (TA) (ankle flexor) were investigated. For the knee, the performance of rectus femoris (RF), vastus medialis (VM), vastus lateralis (VL) (knee extensors) and semimembranosus (SM), semitendinosus (ST) and biceps femoris (BF) (knee flexors) were considered as well.

3 Results

3.1 Muscles' Activation Levels

Figure 2 shows the comparison between the maximum (column A) and the average (column B) of the activation levels of Gas., Sol. and TA. muscles.

In Fig. 2-A1, the maximum activation level of the Gas. muscle in the bi-articular AFO decreased for all stiffness values in comparison to the case without orthosis (w/o case). The lowest activity was seen at the stiffness 25 kN/m, a decrease of nearly 60%. On the other hand, the maximum activation levels of the Gas in mono-articular AFO, had a fluctuating behavior with increase of the stiffness. In general,

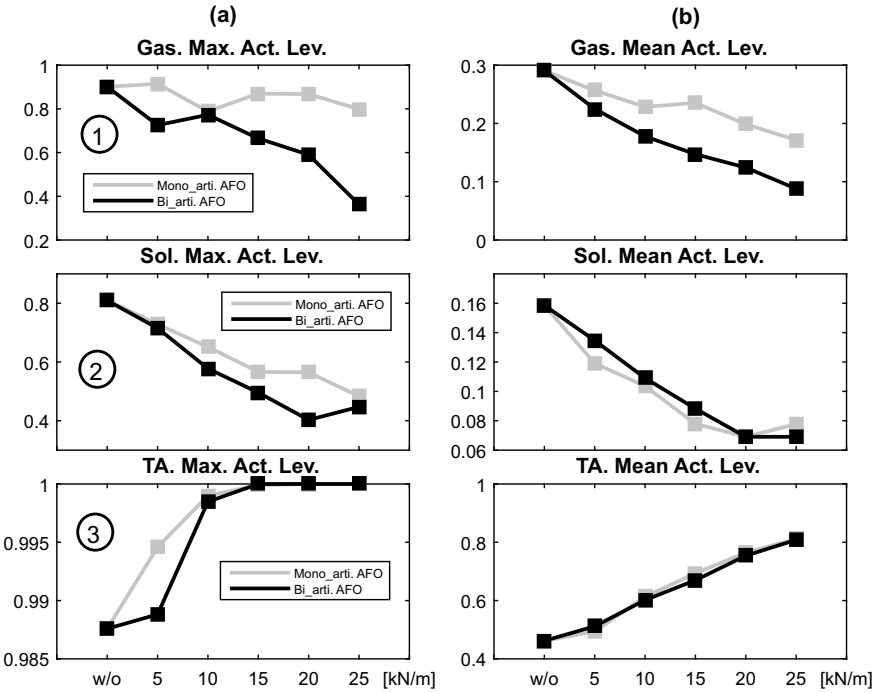

Fig. 2 Comparison between the maximum (column A) and average (column B) activation level of Gas, Sol and TA muscles. The comparison is between the case without AFO (w/o), the mono-articular AFO and the bi-articular AFO with five stiffness values (5–25 kN/m)

the trend was not similar to that of the bi-articular configuration and in addition the reductions of the maximum activation level were not as noticeable as the bi-articular case (highest reduction nearly 13% at 10 kN/m). In Fig. 2-A2, the maximum activation level of the Sol. muscle in the bi-articular AFO decreased for all stiffness values in comparison to the case without orthosis. Such a trend was also observed for the mono-articular AFO, however the reduction caused by the bi-articular AFO was slightly more visible. For the bi-articular AFO, the values continuously reduced in comparison to the case without AFO, however at 25 kN/m the maximum activation level increased with respect to that of the previous stiffness value. In Fig. 2-A3, the values of the maximum activation levels of the TA muscle were very close to each other between the three cases (without, mono- and bi-articular). The trend was relatively similar for both AFO configurations.

Figure 2-B1, shows that the average activation level of the Gas. muscle in the mono- and bi-articular AFO decreased for all stiffness values in comparison to the case without orthosis. The lowest activity was seen at the stiffness 25 kN/m for the bi-articular case, a decrease of nearly 70%. In contrast, the mono-articular AFO led to slightly more reduction of the average activation level of the Sol. muscle in comparison to the bi-articular case (Fig. 2-B2). However, at 25 kN/m, the average

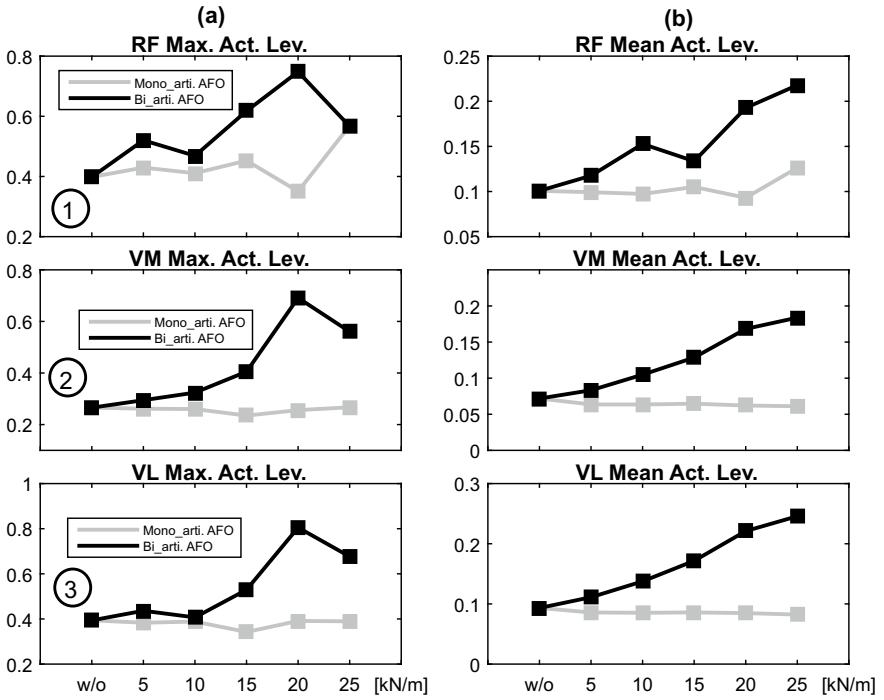

Fig. 3 Comparison between the maximum (column A) and average (column B) activation level of RF, VM and VL muscles. The comparison is between the case without AFO (w/o), the mono-articular AFO and the bi-articular AFO with five stiffness values (5–25 kN/m)

value increased in comparison to the bi-articular AFO. Figure 2-B3, shows that the average activation level of the TA muscle was very similar between mono- and bi-articular cases. The average activation level of the TA. muscle increased for all stiffness values in comparison to the case without AFO (w/o case). The highest increase was at 25 kN/m (about 75%).

Figures 3A-B show the maximum and average activation levels of knee extensors (RF, VM and VL). The maximum activation levels with bi-articular AFO (Fig. 3-A) increased with respect to the case without orthosis. The highest value was seen at 20 kN/m. For mono-articular AFO the maximum activation level of RF was relatively similar until 15 kN/m and then decreased at 20 kN/m and increased at 25 kN/m. The maximum activation level of VM or VL changed very slightly with respect to the case without orthosis. The average activation levels with bi-articular AFO (Fig. 3-B) increased with respect to the case without orthosis. For mono-articular AFO the average activation level of RF was relatively similar until 20 kN/m, and increased slightly at 25 kN/m. The average activation level of VM or VL decreased very slightly with respect to the case without orthosis.

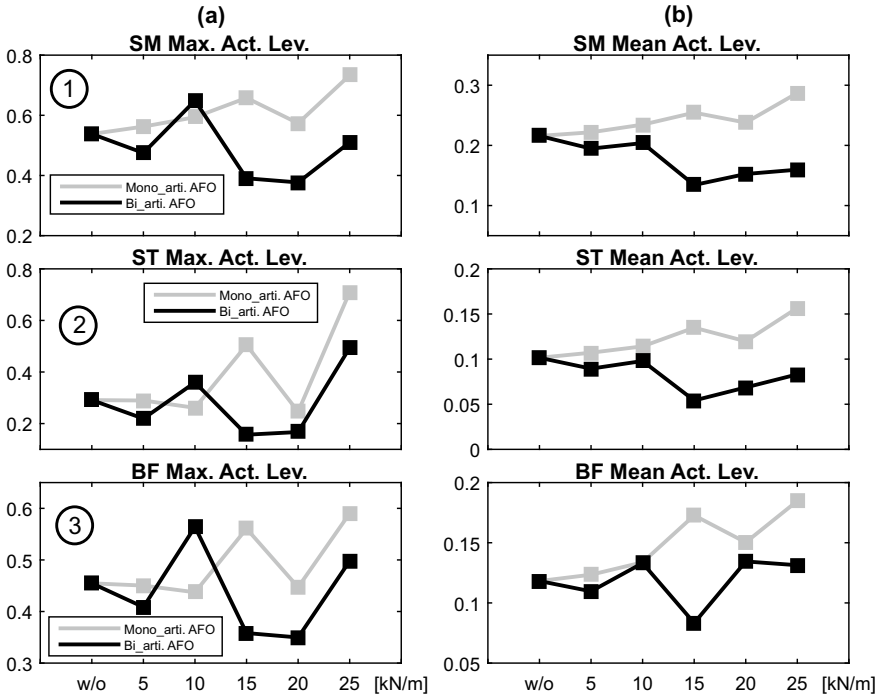

Fig. 4 Comparison between the maximum (column A) and average (column B) activation level of SM, ST and BF muscles

The maximum and average activation levels of knee flexsors (SM, ST and BF) are shown in Figs. 4A-B. The maximum activation levels of SM with bi-articular AFO (Fig. 4-A1) fluctuated with change of the springs and a unique trend was not visible. The maximum activation levels with mono-articular AFO in general increased with the increase of springs. The highest increase was at 25 kN/m. For ST and BF muscles, the maximum activation levels with mono- or bi-articular AFOs did not show a unique trend. The average activation levels of SM with mono-articular AFO (Fig. 4-B1) increased with respect to the case without orthosis. In contrast, for bi-articular AFO, in general the values decreased with respect to the case without orthosis. The trend for the ST muscle (Fig. 4B2) was similar to the SM muscle. The average activation levels of BF with bi-articular AFO (Fig. 4-B3) reached a minimum at 15 kN/m but in general did not change too much with respect to the case without orthosis. For the mono-articular AFO, in general the values increased with respect to the case without orthosis.

3.2 *Muscles' Power*

The maximum and minimum powers of Gas, Sol and TA muscles are shown in Fig. 5A-B. The maximum Gas muscle power (Fig. 5-A1) decreased for all spring values in bi-articular configuration, while the values for mono-articular AFO showed a fluctuating behavior. The maximum Sol power (Fig. 5-A2) decreased for all spring values in mono- and bi-articular AFOs. For TA, the maximum power (Fig. 5-A3) increased in general for both mono- and bi-articular AFOs, however with a fluctuating behavior.

The minimum (negative) Gas muscles power (Fig. 5-B1) increased for all spring values in mono- and bi-articular configurations, however the trend was more obvious for bi-articular AFO. In contrast, for Sol and TA muscles, the power values (Fig. 5-B2 and 3) are relatively similar for both mono- and bi-articular AFOs. For Sol (Fig. 5-B2), the minimum (negative) power values increased until 20 kN/m, however a sudden sharp decrease happened at 25 kN/m. For TA, the decreasing trend of minimum muscle powers (Fig. 5-B3) was relatively similar for both mono- and bi-articular AFOs.

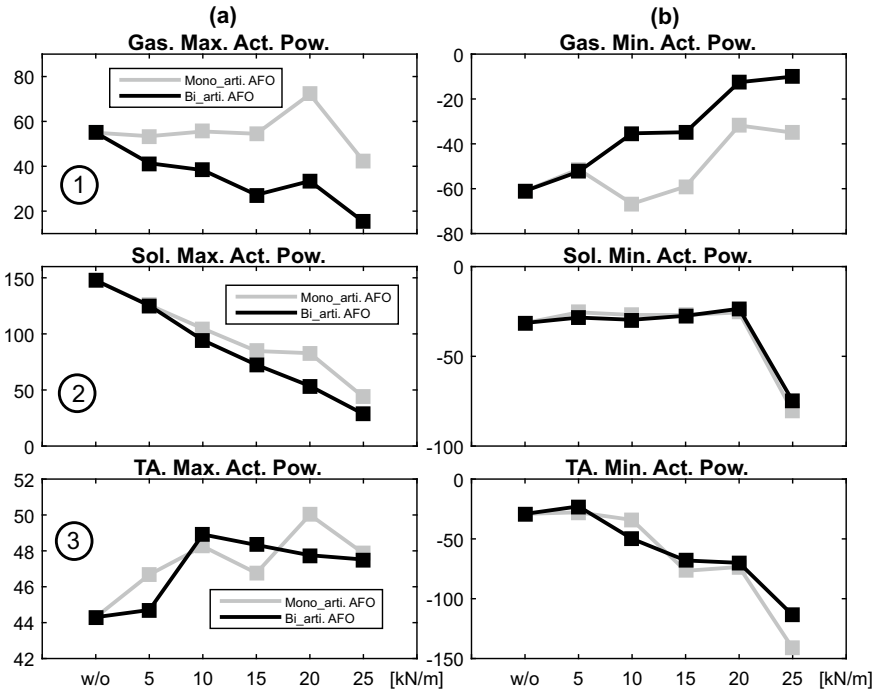

Fig. 5 Muscle actuation power [W]: comparison between the maximum (column A) and minimum (column B) power of Gas, Sol and TA muscles. The comparison is between the case without AFO (w/o), the mono-articular AFO and the bi-articular AFO with five stiffness values (5–25 kN/m)

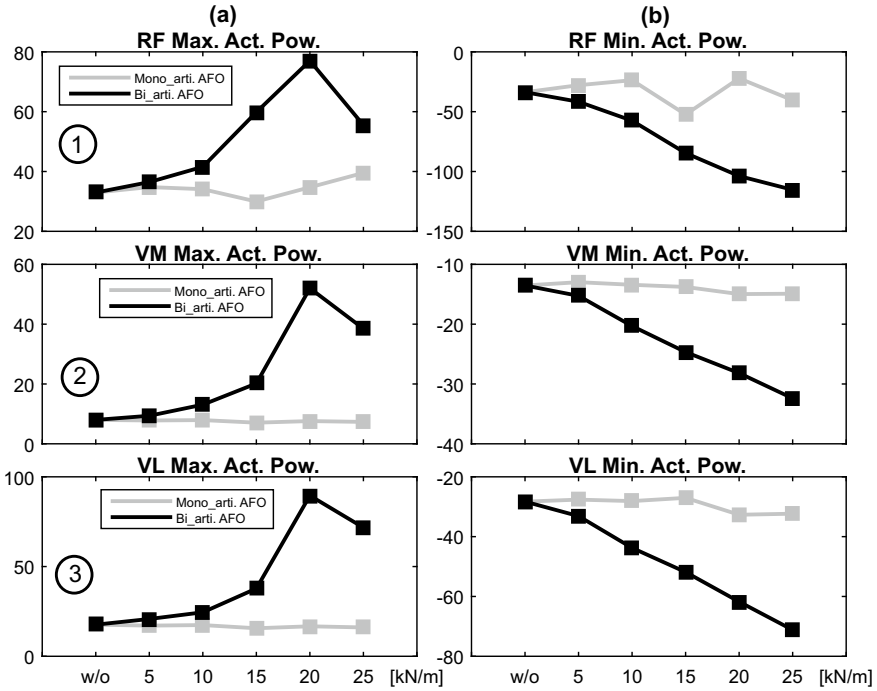

Fig. 6 Muscle actuation power [W]: comparison between the maximum (column A) and minimum (column B) power of RF, VM and VL muscles

The maximum and minimum powers of RF, VM and VL muscles (knee extensors) are shown in Fig. 6A-B. For RF muscle, the maximum power (Fig. 6-A1) increased for the bi-articular configuration, however for mono-articular AFO the maximum values were changing very slightly with respect to the case without orthosis. This trend was also visible for VM and VL muscles (Fig. 6-A2 and 3). For all of those muscles, the minimum values of power were changing very slightly for the mono-articular AFO (Fig. 6-B1 to 3). However, the minimum (negative) values related to the bi-articular AFO were decreasing with the increase of spring stiffness.

Figure 7A-B shows the maximum and minimum powers of knee flexors SM, ST and BF muscles. The maximum power in bi-articular AFO (Fig. 7-A1 to 3) in general decreased however the values show fluctuating behavior and a sudden sharp increase was seen at 10 kN/m. In contrast, the values related to the mono-articular AFO were changing very slightly with respect to the case without orthosis. For mono-articular AFO, for ST and BF, an increase was seen at 15 kN/m, however in general very slight changes were observed in comparison to the case without orthosis.

The minimum power values of SM (Fig. 7-B1) in the bi-articular configuration were increasing toward zero, however at 20 kN/m a sudden sharp decrease was observed. The same sudden decrease was also seen for ST and BF. For all of these

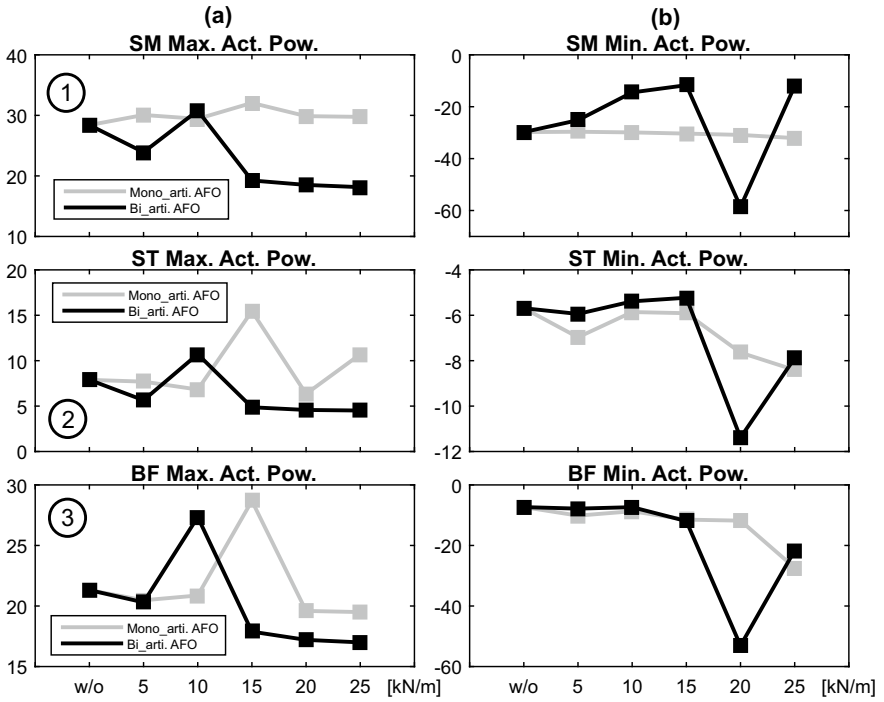

Fig. 7 Muscle actuation power [W]: comparison between the maximum (column A) and minimum (column B) power of SM, ST and BF muscles

muscles, the lowest (negative) minimum values happened at 20 kN/m (Fig. 7-B1 to 3). For mono-articular AFO, in SM muscle the minimum power values were changing only very slightly, however for ST and BF the value were further decreasing in general (getting more negative). Their lowest value was seen at a spring stiffness of 25 kN/m.

4 Discussions and Conclusions

We compared the activation levels and power of Gas, Sol and TA muscles (ankle extensors and flexors), RF, VM and VL (knee extensors) and SM, ST and BF (knee flexors) between normal walking without AFO, and with mono-articular AFO and bi-articular AFO at five different stiffness values.

The simulations showed that both mono- and bi-articular AFOs reduced the maximum and average activation levels of Sol and Gas in comparison to the case without orthosis. For these two muscles, the reductions caused by the bi-articular AFO were more obvious in three out of four results (A1, B1, A2). The only case where the reduction in mono-articular AFO was very slightly more pronounced than that of

the bi-articular AFO, was related to the mean (average) activation level of the Sol muscle (Fig. 2 B2, excluding 25 kN/m).

Looking at Figs. 3 and 6, it seems that this relief of the lower leg muscles through the bi-articular AFO is compensated by a stronger activation of the knee extensors (RF, VM and VL, up to 3.4-fold negative RF power decrease for 25 kN/m vs. no AFO, Fig. 6-B1). On the other hand, the mono-articular AFO, only shows a very slight compensatory activation of these muscles. On the knee flexors (SM, ST and BD), the bi-articular AFO did not have a clear decreasing or increasing effect on the activation levels and maximum power values (Figs. 4 and 7). Therefore, as a conclusion, it may be possible to support lower leg muscle power with upper leg muscle power when using bi-articular AFOs, however possibly at additional metabolic costs.

Both mono- and bi-articular AFOs led to relative increase of the TA's activation levels at all stiffness values (Fig. 2 A3 and B3). The maximum power values (Fig. 5A-3) did not show a considerable increase with respect to the case without orthosis, though. However, the negative power values changed considerably in which at 25 kN/m the value reached approximately 110 W (bi-articular case). Figure 8 shows that negative power values were more notable during late stance and start of the swing phase (appr. 50–70%), where the TA consumes power to counteract with the orthosis and regulate the required moment on the ankle joint. In real-world applications, this may lead to muscle fatigue and the user may fail to perform an appropriate dorsiflexion. This may eventually result in a drop-foot condition.

A clutchable AFO, may possibly solve this. A high-level controller (motion planner) would be needed in this case to define where in the gait cycle the clutch should engage/disengage the AFO, in order to lessen the load on the TA. Clutchable mechanisms are already used in the context of assistive devices [20]. To use such a mechanism for different speeds a motor (actuator) may be required as well.

A main limitation of this study was that it lacked the *human-in-the-loop* considerations. The current model assumed that the joints' motions using AFOs would

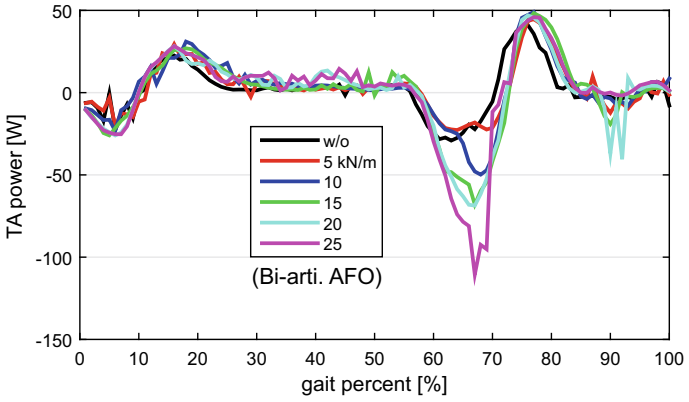

Fig. 8 TA power curves (comparison between without orthosis and bi-arti. AFO 5–25 kN/m)

be similar to the case without orthosis. It was not possible to simulate the human interaction in Opensim software, e.g., to check if the subject is really interested to actuate his/her ankle joint at stiffer 25 kN/m springs similar to the case they don't wear an AFO.

Therefore, in reality the subjects may possibly change their ankle joint motion to avoid muscle fatigue and associated negative feelings. Thus, the maximum and minimum TA power level (Fig. 5-A3 and B3), may possibly differ from what would happen in real world.

In conclusion, the general results show that AFOs with softer springs (based on our results, <10 kN/m) may potentially lead to some benefits in both muscle activation and power decrease of the lower leg muscles. However it needs to be validated with different human subjects walking at different speeds. A customized patient-specific AFO may allow to further facilitate muscular interactions.

Acknowledgements This work was supported by the Grant from the Bundesministerium für Bildung und Forschung (BMBF-INOPRO-16SV7656).

References

1. D.A. Winter, Energy generation and absorption at the ankle and knee during fast, natural, and slow cadences. Clin. Orthopaedics Related Res. **175**, 147–154 (1983)
2. A. Hreljac, Preferred and energetically optimal gait transition speeds in human locomotion. Med. Sci. Sports Exer. **25**(10), 1158–1162 (1993)
3. G.S. Sawicki, D.P. Ferris, Powered ankle exoskeletons reveal the metabolic cost of plantar flexor mechanical work during walking with longer steps at constant step frequency. J. Exp. Biol. **212**(1), 21–31 (2009)
4. P. Malcolm, W. Derave, S. Galle, D. De Clercq, A simple exoskeleton that assists plantarflexion can reduce the metabolic cost of human walking. PloS One **8**(2), e56137 (2013)
5. J. Hitt, A.M. Oymagil, T. Sugar, K. Hollander, A. Boehler, J. Fleeger, Dynamically controlled ankle-foot orthosis (dco) with regenerative kinetics: Incrementally attaining user portability, in *IEEE International Conference on Robotics and Automation* (2007), pp. 1541–1546
6. M. Wiggin, G. Sawicki, S. Collins, An exoskeleton using controlled energy storage and release to aid ankle propulsion, in *IEEE International Conference on Rehabilitation Robotics (ICORR)* (2011), pp. 1–5
7. A. Danielsson, K.S. Sunnerhagen, Energy expenditure in stroke subjects walking with a carbon composite ankle foot orthosis. J. Rehabil. Med. **36**(4), 165–168 (2004)
8. G. Sawicki, C. Lewis, D. Ferris, It pays to have a spring in your step. Exer. Sport Sci. Rev. **37**(3), 130 (2009)
9. E.S. Arch, S.J. Stanhope, J.S. Higginson, Passive-dynamic ankle-foot orthosis replicates soleus but not gastrocnemius muscle function during stance in gait: insights for orthosis prescription. Prosthetics Ortho. Int. **40**(5), 606–616 (2016)
10. S.H. Collins, M.B. Wiggin, G.S. Sawicki, Reducing the energy cost of human walking using an unpowered exoskeleton. Nature **522**(7555), 212–215 (2015)
11. J.A. Norris, K.P. Granata, M.R. Mitros, E.M. Byrne, A.P. Marsh, Effect of augmented plantarflexion power on preferred walking speed and economy in young and older adults. Gait Posture **25**(4), 620–627 (2007)
12. L.M. Mooney, E.J. Rouse, H.M. Herr, Autonomous exoskeleton reduces metabolic cost of human walking. J. Neuroeng. Rehabil. **11**(1), 151 (2014)

13. J. Babič, B. Lim, D. Omrčen, J. Lenarčič, F. Park, A biarticulated robotic leg for jumping movements: theory and experiments. ASME J. Mech. Robot. (2008)
14. G.V. van Ingen Schenau, M. Bobbert, R. Rozendal, The unique action of bi-articular muscles in complex movements. J. Anatomy **155**, 1 (1987)
15. M. Eslamy, M. Grimmer, A. Seyfarth, Adding passive biarticular spring to active mono-articular foot prosthesis: effects on power and energy requirement, in *IEEE-RAS International Conference on Humanoid Robots* (2014), pp. 677–684
16. J. Cleland, On the actions of muscles passing over more than one joint. J. Anatomy Physiol. **1**(1), 85 (1867)
17. S.L. Delp, F.C. Anderson, A.S. Arnold, P. Loan, A. Habib, C.T. John, E. Guendelman, D.G. Thelen, Opensim: open-source software to create and analyze dynamic simulations of movement. IEEE Trans. Biomed. Eng. **54**(11), 1940–1950 (2007)
18. C.T. John, A. Seth, M.H. Schwartz, S.L. Delp, Contributions of muscles to mediolateral ground reaction force over a range of walking speeds. J. Biomech. **45**(14), 2438–2443 (2012)
19. M.Q. Liu, F.C. Anderson, M.H. Schwartz, S.L. Delp, Muscle contributions to support and progression over a range of walking speeds. J. Biomech. **41**(15), 3243–3252 (2008)
20. E.J. Rouse, L.M. Mooney, H.M. Herr, Clutchable series-elastic actuator: implications for prosthetic knee design. Int. J. Robot. Res. **33**(13), 1611–1625 (2014)

Ultrasound Imaging of Plantarflexor Muscles During Robotic Ankle Assisted Walking: Effects on Muscle Tendon Dynamics and Application Towards Improved Exoskeleton and Exosuit Control

Richard W. Nuckols, Sangjun Lee, Krithika Swaminathan, Conor J. Walsh, Robert D. Howe, and Gregory S. Sawicki

Abstract Ankle exosuits/exoskeletons can improve gait but the assistance needs to be tuned to the individual. We suspect that ankle assistance can affect underlying muscle-tendon dynamics and should be accounted for in the control design. We highlight two complementary studies that begin to address these issues. First, we use ultrasound imaging to directly measure the effect of ankle exoskeleton rotational stiffness on soleus contractile dynamics. With increasing stiffness, the soleus operating length and muscle economy increased in early stance, but this was offset by increased shortening velocity and reduced muscle economy in late stance. Second, we demonstrate an approach to rapidly estimate muscle contractile state and its application in prescribing assistance profiles. These results provide evidence for the importance of muscle dynamics and how it can be used to inform design of wearable devices.

Part of this work was supported by grants to G.S.S from the National Institute of Nursing Research of the National Institutes of Health (R01NR014756) and the U.S. Army Natick Soldier Research, Development and Engineering Center (W911QY18C0140). Part is based upon the work supported by the Harvard John A. Paulson School of Engineering and Applied Sciences TEAM initiative, National Institutes of Health (BRG R01HD088619) and the National Science Foundation (CNS-1446464) to C.J.W and the Wyss Institute for Biologically Inspired Engineering. K.S. is also supported by a National Science Foundation Graduate Research Fellowship, and S.L. is supported by Samsung Scholarship.

R. W. Nuckols (✉) · S. Lee · K. Swaminathan · C. J. Walsh · R. D. Howe
John A. Paulson School of Engineering and Applied Science,
Harvard University, Cambridge, MA, USA
e-mail: rnuckols@g.harvard.edu

G. S. Sawicki
Georgia Tech, Atlanta, GA, USA

J. C. Moreno et al. (eds.), *Wearable Robotics: Challenges and Trends*,
Biosystems & Biorobotics 27, https://doi.org/10.1007/978-3-030-69547-7_67

1 Introduction

Ankle exoskeletons/exosuits are capable of improving metabolic demand [1], but the correct assistance timing and magnitude must be provided for the user to effectively interact with the device. Models of walking predict that assistance can disrupt the normally tuned interaction of the ankle plantarflexors and Achilles Tendon [2], but no study had validated the effect of exosuit assistance on muscle dynamics experimentally. Understanding how assistive devices affect muscle dynamics is crucial because the coordinated interaction of the ankle plantarflexors and the Achilles tendon allows for efficient force and power production during walking.

In the PoWeR Lab (Sawicki), we directly measured soleus muscle fascicle dynamics using B-mode ultrasound imaging during exoskeleton assisted walking [3]. We hypothesized that increasing exoskeleton stiffness would result in longer fascicle lengths, increased shortening velocity, and altered soleus muscle economy. Furthermore, we expected that the change in fascicle dynamics would help explain why too much assistance is detrimental to exoskeleton effectiveness.

In a later study in the Harvard Biodesign and Biorobotics Lab (Walsh, Howe), we extended these ideas towards development of exosuit assistance profiles that account for muscle dynamics [4]. We hypothesized that we could measure the onset time of muscle concentric contraction using B-mode ultrasound imaging, and use that time to inform individualized exosuit control for level and incline walking.

2 Materials and Methods

2.1 PoWeR Lab

Eleven individuals walked at 1.25 m s^{-1} for 5 exoskeleton stiffnesses (0, 50, 100, 150 and 250 Nm rad^{-1}). We measured metabolic demand, joint dynamics, and muscle activation. We calculated force per activation by dividing the estimated muscle force (derived from joint dynamics) by activation. We recorded B-mode ultrasound images of the soleus with a low-profile ultrasound probe. We tracked the fascicles using an automated tracking software [5] and calculated the length and velocity of the soleus fascicles for the 5 conditions.

2.2 Harvard Biodesign and Biorobotics

Our sensing/measurement approach used B-mode ultrasound to detect, at real-time rates, when the muscle begins to concentrically contract and generate positive power before push-off. For this, we modeled the ankle soleus-AT complex as an elastic element and contractile element in series. While subjects walked on a treadmill, we

captured B-mode images of the soleus ($n = 7$ at 1.5 m s^{-1} on level ground; $n = 4$, 1.25 m s^{-1} level and 10% incline). We then calculated the optical flow velocity of the soleus along the superficial aponeurosis to determine when the muscle was displacing proximally (away from the ankle) and shortening against the distal Achilles tendon. Finally, we performed an initial ($n = 1$) exosuit evaluation where we generated assistance profiles based on the detected onset of muscle contraction.

3 Results

3.1 PoWeR Lab

Increasing exoskeleton rotational stiffness resulted in an increase in fascicle operating lengths by 4.4 mm and an increase in force per activation by 27% in the highest stiffness compared to no assistance (Fig. 1) [3]. Increasing stiffness also resulted in an increase in shortening velocity by 3.7 mm s^{-1} and a reduction in muscle force per activation by 24% in the highest stiffness compared to no assistance. User metabolic demand was minimized at an intermediate stiffness of 50 Nm rad^{-1} and increased for the highest stiffness.

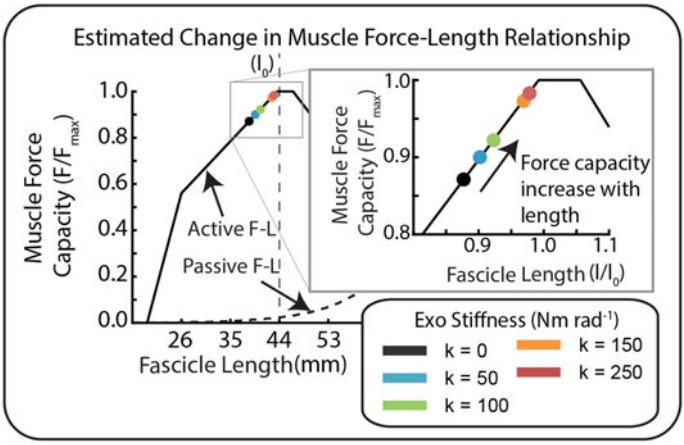

Fig. 1 Effect of exoskeleton stiffness on fascicle length at peak force and and estimated effect of fascicle length change on force production capacity

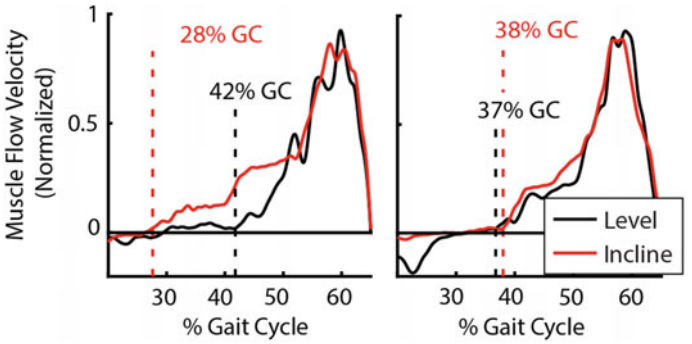

Fig. 2 Estimated onset time of concentric contraction for level and 10% walking for two subjects. Muscle response to incline varied with individuals

3.2 Harvard Biodesign and Biorobotics

The semi-automated routine using optical flow segmented the data to a normalized gait cycle and estimated the onset of concentric contraction at real-time rates (~130 Hz) [4]. Estimation of the onset of concentric contraction had a high correlation ($R^2 = 0.92$) and an RMSE of 2.6% gait cycle relative to manual estimation. The onset of muscle contraction at 1.5 ms^{-1} walking ranged from 39.3 to 45.8% of the gait cycle with an average of 42.8% gait cycle. The onset of muscle contraction was estimated to be 7% earlier in 10% incline walking but was variable across individuals (Fig. 2). Finally, when comparing to a fixed assistance profile, we found that updating the onset of exosuit assistance using muscle contraction timing improved metabolic energy demand in incline walking.

4 Discussion

4.1 PoWeR Lab

The results supported the hypothesis that increasing exoskeleton stiffness alters soleus muscle dynamics and helps explain why increasing assistance does not continually improve performance. We found that increasing exoskeleton stiffness resulted in increased fascicle lengths and improved muscle economy (force/activation) in early stance; however, the benefit was offset by increased fascicle shortening velocity and reduced muscle economy in late stance. This apparent trade-off resulted in a metabolic 'sweet-spot' at intermediate exoskeleton stiffness where metabolic energy consumption was minimized. For the first time, we are capable of providing experimental evidence that supports previous modeling and simulations studies that

predict changes to muscle fascicle dynamics resulting from exoskeleton assistance. These experimental results provides insight into how muscle-tendon dynamics can be incorporated into design for wearable devices.

4.2 Harvard Biodesign and Biorobotics

The transition to muscle concentric contraction shown from this technique aligns with reported group average data from prior studies [6]. The determination that the onset of muscle concentric contraction is variable may help explain why individual response to fixed exosuit assistance is so varied. Though preliminary, the exosuit pilot demonstrates that we may be able to improve exosuit performance by accounting for biomechanical changes in the user's muscle dynamics.

5 Conclusion

This work highlights the importance of understanding muscle-tendon dynamics for developing effective exoskeleton/exosuit controllers. We highlight some recent work that suggest how muscle tendon dynamics might be used for individualized assistance profiles that are adaptive to the task demands. In the future, exosuit controllers that sample the individual's muscle-tendon state may enable muscle-in-the-loop controllers capable of offloading muscle force while maintaining efficient contractile dynamics.

References

1. G.S. Sawicki, O.N. Beck, I. Kang, A.J. Young, The exoskeleton expansion: improving walking and running economy. J. Neuroeng. Rehabil. **17**(1), 25 (2020)
2. R.W. Jackson, C.L. Dembia, S.L. Delp, S.H. Collins, Muscle-tendon mechanics explain unexpected effects of exoskeleton assistance on metabolic rate during walking. J. Exp. Biol. **220**(Pt 11), 2082–2095 (2017)
3. R.W. Nuckols, T.J.M. Dick, O.N. Beck, G.S. Sawicki, Ultrasound imaging links soleus muscle neuromechanics and energetics during human walking with elastic ankle exoskeletons. Sci. Reports **10**(1), 3604 (2020)
4. R.W. Nuckols et al., Automated detection of soleus concentric contraction in variable gait conditions for improved exosuit control, in *IEEE International Conference on Robotics and Automation (ICRA)* (2020)
5. D.J. Farris, G.A. Lichtwark, UltraTrack: software for semi-automated tracking of muscle fascicles in sequences of B-mode ultrasound images. Comput. Methods Programs Biomed. **128**, 111–8 (2016)
6. N.J. Cronin, J. Avela, T. Finni, J. Peltonen, Differences in contractile behaviour between the soleus and medial gastrocnemius muscles during human walking. J. Exp. Biol. **216**(5), 909–914 (2013)

Simulation Platform for Dynamic Modeling of Lower Limb Rehabilitation Exoskeletons: Exo-H3 Case Study

Sergey González-Mejía, José M. Ramírez-Scarpetta, Juan C. Moreno, and José L. Pons

Abstract A flexible simulation platform for human gait with exoskeletons is presented to support the analysis of the human-robot interaction and performance assessment of control strategies design, e.g., assist-as-needed. The platform includes the dynamic modeling of the lower limb's exoskeleton-human with six degrees of freedom in sagittal plane, actuated by servomotors, where the movement equations are explicitly obtained through the Euler-Lagrange approach. The full model is hybrid and it contains four sub-models that are switched between themselves according to the gait cycle phases; also, it comprises the joint actuators dynamics and the low level control system, this modeling was assembled in Simulink-Matlab. It is shown that the proposed platform is a useful tool for assistance control strategies in the gait rehabilitation. Furthermore, simulation results for the Exo-H3 exoskeleton show the successful tracking of angular trajectories, the level of human participation, and the realistic torques.

1 Introduction

Most of the foundational concepts and control techniques for human gait exoskeletons are inspired or emerge from the bipedal robotics field. Wearable exoskeletons are characterized by their kinematic and dynamic behavior, which in turn determine the design of mechanical structures and model-based control systems [1, 2]; these features can be modeled and implemented to run dynamic simulations for

S. González-Mejía (✉) · J. M. Ramírez-Scarpetta
Industrial Control Research Group of Universidad del Valle, Cali, Colombia
e-mail: sergey.gonzalez@correounivalle.edu.co

J. C. Moreno
Neural Rehabilitation Group of the Spanish National Research Council, Madrid, Spain
e-mail: jc.moreno@csic.es

J. L. Pons
Shirley Ryan Ability Lab, Chicago, IL, USA
e-mail: jpons@ric.org

J. C. Moreno et al. (eds.), *Wearable Robotics: Challenges and Trends*,
Biosystems & Biorobotics 27, https://doi.org/10.1007/978-3-030-69547-7_68

further offline assessment of gait function [3]. The gait cycle process of the human-exoskeleton coupled system can be divided into four different contact phases, which generates continuous and discrete states, and can be described through a hybrid model. The work [1] proposes a hybrid model of exoskeleton and each phase of the full model is triggered with the time data. In other similar research [4], a mathematical hybrid 3D-model was developed and it is characterized by a continuous swing and an instantaneous double support phase, and there is a discrete event to trigger the transition to the next phase.

This contribution presents a simulation platform for the dynamic modeling of exoskeleton for human gait. The Mathematical approach of dynamic modeling and its considerations, conception of the model switching estimator and computation of the interaction torque are explained. Finally simulation results for the Exo-H3 exoskeleton are presented.

2 Material and Methods

A. Mathematical approach of dynamic modeling and its considerations

The conception of the mathematical model of a lower limbs exoskeleton with human along the sagittal plane is developed. The phases of the gait cycle for the kinematic modeling are taken into account, and it is important to emphasize that the reference system is variable in time according to the leg in support. The equations of motion of the dynamic models for each phase of the gait cycle were conceived through the Euler-LaGrange representation.

B. Conception of the model switching estimator and computation of the interaction torque

The models are switched to generate a smooth and single output signal for a joint. Thus, a model switch indicator is built to show the current phase of the gait cycle, and it is calculated online using the relative distances between the feet.

The interaction torque, (τ), in a joint is the sum of the motor torque; torques produced by other motors, torques due to static, Coulomb and viscous friction; human torque (τ_h); and torque by external forces. τ_h is an input to the system, therefore, it must be generated according to the desired profile. However, it can be calculated as indicated by (1).

$$\begin{aligned} \tau &= \tau_m + \tau_{m-up/down} - \tau_{fs}(1 - |sign(\dot{q})|) + \ldots \\ &\quad - \tau_{fc} sign(\dot{q}) - C_{fv}\dot{q}_{joint} + \tau_h + Fd \\ \tau_h &= M(q)\ddot{q} + C(q,\dot{q})\dot{q} + g(q) + \sum(-\tau_m + T_{Fr} - Fd) \end{aligned} \tag{1}$$

3 Results and Discussion

The simulation platform, Fig. 1a, is assembled in Simulink-Matlab and describes the dynamic behavior of the Exo-H3 exoskeleton [5], Fig. 1b. The platform calculates signals per joint such as the motor/interaction torque; positions, speeds, and angular accelerations; there is the possibility of applying for friction torque compensation.

Four continuous dynamic models are generated with the Euler-LaGrange formulation, which represent the phases of the gait cycle and are switched to describe the dynamics based on the torques applied to joints. Simulations of bipeds in sagittal plane with respect to a reference system allow testing the feasibility of trajectories that are conceived on other platforms. The obtained results by the kinematic and dynamic modeling fit satisfactorily with the observed data in the literature [6, 7]. The motor torque levels are low during the double support and single support phase, and they are within the physical ranges of action. The transitions between phases are smooth, Fig. 1c. There is still a lot of current research in the control laws design

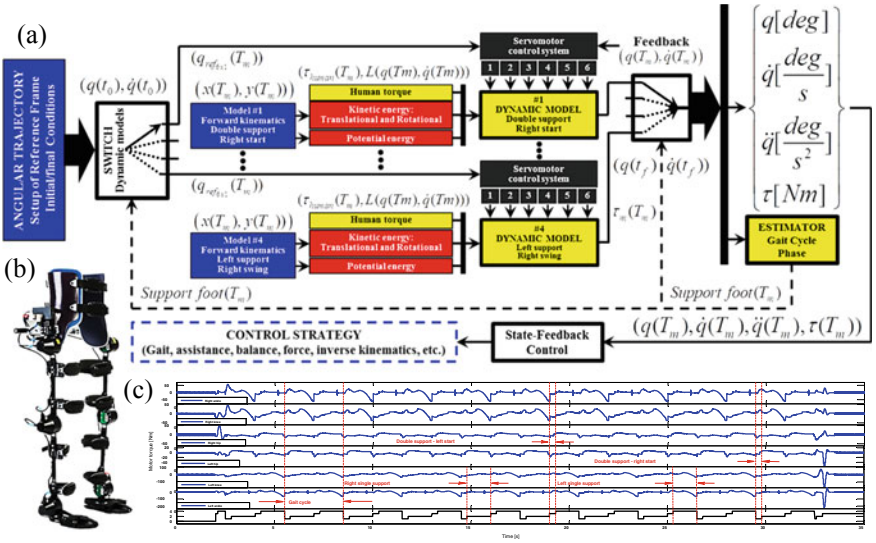

Fig. 1 **a** The simulation platform for dynamic modeling of lower limb rehabilitation exoskeleton. The Lagrangian calculation ($\boldsymbol{L}$) is the difference between the kinetic and potential energy and it is a function of the positions ($\boldsymbol{q}$) and angular velocities ($\dot{\boldsymbol{q}}$). The sampling time ($\boldsymbol{T_m}$) allows the adequate synchronization of the information flow through the Simulink blocks. The dotted lines show the activation of the models switch. The joint angles ($\boldsymbol{q}$) are the inputs of the kinematic models, and the motor torques ($\boldsymbol{\tau_m}$) applied to the joints are the control inputs for the dynamic models. **b** The Exo-H3 robotic exoskeleton (Technaid S.L.) has six degrees of freedom (sagittal plane) and it is operated by DC servomotors. **c** The motor torques for 100% assistance of full system, and switching indicator from 1 to 4 to indicate the phases. The open-loop simulation was for ten gait cycles, each gait cycle lasts three seconds. The model parameters are the height and mass of the human, the positions of the COMs, moments of inertia passing through the COMs, and mass of the mechanical structure and motors

for an exoskeleton assisting a patient, including the treatment of constraints and disturbances to add robustness to the control system.

4 Conclusions and Outlook

The simulation platform shows that it is a versatile and flexible tool for research in assisted rehabilitation of the human gait. Therefore, the platform is useful for the analysis of gait, and control strategies design; it is used to simulate control condition for static and dynamic balance, gait assist, impedance, force feedback, etc.; the validation of the forward kinematic modeling achieves a successful tracking of the experimental displacement trajectories, which were previously applied to the inverse kinematics model; the transfer of final conditions during the models switching and the synchronized resetting of the integrators allow obtaining smooth and bounded outputs at the beginning of double support; for future works, assist-as-needed control will be developed to measure the rehabilitation effectiveness of patients and various clinical protocols to validate them.

Acknowledgements This work was sponsored by the Administrative Department of Science, Technology and Innovation (Colciencias) under grant agreement No. 647-2014 at the Universidad del Valle, Colombia; and it was supported through computational and processing resources provided by Neural Rehabilitation Group and Technaid S.L. at the Cajal Institute, CSIC, Spain.

References

1. X. Wang, H. Wang, Y. Tian, Gait planning and hybrid model based tracking control of lower extremity exoskeleton, in *2016 35th Chinese Control Conference (CCC)*, July 2016, pp. 6019–6024
2. Z. Yang, W. Gu, J. Zhang, L. Gui, *Force Control Theory and Method of Human Load Carrying Exoskeleton Suit* (Springer, Berlin, Heidelberg, 2017).
3. Y. Zhu, G. Zhang, C. Zhang, G. Liu, J. Zhao, Biomechanical modeling and load-carrying simulation of lower limb exoskeleton. Bio-Med. Mater. Eng. **26**(s1), S729–S738 (2015)
4. A. Agrawal et al., First steps towards translating HZD control of bipedal robots to decentralized control of exoskeletons. IEEE Access **5**, 9919–9934 (2017)
5. Technaid—Leading Motion, Exoesqueleto Exo-H3 (2020). https://www.technaid.com/es/productos/robotic-exoskeleton-exo-h3/. Accessed 28 July 2020
6. J. Fan Zhang, Y. Ming Dong, C. Jun Yang, Y. Geng, Y. Chen, Y. Yang, 5-link model based gait trajectory adaption control strategies of the gait rehabilitation exoskeleton for post-stroke patients. Mechatronics **20**(3), 368–376, 2010
7. Y. Long, Z. Du, L. Cong, W. Wang, Z. Zhang, W. Dong, Active disturbance rejection control based human gait tracking for lower extremity rehabilitation exoskeleton. ISA Trans. **67**, 389–397 (2017)

Understanding Technology-Induced Compensation: Effects of a Wrist-Constrained Robotic Hand Orthosis on Grasping Kinematics

Jan T. Meyer, Charlotte Werner, Sarah Hermann, László Demkó, Olivier Lambercy, and Roger Gassert

Abstract Robotic hand orthoses have the potential of supporting grasp function of people with sensorimotor impairments. To achieve lightweight and simple solutions, most devices focus on supporting only a subset of the functional abilities of the hand. This study investigates the effect of such a design trade-off in a wrist-constrained robotic hand orthosis and its effects on upper limb kinematics and grasping abilities of seven able-bodied subjects. Using wearable, inertial sensors on hand, arm, and shoulder we quantified how a reduction of degrees of freedom affected movement strategies in eleven grasping tasks. This analysis helps to understand how simplified design solutions may affect movement patterns of the target end-users, depending on their residual level of functionality. Also, this further highlights the issue of usability-related design trade-offs between compact and lightweight solutions, and more complex multi-degree of freedom devices.

1 Introduction

In early rehabilitation, functional recovery of patients with sensorimotor deficits resulting from, e.g. a spinal cord injury (SCI) is mainly driven by neuroplasticity and the learning of compensation strategies [1]. This enables the persons with disabilities to perform activities of daily living and thereby increase their independence. During prehension tasks, this compensation is often realized by grip alterations such as the tenodesis grasp, or by strategies that involve shoulder abduction. However, depending on the impairment and potential neuromuscular restrictions, such alternative grasping strategies are not always applicable.

The first two authors contributed equally to this work.

J. T. Meyer (✉) · S. Hermann · O. Lambercy · R. Gassert
Rehabilitation Engineering Laboratory, Department of Health Sciences and Technology, ETH Zurich, Zurich, Switzerland
e-mail: relab.publications@hest.ethz.ch

C. Werner · L. Demkó
Spinal Cord Injury Center, Balgrist University Hospital, Zurich, Switzerland

J. C. Moreno et al. (eds.), *Wearable Robotics: Challenges and Trends*,
Biosystems & Biorobotics 27, https://doi.org/10.1007/978-3-030-69547-7_69

In order to further improve the functional independence of people with a limited hand function, promising robotic hand orthoses (RHO) have been proposed and tested in a variety of target users [2]. The aim of novel RHO is to restore functional and potentially natural grasping patterns. Most user studies of RHO focus on the functional benefit gained through device usage by comparing the immediate interventional effect with clinical measures, such as the Action Research Arm Test (ARAT), the Toronto Rehabilitation Institute Hand Function Test (TRI-HFT) and the Jebsen Taylor Hand Function Test (JTHFT) [3–5]. However, the effects on upper limb kinematics, such as grasping strategies and either trained, or unnatural compensatory movements are often neglected. As RHOs become more advanced, it is important to also consider the effect of potential movement constraints while aiming for particularly lightweight and compact solutions.

In this study, we aimed to investigate the effect of a RHO with a constrained wrist on upper limb movement kinematics in able-bodied subjects. With the use of wearable sensors, we analyzed to what extend a compromise in degrees of freedom (DOF) affects the ability and naturalness of handling objects of daily living. These insights help us to weigh off design trade-offs for RHOs and further understand their effects on target-user performance.

2 Methods

2.1 Robotic Hand Orthosis

For this study, a lightweight RHO (148g) developed for people with hand sensorimotor deficits was used. The prototype can assist various grasp types through active finger flexion and extension [5]. To simplify the design of the RHO, the wrist joint was fixed at a 25° extension angle. This was also intended to provide target users with SCI with further grasping stability. A large-diameter push button was used to trigger opening/closing movements of the orthosis.

2.2 Participants

Seven able-bodied participants (28.4 $\pm$ 11.4 years, 3 female, 5 right-handed) were recruited and tested with compliance to SARS-CoV-2-related interaction restrictions and precautions. All subjects gave written informed consent and all experimental procedures were approved by the local ethics committee (Ref. 2018-N-90).

Fig. 1 Experimental setup: able-bodied subject wearing the robotic hand orthosis (RHO) and three wearable sensors (shoulder, lower arm and hand) while performing various grasp types and activities of daily living

2.3 Wearable Sensor Device and Outcome Measures

To assess upper limb kinematics, custom-made inertial measurement units [6] containing 3D gyroscopes and 3D accelerometers were attached to the back of the palm, to the lower arm (behind the RHO), and on top of the ipsilateral shoulder as shown in Fig. 1. Data were recorded at a sampling frequency of 200 Hz. For each sensor, the pitch angle, which describes the angle between the pointing direction of the corresponding limb segment and the gravity vector, was computed using the open-source sensor fusion algorithm of Madgwick et al. [7]. The spread of these pitch angles can quantify compensatory movements [8] and was determined as the main outcome measure through the central range (CR): $CR = 97.5\text{th}–2.5\text{th}$ percentile.

2.4 Experimental Setup and Task Protocol

Eleven tasks adapted from the ARAT [9] and graded redefined assessment of strength, sensibility and prehension (GRASSP) [10] were grouped according to the 3 grasp types (pinch, grip and grasp based on the ARAT subscales). Besides the daily activities "key" = insert and turn key in lock, "bottle" = pour water from 0.5l bottle in cup, "cups" = pour water from cup to cup, and "jar" = open lid of jar, all other tasks (2.5, 5, 7.5 and 10 cm cube, as well as marble, rubber and ball) consisted of a pick-and-place procedure. All tasks were repeated five times, with the right hand only, with and without the RHO. Before starting the testing procedure, all participants were given five minutes to familiarize with the device and its use.

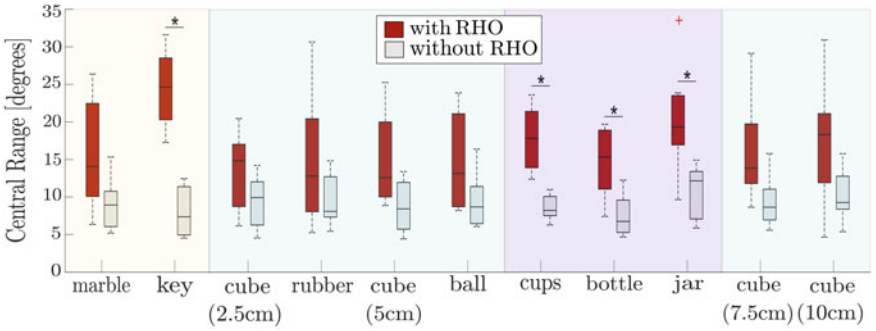

Fig. 2 Shoulder kinematics during grasping movements: the central range (CR) values of all 11 tasks of the conditions with and without the robotic hand orthosis (RHO). The tasks are grouped by object size and grasp type: pinch (marble, key), grasp (rubber, ball, and cubes) and power grip (cups, bottle, jar). Significant differences between conditions are indicated by * ($p < 0.05$)

2.5 Statistical Analysis

The CR of the conditions with/without RHO were compared using the Wilcoxon signed rank test with a significance level of 0.05. The post-processing of the sensor data as well as all statistical analyses were computed in MATLAB R2019b (MathWorks, MA, USA).

3 Results

The inter-subject mean CR values of the shoulder pitch angle for all tasks are shown in Fig. 2. The usage of the RHO increased the angular span of shoulder movements significantly in the tasks key ($p = 0.016$), bottle ($p = 0.016$), jar ($p = 0.031$) and cup ($p = 0.016$). While there was an increasing trend in the CR of pick-and-place tasks, no significant differences were observed.

4 Discussion and Conclusion

In this study, we investigated the effects of a wrist-constrained robotic hand orthosis on the upper limb kinematics of able-bodied subjects during different grasping tasks. We identified a wider span in shoulder pitch angles, predominantly during tasks that resemble daily life prehension activities. This indicates that for more complex tasks, compensatory movements and changes in grasping strategies were needed when using the RHO. These findings are similar to the ones of Schneider et al. [8], where compensatory strategies of SCI patients resulted in a higher CR of the

forearm pitch angle. Purely soft, such as textile- or silicone-based hand orthoses [3, 4] which do not restrict the wrist joint may allow for more natural grasping patterns than fixed-wrist approaches. However, a stabilized wrist can be important for target populations with minimal residual wrist function such as tetraplegic users. Moreover, using compensatory strategies and thereby an unnatural grasping pattern when wearing a lightweight, fixed-wrist RHO might be acceptable for the user due to the increase in functional independence. The advantages of such devices might outperform more complex, often heavy, and expensive solutions that allow for more natural grasping movements.

With this study we aim to underline the importance of understanding upper limb kinematics when investigating the benefits and constraints of wearable robotic assistive technology.

Acknowledgements The authors would like to thank the study participants for their time and dedication. This work is supported by the Vontobel Foundation and the Swiss National Science Foundation through the National Centre of Competence in Research on Robotics.

References

1. S. Mateo, A. Roby-Brami et al., Upper limb kinematics after cervical spinal cord injury: a review. J. Neuroeng. Rehabil. **12**(1), 9 (2015)
2. R.A. Bos, C.J. Haarman et al., A structured overview of trends and technologies used in dynamic hand orthoses. J. NeuroEng. Rehabil. **1**, 1–25
3. C. Correia, K. Nuckols et al., Improving grasp function after spinal cord injury with a soft robotic glove. IEEE Trans. Neural Syst. Rehabil. Eng. (2020)
4. B.A. Osuagwu, S. Timms et al., Home-based rehabilitation using a soft robotic hand glove device leads to improvement in hand function in people with chronic spinal cord injury: a pilot study. J. Neuroeng. Rehabil. **17**(1), 1–15 (2020)
5. T. Bützer, O. Lambercy et al., Fully wearable actuated soft exoskeleton for grasping assistance in everyday activities. Soft Robot. (2020)
6. ZurichMOVE (2019). Available http://zurichmove.com
7. S.O. Madgwick, A.J. Harrison, R. Vaidyanathan, Estimation of IMU and MARG orientation using a gradient descent algorithm, in *IEEE International Conference on Rehabilitation Robotics* (2011)
8. S. Schneider, W.L. Popp et al., Predicting upper limb compensation during prehension tasks in tetraplegic spinal cord injured patients using a single wearable sensor, in *IEEE International Conference on Rehabilitation Robotics* (2019)
9. D. Carroll, A quantitative test of upper extremity function. J. Chron. Diseases **18**(5), 479–491 (1965)
10. S. Kalsi-Ryan, A. Curt et al., Development of the graded redefined assessment of strength, sensibility and prehension (grassp): reviewing measurement specific to the upper limb in tetraplegia. J. Neurosurg. Spine **17**(Suppl 1), 65–76 (2012)

The Effects of Vestibular Stimulation to Enhance Rehabilitation and Enable Robotic Exoskeleton Training for Persons with CP

Ghaith J. Androwis, Peter A. Michael, and Richard A. Foulds

Abstract Reduction of spasticity in persons with cerebral palsy is possible using the application of non-invasive mechanical vestibular stimulation (VS) to the otoliths (in the inner ear). In this study we examined the effects of providing a single session of VS (15 min of a 3-in. of vertical oscillation) to a 35-year old male with spasticity due to CP. This investigation shows promising results of VS application as an intervention that could magnify the effectiveness of conventionally prescribed rehabilitation training/exercises, and can even unlock newly established rehabilitation options (e.g. gait training using robotic exoskeleton).

1 Introduction

Cerebral palsy (CP) is a group of disorders that affect a person's ability to move, maintain balance and posture [1–3]. CP is the most common motor disability of childhood as 1 in 323 children has been identified with CP in the US [3]. There are approximately 764,000 individuals living with CP in the US, and most of them (~75–85%) have spastic CP resulting in significant movement impairments [2, 4]. The US CDC estimates that between 50 and 79% have difficulty walking [5], and about 10% of children with CP walk using a hand-held mobility device [2].

Spasticity is a velocity dependent hypersensitivity of reflexes, and increased muscle tone [6]. It is considered as a major disabling state which alters functional activities. Andersson and Mattsson found that 79% of children with spastic diplegia were able to walk with or without walking aids [7], with a reduction in walking speed and limited control of posture and coordination that result in falls, and increased double support time [6, 8, 9]. More than half, their independent ambulation dramatically decreased with age [7]. Thus, it is crucially important to utilize new strategies,

G. J. Androwis (✉)
Rehabilitation Robotics and Research Laboratory- CMRER, Kessler Foundation, West Orange, NJ, USA
e-mail: ghaith.j.androwis@njit.edu

G. J. Androwis · P. A. Michael · R. A. Foulds
Biomedical Engineering Department, New Jersey Institute of Technology, Newark, NJ, USA

J. C. Moreno et al. (eds.), *Wearable Robotics: Challenges and Trends*,
Biosystems & Biorobotics 27, https://doi.org/10.1007/978-3-030-69547-7_70

interventions and techniques that emphasize lifelong walking and enable enhanced rehabilitation. Importantly, many children with CP, who exhibit high levels of spasticity are excluded from participating in newly emerging gait training using robotic therapy [10, 11]. We believe that results found in this investigation may allow these children to benefit from state of the art therapeutic interventions in which they may otherwise be unable to participate.

2 Material and Methods

A. The vestibular stimulation system

To address spasticity in persons with CP, we have constructed a novel biomechanical apparatus to provide vestibular stimulation (VS) that is capable of providing 2 Hz of non-invasive mechanical stimulation to the saccule of the otolith organ, in the inner ear (Fig. 1). In contrast to the three semicircular canals, which sense the head's angular acceleration, the otoliths (utricle and saccule) sense the head's linear acceleration, its orientation with respect to gravity and the direction and magnitude of acceleration [12, 13]. In particular, the saccule senses vertical accelerations, and contributes to the tone of antigravity muscles [9].

The mechanical vestibular stimulation consisted of a 15 min of vertical oscillation at frequency of 2 Hz and 3 in. of amplitude.

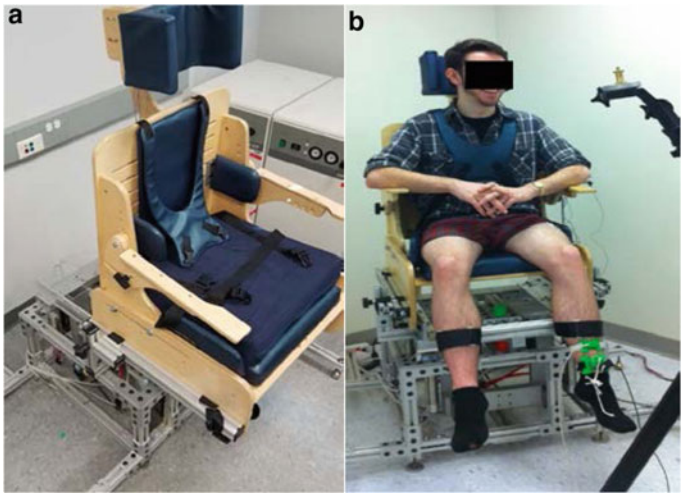

Fig. 1 **a** The developed vestibular stimulation system for providing (2 Hz) of mechanical motion (in the vertical direction while seated) and **b** a participant while receiving a vestibular stimulation session)

B. Experimental Procedure

The data analyzed in this paper consist of the knee's angular displacement of a 35 year old CP male subject. Subject was seated on the examining chair of the vestibular stimulation platform (Fig. 1) while the femur is stabilized in the horizontal orientation and the lower leg hanging freely. The platform is constructed out of 80/20 aluminum material and is computer-controlled to four pneumatic Bimba cylinders, and two Isonic-MOD3 valves.

C. Spasticity Assessment

We evaluated changes in knee spasticity using the Wartenberg pendulum test (PKD) which is a technique commonly used to precisely measure changes of the passive knee angular displacement, stiffness and viscosity with the aim to assess spasticity. To administer this test, a single sensor of an Ascension Technologies trakSTAR electromagnetic tracker was attached to the subject's shank to measure the angler knee joint movement at 100 f/s. The holding force exerted on the shank by the experimenter was measured using a force transducer (ATI-Mini 20/40) that was attached to the subject's shank. The PKD test was administered pre and post VS by the same examiner. The test started by lifting the limb under examination against gravity to full extension and, when relaxed, releasing it, causing it to fall and swing freely. The test is performed while the limb in a relaxed state [8–11].

3 Results

Our results show a promising reduction in spasticity after a single session (15 min) of VS in persons with CP [14–17]. Knee stiffness and damping were significantly reduced (~50%) using an optimization model that allows us to extract stiffness and damping numerically from the PKD data of the knee joint [16, 17], and range of motion (ROM) and angular velocity post VS increased. These results suggest a potential improvement in function in community living [14] (Fig. 2).

4 Discussion and Conclusions

We believe that the provided 2 Hz VS is able to alter the descending control of muscle tone in persons with spasticity due to CP and possibly other clinical diagnoses (stroke, SCI). This may further enable taking advantage of this non-invasive intervention to reduce spasticity and muscle tone in levels that could magnify the effectiveness of the conventionally prescribed rehabilitation training/exercises, and can even unlock newly established rehabilitation options (e.g. gait training using over-ground robotic exoskeleton, RGT), thereby improving the person's quality of life and allow participation in the community and activity of daily living. A larger sample-size, including additional persons with CP, is being analyzed to confirm findings in this study.

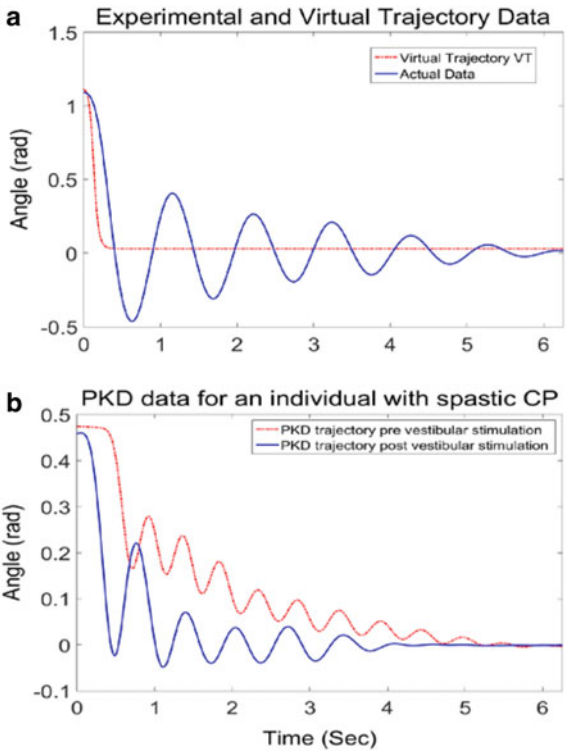

Fig. 2 **a** An example of PKD test for an individual without disability. The virtual trajectory (VT) is a modeled representation of a trajectory passing through the inflection points of the collected data. **b** The PKD trajectory of an individual with spastic CP Pre and post 2 Hz vestibular stimulation

Acknowledgements Research funded by New Jersey Institute of Technology—Kessler Foundation RERC on Wearable Robotics (NIDILRR grant # 90RE5021).

References

1. G. Flores-Mateo, J.M. Argimon, Evidence based practice in postgraduate healthcare education: a systematic review. BMC Health Serv. Res. **7**, 1 (2007)
2. J. Garfinkle, P. Li, Z. Boychuck, A. Bussières, A. Majnemer, Early clinical features of cerebral palsy in children without perinatal risk factors: a scoping review. Pediatr. Neurol. **102**, 56–61 (2020)
3. F. Taylor, "National Institute of Neurological Disorders and Stroke (US), Office of Science and Health Reports. Cerebral palsy: hope through research. Bethesda, Md.: The Institute, 2001. Accessed online September 28, 2005," ed, 2006.
4. D. Podsiadlo, S. Richardson, The timed "Up & Go": a test of basic functional mobility for frail elderly persons. J. Am. Geriatr. Soc. **39**, 142–148 (1991)
5. P. Haak, M. Lenski, M.J.C. Hidecker, M. Li, N. Paneth, Cerebral palsy and aging. Dev. Med. Child Neurol. **51**, 16–23 (2009)
6. J.W. Lance, Symposium synopsis, in *Spasticity: Disordered Motor Control,* vol. 487 (1980)
7. C. Andersson, E. Mattsson, Adults with cerebral palsy: a survey describing problems, needs, and resources, with special emphasis on locomotion. Dev. Med. Child Neurol. **43**, 76–82 (2001)

8. S.M. Day, Y.W. Wu, D.J. Strauss, R.M. Shavelle, R.J. Reynolds, Change in ambulatory ability of adolescents and young adults with cerebral palsy. Dev. Med. Child Neurol. **49**, 647–653 (2007)
9. J. Hutton, P. Pharoah, Effects of cognitive, motor, and sensory disabilities on survival in cerebral palsy. Arch. Dis. Child. **86**, 84–89 (2002)
10. L. Ahlborg, C. Andersson, P. Julin, Whole-body vibration training compared with resistance training: effect on spasticity, muscle strength and motor performance in adults with cerebral palsy. J. Rehabil. Med. **38**, 302–308 (2006)
11. E. Garcia, M. Cestari, D. Sanz-Merodio, Wearable exoskeletons for the physical treatment of children with quadriparesis, in *Humanoid Robots (Humanoids), 2014 14th IEEE-RAS International Conference on* (2014), pp. 425–430
12. K Cullen, Understanding space sickness, Department of Physiology, McGill University (2006)
13. J. Goldberg, G. Desmadryl, R. Baird, C. Fernandez, The vestibular nerve of the chinchilla. IV. Discharge properties of utricular afferents. J. Neurophysiol. **63**, 781–790 (1990)
14. G.J.M. Androwis, A. Peter, D. Jewaid, K.J. Nolan, R. Pilkar, A. Strongwater, R.A. Foulds, The effect of mechanical vestibular stimulation on electromyography onset in a child with cerebral palsy: a case study (2015)
15. G.J. Androwis, P.A. Michael, K.J. Nolan, A. Strongwater, R.A. Foulds, The effect of vestibular stimulation on knee angular trajectory and velocity in children with cerebral palsy, in *Biomedical Engineering Conference (NEBEC), 2015 41st Annual Northeast* (2015), pp. 1–2
16. G.J. Androwis, A. Strongwater, R.A. Foulds, Spasticity and dystonia differentiated via the equilibrium point hypothesis, in *Bioengineering Conference (NEBEC), 2014 40th Annual Northeast* (2014), pp. 1–2
17. G.J. Androwis, R.A. Foulds, A. Strongwater, D. Stone, Quantifying the effect of mechanical vestibular stimulation on muscle tone and spasticity, in *Bioengineering Conference (NEBEC), 2013 39th Annual Northeast* (2013), pp. 17–18

Digitalization and Artificial Intelligence Applied to Wearable Technologies and Ergonomics

A New Terrain Recognition Approach for Predictive Control of Assistive Devices Using Depth Vision

Ali H. A. Al-dabbagh and Renaud Ronsse

Abstract Vision based systems for terrain detection play important roles in mobile robotics, and recently such systems emerged for locomotion assistance of disabled people. For instance, they can be used as wearable devices to assist blind people or to guide prosthesis or exoskeleton controller to retrieve gait patterns being adapted to the executed task (overground walking, stairs, slopes, etc.). In this paper, we present a computer vision-based algorithm achieving the detection of flat ground, steps, and ramps using a depth camera. Starting from point cloud data collected by the camera, it classifies the environment as a function of extracted features. We further provide a pilot validation in an indoor environment containing a rich set of different types of terrains, even with partial occlusion, and observed that the overall system accuracy is above 94%. The paper further shows that our system needs less computational resources than recently published concurrent approaches, owing to the original transformation method we developed.

1 Introduction

The biomechanics of locomotion reveals that leg joints often produce mechanical energy in various locomotion tasks like walking or stair ascending. Moreover, each of these tasks corresponds to different kinetic and kinematic patterns, even in steady-state. As consequence, active prostheses or exoskeletons are necessary to provide disabled users with the capacity to display healthy gait patterns. The control of such devices should be adaptive to the task being executed (walking, taking stairs, etc.) and several researchers recently developed such adaptive algorithms, for instance

This work was supported by the Conseil de l'action internationale of UCLouvain.

A. H. A. Al-dabbagh (✉) · R. Ronsse
Institute of Mechanics, Materials, and Civil Engineering Institute of Neuroscience; and Louvain Bionics, Université catholique de Louvain, Louvain-la-Neuve, Belgium
e-mail: ali.aldabbagh@uclouvain.be

R. Ronsse
e-mail: renaud.ronsse@uclouvain.be

J. C. Moreno et al. (eds.), *Wearable Robotics: Challenges and Trends*,
Biosystems & Biorobotics 27, https://doi.org/10.1007/978-3-030-69547-7_71

by using finite state controllers [1]. However, switching from one locomotion mode to another, requires a timely transition, sometimes even before the critical time or event. Interestingly, computer vision-based terrain detection systems can provide such predictive information about the surrounding environment for some steps in advance. More specifically, systems with depth sensing can accurately detect and locate environmental features in 3D spaces [2].

2 Methods

We implemented a computer vision-based algorithm for terrain recognition using a depth camera. The raw point cloud data obtained from the depth camera passes through multiple processing steps to extract environmental features, and thus achieve terrain detection. These steps are shown in Fig. 1. First data are down-sampled and cropped in order to reduce computational load, since not all points bring a significant part of new information. Then, for each point, a normal vector is estimated from its

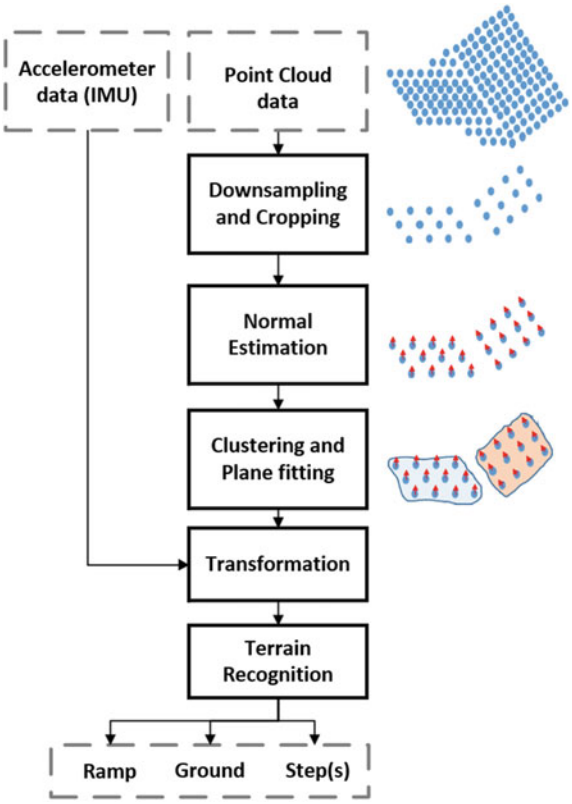

Fig. 1 Block diagram illustrating the overall terrain detection algorithm. Point cloud data acquired from a depth camera and its orientation obtained from an IMU sensor are its inputs. It provides a detection of the locomotion terrain(s), i.e. flat ground, stairs, and/or ramp, as output

neighboring points based on a Principal Component Analysis (PCA) [3]. After that, the point cloud data with their normals are passed to a clustering and plane fitting step. The point cloud data is clustered into several groups using a regional growing algorithm. It starts from a point with minimum curvature called *seed*, and expands the region to include neighboring points having quasi-parallel normals and similar curvature [3]. Next, a plane is fitted over each cluster using the RANdom SAmple Consensus (RANSAC) algorithm [4]. At the end of this step, the environment is thus segmented into several planes, whose 3D location is given by their centroid, and orientation is given by the orientation of their averaged normal vector. However, point cloud data acquired from a depth sensor are provided in a coordinate frame being centered on and oriented with the camera. This causes issues for proper in terrain detection, for instance in order to discriminate between a slope and ground. We mechanically fixed an IMU to the depth sensor in order to retrieve an estimate of its global orientation in space. The feature of the identified planes can then be rotated in the inertial frame. This approach is expected to be less computationally greedy than more classical transformations rotating the whole point cloud before feature extraction [3, 5, 6]. Finally, a classification tree is used for terrain recognition. It tests the transformed features of each plane with respect to several constraints, in order to detect the ground, ramp and step(s). We assigned specific colors to each detected type of terrains for visualization purpose. The algorithm was implemented in the Robot Operating System (ROS), and using the Point Cloud Library (PCL) [7]. The system was tested with six healthy subjects (4 males and 2 females aged between 27 and 32 years) by mounting the sensor and processing unit on subject's chest with a wearable tool. The subjects were asked to follow a pre-specified indoor path which contains stair and ramp in the UCLouvain campus. During the test, the path was cleared from obstacles and people.

3 Results and Discussion

Samples of the recognition results are shown in Fig.2a. The average detection accuracy for different locomotion modes is shown in Fig3. Our method reached above 90% average detection accuracy for all locomotion modes while the grand average accuracy is above 94%. In a second set of experiments, we quantified the computational cost of our algorithm, with a fixed camera on the same scene. We further compared it with a more standard approach consisting in rotating the point cloud back to the inertial frame before the feature extraction. Based on multiple trials, we observed that our method is about 20% cheaper in computational resources than an "all cloud transformation" method, at least for cloud sizes above 10^5 points. Finally, we conducted some pilot tests at stand still to assess the detection robustness with partially occluded terrains. This is important since real urban environments will likely be cluttered with other people or obstacles. Preliminary results showed that the algorithm is robust even if the terrain is partially occluded by an obstacle (see e.g. Fig. 2b), but further quantification is needed.

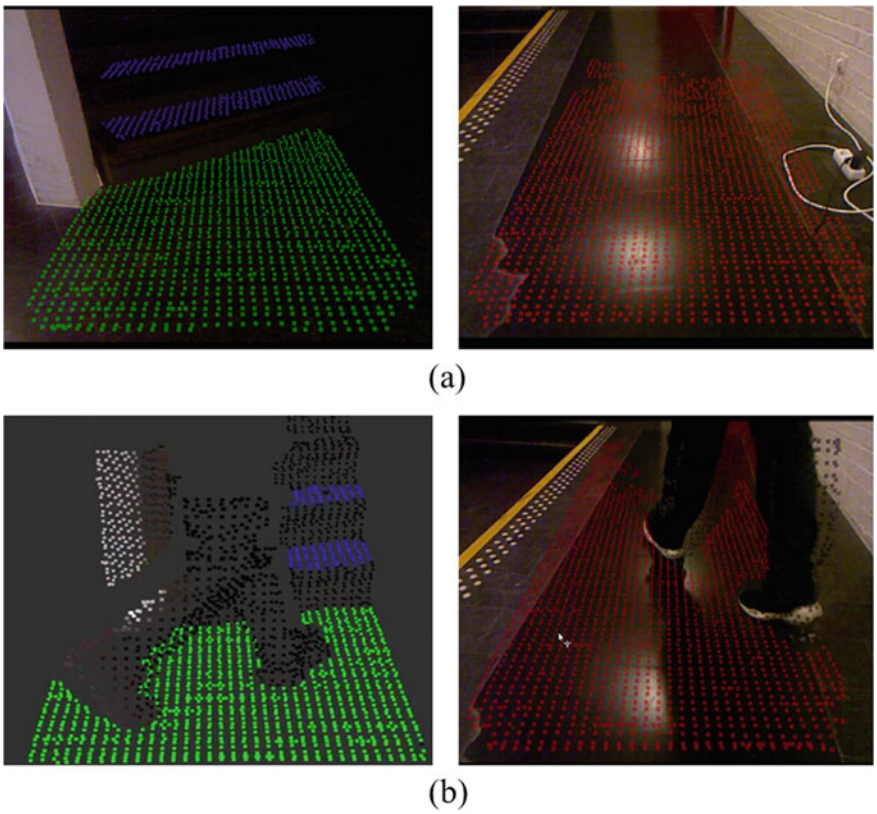

Fig. 2 Terrains recognition samples. Red points for ramp detection, blue points for capture step detection, and green points capture the main ground detection. **a** Clean environment. **b** Environment partly occluded by another walker

4 Conclusion

In this paper, a new terrain detection algorithm based on a depth sensing camera is presented. The system detects the main ground, steps and ramps with above 90% accuracy. It requires less computational time because we only transformed the plane features rather than the whole point cloud. Consequently, this approach is promising for wearable systems with limited processing capabilities. Further testing is ongoing in several indoor and outdoor environments in order to precisely quantify its detection abilities.

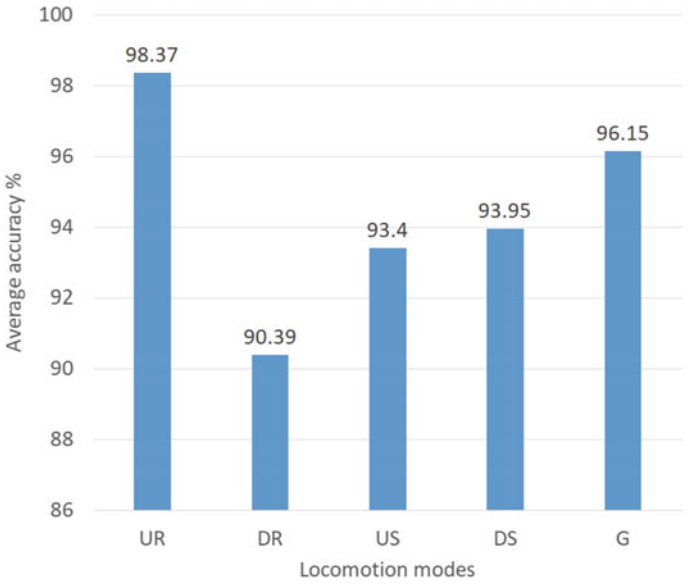

Fig. 3 Average accuracy for different locomotion modes for the all six subjects (UR: up ramp, DR: down ramp, US: up stairs, DS: down stairs, and G: ground-level)

References

1. M.R. Tucker, J. Olivier, A. Pagel, H. Bleuler, M. Bouri, O. Lambercy, J.R. Millán, R. Riener, H. Vallery, R. Gassert, Control strategies for active lower extremity prosthetics and orthotics: a review. J. Neuroeng. Rehabil. **12**(1), 1 (2015)
2. A.H. Al-dabbagh, R. Ronsse, A review of terrain detection systems for applications in locomotion assistance. Robot. Auton. Syst. 103628 (2020)
3. A. Perez-Yus, D. Gutiérrez-Gómez, G. Lopez-Nicolas, J. Guerrero, Stairs detection with odometry-aided traversal from a wearable rgb-d camera. Comput. Vision Image Understand. **154**, 192–205 (2017)
4. R.S. Consensus, M.A. Fischler, R.C. Bolles, A paradigm for model fitting with applications to image analysis and automated cartography **6**, 381–395 (1981)
5. N.E. Krausz, T. Lenzi, L.J. Hargrove, Depth sensing for improved control of lower limb prostheses. IEEE Trans. Biomed. Eng. **62**(11), 2576–2587 (2015)
6. K. Zhang, C. Xiong, W. Zhang, H. Liu, D. Lai, Y. Rong, C. Fu, Environmental features recognition for lower limb prostheses toward predictive walking. IEEE Trans. Neural Syst. Rehabil. Eng. **27**(3), 465–476 (2019)
7. R.B. Rusu, S. Cousins, Point cloud library (pcl), in *IEEE International Conference on Robotics and Automation* (2011), pp. 1–4

Simulation-Based Optimization Methodology for Designing a Workspace with an Exoskeleton

Zohar Potash, Jawad Masood, and Raziel Riemer

Abstract We present a preliminary concept of simulation-based optimization methodology framework for designing workspace with exoskeleton. The framework consists of three main elements human (ergonomic performance), workspace (industrial tasks, sub-tasks, environment, safety) and exoskeleton (assistance levels, robustness, workspace, imposed constraints), mathematical models and interactions that can converge to an optimal solution i.e. workspace design recommendations. We select the changing the drill bit in for the vertical drilling machine as an industrial task. The human and workspace mathematical modelling is performed using the Jack software and Process Simulate software. In future, we will focus on developing exoskeleton mathematical model and establish mathematical interaction between human model and the exoskeleton model.

1 Introduction

Work-related musculoskeletal disorders (MSDs) are responsible for 30% of lost workdays due to injury and result in annual costs of up to $54 billion in the US alone [1]. The major source of work-related costs due to MSDs is manual material handling tasks, such as lifting, carrying and lowering objects accounting for 36% of costs [2]. One way to reduce workloads and injuries is to change the workplace design. However, using method such as NIOSH lifting equation [3] or digital human model software's and changing the workplace design parameters require the design iterations that takes relatively along time thus in many cases the solution found although meet the ergonomics guideline may not be optimal in terms of productivity.

Z. Potash (✉) · R. Riemer
Biomechanics and Robotics Laboratory of the Ben-Gurion, University of the Negev, Beer-Sheva 84105, Israel
e-mail: zoharpo@post.bgu.ac.il

J. Masood
Processes and Factory of the Future Department of CTAG, Centro Tecnológico de Automoción de Galicia, O Porriño, Spain
e-mail: jawad.masood@ctag.com

J. C. Moreno et al. (eds.), *Wearable Robotics: Challenges and Trends*,
Biosystems & Biorobotics 27, https://doi.org/10.1007/978-3-030-69547-7_72

In order to keep the balance between the productivity and the ergonomic needs, a simulation-based optimization methodology for manual material handling tasks has been used to improve productivity while keeping the risk of injury below the ergonomic threshold [4]. Another popular approach in recent years is the adoption of exoskeleton that can assist in reducing the load from the worker [5, 6]. Yet the most common way to evaluate the exoskeletons is by conducting laboratory experiments that simulate the required work environment and task [7, 8], or by performing the field study with workers in several workplaces [9]. Industry experience can alleviate the obstacles to worker's acceptance that are not evident in a controlled laboratory environment [10]. However, these evaluations are time consuming and very expansive. Furthermore, many of the current exoskeletons are design for a single sub-task (e.g. lifting and depositing) and are inefficient for rest of the sub-tasks.

In this study, we will introduce the conceptual framework for simulation-based optimization methodology by integrating digital models of human and an exoskeleton including their interaction.

2 Method

The framework for integration of the exoskeleton into the design (as shown in Fig. 1) is based on three main components and their integration.

2.1 Digital Humans Motion (DHM)

It uses digital humans as representations of the workers inserted into a virtual environment or simulation to assist the prediction of performance and safety [11]. DHM

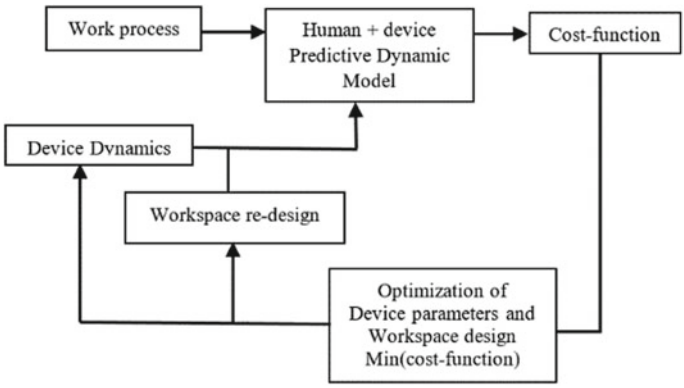

Fig. 1 Optimization-based design for a workplace with exoskeleton

includes biomechanics model, range of motion (ROM), visualizations of the human (appearance, skin, body dimensions).

2.2 Exoskeleton Modeling

We will develop an exoskeleton model that includes parameters such as assistive joint torques, forces, changes in the ROM and additional mass carried by the human and its relative position.

2.3 Optimization Methodology

Uses a framework for formulating workplace design as an optimization problem that maximizes productivity while maintaining ergonomic thresholds. Application of constraint optimization using genetic algorithm could be the best solution [4].

By using the exoskeleton and the human modeling it will be possible by test the effect of the different design parameter of the exoskeleton on the biomechanical loads in this optimization framework. The simulation will enable to examine the exoskeleton impact in the existing workspace. Furthermore, using the optimization problem will enable us to test both the possibility of changing the workspace with or without the exoskeleton to reveal the best possible solution. Further, we could also change the exoskeleton parameter with the aim of giving guideline for better design of an exoskeleton before acutely building and testing. Here we will demonstrate the idea of how results of such framework could assist the workspace and the exoskeleton design.

2.3.1 Step 1: Feeding Industrial Task Information

The figure performs lift of tool (15 kg) from a platform (table height 91.4 cm), carrying several meters, lifting to a machine (height 170 cm), re-grasp with the left hand and pressing a button located on the side (height 200 cm) with the right hand.

2.3.2 Step 2: Enriching the Mathematical Model

In the second step we will build a simulation that represents the task and add the forces acting on the body with the addition of the exoskeleton. This will be performed by modeling the rigid links and mechanism of the shoulder exoskeleton (support lifting tasks) and finding the location of the center of mass and inertia distribution of the device. We will include the information of the individual link mass-inertia to the corresponding body part of the human model. One interesting aspect is to consider

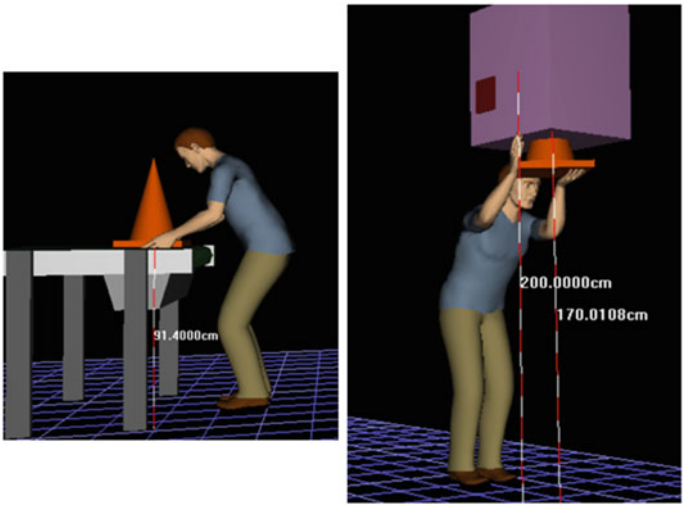

Fig. 2 Task demonstration in Jack software. Left-hand figure shows the worker is picking the drill bit from the storage bench. Right-hand figure shows the worker is mounting the drill bit in the vertical drilling machine

the mass distribution as close to the real exoskeleton device as possible. We can also estimate the physical joint constraints imposed by the exoskeleton on the human body. By limiting the human model joints can simulate the ROM effects of the exoskeleton. We will examine the forces acting on the shoulder with the help of the exoskeleton and examine the secondary effect on the lower back (due to weight gain). We will find the pressure points and the force/toque transfer points i.e. the interaction forces between the exoskeleton and the human. In this way we can generate a mathematical human model with exoskeleton information embedded. We can include the human anthropometry, exoskeleton and environmental constraints in step by step manner to increase the dimension of complexity of the optimization problem. The objective function will be to minimize metabolic cost and assembly time. The output will be the recommended trajectories of the human performing tasks by keeping the human in ergonomic limits and minimizing the metabolic consumption of the worker and maintenance time.

2.3.3 Step 3: Adjusting Exoskeleton Configuration Settings

In the third step, we will explore the possibilities of changing exoskeleton parameters and redesigning the workspace to maximize productivity while keeping the boundaries of the ergonomics away.

3 Conclusion

The preliminary conceptual framework for simulation-based optimization methodology for designing a workspace with an exoskeleton is presented. We have already verify the workspace and human simulation using Jack and Process. Future research is needed to validate and verify the full framework and understand the shortcoming of the approach. Future efforts will consists of development of the exoskeleton mathematical model and defining constraints to generate a high fidelity exo-human digital interaction.

Acknowledgements This work was supported by the Processes and Factory of the Future Department of CTAG—Centro Tecnológico de Automoción de Galicia.

References

1. P.M. Harris, *Nonfatal Occupational Injuries Involving the Eyes, 2004* (Compensation and working conditions online US Department of Labor, Bureau of Labor Statistics, 2008)
2. P.L. Murphy, G.S. Sorock, T.K. Courtney, B.S. Webster, T.B. Leamon, Injury and illness in the American workplace: a comparison of data sources. Am. J. Ind. Med. **30**(2), 130–141 (1996)
3. H. D. of Biomedical and B. Science, *Work Practices Guide for Manual Lifting* (US Department of Health and Human Services, Public Health Service, Centers..., 1981), no. 81–122
4. Y. Harari, A. Bechar, R. Riemer, Simulation-based optimization methodology for a manual material handling task design that maximizes productivity while considering ergonomic constraints. IEEE Trans. Human-Mach. Syst. **49**(5), 440–448 (2019)
5. M. Wehner, D. Rempel, H. Kazerooni, Lower extremity exoskeleton reduces back forces in lifting, in *Dynamic Systems and Control Conference*, vol. 48937 (2009), pp. 49–56
6. N. Sylla, V. Bonnet, F. Colledani, P. Fraisse, Ergonomic contribution of able exoskeleton in automotive industry. Int. J. Ind. Ergon. **44**(4), 475–481 (2014)
7. P.H. Crowell, J.H. Park, C.A. Haynes, J.M. Neugebauer, C.A. Boynton, Design, evaluation, and research challenges relevant to exoskeletons and exosuits: a 26-year perspective from the us army research laboratory. IISE Trans. Occupational Ergon. Human Fact. **7**(3–4), 199–212 (2019)
8. T. Luger, T.J. Cobb, R. Seibt, M.A. Rieger, B. Steinhilber, Subjective evaluation of a passive lower-limb industrial exoskeleton used during simulated assembly. IISE Trans. Occupational Ergon. Human Fact. **7**(3–4), 175–184 (2019)
9. R. Hensel, M. Keil, Subjective evaluation of a passive industrial exoskeleton for lower-back support: a field study in the automotive sector. IISE Trans. Occupational Ergon. Human Fact. **7**(3–4), 213–221 (2019)
10. S. Spada, L. Ghibaudo, S. Gilotta, L. Gastaldi, M.P. Cavatorta, Investigation into the applicability of a passive upper-limb exoskeleton in automotive industry. Proc. Manuf. **11**, 1255–1262 (2017)
11. H.O. Demirel, V.G. Duffy, Applications of digital human modeling in industry, in *International Conference on Digital Human Modeling* (Springer, 2007), pp. 824–832

Optimizing Active Spinal Exoskeletons to Minimize Low Back Loads

Giorgos D. Marinou and Katja D. Mombaur

Abstract The design and control of exoskeletons is not a straight forward task and presents a lot of challenges. Especially in cases of preventing biomechanical damages, for example low back loads, exoskeletons should be able to provide the necessary amount of support without hindering or hurting the user in any way. To this extend, this study exploits optimal control to evaluate cost functions that minimize (a) cumulative low back loads, (b) peak low back loads and (c) a combination of the previous, while constraining contact (interaction) forces between human and exoskeleton. The results are compared to a kinematic reconstruction from a human without exoskeleton performing the same task of lifting a 10 kg box. Cost function (c) performs the best in terms of achieving an equilibrium between minimizing cumulative and peak lumbar torques—subject to the actuator's torque and speed limit—reducing the peak torque by 48%.

1 Introduction

LOWER back injuries and consequently low back pain is one of the most prevalent hazards within the working environment and especially in industrial settings [1]. Recent developments and potential applications of wearable assistive technologies are exponentially increasing. In the context of alleviating lower back loads a few solutions have been researched or even commercialized, including passive [2–4] and active [5–7] exoskeletons. One of the current challenges still, is predicting appropriate support torques for both the passive and active elements of exoskeletons as to alleviate low back loads whilst ensuring comfort of the user. By the means of optimization,

G. D. Marinou (✉)
Optimization, Robotics and Biomechanics Lab, Institute of Computer Engineering (ZITI), Heidelberg University, Heidelberg, Germany
e-mail: giorgos.marinou@ziti.uni-heidelberg.de

K. D. Mombaur
Canada Excellence Research Chair in Human-Centre Robotics and Machine Intelligence, Systems Design Engineering & Mechanical and Mechatronics Engineering, University of Waterloo, Waterloo, Canada

J. C. Moreno et al. (eds.), *Wearable Robotics: Challenges and Trends*,
Biosystems & Biorobotics 27, https://doi.org/10.1007/978-3-030-69547-7_73

the mechanical design of the passive elements can be informed as to provide optimal support [8]. For the active parts of the exoskeleton, optimal control can provide optimal torque profiles for specific motions, such as the stoop lift investigated in this paper.

Based on the development of spinal exoskeletons in the European project SPEXOR [9] and building upon previous work on predicting human lifting motions using optimal control to minimize muscle activation at all joints [10], this study aims to use appropriate cost functions in order to minimize both cumulative and peaks torques [11] about the lumbosacral joint L5/S1 and produce optimal torque profiles for a hip joint hydraulic actuator. We evaluate and present the results in terms of lumbar moments reduction compared to an unassisted motion and moreover investigate the torque profiles yielded for the hip actuator.

2 Methods

Dynamic multibody system models of human and exoskeleton are created according to mass, inertia properties and segment lengths. A stoop lift has been recorded and according to that we track the kinematics and reconstruct the motion using optimal control and a least squares objective function on errors in the trajectory. We also use optimal control to predict a stoop lift with minimum lumbar moments, according to the cost functions detailed below. The following sections describe the modeling pipeline, optimal control problem (OCP) formulations and the evaluation of the cost functions used.

A. *Modeling*

Through collecting anthropometric data, subject-specific dynamic models of the human are created. They are combined with a corresponding spinal exoskeleton model of an active prototype developed in SPEXOR. Both models are represented by rigid 2D multibody systems that are projected in the sagittal plane. We model the human body as a planar floating base, that consists of 11 segments (pelvis, trunk, head, thighs, shanks, feet, upper arms forearms incl. Hands) and has 13 degrees of freedom (DOF), including a complex lumbar joint which resembles the L1–L5 vertebrae and assumes symmetry. For actuating the human, we use direct torques at each joint, limited by the estimated maximum torques in positive and negative direction. The exoskeleton model consists of 5 segments (pelvis, thigh and upper torso brace modules, torso beams, thigh interface carrying the actuator) with a total of 8 DOF. Unique to the SPEXOR exoskeleton model are three passive beams—placed at the back of the torso—with a spring-like behavior which produce a torque between lumbar and torso module, and two hydraulic actuators which produce torques at the level of the hips. The dynamics governing the motion are solved using the Rigid Body Dynamics Library (RBDL) [12]. We use kinematic constraints to attach the exoskeleton to the body, the feet to the ground and the hands on the box.

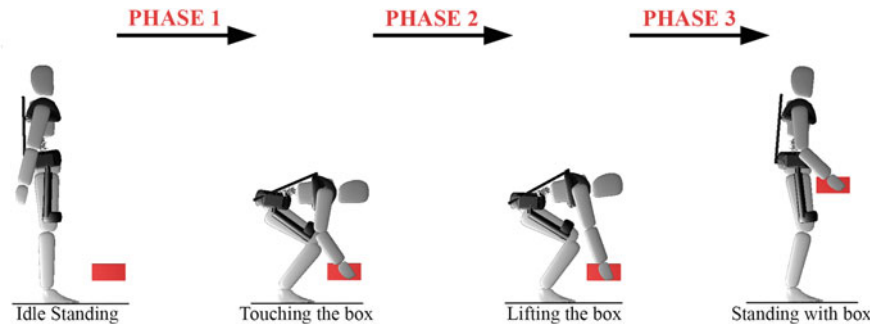

Fig. 1 The stoop lifting motion as formulated in the three different phases of the OCP: standing, lifting and standing back up again.

B. *OCP Formulation*

We use optimal control to solve two different types of problems: (A) Kinematic reconstruction of motion capture data and (B) Optimization and prediction of a stoop type lifting motion. Identical to both problems is the number of phases the problem is split in (Fig. 1).

For *problem (A)* and the human-only OCP, we solve a least-squares fitting problem where the experimental motion is tracked and the distance between the computed and captured positional coordinates is minimized.

For *problem (B)* we explore three different types of cost functions:

- Minimization of cumulative lumbar torques

$$\int_{t_i}^{t_{i+1}} \left\| \boldsymbol{u}^{lum} \right\|_2^2 \mathrm{d}t \tag{1}$$

- Minimization of peak lumbar torques

$$\int_{t_i}^{t_{i+1}} \left\| \boldsymbol{u}^{lum} \right\|_2^4 \mathrm{d}t \tag{2}$$

- Minimization of cumulative and peak lumbar torques

$$w_1 \int_{t_i}^{t_{i+1}} \left\| \boldsymbol{u}^{lum} \right\|_2^2 + w_2 \left\| \boldsymbol{u}^{lum} \right\|_2^4 \mathrm{d}t \tag{3}$$

where w_1 and w_2 are given weights to the objective function terms to emphasize the importance of each and $\boldsymbol{u}^{lum}$ are the controls of the lumbar vertebrae L1–L5. Identical to both problems, are the contact constraints we enforce between the human and the exoskeleton, to ensure comfort well under pain limits. For the prediction of the motion, we suggest the initial values of the state vector in our OCP with the data captured in the experiment. For optimizing we use the direct multiple shooting method implemented in MUSCOD-II [13].

3 Results and Discussion

In investigating the effect of the exoskeleton through cost functions (2)–(4), it is clear that there is an evident reduction in both cumulative and peak lumbar moments. For the cumulative-OCP we can see a reduction to a peak moment of 180 Nm and cumulative moments of 119 Nm. For the peak-OCP, peak moments were reduced to 110 Nm and cumulative moments to 150 Nm. Finally, for the hybrid-OCP, peak moments were reduced to 140 Nm and cumulative ones to 135 Nm. In Fig. 2b it is clear that the human subject had a small range of motion when it comes to lumbar flexion as the angle is much lower than for the optimized with-exoskeleton OCPs. The lumbar flexion angles for the with-exoskeleton OCP resemble the L5 moments in terms of magnitude, as we can see that the highest peaks in moments were performed by the cumulative-OCP where we can also see the highest lumbar flexion angles at the point lifting the box from the ground.

Figure 2c shows the contributions of the hydraulic actuator at the hip and the beams at the back of the torso. We can see that they follow a similar shape throughout the motion of lifting the box, with the highest contributions being at the second phase between touching and beginning to lift the box. Figure 2c shows that with higher actuator output, for example the hybrid-OCP, the lumbar flexion angle observed in Fig. 2b is smaller throughout the motion, so the actuator manages to reduce the human lumbar flexion.

Especially when observing Fig. 2a, it is clear that the hybrid OCP performs in the best way in terms of concluding to a desired equilibrium between minimum peak and cumulative torques. In terms of cumulative low back loads, the area under the graph is less than the cumulative OCP and the peak moment is less than the peak of the cumulative OCP.

4 Conclusions

Based on the study performed in evaluating three different cost functions for minimizing cumulative and peak lumbar torques, we have successfully managed to identify a hybrid cost function that minimizes both with respective weights. We successfully predicted and tailored the torque profiles of exoskeleton actuators according to

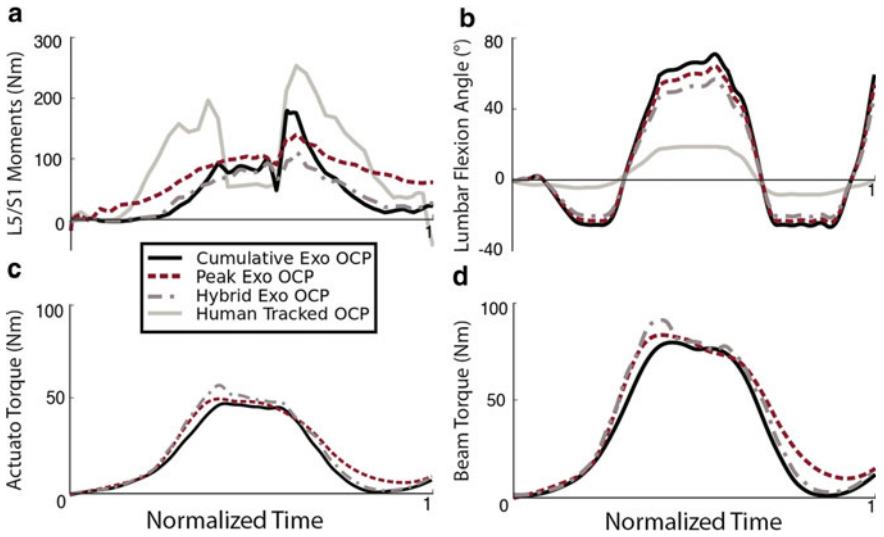

Fig. 2 Effect of exoskeleton through the different cost functions on **a** Lumbar moments and **b** lumbar flexion angles compared to the tracked motion of only human. **c** and **d** represent contributions from hydraulic actuator and torso beams respectively

reconstructed human lifting motions. Lumbar loads are significantly reduced with respect to unassisted human movement and also previous work done with equally minimizing muscle activations on all joints. This work motivates further research in using optimization and optimal control for predicting the control and assistance levels for active exoskeletons.

Acknowledgements This project has received funding from the European Union's Horizon 2020 research and innovation program under grant agreement No. 687662.

References

1. Murtezani, Folia Medica **53**(3), 68–74 (2011)
2. Koopman, J. Biomech **83**, 97–103 (2019)
3. Abdoli-Eramaki, J. Biomech. **40**, 1694–1700 (2007)
4. Ulrey, J. Electromyogr. Kinesiol. **23**, 206–215 (2013)
5. Luo, *IEEE International Conference on Mechatronics and Automation* (2013), pp. 230–236
6. Kozlowski, *Mobile Service Robotics*, 1st ed. (2014), pp. 53–60
7. Muramatsu, *Proceedings of the 35th International Conference on the IEEE Engineering Medicine and Biology Society* (2013), pp. 2844–2849
8. M. Harant, *IEEE-RAS 17th International Conference on Humanoid Robotics* (2017), pp. 535–540
9. Millard, *Frontiers in Robotics and AI*, vol. 4 (2017), p. 41
10. Coenen, J. Occup. Rehabil. **23**(1), 11–18 (2013)

11. J. Babič, SN Appl. Sci. 262 (2019)
12. M.L. Felis, RBDL: an efficient rigid-body dynamics library using recursive algorithms. Auton. Robot. **41**(2), 495–511 (2016). https://doi.org/10.1007/s10514-016-9574-0
13. D.B. Leineweber et al., Comput. Chem. Eng. (2013)

LSTM and CNN Based IMU Sensor Fusion Approach for Human Pose Identification in Manual Handling Activities

Enrique Bances, Adnan Mushtaq Ali Karol, and Urs Schneider

Abstract In recent years, human pose estimation has become a very important research topic in the context of control engines, and exoskeletons. In this paper, we propose a Long Short-Term Memory (LSTM) and Convolutional Neural Networks (CNN) based Hybrid Deep Neural network, aimed to estimate human pose while handling of loads. The proposed model is capable to identify three such activities, i.e. load lifting from the ground, load shifting, and uplifting of the load. For this purpose, a inertial sensor unit (IMU)-based system was developed to collect the raw data. Next, to obtain more robust and accurate results, Kalman filtering has been used as a fusion technique. Rigorous fine-tuning and simulations show that the model obtained from the Kalman filtering achieves better results as compared to the raw data. Our proposed model can classify the target activities with a test accuracy of 86%.

1 Introduction

Industries, like logistics and warehouses, are labor-intensive as well as physically demanding, where heavy manual material handling is often required which introduces unhealthy work postures. Hence, the workers are exposed to the danger of developing work-related musculoskeletal disorders (MSD). MSDs are one of the most common work-related complaints, affecting millions of workers and costing billions of euros. For instance, in 2015, more than 61% of workers reported some kind of MSD in Europe [8], increasing by 21% compared to the previous study carried out in 2012 [9]. Wearable exoskeletons could offer an alternative solution to this problem of heavy weight-lifting since it helps to reduce fatigue.

One of the powered exoskeletons challenges in the development is the complex algorithms to assure security, confort and, energy efficiency. An AI model could help to optimize the control system implementation. Once the activities that are being

E. Bances (✉) · A. M. A. Karol · U. Schneider
Institute of Industrial Manufacturing and Management-IFF, University of Stuttgart, Nobelstr 12, 70569 Stuttgart, Germany
e-mail: nelson-enrique.bances-purizaca@iff.uni-stuttgart.de

J. C. Moreno et al. (eds.), *Wearable Robotics: Challenges and Trends*,
Biosystems & Biorobotics 27, https://doi.org/10.1007/978-3-030-69547-7_74

performed are identified, it is possible for the exoskeleton to infer information and change the state of the mechanical system, like the torque and the angular velocity of motors for an activity.

In this work, we identify three such activities, i.e. holding (label '0'), carrying (label '1'), and lifting (label '2'), based on a long short-term memory (LSTM) [4], as well as convolutional neural networks (CNN) model using IMU sensor fusion data.

2 Related Work

Sensor Fusion was used for human activity recognition such as sitting, lying, standing, washing dishes, vacuuming, sweeping, walking, ascending stairs, descending stairs, treadmill running, and bicycling. After the analysis of different types of filters for the sensor, Kalman filter and complimentary filter were suggested [1].

Human activities pose identification, like, eating, driving, and cooking are predicted using an Apple watch on the right-hand using LSTM architecture. The proposed dataset HAD-AW with LSTM gave an accuracy of 0.953 as compared to the existing datasets [2]. In addition, work involving exoskeletons and classification use additional force sensors for task classification, to lift and to lower, with FSR (Force Sensing Resistor) to dynamically detect weight differences in an exoskeleton device [3].

3 Model Architecture and Description

An IMU-based suit was implemented to collect data. Two IMU sensors were used to record data, which were placed on the spinal cord and the right arm of the person. IMU 9DoF was used, which measures the accelerometer, gyroscope, and the magnetometer values along the three-axis. The model consists of LSTM layers with Adam algorithm (adaptive moment estimation) as the optimizer and the learning rate of 0.0001. Convolution layers were also used to increase overall accuracy. Two different models were created, one for the sensor raw values and another for sensor fusion values. Categorical-cross entropy was used as the loss function in both models. For training and validation, the dataset was divided into 0.8 and 0.2 ratios. All the experiments have been performed in Google Colab with GPU and 12GB RAM.

4 Model Implementation

No relatable data with respect to the problem statement was available and thus a dataset had to be created. The dataset was recorded by 20 people performing each activity to be recognized 10 times with a proper hardware setup. The data was then

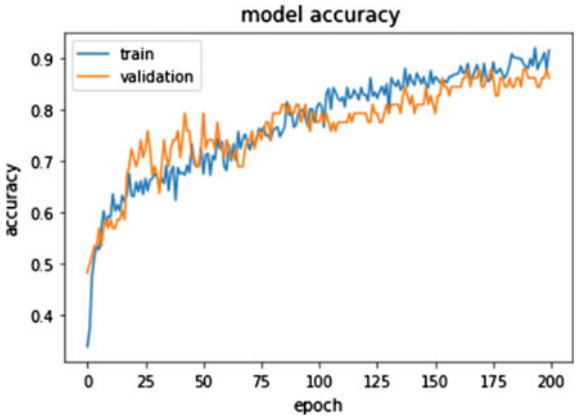

Fig. 1 Training performance of sensor fusion model

preprocessed following steps like data cleaning, a grouping of sequential data, missing values imputation, and normalization. Two different datasets were obtained: one consisting of the raw values and one consisting of the Kalman filter-based sensor fusion values. Finally, these datasets were used to train the Neural Network model for Classification. To establish the potential of the sensor fusion data, two different models were trained, i.e. one model for sensor fusion data and another model for the raw data. Finally, the model's performance was compared based on the accuracy and time complexity.

5 Results

With the models, the accuracy in the case of raw data was 35.2% and in the case of sensor fusion data, it was 85.7%. The model was also deployed in real-time on a raspberry pi IV and the time complexity was 3.649 s. Figure 1 shows the accuracy as a function of a number of epochs for the training and the validation set. It shows when training accuracy is bigger than the validation accuracy, there is no overfitting.

6 Analysis of Results

From the confusion matrix shown in Fig. 2, for the sensor fusion data, we infer that the model is able to distinguish class label '1', i.e. carrying the load, more accurately as compared to the other two class labels.

In 20.8% test cases, the model predicts class label '2', but the ground truth is the class label '0'. Similarly, in 21.2% test cases the model predicts class label '0' when the ground truth is the class label '2', i.e. lifting the load above the shoulder.

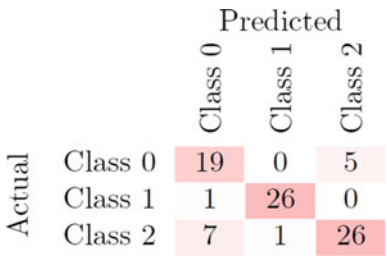

Fig. 2 Confusion matrix—fusion model

One probable reason for this is due to the overlapping of data for some particular cases. The class label '0' indicates holding a box (and then to keep it in front of him), whereas the class label '2' indicates lifting the box above the shoulder. Clearly there can be cases where the person while holding the box and keeping it in front (class label '0'), keeps the box higher than other people, and the activity becomes close to class label '2'. This results in the model getting confused between the class labels '0' and '2'. The Confusion matrix for the sensor fusion data is shown in Fig. 2.

The model having a relatively small dataset as compared to previous activity recognition system performs well enough. We also conclude that usage of sensor fused data significantly improves the models accuracy.

7 Conclusions

In this project, an LSTM and CNN based architecture was adopted to classify the activities. The evaluation results show that the model performs better on the sensor fusion data as compared to the raw data. Also, with the raw data more variable's come into the picture leading to memory constraints.

One of the major drawbacks is the lacked data set. Different people can perform the activity at different speeds, orientations, manners, etc. This leads to the dropin test accuracy. Larger data set can be a key feature to improve the performance of the model.

Another future scope is to improve the speed of classification. This can be done by using data quantization to generate a TensorFlow lite model which can be run on the Raspberry Pi.

After successful classification of the activity, another significant extension of this project is to automatically adjust the parameters of the motor according to the activity being performed in order to avoid injuries and to increase the efficiency of the exoskeleton. With proper activity recognition, the control algorithms for the exoskeleton can be more robust and digitize the system to an even further extend.

Acknowledgements Supported by the Deutsche Forschungsgemeinschaft (DFG, German Research Foundation) under Germany's Excellence Strategy - EXC 2120/1 - 390831618.

References

1. H.F. Nweke, Y.W. Teh, G. Mujtaba, U.R. Alo, M.A. Al-garadi, Multi-sensor fusion based on multiple classifier systems for human activity identification. Human-Centric Comput. Inf. Sci. **9**(1), 34 (2019)
2. S. Ashry, R. Elbasiony, W. Gomaa, An LSTM-based descriptor for human activities recognition using IMU sensors, in *Proceedings of the 15th International Conference on Informatics in Control, Automation and Robotics, ICINCO*, vol. 1 (2018), pp. 494–501
3. L.A. Mateos, Characterizing Lifting and Lowering Activities with Insole FSR sensors in industrial exoskeletons (2017). arXiv:1706.05440
4. S. Hochreiter, J. Schmidhuber, Long short-term memory. Neural Comput. **9**(8), 1735–1780 (1997)
5. Y. Kim, H. Bang, Introduction to Kalman filter and its applications by Submitted: April 26th 2018, Reviewed: July 30th 2018, Published: November 5th 2018. https://doi.org/10.5772/intechopen.80600
6. European foundation for the improvement of living and working conditions, in *First Findings: Sixth European Working Conditions Survey: Résu-mé* (Publications Office, 2015)
7. D. Anxo, C. Franz, A. Kümmerling, Working time and work–life balance in a life course perspective: a report based on the fifth European working conditions survey (Eurofound, 2013)
8. European Foundation, for the improvement of living and working conditions and others, in *First Findings: Sixth European Working Conditions Survey* (Publications Office, 2015). ISBN: 978-92-897-1429-7. https://doi.org/10.2806/59106
9. D. Anxo, C. Franz, A. Kümmerling, Working time and work–life balance in a life course perspective: a report based on the fifth European working conditions survey (Eurofound, 2013). http://urn.kb.se/resolve?urn=urn:nbn:se:lnu:diva-30766

Visual Feedback Strategy Based on Serious Games for Therapy with T-FLEX Ankle Exoskeleton

Angie Pino, Daniel Gomez-Vargas, Marcela Múnera, and Carlos A. Cifuentes

Abstract Therapies with repetitive exercises can result in a lack of interest and motivation of the patient. Therefore, the inclusion of feedback strategies, such as serious games, evidences a significant improvement in those aspects. This paper presents the development and a preliminary validation with a healthy subject of a visual and interactive interface based on serious games for the rehabilitation of patients with ankle dysfunctions. The results show a high level of adaptation of the user to the interface and positive perception in this application.

Keywords Serious games · Ankle exoskeleton · Gait rehabilitation · Visual feedback · Movement intention detection

1 Introduction

Physical therapy aims to counteract stroke after-effects and provide independence to the survivor. However, different studies associated with the inclusion of robotic devices present promising results (e.g., ankle exoskeletons) in the motor recovery of the patient [1].

Specifically, the T-FLEX ankle exoskeleton improved motor recovery during 18 sessions of repetitive movements [2]. Nevertheless, the study exhibited a lack of interaction and patient attention in the session [2]. Considering that repetitive exercises can result in low motivation and tedious experience [3], the use of T-FLEX could have better results.

A. Pino · D. Gomez-Vargas · M. Múnera · C. A. Cifuentes (✉)
Department of Biomedical Engineering, Colombian School of Engineering Julio Garavito, Bogota, Colombia
e-mail: carlos.cifuentes@escuelaing.edu.co

A. Pino
e-mail: angie.pino-l@mail.escuelaing.edu.co

D. Gomez-Vargas
e-mail: daniel.gomez-v@mail.escuelaing.edu.co

M. Múnera
e-mail: marcela.munera@escuelaing.edu.co

J. C. Moreno et al. (eds.), *Wearable Robotics: Challenges and Trends*,
Biosystems & Biorobotics 27, https://doi.org/10.1007/978-3-030-69547-7_75

Several studies evidenced increases in motivation, effort, and active engagement when included visual feedback strategies [4]. In the ankle joint, the inclusion of visual feedback improved patients' balance, which is related to the continuous visual information provided for stimulating the motor area of the brain [4]. Furthermore, interactive feedback strategies, or serious games applied in rehabilitation, proved to be solutions for the discouragement found in long-term therapies and efficient gait rehabilitation [5].

This paper presents the development of a visual and interactive interface based on serious games for the rehabilitation of patients with ankle dysfunctions in three parts: (1) serious game development, (2) user intention strategy, and (3) a preliminary validation.

2 Materials and Methods

The proposed system for the visual feedback strategy (see Fig. 1) includes (1) an ankle exoskeleton to assist the dorsi-plantarflexion movements, (2) a graphic interface based on serious-games to motivate the patient, and (3) an inertial sensor to detect the user's movement intention to control the avatar of the game.

2.1 Visual Interface Design

The interface's virtual environment covers a retro type design based on the open-source game Jumping Guy (see Fig. 2). The game incorporates a calibration stage to assess the user's movement intention, which could be adjusted to increase the difficulty [3]. Moreover, the interface has a tutorial that shows and explains the functionalities and the playing mode looking for easy user adaptation.

The game's goal consists of jumping to avoid enemies through the movement intention explained in the next section. The game has three levels with different characteristics (i.e., the frequency of enemies and graphic design). The first level induces a dorsi-plantarflexion every 3 s, the second every 2 s, and the third every 1.5

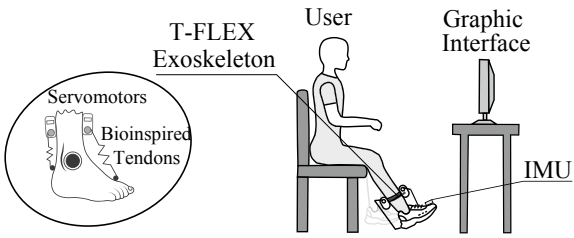

Fig. 1 System setup proposed for the visual feedback strategy

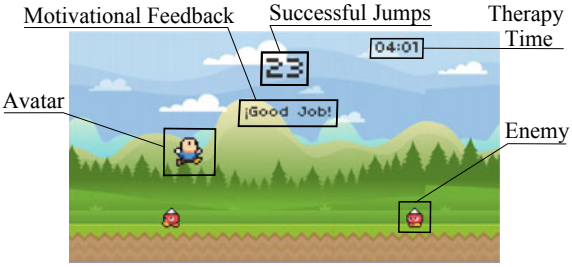

Fig. 2 Interface design based on serious-games for ankle rehabilitation

s. The selected frequencies intend to increase the therapy's intensity and counteract the adaptation period in repetitive exercises [2].

The interface provides feedback for both preserving the motivation and indicating the user's progress and achievement. Finally, a database store the information acquired in the session to compare the session with previous results, as well as encouraging the patient to perform the therapy [3, 5]. The interface and functionalities were developed in Unity (Unity Technologies, Denmark).

2.2 User Movement Intention

An inertial sensor (100 Hz, BNO055, Bosch, Germany), located on the paretic foot tip, estimates the user movement intention. Initially, a 4th-order Butterworth low-pass filter (cutoff 6 Hz) removes the noise from the angular velocity along the sagittal plane. In the calibration stage, the user performs five movements to define the threshold value. Once in the game, the filtered data is compared in real-time with the threshold value calculated in the calibration stage. This way, the avatar jumps, and the exoskeleton executes a repetition when the angular velocity is larger than the threshold. The user intention module runs in the Robotic Operating System (ROS) on a Raspberry Pi 3.

2.3 Preliminary Validation

The experimental protocol intends to assess the healthy subject's usability and adaption (i.e., female, 20 years old, without cognitive and motor-related pathologies) to the graphical interface using the T-FLEX exoskeleton.[1] For that, the participant accomplished the three levels of the game in two conditions: (1) wearing and (1) without using the device. The participant executed each level with both conditions for

[1] The Research Ethics Committee of the Colombian School of Engineering Julio Garavito approved this protocol. The researchers informed the participant about the scope and purpose of the experiment, obtaining her written consent before the study.

5 min, and rested for 5 min between trials. For the wearing state, T-FLEX performed a dorsi-plantarflexion repetition after detecting the user movement intention. This repetition was executed concerning the user's range of motion and with a frequency 1 Hz between movements. In the user adaptation context, the interface registered different parameters of the interaction for each level in both conditions, such as the success rate, the movement detected to trigger the device, and the time response to jump the obstacle. Lastly, the participant completed a QUEST survey to measure the user's perception to the setup proposed.

3 Results and Discussion

The participant exhibited high success rates for the condition without the device (i.e., 98.9% in the first level, 98.0% in the second level, and 96.5% in the third). The inclusion of T-FLEX showed no significant difference in those rates, obtaining values between 94% and 96%. This way, the increase in the repetition frequency (i.e., the game level) led to a higher probability of failures for jumping the obstacle.

Figure 3 shows the participant's response during the first level in terms of the user response to avoid the obstacle (i.e., ideal, late, early, or failure in the jump). The blue elements represent the trial without the device, and the orange indicates the condition using T-FLEX. Concerning the condition using T-FLEX, the response time presented more alterations related to early and late executions (i.e., 0.15 s before and 0.34 s late of the ideal jump, respectively). Nevertheless, the response was enough to jump the obstacle.

In short, the participant accomplished the three levels in both conditions with a high success rate. Therefore, the results indicate a high level of adaptability of the user to the interface proposed. Likewise, the preliminary results show an improvement in comparison with other studies, where the success rate, in the condition using a robotic device, was close to 70% [6]. Nevertheless, this study has one participant. Consequently, an experimental validation with a group of participants is necessary to verify these results.

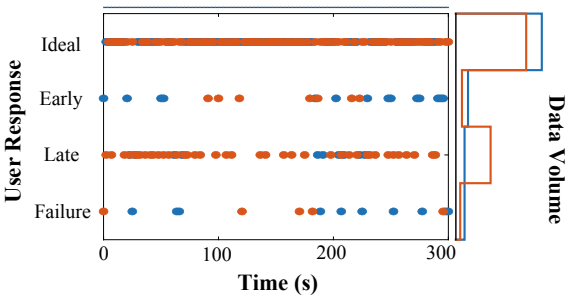

Fig. 3 User progression during the first level. The orange color represents the trial with T-FLEX, and the blue color shows no device condition. The right graph exhibits the data volume for each state

Table 1 QUEST survey responses

QUEST item	Level of satisfaction
Dimensions (size, height, length, width)	5
Weight	4
Adjustments (fixing, fastening)	3
Safety (secure)	5
Ease of use	5
Comfort	3
Effectiveness	4
Device satisfaction	4

For the user perception about the interface, Table 1 resumes the user's QUEST responses after the protocol. The values are assessed on a scale of 0–5, being 0 the lowest score. The device satisfaction was 4 of 5, which evidence an appropriate interaction of the user with the interface proposed. The participant remarked aspects such as ease of use, safety, and effectiveness.

4 Conclusions and Future Works

This paper presented the development of a visual and interactive interface intended to be used in therapies of people with ankle dysfunctions. The results showed a high adaptation of the user to the interface and positive perception in the preliminary validation. Likewise, the system worked properly and did not evidence to be unsafe. However, the experiment showed is only an initial trial with one subject. Hence a validation with a significant group is necessary to verify these promising results. The future works should be focused on assessing of the interface in patients with ankle dysfunctions in a rehabilitation scenario to determine the effectiveness and improvements in motor recovery.

Acknowledgements This work was supported by MinCiencias Colombia (grant ID No. 801-2017) and (grant ID No. 845-2020), and funding from the Colombian School of Engineering Julio Garavito (ECIJG).

References

1. T. Mikolajczyk, I. Ciobanu, D.I. Badea, et al., Advanced technology for gait rehabilitation: an overview. Adv. Mech. Eng. **10**(7) (2018)
2. D. Gomez-Vargas, M.J. Pinto-Bernal, F. Ballen-Moreno, et al., Therapy with t-flex ankle-exoskeleton for motor recovery: a case study with a stroke survivor, in *8th IEEE RAS & EMBS*

International Conference on Biomedical Robotics and Biomechatronics (BioRob) (2020)
3. N. Barrett, I. Swain, C. Gatzidis, et al., The use and effect of video game design theory in the creation of game-based systems for upper limb stroke rehabilitation. J. Rehabil. Assist. Technol. Eng. **3** (2016)
4. S.-N. Jeon, J.-H. Choi, The effects of ankle joint strategy exercises with and without visual feedback on the dynamic balance of stroke patients. J. Phys. Therapy Sci. **27**(8), 2515–2518 (2015)
5. K. Lohse, N. Shirzad, A. Verster et al., Video games and rehabilitation: using design principles to enhance engagement in physical therapy. J. Neurol. Phys. Therapy **37**(4), 166–175 (2013)
6. G. Asín-Prieto, A. Martínez-Expósito, F.O. Barroso et al., Haptic adaptive feedback to promote motor learning with a robotic ankle exoskeleton integrated with a video game. Front. Bioeng. Biotechnol. **8**, 113 (2020)

The Utilization Effects of Powered Wearable Orthotics in Improving Upper Extremity Function in Persons with SCI: A Case Study

Ghaith J. Androwis, Steven Kirshblum, and Guang Yue

Abstract Persons with upper extremity (UE) impairments due to spinal cord injury (SCI) have limited capacity to move or perform basic activities of daily living (ADL). Such movement limitations significantly reduce a patient's quality of life (QOL) and level of independence. Restoration of UE motor function in people with SCI remains a high priority in rehabilitation and in the field of assistive technology. UE myoelectric powered wearable orthoses (UE-MPWO) specifically designed to restore wrist/hand movements may help fill the gap by increasing strength of the participating muscles, range of motion (ROM) of the joints, and ability to perform daily tasks involving using wrist/hand in persons with SCI. The goal of this study was to evaluate the effects of the UE-MPWO (MyoPro) in ameliorating wrist/hand/UE movement capability, and increasing ADL and QOL in people with SCI.

1 Introduction

Spinal cord injury (SCI) is a medically complex and life-disrupting condition. An estimated incidence of 17,700 new traumatic SCI cases are reported each year in the United States [1]. In about half of those, the injury involves some part of the arm and hand, representing significant disability and dependence for those patients [1–4]. Following an SCI there is also often loss of sensory and/or motor control of the upper and lower limbs. The characteristics of the impairment depends on the extent and level of the SCI [5, 6]. Individuals with higher levels of SCI have limited capacity to move or perform basic activities of daily living (ADL). Such movement

G. J. Androwis (✉) · G. Yue
Rehabilitation Robotics and Research Laboratory- CMRER, Kessler Foundation, West Orange, NJ, USA
e-mail: gandrowis@kesslerfoundation.org

G. J. Androwis
Bioengineering Department, New Jersey Institute of Technology, Newark, NJ, USA

S. Kirshblum
Physical Medicine and Rehabilitation, Kessler Institute for Rehabilitation, West Orange, NJ, USA

J. C. Moreno et al. (eds.), *Wearable Robotics: Challenges and Trends*,
Biosystems & Biorobotics 27, https://doi.org/10.1007/978-3-030-69547-7_76

Fig. 1 A myoelectric upper extremity orthosis (MyoPro)

limitations significantly reduce a patient's quality of life (QOL) and level of independence, particularly when the UEs are impaired [7]. UE myoelectric powered wearable orthoses (UE-MPWO) specifically designed to restore wrist/hand movements (that are most difficult to recover after injury) may help fill the gap by increasing strength of the participating muscles, range of motion (ROM) of the joints, and ability to perform daily tasks involving using wrist/hand in persons with SCI [3]. Researchers have recently adopted task-specific methods of improving function and independence in individuals with SCI who have upper limb paralysis [3, 7, 8], for example, robotic assisted training for UE in individuals with incomplete SCI [9–11]. The overall goal of this study was to evaluate the effects of the UE-MPWO (MyoPro) in ameliorating wrist/hand/UE movement capability, and increasing ADL and QOL in people with incomplete SCI.

2 Material and Methods

2.1 Upper Extremity Robotic Orthosis (MyoMo)

The MyoPro (Myomo Inc., Cambridge, Massachusetts) (Fig. 1) is a noninvasive, lightweight (approximately 4lbs), wearable system currently available in numerous rehabilitation facilities across the nation [12]. The orthosis provides 0–130 ° of motion and 7 Nm of torque at the elbow and 1–2.7 Nm torque for the fingers. This translates into the ability to lift approximately 5–8 lbs (depending on the user's clinical presentation) [12]. This orthotic device uses surface electromyography (sEMG) signals from affected muscle groups to control a powered orthosis, providing powered assistance for elbow flexion and extension and gross grasp motions via motors attached to the exterior of the brace. It functions by continuously monitoring the sEMG signals of the user's bicep and triceps muscles for elbow motion and the forearm flexor and extensor muscle groups for grasp motion (a 3 jaw-chuck grip

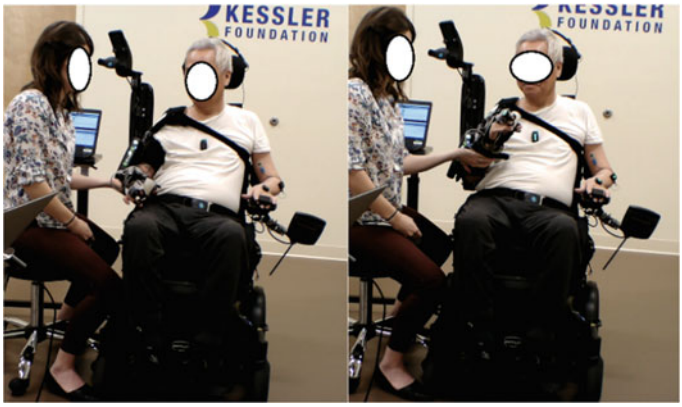

Fig. 2 A participant with SCI is utilizing the UE-MPWO (Myo-Pro) to hold on to an object and bring it closer to his face

pattern). These signals are filtered and processed to provide a desired joint torque proportional to the exerted effort of the user.

2.2 Experimental Procedure

The data analyzed in this paper consist active elbow-joint angler ROM 75 year old male subject with SCI (ASIA Impairment Scale (AIS) C level (C3-C4). Subject was tested with and without the UE-MPWO while seated in his wheelchair (Fig. 2) using Trigno Wireless system (Delsys, Massachusetts, USA) and 9-axis Inertial measurement unit (IMU) and EMG sensors. IMU data were analyzed using a bidirectional zero-lag Butterworth low-pass filter (cutoff frequency = 10 Hz) using MATLAB 2020 (The MathWorks, Inc).

3 Results

Our pilot randomized controlled trial compared the immediate orthotic effects using an UE-MPWO during ADL tasks. The participant received training sessions in an outpatient therapy gym 3 times per week over a 6-week period. Each session was supervised by a licensed therapist, over 60 min, and involved a customized level of training and assistance using the UE-MPWO orthosis. The participant demonstrated a 359% improvement in elbow-joint ROM with the UE-MPWO compared to without it (i.e. 10.6° without and 48.9° with UE-MPWO) (Fig. 3). Further, while utilizing the UE-MPWO, the participant was able, for the first time after his SCI, to drink from a bottle of water and was able to touch his face independently.

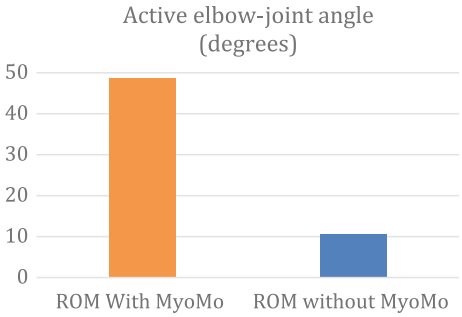

Fig. 3 The active ROM of elbow-joint against gravity with and without UE-MPWO (Myo-Pro)

4 Discussion and Conclusions

Applying the UE-MPWO condition was successful, given that, the participant demonstrated a 359% improvement in elbow-joint ROM with the UE-MPWO (i.e. 10.6º without and 48.9° with UE-MPWO). This may be explained due to the robotic training effects received over six weeks of participation in this study where UE muscles showed increased strength which was also translated to a better coordination and control of participants' UE while using the UE-MPWO to complete ADL tasks. This increase in elbow ROM was further translated to other immediate assistance in completing functional tasks (i.e. drink from a bottle of water and was also able to touch his face). The UE-MPWO enabled the participant to use his own motor control signal (as captured from the upper and lower arm muscles by the UE-MPWO sEMG sensors) to self-initiate and control movement of his UE for completing these ADL tasks that have significant impact on the participant's self-esteem and ability to be engaged in daily self-care activities. Data analysis of a larger sample is underway to confirm the findings.

Acknowledgements Research funded by Department of Defense (DoD), Congressionally Directed Medical Research Programs (DoD award#:W81XWH-18–1-0728).

References

1. S.C.I. Facts, Figures at a glance. *2019 SCI Data Sheet*, ed (2020)
2. P. Rosenbaum, N. Paneth, A. Leviton, M. Goldstein, M. Bax, D. Damiano et al., A report: the definition and classification of cerebral palsy April 2006. Dev. Med. Child Neurol. Suppl. **109**, 8–14 (2007)
3. R. Martin, J. Silvestri, Current trends in the management of the upper limb in spinal cord injury. Curr. Phys. Med. Rehabil. Rep. **1**, 178–186 (2013)
4. N.-H. White, N.-H. Black, Spinal cord injury (SCI) facts and figures at a glance (2016)
5. W.H. Organization, I.S.C. Society, *International perspectives on spinal cord injury*. World Health Organization (2013)

6. M. J. Kuipers, Functional Electrical Stimulation as a neuroprosthesis for sitting balance: measuring respiratory function and seated postural control in able-bodied individuals and individuals with spinal cord injury, University of Toronto (Canada) (2013)
7. P. Maciejasz, J. Eschweiler, K. Gerlach-Hahn, A. Jansen-Troy, S. Leonhardt, A survey on robotic devices for upper limb rehabilitation. J. Neuroeng. Rehabil. **11**, 3 (2014)
8. S. Hesse, H. Schmidt, C. Werner, A. Bardeleben, Upper and lower extremity robotic devices for rehabilitation and for studying motor control. Curr. Opin. Neurol. **16**, 705–710 (2003)
9. K.D. Fitle, A.U. Pehlivan, M.K. O'Malley, A robotic exoskeleton for rehabilitation and assessment of the upper limb following incomplete spinal cord injury, in *2015 IEEE International Conference on Robotics and Automation (ICRA)*, pp. 4960–4966 (2015)
10. J.M. Frullo, J. Elinger, A.U. Pehlivan, K. Fitle, K. Nedley, G.E. Francisco, et al., Effects of assist-as-needed upper extremity robotic therapy after incomplete spinal cord injury: a parallel-group controlled trial. Frontiers in Neurorobotics **11** (2017)
11. D. Vanmulken, A. Spooren, H. Bongers, H. Seelen, Robot-assisted task-oriented upper extremity skill training in cervical spinal cord injury: a feasibility study. Spinal Cord **53**, 547 (2015)
12. S. Dunaway, D.B. Dezsi, J. Perkins, D. Tran, J. Naft, Case report on the use of a custom myoelectric elbow–wrist–hand orthosis for the remediation of upper extremity paresis and loss of function in chronic stroke. Mil. Med. **182**, e1963–e1968 (2017)

Exoskeletons in Industry 4.0: Open Challenges and Perspectives

Using a Spring-Loaded Upper-Limb Exoskeleton in Cleaning Tasks: A Preliminary Study

I. Pacifico, F. Aprigliano, A. Parri, G. Cannillo, I. Melandri, F. S. Violante, F. Molteni, F. Giovacchini, N. Vitiello, and S. Crea

Abstract In the next few years, exoskeletons for workers' support are expected to be key players in the global industrial market. Interventional studies to explore the exoskeletons' effectiveness in real and realistic simulated scenarios have to be carried out in the wide variety of use cases. This work introduces a preliminary comprehensive assessment of a spring-loaded upper-limb exoskeleton, carried out using both instrumental and perception-related metrics in a realistically simulated job

N. Vitiello and S. Crea—These authors share the senior authorship.

A. Parri, F. Giovacchini, N. Vitiello and S. Crea have interests in the spin-off company (IUVO S.r.l.). IUVO S.r.l. has developed the MATE technology. The IP protecting the MATE technology is owned by IUVO S.r.l. (Pontedera, Italy) and licensed to COMAU S.p.A. (Grugliasco, Italy) for commercial purposes in the industrial market. F. S. Violante, F. Molteni, N. Vitiello, and S. Crea are scientific advisors of IUVO S.r.l.

I. Pacifico (✉) · N. Vitiello · S. Crea (✉)
The BioRobotics Institute, Scuola Superiore Sant'Anna, viale Rinaldo Piaggio 34, 56025 Pontedera, Pisa, Italy
e-mail: ilaria.pacifico@santannapisa.it

S. Crea
e-mail: simona.crea@santannapisa.it

Department of Excellence in Robotics & AI, Scuola Superiore Sant'Anna, Piazza Martiri della Libertà, 33, 56127 Pisa, Italy

F. Aprigliano · A. Parri · F. Giovacchini
IUVO S.R.L, via Puglie 9, 56025 Pontedera, Pisa, Italy

G. Cannillo · I. Melandri
Formula Servizi, Via Monteverdi, 31, 47122 Forlì, Italy

F. S. Violante
Dipartimento di Scienze Mediche e Chirurgiche, Università di Bologna, Via Massarenti 9, 40138 Bologna, Italy

F. Molteni
Villa Beretta Rehabilitation Center, Valduce Hospital, Via N. Sauro 17, 23845 Costa Masnaga, Lecco, Italy

N. Vitiello · S. Crea
IRCCS Fondazione Don Carlo Gnocchi, 50143 Florence, Italy

J. C. Moreno et al. (eds.), *Wearable Robotics: Challenges and Trends*,
Biosystems & Biorobotics 27, https://doi.org/10.1007/978-3-030-69547-7_77

activity. Results show that the MATE exoskeleton significantly alleviates the strain in the shoulder and reduces the perceived effort in the investigated task. Questionnaires indicated well-above-threshold usability and acceptability indices. Short-term evidence of strain reduction induced by the use of exoskeletal vests paves the way for systematic assessment across different use-cases.

1 Introduction

Industrial exoskeleton technology (IET) is gaining overwhelming attention all over the world. Expectations about the beneficial effects of IET on work performance and quality enhancement, as well as risk reduction of work-related musculoskeletal disorder incidence, have fostered the rise of the global exoskeleton interest [1]. Yet, widespread adoption of IET should be supported by perspective interventional studies needed to verify and validate the benefits and risks of industrial exoskeletons. To date, only few studies have been carried out with experienced operators, and, to the best of the author's knowledge, comprehensive simulated testing in real use-case has not yet been deployed [2].

Nevertheless, the on-field testing phase represents the last link in the IET assessment chain, where experimenters have to face several issues related to gesture and task variability. For this attempt, testing IETs under controlled environmental conditions in simulated job-tasks in real operational environments could match the tradeoff between complexity and repeatability. This process should be reiterated for each one of the identified use cases since all of them are characterized by their own sub-tasks, complexity, range of movement, and flexibility.

This work introduces a preliminary assessment of a spring-loaded upper-limb exoskeleton through instrumental and perception-related metrics during a realistic simulated job activity. The tested device is the MATE (Muscular Aid Technology Exoskeleton, COMAU S.p.A., Grugliasco, Turin, Italy). MATE is a spring-loaded exoskeleton with a kinematic structure highly compliant with the human shoulder physiology and a bio-inspired assistive torque profile that partially compensates the weight of the user's arm [3].

2 Material and Methods

Experiments took place at Formula Servizi (Forlì, Italy; https://www.formulaservizi.it/), an Italian worker cooperative specialized in the provision of various high-quality services. A testing area was created ad hoc to realistically reproduce the *ceiling cleaning* job activity.

One experienced operator, with no prior experience with the use of the MATE, was recruited for the experiments and performed the job task with and without wearing the MATE, namely EXO and NOEXO conditions. The operator participated in the

ceiling cleaning task, which consisted of cleaning up cobwebs from high ceilings (~7 m) using an extensible duster (Fig. 1a). The gesture required to execute two wide brushes by sustaining the pole from the bottom with one arm and directing its movement with the other arm, kept in an elevated position (i.e., ~120–135°). The participant repeated 20 times the gesture sequence, which started and finished with the arms along the trunk. Before taking part in the experiment, the volunteer was informed about the goals of the study and signed a written informed consent form. The measurements were performed following the declaration of Helsinki and the study was approved by The Institutional Review Board of Scuola Superiore Sant'Anna (study n. 10 of year 2020). The electromyographic activity of the anterior deltoid (AD), medial deltoid (MD), upper trapezius (UT), posterior deltoid (PD), and pectoralis major (PM) muscles was acquired on the side of the elevated arm using the BTS FREE EMG 1000 (BTS Bioengineering, Milan, Italy) at a sampling frequency of 1 kHz. A twin-axis electrogoniometer SG150 (Biometrics Ltd, Newport, UK) was placed ipsilaterally on the shoulder joint for signals segmentation. Raw EMG signals were rectified and low-pass filtered (zero-lag 2nd order Butterworth, filter range: 20–450 Hz; zero-lag 2nd order IIR notch filter at 50 Hz; 100 ms moving average filter), normalized to maximum voluntary exertions (nEMG) and then summed to obtain the Total nEMG signal as proposed in [4]. To segment nEMG and Total nEMG signals, time instances corresponding to the beginning and end of the gesture were detected by visually inspecting EGN signals and double-checked with videos captured throughout the trial. Finally, iEMG and Total iEMG were computed from segmented signals by integrating and normalizing them by the task duration. The percentage variation between the muscle activation under the EXO condition and NOEXO condition was calculated. Statistical evaluation of iEMG and Total iEMG differences between the two conditions were performed using a two-sided Wilcoxon rank-sum test with the significance level set to 0.05. The rated perceived exertion (RPE) was monitored using the Borg CR10 scale [5], assigned by the participant at the end of the task in both experimental conditions. The System Usability Scale [6] and the Technology Acceptance Model [7] questionnaires were administered to the operator.

3 Results

The results of the EMG analysis are shown in Fig. 1b, c. Completing the *ceiling cleaning* task with the exoskeleton support significantly reduced individual and overall muscle activities. The EXO condition produced the largest reductions at the AD, MD, and UT (reduction of 23, 29, and 13% compared to the NOEXO condition, $p = 0.003$, $p < 0.001$, and $p = 0.01$,for AD, MD, UT, respectively see Fig. 1b), which were the most active among the recorded muscles during the NOEXO condition (8–13% MVC). PD also significantly reduced in the EXO compared to the NOEXO condition (reduction of 11%, $p = 0.016$), whereas a minor non-significant variation was observed in PM (reduction of 9%, $p = 0.08$). A reduction trend was also recorded

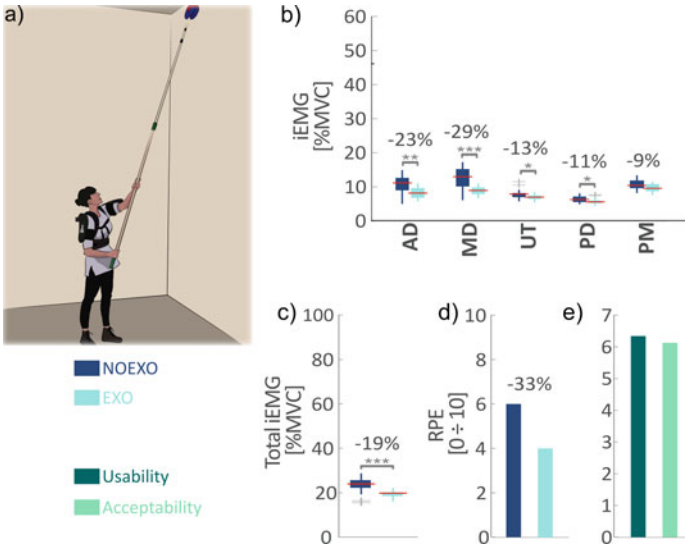

Fig. 1 **a** Illustration of the *ceiling cleaning* task. **b**, **c** Muscle activity. Boxplots show the across-gesture statistics of **b** iEMG and **c** total iEMG parameters. **d** Rated perceived effort (RPE). Numbers in percentage value indicate the relative variation of iEMG, Total iEMG, and RPE between the EXO (turquoise boxes) and NOEXO condition (blue boxes). **e** Usability (green) and acceptability (light green) indices. Muscle acronyms: anterior deltoid (AD), medial deltoid (MD), upper trapezius (UT), posterior deltoid (PD), and pectoralis major (PM)

in the Total iEMG index, which lowered by 19% ($p < 0.001$, Fig. 1c). The operator scored a relatively high RPE value in the NOEXO condition (6/10) and reported 33% less perceived effort when using the MATE (4/10) (Fig. 1d). Questionnaire results also indicated well-above-threshold usability and acceptability indices (6.33/7 and 6.14/7, Fig. 1e).

4 Discussion

This work introduces a preliminary evaluation of the short-term effect of the MATE exoskeleton on an experienced worker performing realistically simulated job activities. Results from this study show that the MATE exoskeleton has the potential to significantly alleviate the strain in the shoulder and reduce the perceived effort in the investigated task.

Assessment of instrumental (sEMG) and perception-related (RPE, Usability, and Acceptability) metrics suggests that industrial upper-limb exoskeletons can offer a valuable solution to perform shoulder demanding work activities with reduced upper-limb physical strain. While promising, this study is limited by its short-term nature. Longer use of the technology may raise issues which would be not evident in short

studies. Future works will focus on the systematic assessment of IET via monitoring the persistency of the device's effectiveness over time and possible long-term side effects.

Acknowledgements This work has been supported in part by Formula Servizi and Scuola Superiore Sant'Anna.

References

1. W. Rian, An exciting future for exoskeletons [WWW Document] (2019). https://www.abiresearch.com/blogs/15J/ (accessed 12.03.21)
2. T. McFarland, S. Fischer, Considerations for industrial use: A systematic review of the impact of active and passive upper limb exoskeletons on physical exposures. IISE Trans. Occup. Ergon. Hum. Factors **7**(3–4), 322–347 (2019)
3. I. Pacifico et al., Experimental evaluation of the proto-MATE: a novel ergonomic upper-limb exoskeleton for reducing the worker's physical strain. IEEE Robot. Autom. Mag. 0 (2020)
4. D.C. Lee, H.K. Lim, W.B. McKay, M.M. Priebe, S.A. Holmes, A.M. Sherwood, Toward an objective interpretation of surface EMG patterns: A voluntary response index (VRI). J. Electromyogr. Kinesiol. **14**(3), 379–388 (2004)
5. G. Borg, *Borg's Perceived Exertion and Pain Scales.* (Human Kinetics, 1998)
6. J. Brooke, SUS-a quick and dirty usability scale. Usability Eval. Ind. (1996)
7. V. Venkatesh, F.D. Davis, Theoretical extension of the technology acceptance model: Four longitudinal field studies. Manage. Sci. **46**(2), 186–204 (2000)

Methods for User Activity Recognition in Exoskeletons

Iñaki Díaz, Juan Martín, Xabier Justo, Carlos Fernández, and Jorge Juan Gil

Abstract Exoskeleton technology is making its way into the industry as an assistance tool to prevent workers from suffering musculoskeletal disorders. However, current control algorithms do not yet allow for a natural human-robot collaboration interface. A key issue to develop efficient exoskeleton controllers resides in the user's activity recognition. This work describes several exoskeleton sensorization options and Machine Learning methods tested on GOGOA's ALDAK active exoskeleton to identify user activity type.

1 Introduction

MUSCULOSKELETAL disorders (MSDs) are injuries and disorders that affect the human body's musculoskeletal system. They represent the main occupational risk factor and usually result in a loss of productivity while also posing a risk to the employee's health. Exoskeletons can assist workers in repetitive lifting of heavy objects that is one of the most common risk factors for MSDs. Everyday many workers have to lift heavy loads during the working day. The sixth European Working

I. Díaz (✉) · X. Justo · J. J. Gil
Smart Systems for Industry 4.0 Group of CEIT-Basque Research and Technology Alliance (BRTA), San Sebastián, Spain
e-mail: idiaz@ceit.es

Universidad de Navarra, San Sebastián, Spain

X. Justo
e-mail: xjusto@ceit.es

J. J. Gil
e-mail: jjgil@ceit.es

J. Martín · C. Fernández
GOGOA Mobility Robots S.L, Abadiano, Spain
e-mail: jmartin@gogoa.eu

C. Fernández
e-mail: cfisoird@gogoa.eu

J. C. Moreno et al. (eds.), *Wearable Robotics: Challenges and Trends*,
Biosystems & Biorobotics 27, https://doi.org/10.1007/978-3-030-69547-7_78

Conditions Survey carried out in 2015 in 35 countries revealed that 32% of workers perform tasks like carrying or moving heavy loads, and 10% of health and personal care workers are required to lift and carry patients [1].

Active exoskeletons, though more expensive and complex than passive ones, seem more promising in assisting workers reducing MSDs. Several active exoskeletons have been developed for lifting assistance worldwide with good results [2]. However, these systems still need further development in terms of cost, usability and control for industry adoption. Regarding the control of these systems, a key issue not properly solved is the automatic user activity recognition. Currently, user motion activity type is not properly detected, and active exoskeletons are manually triggered by users through control buttons or voice commands. This approach reduces the natural human-robot interaction reducing work efficiency and acceptability.

State of the art work dealing with user activity recognition mainly relies on electromyography (EMG) to detect different user actions [3, 4]. This technology allows evaluating the electrical activity produced by skeletal muscles. Main drawback is that electrodes have to be placed on the user's body, which is not a valid solution for industry acceptance. Research is being carried out to develop non-invasive systems such as the CTRL-kit[1], but yet there is no reliable system on the market. Besides, EMG signals usually vary over time due to sweat, temperature and other factors.

Other approaches [5] have integrated sensors in the shoe to detect foot pressure as a result of lifting actions. The proposed solutions are still too invasive for industrial application. To the best of our knowledge, [6] is the only work that has tried to detect user activity by incorporating non-invasive sensors to the exoskeleton. Specifically, they rely on the hip joint angle measured by two on-board encoders, and the movement of the trunk in the sagittal plane measured by placing an Inertial Measurement Unit (IMU) on the backpack of the exoskeleton.

This work intends to use a wide range of low-cost sensors available in the market to appropriately detect user activity and further develop collaborative exoskeleton controllers. We believe that the analysis of these sensors will allow control engineers optimizing current exoskeleton controllers for improved human-exoskeleton interaction.

2 Material and Methods

2.1 Exoskeleton

The exoskeleton under analysis in this work is GOGOA's active ALDAK exoskeleton for industry (Fig. 1). It is an active hip exoskeleton used as lumbar support in lifting loads (up to 35 kg).

[1] https://www.ctrl-labs.com/ctrl-kit/.

Fig. 1 Active ALDAK exoskeleton from GOGOA

2.2 *Sensors and Measures*

Currently, ALDAK is only equipped with hall sensors coupled to the hip actuators (one in each leg). After a thorough analysis of available sensors and methods to integrate them into the exoskeleton, we have selected the following ones for further implementation (Fig. 2):

Fig. 2 ALDAK exoskeleton sensorization

- Load cells: 2 load cells per bar connected to the hip joint.
- Pressure Sensors: Four in each of the two clamps that tight the exoskeleton to the user's legs. Two types of sensors are tested, resistive and piezo-resistive.
- Inertial Measurement Unit (IMU): An IMU has been placed at the backpack of the exoskeleton to measure 3D accelerations of the user.

2.3 Data Acquisition

21 users (21–47 years old, 1.71–1.92 m height) equipped with the exoskeleton have carried out the same lifting tasks in a sequential way: (1) Standing up (sensor power on, wait few seconds), (2) walk 1.5 m, (3) bend, (4) hold a 5 kg box, (5) lift it, (6) Standing up (wait few seconds and power-off).

Data acquisition is carried out by an Arduino Mega 2560 board, powered by batteries and equipped with a log shield in order to measure all sensors data. Data is acquired at a sampling rate of 500 S/s.

3 Results

Figure 3 shows as example of the data acquired over time by the four piezo-resistive pressure sensors placed at the user's right leg in one of the trials. This sensor acquires well motion task transitions and it seems very relevant for user activity recognition. However, its initial value and performance are highly dependent on how well they are adjusted to the leg of the user at setup.

Supervised Machine Learning Classifiers are used to test and predict the activity type (standing, walking, bending and lifting) in each data sample of all experiments, after labelling them manually. The 21 experiments provide a dataset of 66463 measures per sensor, 80% are used for training (4-fold-cross validation is used), and 20% for testing. The analysis is repeated with different combinations of sensors.

The optimal sensor combination results from: 1 piezo-resistive sensor, 2 load cells (one in each leg), 2 hall sensors, and the IMU (only Y and Z axis). Best precision results for this combination of sensors are obtained with: Decision Trees (99.6%), KNN (99.8%) and Cubic SVM (99.8%).

4 Conclusion

User motion activity recognition at the earliest moment is key to build a smart exoskeleton controller. This work gives insight over a wide range of low-cost sensors

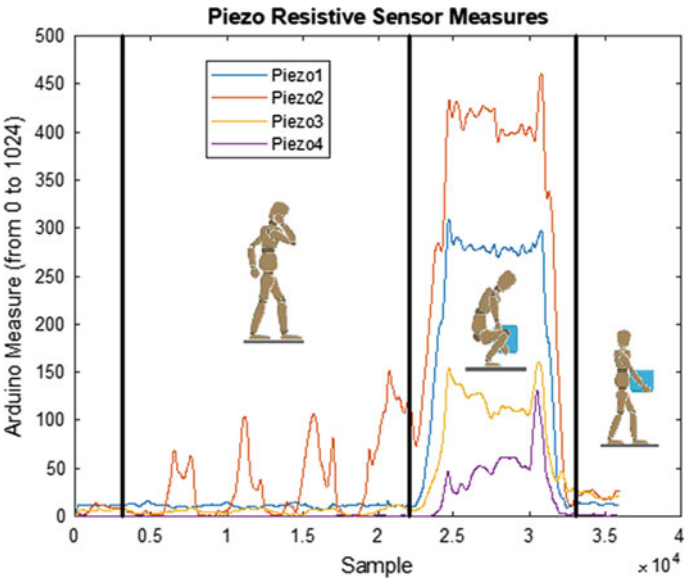

Fig. 3 Picture of the signal measured by the 4 piezo-resistive sensors at the user's right leg over time and task sequence in one of the trials.

that can be integrated with this purpose. With the right choice and location of a piezo-resistive sensor, two load cells, two hall sensor for rotation measurement and one IMU, user activity type can be recognized with a 99.8% precision. Further work will analyze Deep Learning methods such as Long Short-Term Memory (LSTM) neural networks for improved prediction performance. This information will allow developing truly natural human-exoskeleton interaction algorithms.

Acknowledgements This work has been supported by the Spanish project EXOXUTIK (CDTI IDI-20190777).

References

1. Eurofund, Sixth european working conditions survey, overview report, *Publications Office of the European Union*, Technical Report (2016)
2. J. Theurel, K. Desbrosses, Occupational exoskeletons: Overview of their benefits and limitations in preventing work-related musculoskeletal disorders. IISE Trans. Occup. Ergonomics Hum. Factors **7**(3–4), 153–162 (2019)
3. S. Kawai, H. Yokoi, K. Naruse, Y. Kakazu, Study for control of a power assist device. Development of an EMG based controller considering a human model, in *2004 IEEE/RSJ International Conference on Intelligent Robots and Systems (IROS)*, vol. 3 (2004), pp. 2283–2288

4. H. Kawamoto, Suwoong Lee, S. Kanbe, Y. Sankai, Power assist method for hal-3 using EMG-based feedback controller, in *IEEE International Conference on Systems, Man and Cybernetics*, vol. 2 (2003), pp. 1648–1653
5. L. A. Mateos, J. Ortiz, S. Toxiri, J. Fernandez, J. Masood, D.G. Caldwell, Exoshoe: A sensory system to measure foot pressure in industrial exoskeleton," in *6th IEEE International Conference on Biomedical Robotics and Biomechatronics (BioRob),* (2016), pp. 99–105
6. B. Chen, L. Grazi, F. Lanotte, N. Vitiello, S. Crea, A real-time lift detection strategy for a hip exoskeleton. Front. Neurorobot. **12**, 1–7 (2018)

A Topology-Optimization-Based Design Methodology for Wearable Robots: Implementation and Application

Lorenzo Bartalucci, Matteo Bianchi, Enrico Meli, Alessandro Ridolfi, Andrea Rindi, and Nicola Secciani

Abstract Robotic-based human assistance is increasingly spreading both in clinical practice and in the industrial sector. The use of wearable robots, such as exoskeletons, is considered one of the most promising applications since it allows for merging human flexibility and creativity with machine endurance. Such devices shall be comfortable and lightweight to be as transparent as possible to the user's perception. At the same time, they shall also be stiff enough to drive body parts while bearing the exchanged forces efficiently. The gold standard methodology to achieve such results is the topology optimization, which, even if used mainly in structural optimization, is still relatively new to wearable robots. In this paper, the authors propose a topology-optimization-based design strategy suitable to be applied, if adapted case by case, to a generic design of a wearable system. The presented test case, used as a benchmark to assess the optimization-based design process, focuses on a hand exoskeleton made of aluminum alloy, resorting to an additive manufacturing process.

1 Introduction

Structural-optimization problems are faced in many areas of engineering. Several mathematical methods have been exploited in tackling these issues, among them also the topology optimization. By definition "*topology*" refers to "*the way the parts of something are organized or connected*" (Cambridge Dictionary), and, in fact, topology optimization differs from the other structural techniques because it optimizes material density rather than shape, leading to an optimal distribution of a given amount of material into a fixed design space to get optimal structural characteristics.

The authors would like to thank CERTEMA Multidisciplinary Technological Laboratory and the IRCSS Don Gnocchi in Florence for the precious and fundamental collaboration, and for logistic and research support.

L. Bartalucci (✉) · M. Bianchi · E. Meli · A. Ridolfi · A. Rindi · N. Secciani
Department of Industrial Engineering (DIEF), University of Florence, Via di Santa Marta 3, 50139 Florence, Italy
e-mail: lorenzo.bartalucci@unifi.it

J. C. Moreno et al. (eds.), *Wearable Robotics: Challenges and Trends*,
Biosystems & Biorobotics 27, https://doi.org/10.1007/978-3-030-69547-7_79

The high flexibility and customizability of this procedure make it particularly suitable to be exploited in user-oriented applications, like the design of wearable robots (e.g., exoskeletons), especially considering the space and weight constraints deriving from the necessity to apply the optimized components to the human body. However, while it is widely used in civil and automotive engineering applications, its exploitation is still relatively new in the medical field [1].

The research work presented in this paper hence investigates the potentialities of topology optimization in the specific field of wearable robotics for biomedical applications (e.g. robotic-based rehabilitation and assistance, or strength enhancing). This approach can indeed lead to a remarkable impact on the patient, who will be able to wear a lightweight and comfortable but still high performing device.

2 Background

In [2], three rigid hand exoskeleton prototypes developed by the Department of Industrial Engineering of the University of Florence (DIEF) are presented, and their main features discussed. They are all 3D-printed in Acrylonitrile Butadiene Styrene (ABS) and, if on the one hand, their high portability and usability are strictly related to this very material, on the other hand, its use also results in the main performance limitations. As a matter of fact, since the exoskeleton functioning is based on rigid kinematic chains acting on the user's fingers, the stiffness of the device plays a crucial role in applying suitable forces on the hand for the fulfillment of Activities of Daily Living (ADLs). This paper will then show how by making use of metal alloys (e.g., aluminum alloys) and exploiting topology-optimization-based procedures, it is possible to guarantee increased performances—in terms of stiffness, and bearable and

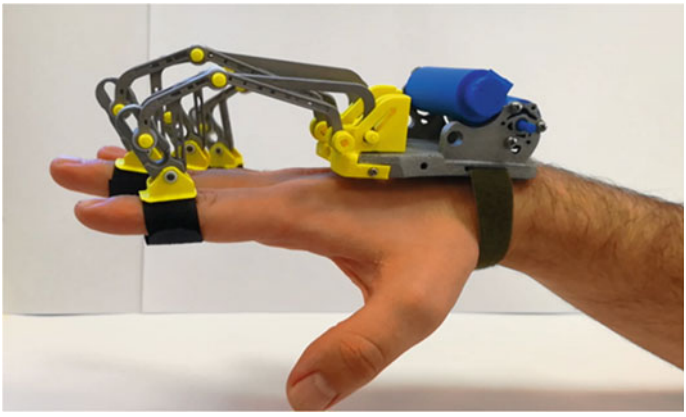

Fig. 1 The final version of the hand exoskeleton prototype resulting from the proposed topology-optimization-based design procedure

transferable forces—maintaining an acceptable weight. Figure 1 shows the resulting prototype, which has been produced with additive manufacturing techniques since the geometries deriving from topology optimization are not suitable for standard production processes.

3 Topology Optimization Process

The test case is a generic finger mechanism used in the hand exoskeleton prototypes introduced in Sec. 2. In the test case definition, four different aspects are considered: (i) the geometry, which has been identified as the base geometry of a finger mechanism (Fig. 2); (ii) the material, which has been identified as Cl31Al aluminum alloy and assumed having linear elastic isotropic properties; (iii) the boundary conditions, which have been assigned replicating the joints' couplings of the mechanism; (iv) the loads applied to the device, which, according to Fig. 2, have been reasonably chosen as a 20 N vertical force, and a ± 2 N lateral force along z direction, both applied at joint 4.

The remainder of this section will briefly cover the other vital aspects of the optimization procedure.

3.1 Design Space

Design spaces (or design areas) indicate the set of elements that can be targeted by the optimization; non-design areas shall have instead to remain unchanged. In this case study—starting from the original structure reported in Fig. 2—the only non-design

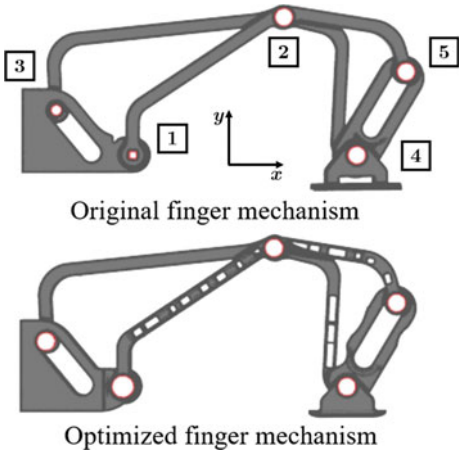

Fig. 2 Above, the kinematic scheme of the test case: the numbers indicate the different joints (the red circles) that make it up. Below, the same kinematic scheme at the end of the optimization process

areas have been defined as the regions around each joint, which should have had to be left unchanged not to change the kinematics.

3.2 Objective Function and Optimization Constraints

the compliance minimization [3] has been carried out in the presented framework. Optimizing this quantity means looking for the material density distribution that minimizes the structure deformation under the defined loading conditions. The compliance, $l(\boldsymbol{u})$, is calculated as follow:

$$l(\boldsymbol{u}) = \int_{\Omega} \boldsymbol{f} \cdot \boldsymbol{u} \, d\Omega + \int_{\Gamma_T} \boldsymbol{t} \cdot \boldsymbol{u} \, ds, \tag{1}$$

where $\boldsymbol{f}$ are the body forces on the domain Ω, $\boldsymbol{t}$ are the external forces on the traction part of the boundary $\Gamma_T \subset \partial\Omega$, $\boldsymbol{u}$ is the vector collecting the displacements, and ds is the infinitesimal part of Γ_T. Finally, the maximum allowable stress values, displacements, and volume fraction have been set as the optimization constraints.

3.3 Optimization Algorithm

the algorithm used has been the density method, also known as the Solid Isotropic Material with Penalization (SIMP) method [4]. A pseudo-density function $\rho_f \in [0\ 1]$ is defined as the design variable and assigned to different portions of the material. Such density varies continuously between 0 and 1, defining the element as being either void or solid. The solver, OptiStruct (Structural Analysis Solver), hence removes material where the pseudo-density drops below a fixed threshold.

4 Results and Conclusion

The optimization problem thus set has been solved for the entire index mechanism. A comparison between the mass of the original mechanism and the optimized one is reported both in absolute terms and as a percentage in Table 1.

Such a comparison has been accompanied by a detailed static Finite Element Analysis (FEA) aiming to assess the maximum deformation for each of the components that make up the mechanism. It has been seen that, when taken individually, the components can deform up to 6 mm under the same loading conditions reported in Sect. 3, against a maximum value of 2.5 mm of the non-optimized component;

Table 1 Mechanism mass before and after the topology optimization

Component	Original mass (g)	Optimized mass (g)	Reduction mass %
Finger mechanism	13.34	10.6	20.5

however, a maximum displacement of 0.8 mm has been recorded while analyzing all the components coupled together.

To mention that the geometries of the optimized models of each component, directly obtained by the solver, are dependent on the mesh and do not have a homogeneous surface. The last stage of the process involved a smoothing of the surfaces, resulting in what is visible in Fig. 2.

Lightness and stiffness are crucial characteristics of wearable robots, whatever the field of application (e.g., healthcare as well as the construction industry) and whatever part of the body is concerned (e.g., upper or lower limbs). The work reported in this paper aimed to assess the efficacy of topology optimization for the design of such devices for which even a small reduction in weight translates into significant energy savings for the wearer. The exploitation of the SIMP method allows for a fine tuning of the stiffness to lightness ratio by varying the way the solver interprets different values of pseudo-density. The use of such a strategy for the proposed test case showed promising results, culminating in a mass reduction of the 20%, without compromising rigidity.

References

1. M. Bianchi, F. Buonamici, R. Furferi, N. Vanni, Design and optimization of a Flexion/extension mechanism for a hand exoskeleton system, in *ASME 2016 International Design Engineering Technical Conferences and Computers and Information in Engineering Conference*, August 2016
2. N. Secciani, M. Bianchi, A. Meschini, A. Ridolfi, Y. Volpe, L. Governi, B. Allotta, Assistive hand exoskeletons: the prototypes evolution at the university of florence, in *Advances in Italian Mechanism Science*, ed. by G. Carbone, A. Gasparetto (Springer International Publishing, Cham, 2019), pp. 307–315
3. S. Wang, K. Lim, B. Khoo, M. Wang, An extended level set method for shape and topology optimization, J. Comput. Phys. **221**(1), 395–421 (2007). (Online). Available: http://www.sciencedirect.com/science/article/pii/S0021999106002968
4. L. Shu, M.Y. Wang, Z. Fang, Z. Ma, P. Wei, Level set based structural topology optimization for minimizing frequency response. J. Sound Vib. **330**(24), 5820–5834 (2011). (Online). Available: http://www.sciencedirect.com/science/article/pii/S0022460X11006079

Lifting and Carrying: Do We Need Back-Support Exoskeleton Versatility?

Tommaso Poliero, Maria Lazzaroni, Stefano Toxiri, Christian Di Natali, Darwin G. Caldwell, and Jesús Ortiz

Abstract In recent years, back-support exoskeletons have shown potential to mitigate the ergonomic risk associated with *lifting* activities. In addition to lifting, *carrying* is known to represent a risk for the workers. In this work, we elaborate on the effects of an active back-support exoskeleton (*XoTrunk*) assisting with carrying activities, using the same control strategy adopted in lifting-assistance. The results show that for most of the users (7 out of 9) such assistance is hindering the leg movements. As a consequence, exoskeletons should embed task recognition capabilities in order to switch control strategies according to the performed task.

1 Introduction

Back-support exoskeleton usage can be related to a reduction of lower-back muscle activation that, in turn, can be linked to a mitigated risk of injuries [1–3]. At first, studies have focused on understanding the effects that the assistance delivered by these devices could have on the *erector-spinae* muscles, while performing lifting activities or static bending [4]. Nevertheless, in the manual material handling (MMH) framework, the International Standard ISO 11228 establishes ergonomic guidelines not only to mitigate lifting but also activities such as carrying, pushing and pulling. So, the first question that arises is whether exoskeletons should be *designed specifically for a task* or should they be intrinsically *versatile* to support different activities. Of course, the choice of how to actuate the exoskeleton plays a paramount role in this context. Indeed, exoskeletons relying on purely passive elements such as gas/coil springs or elastic bands, cannot tune, according to the task, the amount of

T. Poliero · M. Lazzaroni · S. Toxiri · C. D. Natali · D. G. Caldwell · J. Ortiz
Department of Advanced Robotics, Istituto Italiano di Tecnologia, Genoa, Italy

T. Poliero (✉)
Department of Informatics Bioengineering Robotics and Systems Engineering, University of Genoa, Genoa, Italy
e-mail: tommas.poliero@iit.it

M. Lazzaroni
Department of Electronics, Information and Bioengineering, Politecnico di Milano, Milan, Italy

J. C. Moreno et al. (eds.), *Wearable Robotics: Challenges and Trends*,
Biosystems & Biorobotics 27, https://doi.org/10.1007/978-3-030-69547-7_80

assistance they provide. On the other hand, exoskeletons that exploit active elements such as motors or electro-magnetic clutches, can generate torques congruously with the task being performed and, thus, make the best of the versatility provided by their actuators. As a consequence, recent research has started focusing on how to apply Human Activity Recognition (HAR) to back-support exoskeletons in order to properly control the exoskeleton according to the task being executed [5–7].

In this work, we elaborate on the need to design back-support exoskeleton controllers that are aware of the performed task and can distinguish lifting activities from carrying ones. To this end, we investigated the subjective perceptions of 9 users performing carrying while being assisted according to a control strategy designed for symmetric lifting tasks and presented in [8].

2 Materials and Methods

Nine male healthy subjects (1.78 ± 0.04 m, 76.55 ± 8.22 kg, 31 ± 3.46 years old) were recruited and signed an informed consent. The experimental task consisted of *carrying*, i.e., straight level walking for 7.5 m, while holding a 15 kg box close to the trunk at a self-selected speed. This task was repeated 3 times, with and without exoskeleton, in randomized order. The back-support exoskeleton used in this assessment was XoTrunk, an improved version of the Robo-Mate prototype, presented in [8] and discussed in further details concerning actuators and kinematics in [9] and [10], respectively.

In [8], the authors presented a control strategy that provides assistance proportionally to the wearer's trunk inclination and forearm muscle activity. In the carrying task analysed in this work, the trunk inclination can be neglected, whereas forearm muscle activity can be considered constant as the payload did not change. Therefore, the control strategy running on the exoskeleton was simplified for these experiments. Specifically, motors were set to produce a constant torque of 10Nm per side. As motors generate torques, these result in a simultaneous extension moment at the back and both hips.

To understand whether there is a need to design different controllers according to the task or it is sufficient to use the same controllers developed for lifting, an analysis was made on the users' subjective perception of the assistance. In particular, filling-in a simplified rating of perceived exertion questionnaire, each user indicated if executing the task with the exoskeleton they could perceive a benefit or a discomfort/hindrance with respect to the no-exoskeleton case. The analysed body regions were shoulders, arms, back/trunk, waist and legs.

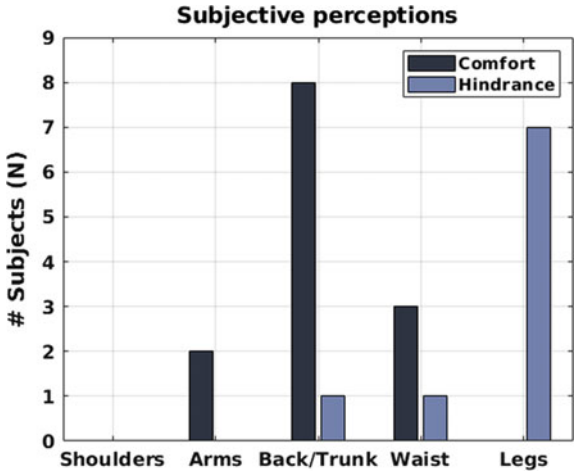

Fig. 1 Bar plot of the questionnaire result. Each group is divided in those who reported comfort (black) and those who reported hindrance/discomfort (blue)

3 Results

Figure 1 displays the results for each of the body regions under analysis. Almost all the users reported benefit in the back/trunk region (8 out of 9) and discomfort in the legs (7 out of 9). No user reported perceived benefit in the legs whereas 1 subject felt hindrance also for the trunk region. It is also interesting to report that on the waist (where the exoskeleton is anchored) 3 users could feel a benefit from the exoskeleton usage and 1 experienced discomfort. Even though the exoskeleton is not assisting the arms, 2 subjects felt a benefit also in this body region. Consistently with the exoskeleton action, no user reported effects on the shoulder region.

4 Discussion

The data clear polarity suggests that assisting carrying exploiting the same strategies developed for symmetric lifting can be effective but has some drawbacks. Indeed, the exoskeleton action resulted in a perceived support for the back, but it also yielded hindrance and discomfort in the lower limbs. This discomfort might be strictly related to the motors generating simultaneous extension moments at both hips. Indeed, such assistance seems appropriate when performing lifting as every time there is back flexion or back extension, there is also a corresponding flexion or extension of the hips. On the contrary, applying the same approach to carrying, the extension moments acting simultaneously on both hips interfere with the leg movements. In particular, this support might have been beneficial during hip extension (stance phase), but perceived as hindering the hip flexion (swing phase). Data seem to confirm this supposition. As a result of this hindrance, balance and walking speed might be

significantly affected, resulting both in productivity losses and limited acceptance of the exoskeleton. Using transparency (zero-torque) control during carrying would solve/reduce hindrance, but correspondingly give up the positive support for the back during a task that the International Standard marks as worthy of attention. Transparency control can be achieved both by active and quasi-passive/semi-active exoskeletons. These latter are devices that exploit actively controlled elements such as electro-magnetic clutches for the engagement or dis-engagement of the passive elements. On the contrary, to provide support also during carrying, it is necessary to use active exoskeletons. Anyhow, to fully exploit active back-support exoskeleton capabilities and versatility it is important to introduce task awareness (HAR). Indeed, once the task being performed is recognized, it would allow to activate the best control strategy. As an example, in this study, it would have been possible to switch between a strategy that has been implemented taking inspiration from symmetric lifting tasks to a novel control strategy specifically designed for carrying assistance. As presented in recent works, HAR can be achieved by exploiting common exoskeleton on-board sensors (such as encoders and IMUs) and, so, most exoskeletons could implement it, [5–7]. In particular, in [6], we showed how XoTrunk control strategy can be expanded to include on-line task recognition to distinguish between *walking*, *lifting*, *standing* and *carrying*.

Finally, to effectively understand the importance of supporting carrying activities and the exoskeleton effects, future works should present a rigorous analysis on muscle activation and kinematics.

5 Conclusion

In this work, we have presented the subjective perceptions from 9 subjects performing carrying tasks while being assisted by an active back-support exoskeleton. A control strategy suited for symmetric lifting tasks was adopted. The results show that the exoskeleton action was perceived as beneficial for the back but hindering the natural leg movement patterns occurring while walking. This highlights the importance of control strategies suited to different tasks, as well as of the capability to distinguish the activity being performed to select the most appropriate strategy.

Acknowledgements This work has also been funded by the Italian Workers' Compensation Authority (INAIL).

References

1. M.P. de Looze, T. Bosch, F. Krause, K.S. Stadler, L.W. O'Sullivan, Exoskeletons for industrial application and their potential effects on physical work load. Ergonomics **59**(5), 671–681 (2016)

2. J. Theurel, K. Desbrosses, Occupational exoskeletons: overview of their benefits and limitations in preventing work-related musculoskeletal disorders. IISE Trans. Occup. Ergonomics Hum. Factors, 1–17 (2019)
3. S. Toxiri, M.B. Nöf, M. Lazzaroni, J. Fernndez, M. Sposito, T. Poliero, L. Monica, S. Anastasi, D.G. Caldwell, J. Ortiz, Back-support exoskeletons for occupational use: an overview of technological advances and trends. IISE Trans. Occup. Ergonomics Hum. Factors **7**(3-4), 237–249 (2019). (Online). Available: https://doi.org/10.1080/24725838.2019.1626303
4. L. Grazi, B. Chen, F. Lanotte, N. Vitiello, S. Crea, Towards methodology and metrics for assessing lumbar exoskeletons in industrial applications, in, *II Workshop on Metrology for Industry 4.0 and IoT (MetroInd4. 0&IoT)*. (IEEE, 2019) **2019**, pp. 400–404
5. B. Chen, F. Lanotte, L. Grazi, N. Vitiello, S. Crea, Classification of lifting techniques for application of a robotic hip exoskeleton. Sensors **19**(4), 963 (2019)
6. T. Poliero, S. Toxiri, S. Anastasi, L. Monica, D.G. Caldwell, C.J. Ortiz, Assessment of an on-board classifier for activity recognition on an active back-support exoskeleton, in *2019 IEEE 16th International Conference on Rehabilitation Robotics (ICORR)*. (IEEE, 2019), pp. 559–564
7. M. Jamšek, T. Petrič, J. Babič, Gaussian mixture models for control of quasi-passive spinal exoskeletons. Sensors **20**(9), 2705 (2020)
8. S. Toxiri, A.S. Koopman, M. Lazzaroni, J. Ortiz, V. Power, M.P. de Looze, L. O'Sullivan, D.G. Caldwell, Rationale, implementation and evaluation of assistive strategies for an active back-support exoskeleton. Front. Robot. AI **5**, 53 (2018)
9. C. Di Natali, S. Toxiri, S. Ioakeimidis, D.G. Caldwell, J. Ortiz, Systematic framework for performance evaluation of exoskeleton actuators, in *Wearable Technologies* (2020, in press)
10. M. Sposito, C. Di Natali, S. Toxiri, D.G. Caldwell, E.De Momi, J. Ortiz, Exoskeleton kinematic design robustness: an assessment method to account for human variability, *Wearable Technologies* (2020, in press)

Exoskeletons Introduction in Industry. Methodologies and Experience of Centro Ricerche Fiat (CRF)

Massimo Di Pardo, Rossella Monferino, Francesca Gallo, and Felice Tauro

Abstract Exoskeletons and other technologies for aiding work need to be tested and selected before starting the implementation plan or further evaluation phases. Innovation in this field is highly dynamic and new products are frequently proposed at prototype level so discriminating phase is important. This paper aims to explain how FCA–CRF is approaching the evaluation of new products and the new technologies for aiding work. The evaluation is based on applicative cases and on testing procedures as well as on testing session results. The selection phase is important to define if exoskeleton or other technology under investigation fits the needs of workstation and tasks to be faced during work activity. In this way an objective performance evaluation of the exoskeleton matching the workplace needs can be operated. The applied testing procedure for this exoskeletons investigation demonstrated its usefulness at laboratory and pilot case level.

1 Introduction

Exoskeletons are external mechanical structures, active or passive, that support the worker in specific work tasks [1]. These systems are designed to give support in certain body districts; those addressed to the industrial world are mainly oriented to assist the back and upper limbs with targets of postural assistance, applied force reduction, manual material handling and supporting tools. CRF is working in the

M. Di Pardo (✉) · R. Monferino · F. Gallo
Centro Ricerche Fiat (CRF), Orbassano, Italy
e-mail: massimo.dipardo@crf.it

R. Monferino
e-mail: rossella.moferino@crf.it

F. Gallo
e-mail: francesca.gallo@fiatgroup.com

F. Tauro
Centro Ricerche Fiat (CRF), Melfi, Italy
e-mail: felice.tauro@crf.it

J. C. Moreno et al. (eds.), *Wearable Robotics: Challenges and Trends*,
Biosystems & Biorobotics 27, https://doi.org/10.1007/978-3-030-69547-7_81

research of technological solutions for supporting workers (for instance by modification of workstation and work methods, or by implementation of tools, equipment, exoskeletons). These solutions are sought in order to bring benefits both for the improvement of the operator's working conditions and in terms of efficiency and quality of the production process. The procedures for exoskeleton evaluation are mainly focused on performances assessment of the device [2]. SEMG (Surface Electro Myography) is often the discriminating instrument used for effectiveness estimation, but it's complicated to apply it in the real environment [3]. Several methods developed for practical evaluation are available according to the experience of the case [4], but need to be generalized and linked to the needs of the workstation. Since no standard evaluation method is available in the literature at present, we propose a methodology (this is the novelty in respect to the state of art) that assesses and compares functionalities, performances, usability and applicability of passive devices in simulated and real workplaces. The result of this work, improves the exoskeletons evaluation because based on numerical, objective and standard criteria linked to the workstation needs. It makes possible a comparison among different devices.

2 Methodology and Instruments

2.1 Objectives

The first objective is to detect the most suitable exoskeleton for the workstation appointed for a specific task. This objective is focused on the fulfillment of the needs of the work task and the related workstation including the equipment.

The second objective is to estimate the level of fitting and the compliance degree between the selected exoskeleton and the workstation under analysis. This means to know the performances and functionalities of the exoskeletons available on the market, and put them in relationship with the workstation needs. Finally, the third objective is to improve the workstation ergonomics increasing the worker wellbeing. This objective is achievable by the fulfillment of the previous two objectives, and by the fulfillment of usability requirements for the selected exoskeleton.

2.2 Methodology

The methodology aims to mathematize qualitative evaluation and to make a correlation between the needs of the production system (made of workstation, work task and worker) and the exoskeleton performances. The best matching between production system needs and exoskeleton performances helps the worker in his task, increasing ergonomics and wellbeing perception. The methodology is made of two phases: the *first phase* is the *exoskeleton selection* through laboratory testing. The *second phase*

is the *exoskeleton evaluation in real environment* by its application to a pilot case. The ***first phase*** is based on three main steps. The first step (a) focuses on the detection of the workstation needs, in collaboration with the Manufacturing Engineering team. We consider the following main items: ergonomics postures, workplace geometrical characteristics, work cycle time, loads to be moved. This is the workstation characterization. The second step (b) investigates performances and functionalities of exoskeletons to define effects on the human body, through objective evaluations. Two items of the usability analysis (efficacy and efficiency) are considered. This evaluation is carried out by measurement instruments and biomechanical simulation tools, in comparative tests on working tasks performed with and without the exoskeleton. This part of the work is carried out in the CRF laboratory on real-like tasks, in order to classify exoskeletons and build a database of the main functionalities. Filling a *correlation matrix* for crossing workstation needs and exoskeleton performances (Fig. 1) is the last step (c). The correlation matrix is based on a scoring, giving the level of fulfillment of exoskeleton performances in respect to the needs of the workstation. This step is developed by routine that fill in the matrix automatically gathering info from the database about workstation characteristics. It is an iterative process that leads to the exoskeleton selection. The ***second phase*** consists in exoskeletons testing on real workplaces in production line (in particular on those from which the real-like tasks derive). This is made to gather operators' feedback about the support received by the device, and its usability (subjective item: satisfaction), applicability (vs. Technical and managerial constraints) and acceptability (by the social environment).

2.3 Procedures and Instruments

Test procedures, developed at CRF, focuses on task execution and measurement by instruments. Measurements of usability are carried out with the aim of evaluating the support provided by the investigated exoskeletons under different conditions of use, through static and dynamic work tests. Tests are carried out in a controlled environment with the aim of studying the task/exoskeleton binomial on the aspects of interaction, subjective evaluation and compatibility with the chosen set up. For this purpose, real work tasks are chosen and performed under appropriate conditions, at first in lab and after replied in manufacturing plant (workstation pilot case).

The assessment team is composed by experts: ergonomists, safety managers, production engineers, psychologists and physicians. For the three items of usability test (efficacy, efficiency and satisfaction) we use the following instruments. *Efficacy* is evaluated by the *reduction of biomechanical load* due to the exoskeleton use (compared to the same task without exoskeleton); for this evaluation the software "AnyBody Modeling System" is used. *Efficiency* is evaluated by the measurement of the level of interaction between exoskeleton and human body. We use motion capture system (Xsens-Awinda and Sony video cameras), and contact pressure sensors (Xsensor PX200:20.40.05). We detect body postures angles, movement and

Fig. 1 Cross matrix: exoskeleton performances versus workstation needs

localized pressure between exoskeleton and human body. We measure also the *task execution time* for a comparison among devices efficiency and in respect to the task without exoskeleton. In addition we use also a smart watch (TomTom) to value *energy expenditure* during work task. For the *satisfaction,* some questionnaires based on TAM (Technology Acceptance Model), VADS (Visual Analysis Discomfort Scale) forms and structured interview, are used. In the pilot case "acceptability" is based on an interview to assess how the worker perceive the device use in respect to the factory social environment (other workers, organization).

2.4 Results

We carried out more than 20 workstation analysis in "CNH-Industrial" production plants. With the help of the methodology we obtained only one number (score) that summarize the goodness of the coupling between exoskeleton and workstation. The methodology can properly select exoskeletons useful for workstations under examination. The methodology is also useful for generating a data base of exoskeletons performances, speeding up further evaluations and analysis including comparison among devices. The first phase (in the laboratory) help the second phase (in plants) reducing the number of problems that could be found in the pilot case. Finally, "acceptability item" is a key element and if is not good it can compromise the successful exoskeleton implementation.

3 Conclusion

All these measurements gives us the global effect of introducing an exoskeleton on a specific workstation considering the realistic context of use. Based on the whole methodology we are able to provide guideline to the production sectors of FCA/CNHI for exoskeleton choice and application. This is an important help for keeping standard production aligned with the Word Class Manufacturing rules. An important extension of the methodology could be its automatization through sensors and software tools for speed up the analysis and increase precision.

References

1. DeLooze et al, 2016. Exoskeletons for industrial application and their potential effects on physical work load. Ergonomics 59(5):671–81
2. Spada et al, 2018. *Analysis of exoskeleton introduction in industrial reality*. International Conference on Applied Human Factors and Ergonomics AHFE 2017, pp. 236–244
3. Bostelman et al., Cross-industry standard test method developments. Frontiers of Information Technology and Electronic Engineering **18**(10), 1447–1457 (2017)
4. Bosch et al, 2016. The effects of a passive exoskeleton on muscle activity, discomfort and endurance time in forward bending work. Applied ergonomics 54:212–217

Quantifying the Impact of a Lower Limb Exoskeleton on Whole-Body Manipulation Tasks. Methodological Approach and First Results

Yaiza Benito Molpeceres, Guillermo Asín-Prieto, Juan Carlos García Orden, and Diego Torricelli

Abstract In recent years, back-support exoskeletons have been postulated as a competitive solution to reduce mechanical loading during lifting tasks, contributing to the prevention of low back pain. However, little research involving lower body exoskeletons has been done on this matter. The present study evaluates the impact of the H2 robotic exoskeleton on whole-body manipulation tasks, through a standardized experimental protocol and a set of objective metrics. Wearing the exoskeleton allowed the subject to perform the tasks successfully, occasionally showing magnified range of movement values at certain joints. In addition, its use reduced back mechanical loading of loaded-box lifts. However, the device also had a non-desirable impact on functional performance, increasing postural instability, slowing down tasks completion, and diminishing movement smoothness.

1 Introduction

During the last decade, the increasing availability of exoskeletons have started a new exciting era for robotics. Companies are considering the use of such devices to improve workers' safety and ergonomics, and the scientific community is more than ever active in this field [1]. Nowadays, most of the exoskeletons aimed at reduc-

Y. B. Molpeceres (✉) · J. C. G. Orden
Department of Continuum Mechanics and Theory of Structures of the Universidad Politécnica, de Madrid, Spain
e-mail: yaiza.benito44@gmail.com

J. C. G. Orden
e-mail: juancarlos.garcia@upm.es

G. Asín-Prieto · D. Torricelli
Neural Rehabilitation Group of the Spanish National Research Council, Madrid, Spain
e-mail: guillermo.asin.prieto@gmail.com

D. Torricelli
e-mail: diego.torricelli@csic.es

G. Asín-Prieto
Gogoa Mobility Robots S.L., Abadiño, Spain

J. C. Moreno et al. (eds.), *Wearable Robotics: Challenges and Trends*,
Biosystems & Biorobotics 27, https://doi.org/10.1007/978-3-030-69547-7_82

ing the spine loading are represented by back-support devices, whereas lower limb exoskeletons are mostly focused on providing gait assistance. Although there are some lower limb systems with useful applications beyond the clinical rehabilitation, little research on their impact on manipulation tasks has been done so far [2].

2 Materials and Methods

2.1 H2 Exoskeleton

The present study made use of the H2 lower body exoskeleton [3] whose joints were uncoupled, i.e. not offering any resistance apart from the mechanical limitations inherent to its rigid structure.

2.2 Testbed

The testbed is a non-reflectant modular structure consisting of a fixed frame and 4 mobile shelves; two of them, adjustable to the height of subject's knees, and the other two, to the height of subject's shoulders (Fig. 1).

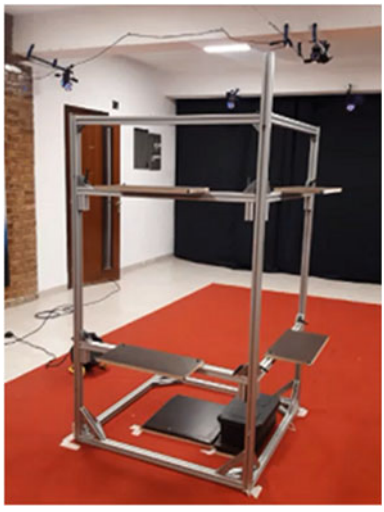

Fig. 1 Built testbed used in the experimental part

2.3 Experimental Protocol

The experimental protocol was approved by the Ethical Committee of the Spanish National Research Council (092/219). It consists of two tasks vinculated to manipulation skills from bipedal standing: *Sagittal Lifting* and *Lateral Box Transfer*. The three factors involved in the experiment are: System *(No exoskeleton/ Exoskeleton)*, Load *(0 kg/ 10% of subject's body weight)* and Lift Type (for sagittal lifting, *Floor-to-Knee* (F2K)/ *Floor-to-Shoulder* (F2S)/ *Knee-to-Shoulder* (K2S); and for lateral box transfer, *Knee-to-Knee* (K2K)/ *Shoulder-to-Shoulder* (S2S)). Lateral box transfer task results are not presented in this paper.

2.4 Testing Procedure

By the moment, one young healthy male subject has been tested. Human motion in the sagittal plane was recorded at 100 Hz using a photogrammetric marker-based motion capture system (Vicon, Oxford Metrics), and the kinematic data were low-pass filtered with a zero-phase lag 4th order Butterworth filter at 8 Hz. Prior to the start of the experiment, the exoskeleton was fitted to the subject and the mobile shelves of the testbed were adjusted to his knees and shoulders' height. The 14 mm-diameter retroreflective markers were placed according to the Full Body Plug-in-Gait protocol [4]. The dynamic trials were performed in a randomized order, so as to prevent learning effects. Between trials, the subject was asked to close his eyes making him unaware of the boxes' interchange performed by the researchers.

2.5 Movement Quantification: Metrics

We developed the following set of objective metrics based on kinematic data: *A.* Range of movement (RoM); *B.* Postural instability, assessed by computing the deviation between the centre of mass and the centre of the base of support [5]; *C.* Performance time, or required time to complete the task; *D.* Spinal loads estimation, given by the L4-L5 and L5-S1 compression and shear forces [6]; and *E.* Smoothness, obtained by computing the arc length of the joint's speed spectral profile [7].

3 Results

All the results described below refer to Table 1

3.1 Range of Movement

Despite the mechanical constraints, the range of movement at the lower-extremity joints was not limited. A larger RoM was occasionally observed at the hip and knee joints in exoskeleton trials as a result of neuromechanical adaptations or due to dynamic effects introduced by the device. In addition, no compensatory effects were observed on upper-limb joints.

3.2 Postural Instability

The H2 increased postural instability, especially in the anterior/posterior direction, although being far from introducing considerable fall risks.

3.3 Performance Time

The H2 exoskeleton increased the total time of task execution. This reflects the reduction of subject's agility while wearing the device.

Table 1 Performance metrics corresponding to the Sagittal Lifting task and to the knee joint

Experimental condition	System	RoM (degrees)	Postural instability (%)	Time (seconds)	Spinal loads (Newtons)	Smoothness (dimensionless)
F2K 0 kg	No exo	94.20	11.48	10.38	1224.70	−3.45
F2K 0 kg	Exo	104.15	–(experimental error)	11.94	1423.50	−4.55
F2S 0 kg	No exo	111.80	12.25	11.18	1039.70	−3.10
F2S 0 kg	Exo	161.65	25.40	13.58	1144.20	−2.25
K2S 0 kg	No exo	58.55	10.70	10.91	848.74	−2.95
K2S 0 kg	Exo	121.05	19.10	10.80	974.93	−3.20
F2K 10%	No exo	154.80	17.39	10.56	2500.60	−1.85
F2K 10%	Exo	167.70	36.62	13.53	1639.50	−4.10
F2S 10%	No exo	132.10	16.13	11.23	2046.80	−2.30
F2S 10%	Exo	164.05	28.92	14.24	1484.50	−3.90
K2S 10%	No exo	70.40	20.12	10.09	2082.10	−3.25
K2S 10%	Exo	167.95	21.50	12.84	1194.70	−5.05

3.4 Spinal Loads Estimation

In empty-box lifts, compression forces are greater in exoskeleton trials than in those performed without the device. However, in loaded-box lifts, although the back forces increased without the exoskeleton, a reduction on them was observed when using the device.

3.5 Smoothness

A slightly smoother trend is observed in the exo-free trials. Smoother manoeuvres correspond to the upper-limb joints, and the more abrupt ones to the hip joint.

4 Discussion

The main goal of this study was to quantify the impact of a lower limb exoskeleton on manipulation tasks. A limitation in the RoM was expected; however, the exoskeleton allowed the subject to perform natural movements. We expected that lifting the loaded box while wearing the exoskeleton will affect subject's stability. It was observed that the loaded box slightly increased instability in the exoskeleton trials. As expected, the exoskeleton increased the performance time. Moreover, the H2 relieved the subject's back loading when lifting the loaded box. Lastly, the exoskeleton slightly decreased the smoothness, which varied across joints.

5 Conclusions

Given our results, even though this study can not be considered definitive in any way as only one subject was tested, the H2 exoskeleton assessed did not negatively affect the subject's RoM nor his back mechanical loading. However, it is responsible for the increase of postural instability and performance time, and for the decrease of movement smoothness. As future work, more subjects should be tested, movement in other planes should be studied, and the effects of the powered exoskeleton should be investigated.

Acknowledgements The work presented in this paper was supported by the European Union's Horizon 2020 research and innovation program under grant agreement No 779963—EUROBENCH.

The authors would like to acknowledge the support of Technaid S.L. for unconditionally providing the exoskeleton for this research.

References

1. D. Torricelli, J.L. Pons, EUROBENCH: preparing robots for the real world. In: *Wearable Robotics: Challenges and Trends*. WeRob 2018. Biosyst. Biorobot. **22**, 375–378, 2018. (Springer)
2. T. Luger et al., Influence of a passive lower-limb exoskeleton during simulated industrial work tasks on physical load, upper body posture, postural control and discomfort. Appl. Ergonomics **80**, 152–160 (2019)
3. M. Bortole et al., The H2 robotic exoskeleton for gait rehabilitation after stroke: early findings from a clinical study. J. Neuroeng. Rehabili. **12**(1), 54 (2015)
4. Vicon, Plug-in-Gait Reference Guide
5. M. Alamoudi, *Investigation and Analysis of the Effects of Manual Lifting and Carrying Activities on Postural and Gait Stability in Normal Subjects* (Research repository of Miami University, 2017)
6. F. Ghezelbash et al., Subject-specific regression equations to estimate lower spinal loads during symmetric and asymmetric static lifting. J. Biomech. **102**, 109550 (2020)
7. S. Balasubramanian et al., A robust and sensitive metric for quantifying movement smoothness. IEEE Trans. Biomed. Eng. **59**(8), 2126–2136 (2012)

Assessment of Exoskeleton Related Changes in Kinematics and Muscle Activity

Fabio V. dos Anjos, Taian M. Vieira, Giacinto L. Cerone, Talita P. Pinto, and Marco Gazzoni

Abstract Work-related musculoskeletal disorders, reported at shoulder and low back regions, rank among the most serious health problems in industry. Owing to their ability in providing support to the shoulder and back regions during sustained and repetitive tasks, passive exoskeletons are expected to prevent work-related disorders. In this work, experimental protocols were conducted for the extraction of relevant information regarding the neuromuscular activation and kinematics during simulated working activities with passive exoskeletons. Our results support the notion these passive exoskeletons have the potential to alleviate muscular loading and therefore to prevent musculoskeletal disorders in the industrial sector.

1 Introduction

EXOSKELETONS have been proposed as a promising solution for the prevention of work-related musculoskeletal disorders (MSD) [1, 2]. However, the current knowledge does not fully clarify the impact of exoskeletons on MSD prevention [3]. *Even if many factors must be considered in MSD prevention,* excessive muscular stress

F. V. dos Anjos
Postgraduate Program of Rehabilitation Sciences, Augusto Motta University (UNISUAM), Rio de Janeiro, Brazil
e-mail: fabioanjos@souunisuam.com.br

T. M. Vieira · G. L. Cerone · T. P. Pinto · M. Gazzoni (✉)
Laboratory for Engineering of the Neuromuscular System (LISiN), Politecnico di Torino, Torino, Italy
e-mail: marco.gazzoni@polito.it

T. M. Vieira
e-mail: taian.vieira@polito.it

G. L. Cerone
e-mail: giacintoluigi.cerone@polito.it

T. P. Pinto
e-mail: talita.peixoto@polito.it

J. C. Moreno et al. (eds.), *Wearable Robotics: Challenges and Trends*,
Biosystems & Biorobotics 27, https://doi.org/10.1007/978-3-030-69547-7_83

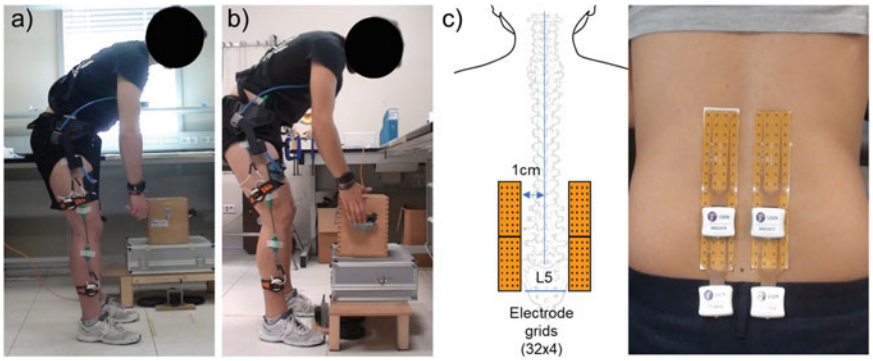

Fig. 1 The static **a** and dynamic **b** tasks used to evaluate changes in muscle activity induced by the Laevo exoskeleton. **c** Surface EMG was acquired using four matrices (16 × 4 electrodes) positioned over the lumbar muscles bilaterally

is a predominant risk factor. *Consequently,* surface electromyography (sEMG) is an important tool for the evaluation of exoskeleton effectiveness, providing information about changes in muscle efforts. Exoskeletons showed a clear potential in limiting local muscular demand, however, great differences in the reduction of muscle activity are reported in literature [3]. *In this work w*e studied the changes in EMG activity and kinematics induced by the use of two passive exoskeletons: one for lumbar support (Laevo V2.5—Laevo B.V., Delft, Netherlands) and one for upper limb support (MATE, Comau S.p.a, Turin, Italy).

2 Material and Methods

2.1 Lumbar Support—Laevo

Ten male volunteers were recruited (age: 22–32 years).

(1) *Tasks*

Participants were asked to perform one static and one dynamic task, with and without the passive exoskeleton. The static forward bending task consisted in maintaining a 45° trunk flexion posture (Fig. 1a) until exhaustion. In the dynamic task, participants were instructed to repetitively lift and lower a box (mass: 10 kg) between two surfaces at 50 cm and 100 cm from the ground level (Fig. 1b). The task was repeated for 10 min with a frequency of 15 times per minute. A digital metronome was used to assist subjects in complying with the requested cadence.

(2) *Electromyography and kinematics*

Monopolar sEMG signals were collected *from the low back muscles bilaterally with four electrode grids (8 × 4 electrodes, inter-electrode distance:* 10 mm*;* Fig. 1c) *organized in two groups of 32 × 4 electrodes. Signals were conditioned and sampled using four* 32 channel acquisition systems for HD-sEMG (2048 samples/s; 16-bit) (LISiN, Politecnico di Torino and OT Bioelettronica) [4]. Hip and knee joint angles of the right leg were collected from two electrogoniometers (Twin-Axis Electrogoniometer SG150, Biometrics Ltd., Newport, United Kingdom), with zero degrees corresponding to full knee and hip extension.

(3) *Data processing and statistical analysis*

For the static task, Root Mean Square (RMS) values were computed from single-differential EMGs over 1s epochs, while for the dynamic task, RMS values and maximum and minimum joint angles were calculated over individual lifting -lowering cycles. RMS maps were obtained by averaging RMS values at 10% increments in time over the duration of task. For each task, the degree of activity was computed from the maps at the beginning, mid and end of task as the average RMS over the channels showing an RMS value higher than 70% of the maximum RMS in the map [5]. The coordinates of the centroid of RMS distribution along the cranial-caudal direction were also computed. About the kinematic data, the average maximum and minimum angles were extracted from the first, middle and last decile of task for both lifting and lowering. A 2-way and 3-way ANOVA were applied separately for each cycle phase to respectively assess the effect of Time and Device on the joint angles and the effect of Time, Device and Side on the degree of activity and the centroid of RMS distribution (*post-hoc* Tukey and significance level of 5%).

2.2 Upper Limb Support—MATE

Twelve young healthy volunteers (age: 20–30 years) participated in the study.

(1) *Tasks*

Subjects were instructed to maintain four static postures (Fig. 2a) for 20s in two conditions (without and with the passive exoskeleton MATE). The considered postures were: (P1) shoulder abducted at 90°, elbow flexed at 90°, elbow pronated at 90°; (P2) shoulder flexed at 90°, elbow flexed at 90°, elbow pronated at 90°; (P3) shoulder flexed at 90°, elbow pronated at 90°; (P4) shoulder abducted at 90°, elbow pronated at 90°. Each task was repeated 5 consecutive times. The assistance level was set as recommended by the manufacturer in relation to height and weight of the user.

(2) *Electromyography and kinematics*

Bipolar EMGs were collected from the anterior, medial and posterior deltoids and the upper trapezius of the right upper limb using pairs of surface electrodes (30 mm

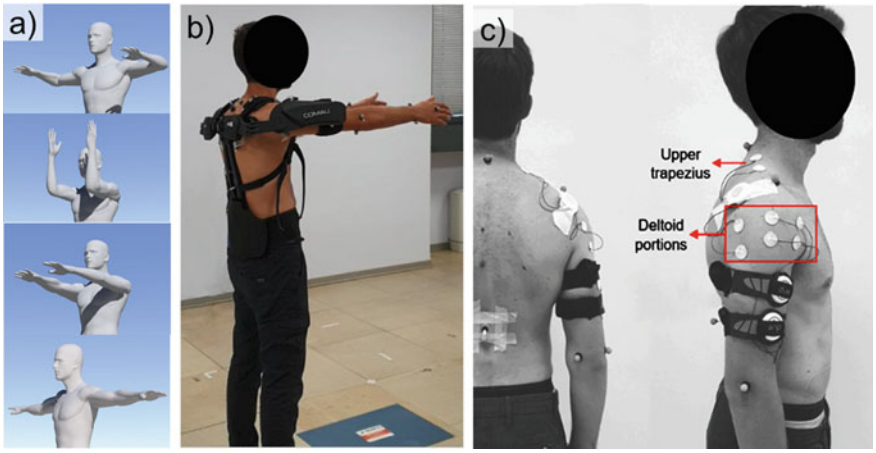

Fig. 2 **a** shows the four static postures considered in the study. **b** shows one subject wearing the MATE exoskeleton in posture P3. **c** The positioning of EMG electrodes

inter-electrode distance, 24 mm diameter, Spes Medica, Battipaglia, Italy) and digitized at 2048 Hz with a 16 bits A/D converter (DuePro, OTBioelettronica and LISiN, Politecnico di Torino, Turin, Italy). Kinematic of upper limbs were recorded simultaneously with EMGs by a 12 camera VICON system (100 Hz, Vero v2.2, Oxford, UK), positioning the markers according to the protocol proposed by Hebert et al. [6].

(3) *Data processing and statistical analysis*

For each investigated muscle and posture the average RMS amplitude was computed across the 5 repetitions. Differences in RMS amplitude were assessed with 2-way ANOVA separately for each posture, with condition (with and without exoskeleton) as repeated measures (2 conditions × 4 postures). Whenever any significant difference was revealed paired comparisons were assessed with Tukey-HSD post-hoc test.

3 Results and Discussion

3.1 Lumbar Support—Laevo

Statistical analysis revealed lower level of lumbar muscles' activity (~10%) with than without exoskeleton throughout static task ($F = 10.61$, $p < 0.01$) together with a redistribution of muscle activity (~0.5 cm) in the caudal direction toward the end of task ($F = 4.11$, $p < 0.02$). In the dynamic task, a significant attenuation effect of exoskeleton on muscle activity was observed at the beginning of task ($F > 4.97$, $p < 0.01$ in both phases) during both lifting (~5%; $p = 0.01$) and lowering (~8.5%; $p <$

0.01). A trend toward a redistribution of muscle activity to the distal muscle region during the task (~0.5 cm; $F = 2.60$, $p < 0.09$) was observed without than with the use of exoskeleton. This finding seems to indicate that exoskeleton may reduce muscle loading at the beginning of the task. Moreover, for the knee joint, a lower maximum angular position (~6.5°) was observed with than without exoskeleton, regardless of cycle phase (Device effect: $F > 8.72$, $p < 0.01$; *post-hoc*: $p < 0.01$), suggesting exoskeleton might affect the range of motion during the dynamic task.

3.2 Shoulder Support—MATE

A main Device effect was observed for anterior and medial deltoids and upper trapezius, with lower RMS values with than without exoskeleton ($F > 6.10$; $p < 0.018$ for all cases). Significant interaction was observed for posterior deltoid, with lower amplitude values with than without exoskeleton for P1 and P4 (*post-hoc* $F > 3.53$ and $p < 0.025$). These findings revealed the attenuation effect of exoskeleton on muscle activity was manifested at all muscles evaluated, though not for all postures when considering posterior deltoid.

4 Conclusion

The results suggest the passive exoskeletons tested seem to be potentially relevant to attenuate the muscular effort, with implications for the prevention of work-related musculoskeletal disorders. The extension of the study to dynamic conditions with the MATE exoskeleton is ongoing.

Acknowledgements This work was supported by Regione Piemonte and the Ministry of Education, University, and Research in the POR FESR 2014/2020 framework Project "Human centered Manufacturing Systems (HuManS)" and by IUVO Srl.

References

1. T. Bosch, J. van Eck, K. Knitel, M. de Looze, The effects of a passive exoskeleton on muscle activity. Appl Ergon. **54**, 212–217 (2016)
2. K. Huysamen, T. Bosch, M. de Looze, K.S. Stadler, E. Graf, L.W. O'Sullivan, Evaluation of a passive exoskeleton for static upper limb activities. Appl. Ergon. **70**, 148–155 (2018)
3. J. Theurel, K. Desbrosses, Occupational exoskeletons: overview of their benefits and limitations in preventing work-related musculoskeletal disorders. IISE Trans. Occup. Ergon. Hum. Factors (2019)
4. G.L. Cerone, A. Botter, M. Gazzoni, A modular, smart, and wearable system for high density sEMG detection. IEEE Trans. Biomed. Eng. Eng. **66**(22), 3371–3380 (2019). https://doi.org/10.1109/TBME.2019.2904398

5. T.M.M. Vieira, R. Merletti, L. Mesin, Automatic segmentation of surface EMG images: Improving the estimation of neuromuscular activity. J. Biomech. (2010). https://doi.org/10.1016/j.jbiomech.2010.03.049
6. J.S. Hebert, J. Lewicke, T.R. Williams, A.H. Vette, Normative data for modified Box and Blocks test measuring upper-limb function via motion capture. J. Rehabil. Res. Dev. **51**(6), 918–932 (2014)

Exoskeletons for Military Applications

Exoskeletons for Military Logistics and Maintenance

Mona Hichert, Markus Güttes, Ines Bäuerle, Nils Ziegenspeck, Nico Bölke, and Jonas Schiebl

Abstract Field studies were performed at various logistics and maintenance facilities of the German armed forces, with the aim to develop a set of design requirements for novel exoskeletons in military logistics applications. This led to an improved understanding of common logistics tasks and a list of design requirements including main and secondary activities, ranges of motion and environmental parameters. From these design requirements, designs and first prototypes were derived.

1 Introduction

In many areas of logistics and maintenance, workers have to perform physically strenuous work, such as lifting and carrying heavy objects, as well as working in forced postures (e.g. forward bent posture or overhead work) or while standing. The strain on the musculoskeletal system can lead to serious damage of the back or shoulders resulting in a reduced quality of life, increased sick days and reduced productivity [1].

M. Hichert (✉) · M. Güttes · I. Bäuerle
Fraunhofer FKIE–Fraunhofer Institute of Communication Information Processing and Ergonomics, Bonn, Germany
e-mail: mona.hichert@fkie.fraunhofer.de

M. Güttes
e-mail: markus.guettes@fkie.fraunhofer.de

I. Bäuerle
e-mail: ines.baeuerle@fkie.fraunhofer.de

N. Ziegenspeck · N. Bölke · J. Schiebl
Fraunhofer IPA–Fraunhofer Institute for Manufacturing Engineering and Automation, Stuttgart, Germany
e-mail: nils.ziegenspeck@ipa.fraunhofer.de

N. Bölke
e-mail: nico.boelke@ipa.fraunhofer.de

J. Schiebl
e-mail: jonas.schiebl@ipa.fraunhofer.de

J. C. Moreno et al. (eds.), *Wearable Robotics: Challenges and Trends*,
Biosystems & Biorobotics 27, https://doi.org/10.1007/978-3-030-69547-7_84

Musculoskeletal disorders are one of the major reasons for work incapacity [2]. Sick days are not only costly, but are also accompanied by loss of knowledge, experience and routine of specialized workers. Exoskeletons are innovative ergonomic tools, which potentially decrease the strain on the body [3]. Exoskeletons can be categorized in passive systems that support by mechanical elements like springs or elastic bands and active systems that provide support from e.g. electric motors. An intermediate approach are adaptive or semi-active exoskeletons that use motors to activate or adjust a passive support system.

To investigate the potential benefits of exoskeletons in the logistics of the German armed forces, the project "ExoLog" was launched in June 2019. The two Fraunhofer Institutes FKIE (Fraunhofer Institute for Communication, Information Processing and Ergonomics) and IPA (Fraunhofer Institute for Manufacturing Engineering and Automation) are developing novel exoskeletons in close cooperation with partners of the German armed forces until the end of 2021. First, design requirements for the stationary military logistics base were set, followed by a comparison to the mobile logistic tasks and the corresponding changes in requirements. This extended abstract focuses on the stationary military logistics.

2 Method

Different military stationary logistics facilities, like ammunition depots, material warehouses materials management center deployment and naval bases, were examined. Inspection of workspaces led to a selection of activities, in which soldiers and civilian workers can potentially benefit from exoskeletons. The focus was on overhead work, lifting and carrying, and tasks in forward bent postures. Movements during these selected tasks were recorded by a mobile motion capture system (MTw Awinda, Xsens, Enschede, the Netherlands). Resulting joint angles were calculated from the generated movement data and compared to occupational safety recommendations [4]. According to the soldiers subjective rating, the lower back and shoulders are the areas that experience the highest strain.

Furthermore, some soldiers were introduced to and fitted with commercially available exoskeletons and were asked to execute their tasks wearing exoskeletons. The used exoskeletons included several passive exoskeletons for overhead work and for lifting tasks. After completing the tasks, their judgement was recorded through questionnaires and interviews. This was a first exploratory investigation into the subjective perception of the application of exoskeletons. The small number of participants, short duration and variability of tasks do not allow statistical conclusions. The aim was to get an indication of the potential benefits in stationary military logistics and room for improvement for novel devices.

Subsequently, the observations of the visits were summarized in a list of requirements.

3 Results

Derived from the observations, two novel exoskeletons that fulfill the summarized requirements and provide better functionality as well as user acceptance of commercial exoskeletons are being developed in the scope of this project. The first novel device is focused on the shoulder area, supporting overhead work as well as lifting between hip height and overhead height, while the second device is focused on lifting tasks between floor and hip height as well as forward bent work. The list of requirements for exoskeletons in the stationary military logistics was subcategorized into main activities that can be supported by, and secondary activities that should be feasible with the exoskeleton.

The main activities included lifting and laying down at and from waist level (with and without mesh stillages), carrying at waist level, lifting up to and down from shoulder level, overhead work and forward bent tasks. Joint angles, which could lead to musculoskeletal diseases when they occur often or over a prolonged period of time were found in several tasks. Affected areas were hip flexion, shoulder flexion and abduction and in some cases head extension.

In addition, environmental parameters, available infrastructure, users and their anthropometric data, executed range of motion during the main activities, performance data, usability, comfort, and safety requirements were identified. Usability, comfort and safety requirements included weight of the device, time and ease to don and doff, adaptability to different user sizes, size of the device, noise levels, power supply and compatibility with everyday equipment and clothing of the worker.

4 Discussion

Visits at different military stationary logistics facilities resulted in a list of requirements for novel exoskeletons.

The presented joint angle data underlines the potential benefits utilizing ergonomic tools, like exoskeletons, in the execution of these tasks.

The measured data allow us to formulate specific joint angles which workers should be able to execute while wearing an exoskeleton without restriction of movement, as well as certain specific movements that should be supported.

Furthermore, the developed list of design requirements with all its categories, which were not discussed in detail here, gives an informed starting point for the development of novel exoskeletons.

Ongoing work as part of the project includes laboratory experiments and exoskeleton development and engineering. An experimental methodology has been developed to evaluate existing commercial exoskeletons, followed by newly developed prototypes, by imitating the main field test tasks in the Fraunhofer human performance laboratory under controlled conditions. Muscle activity (EMG), metabolic

cost and kinematics will be recorded. By inverse dynamic calculations resulting joint moments will be evaluated.

Novel exoskeleton development focuses on passive, semi-active and adaptive exoskeletons for shoulder and back support. Overall, the aim is to investigate the exoskeletons benefits for logistic workers by quantifying physiological and biomechanical data in the scope of occupational health and safety. Reducing the physical strain might also enable the soldiers and civilian workers to perform tasks under more healthy conditions for longer periods of time.

For now, the focus is on stationary military logistics, but applications are intended for mobile logistics as well. We observed similarities in stationary military logistics and civil logistics. However, differences were found in more Personal Protection Equipment (PPE, e.g. bulletproof vests), higher time pressure, higher weight of manually transported objects and longer task duration in the military setting.

5 Conclusion

A set of design requirements, derived from field experiments and interviews with staff of the German armed forces has been developed for the application of exoskeletons in military logistics. Next steps include the development of passive and semi-active adaptive exoskeletons and laboratory test methodology to evaluate and compare exoskeletons (existing and new), and improve understanding about the physiological performance of humans using exoskeletons during military logistics tasks.

Acknowledgements This work was supported by the Exolog Project funded by the German Armed Forces (Bundeswehr) under Grant No E/U2Ci/KA225/JF080.

The authors like to thank the soldiers and civil workers at the military stationary logistics facilities for participating in the field tests and our partners in the German armed forces for their valuable input.

References

1. L.L. Andersen, N. Fallentin, J.Z.N. Ajslev, M.D. Jakobsen, E. Sundstrup, Association between occupational lifting and day-to-day change in low-back pain intensity based on company records and text messages. Scand. J. Work Environ. Health **43**(1), 68–74 (2017).
2. H.F. van der Molen, C. Foresti, J.G. Daams, M.H.W. Frings-Dresen, P.P.F.M. Kuijer, Work-related risk factors for specific shoulder disorders: A systematic review and meta-analysis. Occup. Environ. Med. **74**(10), 745–755 (2017).
3. M.P. de Looze, T. Bosch, F. Krause, K.S. Stadler, L.W. O'Sullivan, Exoskeletons for industrial application and their potential effects on physical work load. Ergonomics **59**(5), 671–681 (2016).
4. Deutsche Gesetzliche Unfallversicherung e.V. (DGUV), *DGUV Information 208–033: Belastungen für den Rücken und Gelenke - was geht mich das an?* (2016). (Online). Available: https://publikationen.dguv.de/widgets/pdf/download/article/458

Aerial Porter Exoskeleton (APEX) for Lifting and Pushing

W. Brandon Martin, Alexander Boehler, Kevin W. Hollander, Darren Kinney, Joseph K. Hitt, Jay Kudva, and Thomas G. Sugar

Abstract A hip exoskeleton was designed that can assist hip extension during squat lifting and pushing. The device incorporates a motor, ball screw in a compact lightweight package. The total weight of the system including the battery is 3.94 kg and the system can supply over 30 Nm of torque to each leg. The device assists lifting and pushing and is not engaged during walking, running or other tasks.

1 Introduction

WEARABLE robotic systems are being developed to assist at the hips [1–6]. These systems must be lightweight, energy efficient, and must conform to the human. For systems to assist during load handling tasks, they must not interfere with the human gait such as walking and jogging.

We have developed a hip exoskeleton, APEX (Aerial Porter Exoskeleton). A similar system, HeSA, was designed in 2016–2018 to assist soldiers walking on patrol, wearing a tactical vest that holds body armor. The current system is designed for logistics handling and will only operate during lifting and pushing. The design and testing of the system will be described.

USAF, Contract FA8606–19-C-0018.

W. Brandon Martin · A. Boehler · T. G. Sugar
Human Machine Integration Laboratory, Arizona State University, Tempe, AZ, USA

T. G. Sugar (✉)
Arizona State University, Tempe, AZ, USA
e-mail: thomas.sugar@asu.edu

K. W. Hollander · D. Kinney
Augspurger Komm Engineering Inc., Phoenix, AZ, USA

J. K. Hitt
GoX Labs, Phoenix, USA

J. Kudva
Nextgen Aeronautics, Torrance, USA

J. C. Moreno et al. (eds.), *Wearable Robotics: Challenges and Trends*,
Biosystems & Biorobotics 27, https://doi.org/10.1007/978-3-030-69547-7_85

2 Design Goals

The goal is to develop a lightweight, hip exoskeleton to reduce workplace injuries and improve productivity, efficiency, and quality during logistics operations. We will focus on pushing large pallets (4500 kg) onto cargo aircraft and the lifting of some light (1–4.5 kg), medium, (4.5–13.6 kg) and heavy objects (13.6–22.7 kg), specifically:

1. A comfortable, lightweight design is proposed that is easily donned and doffed. The current system can be donned in less than 1 min.
2. Utilizing the unique "catch and release lever arm" approach, the system will not constrain postures or walking.
3. With the unique catch and release lever arm, the system will allow operators to get in and out of vehicles and sit on a forklift.
4. The device is intuitive to operate with no need for user input. There is no extended training period for the control system that is always in-phase with the user based on our unique phase-oscillator controller.
5. The system will be adjustable to accommodate small and large workers.
6. The powered system is very efficient and will only be used to assist pushing and lifting.

Powered System versus Passive System: Passive back exoskeletons are functioning very well. Current commercial systems include SuitX, Laevo, Hunic, and HeroWear. Passive back exoskeletons have been shown to reduce metabolic cost and assist the user in performing more ergonomic lifts, decreasing injury potential. A passive system is lighter and more cost effective than a powered system as well. However, a passive system cannot supply extra power and torque when needed to perform heavy lifting and pushing all-day. A passive system can only return the amount of stored energy that the person puts into it. Most importantly, most passive systems cannot get out of the way when walking or running.

We do not feel that a passive system can assist in heavy pushing tasks. If the worker just cannot push the pallet, without the need for extra crew members, then a passive system will not help because it cannot supply any extra enhancement. However, a powered system will supply extra hip extension torque for pushing tasks. Our main benefit is to increase the leg extension torque reducing muscle fatigue.

3 Design

We had discussions with airport logistics companies about pushing and loading cargo onto aircraft. Firstly, we were informed that nothing should be at the feet/shoes since the worker is moving inside of cramped areas and there can be objects on the ground such as transfer balls.

Secondly, we learned that turning around and pushing with your back is easier on the legs. This occurs because the lumbar region is supported; some of the weight

of the user is supported by friction between the object and the back; the heels are touching the ground, and the large muscles in the front of the leg and the calf muscles are used to extend the shank. However, this motion is not recommended because the user is not holding onto the cargo.

Pushing a large object is difficult because the legs must support the mass of the body; the heel is off of the ground, the pelvis and lumbar region must resist the pushing force; and *it is difficult to extend the thigh and knee from a flexed position*, shown in the right illustration of Fig. 1.

Lifting objects is difficult as well because *it is hard to extend the thigh and knee from a flexed position when performing a squat lift.* Many users prefer a stooped lift because it is a less energetic movement requiring less muscle work from the legs. The squat lift is better for the lower back, but it takes more energy to perform the motion.

The APEX device provides unidirectional torque support for hip extension to each hip, see Fig. 1.

Peak torque for hip extension per leg	30 Nm
Total device weight without battery	3.26 kg
Battery weight, 36 V 72 Whr	0.68 kg
Motor/ball screw/spring actuator	

The hip actuator can disengage from the thigh attachment to allow for free range of motion during walking and jogging. The free motion allows the user to flex and extend the hip to walk naturally, ascend and descend stairs and get easily in and out of vehicles.

The actuator is attached to a carbon fiber structure that has two purposes. Firstly, it resists the reaction torque of the motor so that the hip can be assisted to push the user forward or push the user upward during lifting. Secondly, the hip structure helps to maintain better posture. The motor unit is attached to the carbon fiber structure with pin joints to allow hip abduction and adduction, see Fig. 2.

4 Testing

The device was worn and tested. We are primarily focused on two tasks. Pushing a 227 kg cart at a travel rate of 1 m/s for 100 m. The second task is to lift 13.6 kg and walk 6.1 m and set the object down. This task will be repeated 30 times over 15 min. We will be measuring lift kinematics and metabolic cost using the GoX Ergo Kit seen in Fig. 3.

The supplied torque for the APEX mechanism was tested with two devices, a spring gauge and a force plate. Both tests returned 30 Nm of torque when the assist mechanism was activated.

Fig. 1 The hip exoskeleton assists lifting and pushing. (Version 2 with improved thigh cuffs)

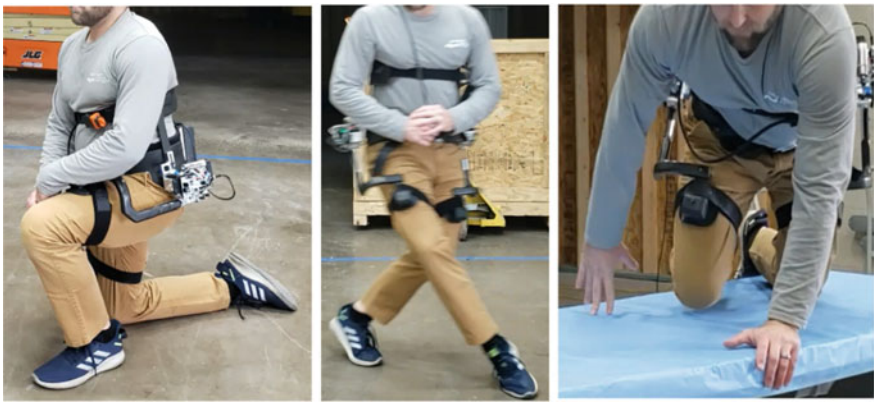

Fig. 2 The hip exoskeleton has free range of motion. (Version 1)

5 Conclusion

We have designed a lightweight hip exoskeleton that can apply 30 Nm of assistive hip extension per leg in concert with the user. When the system is disengaged, the user can walk, run, and climb over objects. Further developments will include the ability to assist stair climbing and sit-to-stand tasks.

Fig. 3 GoX Ergo Kit used to measure metabolic cost, heart rate, and lift kinematics

Acknowledgements A patent application has been filed on the mechanical design "Hip Exoskeleton for Lifting and Pushing," by Thomas Sugar and Kevin Hollander. Any opinions, findings, and conclusions or recommendations expressed in this material are those of the authors and do not necessarily reflect the views of the funding agency.

References

1. A. Asbeck, K. Schmidt, C. Walsh, Soft exosuit for hip assistance, Robot. Auton. Sys. (2014)
2. K. Seo, J. Lee, Y. Park, Autonomous hip exoskeleton saves metabolic cost of walking uphill, ICORR (2017)
3. K.W.Hollander, N. Cahill, R. Holgate, R.L. Churchwell, Clouse, P.C., D. Kinney, A. Boehler, A passive and active joint torque augmentation robot (JTAR) for hip gait assistance, *ASME IDETC 2014, DETC2014-35654*, Buffalo, NY
4. K.W. Hollander, N. Cahill, R. Holgate, R.L. Churchwell, P.C. Clouse, D. Kinney, A. Boehler, J. Ward, A joint torque augmentation robot (JTAR) for ankle gait assistance, *ASME IDETC 2014, DETC2014-35653*, Buffalo, NY
5. K.W. Hollander, P. Clouse, N. Cahill, A. Boehler, T.G. Sugar, A. Ayyar, Design of the orthotic load assistance device (OLAD), dynamic walking, Pensacola, FL.
6. J. Kerestes, T.G. Sugar, M. Holgate, Adding and subtracting energy to body motion—phase oscillator, IDETC (2014)

Exoskeletons for Unarmed Military Use: Requirements and Approaches to Support Human Movements Using an Example of Protection Against Unknown CBRN Dangers

C. Linnenberg, J. Klabunde, K. Hagner, and R. Weidner

Abstract Using individual protective equipment (IPE) while handling unknown chemical, biological, radiological and nuclear (CBRN) dangers can lead to high physical stress on the user. The use of exoskeletons may be a good approach to help relieving the user and may increase the overall wear time of the IPE. Due to the unique environment and equipment, this use case applies additional requirements on the exoskeletal functions, design and interaction with the IPE. By the example of disposal of unknown CBRN dangers, this contribution observes and analyses the different tasks in the field of handling unknown CBRN dangers and deduces requirements for the combination of the IPE and exoskeletons. The results recommend the use of exoskeletons combined with the IPE, especially the gas-tight protective suit and a few approaches to include exoskeletal systems in the security measures.

1 Introduction

HANDLING CBRN hazardous substances requires a high degree of safety precautions. In order to be able to comply with these, it is necessary to use protective suits with an adequate protection level and hazard-depending respiratory protection. The

The research is funded by Bundeswehr Research Institute for Protective Technologies and NBC Protection, Project: "Entlastung beim Tragen von CBRN-Schutzausrüstung", (grant number E/E590/IZ014/HF120). The sole responsibility for the manuscript contents lies by the authors. We thank the partners for their support and cooperation.

C. Linnenberg (✉) · R. Weidner
Production Technology, Institute for Mechatronics, University Innsbruck, Innsbruck, Austria
e-mail: Christine.Linnenberg@uibk.ac.at

J. Klabunde · R. Weidner
Laboratory for Production Technology, Helmut Schmidt University, University of the German Federal Armed Forces Hamburg, Hamburg, Germany

K. Hagner
Department of Individual and Collective Protection, Bundeswehr Research Institute for Protective Technologies and NBC Protection, Munster, Germany

J. C. Moreno et al. (eds.), *Wearable Robotics: Challenges and Trends*,
Biosystems & Biorobotics 27, https://doi.org/10.1007/978-3-030-69547-7_86

highest possible protection level is used to deal with unknown hazardous substances, where gas-tight impermeable protective suits and self-contained breathing apparatus (SCBA) are used. This can lead to a high physical strain due to the limited mobility, the additional weight of the SCBA, the flexing resistance caused by the suit's material and the SCBA [1]. The use of exoskeletal systems may be suitable to counteract these stresses and reduce overload on the user. Field and biomechanical laboratory studies were carried out as a basis for deriving key stress factors of the strenuous tasks and requirements on exoskeletal systems. To comply with the high protection level of the IPE, the use of exoskeletons has to meet special requirements.

2 General Analysis

2.1 Field Analysis

The field analysis took place in a save area that was already decontaminated. Experts in handling and disposing unknown CBRN dangers were accompanied and interviewed while simulating their daily working tasks. Camera recordings were taken to determine working steps and approximate range of motion. The key tasks are categorized into five basic activities, covering the majority of the work activities. These activities include (1) chopping, (2) shoveling (3) lifting contaminated or explosive material, (4) recovering explosives, (5) walking with the IPE into or out of contaminated areas. Fig. 1 shows examples from the camera analysis.

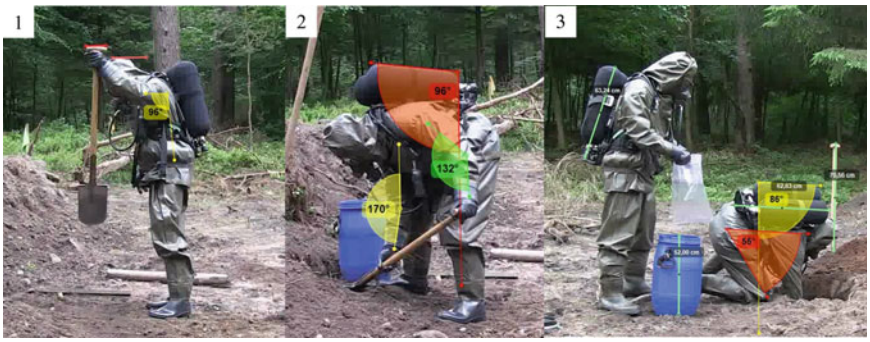

Fig. 1. Basic activities observed in the field: e.g. chopping (1), shoveling (2) and recovering (3)

2.2 Laboratory Study

The results of the field analysis were used to set up the laboratory test environment. The five basic activities from the field study were each performed in three different conditions: (1) without any equipment, to capture the strain of the actual activity itself (2) with SCBA to detect strains caused by the additional weight and (3) in full gear with SCBA and IPE (suit, boots and gloves) to record total strains. The tests carried out in the study contain kinematic, electromyographic (EMG), electrocardiographic (ECG) and posturographic measurements to draw conclusions on the change in the movement pattern, muscle activity, cardio-pulmonal stress and postural control. EMG-Data were standardized by maximal voluntary contractions (MVC) on the observed muscles. The test set was carried out by six subjects with an average age of 32.5 years. Methodological details are published in [2].

Performance duration prolonged over the test condition in every test set, e.g. lifting contaminated material took 31% longer with SCBA and IPE. On average ECG frequency increased for 14% in condition with SCBA&IPE compared to basic condition with a mean frequency of 102 bpm. Wearing SCBA caused higher fluctuations of body's center of gravity for 23%, wearing IPE additionally caused 50% higher fluctuations compared to basis. It can be assumed that the influence of the backpack weight is about as strong as the influence of the protective suit on the motoric and postural control. Kinematic and EMG data are quite task specific and detailed. Over all it can be summarized that, among others, the most strenuous body part is the shoulder neck region especially in the chopping and recovering tasks with up to 81%MVC mean activity of the trapezius muscle. It is followed by the lower back that shows mean activities of the erector spinae muscle up to 34% at lifting and recovering tasks. Kinematic data for instance show obviously restrictions in mobility caused by the suit. Then again, kinematic data revealed the positive influence of the SCBA backpack, serving as a counteracting balancer at the lifting task by the means of smaller back angles and less erector muscle activity in condition SCBA and SCBA&IPE.

3 General Results

There are different measures to improve the actual work. One is using organizational measures as optimized workflows or specification of work processes. This includes, e.g., work specific personal training, ergonomic positioning of the equipment. Another approach using technological improvements utilizes, e.g., an optimized backpack structure, implementing lifting gear and transportation systems, a customized excavator or exoskeletal systems. Due to the large variety of operation areas, most technological measures are only suitable for a very limited number of scenarios. Using active exoskeletons with an adaptable range of functions and support power turns out to be the most suitable solution.

According to the laboratory study there are mainly two overloaded body areas that offer a good starting point for relief with exoskeletons. One is the shoulder-neck-area and the other one is the lower back. Since the body parts are apart from one another, two different approaches may be implemented in one exoskeletal system.

4 Requirements for the Use of Exoskeletons in Combination with CBRN Protective Gear

There are mainly four influencing variables of exoskeletal support: human, activity, social surrounding and work environment. Typical examples are the different anthropometry of humans or physical precondition, range of motion of an activity or work content that requires different support. The work environment must be taken into account, e.g., with different local climatic conditions or workstations, as well as the social environment with its staff and different affinity to technology.

Handling unknown CRBN dangers requires additional factors of the influencing variables: First, the working environment is characterized by the risk of contamination. In particular, requirements arise from weather condition, the breathing protection (SCBA/powered air purifying respirator PAPR) and the impacts of the suit itself, that are inhibited vaporization, high humidity inside the suit because of the impermeable and gas-tight material, limited mobility and field of view. Second, the activity tasks themselves are characterized especially by the high backpack weights (SCBA/PAPR), the permanent change of tools and breathing protection depending on the security level.

Accordingly, safety demands arise and the safety functions, according to DIN EN ISO 13482, and the integrity of the suit must be met. Realizing a lightweight system would decrease the load and improve the breathing by using accessory respiratory muscles. To prevent further limited mobility of the suit, the exoskeleton has to be integrated within the suit. On the other hand, the suit must fully cover the exoskeleton and has to be detachable from one another while taking off the IPE to prevent contamination of the exoskeleton and the user. A high resistance of the exoskeletons main parts against humidity and sweat has to be given to ensure a high reliability and action safety. Integration of the exoskeleton and a functional back structure is necessary to switch or change the breathing protection, transfers the load to the lower extremity and relieves shoulders, neck and breathing. This also ensures fewer restrictions when performing different kinds of movements, that need to be e.g., empowered, facilitated or stabilized [3]. Providing the best postural results in stance, SCBA/ PAPR should have a high center of gravity on the body, respectively the shoulders. Dynamic actuators that meet the natural movements, movement velocity and acceleration as well as joint specific and position depended application of force until joints end positions should be approached to lower energy consumption and increase the metabolic efficiency.

5 Conclusion

In this contribution, special requirements for exoskeletons in the use of unarmed military CBRN handling and their determination were described and conclusions for general approaches of exoskeleton systems within the working area were drawn. One of the main points are the special demands of the IPE for the functionalities of the exoskeleton. The protective function has to be preserved under any circumstances while the gear affects the user with additional strains due to its function-related limitations. As mainly overloaded body areas the shoulder-neck-area and the lower back were addressed. Thus, exoskeletal approaches for each of the corresponding tasks have to be implemented. The field and laboratory tests carried out serve as a comparison to validate the use and effectiveness of possible support systems. Nevertheless, it is necessary to consider the user of the IPE in the implementation as well in order to achieve a high level of acceptance of the system combination. Further steps include the implementation of exoskeletal approaches in the suit and the testing of the functionalities in the laboratory and field tests.

References

1. K.J. Glitz, U. Seibel, W. Gorges, C. Piekarski, D. Leyk, *Gesundheit und Leistung im Klima*, vol. 12, Wehrmedizin und Wehrpharmazie (2011)
2. K. Hagner, C. Linnenberg, A. Werner, R. Tandon, A. Overkamp, Entlastungsmöglichkeiten beim Tragen impermeabler ABC-Schutzausrüstung, in *3. transdisziplinäre Konferenz "Tdchnische Unterstützungssysteme, die die Menschen wirklich wollen* (2018)
3. A. Karafillidis, R. Weidner, Distinguishing support technologies. A general scheme and its application to Exo-skeletons, in *Developing Support Technologies*, pp. S.85–100. Springer (2018)

Analysis of a Passive Ankle Exoskeleton for the Reduction of the Metabolic Costs During walking—A Preliminary Study

Luís P. Quinto, Pedro Pinheiro, Sérgio B. Gonçalves, Ivo F. Roupa, and Miguel T. Silva

Abstract The present study has as main objective the design and development of a passive exoskeleton for the reduction of the metabolic costs during gait. The prototype was designed based on an existing concept, exploring specific issues related to ankle mobility, user's ergonomics and structural customization. The evaluation of the exoskeleton performance was performed by 15 volunteers belonging to the Portuguese Army, based on the 6MWT. The exoskeleton was tested considering three force elements with different stiffnesses to assess the influence of this parameter in its performance. A qualitative analysis was also performed to assess the users' perception during the trials. Results showed a reduction of the metabolic costs in 10 subjects, presenting an average value of 3%. Moreover, the results indicate that the selection of the force elements and the tuning of the spring-engaging mechanism plays a key role in the efficiency of the developed solution.

1 Introduction

In recent years, the interest for human enhancing systems has grown significantly, particularly in the areas of defence, industry and rehabilitation. Military operations require a high energy expenditure, which could result in high exhaustion rates and

The authors would like to thank the Portuguese Army, though CINAMIL (ELITE/2019/CINAMIL) and FCT through IDMEC, under LAETA, project (UIDB/50022/2020).

L. P. Quinto (✉) · P. Pinheiro
CINAMIL, Academia Militar, Instituto Universitário Militar, Lisbon, Portugal
e-mail: luis.quinto@academiamilitar.pt

P. Pinheiro
e-mail: pinheiro.pmb@exercito.pt

L. P. Quinto · P. Pinheiro · S. B. Gonçalves · I. F. Roupa · M. T. Silva
IDMEC, Instituto Superior Técnico, Universidade de Lisboa, Lisbon, Portugal
e-mail: sergio.goncalves@tecnico.ulisboa.pt

M. T. Silva
e-mail: miguelsilva@tecnico.ulisboa.pt

J. C. Moreno et al. (eds.), *Wearable Robotics: Challenges and Trends*,
Biosystems & Biorobotics 27, https://doi.org/10.1007/978-3-030-69547-7_87

in an increase of the injury risk of soldiers [1, 2]. In these cases, exoskeletons can be a useful resource, as they can reduce the metabolic costs associated to the performance of a given task, increase the human capabilities and reduce the risk of derived musculoskeletal pathologies [1]. The main objective of this study is the development of a passive ankle exoskeleton to be applied in a military context, which allows for the reduction of the metabolic costs during walking. Hence, the developed solution should be versatile and compliant with a wide variety of terrains. It should also be easily adaptable to other applications aiming its use by a broad spectre of users. To do so, specific requirements should be taken into consideration like comfort, ergonomics, range of motion of the actuated joint and adaptability to the user's anthropometry and footwear. The main contributions of this work are the identification of the product requirements aiming its final application and the development of a functional prototype for laboratory tests (TRL 4) using additive manufacturing. The solution should take into consideration specific military requirements, such as comfort for long periods of time, range-of-motion of the ankle joint, no electromagnetic signatures, among others. While complying with these requirements, the exoskeleton should allow for the reduction of the metabolic cost during gait, one of the critical activities in military operations.

2 Materials and Methods

In order to achieve a final prototype that could be tested in a laboratory, the development of the exoskeleton followed four major steps:

(1) Exoskeleton Requirements: a concept development process, based on [3], was implemented to define the exoskeleton technical specifications. A set of interviews was conducted with individuals with experience in military operations to identify the major specifications. The guidelines proposed by the major military agencies, such as the North Atlantic Treaty Organization (NATO) or European Defence Agency (EDA), were also taken into consideration during this phase [4]. The relevance of each specification was analysed by applying a Mudge diagram and a Kano model. At the end of this process, a set of requisites were defined as mandatory, and the project evolved for the concept design.

(2) Concept Generation: the development of the exoskeleton considered two major activities, the development of the structural part and the development of the actuation unit. The structural part considered a novel approach with one lateral rod and a planar spherical bearing to allow for the free movement of the ankle joint. An external fixation to the shoe was also developed to maintain the footwear ergonomics. For the actuation unit, the mechanism proposed by Collins et al. [5] was adopted with the required modifications to fit in the developed structure.

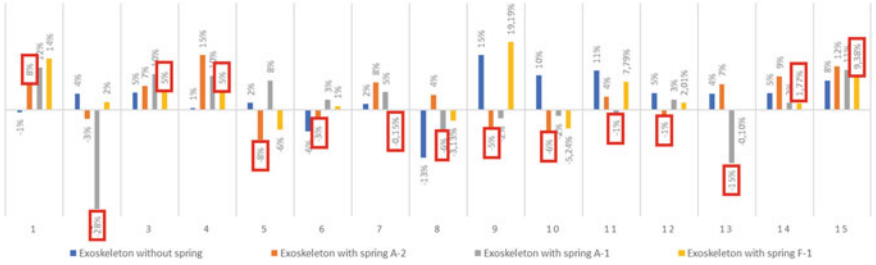

Fig. 1. Percentual variation in metabolic costs for each subject

(3) Manufacturing of the Prototype: a prototype based on the concept developed in point 2 was produced using 3D scanning and additive/subtractive manufacturing techniques. The system was posteriorly tuned based on preliminary tests made with the reference subject.
(4) Experimental analysis: 15 subjects belonging to the Portuguese Army, with no identified musculoskeletal pathologies, were selected to perform the laboratory trials.

A quantitative analysis, based on the evaluation of the metabolic costs during walking, was performed using a gas analyser system. The experimental protocol was defined according to the 6 min Walk Test (6MWT) [6] and the compendium of physical activities [7]. Three springs with different stiffnesses were used to evaluate the influence of this parameter on the exoskeleton performance. Additionally, a questionnaire was also applied to assess subjective variables, such as the mobility of the ankle, comfort, and overall perception of the system functionality.

3 Results and Discussion

The quantitative results, illustrated in Fig. 1, indicate that the use of a passive exoskeleton can lead to a reduction of the metabolic costs while walking. 10 of the 15 volunteers presented a reduction of the expended energy, with values varying between −27.9 and −0.1%. However, it is important to note that the observed reductions did not occur for the same spring, indicating that the properties of the passive elements should be selected according to the user's anthropometric properties. Considering the best results for each volunteer, obtained with the spring that better fitted their characteristics, the study registered an average reduction in metabolic costs of 3.0%. Considering only the results of the subjects who registered a reduction of the metabolic costs, this value rose to 4.9%. Three volunteers revealed a reduction in the metabolic costs during walking with the exoskeleton without actuation. No specific reason was identified for such results, requiring further analysis. Qualitative analysis indicated that the exoskeleton did not interfere with the ergonomic of the footwear and ankle range-of-motion. Also, most of the subjects could correctly identify if the exoskeleton was

reducing or increasing the metabolic costs during walking. Limited efficiency or ergonomic issues could have resulted from the fact that, for practical reasons, every subject performed the trials with a structure modelled to best fit the physical characteristics of subject zero (reference subject). Preliminary tests also showed that the tuning of the spring-engaging mechanism plays a vital role in the exoskeleton performance.

4 Conclusion

The findings achieved in this work suggest that the use of a solution as the one proposed in this work can lead to a reduction of the metabolic costs, with 10 of the 15 individuals, revealing a decrease of metabolic costs. The developed structure maintains the ergonomics of the footwear and the range of motion of the ankle. The use of additive manufacturing to build the exoskeleton structure allows for a custom-made structure with a low acquisition cost. Future work will address the selection of different structural materials for a lighter and less bulky structure, and the evolution of the spring-engaging mechanism. A methodology for the selection of the force unit will also be addressed in future studies.

Acknowledgements To all the volunteers that participated in this project and to the Lisbon Biomechanics Laboratory, for the support and availability in the collection of anthropometric data.

References

1. H.P. Crowell et al., Methodologies for evaluating the effects of physical augmentation technologies on soldier performance, *US Army Res. Lab. Aberdeen Proving Gr. United States*, no. May, p. 78 (2018). doi: https://doi.org/10.13140/RG.2.2.13662.48961
2. J.J. Knapik, K.L. Reynolds, E. Harman, Soldier load carriage: historical, physiological, biomechanical, and medical aspects. Mil. Med. **169**(1), 45–56 (2004). https://doi.org/10.7205/milmed.169.1.45
3. K.T. Ulrich, S.D. Eppinger, *Product Design and Development*, 5th edn. (McGraw-Hill/Irwin, New York, 2012).
4. Report from the 2nd Integration of the Exoskeleton in the Battlefield Workshop (2nd IEB WS) (2018)
5. S.H. Collins, M.B. Wiggin, G.S. Sawicki, Reducing the energy cost of human walking using an unpowered exoskeleton. Nature **522**(7555), 212–215 (2015). https://doi.org/10.1038/nature14288
6. R.O. Crapo, P.L. Enright, R.J. Zeballos, ATS Statement: guidelines for the six-minute walk test. Am. J. Respir. Crit. Care Med. **166**(1), 111–117 (2002). https://doi.org/10.1164/ajrccm.166.1.at1102
7. B.E. Ainsworth et al., Compendium of physical activities: a second update of codes and MET values. Med. Sci. Sport. Exerc **43**(8), 1575–1581 (2011). https://doi.org/10.1249/MSS.0b013e31821ece12

A Multivariate Analysis for Force Element Selection in Passive Ankle Exoskeletons

Nuno A. Ribeiro, Luís P. Quinto, Sérgio B. Gonçalves, Ivo F. Roupa, Paula P. Simões, and Miguel T. Silva

Abstract Exoskeletons performance is influenced by several factors such as ergonomics, actuation force or actuation timing. In particular, for passive exoskeletons, the force element specifications are crucial for its performance. This study aims to infer the existence of a relation between the stiffness of the force element installed on an ankle exoskeleton and the anthropometric parameters of its user. Multivariate statistical techniques were applied to analyse the relevance of the anthropometric data in the energy expenditure of 15 subjects, during the execution of the six-minute walk test using a passive ankle exoskeleton. Results suggest a multiple linear relation between the anthropometric data and the metabolic results obtained for each volunteer. In conclusion, the presented methodology enables the selection of the most appropriate spring for each user, without resorting to time-consuming laboratory or field tests.

The authors would like to thank the Portuguese Army, though CINAMIL (ELITE/2019/CINAMIL) and FCT through IDMEC, under LAETA, project (UIDB/50022/2020).

N. A. Ribeiro · L. P. Quinto (✉) · P. P. Simões
CINAMIL, Academia Militar, Instituto Universitário Militar, Lisbon, Portugal
e-mail: luis.quinto@academiamilitar.pt

N. A. Ribeiro
e-mail: ribeiro.ngmfa@exercito.pt

P. P. Simões
e-mail: paula.simoes@academiamilitar.pt

L. P. Quinto · S. B. Gonçalves · I. F. Roupa · M. T. Silva
IDMEC, Instituto Superior Técnico, Universidade de Lisboa, Lisbon, Portugal
e-mail: sergio.goncalves@tecnico.ulisboa.pt

M. T. Silva
e-mail: miguelsilva@tecnico.ulisboa.pt

P. P. Simões
CMA-Faculdade de Ciências E Tecnologia, Universidade Nova de Lisboa, Lisbon, Portugal

J. C. Moreno et al. (eds.), *Wearable Robotics: Challenges and Trends*,
Biosystems & Biorobotics 27, https://doi.org/10.1007/978-3-030-69547-7_88

1 Introduction

Soldiers are assigned functions that are associated with intense physical efforts, such as long marches or the handling and transportation of heavy loads. These efforts are aggravated by exposure to unpredictable situations, inherent to the complexity of a theatre of operations. The increase in the likelihood of injury and the reduction of the readiness level of the force [1] concerns both political decision-makers and military officials. Exoskeletons are a possible solution to these issues, since they reduce the metabolic costs of the military, increasing their readiness level and reducing their risk of injury [2–4].

Most of the exoskeleton solutions require the identification of several biomechanical and anthropometric parameters of its user to design and tune different components. This customisation will significantly improve the overall performance of the system [3, 5].

In the case of passive solutions used to reduce the metabolic costs during walking, the selection of the force element plays a vital role. In ankle exoskeletons that use springs the stiffness of its force elements must be carefully selected accordingly to the user. This feature is vital since this element will store the energy during certain phases of the gait, releasing it in others, providing adequate support to the exoskeleton user.

However, the identification of the force element stiffness is usually based in protocols which are both complex and time-consuming [3, 5]. Therefore, these protocols are difficult to use in field conditions, which limits the overall use of these exoskeletons.

The main objective of this work is to infer the existence of a relationship between the anthropometric parameters of each volunteer and the stiffness of the force element during walking, to define a selection procedure for this element taking into account the physical characteristics of the user.

2 Methods

Initially, a passively actuated ankle exoskeleton was developed and built, based on the working principle proposed by Collins et al. [3]. Afterwards, this solution was tested by fifteen subjects belonging to the Portuguese Army, in the Lisbon Biomechanics Laboratory comprising quantitative and qualitative analysis.

The experimental protocol involved the evaluation of the metabolic costs of each subject during the execution of the six-minute walk test [5] using three force elements with different stiffness values (see Table 1).

The metabolic expenditure was measured through the Metabolic Equivalent Task (MET). After the trials, each subject filled in a survey to evaluate several aspects related to the exoskeleton like its comfort, ankle range of motion or the support provided by each of the springs, amongst others. Additionally, a specific protocol

Table 1 Force elements specifications

Spring	Weight (kg)	Dimensions (mm)	Stiffness (N/m)
F-1	0.065	Ø20.0 × 97	8422
A-1	0.015	Ø14.9 × 52.5	7058
A-2	0.020	Ø14.1 × 65.5	4801

was developed for the collection of the anthropometric data and gait space-time parameters of each subject, based on the methodology developed by Norton [6]. This protocol involved the collection of the following anthropometric data: height, thigh length, weight, tibial length, calf girth, ankle to heel length (anterior side), ankle to ground length (posterior and anterior sides), bimalleolar breadth, foot length, cadence and walking speed, step length and distance covered in the Cooper test.

After data collection, a multivariate statistical analysis was performed to analyse the relevance of anthropometric data (explanatory variables) in the metabolic results (variable of interest) obtained during the experimental trials [5]. To evaluate the magnitude and direction of the relationship between the variables under study, Pearson Correlation Coefficient was considered [7]. Spearman Correlation Coefficient was also analysed to validate the evaluation of the degree of association between the variables [8]. Finally, several multiple linear regression models, under different scenarios, were adjusted, using the IBM SPSS® Statistics 26 software, considering the general data and grouped by type of spring (F-1, A-1, A-2).

3 Results and Discussion

Several multiple linear regression models were fitted to springs A-1 and A-2 groups. For F-1 spring group, due to the low number of available observations, it was not considered in this phase of the current study. According to the obtained model for the A-1 spring, the most significant factors are the length from the ankle to the ground—anterior side (x_1) (positive correlation—increases proportionally with the metabolic costs) and the bimalleolar breadth (x_2) (negative correlation—decreases proportionally with the metabolic costs). The height variable (x_3) was also integrated into the model since it improves the model goodness of fit [9]. Therefore, it is possible to estimate the results of the metabolic costs with the A-1 spring, through the following model, as in (1), with a corresponding R^2 of 0.795:

$$MET = 3.524 + 0.021x_1 - 0.045x_2 - 1.211x_3 \quad (1)$$

For the A-2 spring, the significant variables were found to be the *length* from the ankle to the ground—anterior side (x_1), the bimalleolar breadth (x_2) and the length from the ankle to the ground—posterior side (x_4). The first correlates positively with metabolic expenditure, while the last two correlate negatively. Thus, it is possible to estimate the value of metabolic results with the use of the A-2 spring, using the

following model, as in (2), with a corresponding R^2 of 0.999:

$$MET = 1.475 + 0.003x_1 - 0.025x_2 - 0.002x_4 \quad (2)$$

For both adjustments, a residual analysis was performed, and no limitations were identified (Durbin-Watson close to 2 and residuals mean close to 0). In summary, the obtained results confirm the existence of a multiple linear relationship between the anthropometric data and the metabolic results obtained for each volunteer. In a second phase of the work, new results were achieved for the F-1 spring, enabling its study. The most significant factor was: time to walk 100m (x_5). This enabled to estimate the value of the metabolic results with the use of the F-1 spring, as in (3), with a corresponding R^2 of 0.842:

$$MET = 8.294 - 1.037x_5 \quad (3)$$

4 Conclusion

This study proposes a new method for the selection of the most appropriate force element to install on a passive ankle exoskeleton for each volunteer, based on their anthropometric data. This aspect is of particular interest since the adjustment of the solution to the user is a crucial point to ensure proper performance and comfort of the exoskeleton. The importance of this study is related to the definition of an innovative methodology based on individual quantitative and qualitative metrics. The obtained results confirm that the proposed method is suitable for the selection of the most appropriate spring for each user, without resorting to time-consuming laboratory or field trials. Future work will involve the application of this study to a more significant group and the evaluation of the exoskeleton in field trials.

Acknowledgments To all the volunteers that participated in this project and to the Lisbon Biomechanics Laboratory, for the support and availability in the collection of anthropometric data.

References

1. S.A. Birrell, R.H. Hooper, Initial subjective load carriage injury data collected with interviews and questionnaires. Mil. Med. **172**(3), 306–311 (2007). https://doi.org/10.7205/MILMED.172.3.306
2. HULC^{TM} | Berkeley Robotics and Human Engineering Laboratory. https://bleex.me.berkeley.edu/research/exoskeleton/hulc/. Accessed 2 Jun 2020
3. S.H. Collins, M.B. Wiggin, G.S. Sawicki, Reducing the energy cost of human walking using an unpowered exoskeleton. Nature **522**(7555), 212–215 (2015). https://doi.org/10.1038/nature14288

4. L.M. Mooney, E.J. Rouse, H.M. Herr, Autonomous exoskeleton reduces metabolic cost of human walking during load carriage. J. Neuroeng. Rehabil. **11**, 80 (2014). https://doi.org/10.1186/1743-0003-11-80
5. P. Pinheiro, L. Quinto, S.B. Gonçalves, M.T. Silva, Analysis of the Performance of a Passive Ankle Exoskeleton for Reduction of the Metabolic Costs in Gait (2019), p. 2
6. K. Norton, Standards for anthropometry assessment, in *Kinanthropometry and Exercise Physiology*, 4th ed. (2018), pp 68–137
7. J. Cohen, P. Cohen, S.G. West, L.S. Aiken, *Applied Multiple Regression/Correlation Analysis for the Behavioral Sciences*, 3rd Ed., no. 1. (2003)
8. J.O. Rawlings, S.G. Pantula, D.A Dickey, *Applied Regression Analysis : A Research Tool, Second Edition Springer Texts in Statistics* (1998)
9. A. Field, *Discovering Statistics using SPSS*, 3rd ed., vol. 622. (SAGE Publications Inc., 2009)

Application Industrial Exoskeletons

On the Design of Kalman Observers for Back-Support Exoskeletons

Erfan Shojaei Barjuei, Darwin G. Caldwell, and Jesús Ortiz

Abstract This paper presents the synthesis of a Kalman state observer for an industrial back-support exoskeleton. The design of a state observer always should be based on a model providing an adequate description of the system dynamics; however, when back-support exoskeletons are considered, the synthesis of a state observer becomes very challenging, since only nonlinear models may be adopted to reproduce the system dynamic response with adequate accuracy. In this work, the possibility of employing a Kalman state observer together with a suitable linear model is investigated. Simulated results illustrate the effectiveness of the proposed approach when it is applied to the synthesis of a state observer for a back-support exoskeleton.

1 Introduction

Considerable research effort has been recently devoted to the development of adequate models and control approaches for wearable robots such as exoskeletons [1]. Moreover, exoskeletons might be profitably employed in in the industrial field and also in military and rehabilitation applications [2]. Basically, an industrial exoskeleton is worn by a user to provide support and reduce the risk of musculoskeletal disorders (MSD) due to physically demanding activities by generating appropriate assistive force(s) and torque(s). An example of an industrial back-support exoskeleton is shown in Fig. 1a.

In general, muscle impedance properties are neutrally modulated to generate appropriate bio-mechanical energies in biological systems. This fact needs to sense the torque due to human-robot interaction [3]. On this basis, the synthesis of a state observer based on Kalman filter [4] for a back-support exoskeleton for estimating interaction force/torque has been proposed and developed in this paper. Kalman filters are usually very sensitive to modeling errors. Despite this problem they can work well in a closed loop environment providing closed loop stability and good performance despite of large errors in the estimated values. The proposed state observer

E. Shojaei Barjuei (✉) · D. G. Caldwell · J. Ortiz
Advanced Robotics, Istituto Italiano di Tecnologia, 16163 Ge Genoa, Italy
e-mail: erfan.shojaei@iit.it

J. C. Moreno et al. (eds.), *Wearable Robotics: Challenges and Trends*,
Biosystems & Biorobotics 27, https://doi.org/10.1007/978-3-030-69547-7_89

requires the measurement of only the angular velocity of the electrical motor and the instant value of the torque signal from the output of the transmission section. Hence, the state observer does not need the use of other sensors such as strain gauge bridges or accelerometers.

2 The Dynamic Model

In order to formulate the motion of the human trunk with a back-support exoskeleton, the linear biomechanical model, developed in [5], has been used in this work (Fig. 1b). In this model, the equivalent rotational stiffness including stiffness parameters between the human trunk and the exoskeleton is represented by a rotational spring k_{eh} (N m rad^{-1}). In a similar way, the equivalent rotational damping between the human trunk and the exoskeleton is shown by a rotational damper d_{eh} (N m s rad^{-1}), the damper of the human hip which corresponds to rotation axis of the human upper-body is represented by b_h (N m s rad^{-1}) and the center of mass locations of the human upper-body and the exoskeleton relative to their axis rotations are given by CM_{hu} (m) and CM_{exo} (m) respectively.

As some system parameters can be identified from data-sheet of components (provided by manufacturers), the information related to some parameters such as gearbox damping and friction are not reported anywhere. Hence, the experimental setup used for the identification of these parameters has been developed. This experimental setup comprises the same components used in our exoskeleton.

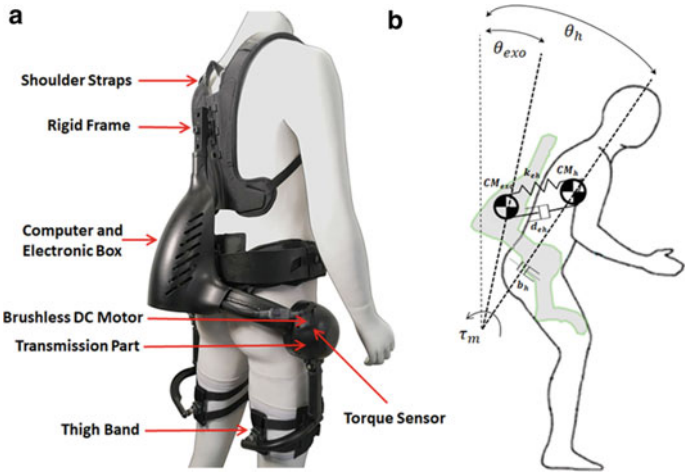

Fig. 1 **a** A back-support exoskeleton with indications to main components. **b** Graphical representation of the sagittal plane of a upper-body exoskeleton and its operator based on the mass-spring-damper modeling

3 State Observer Design

In our application, there is no direct measurement for the torque on the human body, which is defined as the ratio of the applied torque to the deformation of the trunk muscles. Hence there is a need of the state observer to obtain an estimation of the torque on the human body. The first step to design Kalman observer is considering the state vectors and reforming the dynamic equation of the system accordingly. Then the necessary condition for the Kalman Filter observer to work correctly is that the system for which the states are to be estimated, is observable [4].

4 Implementation of the State Observer and Performance Analysis

The performance of the observer has been evaluated by comparing the values of the simulation state variables over the observer on a test case by means of a linear quadratic regulator (LQR) controller with the integral action. The block diagram of the closed-loop control system is shown in Fig. 2.

The first evidence of the observer effectiveness is reported in Fig. 3 where a comparison is made between the step responses of the closed-loop control system using the proposed state observer and the linear dynamic model of the system. Figure 4 shows the error between the linear model and the estimator in terms of torque on the human body which is very small. That is, the mean-squared of the error is about 0.1×10^{-3} (N m) and approaches zero over time.

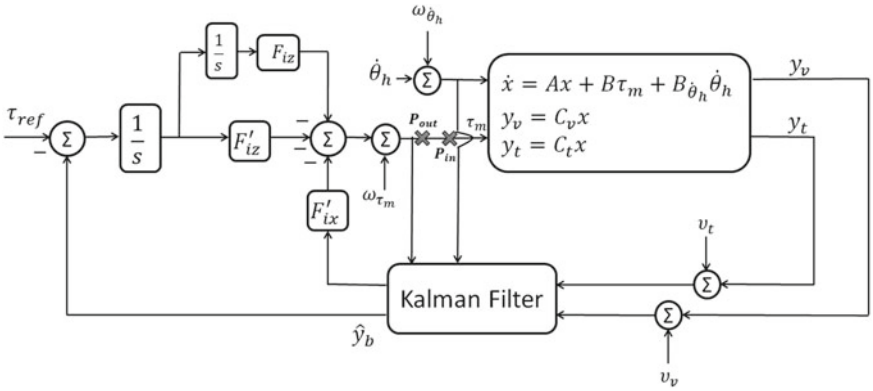

Fig. 2 Block diagram of the closed-loop control system

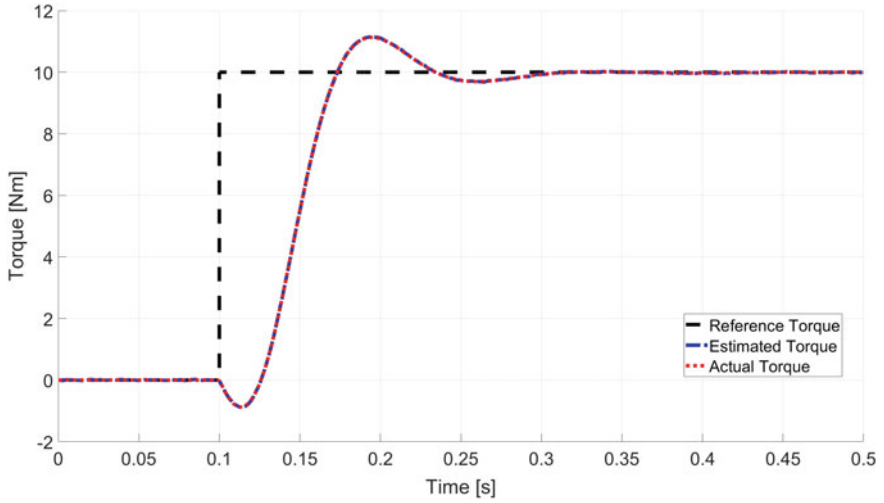

Fig. 3 Step response of the system for estimated and actual torque on the human body

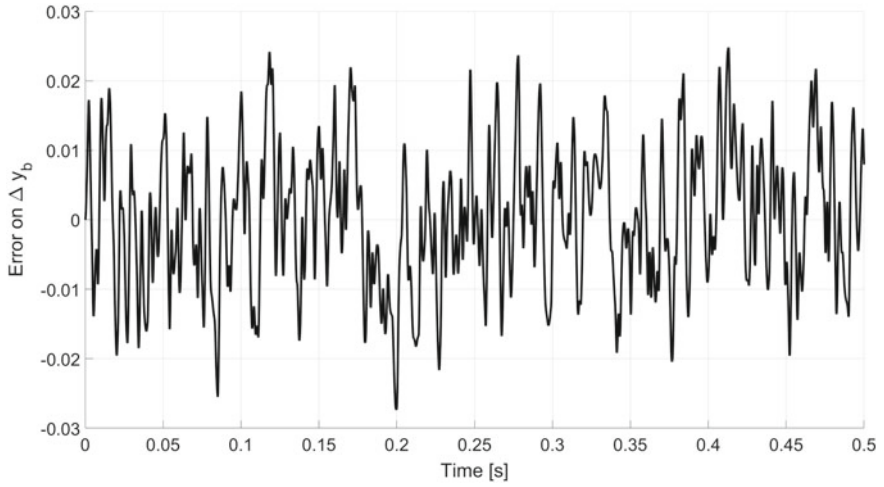

Fig. 4 Error between the actual and the estimated values of the torque on the human body

Furthermore, stability margins have been evaluated by Nyquist plot (Fig. 5 of the loop gain, from the motor plant input (point P_{in} in Fig. 2) to the computed torque signal from the controller (point P_{out} in Fig. 2). We can see that the plot in Fig. 5, does not encircle the critical point $(-1 + 0j)$, so the system is stable.

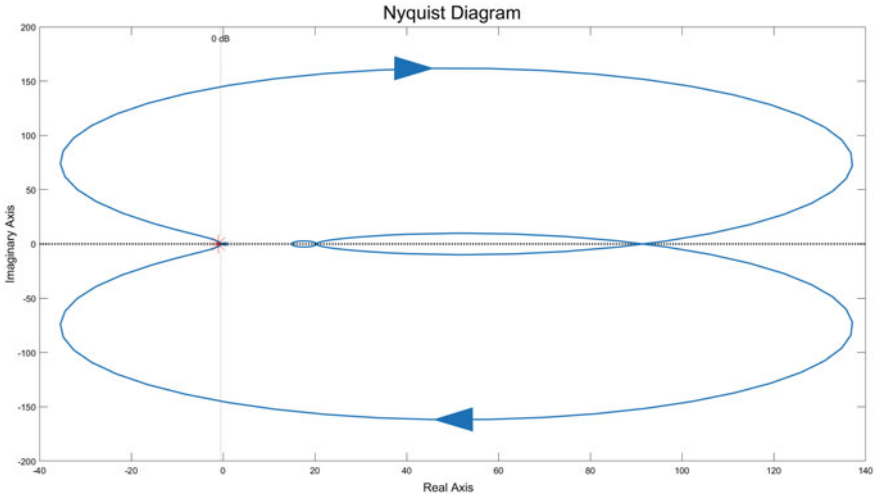

Fig. 5 Nyquist diagram of the open-loop system from the motor plant input to the computed torque signal from the controller

5 Conclusion

In this work a general approach for designing effective state observers for industrial back-support exoskeletons has been presented. The results achieved from the simulation environment through a Linear-Quadratic-regulator (LQR) control [6] with double integrator action and the full state feedback illustrate that the estimation is accurate and the estimation error is closed to zero.

Acknowledgements This work has been funded by Italian Workers' Compensation Authority (INAIL) for the development of wearable assistive exoskeletons and hosted by Istituto Italiano di Tecnologia (IIT).

References

1. E.S. Barjuei, S. Toxiri, G.A. Medrano-Cerda, D.G. Caldwell, J. Ortiz, Bond graph modeling of an exoskeleton actuator, in *10th Computer Science and Electronic Engineering (CEEC)*, vol. 2018. (IEEE, 2018), pp. 101–106
2. E.S. Barjuei, M.M. Ardakani, D.G. Caldwell, M. Sanguineti, J. Ortiz, On the optimal selection of motors and transmissions for a back-support exoskeleton, in *2019 IEEE International Conference on Cyborg and Bionic Systems (CBS)* (IEEE, 2019), pp. 42–47

3. J. Li, E.S. Barjuei, G. Ciuti, Y. Hao, P. Zhang, A. Menciassi, Q. Huang, P. Dario, Magnetically-driven medical robots: An analytical magnetic model for endoscopic capsules design. J. Magn. Magn. Mater. **452**, 278–287 (2018)
4. E.S. Barjuei, A. Gasparetto, Predictive control of spatial flexible mechanisms. Int. J. Mechan. Control (JoMaC) **16**(01), 85–96 (2015)
5. E.S. Barjuei, M.M.G. Ardakani, D.G. Caldwell, M. Sanguineti, J. Ortiz, Optimal selection of motors and transmissions in back-support exoskeleton applications. IEEE Trans. Med. Robot. Bionics **2**(3), 320–330 (2020)
6. E.S. Barjuei, J. Ortiz, A comprehensive performance comparison of linear quadratic regulator (lqr) controller, model predictive controller (mpc), h_∞ loop shaping and μ-synthesis on spatial compliant link-manipulators." Int. J. Dyn. Control (2020)

Subjective Perception of Shoulder Support Exoskeleton at Groupe PSA

Jawad Masood, Erika Triviño-Tonato, Maria Del Pilar Rivas-Gonzalez, Maria Del Mar Arias-Matilla, and Ana Elvira Planas-Lara

Abstract The emerging Industrial Exoskeleton Technology (IET) adoption in industry requires an assessment of its long duration impact. We present the subjective assessment of the shoulder support exoskeleton (Levitate AIRFRAME) at Groupe PSA Vigo factory by setting-up evaluation phases in the assembly line under industrial conditions. These phases are the preliminary-term [28 workers, 14 h], short-term [8 workers 75 h] and the medium-term [11 workers, 240 h]. We continuously monitored the workers and gradually increased the usage time until full autonomy was achieved for full shift. We discovered that searching the initial static fit of the exoskeleton is a non-trivial task. In addition, we noted that the usability and reliability aspects which were absent in preliminary-term and short-term testing are influential in medium-term testing such as body temperature elevation and exoskeleton mechanical wear and tear. Finally, we observed the gradual decrease in the exoskeleton usage among workers contrary to our hypothesis.

1 Introduction

Work-related musculoskeletal disorders (WRMSDs) show symptoms of constant pain of muscles, tendons, nerves and blood vessels, which is mostly caused by repetitive motion or overexertion [1]. In Spain, according to data from Communication

The authors acknowledge the contributions of the F4.0 Automation consortium in general and Groupe PSA in particular.

J. Masood (✉) · E. Triviño-Tonato
Processes and Factory of the Future Department of CTAG, Centro Tecnológico de Automoción de Galicia, O Porriño, Spain
e-mail: jawad.masood@ctag.com

M. D. P. Rivas-Gonzalez
Ergonomics Area at Groupe PSA Vigo Factory, Groupe PSA Centro de Vigo, Avda. Citroën 3 y 5, Vigo, Spain

M. D. M. Arias-Matilla · A. E. Planas-Lara
Mutua Universal, Av. Tibidabo 17–19, 08022 Barcelona, Spain

J. C. Moreno et al. (eds.), *Wearable Robotics: Challenges and Trends*,
Biosystems & Biorobotics 27, https://doi.org/10.1007/978-3-030-69547-7_90

of Occupational Diseases in Social Security (CEPROSS) [2], 2019 was closed with 23,146 reported cases of occupational disease (group 2: physical agents), an increase of 16.7% from 2018.

This growing WRMSDs rate in recent years calls for a solution. Exoskeletons are one of the most promising solutions to reduce WRMSDs. These devices facilitate assistance to certain anatomical areas that receive more biomechanical loading. Today, there are 30 commercial industrial exoskeleton manufacturers, whereas 12 of them provide shoulder support exoskeletons [3]. However, their usage is minimal due to the gap between end-user needs and specification, lack of standardization, and benchmarking [4].

The literature review reveals that the testing of the industrial exoskeletons mainly focuses on analyzing the variation in muscle activity by measuring the Electromyography level (EMG) of the primary muscles involved in the workplace. The standard practice is to collect this data by simulating the workstation in ergonomic laboratories or perform short tests within a controlled environment. Subjects who carry out the tests often have no experience performing the workstation activities, therefore, you cannot verify the fidelity of exoskeleton impact. Currently, there is no study in the literature that demonstrate the evolution of the device's acceptability by the larger worker population or long-duration testing case study of the shoulder support exoskeleton [5].

CTAG, Mutua Universal and Groupe PSA Vigo factory have been working on a project since 2016. The aim of the project is to find a device that mitigated the WRMSDs and achieving its implementation on the assembly line. We selected the Levitate Airframe, which is a wearable exoskeleton to improve upper extremity musculoskeletal health for workers by following our previously developed protocol [4]. In this work, we present a subjective perception with regards to the usability, impact and utility. It was carried by experienced workers at Groupe PSA Vigo factory.

2 Development

The testing process at Groupe PSA [4] was structured in four phases, (I) Selection of the exoskeleton (Expression of needs), (II) Laboratory Test, (III) Simulated Test (Offline Emulated Task), (IV) In-line test (Assembly line Real tasks). In this paper, we will focus on phase IV.

2.1 Scope and Planning

Phase IV was developed at Groupe PSA facilities. It corresponded to the in-line test under real production conditions. The objective was to achieve a progressive implementation process, in which workers were accompanied throughout the process and their level of acceptance and adaptation to exoskeleton were assessed. The selected

operations were from workstations called "Under Box". It involved repetitive tasks with the elevation of upper limbs, with operations at or above the head. The results were evaluated by subjective questionnaires and an interview with workers.

2.2 Subjective Perception Methods

The questionnaires developed for this study were structured in three sets: (I) Usability (flexibility and adaptability of the exoskeleton), (II) Impact (impact of the exoskeleton on the subject's body), (III) Utility (device performance during work and possible interference). These questionnaires were multiple-choice polytomous type, where the subjects can answer each question as positive or negative or indifferent.

2.3 Phase 1V—In-Line Test (Real Production)

This phase consisted of three testing terms: (a) Preliminary-term, (b) Short-term and (c) Medium-term. All subjects participants gave full consent and without a clinical history of back or shoulder pain. The parameters of the subjective evaluation can be seen in the Table 1. **Preliminary-term:** The objective of the preliminary term was to perform rapid testing for (maximum 30 min per subject) involving a large group of workers. We aimed to gather a first impression of the device and to detect its shortcoming, which was not evident in the previous phases. **Short-term:** The objective of the short-term was to gradually increase the device usage time to address the concerns raised in the preliminary term. Subjective perception showed the device support. **Medium-term:** The objective was to daily monitor each worker and increase the usage time until autonomy was achieved. To address the device adjustment problem, we frequently invited the device manufacturer for worker training.

Table 1 Summary of subjective analysis questionnaires (validated by the experts panel from Mutua Universal and Groupe PSA)

Phase IV terms	Worker (Gender)	Usage time (h)	Questionnaire items [Phase IV terms]—Set I: Usability (1–5), Set II: Impact (6–11), Set III: Utility (12–16)
a. Preliminary	28 (24M, 4W)	14	1. Wearability (donning/doffing) [a, b, c], 2. Wearability (fit) [a, b, c], 3. Usability (comfort) [a, b, c], 4. Usability (weight) [a, b, c], 5. Adaptability (walking/sitting) [b, c], 6. Assistance (general) [a, b, c], 7. Assistance (static posture) [c], 8. Assistance (dynamic movements) [a, b, c], 9. Assistance (body .. support) [a (shoulder), b (shoulder, neck, arms, back), c (shoulder, neck, upper back, lower back, arms)], 10. Impact (other body parts) [a, b, c], 11. Impact (cognitive) [b], 12. Utility (general) [a, b, c], 13. Utility (accessibility) [a, b, c], 14. Utility (compatibility with EPI's) [c], 15. Maintainability (storage) [c], 16. Safety (environmental interference) [c]
b. Short	8 (8M , 0W)	75	
c. Medium	11 (11M, 0W)	140	

3 Results and Discussion

Term-a results (Table 2) verify the subjective positive response for usability (73.25%), impact (74%) and utility (57%). We hypothesized the usage experience can improve by device utility and moved to term-b. We observed the improved results during term-b i.e. usability (93.5%), impact (77.5%) and utility (93.5%). This encouraging subjective perception compeled us to move forward to the term-c. Term-c results showed a positive response for usability (68.75%) and impact (67%), which was lower than the previous two terms. The most significant drop was in the utility of the device (37.5%). The major drawbacks were the body temperature elevation and environmental interference. The overall results of all subjects and terms are shown in Fig. 1. We observed the overall positive response from 70% to 88% between term-a to term-b that reduces to 60% after term-c. The main factor was the device utility, where the positive responses decrease from 57 to 37.5%. Moreover, we observed a similar pattern in usability and utility. We noted the increase in indifferent responses from 9.25 to 37.5% in term-c. Finally, the negative responses tend to increase in the term-a (22%) from term-c (25%).

Table 2 Usability, impact and utility results

Questionnaire items		Set I (%)	Set II (%)	Set III (%)
Positive	Term-a	73.25	74	57
	Term-b	93.50	77.50	93.50
	Term-c	68.75	67	37.50
Indifferent	Term-a	17	10	21.50
	Term-b	6.50	18.50	6.50
	Term-c	9.25	24.25	37.50
Negative	Term-a	10	16	21.50
	Term-b	0	4	0
	Term-c	22	8.75	25

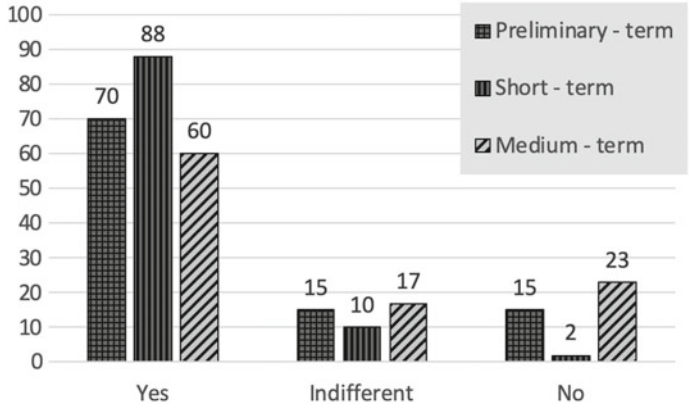

Fig. 1 Overall subjective perception

4 Conclusion

We present a subjective perception of the shoulder support exoskeleton under actual working conditions. We observed the gradual decrease in utility, usability and impact during term-c. However, the most significant subjective perception drop was observed in device utility. We noted the body temperature elevation concerns during the term-b and the term-c. Despite the term-c lack of yielding the expected results that can allow the widespread implementation of the exoskeleton, overall, the subject perception showed the reduction of physical fatigue in the shoulder, neck and arms.

References

1. O. Korhan, A. Mackieh, A model for occupational injury risk assessment of musculoskeletal discomfort and their frequencies in computer users. Saf. Sci. **48**(7), 868–877 (2010)
2. CEPROSS. 2019 Statistics yearbook preview: Occupational disease. http://www.mites.gob.es/ficheros/ministerio/estadisticas/anuarios/2019/EPR/EPR.pdf (2019). (Online). Accessed 23 Sep 2020
3. A. Voilqué et al., Industrial exoskeleton technology: classification, structural analysis, and structural complexity indicator, in *2019 Wearable Robotics Association Conference (WearRAcon)* (2019), pp. 13–20
4. J. Masood et al., Industrial wearable exoskeletons and exosuits assessment process, in *International Symposium on Wearable Robotics* (Springer, 2018), pp. 234–238
5. N. Sylla et al., Ergonomic contribution of able exoskeleton in automotive industry. Int. J. Indus. Ergonomics **44**(4), 475–481 (2014)

MH-Forces, a Motion-Capture Based Method to Evaluate Workplace Ergonomics: Simulating Exoskeleton Effects

Javier Marín, Juan de la Torre, and José J. Marín

Abstract In this document, we explain the MoveHuman-Forces (MH-Forces) method, which aims to evaluate the ergonomics of a specific workplace. This method provides the level of risk to suffer an injury on each body joint. The risk calculation is based on a motion-capture measurement in the workplace. This method can be used for the assessment of existing workplaces and the validation of new ones. After introducing their foundations, we introduce how MH-Forces can be used to assess the inclusion of exoskeletons in workplaces.

1 Introduction

The repetitive strain injury (RSI) is an occupational disease with the highest incidence in the workplace and entails high costs for companies [1]. Ergonomic evaluations are especially helpful in preventing RSIs. They aim to improve workers' health and productivity.

To conduct ergonomic evaluations, observational methods, such as REBA (postural load), NIOSH (load manipulation), or OCRA (repetitive tasks), are usually applied. However, these methods are generally not automated, require considerable evaluator time, and have an important subjective factor. Therefore, methods based on objective information that can be applied in an automated manner are required [2].

Likewise, exoskeletons have become an interesting solution to reduce the number of injuries and improve the ergonomic factors of particular workplaces. However,

J. Marín (✉) · J. de la Torre · J. J. Marín
IDERGO (Research and Development in Ergonomics) Research Group, I3A (Aragon Institute of Engineering Research), Department of Design and Manufacturing Engineering, University of Zaragoza, C/Mariano Esquillor s/n, 50018 Zaragoza, Spain
e-mail: 647473@unizar.es

J. de la Torre
e-mail: 627471@unizar.es

J. J. Marín
e-mail: jjmarin@unizar.es

J. C. Moreno et al. (eds.), *Wearable Robotics: Challenges and Trends*,
Biosystems & Biorobotics 27, https://doi.org/10.1007/978-3-030-69547-7_91

due to its incipient development, evaluation methods are still required to ensure its effective integration in the industry.

In this document, we present a general scheme of the MH-Forces method [3], which is based on motion capture and serves to assess the risk of suffering an RSI in each joint in a workplace. Additionally, we introduce how the method can predict the effects of using an exoskeleton.

2 MH-Forces

2.1 Definition of Risk in MH-Forces

The risk of suffering an RSI is a score that represents how harmful a specific task is for the worker. In this manner, UNE-EN 1005–5: 2007 identified certain factors whose presence can increase the risk of injury: (1) strength, (2) posture and movement, (3) repetitiveness, (4) duration of work, (5) insufficient recovery time, and (6) so-called additional factors (i.e. vibration, adverse environmental conditions, and others).

MH-Forces scores these factors to calculate a risk index in a repetitive-task workplace using the process described in Fig. 1. The risk calculation derives from motion-capture data recorded in the workplace, information entered by the user about the workplace, and databases on human models and anatomical data included in the programme. This method began to be developed 10 years ago, and it has been created in WorldViz-Vizard based on python. The term 'forces' comes from the importance of external forces executed by the worker and internal forces on the joints.

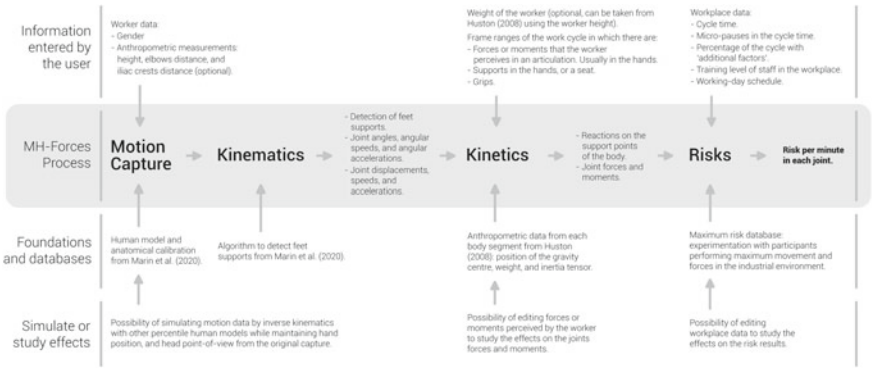

Fig. 1 MH-Forces scheme. Risks for a repetitive-task workplace

2.2 Motion Capture and Kinematics

The MH-Forces method does not impose the use of a specific motion-capture system. In our case, we use the MH-Sensor system [4]. This system uses magnetometer-free inertial sensors to avoid magnetic disturbances, which are common in industrial environments. Marin et al. [4] assessed and described how this system calculates the kinematics, including angles and displacements, and how it detects the support points when the worker is standing or walking.

2.3 Calculating Kinetics

MH-Forces computes the forces and torques in each joint and posture using Huston equations [5]. To accomplish this, the method uses the information from the human model (i.e. the length, weight, position of the gravity centre, and inertia tensor of each body segment), and the forces and torques that the worker performs during the work cycle, which has to be introduced by the user (e.g. a vertical load of 5 kg between the second 5 and 21 of the motion recording).

2.4 Calculating Risks

For the risk calculation in each joint and posture (i.e., one frame of the capture), we propose a logic based on the risk factors of UNE-EN 1005–5:2007. Factors 1 and 2 are scored according to the kinematics and kinetics data, and factors 3–6, which depend on the worker schedule, penalise the result. To calculate a value derived from factors 1 and 2 we multiply the 'angle' (weighted from 1–2), 'angular acceleration' (from 1–1.5), 'force' (from 1–2), 'torque' (from 1–2.5), and 'grip' (from 1–2; only applicable to the wrist joint). We assign the maximum weight to each factor when the recorded measurement approaches the maximum possible value of the 'maximum risk database' and the minimum score when the measurement approaches zero. The 'maximum risk database' was obtained recording volunteers moving their joints with the maximum loads and speeds that occur in the industrial environment. Then, to consider the full capture and the 3–6 factors, the values for each posture are added and multiplied by a receptiveness factor (from 1–9; one if the value in the posture is the minimum possible, and nine if it is the maximum). In this manner, those positions with high risk affect more. Subsequently, the resulted score is multiplied by a recovery factor (from 1–2.6) and a duration factor (from 0.5–2), which depend on the time assigned to the worker for that task during the working day, and a penalty for additional factors (from 1–1.18) that exists on the workplace. Finally, the result is multiplied by 60 and divided by the cycle time to calculate the risks per minute. The final value of the risk is presented as a percentage of the maximum achievable value

(sum of the maximum scores described in a minute), and it is transformed into a three-level score: acceptable <25%, conditional 25–40%, and non-acceptable >40%.

2.5 Simulating Exoskeleton Effects

The effect of an exoskeleton has to be considered in the 'Calculating Kinetics' stage, and the exoskeleton has to be modelled as a set of forces and moments applied on the body in specific instants. In a preliminary study, we modelled the Laevo V2.5, which is a passive exoskeleton designed to support bent-forward work and repetitive lifting movements. Our model included a vertical load on the hips (weight of the device), and three forces, one applied on the reference system of the chest and the others on the reference system of the tights. These forces only occur when the user bent-forward more than an adjustable angle (from 0 to 35°). Their value was calculated measuring the torque of the mechanical joint and the distances to the application points. In these pilot tests, the user lifted 6 kg from the ground several times, and the exoskeleton implied a substantial reduction of the risk in the lower back and a slight increment of the risk in the knees.

3 Discussion and Conclusions

In this document, we present the scheme of the MH-Forces method [2] and explain its foundations. This method can have a relevant practical utility to prevent RSI. When the MH-Forces method is applied to various workplaces, it provides the so-called 'risk map' (i.e., a matrix with one risk score for each joint and workplace). This risk map is a valuable result, in the first place, to manage the rotations of workers, in a balanced manner, without overload certain joins. Additionally, the risk map is also valuable, to visualise those workplaces with non-acceptable risk, which has to be improved. For this second application, many solutions may be considered, among we found the exoskeletons. In this regard, MH-Forces can assess the risk reduction that an exoskeleton may suppose. Nevertheless, to integrate this technology in the industry, the risk reduction has to be combined with other factors that have to be studied, such as the mental stress related with it, or other subjective or organisational factors.

Acknowledgements We would like to thank Mutua Universal, BSH, Quiron Prevencion, Volkswagen, and recently Gesinor, which have contributed to developing and adjusting this method.

The project was co-financed by the Government of Aragon, the European Regional Development Fund, and the University of Zaragoza (Spain).

References

1. Eurofound. *Sixth European Survey on Working Conditions: General Report* (Publications-Office-of-the-European-Union, Luxembourg, 2018)
2. J. Diego-Mas, R. Poveda-Bautista, D. Garzon-Leal, Influences on the use of observational methods by practitioners when identifying risk factors in physical work. Ergonomics **58**, 1660–1670 (2015)
3. M.J. Bone-Pina, *Método de Evaluación Ergonómica de Tareas Repetitivas, Basado en Simulación Dinámica de Esfuerzos con Modelos Humanos*. PhD thesis, University of Zaragoza, 2016
4. J. Marín, T. Blanco, J. Torre, J.J. Marín, Gait analysis in a box: a system based on magnetometer-free IMUs or clusters of optical markers with automatic event detection. Sensors **20**, 3338 (2020)
5. R. Huston, *Principles of Biomechanics* (CRC, 2008)

A Methodology to Assess the Effectiveness and the Acceptance of the Use of an Exoskeleton in a Company

J. A. Tomás-Royo, M. Ducun-Lecumberri, A. E. Planas-Lara, and M. Arias-Matilla

Abstract The integration of new technologies in the workplace and, in particular, the use of exoskeletons, requires a precise analysis of the effects these devices have on the workers and their environment. This analysis will allow us to assess the advantages and effectiveness of the implementation. A structured and systematic methodology for the subjective and objective analysis of the use of exoskeletons in the field is presented in this work, as a result of years of experience working with different companies. The methodology is developed in four phases of work, from a preliminary needs analysis to the implementation of the exoskeleton in the workplace.

1 Introduction

The reduction of musculoskeletal disorders (MSD) is one of the main challenges that companies and society face worldwide nowadays. Instead of reducing, the incidence of musculoskeletal accidents and illnesses remains constant over time [1] and it will probably worse due to the growing ageing of the workforce [2]. Industry 4.0 and the development of new wearable technologies may contribute to preventing MSD [3].

Many exoskeletons available in the market are supposed to be effective in reducing physical load and improving working conditions. However, laboratory conditions in

J. A. Tomás-Royo (✉) · M. Ducun-Lecumberri · A. E. Planas-Lara
Ergonomics Laboratory, R&D Technical Management of Mutua Universal, Barcelona, Spain
e-mail: jtomasro@mutuauniversal.net

M. Ducun-Lecumberri
e-mail: mducunle@mutuauniversal.net

A. E. Planas-Lara
e-mail: aplanasl@mutuaunivesal.net

M. Arias-Matilla
Psychosociology Area at Occupation Risk Prevention, Department of Mutua Universal, Barcelona, Spain
e-mail: mariasma@mutuauniversal.net

J. C. Moreno et al. (eds.), *Wearable Robotics: Challenges and Trends*,
Biosystems & Biorobotics 27, https://doi.org/10.1007/978-3-030-69547-7_92

which their trials were made at the design phase are generally different from field conditions in the industry.

The use of an exoskeleton supposes a close interaction between the user and the assistance device, as well as an interaction between them and the work environment. Hence, it seems reasonable the need for a structured, methodological and systematic analysis to assess the impacts and potential consequences on both the worker and company management.

2 Materials and Methods

This methodology is developed from the experience in the field, after more than three years of work, in which the implementation of exoskeletons in the workplace has been studied and put into practice in collaboration with several associated companies.

The observation of needs expressed by the companies leads us to suggest that, in order to assess the real impact of the exoskeleton on a workplace, it is necessary to know:

(A) On one hand, the "objective" effect of the exoskeleton on the user´s body to assess the reduction in their muscular effort, the smoothness of their motion and the lack of overloads in their body.
(B) On the other hand, the "subjective" effect on the worker to assess their comfortability, acceptance and adaptation to the exoskeleton that confirms the assistance device will not be rejected.
(C) Moreover, the effect of the use of the exoskeleton on the production pace, the environment and the manufactured product that will ensure the company a balance between the potential advantages and disadvantages.

3 Results

The main aim of the developed methodology is to assess whether the implementation of an exoskeleton in the workplace will reduce workers´ physical load, will not damage users nor generate any disturbance in the work environment and will improve the work conditions ostensibly. It is recommended a multidisciplinary work team to participate throughout all the study. The team should be consisted of, at least, some company technical department, the medical service, workers representatives, experts on ergonomics, biomechanics and psychosociology and the support of the assistance device supplier.

The methodology establishes 4 phases of work. After each phase, the multidisciplinary team evaluates, depending on the results obtained, whether or not to proceed to the next phase (Fig. 1).

Each phase duration depends on the size and complexity of the company, the time and the resources available.

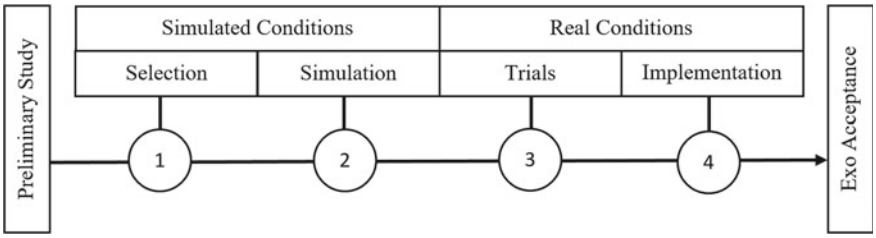

Fig. 1. Scheme with 4-phase methodology

3.1 Phase 1—Selection of the Exoskeleton

Firstly, a preliminary study of the workplace is carried out to assess the risk to suffer musculoskeletal disorders and consider the possible alternatives to eliminate or reduce it (workplace redesign, auxiliary aids, etc.) [4]. When an exoskeleton is confirmed to be the best option, we proceed to the selection of an appropriate device. An available benchmark to compare with other studies in companies with similar tasks and exoskeletons is https://eurobench2020.eu.

The most suitable exoskeleton is selected regarding both the kind of tasks developed in the workplace and the body area to protect (back, neck, arms, hands or legs). Subsequently, the multidisciplinary work team has a first contact with the exoskeleton to get their first impressions about its usability and functionality that are registered with a rapid questionnaire.

3.2 Phase 2—Simulation (Off-line)

This phase aims to check the exoskeleton behaviour for the work conditions for what has been prescribed. Several off-line trials are carried out to analyse objectively and subjectively the task performance with and without the exoskeleton. Trials are designed according to the exoskeleton type. Thus, we perform static, dynamic, load manual handling tests, etc.

The objective assessment is conducted through the register of those biophysical parameters considered of interest for each situation, such as muscular activity, body segments movements and postures, balance, metabolic rate, etc.

The subjective assessment is completed through perception questionnaires [5]. The user answers to items related to the exoskeleton usability, adjustments, functionality and effectiveness. If the evaluations results mostly positive, we proceed to the next phase. Potential negative scores are taken into account to improve the device adaptation.

3.3 Phase 3—In-line Trials

This phase aims to verify the exoskeleton behaviour in the real work conditions, with the regular production paces, to detect the effect on the worker (degree of acceptance), on the work environment (safety, quality and layout) and on the work organization (cycle times, production rates, etc.)

We ask voluntary workers, as many ones as possible, for performing their usual tasks wearing the exoskeleton for a brief time (less than 1 h) and under some members of the multidisciplinary work team face-to-face supervision. Then, the user answers a subjective perception questionnaire about their impressions during the exoskeleton use (adjustments, interferences, discomfort, etc.). If a high percentage of users consider the device inadequate, the company will probably reject it.

3.4 Phase 4—Implementation

This phase, likewise the previous one, is executed under usual production conditions. Some trials are carried out with a limited number of voluntary workers who have valued the use of the exoskeleton positively in Phase 3.

The aim is to assess performance after the extended use of the exoskeleton. For that purpose, initially, the users wear the exoskeleton for a short time (1 h), progressively increasing this time for several weeks (until 4, 6 or 8 h of use per shift). After each period of use, the worker fulfils a subjective perception questionnaire with their impressions and is interviewed by the multidisciplinary team psychologist.

Once the adaptation and appropriation period of the user with the exoskeleton has finished, a new objective analysis is conducted. Namely, biophysical parameters of interest are recorded to assess the performance of the tasks in the workplace carried out without and with the exoskeleton.

To conclude, the company decides, according to the results from the objective and subjective assessment and the overall evaluation of the experience, whether the introduction of the exoskeleton is approved or not for the usual development of tasks in that workplace.

4 Discussion

This methodology requires time and resources from the company. However, they are much less than those that the incorporation of an inappropriate device would imply, avoiding unnecessary investments. Obviously, a balance should be found between time spent on testing and the prevention of potential negative impacts.

On the other hand, to avoid workers can potentially reject the use of an exoskeleton considered adequate, the implementation process should be conducted in a progressive, structured and participatory way.

Furthermore, the effects of the continuous use of the exoskeleton in the medium and long term are unknown. Therefore, it is essential to go on evaluating the impacts of the device on the workers´ health throughout the time it is being used.

5 Conclusion

Issues such as an exoskeleton inappropriate for the tasks performed, poorly adjusted to the worker, a lack of an adaptation period or inadequate periods of use, can negatively affect both the health of the workers and the management of the company. Thus, the implementation of an exoskeleton in a workplace should be done with caution.

A systematic methodology involving an objective and subjective analysis is a tool that provides the needed feedback about how the exoskeleton influences on the muscular activity, the working postures and movements, the perceived efforts, just as the comfortability, functionality and effectiveness of the exoskeleton.

References

1. J.O. Crawford, R. Graveling, A. Davis, E. Giagloglou, M. Fernandes, A. Markowska, M. Jones, E. Fries-Tersch, *Work-Related Musculoskeletal Disorders: From Research to Practice. What can be Learnt? European Risk Observatory Report* (European Agency for Safety and Health at Work—EU-OSHA, 2020)
2. B. Rechel, E. Grundy, J.-M. Robine, J. Cylus, J.P. Mackenbach, C. Knai, M. McKee, Ageing in the European Union. Lancet **181**, 1312–1322 (2013)
3. B.A. Kadir, O. Broberg, Human well-being and system performance in the transition to industry 4.0. Int. J. Ind. Ergon. **76**, 102936 (2020)
4. A.E. Planas-Lara, J.A Tomás-Royo, M. Ducun-Lecumberri, *Ergonomics 4.0 and Exoskeletons. Myths, Legends and Truths* (Ed. Mutua Universal, 2020)
5. J. Masood, E. Triviño-Tonato, P. Rivas-González, M. Arias-Matilla, A.E. Planas-Lara, Subjective Perception of Shoulder Support Exoskeleton at Groupe PSA (WeRob2020) (Chapter 90, this volume)

Objective Techniques to Measure the Effect of an Exoskeleton

A. E. Planas-Lara, M. Ducun-Lecumberri, J. A. Tomás-Royo, Javier Marín, and José J. Marín

Abstract Know in advance the effects of an exoskeleton on the worker's body, before its implementation in the workplace, will give us valuable information to make decisions and optimize company resources. Three objective techniques (surface electromyography, 3D motion capture and dynamometry for the biomechanical analysis with the MH-Forces ergonomics assessment method) are used for this aim. Measurements results will show how the use of an exoskeleton while performing a task can modify the efforts, the muscular activity, the postures, the movements and the forces on the worker's joints. These objective techniques can provide quantitative and reliable data to prevent potential exoskeleton users from suffering musculoskeletal disorders.

1 Introduction

Exoskeletons can be a satisfactory option to tackle musculoskeletal disorders (CTD) [1]. However, the implementation of an exoskeleton means changes [2] in the workplace that will affect the user, their workmates and their environment [3].

Mutua Universal has developed a methodology to assess the effectiveness and the acceptance of the use of exoskeletons in a company [4]. One of the axes of this methodology is the objective analysis of the effect of the exoskeleton on the worker's body. This analysis tries to verify whether the exoskeleton generates neither overload nor unnecessary effort on the worker.

A. E. Planas-Lara (✉) · M. Ducun-Lecumberri · J. A. Tomás-Royo
Ergonomics Laboratory at Mutua Universal, Av. Tibidabo 17-19, 08022 Barcelona, Spain
e-mail: aplanasl@mutuauniversal.net

J. Marín · J. J. Marín
IDERGO (Research and Development in Ergonomics) Research Group, Department of Design and Manufacturing Engineering, I3A (Aragon Institute of Engineering Research), University of Zaragoza, C/Mariano Esquillor s/n, 50018 Zaragoza, Spain
e-mail: 647473@unizar.es

J. J. Marín
e-mail: jjmarin@unizar.es

J. C. Moreno et al. (eds.), *Wearable Robotics: Challenges and Trends*,
Biosystems & Biorobotics 27, https://doi.org/10.1007/978-3-030-69547-7_93

The aim of the objective techniques is to confirm that the exoskeleton does not involve overexertion or unnecessary strain on the worker's body. Accordingly, we need to register biophysical parameters such as the muscular activity performed, postures, body segments motion or internal forces on the joints caused by the weight, the loads handled and other external forces the worker does.

The purpose of this work is not to present a specific data analysis from a given trial, but to offer the instrumental techniques on which a researcher can rely on to perform an objective analysis of the impact of the exoskeleton on the user in real working conditions.

2 Measuring Techniques

This document presents three measuring techniques to register biophysical parameters that can be applied to the ergonomic study of exoskeletons. These techniques are surface electromyography, 3D motion capture and dynamometry for biomechanical analysis.

2.1 Surface Electromyography

Surface electromyography (SEMG) is a non-invasive measuring technique that, when applied in ergonomics, allows, among other applications, to identify the muscular groups having the principal role in the tasks performed, analyse muscular activity in each muscular group of interest or compare the muscular behaviour when the same tasks are executed throughout different processes [5].

When applied to exoskeleton analysis, it permits us to compare the muscular activity developed by the worker when performing the task with and without the exoskeleton.

The protocol to perform the measurements consists of: (1) identifying the muscles involved in the actions the worker carries out, (2) placing the electrodes on their skin, (3) recording the Maximum Voluntary Contraction (MVC) for every muscle to use them as a reference and finally (4) recording the electromyographic signals while the worker is developing the working tasks. A significant number of workers will be established for the analysis depending on the resources available and the scope of the study.

The results obtained through SEMG show if the activity required by a particular muscular group is higher or lower with the use of the exoskeleton.

The percentage of difference in the muscular activity between with and without exoskeleton considered significant is established according to the muscular group and the type of exoskeleton. For example, a 9% of the difference in the trunk extensor activity is considered significant in the case of using a passive exoskeleton for assistance for the back [6].

Based on these results, and depending on the quantity each muscle contributes to the task, a study is carried out whose conclusions guide the decision-making in terms of implementation or not of the exoskeleton in the workplace.

2.2 3D Motion Capture

The ranges of motion for the different joints constitute another one fundamental parameter of analysis. They allow us to verify how postures and movements are altered with the use of the exoskeleton and if comfort areas are surpassed.

One of the most practical techniques to register the motion of all body segments is through inertial sensors.

In this sense, it is possible to apply the MH-Sensors motion-capture system based on inertial sensors [7]. This system has significant advantages for application in the workplace: (1) portability, which allows real-time capturing in the workplace, (2) a straightforward process of anatomical calibration or sensor-to-segment alignment, which adjusts the human model to the anthropometric measurements of the analysed subject in-situ, (3) non-influence of magnetic disturbances, which could negatively affect this type of technology, especially in production environments.

The protocol followed to measure motion consists of: (1) identifying the body joints involved in the actions carried out by the worker, (2) placing the inertial sensors on the relevant body segments under study, (3) recording the initial posture as a reference to calibrate the system, (4) recording the motion signal during the performance of the tasks and (5) creating a biomechanical model to reproduce worker's movements to obtain the ranges of motion for each joint.

The outcomes obtained through this instrumental technique allow us to conclude whether the movements executed by the worker are less or more demanding with the use of the exoskeleton. The percentage of difference in the range of motion between with and without exoskeleton that is considered significant is established according to the body area and the type of exoskeleton.

2.3 Dynamometry for the Biomechanical Analysis

Another remarkable aspect to analyse is how the weight and the stiffness of the exoskeleton can influence the worker's joints and if this impact might cause damage in the medium and the long term.

In this sense, to assess the ergonomics of the workplace, the MH-Forces [8] method uses motion capture to calculate joint forces and moments and, with this information, estimates a joint risk index (0 minimum risk to 5 maximum risk). For its application, the forces and moments that the worker performs during the work cycle must be introduced. Similarly, this method would allow the consideration of the forces and moments caused by the exoskeleton acting on the body. In this way,

the expected effect of the exoskeleton on the biomechanics (kinematics and kinetics) of the worker during the execution of the task can be objectified by simulation.

3 Challenges

Despite the fact that the objective measuring techniques provide valuable results that help the decision-making in terms of the convenience or not to implement an exoskeleton, they involve some difficulties in practice.

Wearing an unfamiliar element on the body, such as an exoskeleton, is a challenge for the worker because of the addition of weight, the extra volume and the resistance to movement that it supposes. It causes physical interferences in the environment and hinders worker mobility.

Furthermore, sensors and elements attached to the worker's body that are required to monitor the performance increase this feeling of uncomfortability.

We require small, light and flexible devices that can be placed between the worker's body and the exoskeleton and be as unnoticeable as possible to achieve the least invasive possible measurement for the worker performing the activity.

Long-term studies entail time and resources, thus, they are difficult to carry out. The development of versatile and practical software will let the researchers achieve objective and reliable results with the minimal time investment.

4 Conclusion

The implementation of an exoskeleton in a company is costly in terms of time, staff and other resources involved.

The use of measuring objective techniques to analyse the effects of an exoskeleton on a user allows us to achieve reliable results and establish a precise diagnosis of the situation. It is possible to objectify the potential percentage in muscular activity reduction, the force reaction magnitude on the different joints and the periods during which the worker is adopting awkward postures.

In addition to this, it avoids false expectations about the convenience of the exoskeleton and confirms that it does not physically harm in the short term. The use of these instrumental techniques let us know in advance these effects will allow the decision-making and optimise the company resources before a potential implementation.

Acknowledgements Mutua Universal wishes to thank its associated companies for the collaboration provided in the studies with exoskeletons that have served as the basis for this work.

References

1. OSHA-EU, The impact of using exoskeletons on occupational safety and health (2019). https://osha.europa.eu/en/publications/impact-using-exoskeletons-occupational-safety-and-health/view
2. S. Kim et al., Assessing the potential for "undesired" effects of passive back-support exoskeleton use during a simulated manual assembly task: muscle activity, posture, balance, discomfort, and usability. Appl. Ergon. **89**, 103194 (2020)
3. A.E. Planas-Lara, J.A Tomás-Royo, M. Ducun-Lecumberri, *Ergonomics 4.0 and Exoskeletons: Myths, Legends and Truths* (Ed. Mutua Universal, 2020)
4. J.A. Tomás-Royo, M. Ducun-Lecumberri, A.E. Planas-Lara, M.M. Arias-Matilla, in *A Methodology to Assess the Effectiveness and the Acceptance of the Use of an Exoskeleton in a Company*, ed. by JuanC. Moreno et al. Biosystems & Biorobotics, Wearable Robotics: Challenges and Trends, 978-3-030-69546-0, vol. 27
5. S. Kumar, A. Mital, *Electromyography in Ergonomics* (Ed. Taylor & Francis, 1996)
6. S. Madinei, Biomechanical assessment of two back-support exoskeletons in symmetric and asymmetric repetitive lifting with moderate postural demands. Appl. Ergon. **88**, 103156 (2020)
7. J. Marín, T. Blanco, J. de la Torre, J.J. Marín, Gait analysis in a box: a system based on magnetometer-free IMUs or clusters of optical markers with automatic event detection. Sensors **20**, 3338 (2020)
8. M. Boné, *Método de evaluación ergonómica de tareas repetitivas, basado en simulación dinámica de esfuerzos con modelos humanos.* Ph.D. Thesis. University of Zaragoza, Spain, 2016

Designing an Integrated Tool Set Framework for Industrial Exoskeletons

O. A. Moreno, F. Draicchio, L. Monica, S. Anastasi, D. G. Caldwell, and J. Ortiz

Abstract The main objective of industrial exoskeletons is to provide physical assistance to prevent musculoskeletal disorder in workers. A group of active exoskeletons are powered by electrical actuators, in this scenario different challenges appear when modulating the effective active assistance. This paper presents a digital tool set framework as a strategy to improve the industrial exoskeleton performance during testing sessions and real scenarios. The design considerations are based on the required visual interfaces of this framework. The proposed human-machine interface is composed by (i) the user-command interface, a wearable device for user settings input (ii) the monitor-system, a desktop visual interface, and (iii) the gain-system interface, a mobile parameter configuration manager. Case studies where the framework potentially can be implemented are presented; the framework is designed to be compatible with the industrial exoskeleton XoTrunk.

O. A. Moreno (✉) · D. G. Caldwell · J. Ortiz
Advanced Robotics Department, Istituto Italiano di Tecnologia,
Via Morego 30, 16163 Genova, Italy
e-mail: olmo.moreno@iit.it

F. Draicchio
Department of Occupational Environmental Medicine, Epidemiology and Hygiene, INAIL,
Monte Porzio Catone, Rome, Italy
e-mail: f.draicchioi@inail.it

L. Monica · S. Anastasi
Department of Technological Innovation and Safety Equipment, INAIL, Monte Porzio Catone,
Rome, Italy
e-mail: l.monica@inail.it

S. Anastasi
e-mail: s.anastasi@inail.it

J. C. Moreno et al. (eds.), *Wearable Robotics: Challenges and Trends*,
Biosystems & Biorobotics 27, https://doi.org/10.1007/978-3-030-69547-7_94

1 Introduction

The exoskeleton is an external system suit that generates appropriate assistive forces, providing support and protection to the user who wears it [1]. A relevant interest for the manufacturing sector is to avoid the difficulties for workers during manual handling tasks [2].

One objective of industrial exoskeletons is to prevent musculoskeletal disorders (MSD) [3] such as articulation rigidity, pain, and loss of strength. An exoskeleton could be a passive (non-actuated) or an active (actuated) device. In [2], it is shown a list with 52% of active exoskeletons, in contrast of 48% passive ones. Toxiri et al. [4] describe active exoskeletons are likely to be more effective and versatile than passive ones, but it's design entails challenges reflected in the control methods and the active assistance modulation.

Different studies on control approach [5], and activity recognition [6] showed the variety of gains, variables and signals involved in the process to achieve a robust active exoskeleton controller. In this scenario, it is important to design an essential supporting digital structure to configure, calibrate, and tune up the system capabilities. This work presents the design of a standardized digital tool set as a human-machine interface (HMI) framework compatible with the next generation of industrial exoskeleton XoTrunk [7], to command, monitor and control back support system properties.

2 The Framework Structure

The tool set framework is a strategy to improve the capabilities of industrial exoskeletons based on the integration of data management, a monitoring system and a customized hardware. The framework structure will not process nor store any personal data of the user, such as daily activities or work performance.

2.1 User-Command Interface (UCI)

The UCI objective is to provide an adaptable setup system considering the variability between tasks and users. Since the assistive force/torque provided by the exoskeleton is user/task dependent, it is necessary an interface to adjust system configuration parameters for instance torques. Besides, it gives simple access to personalize different profiles according to the user's characteristics such as height and weight.

2.2 Monitor-System Interface (MSI)

The MSI is a data visualization tool which presents an intuitive graphical interface for monitoring signals such as velocity and force of an exoskeleton or a group of exoskeletons. The MSI tasks are: (a) monitor the performance and status of the system, (b) prevent user injuries (system misuse, overload, etc.), (c) coordinate the work between exoskeletons and (d) integrate the exoskeletons in the current production line.

2.3 Gain-System Interface (GSI)

The GSI is a mobile device implemented in an embedded system with component peripherals (sliders, push-buttons, and a touchscreen) that connects wirelessly to the exoskeleton. The developer is capable of modifying gain variables such as stiffness, this presents a solution to configure-calibrate parameters.

3 Hardware-Software Interfaces Architecture

The system presents modularity properties among the interfaces as depicted in Fig. 1. First, the UCI (wearable) has a navigation wheel, a fingerprint sensor and a touchscreen; the device is attached to the exoskeleton. According to the user input (position and activity), the UCI configures the exoskeleton functional parameters to improve performance in the activity frame. Second, the MSI (desktop) is a visual interface that tracks data signals (torque, current and velocity) generated in the exoskeleton and observes the status of the system. The connectivity of the MSI is through a wireless network to the exoskeleton. Finally the GSI (mobile), this module is a portable hardware that contains sensors and a visual interface connected to an embedded system. Since there is a wireless connection to the exoskeleton, a cross-platform property is linked between the UCI and the GSI; that means accessibility to the UCI frames and database for adjusting and configuration.

4 Application Study

The intention of this study is to show areas of opportunity where the framework can be adapted to improve the exoskeleton's performance. The following case studies show the use of the industrial exoskeleton: RoboMate [7]. A study on exoskeleton versatility based on human activity recognition [6] shows how working performance is affected when using an active exoskeleton. Since the actuators tend to hinder the

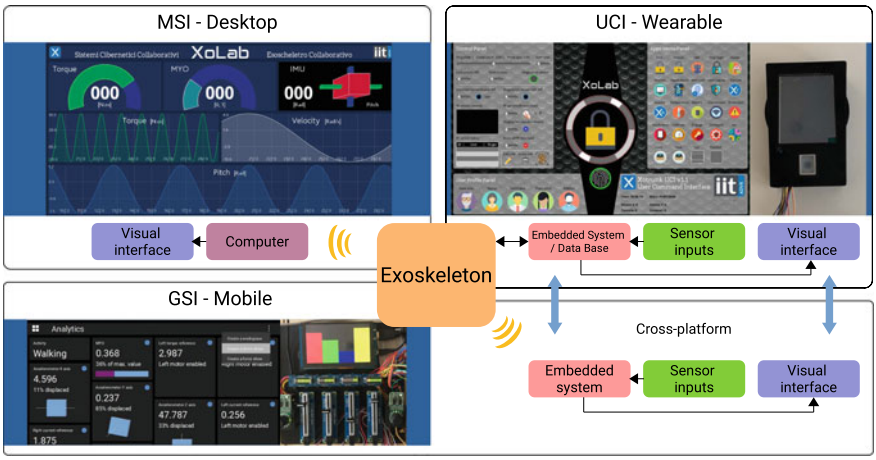

Fig. 1 Hardware-Software Interfaces Architecture. The digital tool set framework as desktop, wearable and mobile interfaces. The toolchain selected is: *Processing* [8], a visual programming framework for designing and prototyping. XoLab is the Exoskeleton Laboratory of Advanced Robotics Department at Istituto Italiano di Tecnologia

user's movements, it is a common practice to switch off the assistance manually by the user. The study goal is to improve user activity recognition, and automate the active assistance. In this case, using the UCI permits to select diverse operation modes according to the user activity task, even the activity recognition option.

In [5], is presented a new strategy to improve control active assistance in dynamic situations, in this case, the beginning and end of lowering and lifting movement. Since an inertial measurement unit (IMU) was attached to detect the user's inclination, the MSI is the plotting tool to track and visualize in real time the IMU's signal feeding the controller.

At last, a study on energy consumption during industrial lifting tasks [9] reports how actuator design affects properties such as weight and user comfort when using the exoskeleton. The aim is to modulate the torques to reduce the overload on the exoskeleton joints, this is interpreted as a comfortable movement when wearing the exoskeleton. For this scenario, the GSI interacts directly with the controller for configuring the gains such as stiffness during the test session.

5 Future Development

The future development for the digital tool set framework is divided in two sections: (a) testing prototype, and (b) system validation. In the testing section the aim is to specify scenarios, tasks, users, measurements and desired outcomes to prove the system capabilities and improve the framework performance. Later on, the valida-

tion section will include locations, environment conditions, tasks, subject requisites, metrics and evaluation forms, the system should be successfully used in the defined environment in certain tasks.

6 Conclusion

The digital tool set framework design shown in this work presents a potential utility for industrial active exoskeletons. Initially, the UCI as wearable device attached to the exoskeleton configures user settings for better performance. Second, the MSI is a desktop monitoring system to track the exoskeleton signals. Lastly the GSI, a mobile interface with sensors and a graphic environment used to configure the exoskeleton parameters during testing. The case studies presented belong to the industrial exoskeleton RoboMate and the framework aims to be part of the next exoskeleton generation called XoTrunk. Testing and validating the system features will improve the performance of the exoskeleton in real task scenarios.

Acknowledgements This work has been funded by the Italian Workers' Compensation Authority (INAIL).

References

1. E.S. Barjuei, M.M.G. Ardakani, D.G. Caldwell, M. Sanguineti, J. Ortiz, Optimal Selection of motors and transmissions in back-support exoskeleton applications. IEEE Trans. Med. Robot. Bionics 1 (2020)
2. A. Voilqué, J. Masood, J. Fauroux, L. Sabourin, O. Guezet, Industrial exoskeleton technology: classification, structural analysis, and structural complexity indicator, in *2019 Wearable Robotics Association Conference (WearRAcon)* (2019), pp. 13–20
3. H.-W. Choi, Y.-K. Kim, D.-M. Kang, J.-E. Kim, B.-Y. Jang, Characteristics of occupational musculoskeletal disorders of five sectors in service industry between 2004 and 2013. Annals Occup. Environ. Med. **29**, 41 (2017)
4. S. Toxiri, A.S. Koopman, M. Lazzaroni, J. Ortiz, V. Power, M.P. de Looze, L. O'Sullivan, D.G. Caldwell, Rationale, implementation and evaluation of assistive strategies for an active back-support exoskeleton. Front. Robot. AI **5**, 53 (2018)
5. M. Lazzaroni, S. Toxiri, D.G. Caldwell, S. Anastasi, L. Monica, E.D. Momi, J. Ortiz, Acceleration-based assistive strategy to control a back-support exoskeleton for load handling: preliminary evaluation, in *2019 IEEE 16th International Conference on Rehabilitation Robotics (ICORR)* (2019), pp. 625–630. ISSN: 1945-7901
6. T. Poliero, L. Mancini, D.G. Caldwell, J. Ortiz, Enhancing back-support exoskeleton versatility based on human activity recognition, in *2019 Wearable Robotics Association Conference (WearRAcon)* (2019), pp. 86–91
7. J. Ortiz, S. Toxiri, D.G. Caldwell, Beyond robo-mate: towards the next generation of industrial exoskeletons in Europe, in *Wearable Robotics: Challenges and Trends*, ed. by M.C. Carrozza, S. Micera, J.L. Pons, eds. Biosystems & Biorobotics (Springer International Publishing, Cham, 2019), pp. 365–369

8. C. Reas, B. Fry, J. Maeda, *Processing: A Programming Handbook for Visual Designers and Artists* (The MIT Press, Cambridge, 2007)
9. S. Toxiri, T. Verstraten, A. Calanca, D.G. Caldwell, J. Ortiz, Using parallel elasticity in back-support exoskeletons: a study on energy consumption during industrial lifting tasks, in *2019 Wearable Robotics Association Conference (WearRAcon)* (2019), pp. 1–6

Benchmarking Wearable Robots

Wearable Robots Benchmarking: Comprehending and Considering User Experience

Philipp Beckerle

Abstract In real-world applications, wearable robots need to serve functional requirements, but also satisfy user demands. A systematic evaluation will require multidisciplinary benchmarking methods. Since user experience seems to be of distinct relevance, this paper analyzes how user experience influences wearable robots use and how it can be considered in benchmarking. Focus is set on potential metrics and how we could include them in human-centered benchmarking approaches.

1 Introduction

Currently, we witness wearable robots entering practical applications, e.g., exoskeletons and prostheses [1, 2]. To achieve their application-specific objectives, performance evaluation needs reliable and replicable testing methods [1].

Going beyond a functional perspective, we should consider the users' needs via appropriate benchmarking methods [3]. Actually, users' experiences and needs are understood to distinctly influence functional outcomes of wearable robot use [4, 5] and even determine whether devices are used at all [6]. Research is just starting to tackle this by multidisciplinary evaluation methods [7, 8], which take perceptual, emotional, and cognitive processes into account [3].

The above-mentioned processes are strongly related to physical and cognitive human-robot interaction. Especially, co-adaptation between user and robot is highly relevant and might be exploited to improve functional, but also experience-related outcomes [4, 5]. Due to these entanglements and the issue that some aspects of experience might not be quantifiable, human-centered approaches in general and human-in-the-loop techniques in particular are promising for the investigation of the users' satisfaction, comfort, body experience in real interaction scenarios [5].

P. Beckerle (✉)
Chair of Autonomous Systems and Mechatronics, Department of Electrical Engineering, Friedrich-Alexander-University Erlangen-Nürnberg, Erlangen, Germany
e-mail: philipp.beckerle@tu-dortmund.de

Department of Mechanical Engineering, Institute for Mechatronic Systems, TU Darmstadt, Darmstadt, Germany

J. C. Moreno et al. (eds.), *Wearable Robotics: Challenges and Trends*,
Biosystems & Biorobotics 27, https://doi.org/10.1007/978-3-030-69547-7_95

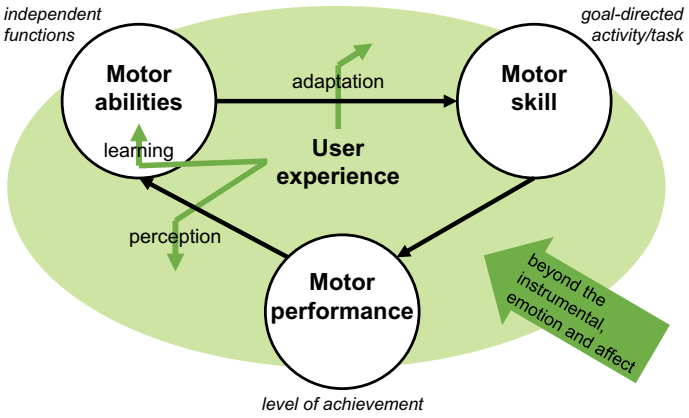

Fig. 1 The benchmarking taxonomy of Torricelli et al. [1] in the context of user experience. Motor skills, motor abilities, and motor performance will be experienced by the user. This experience will, in turn, shape the user's perception, learning, and adaptation behavior. Moreover, non-functional factors like aesthetics, emotion, and affect influence the overall user experience and resulting behavior

This contribution discusses the influence of user experience on wearable robots use and benchmarking. Potential metrics to consider user experience are analyzed and directions to human-centered benchmarking are proposed.

2 User Experience

User experience comprises the perception and reactions of a person using a system [9], which covers direct physical and cognitive interaction in the case of wearable robots [3]. As outlined by Hassenzahl and Tractinsky [10], user experience goes beyond function-related impressions and is strongly influenced by aspects such as aesthetics, emotion, and affect.

Torricelli et al. [1] defined a wearable robot benchmarking taxonomy of intertwined motor aspects (see Fig. 1). Interpreting these functionally-focused aspects regarding user experience indicates its influences on motor skills, abilities, and performance. The experience of motor aspects, which Torricelli et al. suggest for quantitative evaluation [1], shapes users' perception, learning, and adaptation behaviors: on the one hand, the assessment of their own motor capabilities might depend on overall satisfaction and non-functional modulators. On the other hand, learning new control strategies as well as adapting motor abilities are subject to neural plasticity due to mutual adaptation of user and robot [5].

3 Potential Metrics

To comprehend and consider user experience of wearable robots, recent research suggests to integrate associated perceptual, emotional, and cognitive aspects in functional assessment protocols [4]. This needs metrics covering application-specific modulators of device acceptance and satisfaction [4]. Generally, but especially in benchmarking, quantitative metrics are tempting due to providing explicit values. Yet, they might not always suffice: non-functional aspects like aesthetics, emotion, and affect call for qualitative metrics providing insights to individual particularities.

Theoretical models and experimental studies of user experience help to identify possible metrics [3]. For prosthetics, the model by Gauthier-Gagnon et al. describes that some experience-related aspects can be influenced by technical design, while others cannot, i.e., predispositions and psychosocial environment [11]. Yet, aspects which cannot be altered directly, might have strong impact on actual user experience. Questionnaires and interviews explore user satisfaction, e.g., in prosthetics [12, 13], but an approach covering wearable robots in general appears to be missing [3].

Promising candidate metrics are recently researched (see Fig. 2): the users' body experience might be assessed measuring their sense of embodiment [5]. Similarly, the sense of agency over the device can indicate the transparency and intuitivity of assistive control [14]. Subjective cognitive load can indicate how easily users get along with a device and its control [4]. This is of special interest when thinking about learning systems sharing control with their human partner.

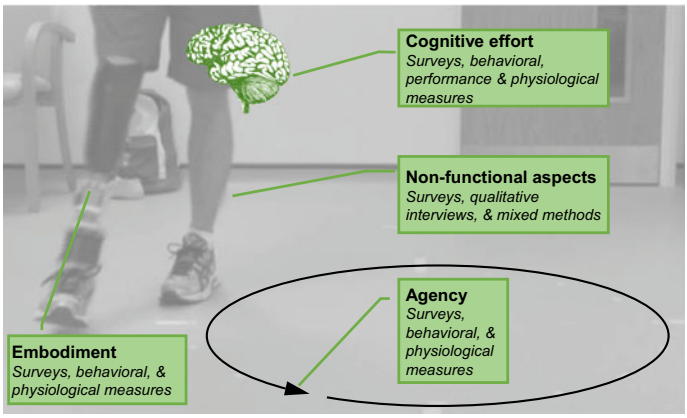

Fig. 2 Metrics assessing user experience in wearable robot benchmarking. Human-in-the-loop experiments might help to understand cause-effect relationships of experience modulators and exploit the full bandwidth of measures. In-the-wild benchmarking might be limited to survey and psychophysiological methods to avoid interferences with experimental design

4 Human-Centered Benchmarking

To holistically consider functional and experience-related aspects, benchmarking might take inspiration from human-centered design [12, 15]. While continuous user involvement appears obvious, benchmarking could benefit from systematic user experience assessment, e.g., to weight functional observations considering non-functional aspects.

Human-in-the-loop experiments are promising to understand cause-effect relations underlying human-robot interaction and user experience [4, 5]. They can systematically vary modulating factors and exploit all potential experience measures. To assess embodiment, agency, and cognitive effort, psychometric [16, 17], psychophysiological [17], performance-related [18], and behavioral [14, 17] measures exist. Since the latter demand specific designs, they are valuable in the laboratory, but might not be feasible outside.

5 Conclusions

Wearable robot benchmarking is highly important to keep track of user outcomes. For a holistic, possibly human-centered, perspective we will need a deep understanding of motor-experience correlations and their metrics in benchmarking. Considering user experience throughout the evaluation process, we might be able to improve user outcomes.

References

1. D. Torricelli, J. Gonzalez-Vargas, J.F. Veneman, K. Mombaur, N. Tsagarakis, A.J. Del-Ama, A. Gil-Agudo, J.C. Moreno, J.L. Pons, Benchmarking bipedal locomotion: a unified scheme for humanoids, wearable robots, and humans. IEEE Robot. Autom. Mag. **22**(3), 103–115 (2015)
2. M. Windrich, M. Grimmer, O. Christ, S. Rinderknecht, P. Beckerle, Active lower limb prosthetics: a systematic review of design issues and solutions. BioMed. Eng. OnLine **15**(3), 5–19 (2016)
3. D. Torricelli, C. Rodriguez-Guerrero, J.F. Veneman, S. Crea, K. Briem, B. Lenggenhager, P. Beckerle, Benchmarking wearable robots: challenges and recommendations from functional (user experience and methodological perspectives (in revision))
4. P. Beckerle, G. Salvietti, R. Unal, D. Prattichizzo, S. Rossi, C. Castellini, S. Hirche, S. Endo, H. Ben Amor, M. Ciocarlie, F. Mastrogiovanni, B.D. Argall, M. Bianchi, A human-robot interaction perspective on assistive and rehabilitation robotics. Front. Neurorobot. **11**(24) (2017)
5. P. Beckerle, C. Castellini, B. Lenggenhager, Robotic interfaces for cognitive psychology and embodiment research: a research roadmap. Wiley Interdiscipl. Rev. Cogn. Sci. **10**(2), e1486 (2019)
6. N. Jiang, S. Došen, K. Müller, D. Farina, Myoelectric control of artificial limbs—is there a need to change focus? IEEE Signal Process. Mag. **29**(5), 148–152 (2012)

7. A.L. Ármannsdóttir, P. Beckerle, J.C. Moreno, E.H.F. van Asseldonk, M.-T. Manrique-Sancho, A. del Ama, J. Veneman, K. Briem, Assessing the involvement of users during development of lower limb wearable robotic exoskeletons: a survey study. Human Fact. **62**, 351–364 (2020)
8. J. Ghillebert, S. De Bock, F. Flynn, J. Geeroms, B. Tassignon, B. Roelands, D. Lefeber, B. Vanderborght, R. Meeusen, K. De Pauw, Guidelines and recommendations to investigate the efficacy of a lower-limb prosthetic device: a systematic review. IEEE Trans. Med. Robot. Bion. **1**(4), 279–296 (2019)
9. DIN Deutsches Institut für Normung e.V., EN ISO 9241-9:2000, Ergonomische Anforderungen für Bürotätigkeiten mit Bildschirmgeräten (2000)
10. M. Hassenzahl, N. Tractinsky, User experience—a research agenda. Behav. Inf. Technol. **25**(2), 91–97 (2006)
11. C. Gauthier-Gagnon, M.C. Grisé, Enabling factors related to prosthetic use by people with transtibial and transfemoral amputation, Arch. Phys. Med. Rehabil. **80**(6), 706–713 (1999)
12. P. Beckerle, O. Christ, T. Schürmann, J. Vogt, O. von Stryk, S. Rinderknecht, A human-machine-centered design method for (powered) lower limb prosthetics. Robot. Auton. Syst. **95**, 1–12 (2017)
13. E.C. Baars, E. Schrier, P.U. Dijkstra, J.H.B. Geertzen, Prosthesis satisfaction in lower limb amputees: a systematic review of associated factors and questionnaires. Medicine **97**(39) (2018)
14. S. Endo, J. Fröhner, S. Music, S. Hirche, P. Beckerle, Effect of external force on agency in physical human-machine interaction. Front. Human Neurosci. **14** (2020)
15. T. Jokela, N. Iivari, J. Matero, M. Karukka, The standard of user-centered design and the standard definition of usability: analyzing iso 13407 against iso 9241-11, in *Proceedings of the Latin American Conference on Human-computer Interaction* (2003), pp. 53–60
16. S.G. Hart, L.E. Staveland, Development of nasa-tlx (task load index): results of empirical and theoretical research. Adv. Psychol. **52**, 139–183 (1988)
17. O. Christ, M. Reiner, Perspectives and possible applications of the rubber hand and virtual hand illusion in non-invasive rehabilitation: technological improvements and their consequences. Neurosci. Biobehav. Rev. **44**, 33–44 (2014)
18. A. Erdogan, B.D. Argall, The effect of robotic wheelchair control paradigm and interface on user performance, effort and preference: an experimental assessment. Robot. Auton. Syst. **94**, 282–297 (2017)

Performance Indicators of Humanoid Posture Control and Balance Inspired by Human Experiments

Vittorio Lippi, Thomas Mergner, Christoph Maurer, and Thomas Seel

Abstract Posture control and maintaining balance are fundamental elements of humanoid robot control and have a significant impact for the performance of robots. The evaluation of robotic performance, at the state of the art, is mostly evaluated at goal level, e.g. with robot competitions. While falling is a typical reason beyond the failure of the humanoid operation, the failure itself does not provide many details about the nature of the underlying problem that can be used to improve the control. In order to provide a more specific analysis of posture control and balance, this contribution presents a set of performance indicators, i.e. indexes that can be used to compare the performance of robots with the human control systems. The inspiration for the proposed tests and indicators comes from human experiments and particular emphasis is placed on human-robot comparison.

1 Introduction

Posture control and balance are required to maintain equilibrium when walking or standing and to provide buttress when performing a motor task. Losing balance is one of the typical reasons of failure for humanoids, often damaging the hardware, as reported for example for the DARPA challenges [1–3]. During such a challenge the robot is evaluated in terms of goal achievement, without (directly) going into details of the reason of the failure. An evaluation system focused on the details of posture control is envisaged to be useful to inspire the improvement of the components of the control system. The study of human posture control can provide inspiration for the control of humanoids [4–7] and, on the other hand, humanoids represent a potential testbed for theories for human neurology [8]. Studies involving human-inspired posture control systems usually include an ad hoc specified test of performance,

V. Lippi (✉) · T. Seel
Fachgebiet Regelungssysteme (Control Systems Group), Technische Universität Berlin, Einsteinufer 17, Berlin, Germany
e-mail: vittorio.lippi@uniklinik-freiburg.de

T. Mergner · C. Maurer
Neurology, University Clinic of Freiburg, Freiburg, Germany

J. C. Moreno et al. (eds.), *Wearable Robotics: Challenges and Trends*,
Biosystems & Biorobotics 27, https://doi.org/10.1007/978-3-030-69547-7_96

while neurology works exploiting the robot as a simulation device for the comparison between human and robot behavior defined on some quantitative basis (e.g. body-sway frequency response to external disturbances). In this work we specify a set of tests and *performance indicators* (PI) that are meant to make such evaluations repeatable and comparable between different robots. This fits in the more general effort of producing benchmarking tools for humanoid robots [6, 9–12].

2 Tests and Performance Indicators

Sinusoidal disturbance. Providing an external disturbance with a sinusoidal profile allows for an evaluation of the performance in terms of disturbance rejection. Different kinds of stimuli can be used, e.g. surface tilt or translation. The response consisting of the induced body sway is used to compute gain on a specific frequency as ratio between response and stimulus [13]. The periodic nature of the stimulus can test the ability of the robot to exploit prediction [14]. Considering that in general the response of the robot is not linear, several frequencies and amplitudes can be tested obtaining several scores. In general, a smaller gain is considered a better performance, nevertheless a more "relaxed" compensation of the disturbances may be more efficient and hence the gain may be evaluated together with energy consumption or mechanical work produced by the actuators [13].

For testing the movement of the support surface with a sinusoidal profile, the pi is the body sway over the stimulus: ***gain****. The smaller the gain the better the performance.*

Raised Cosine. A support surface movement, e.g. translation or tilt, with a velocity profile of a raised cosine represents a smooth version of a step function that can be used safely for humanoids and human subjects [15]. In this way the transient response to external stimuli can be evaluated in terms of characteristics like *rise time, overshoot, settling time, peak time* and *delay-time.*

Raised cosine is a "safe" version of the step function that can be used to evaluate a PI reflecting the transient response characteristics: **rise time**, **overshoot**, **settling time**, **peak time** *and* **delay-time**.

Model parameters. Parametric models of human posture control can be fitted on experimental data. This transforms a series of body sway measures and input stimuli into a set of parameters. In particular we developed a system to fit the nonlinear DEC

(*disturbance estimation and compensation*) model [4] based on convolutional neural networks [16]. The parameters are not a PI by themselves, but they can be used to assess some properties of the humanoid such as joint stiffness and total loop delay. The set of parameters represents a feature set that can be used in the development of machine learning solutions and to define a similarity between two different robots.

Parameters for posture control models are a concise and meaningful representation of robot behavior that can be used for performance evaluation.

Human likeness. A dataset of results from human experiments is provided as a reference for the benchmarking. The set includes healthy subjects and subjects with specific health conditions affecting sensorimotor control such as spasticity or vestibular loss. The experiments consisted in providing the subject with a stimulus consisting of a tilt or a translation of the support surface in the sagittal plane, while body sway was recorded as output. The profile used for the stimulus is a pseudo-random ternary signal, PRTS [17]. The comparison between different behaviors is defined in terms of the norm of the difference between frequency response functions on a set of relevant frequencies (specifically $\boldsymbol{f}_{\boldsymbol{peak}}$ *= [0.0165, 0.0496, 0.0992, 0.1322, 0.1818, 0.2314 0.2975, 0.3636, 0.4463, 0.5785, 0.7273, 0.9256, 1.1736, 1.4545, 1.7686, 2.1983] Hz*). Such frequencies are defined by the structure of the PRTS power-spectrum $P(f)$ that has a "comb" profile with peaks on those frequencies separated by ranges of frequencies with virtually no signal. Furthermore, the peaks of the PRTS power-spectrum have larger values at lower frequencies [18]. This implies a better signal-to-noise ratio for the first components. A weighting proportional to $P\left(\boldsymbol{f}_{peak}\right)$ is applied in the comparison. The distance between two FRFs is defined and the norm of the difference weighted by the precision matrix, i.e. the inverse of the covariance matrix $\sum$, computed on the dataset of normal subjects, this together with the foretold weighting leads to the definition of the norm:

$$D = \sqrt{\boldsymbol{d}^{\boldsymbol{T}} \boldsymbol{S} \Sigma^{-1} \boldsymbol{S} \boldsymbol{d}} \tag{1}$$

where $\boldsymbol{S} = diag\left(P\left(\boldsymbol{f}_{peak}\right)\right)$ is the diagonal matrix representing the reweighting due to the power-spectrum, and $\boldsymbol{d}$ is the difference between the two FRFs.

This approach does not require model identification because it is performed on the basis of the data. The comparison can be performed between the tested robot and the average of the groups (healthy or with special deficient conditions) or between two single samples in order to quantify how much two robots differ from each other.

Human likeness *can be estimated on the basis of a comparison with a dataset from human experiments. Different groups of subjects can provide a reference*

to 'diagnose' a specific behavior. The measure in (1) defines a norm that can be used also to compare two specific trials.

3 Conclusion

In this contribution we presented a set of PIs for posture control and an overview of our humanoid performance benchmarking principles. The human experimental dataset, the software implementing the proposed analysis and the hardware required to perform the proposed tests will be available through the EUROBENCH initiative (https://eurobench2020.eu/). Specifically, the moving platform has been designed for humanoids, but, provided that safety for users is properly ensured, the here described PIs can be applied to the study of wearable robots.

Acknowledgements This work is supported by the project EUROBENCH (European Robotic Framework for Bipedal Locomotion Benchmarking, www.eurobench2020.eu) funded by H2020 Topic ICT 27–2017 under grant agreement number 779963.

References

1. E. Guizzo, E. Ackerman, The hard lessons of DARPA's robotics challenge [News]. IEEE Spectr. (2015). https://doi.org/10.1109/mspec.2015.7164385
2. C.G. Atkeson et al., No falls, no resets: reliable humanoid behavior in the DARPA robotics challenge. in *IEEE-RAS International Conference on Humanoid Robots* (2015). https://doi.org/10.1109/HUMANOIDS.2015.7363436
3. C.G. Atkeson et al., What happened at the DARPA robotics challenge finals. in *Springer Tracts in Advanced Robotics* (2018)
4. V. Lippi, T. Mergner, Human-derived disturbance estimation and compensation (DEC) method lends itself to a modular sensorimotor control in a humanoid robot. Front. Neurorobot. **11**, (2017). https://doi.org/10.3389/fnbot.2017.00049
5. A.V. Alexandrov, V. Lippi, T. Mergner, A.A. Frolov, G. Hettich, D. Husek, Human-inspired Eigen movement concept provides coupling-free sensorimotor control in humanoid robot. Front. Neurorobot. **11**, (2017). https://doi.org/10.3389/fnbot.2017.00022
6. V. Lippi, D. Torricelli, G. Hettich, T. Mergner, Benchmarking human-likeness of robot postural control—suggestions from human experiments. in *Workshop in Benchmarking Human-Like Locomotion Humanoids 2013 Conference*, (2013)
7. C. Ott et al., Good posture, good balance: comparison of bioinspired and model-based approaches for posture control of humanoid robots. IEEE Robot. Autom. Mag. **23**(1), 22–33 (2016). https://doi.org/10.1109/MRA.2015.2507098
8. V. Lippi, T. Mergner, Humanoid neurorobotics-posture, balance and movement control. in *School and Symposium on Advanced Neurorehabilitation (SSNR2016)*, (2016)
9. D. Torricelli et al., Benchmarking human likeness of bipedal robot locomotion: state of the art and future trends. in *Metrics of Sensory Motor Coordination and Integration in Robots and Animals* (Springer, 2020), pp. 147–166

10. R. Conti, F. Giovacchini, L. Saccares, N. Vitiello, J.L. Pons, D. Torricelli, What do people expect from benchmarking of bipedal robots? Preliminary results of the EUROBENCH survey. in *Biosystems and Biorobotics* (2019)
11. D. Torricelli, J.L. Pons, EUROBENCH: preparing robots for the real world. in *Biosystems and Biorobotics* (2019)
12. T. Mergner, V. Lippi, Posture control—human-inspired approaches for humanoid robot benchmarking: conceptualizing tests, protocols and analyses. Front. Neurorobot. **12**, (2018). https://doi.org/10.3389/fnbot.2018.00021
13. V. Lippi, T. Mergner, T. Seel, C. Maurer, COMTEST project: a complete modular test stand for human and humanoid posture control and balance. in *IEEE-RAS International Conference on Humanoid Robots* (2019). https://doi.org/10.1109/Humanoids43949.2019.9035081
14. V. Lippi, Prediction in the context of a human-inspired posture control model. Rob. Auton. Syst. (2018). https://doi.org/10.1016/j.robot.2018.05.012
15. V. Lippi, G. Hettich, T. Mergner, Modeling postural control of support surface translations. in *IEEE Humanoids, Workshop on Cognition, Perception and Postural Control for Humanoids* (Madrid, Spain, 2014)
16. V. Lippi, T. Mergner, C. Maurer, Deep learning for posture control nonlinear model system and noise identification. in Proceedings of the 17th International Conference on Informatics in Control, Automation and Robotics—vol. 1: ICINCO, ISBN 978-989-758-442-8, pages 607–614. (2020) https://doi.org/10.5220/0009148106070614
17. R.J. Peterka, Sensorimotor integration in human postural control. J. Neurophysiol. (2002). https://doi.org/10.1152/jn.2002.88.3.1097
18. D. Joseph Jilk, S.A. Safavynia, L.H. Ting, Contribution of vision to postural behaviors during continuous support-surface translations. Exp. Brain Res. **232**(1), 169–180 (2013). https://doi.org/10.1007/s00221-013-3729-4

Lower-Limbs Exoskeletons Benchmark Exploiting a Stairs-Based Testbed: The STEPbySTEP Project

Nicole Maugliani, Marco Caimmi, Matteo Malosio, Francesco Airoldi, Diego Borro, Daniel Rosquete, Ausejo Sergio, Davide Giusino, Federico Fraboni, Giuseppe Ranieri, Luca Pietrantoni, and Loris Roveda

Abstract Wearable exoskeletons can be valuable assistive robots to physically support humans in a wide variety of daily living activities. However, there is a lack of standards for the devices benchmark and evaluation. The STEPbySTEP project is developing a modular and sensorized reconfigurable staircase testbed for lower-limb exoskeletons benchmarking to be included in the main EUROBENCH project testing facility. In addition, metrics for the benchmark and evaluation of different solutions are defined, including physical interaction metrics, ergonomics metrics, and human factors metrics.

1 Testbed Description

The STEPbySTEP project proposes the development of a modular, sensorized and reconfigurable staircase testbed to be used in a systematic procedure aimed at validating lower-limbs exoskeletons (LLEs) abilities, performance and effects on user experience during ascending/descending stairs. The proposed testbed is shown in Fig. 1. The capability of the setup to reconfigure the inclination of the staircase (i.e., the height of the steps) is of great importance to test the LLEs in different situations. Such inclination can be set by changing the height of the landing through the *Actu-*

N. Maugliani · M. Caimmi · M. Malosio · F. Airoldi
Institute of Intelligent Industrial Technologies and Systems for Advanced Manufacturing (STIIMA) of Italian National Research Council (CNR), via Corti, 12, 20133 Milan, Italy

D. Borro · D. Rosquete · A. Sergio
CEIT-Basque Research and Technology Alliance (BRTA) and Tecnun, (University of Navarra), Manuel Lardizabal 15, 20018 Donostia-San Sebastian, Spain

D. Giusino · F. Fraboni · G. Ranieri · L. Pietrantoni
Department of Psychology, University of Bologna, via Filippo Re, 10, 40126 Bologna, Italy

L. Roveda (✉)
Istituto Dalle Molle di studi sull'Intelligenza Artificiale (IDSIA), Scuola universitaria professionale della Svizzera italiana (SUPSI), Università della Svizzera italiana (USI), via Cantonale, 6928 Manno, Switzerland
e-mail: loris.roveda@idsia.ch

J. C. Moreno et al. (eds.), *Wearable Robotics: Challenges and Trends*,
Biosystems & Biorobotics 27, https://doi.org/10.1007/978-3-030-69547-7_97

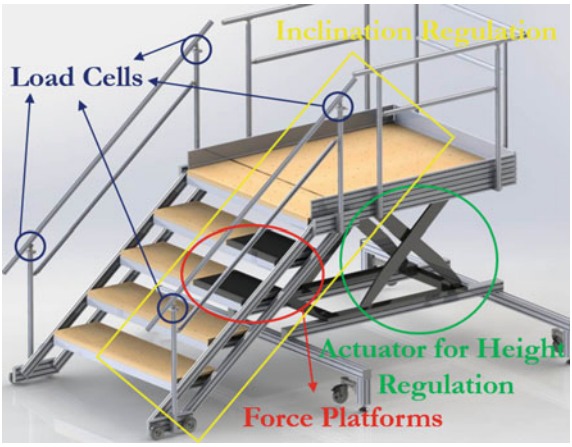

Fig. 1 Proposed reconfigurable and sensorized stair testbed

ator for Height Regulation. The handrail is sensorised with load cells to quantify how much the subject supports himself on the handrail. In addition, two steps are sensorized with a force plate (BTS P-6000) to measure the contact forces between the subject and the steps. Two force plates are in fact enough to evaluate a complete gait cycle; anyway, if necessary, the test bed provides for the possibility of installing up to 4 force plates. Observational measures and performance indicators will be provided along with a set of reference data acquired from a group of healthy subjects ascending/descending stairs with no exoskeleton. Set of data will be provided for two strategies: ascent and descent putting (1) only one foot on each step (classical) or (2) both feet on each step (like patients do). In the paper only strategy 1 is handled.

2 Metrics Definition

2.1 Physical Interaction Metrics

The proposed metrics rely on the use of surface electromyography (sEMG), a technique to record the muscles electrical activity during contraction. The stronger is the contraction, the higher is the electrical activity. The sEMG of tibialis anterior, soleus, rectus femoris, and hamstring muscles will be collected bilaterally. The selection of these muscles is a good compromise between the setup time and the quantity of information extractable from the data, but more muscles may be selected for other kinds of analyses (e.g., muscle synergies). Two kind of metrics will be presented: an index quantifying the amount of activity of the muscle i ${}_AEMG^i$, and an index quantifying the co-contractions between the muscle i and muscle j $ccEMG^{ij}$). The first metric was recently tested to verify the effectiveness of a physical collaborative

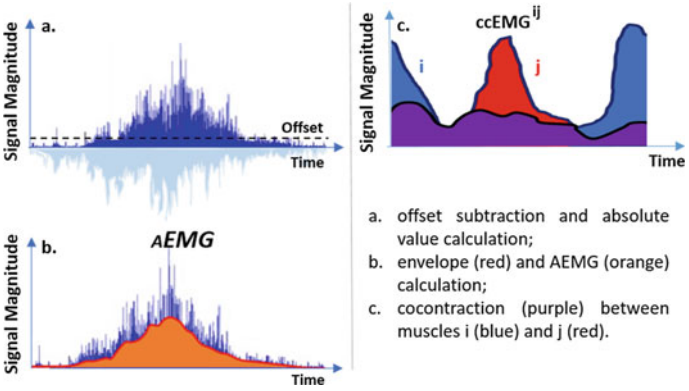

Fig. 2 EMG elaboration (left) and co-contraction index calculation (right)

controller on a KUKA iiwa LBR 14 robot [1, 2]. The second metric was used in a study of proprioception during robot-assisted reaching [3].

Each muscle signal is processed as follows: (i) subtraction of the DC offset; (ii) the calculation of the absolute value; (iii) calculation of the signal envelope ENV^i using of a Hilbert transform filter (Fig. 2 left panel). The index ${}_AEMG^i$ quantifying the activity of the i-muscle is defined as the area underneath the signal envelope:

$$ {}_AEMG^i = \sum_{k=1}^{N} ENV^i(k). \tag{1} $$

The index $ccEMG^{ij}$ quantifying the co-contraction between the muscle i and the muscle j (Fig. 2 right panel) is:

$$ ccEMG^{ij} = 2 \times \frac{\Sigma_{k=1}^{N} \min(ENV^i(k), ENV^j(k))}{{}_AEMG^i +_A EMG^j} \times 100\%, \tag{2} $$

where N is the number of samples and ENV^i the i-muscle signal envelop.

2.2 Biomechanical Metrics

In stair ascent/descent there's no common definition of the phases, sub phases and events of the movement as in gait analysis. Figure 3 shows the definition of phases and subphases made by Harper [4].

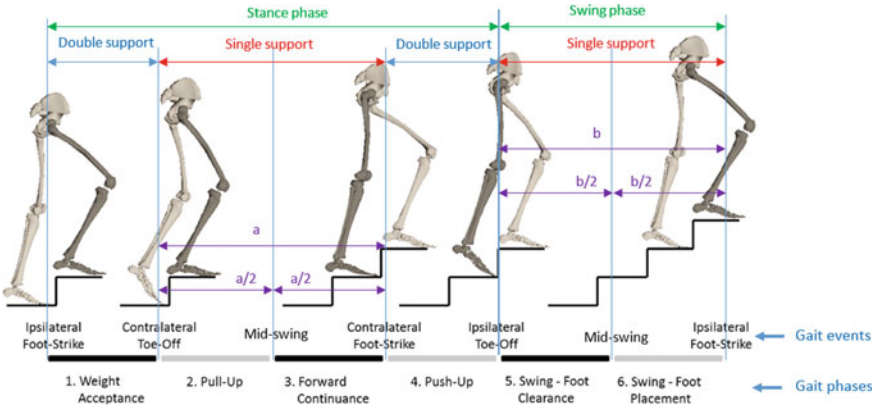

Fig. 3 Figure from [4] and modified by CEIT. The six regions of the ipsilateral (dark shaded) leg gait cycle: **1** weight acceptance (ipsilateral foot-strike to contralateral toe-off), **2** pull-up and **3** forward continuance (contralateral toe-off to contralateral foot-strike divided into two equal sections), **4** push-up (contralateral foot-strike to ipsilateral toe-off), **5** early swing and foot clearance and **6** late swing and foot placement (ipsilateral toe-off to ipsilateral foot-strike divided intro two equal sections)

2.2.1 Simple Metrics

Simple metrics that can be measured easily in clinical setting or a motion capture lab:

- Total time to ascend the stair. Considering only ascend.
- Total time to descend the stair. Considering only descend.

2.2.2 Complex Metrics

We take into account temporal and kinematics parameters.
Temporal Parameters (Time parameters): Subphases of stair climbing (% of gait cycle):

- Weight acceptance phase
- Pull-up phase
- Forward continuance
- Push-up
- Swing-foot clearance
- Swing-foot placement

Subphases of stair descend (% of gait cycle):

- Weight acceptance phase
- Forward continuance phase

- Controlled lowering phase
- Leg pull through
- Foot placement

Kinematic and kinetic parameters:

- Joint angles versus % of gait cycle.
- Peak values of angles and time occurrence (% of gait cycle) at the hip, knee and ankle joint.
- Peak values of vertical ground reaction force, anterior-posterior and medium-lateral center of progression
- Peak value of forces applied on the handrail.

2.3 Human Factors Metrics

Based on previous literature regarding the evaluation of medical LLEs' impact on users'perceptions and behaviors [5], the STEPbySTEP project aims to develop a Human Factors benchmarking framework based on the integration of well-accredited evaluation tools. Two types of metrics will be included. Cognitive metrics will encompass: cognitive-motor interference, measured by the Single-Dual Task Paradigm [6], and perceived musculoskeletal pressure/discomfort, measured by the Local Perceived Pressure Method [7]. Behavioral metric will correspond to an ad-hoc observational checklist measuring user-exoskeleton interaction. The protocol will be divided in three phases. The first phase (before task, 25 min) entails a semi-structured interview (15 minutes) concerning user expectations about his/her experience with the exoskeleton, along with a questionnaire about age, sex, anthropometric features and expertise with assistive devices. The second phase (during task, 20 min) consists of climbing the staircase testbed. In turn, two experimental conditions will be run, such as without and with cognitive-motor interference. The third phase (after task, 30 min) encompasses a semi-structured interview (15 min) regarding user attitudes about his/her experience with the exoskeleton, along with a questionnaire about local perceived pressure.

References

1. L. Roveda et al., Fuzzy impedance control for enhancing capabilities of humans in onerous tasks execution, in *2018 15th International Conference on Ubiquitous Robots (UR)* (IEEE, 2018), pp. 406–411
2. L. Roveda et al., Assisting operators in heavy industrial tasks: on the design of an optimized cooperative impedance fuzzy-controller with embedded safety rules. Front. Robot. AI **6**, 75 (2019)
3. M. Caimmi et al., Proprioceptivity and upper-extremity dynamics in robot-assisted reaching movement, in *2012 4th IEEE RAS & EMBS International Conference on Biomedical Robotics and Biomechatronics (BioRob)* (IEEE, 2012), pp. 1316–1322

4. N. Harper et al., Muscle function and coordination of stair ascent. J. Biomech. Eng. **140**(1) (2017)
5. Ármannsdóttir Anna et al., Assessing the involvement of users during development of lower limb wearable robotic exoskeletons: a survey study. Human Fact. **62**(3), 351–364 (2020)
6. P. Plummer-D'Amato et al., Interactions between cognitive tasks and gait after stroke: a dual task study. Gait Post. **27**(4), 683–688 (2008)
7. H. van Reenen Heleen et al., Does musculoskeletal discomfort at work predict future musculoskeletal pain? Ergonomics **51**(5), 637–648 (20080

Towards a Unified Terminology for Benchmarking Bipedal Systems

Anthony Remazeilles, Alfonso Dominguez, Pierre Barralon, and Diego Torricelli

Abstract In the European project EUROBENCH, we are developing a framework for benchmarking the performances of bipedal systems: from humans to humanoids through wearable robots. Fair benchmarking requires defining and sharing clear and complete protocols so that bipedal systems can be studied and compared within similar and reproducible conditions. Even if the experimental methods and system comparisons are common scientific tasks, the description of the experimental protocols that are followed are rarely complete enough to allow it to be replicated. We list, in this article, the information required to properly define a protocol (e.g. experiment objectives, testbeds, type of collected and processed data, performance indicators used to score and compare experiments). Agreeing on a common terminology for benchmarking concepts will ease the evaluation of new technologies and promote communication between the different stakeholders involved in the development and use of bipedal systems.

1 Introduction

It is widely recognized that the validation of any technological development requires demonstrating experimentally its technical soundness. Furthermore, proper exploitation of scientific results requires replicating someone else experiment, to compare

A. Remazeilles · A. Dominguez · P. Barralon
TECNALIA, Basque Research and Technology Alliance (BRTA), Paseo Mikeletegi 1, 20009 San Sebastian, Spain
e-mail: anthony.remazeilles@tecnalia.com

A. Dominguez
e-mail: alfonso.dominguez@tecnalia.com

P. Barralon
e-mail: pierre.barralon@tecnalia.com

D. Torricelli (✉)
Neural Rehabilitation Group, Spanish National Research Council (CSIC), Cajal Institute, Madrid, Spain
e-mail: diego.torricelli@csic.es

J. C. Moreno et al. (eds.), *Wearable Robotics: Challenges and Trends*,
Biosystems & Biorobotics 27, https://doi.org/10.1007/978-3-030-69547-7_98

its outcomes with new results (e.g. using a different robotic system or control law), using well-chosen performance criteria [3]. In the emerging field of wearable robots and bipedal systems in general, there is still a lack of common methodologies and benchmarking frameworks to effectively compare system performance [4]. Competition events like Cybathlon allow the comparison of bipedal systems, but they only focus on simple metrics like completion time [5], and cannot characterize and compare more precisely the performance of the systems under consideration.

In the European project EUROBENCH we are creating a framework suitable for benchmarking bipedal locomotion systems, including humans and wearable robots, as well as humanoid robots [1]. We are designing a set of protocols and testbeds that will be available in two physical facilities. Protocols are described in sufficient detail to permit any experimenter to reproduce them in his/her own facilities. Fair comparisons are obtained with an automatic scoring mechanism that uses benchmarking algorithms associated to the protocol followed to extract performance scores from the data collected.

Designing a systematic benchmarking system requires a clear and complete definition of the protocols to guarantee that experimenters, later, will conduct their experiments as expected. This is a challenging process, as practices and concerns may vary significantly from one community to another. We are thus sharing in this article the set of information we consider necessary to have a clear and replicable protocol, together with its associated terminology.

2 Terminology

We arbitrarily segment the key concepts as follows: (i) the protocol description, from which an experimenter shall learn all objectives, means and requirements, (ii) the experimentation in which data is collected, and (iii) the scoring, in which the collected data are assessed according to the metrics associated to the protocol.

2.1 Benchmarking Protocol

Per se, a protocol description should provide clear prescriptions on all the concepts introduced in the three categories. By reading it, an experimenter should be able to verify if it fits his needs (objectives and associated metrics), and if he has access to the appropriate material to conduct it (tesbded). We highlight some key features to be provided.

Scenario: Description of the functional task(s) to be performed in a given environment (e.g. “walking on a moving surface”). A scenario can act as a namespace gathering protocols dealing with similar functional task(s), for example.

Objective: Textual description of the features to be characterized through this protocol.

Target subjects: Definition of the subjects that can take part in the experimentation (humanoid, human with prosthesis, …), possibly with inclusion and exclusion criteria (e.g. healthy humans, or those with a given pathology).
Testbed: A description of the equipment required to perform the experiments, which includes the physical objects involved in the tests (e.g. stairs, slopes), with a definition of their location in the scene [6], as well as the hardware required for sensing (e.g. motion capture, force platform) and acting (e.g. treadmill, "pusher"). The software used to control these items and to collect data is part of the testbed. The protocol may accept slightly different types of equipment, as long as the data required to score the experiment is collected.
Performance indicator (PI): A numerical quantity describing the performance of the system under investigation, according to the protocol objectives. A PI can be (i) a measured physical quantity or derived from several such quantities, (ii) dimensional or dimensionless, (iii) a unique value or a time-series. Several PIs may be needed to fully describe a system's level of ability.
Protocol procedure: As in a cooking recipe, the protocol steps should describe all the successive operations an experimenter must follow, from the setup configuration, subject preparation and guidance, to the experiment execution, data collection and preparation for scoring.

2.2 Experimentation-Related Concepts

Following the protocol definition and procedure, the experimenter is ready to conduct an experiment.

According to the procedure, the experiment may include N repetitions, or **runs**. A run is a single execution of the action, but the subject may be requested to repeat exactly the same actions for statistical purposes. The protocol can also suggest evaluating different **variants of the conditions**. If so, the total number of runs is $C \times N$. The experiment can also involve several human subjects. Data collected should be labelled so that anybody can *a posteriori* deduce the participant's ID number, the experiment conditions or variant, and the run number of each datafile.

In an experiment report, the experimenter must provide information on the following items:
Experiment subject: Specification of the subject(s) involved in the experiment. In our context, the bipedal system may be only a human, only a robot (i.e. a humanoid), or a combination of both (human wearing an exoskeleton or a prosthesis). The protocol may require storing specific parameters, such as anthropometric (or robot-metric) measures. The experimenter may also collect additional descriptive information (like clinical/demographic parameters, design or robot control strategies), to enrich the subject description and enable further meta-analysis. All this data collection should comply with privacy and regulatory concerns.
Experimental data: Set of measures needed to compute the PIs. We differentiate the *raw* data and the *pre-processed* data. Raw data is that which is directly collected

by the software of the testbed, in a format that may be specific to the brand of the equipment used. The Pre-processed data is derived from the raw data to describe a relevant physical quantity (e.g. joint angle), irrespective of the sensor(s) used.
Controlled variables: Conditions and parameters that must be logged by the experimenter, as they may not be measured by the instrumented tesbed but are nevertheless needed to fully describe the experimental settings. These variables shall not change during a run execution, and shall remain constant during the N repetitions. They can be related to either: (i) a configuration of the testbed (e.g. slope angle and length for a walking on slope protocol), (ii) a configuration of the robotic system (such as different assistance levels of an exoskeleton, or different tuning parameter sets of an humanoid), or (iii) behavioural instructions provided to the subject (such as "do the action with eyes closed"). Each of the C experimental conditions should be described by well controlled variables.

After experiment completion, a set of files is gathered: (i) the bipedal system involved, (ii) values of the controlled variables per condition, (iii) a set of captured data files, organized per content type, run, condition and subject numbers.

2.3 Computation of Metrics

The benchmarking process consists, then, of computing the PIs (see Sect. 2.1) from the collected data. To be as objective as possible, and following a separation of concerns, the metric computation should not be linked to the experiment itself; it should accept data from any experiments that have followed the same protocol and collected the appropriate data.
Benchmarking algorithm: algorithm able to compute one or more performance indicators from experimental data.
Benchmarking metric routine: Code implementing one or more benchmarking algorithms. This code receives as input the data (preferably pre-processed, for the sake of generality and reusability), the bipedal system specs and the condition settings. It returns as output the PI(s) value(s). Publicly available code is preferred and encouraged to permit code evaluation, contrast and maintenance.
Performance Indicator scope: Ideally, a PI should be computed given the data of a single run. In general, the computation of a score is an iterative evaluation of each data run, followed by an aggregation process.
Performance Indicator aggregation: the PI should provide the means for aggregating scores obtained per run, to combine all PI runs of a same condition setting, to combine PI of each condition, and possibly to combine the PIs obtained by each human subject. A clear separation of the computation for a single run and for the successive aggregations results in code that is much easier to maintain.

3 Conclusion

We have described in this document a set of concepts and information required to define a reproducible protocol for benchmarking robotic systems. It is currently being used and implemented for all the benchmarking protocols developed within Eurobench, and will permit the automatic evaluation and comparison of any experiment following these protocols. We develop the Eurobench framework in collaboration with numerous institutions, and the framework concepts and terminologies are being discussed through publicly visible documentation [2]. Even though this framework is developed specifically for benchmarking bipedal systems, it could be easily extended to other robotic systems and applications.

Acknowledgements Supported by the H2020 EUROBENCH project, grant No. 779963.

References

1. Eurobench. http://eurobench2020.eu/ (2020)
2. Eurobench software documentation. https://github.com/aremazeilles/eurobench_documentation (2020)
3. F. Bonsignorio, A. del Pobil, Toward replicable and measurable robotics research (from the guest editors). IEEE Robot. Autom. Mag. **22**(3), 32–35 (2015)
4. D. Pinto-Fernandez, D. Torricelli, M.D.C. Sanchez-Villamanan, F. Aller, K. Mombaur, R. Conti, N. Vitiello, J.C. Moreno, J.L. Pons, Performance evaluation of lower limb exoskeletons: a systematic review. IEEE Trans. Neural Syst. Rehabil. Eng. **28**(7), 1573–1583 (2020)
5. R. Riener, The cybathlon promotes the development of assistive technology for people with physical disabilities. J. NeuroEng. Rehabil. 49 (2016)
6. C. Shirota, E. van Asseldonk, Z. Matjacic, H. Vallery, P. Barralon, S. Maggioni, J.H. Buurke, J.F. Veneman, Robot-supported assessment of balance in standing and walking. J. Neuroeng. Rehabil. **14**, 80 (2017)

A Methodology for Benchmarking Force Control Algorithms

R. Vicario, A. Calanca, N. Murr, M. Meneghetti, E. Sartori, G. Zanni, and P. Fiorini

Abstract Force control is nowadays a mature technology, widespread in modern robotics systems and commercialized within several application domains. However, assessing the performance of a force-controlled system is not a trivial task because it may be strongly influenced by the environment dynamics. Exerting a force on a soft environment is different from exerting a force on a rigid environment. Indeed, the same force-controlled robot can have different force responses in different environments and a standardized and comprehensive method to assess the performance of a force-controlled system is not available yet. This paper, as part of the Forecast project, aims at filling this gap by proposing a benchmarking method able to define a comprehensive score for a given force-controlled system accounting for its sensitivity to environment uncertainties and variations. This paper describes such benchmarking methodology which allows to compare force control algorithms on a common ground and to determine the preferable control solutions in a specific application domain.

1 Introduction

ONE of the main problems in force control is that performance doesn't only depends on the dynamics of the robot, but also on the dynamics of the environment, which is usually uncertain and possibly time-varying. This can lead to unpredictable force control performance [2]. Many solutions based on advanced control techniques have been proposed in recent years to overcome such performance issues (e.g. *based on disturbance observers, robust control, adaptive control, acceleration feedback*). A force controller that works perfectly for any model and environment does currently not exist. Given these premises, in this abstract we propose a methodology to standardize the benchmarking of force control algorithms applied to different actuation architectures and considering a wide set of possible environments and disturbances, defined by the application of interest.

R. Vicario (✉) · A. Calanca · N. Murr · M. Meneghetti · E. Sartori · G. Zanni · P. Fiorini
Altair Robotics Laboratory, University of Verona, Verona, Italy
e-mail: rudy.vicario@univr.it
URL: http://www.metropolis.scienze.univr.it

J. C. Moreno et al. (eds.), *Wearable Robotics: Challenges and Trends*,
Biosystems & Biorobotics 27, https://doi.org/10.1007/978-3-030-69547-7_99

2 Forecast Project

Experimentally testing control algorithms on different systems and environments may be extremely time consuming and pratically unfeasible. For this reason, we propose an implementation of a simulation framework to comprehensively quantify the performance of force control algorithms in different working conditions. A specific effort is devoted to maximize the informativity of simulations and to provide exhaustive performance metrics, still giving easy-to-read data to the user. In our concept, the system designer only needs to provide data about their own system, the possible environment of interest and some candidate force control implementation to test. Eventually, he/she can choose among a library of force control implementations provided within the benchmarking software. The output of the benchmarking system will be a few plots and values that comprehensively measure the algorithm behaviour in different environments. The evaluation metric calculates the discrepancy between the actual and the desired behaviour within all the interesting working conditions and when the system is subject to disturbances in a well-defined frequency range.

2.1 Simulation Software

The simulation software considers relevant details of force control imprementation (e.g. real-time periodic execution), different electromagnetic motor choices (e.g. voltage or current controlled motors) and specific actuator parameters (motor inertia, friction, saturations, series stiffness). According to most common environment modelling, the benchmarking system takes into account environment stiffness, damping and inertia.

The simulation architecture is object-oriented, written in Matlab and uses the Simulink simulation engine [3]. To run the proper set of simulations, the user must choose:

- The actuator model (from a library of already implemented models);
- A force controller (it's possible to implement a new controller or choose it from a library of already implemented controllers);
- A range of environment parameters.

2.2 Evaluation Software

The proposed benchmarking system records the system behavior in response to a well defined force reference in different environments and computes the performance indicators listed in the Table 1. Mean quantities in Table 1 describe the average value across different environments and standard deviation describes the sensitivity

Table 1 Forecast performance indicators

Name	Symbol
Mean static error	$E[\overline{e}_\infty]$
Static error standard deviation	$\sqrt{Var[\overline{e}_\infty]}$
Mean dynamic error	$E[\overline{e}]$
Dynamic error standard deviation	$\sqrt{Var[\overline{e}]}$
Worst case environments	WCE
Best case environments	BCE
Mean overshoot level	$E[S\%]$
Overshoot level standard deviation	$\sqrt{Var[S\%]}$
Maximum overshoot level	$MAX[S\%]$
Mean bandwidth	$E[\omega_B]$
Bandwidth standard deviation	$\sqrt{Var[\omega_B]}$
Minimum guaranteed bandwidth	$MIN[\omega_B]$
Linearity	LIN

to environments uncertainties. A detailed explanation of the performance indicators can be found in [1].

Two concise representations of the benchmarking output are provided:

- A graphical overview of single-experiment indicators evaluated for any interesting working condition and disturbance, as exemplified in Fig. 1;
- A quantitive summary information regarding the whole interesting working conditions considering the performance indicators of Table 1.

3 Hardware Testbench

In addition to the simulation software, we also designed a hardware testbench, as shown in Fig. 3. It is composed by:

- A motor module with a motor and an encoder;
- A spring module, to implement a serial elastic actuator;
- An environment module with a torque sensor, that can be:
  - a rod with a fixed spring and an encoder;
  - a motor with an encoder controlled by the software to emulate a wide range of different environments.

The testbench is controlled by the Forecast Control Framework [4] which handles the hardware management allowing the user to write a control algorithm and run it on the hardware testbench. The framework provides functions that aim to run the control loop at a user-defined frequency, and for every iteration of the loop, it automatically:

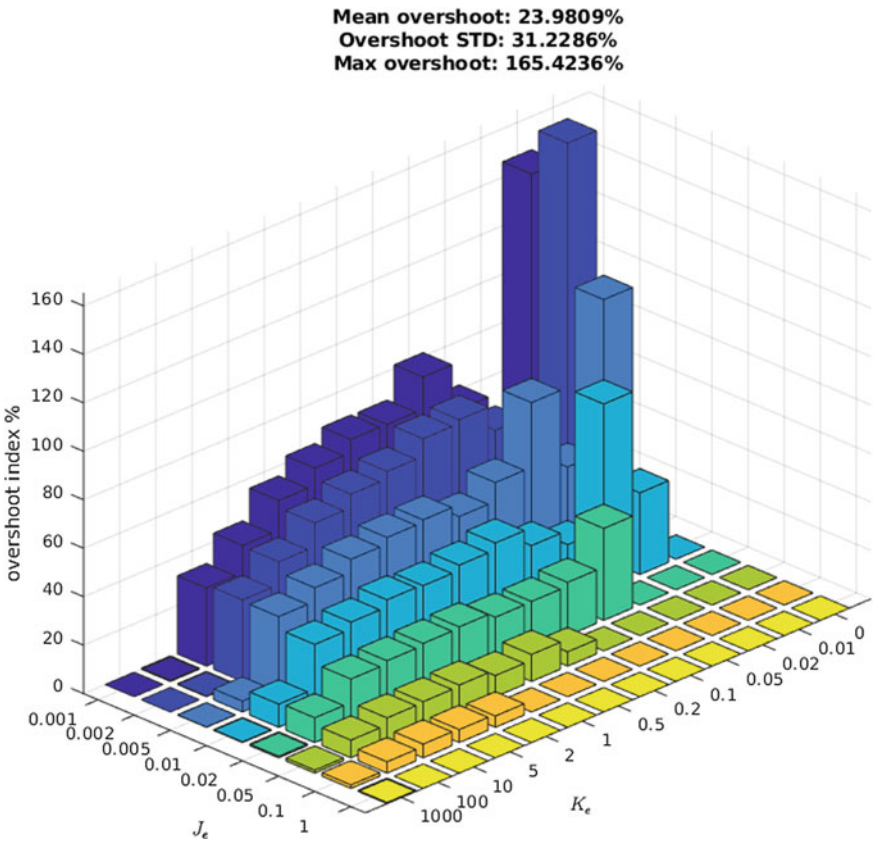

Fig. 1 In this plot each bar is related to a single experiment, which account for a single environment. Horizontal axes represent experiments with different environment stiffness and inertia, while the vertical axis is the overshoot index, in percentage. This is only an illustrative figure

(1) Reads the sensors;
(2) Executes the control algorithm;
(3) Logs selected variables via Serial/USB.

The user just needs to implement a control algorithm and to set some parameters, i.e. the environment damping and stiffness. A simplified class diagram of the framework is shown in Fig. 2. In order to make the testbench simple to use, we have implemented a user interface [5, 6], characterized by high usability and customability, to collect the data from experiments.

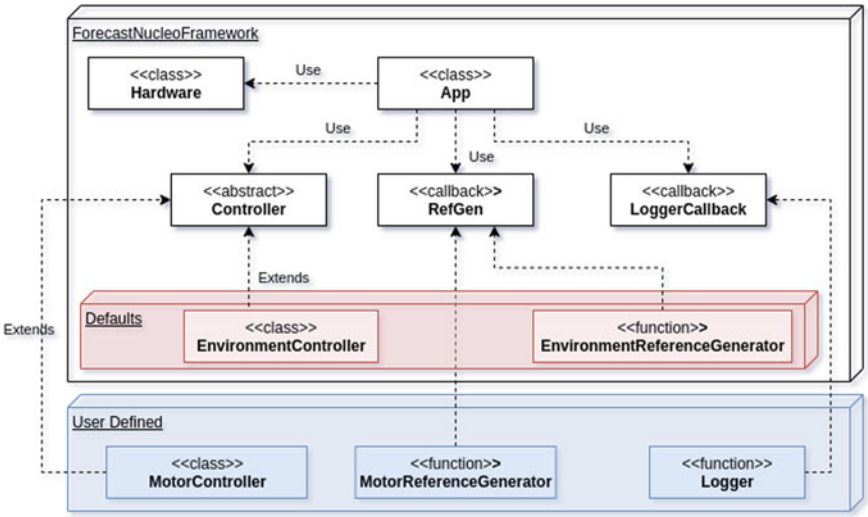

Fig. 2 Class diagram of the forecast nucleo framework. Blue blocks must be implemented by the user, while Red blocks are already implemented with settable parameters

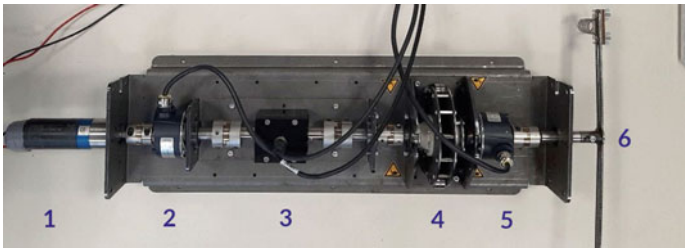

Fig. 3 A preliminary not yet modular version of the physical testbench **a** is the motor, **b** the motor encoder, **c** the torque sensor, **d** the spring in series, **e** the environment encoder, **f** the environment (fixed spring)

4 Conclusion

We proposed a benchmarking system which evaluates the behaviour of a force-controlled system in different environments. The proposed system is simulation-based and includes a modular testbed for experimental validation.

Acknowledgements The research has received funding from the European Union's Horizon 2020 programme under grant agreement EUROBENCH n. 779963.

References

1. R. Vicario, A methodology for benchmarking force control algorithms (2020). https://doi.org/10.13140/RG.2.2.18759.11680
2. R. Muradore, A. Calanca, P. Fiorini, A review of algorithms for compliant control of stiff and fixed compliance robots. IEEE Trans. Mechatron. **21**, 613–624 (2016)
3. Repository of SESim, http://www.gitlab.com/altairLab/elasticteam/SESim
4. Repository of Forecast Control Framework, http://www.gitlab.com/altairLab/elasticteam/forecastnucleoframework
5. Forecast UI showcase video, http://www.youtube.com/watch?v=40l8gGEEiSE
6. Repository of Forecast UI, http://www.gitlab.com/altairLab/elasticteam/forecast/forecast-atlas

Limitation of Ankle Mobility Challenges Gait Stability While Walking on Lateral Inclines

Maarten R. Prins, Nick Kluft, Wieke Philippart, Han Houdijk, Jaap H. van Dieën, and Sjoerd M. Bruijn

Abstract Exoskeletons often allow limited movement of the ankle joint. This could increase the chance of falling while walking, particularly on challenging surfaces, such as lateral inclines. In this study, the effect of a mobility limiting ankle brace on gait stability in the frontal plane was assessed, while participants walked on lateral inclines. The brace negatively affected gait stability when it was worn on the leg that was on the vertically lower side or 'valley side' of the lateral incline, which would indicate an increased risk of falling in that direction.

1 Introduction

STABILITY of gait is challenged by slopes, such as laterally inclined surfaces. Computer controlled walking devices, such as humanoid robots and exoskeletons, should be able to adapt to changes in surface angle to reduce the risk of falling. Many of such devices have limited joint mobility in the lower extremities compared to healthy humans. This could hamper the ability to adapt to slopes while walking. In

This project was sponsored by a grant from the EUropean ROBotic framework for bipedal locomotion bENCHmarking (EUROBENCH), EU Grant 779963.

N. Kluft · W. Philippart · J. H. van Dieën · S. M. Bruijn (✉)
VU University, Amsterdam, The Netherlands
e-mail: s.m.bruijn@vu.nl

N. Kluft
e-mail: n.kluft@tudelft.nl

M. R. Prins
Military Rehabilitation Center Aardenburg, Doorn, The Netherlands
e-mail: mr.prins@mrcdoorn.nl

N. Kluft
Delft University of Technology, Delft, The Netherlands

H. Houdijk
University Medical Center Groningen, Groningen, The Netherlands
e-mail: h.houdijk@umcg.nl

J. C. Moreno et al. (eds.), *Wearable Robotics: Challenges and Trends*,
Biosystems & Biorobotics 27, https://doi.org/10.1007/978-3-030-69547-7_100

this study, we evaluated the effect of a mobility limiting ankle brace on gait stability while walking on laterally inclined surfaces.

2 Methods

2.1 Participants, Equipment and Protocol

Twenty healthy participants (9 female, age 40 (SD 12) years, height 1.78 (SD 0.09) (m), weight 74 (SD 13) (kg)) were recruited for this study. Subjects walked on an instrumented treadmill that is part of a Computer Assisted Rehabilitation ENvironment (CAREN) (as shown in Fig. 1). Retroreflective markers were placed on the subjects to determine the movements of the center of mass and both feet. During the experiment, the speed of the treadmill was fixed at 0.6 (m/s). At the beginning of each trial, the treadmill was oriented horizontally. After a minimal number of 48 strides was recorded, the slope of the treadmill changed to a lateral incline of -3 degrees (i.e. right side up), followed by +3, −6, +6, etc. until a lateral incline of +15 degrees was reached. All subjects completed this experiment without joint mobility limitation. Five subjects performed the same experiment again with a custom made carbon ankle brace on the right ankle that blocked virtually any ankle movements.

2.2 Outcome Metrics

We assessed overall gait changes from wearing the ankle brace using stride time and stride width. Gait stability was expressed in terms of lateral margin of stability [1] (Fig. 2). The margin of stability expresses how close the body, modelled as an inverted pendulum, gets to toppling over the stance leg by taking the position and

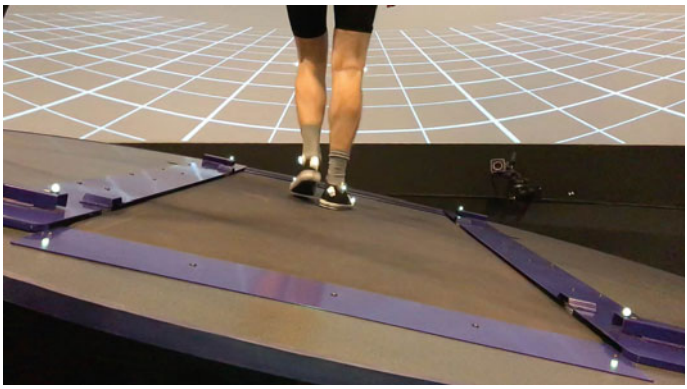

Fig. 1 The CAREN-system. The lateral incline of the treadmill was changed between + and − 15° by a motion base underneath the round platform

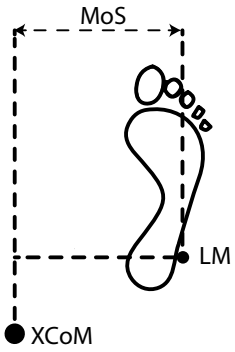

Fig. 2 Visual representation of the lateral margin of stability (MoS). At the start of the swing phase of the contralateral leg, the lateral margin of stability was defined as the mediolateral distance between the extrapolated center of mass (XCoM) and the lateral malleolus (LM) of the stance leg. The XCoM would predict the maximum excursion of the CoM given its current velocity and position. The XCoM would need to remain medial to the LM to prevent the body from toppling over the stance leg

velocity of the center of mass into account. To get further insight into why subjects might have had a reduced lateral margin of stability, we also compared the velocity of the centre of mass, as well as the distance between the center of mass and the base of support.

3 Results

When subjects wore an ankle brace, they walked with shorter and wider strides for all lateral inclines. With the right ankle braced, the lateral margin of stability towards the left side was unaffected. However, margin of stability towards the braced side increased for negative inclines (i.e. braced leg towards the vertically higher side or 'hill side') when compared to normal walking (Fig. 3). When the leg with the ankle brace was on the vertically lower side or 'valley side' (i.e. for positive angles), there was a smaller margin of stability on that side. Analysis of the underlying variables with the braced leg on the 'valley side' showed an increased maximum velocity of the center of mass towards the valley and a smaller distance of the center of mass relative to the base of support at toe off compared to the the ipsilateral leg during the unbraced condition and compared to the contralateral leg during the same trial.

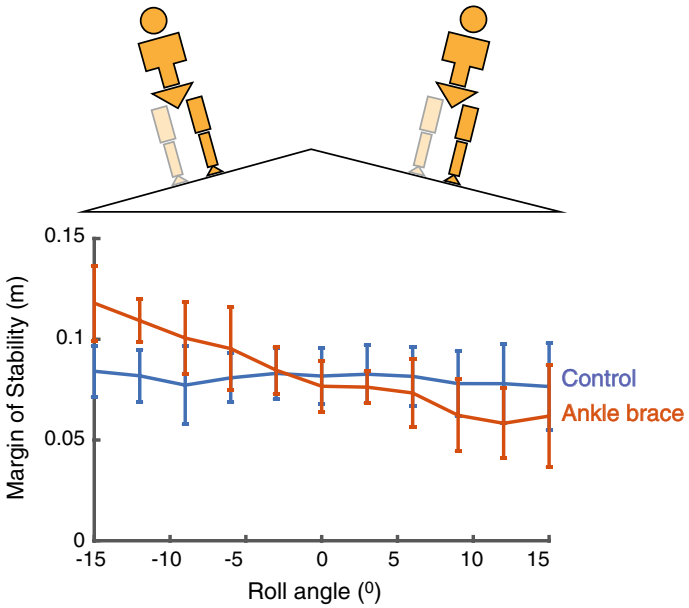

Fig. 3 Margin of stability for the right leg without (blue) and with (red) ankle brace. Negative roll angle indicate slopes to the left (i.e. where the leg represented here is on the 'hill side'), whereas positive roll angles indicate slopes to the right (i.e. where the leg represented here is on the 'valley side')

4 Discussion and Conclusion

Our results suggest that constraining the ankle leads to changes in spatiotemporal gait parameters that are thought to have a stabilizing effect, such as shorter and wider strides [2–4]. When walking on a lateral incline with the braced ankle on the 'hill side', the lateral margin of stability was indeed better for that leg. However, with the brace on the 'valley side', the lateral margin of stability was reduced. A possible explanation for this finding is that the orientation of the foot does not fully adapt to the walking surface while wearing a brace. The stiffness of the ankle brace foot plate was relatively high, and subjects most likely placed their foot horizontally on the inclined treadmill as a result of this stiffness. This means that the effective base of support of the 'valley leg' would be the medial side of the foot (Fig. 4). Hence, the center of pressure off the 'valley leg' would be relatively close to the center of mass, reducing the braking effect on the center of mass in the medial direction, which could explain the relatively high velocity of the center of mass in the direction of the braced 'valley-side' leg. Note that the margin of stability in this study was calculated with the lateral malleolus as base of support and that the reduction in lateral margin of stability with the ankle brace at the 'valley side' would probably be even larger when the effective base of support (the area where the CoP can be located) would be used.

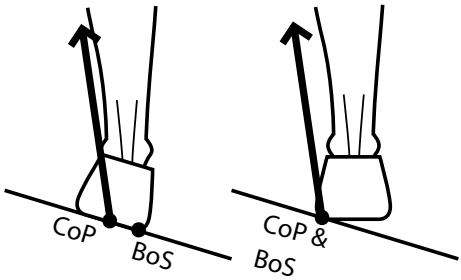

Fig. 4 Left: with unrestrained ankle mobility, the orientation of the foot can be adjusted to the incline of the walking surface. In that case, the center of pressure (CoP) can fluctuate between the medial side of the foot and the lateral side of the foot, or base of support (BoS). Right: with the ankle fixated in a neutral position, the orientation of the foot will not fully adapt to the orientation of the walking surface. As a result, the effective BoS size will be reduced with an upper boundary closer to the medial side of the foot, limiting the area where the CoP can be located

References

1. A.L. Hof, The 'extrapolated center of mass' concept suggests a simple control of balance in walking. Human Movement Sci. **27**(1), 112–125 (2008)
2. L. Hak, H. Houdijk, F. Steenbrink, A. Mert, P. van der Wurff, P.J. Beek, J.H. van Dieën, Speeding up or slowing down? Gait adaptations to preserve gait stability in response to balance perturbations. Gait Post. **36**(2), 260–4 (2012)
3. L. Hak, H. Houdijk, P.J. Beek, J.H. van Dieën, Steps to take to enhance gait stability: the effect of stride frequency, stride length, and walking speed on local dynamic stability and margins of stability. PLoS One **8**(12), e82842 (2013)
4. L. Hak, H. Houdijk, F. Steenbrink, A. Mert, P. van der Wurff, P.J. Beek, J.H. van Dieën, Stepping strategies for regulating gait adaptability and stability. J. Biomech. **46**(5), 905–11 (2013)

A Workaround for Recruitment Issues in Preliminary WR Studies: Audio Feedback and Instrumented Crutches to Train Test Subjects

Matteo Lancini, Simone Pasinetti, Marco Ghidelli, Pietro Padovani, David Pinto-Fernández, Antonio J. del-Ama, and Diego Torricelli

Abstract One of the main problems in studies involving exoskeletons for assisting gait of Spinal Cord Injury (SCI) users is recruitment of a suitable number of subjects, especially when age, gender, and pathologies are considered. Studies involving able-bodied subjects could instead rely on a considerable number of subjects, but the reliability of the results when transferred to real exoskeleton users is limited. This limitation could be partially solved using able-bodied subjects for preliminary tests. In this paper, we describe a first approach to train able-bodied subjects to behave as SCI subjects during walking. An audio feedback driven by a pair of instrumented crutches has been used to train healthy subjects during exoskeleton walking. To test the system, 22 able-bodied subjects have been analyzed during a straight walk with and without the audio feedback. Results show that the audio feedback induces a learning effect and a persistency effect in the participants.

1 Introduction

Lower limb powered exoskeletons used for gait therapy, demonstrated functional improvements and potential to improve the daily life of people with SCI [1]. In the

M. Lancini (✉) · S. Pasinetti · P. Padovani
Department of Mechanical and Industrial Engineering, University of Brescia, Brescia, Italy
e-mail: matteo.lancini@unibs.it

M. Ghidelli
Department of Information Engineering, University of Brescia, Brescia, Italy

D. Pinto-Fernández
Universidad Politécnica de Madrid, Madrid, Spain

Diego Torricelli
Spanish Research Council (CSIC), Madrid, Spain

A. J. del-Ama
National Hospital for Paraplegics, Toledo, Spain

Rey Juan Carlos University, Madrid, Spain

J. C. Moreno et al. (eds.), *Wearable Robotics: Challenges and Trends*,
Biosystems & Biorobotics 27, https://doi.org/10.1007/978-3-030-69547-7_101

available scientific literature, the tests in these topics are often limited to a small number of participants [2, 3], due to the difficulties in recruiting subjects.

When conducting a study with a large population, subjects with SCI will have different lesions, gender and age, making it difficult to obtain a uniform population, as specified in [4]. To limit this variability and solve logistics issues, some tests are conducted with only one patient as seen in [5] and [6].

These limitations could be solved using able-bodied subjects trained to behave as SCI subjects for a certain physical task, which we propose to call "pseudo-SCI-subjects". This would allow several rounds of tests in the early stages of a new device design, when the aim is safety assessment, before involving frail, SCI subjects in more advanced tests.

In this paper, we propose a method to train healthy subject to mimic the gait pattern and the physical compensation of a SCI subject during exoskeleton-assisted walking. Impaired subjects require a minimum load, functional to balance, to be transferred to the crutches, while they are trained to avoid overloading them, to protect the shoulders from chronic pain. The main objective of this paper is to verify the feasibility of the proposed method to replicate this behavior.

2 Materials and Methods

2.1 Experimental Setup

The instrumentation used in the experiments is composed of an exoskeleton (H2, Technaid, Spain) [7], a pair of instrumented crutches [8], and a pair of commercial in-ears Bluetooth earphones (Taotronics TTBH026).

The instrumented crutches allow monitoring the axial forces and the antero-posterior and medio-lateral orientations in real time. As shown in Fig. 1, each crutch transmits force readings to a readout unit. This readout unit controls the audio feedback using a Bluetooth earphone worn by the user. The exoskeleton was in passive

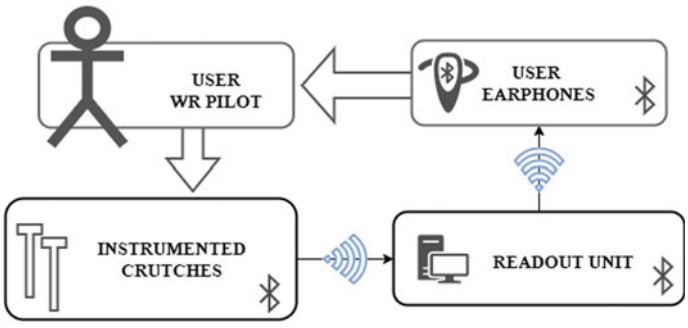

Fig. 1. Overview of the feedback system used

mode to constrain the motion of the user, without adding to the tests the variability due to the control strategy of the exoskeleton.

To avoid confusing the user, the audio feedback is driven only by the load measured on the dominant-side crutch, which is compared with two force thresholds: while the force is higher than the lower limit, a low-pitch sound is reproduced, if the upper limit is crossed a high-pitch sound is used. Kinematic data was also recorded using a marker-based mocap (Vicon Nexus 2.9.0 by Vicon Motion Systems, UK) and a subset of the plug-in gait protocol.

2.2 Experimental Protocol

After wearing the exoskeleton, users were asked to walk at a self-selected speed for 5-min. The lower threshold was set to the 60^{th} percentile of force peaks recorded in this phase, or 24% of the body weight, whichever lower, while the upper threshold was set to 35% of the body weight, following [6]. Then subjects performed a 10 m Walking Test (10MWT) without audio feedback (baseline test). Subjects were split randomly into two groups: the FN group (feedback/no feedback) performed 10 repetitions of the 10MWT, at first with, then without the audio feedback; the NF group (no feedback/feedback) performed the same test, at first without, then with the audio feedback. Before the tests with feedback, a familiarization phase of 5-min walking was carried out.

2.3 Data Analysis

Heel contact events and the toe off events were identified using the difference between the coordinate y of the markers TOE and HEEL: the peaks have been considered as heel contact events, while the minimums as toe off events.

Cadence was normalized by dividing by the baseline test cadence, while force was normalized on the body weight.

3 Results

22 able-bodied subjects were recruited for the study (10 women and 12 men, 21 to 41 years old). Figure 2 shows the boxplots of the normalized cadence of both groups. The NF group undergoes a decrease in the median cadence up to 29% of the baseline from the tests without the audio feedback to the tests with the feedback. In the FN group, the decrease in cadence persists even after removing the audio feedback. The NF group, instead, shows a cadence in the trials without the audio feedback close to 1 (the value of the baseline test).

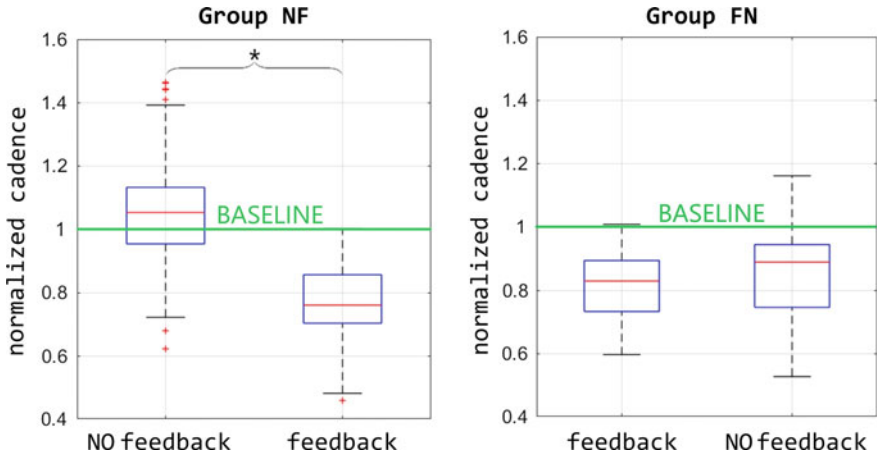

Fig. 2. Boxplots of the normalized cadence for the NF group (left image) and for the FN group (right image). The value 1 correspond to the baseline's cadence. * indicates a statistically significant difference

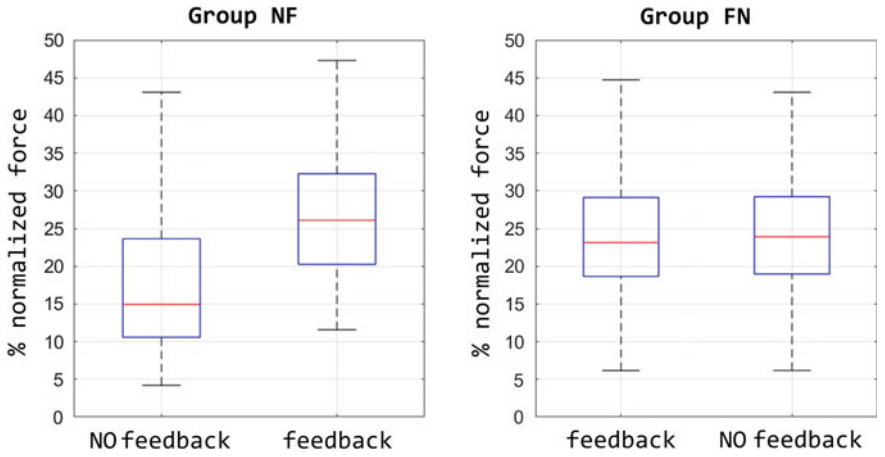

Fig. 3. Boxplots of the peaks of the crutch force of the dominant limb normalized on the weight of the subject and the exoskeleton for the NF group (left image) and for the FN group (right image)

Figure 3 shows the boxplot of the load applied on the dominant-side crutch for the NF and the FN group. The load applied increases by about 11% in the NF group and the load is kept at around 24% in both types of trial in the FN group.

4 Discussion

The audio feedback showed an influence on cadence. The analysis of the NF group indicates that the audio feedback produces stronger variation in gait parameters that simple instructions given to the user, since tests with no feedback are closer to the baseline of self-selected speed. The analysis of the FN group suggests that there is a learning effect that persists even after the feedback is removed, at least for the hour needed to repeat the tests. This demonstrate the feasibility of training the subjects for tests with exoskeletons prototypes, by having them perform a short training session with the instrumented crutches before the actual tests.

Similar conclusions are drawn by looking at the force: as for the cadence, the force induced by the feedback persists even without the audio feedback. This shows how the change induced involves both dynamic and kinematic gait parameters. Further experiments must be performed to analyze the effective performances of our method, focusing on *(i)* the recruitment of more able-bodied subjects and *(ii)* the comparison between kinematics of pseudo-SCI and SCI subjects.

Acknowledgements The authors would thank Marcello Domenighini for the preliminary tests and Technaid srl for the logistic support. This work was supported by COST Action CA16116, and by European project EUROBENCH (grant 779963).

References

1. H. Fritz, D. Patzer, S.S. Galen, Robotic exoskeletons for reengaging in everyday activities: promises, pitfalls, and opportunities. Disab. Rehab. **41**, 560–563 (2019)
2. D.R. Louie, J.J. Eng, T. Lam, Spinal Cord Injury Research Evidence (SCIRE) Research Team, Gait speed using powered robotic exoskeletons after spinal cord injury: a systematic review and correlational study. J. NeuroEng. Rehab. **12**(82), (2015)
3. M. Arazpour, M. Samadian, K. Ebrahimzadeh, M. Ahmadi Bani, S.W. Hutchins, The influence of orthosis options on walking parameters in spinal cord-injured patients a literature review. Spinal Cord **54**, 412–422, (2016)
4. L.E. Miller, A.K. Zimmermann, W.G. Herbert, Clinical effectiveness and safety of powered exoskeleton-assisted walking in patients with spinal cord injury: systematic review with meta-analysis. Med. Devices (Auckl) **9**, 455–466 (2016)
5. J.L.A. Contreras-Vidal, N. Bhagat, J. Brantley, J.G. Cruz-Garza, Y. He, Q. Manley, S. Nakagome, K. Natham, S.H. Tan, F. Zhu, L. Pons, Powered exoskeletons for bipedal locomotion after spinal cord injury. J. Neural Eng. **13**(031001), (2016)
6. M. Lancini, S. Pasinetti, V. Montini, G. Sansoni, Monitoring upper limbs during exoskeleton-assisted gait outdoors. Biosys. Biorob. **22**, 127–131 (2019)
7. M. Bortole, A. Venkatakrishnan, F. Zhu, J.C. Moreno, G.E. Francisco, J.L. Pons, J.L. Contreas-Vidal, The H2 robotic exoskeleton for gait rehabilitation after stroke: early findings from a clinical study. J. NeuroEng. Rehabil. **12**(54), (2015)
8. E. Sardini, M. Serpelloni, M. Lancini, S. Pasinetti, Wireless instrumented crutches for force and tilt monitoring in lower limb rehabilitation. Procedia Eng. **87**, 348–351 (2014)

3D Relative Motion Assessment in Lower-Limb Exoskeletons: A Case of Study with AGoRA Exoskeleton

Felipe Ballen-Moreno, Carlos A. Cifuentes, Thomas Provot, Maxime Bourgain, and Marcela Múnera

Abstract Different studies have been conducted to assess the performance of several features of exoskeletons. One of the most critical component is the physical interfaces which transfer the energy to the user. Nevertheless, they have been isolated within the assessment process. In this sense, this work presents a 3D relative motion methodology to evaluate a lower-limb exoskeleton's physical interfaces. One male subject wore the AGoRA exoskeleton to apply the proposed methodology using an optoelectronic system. Kinematic results showed the 3D human-robot interaction (HRI) of the user's thigh, identifying an undesired degree of freedom of 36.5° among the gait cycle. Hence, the implications of this analysis provide a comprehensive indicator of physical interface's performance.

1 Introduction

Physical interfaces are defined as attachments between the user and the exoskeleton securing the device to the main plane of operation, force transmission, and comfort [1]. They are designed using a variety of materials (e.g., 3D printed PLA or ABS, carbon fiber interfaces or velcro strips) which can be made as a customized or generic interface [1, 2]. As a result of their extensive designs, further analysis in this topic is required to understand user-device interaction [2].

F. Ballen-Moreno · C. A. Cifuentes (✉) · M. Múnera
Department of Biomedical Engineering, Colombian School of Engineering Julio Garavito, Bogotá, Colombia
e-mail: carlos.cifuentes@escuelaing.edu.co

T. Provot · M. Bourgain
EPF Graduate School of Engineering, Sceaux, France
e-mail: thomas.provot@epf.fr

Institut de Biomécanique Humaine Georges Charpak, Arts et Metiers Institute of Technology, Paris, France

J. C. Moreno et al. (eds.), *Wearable Robotics: Challenges and Trends*,
Biosystems & Biorobotics 27, https://doi.org/10.1007/978-3-030-69547-7_102

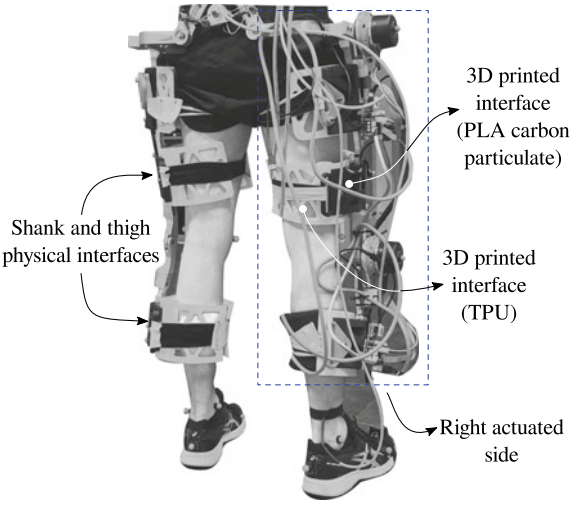

Fig. 1 AGoRa exoskeleton. Uni-lateral actuation is transferred to the user by three physical interfaces along the leg

Kinematic and kinetic analysis is used to assess the physical interface's performance. Internal forces and torque identify the sinks of energy among the physical interfaces [3]. Furthermore, ergonomic indicators can also relate to energy sinks through 2D approaches [4]. However in the literature, rotations and translations are not considered among other planes affecting exoskeleton's performance. Besides, ergonomic indicators found by Pinto et al. overlooked the stability and misalignment of the exoskeleton compared to the human joints [2]. To fully comprehend and assess the physical interface's performance through relative motion is essential to follow a three-dimensional approach [1, 2].

In this sense, this work presents a 3D relative motion methodology based on the difference of orientations between the user limb and the exoskeleton link. A case of study is presented wearing a uni-lateral set-up of the AGoRA exoskeleton [5], as shown in Fig. 1.

2 Methods

One healthy male subject participated in this study (26 years old, 65 kg, 1.77 m). The AGoRA exoskeleton used an impedance controller. The actuated side is assessed through a 6-m walk test, focusing on the thigh's physical interfaces. Kinematic data is acquired through 11 cameras (100 Hz, accuracy 0.1 mm, Vicon Motion System, Oxford, UK) using 28 reflective markers (14 mm diameter) on the subject, following the modified Helen Hayes for lower-limb [6]. Moreover, the exoskeleton was also fitted with 20 markers distributed per leg as: four markers in the lower thigh physical interface, one marker per motor joint (i.e., hip and knee exoskeleton joint) and four markers in the shank physical interface. The placement of the markers were the same

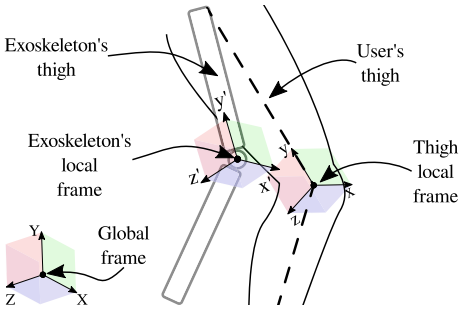

Fig. 2 2D-projection of the descriptive scheme of rotation matrices. The user's local frame is located in the center of the knee joint. The exoskeleton's local frame is placed in the corresponding hinge knee joint

for all the trial, as well as the exoskeleton was donned once. The 3D methodology used this markers set-up to quantify the interaction between the user and the device.

The proposed methodology was aimed at the interaction between the exoskeleton and the user's thighs. Through the markers location in the global reference frame, two local frames were created as showing in Fig. 2. These frames' origin was located in the middle of the knee joint and the exoskeleton link for the user's thigh and the exoskeleton's thigh, respectively. Two rotation matrices $R_{th/O}$ and $R_{exo/O}$ were defined to describe user's thigh and exoskeleton thigh. The difference of orientation of the exoskeleton compared to the user's thigh ($R_{exo/th}$) was then computed as Eq. 1. This outcome is used to estimate three bias angles referenced to: (1) the frontal plane around the mediolateral axis (Rot. X), (2) the transversal plane around the longitudinal axis (Rot. Y), and (3) the sagittal plane around the mediolateral axis (Rot. Z). All this procedure followed the International Society of Biomechanics recommendations.

$$R_{exo/th} = R_{exo/O} \wedge R_{O/th} \tag{1}$$

3 Results and Discussion

As mentioned above, the 3D relative motion methodology was executed to determine the physical interfaces' performance. The difference of orientations were analyzed regarding eighteen gait cycles, shown in Fig. 3. The highest difference of orientation was obtained on Rot. Y of 36.5° (−24° to 12.5°) among the swing phase. This outcome was unexpected, given that the hip and knee actuators should only influence the sagittal plane causing a loss of transmission to the knee joint. Therefore, the physical interfaces allowed an undesirable degree of freedom including additional forces and torques to the user and the device. The Rot. Z presented a scatter behavior characterized by differences of orientation lower than 10°. This behavior might be caused by a lack of adjustment to the user's thigh, in contrast to the Rot. X presented the smoothest behavior between the user and the exoskeleton.

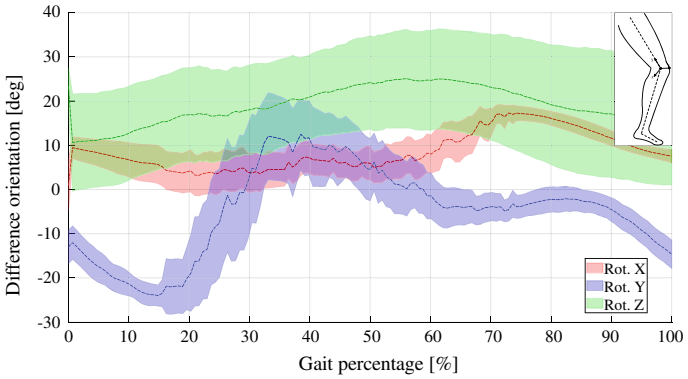

Fig. 3 3D relative motion analysis. The difference of orientation of the exoskeleton thigh link compared to the user's thigh. Each zone represents their behavior consider the standard deviation given by 18 gait cycles

Differences of orientations involve an in-depth insight into the physical HRI during the task, which the 3D methodology might show the stability of the interaction. Even though the variation of Rot. Z and Rot. X were similar; the distance between their mean curves at the same gait percentage directly affects the Rot. Y. In this sense, the Rot. Y is higher while the distance between the mean curves of Rot. Z and Rot. X increase along with the gait percentage.

The outcomes provide new information about human-robot interaction which could identify losses of transmission along three planes. For instance, higher differences of orientation could lead to translations which generate undesired torques for the user or within the physical interfaces. These losses can also be related to selected material for the physical interfaces bringing a comprehensive view of the physical interface's design improving the selection of materials and their response. It could also delimit the number of fixtures per segment needed to a specific task, allowing a minimum difference of orientation.

In comparison with the study of [4], they aimed to analyze the sagittal plane using a referenced distance between the user and the physical interface. They only considered one part of the interaction and discarded rotations within the points of reference. According to the literature evidence, 3D relative motion analysis did not have a comparable performance indicator.

4 Conclusion

This work presented a novel 3D relative motion methodology to assess lower-limb exoskeletons. It was used to perform a case of study using the AGoRA exoskeleton, where it was quantified the response of the physical interfaces regarding the gait cycle.

Besides, this methodology gave significant insights. Future works will be focused on increase the number of subjects enrolled in the study to analyze the impact of subjects' anthropometric variation within the methodology.

Acknowledgements This work was financially supported by the Minciencias grant (801-2017) and (845-2020), and internal fundings from the Colombian School of Engineering Julio Garavito, EPF Graduate School of Engineering, and Institut de Biomécanique Humaine Georges Charpak.

References

1. M.D.C. Sanchez-Villamañan, J. Gonzalez-Vargas, D. Torricelli, et al., Compliant lower limb exoskeletons: a comprehensive review on mechanical design principles. J. NeuroEng. Rehabil. (2019)
2. D. Pinto-Fernandez, D. Torricelli, M.D.C. Sanchez-Villamanan, et al., Performance evaluation of lower limb exoskeletons: a systematic review. IEEE Trans. Neural Syst. Rehabil. Eng. (2020)
3. J. Li, S. Zuo, C. Xu et al., Influence of a compatible design on physical human-robot interaction force: a case study of a self-adapting lower-limb exoskeleton mechanism. J. Intell. Robot. Syst. Theory Appl. **98**, 525–538 (2020)
4. K. Langlois, M. Moltedo, T. Bacek, et al., Design and development of customized physical interfaces to reduce relative motion between the user and a powered ankle foot exoskeleton, in *2018 7th IEEE International Conference on Biomedical Robotics and Biomechatronics (Biorob)* (IEEE, 2018), pp. 1083–1088
5. M. Sanchez-Manchola, D. Gomez-Vargas, D. Casas-Bocanegra, Development of a robotic lower-limb exoskeleton for gait rehabilitation: AGoRA exoskeleton, in *IEEE ANDESCON* (IEEE,2018), pp. 1–6
6. M.P. Kadaba, H.K. Ramakrishnan, M.E. Wootten, Measurement of lower extremity kinematics during level walking. J. Orthop. Res. 383–392 (1990)

Robotic Rehabilitation in Cerebral Palsy: A Case Report

Beatriz Moral, Óscar Rodríguez, Elena García, Eduardo Rocón, and Sergio Lerma

Abstract Cerebral palsy includes several posture and movement disorders which produce limitations in functional activities such as gait. In recent years robotics have been used as a complement of the treatment of neurological pathologies. The exoskeleton Ekso bionics enables professionals to perform treatments to improve gait in patients with cerebral palsy. After 24 sessions many spatiotemporal and kinematic parameters were improved in one patient with cerebral palsy.

1 Introduction

Cerebral palsy (CP) includes a number of posture and movement disorders which appear after an injury in an immature cerebellum during the fatal development or during the first year of life. It causes limitations in many daily life activities including gait [1]. Gait impairment is one of the most important difficulties that a child with CP can face. Thus, improving gait is one of the most important treatments within rehabilitation, as it contributes the patient's independence and an improvement in

B. Moral (✉) · Ó. Rodríguez · E. García
Instituto de Rehabilitación, Funcional La Salle, Madrid, Spain
e-mail: beatriz@irflasalle.es

Ó. Rodríguez
e-mail: oscarrl@irflasalle.es

E. García
e-mail: egarcia@irflasalle.es

Ó. Rodríguez
Universidad CEU San Pablo, Madrid, Spain

E. Rocón
Consejo Superior de Investigaciones Científicas, CSIC, Madrid, Spain
e-mail: e.rocon@csic.es

S. Lerma
Centro Superior de Estudios Universitarios La Salle, Madrid, Spain
e-mail: sergio.lerma@lasallecampus.es

J. C. Moreno et al. (eds.), *Wearable Robotics: Challenges and Trends*,
Biosystems & Biorobotics 27, https://doi.org/10.1007/978-3-030-69547-7_103

his quality of life [2]. The use of robotics as a complement in gait rehabilitation in adults and children with neurological pathologies has been implemented recently, showing good results in patients with spinal cord injury or brain damage such as strokes [3, 4].

2 Material and Methods

2.1 Subject

The subject of the present study is an 18 years old male diagnosed with spastic diplegia and a Gross Motor Functional Classification System III (GMFCS III).

2.2 Treatment

The gait rehabilitation was supported with Ekso GT, with the Software SmartAssist™, a robotic exoskeleton made by EksoBionics. The treatment consisted of two 60 min sessions each week. A total number of 24 sessions were conducted, using 10–15 min of each of them to calibrate the device and record all data. The sessions took place in Instituto de Rehabilitación Funcional La Salle (Madrid). In addition, the patient was doing one 60 min session of in-group therapeutic exercise designed by physiotherapists.

In the 16th session the centre where the sessions were carried out was closed for 3 months due to the sanitary crisis caused by COVID-19. During that time, the patient hardly did any exercise at home. When the restrictions ended the sessions were resumed, but without the in-group sessions, as the centre where they were carried out was still closed.

During the treatment, the exo-skeleton aids for the oscillation phase were decreased gradually session by session. Once the patient reached the minimal aid values, ankle weights were added (1 kg for 14th and 15th sessions and 2 kg for 21st, 22nd, 23rd and 24th sessions).

2.3 Assessment Method

The assessments were carried out pre and post treatment. A 3D gait analysis was recorded at 200 Hz using a motion capture system Smart-DX (BTS Bioengineering, Italy). In order to obtain gait kinetics, a set of reflective markers were placed over the skin on discrete anatomical sites according to the Helen Hayes Model. Also the values from the Ekso device were recorded each session.

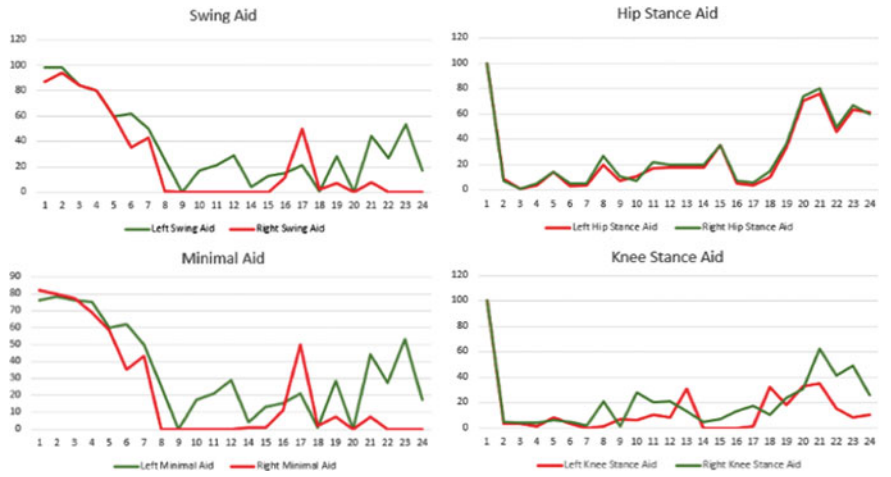

Fig. 1 Data collect by Ekso exoskeleton

3 Results

3.1 Regarding the Data Collected by Ekso

The swing aid is the grade of assistance the device offers during the swing phase expressed in percentage. It can be observed how this value decreases gradually during the sessions, reaching the value 0 for left lower limb in some sessions (Fig. 1). After the lockdown, (session 16) an increase in this value can be observed specially in right lower limb. This is probably due to the lack of exo-skeleton and in-group exercise done during this period. A tendency to decrease in the next sessions can be observed as exercise was resumed.

The stance aid is the grade of assistance the device offers to achieve a total active extension for knees and hips. This parameter was previously fixed by the therapists. In this case, it can be observed how before the lockdown this percentage was decreasing. In contrast to this, after the three months without any treatment, these values increase, especially for hip assistance (Fig. 1).

3.2 Spatio-Temporal Parameters

Regarding these variables, an improvement is shown during the stance phase and in the swing phase, inferring an increase in stride length bilaterally and step cadence (Tables 1, 2 and 3). There were no changes regarding the mean velocity.

Table 1 Spatio-temporal parameters. Right limb

Right limb	Normal values	Pre	Post	Changes
Stance phase (%)	60	78.27	63.63	−14.64
Swing phase (%)	40	21.73	36.37	14.64
Stride length	1.36	0.58	0.65	−0.07

Table 2 Spatio-temporal parameters. Left limb

Left limb	Normal values	Pre	Post	Changes
Stance phase (%)	60	72.93	66.91	−6.02
Swing phase (%)	40	27.06	33.09	6.03
Stride length	1.36	0.6	0.61	0.01

Table 3 Spatio-temporal parameters

	Normal values	Pre	Post	Changes
Cadence (Step/min)	114	60.3	64.8	4.5
Velocity (m/s)	1.2	0.3	0.3	0

3.3 Kinematic Analysis

An improvement in the sagittal plane can be observed in the hip kinematic analysis. Both lower limbs show a decrease in flexion in the last part of the swing phase and in the initial contact (heel strike), apart from an increase in extension during the stance phase of both lower limbs (Fig. 2). Regarding the knee joint, an improvement can be observed during the whole gait cycle. Regarding the ankle, a decrease in the dorsal flexion can be observed during the whole gait cycle (Fig. 2).

3.4 Gait Deviation Index (GDI)

GDI is a score derived from three-dimensional gait analysis. The GDI provides a numerical value that expresses overall gait pathology (ranging from 0 to 100, where 100 indicates the absence of gait pathology). It is one of the most used variables of gait in children with CP. An improvement can be observed for this parameter in both lower limbs (Table 4).

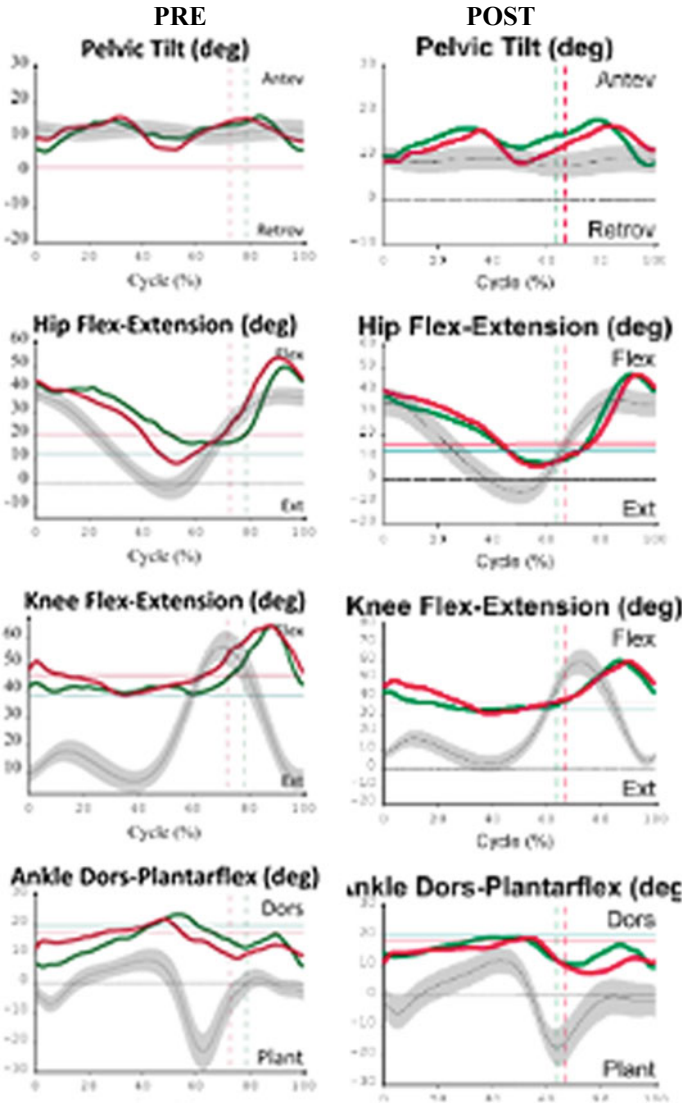

Fig. 2 Kinematic analysis

Table 4. Gait deviation index

	Right limb	Left limb
Pre	69.7	72.39
Post	70.86	76.43
Change	1.16	4.04

3.5 Patient's Feedback

The patient and family satisfaction are other values to take into account. Both family and patient were very thankful during the whole procedure as they perceived an improvement in his gait and had a feeling of having made a medium/high physical effort during each session.

4 Discussion

A larger sample size is needed so that the results in this investigation are comparable to other studies using this exoskeleton but with different pathologies such as spinal cord injury or brain damage. It would also be useful to study how changing the number of sessions affects the results and the influence of psychosocial parameters on gait-related parameters [3–5].

5 Conclusion

The use of the Ekso exoskeleton in patients with cerebral palsy might be promising as a complement to gait rehabilitation. In this case, an improvement in gait kinematics, spatiotemporal parameters and GDI, have been shown. Future investigations should include a larger sample size to extrapolate the results more reliably.

References

1. M. Bax, M. Goldstein, P. Rosenbaum, A. Leviton, N. Paneth, B. Dan, B. Jacobsson, D. Damiano, Proposed definition and classification of cerebral palsy, April 2005. Dev. Med. Child. Neurol. **47**(8), 571–576 (2005)
2. N.G. Moreau, A.W. Bodkin, K. Bjornson, A. Hobbs, M. Soileau, K. Lahasky, Effectiveness of rehabilitation interventions to improve gait speed in children with cerebral palsy: systematic review and metaanalysis. Phys. Ther. **96**(12), 1938–1954 (2016)
3. Physiotherapists' Experiences Using the Ekso Bionic Exoskeleton with Patients in a Neurological Rehabilitation Hospital: A Qualitative Study.
4. E. Read, C. Woolsey, C.A. McGibbon, C. O'Connell, Rehabil Res Pract. **2020**, 2939573 (2020). C. Fisahn et al., Gait training after spinal cord injury: safety, feasibility and gait function following 8 weeks of training with the exoskeletons from Ekso bionics. Global Spine J. **6**(8), 822–841 (2016)
5. S.-H. Chang, T. Afzal, J. Berliner, G.E. Francisco, Exoskeleton-assisted gait training to improve gait in individuals with spinal cord injury: a pilot randomized study. Pilot Feasibility Stud. **4**, 62 (2018)

Test Method for Exoskeleton Locomotion on Irregular Terrains: Testbed Design and Construction

A. Torres-Pardo, D. Pinto-Fernández, E. Belalcázar-Bolaños, J. L. Pons, J. C. Moreno, and D. Torricelli

Abstract This work aims to define a benchmarking scenario for the evaluation of the performance of lower limb exoskeletons while walking on irregular terrains. We designed a modular testbed that can be easily configured to replicate a wide range of uneven terrains. The testbed, based on several design criteria such as modularity, reproducibility, robustness and low-cost, aims to be a concrete solution to researchers and developers to test their systems according to a standardized method. The long term goal is to provide means to demonstrate the ability of new exoskeletal systems to operate safely and reliably in realistic out-of-the-lab conditions.

1 Introduction

Robotics is undergoing an unprecedented era due to the increased abilities of robotic systems to work in close interaction with humans. This is especially the case for wearable robots, which are generating high expectations in several applications domains. Nevertheless, wearable robots are yet to demonstrate their ability to operate safely

A. Torres-Pardo · D. Pinto-Fernández · J. C. Moreno · D. Torricelli (✉)
Neural Rehabilitation Group of the Spanish National Research Council, Madrid, Spain
e-mail: diego.torricelli@csic.es

D. Pinto-Fernández
Universidad Politécnica de Madrid, Madrid, Spain

E. Belalcázar-Bolaños
Technaid S.L, Madrid, Spain

J. L. Pons
Legs and Walking Lab, Shirley Ryan AbilityLab (Formerly Rehabilitation Institute of Chicago), Chicago, IL, USA

Department of Physical Medicine and Rehabilitation, Feinberg School of Medicine, Northwestern University, Chicago, IL, USA

Department of Biomedical Engineering, McCormick School of Engineering and Applied Science, Northwestern University, Chicago, IL, USA

J. C. Moreno et al. (eds.), *Wearable Robotics: Challenges and Trends*,
Biosystems & Biorobotics 27, https://doi.org/10.1007/978-3-030-69547-7_104

in real world conditions outside the laboratory. In the case of lower limb exoskeletons, one of the major and still unsolved challenges is achieving stable locomotion over the variety of terrains that characterize outdoor environments, which include irregularities, inclined surfaces, or soft terrains [1].

Unfortunately, there are still no quantitative methods to test the performance of exoskeleton in these conditions, being most of the tests realized during flat ground or treadmill walking [2]. From a preliminary analysis of the literature in human biomechanics and robotics locomotion, we found that there is no clear agreement on how to characterize irregular terrains. Existing literature does not converge into a common specification of roughness, softness, types of materials or experimental procedures. The lack of this information is hindering the development and consolidation of common setups that can be shared across laboratories and robotic platforms.

To fill this gap, in this paper we present our preliminary work towards the creation of a standardized benchmarking method that will allow the evaluation of the performance of lower limb wearable robots on irregular terrains.

In particular, this work is focused on the design and construction details of the practical testbed.

2 Material and Methods

The testbed is composed of a flat commercial rehabilitation walking platform (Chinesport [3]) modified to reach 1m width, with a wooden board on top. This board has equally distanced holes where a set of modules can be fitted. The modules include: forty-eight square wooden blocks with different heights and inclinations (see Fig. 1); twelve soft-irregular modules (from the company Terrasensa [4]) and two soft flat mats (from the company Tamdem) with different densities. Each wooden block is made up of an anti-slip 1.8x50x50cm plywood board, two wedges of 5º, 10º or 15º or a flat strip of 2.2, 4.4, 6.6 or 8.8cm (see Fig. 1).

The combination of these modules of different inclinations, heights and softness can lead to a range of irregular surface patterns. Among all the possible combinations, we propose the following six configurations (see Fig. 2):

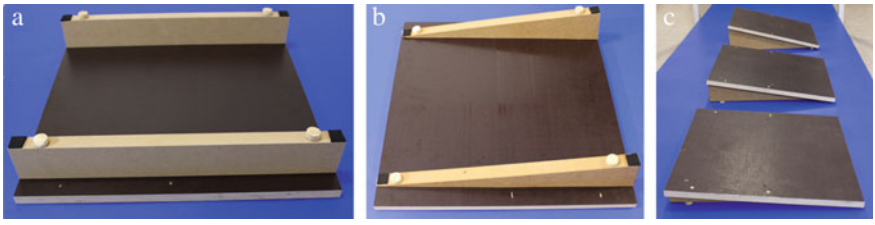

Fig. 1 Wooden modules: flat (**a**) and slopes at different inclinations (**b**, **c**)

A-like: The inclined wooden modules are placed with the angles at the sides of the walkway, creating a "mountain" in the middle of it. Three configurations can be achieved, one per each inclination.

V-like: The inclined modules are placed towards the middle of the platform, creating a depression in the center. Again, one configuration per inclination is available.

M-like: The inclined modules are placed in an alternated pattern, creating three mountains and two depressions. Three configurations can be achieved by implementing the three different inclinations.

Steps: This configuration combines flat wooden blocks of four different heights (2.2, 4.4, 6.6 and 8.8 cm) to simulate small steps (typically lower than a stair step). A specific sequence is proposed to force the subject to ascend and descend all heights.

Soft terrains: Two mats of different densities (100 and 30 kg/m^3) and heights (5 cm and 7 cm respectively) to achieve two different levels of softness.

Soft irregularities: Commercial square modules with soft irregularities (Terrasensa [4]) are placed in the walkway to simulate an unstructured irregular pattern.

3 Results

The result of our work is a benchmarking testbed that replicates a wide range of simplified, yet challenging, scenario irregular terrain patterns. The main characteristics of the developed testbed are:

Modularity: The same modules can be combined together to achieve different terrain setups.

Replicability: The chosen design can be easily reproduced by anyone without any particular technical skills.

Robustness: The platform is strong and stable enough to ensure secure gait with or without wearing an exoskeleton.

Ease of sensorization: The platform can be easily sensorized as it does not include any occlusion to optical motion capture systems and is compatible with pressure sensors.

Easily reconfigurable: The proposed modules can be placed and removed very quickly by one operator.

Safe: The structure has two lateral bars to serve as support for stability if needed.

Low cost: The materials used in the testbed building are not expensive, making it affordable for most research centers and exoskeleton designers and manufacturers.

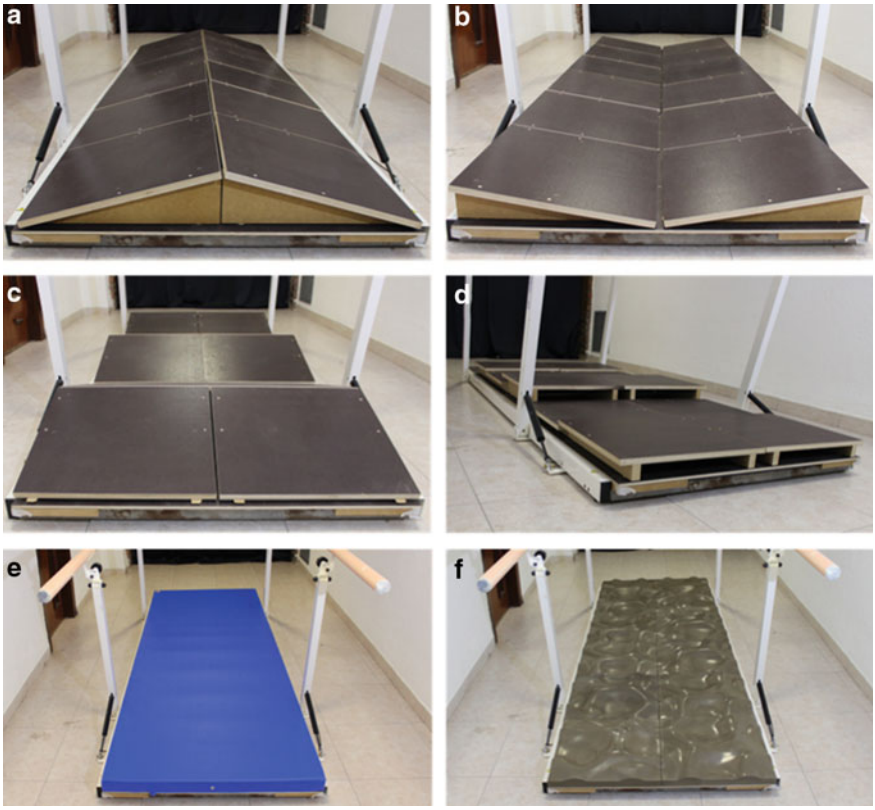

Fig. 2 Terrain configurations: A-like (**a**), V-like (**b**), M-like (**c**), steps (**d**), soft terrains (**e**), and unstructured irregularities (**f**)

4 Discussion

Nowadays no standardized methods for exoskeletons' performance evaluation exist. The testbed here proposed is a first step towards a solution that can be usable across different exoskeleton systems. The testbed can be configured and re-configured easily, allowing at least 14 different terrain configurations with different levels of difficulty by combining modules with various inclinations, heights and softness. With this testbed, most of the irregular terrain conditions encountered in everyday-life scenarios are covered, as (1) irregular structured terrains, (2) obstacles and steps, (3) soft terrains and (4) unstructured ecological-like terrains. Future experiments should be conducted to answer a number of questions necessary to progress toward a full definition of this standardized test method:

- Does the combination of 5º, 10º, and 15º slopes constitute sufficiently challenging conditions for exoskeletons? Should other slope angles be considered?

- What metrics and performance indicators can/should be calculated over these terrains to properly quantify walking performance?
- Will the values of softness be sufficient to span the range of soft terrains that can be found out of the lab?
- How many runs over these terrains should be performed to obtain statistically relevant results?
- What sensors are needed to extract the relevant information across a wide variety of exoskeleton solutions?

5 Conclusion

The testbed here presented aims to be the first step towards a unified benchmarking tool for the evaluation of performance of robotic systems on irregular terrain conditions.

This testbed, together with a set of clear performance indicators, is expected to facilitate the decision-making process during the process of technical development as well as during the purchasing of exoskeleton products by end-users. The testbed, designed to be easily replicated by different laboratories, is one of the first concrete efforts in reproducing real-life unstructured conditions in a standardized way in the field of wearable robots. We expect that the availability of such standard platform will promote the evaluation of exoskeletons in realistic scenarios as a common practice, facilitating the introduction of new solutions beyond clinical rehabilitation, e.g. in the workplace or in outdoor environments.

Acknowledgements This work has been supported by the H2020 Project EUROBENCH (grant number 779963, https://eurobench2020.eu/).

References

1. A. Abouhossein, U. Martinez-Hernandez, M.I. Awad, I. Mahmood, D. Yilmaz, A.A. Dehghani-Sanij, Assistive gait wearable robots—from the laboratory to the real environment. In: *Reinventing Mechatronics*, (Springer International Publishing, 2020), pp. 75–92
2. D. Pinto-Fernandez et al., Performance evaluation of lower limb exoskeletons: a systematic review. IEEE Trans. Neural Syst. Rehabil. Eng. 1 (2020)
3. Chinesports Webpage. PARALELA PLUS 3M. Available: https://www.chinesport.es/catalogo-general/paralelas-y-escaleras-para-rehabilitacion/paralelas-para-rehabilitaci--n-l--nea-plus/01326-paralela-plus-3m. Accessed: 01-Sep-2019.
4. Terrasensa Webpage. Terrasensa® New ways in therapy and training with the terrasensa® system English brochure. Available: https://www.blackroll.no/wp-content/uploads/2013/08/Terrasensa-brosjyre.pdf. Accessed: 01-Sep-2019

Small–Medium Enterprises in the Wearable Robotics Field: Tools and Opportunities to Create a Successful Company

Private/Public Funding Strategies for Interactive Robotics Companies

Arantxa Rentería-Bilbao

Abstract The aim of is paper is to provide a structured view of funding possibilities for companies in the field of interactive robotics. The paper presents a set of funding sources which are of interests for start-ups, spin-off and young companies working in the design and development of interactive robots, including wearable devices. This paper is divided into three chapters, covering private funding (types of existing funding sources, their specific target companies and requirements, and the reasons on how and why investors invest), public funding (mainly coming from European grants under several programs) and the conclusions.

1 Introduction

The world of start-ups dealing with interactive robotics (IR) is full of researchers with good ideas, willing to go ahead with the new company. But they lack funds to transform their inspiration and push into a successful business.

Others, on the contrary, have the money and are looking for that spark of entrepreneurial creativity, which aims to connect the needs of our society with effective technological solutions. Most entrepreneurs agree on the idea that the collaboration between private and public support is of key importance [1].

One of the main outcomes of the survey carried out in INBOTS project [2] shows the importance of the access to funding, financial resources, potential investors and business networks. There are economic barriers, including the accurate identification of the real needs of the target market, access to funding, and various legal services such as those related to intellectual property.

A. Rentería-Bilbao (✉)
Medical Robotics Group of Tecnalia, Basque Research Alliance, Derio, Spain
e-mail: arantxa.renteria@tecnalia.com

J. C. Moreno et al. (eds.), *Wearable Robotics: Challenges and Trends*,
Biosystems & Biorobotics 27, https://doi.org/10.1007/978-3-030-69547-7_105

2 Private Fund Raising

2.1 How to Identify the Opportunity

In order to attract potential investors to fund the innovative new companies developing IR, the entrepreneurs need to know how to identify the opportunity for their new business related to integrating/using IRs. The open questions include:

- Customer-Problem-Solution
- Does the opportunity match the founders experience, skills and interests?
- Can they recruit and lead the team needed to exploit the opportunity?
- Do the resource needs of the opportunity shorten the odds-on success?
- Is the timing of the opportunity, right?
- Do they need to comply with legal requirements?
- Does the opportunity constitute a scalable (and saleable) business?

2.2 Why Investors Invest

It is also important to know why investors invest, they must believe in the proposed business/idea:

- Trustworthiness of the entrepreneur
- Expertise of the entrepreneur
- Enthusiasm of the entrepreneur
- Track record of the entrepreneur
- Perceived rewards for the investors
- Sales potential of the market.

Some things the entrepreneur should know about potential investors include:

- What kinds of investments have they made in the past?
- What kinds of deals are they looking for currently?
- How do they make investment decisions? What kinds of deals do they like?

The entrepreneur must be ready to answer to potential questions the investors ask:

- Can the new company accomplish the tasks described in the business plan?
- How does the new company and IR product fit into the industry?
- What are the trends in the IR market?
- What are the drivers to success in the IR industry?

2.3 Some Private Funding Sources

While startups in the United States have sought funding from private entities, new companies in the European Union have relied on credits from banks in order to fund their growth. More recently, mainly from the 2008 crisis, the companies seek funding from business angels and venture capitalists.

One example is Tecnalia Ventures [3], which develops business opportunities for the valorization and commercialization of technology by connecting the main pillars of an entrepreneurial ecosystem: minds, management and money. When the results of a research project reach a certain Technology Readiness Level (TRL), they look for:

- people with an entrepreneurial profile / business vision capable of transferring the developed technology to the market, thus generating real business opportunities. These are profiles to which the value proposition of transforming a technological spin-off into a growing Small and Medium Enterprise (SME) is attractive to them.
- smart investors that not only provide the necessary financial muscle to transform technologies into revenues but who are also committed to support the development of the company.

Angel investing is equity finance. An angel investor is a high net worth individual who makes use of their personal disposable finance and makes their own decision about making the investment. The investor would normally take shares (an equity stake) in your business in return for providing equity finance (funds). The angels normally seek to not only provide the business with money to grow, but also bring their experience and knowledge to help the company achieve success. They can invest alone, or as part of a syndicate (a group of angels) [4].

Venture capital differs from angel investing because it invests in businesses through managed funds, coming from private or public money. The venture capitalist manager invests the money on behalf of the fund which has to be profitable and make a return for the fund's investors. Due to high costs of administration and the need to be very selective to ensure a return on the fund, VC funds are more risk averse and thus make fewer small investments in start and seed stage.

There are also tax reductions at national level in EU for startups. Different requirements (company´s age and nature, number of workers, etc.) and funding schemes (income tax reduction, grants for investors, etc.), apply in each country.

3 Public Fund Raising in H2020 and Horizon Europe

Funding opportunities under Horizon 2020 are set out in multiannual work programmes which cover the large majority of support available. The work programmes are prepared by the European Commission within the framework provided by the Horizon 2020 legislation and through a strategic programming

process, integrating EU policy objectives in the priority setting. Robotics can be found on many of the current H2020 programmes and calls.

3.1 Robotics in LEIT-ICT Program

The topics addressed in this Work Programme part cover the ICT technology in a comprehensive way, from technologies for Digitising European Industry, HPC, Big Data and Cloud, 5G and Next Generation Internet. This Work Programme supports core ICT industries through roadmap-based Public Private Partnerships (PPs).

3.2 Robotics in NMBP and FET Programs

This program covers different areas: Nanotechnologies, Advanced materials, Advanced manufacturing and processing and Biotechnology. Activities of the work programme will address the whole innovation chain with technology readiness levels spanning the crucial range from medium levels to high levels preceding mass production and helping to bridge the gaps ("valley of death") in this range.

Future and Emerging Technologies (FET) Open, which represents 40% of the overall FET budget in Horizon 2020, is entirely non-prescriptive with regards to the nature or purpose of the technologies that are envisaged. FET Open covers all technological areas and no budget is specifically earmarked for ICT or Robotics.

3.3 Robotics in EIC PILOT and Societal Challenges Programs

SME participation is encouraged throughout the work programme and in particular in the priorities 'Industrial Leadership' and 'Societal Challenges'. Dedicated SME support is channeled through the SME Instrument, introduced in the Work Programme 2014–2015, which promotes SMEs' innovation activities from concept to market. In 2016–17, all topics using the SME instrument were grouped in a continuously open common call. For 2018–20, this consolidation is pursued and the support to SMEs through this dedicated instrument takes the form of a single topic with a fully bottom-up approach (still with continuously open call with four deadlines per year).

Robotic research is expected to continue under the new Horizon Europe funding program of the European Commission, with a general proposed budget of 100 B€. Specific area of intervention of artificial intelligence and robotics, and clusters related

to health, digital industry, space, etc., could be the umbrella to new research projects on interactive robotics.

4 Conclusion

The investment risks depend on the TRL of the product: high risk for early stage (TRL 1–3), low risk for market ready (TRL 7–9). Usually the financing follows these three main stages:

1. Financing early stage technologies to make ready for license or sale (pre-seed or seed funding).
2. Financing a start-up.
3. Financing a company for growth and exit by investors.

Main outcomes of the HUM and WRs fields are that these two fields are very attractive both in terms of companies founded in the last 5 years and in terms of potential market. Indeed, one of the main aspects that emerges by the interviews carried out with founders of companies is that the market seems to be enough mature to accept humanoid robots or wearable products. However, some negative issues still remain: the lack of clear normative framework and the selection of the right business model to guarantee self-sustainability as well as some residual psychological barriers in accepting new technologies.

Acknowlegements This work has received the financial support of INBOTS project, which has received funding from the European Union's Horizon 2020 research and innovation programme under grant agreement No 780073.

References

1. C. Benito, B-Venture busca en su cuarta edición ser un punto de inflexión para los emprendedores. El Correo J. (2019)
2. INBOTS, Inclusive Robots for a Better Society, https://inbots.eu
3. https://www.tecnaliaventures.com/?lang=en. Last accessed 6 February 2020
4. The UK Angel Market Survey, https://www.ukbaa.org.uk/. Last accessed 7 February 2020

RobotUnion Project: Accelerating Startups in Robotics

Leire Martínez and Arantxa Rentería-Bilbao

Abstract RobotUnion discovers, supports and funds 20 European scaleups confirmed by venture capital investors and global corporates of four market domains for robotics: manufacturing, agriculture, healthcare and civil infrastructure. 40 companies developing selected out of a pan-European deal flow of 300 scaleups through 2 Open Calls. The top 20 have joined an acceleration programme that helps them progress from TRL4 to TRL7 onwards. The programme provides them with technical and non-technical support services: researchers in residence, entrepreneurs in residence, vouchers to access to facilities and technical services, public and private funding.

1 Introduction

The main goal of *RobotUnion* [1] is to stimulate small and medium enterprises (SME) in the robotics sector and to develop novel and challenging technology and systems applicable to markets. *RobotUnion* is supporting Scaleups: companies presenting high growth potential in developing and providing robotics. As Scaleups companies, we consider both emerging start-ups presenting disruptive technologies and business models, but also more established companies with existing activities that plan to transform their industries and markets through robotics solutions.

The consortium was designed to contribute to the overcoming of the systemic challenges (# innovation barriers) that are constraining the capability of European promising companies to develop novel and innovative technology that has the potential to open new markets for Robotics in domains like Manufacturing, Agri-Food, Healthcare and Civil infrastructure.

L. Martínez · A. Rentería-Bilbao (✉)
Medical Robotics Group of Tecnalia, Basque Research Alliance, Derio, Spain
e-mail: arantxa.renteria@tecnalia.com

L. Martínez
e-mail: leire.martinez@tecnalia.com

J. C. Moreno et al. (eds.), *Wearable Robotics: Challenges and Trends*,
Biosystems & Biorobotics 27, https://doi.org/10.1007/978-3-030-69547-7_106

RobotUnion is investing €4 million in 40 companies during 2 Open Calls from 2018 to 2020. In each Open Call, the consortium is selecting 40 companies from which 8 top performing are about to reach 1M of private investment.

RobotUnion is the consortium made by top accelerators, global brands and venture capital (VC):

- Mobile World Capital, host of Mobile World Congress and 4YFN events.
- 4 top corporates: FENIN, Ferrovial, ARLA and MADE, each of them leading one of the verticals.
- VTT, DTI, TU Delft, TECNALIA, and PIAP, the top Research and Technology Organizations who will provide State-of-the-art technical support and access to "premier-class" technology.
- CHRYSALIX and 'Odense Seed and Venture' as top VCs.
- ISDI First Digital Native Business School.
- FundingBox as the leading European funding platform for Scaleups (Startups and SMEs).
- Blumorpho links innovation providers with private investors. Blumorpho delivers the relevant support to Scaleups that enables them to reach the maturity expected by private investors.

RobotUnion applies a funnel approach: 20 Scaleups start the journey but only 10 get access to the full technology and business mentoring package. Selected companies are able to participate in a 16 month online Premium Acceleration Service, which is articulated through a 4-Stages Acceleration Programme ('Feasibility Phase', 'Product Development', 'Live Due Diligence' and 'Go-to-Market'). See Fig. 1.

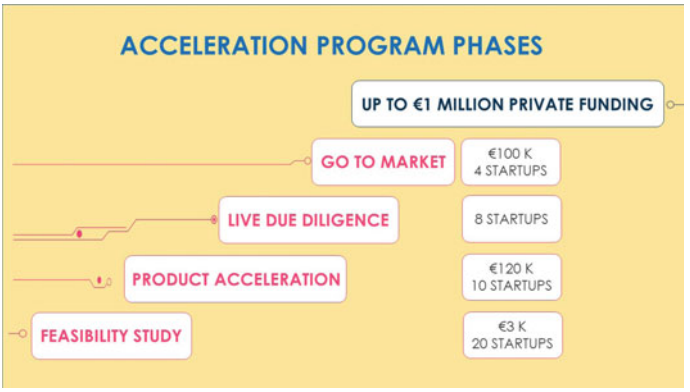

Fig. 1. Scheme of the funding phases

2 Value Proposition for Startups

RobotUnion offers an attractive full package of services for Startups at growth stage, composed by:

- Financial support up to €1,2M (€223K EU Funding equity free and €1M by top VC's in Robotics field such as CHRYSALIX and Odense Seed and Venture).
- State-of-the-art technical support and access to "premier-class" technology provided by VTT, DTI, DELFT, TECNALIA and PIAP.
- World class Training and high-level Mentoring by the pool of 1st level mentors from Google, Airbnb, Ikea, Yahoo, Prisa, Microsoft, among others, provided by ISDI.
- Presence in top EU Scaleups events such as 4YFN@Mobile World Congress, Slush, Web Summit
- International PR exposure powered by Mobile World Congress.
- Fundraising services provided by Blumorpho (private funding) and FundingBox (public funding). Contact with top VC's and equity-based crowdfunding platforms at EU level
- A Direct access to world top industry leaders such as MADE representing world Manufacturing leaders like Danfoss, Grundfos, Vestas and LEGO and among others plus ARLA in Agri Food; FENIN in Healthcare and FERROVIAL in Civil Infrastructure.

3 Developed Work

The work performed in the project was clustered around 6 main work packages.

3.1 WP1 Community Building and Marketplace

RobotUnion awareness strategy includes a campaign that strongly communicates the project's activities and results, with a view of optimizing their value and impact. The project has been present at 33 international Startups and robotic related events and has organized 31 info sessions to disseminate the Open Calls. As support to the Dissemination Strategy a RobotUnion Community (1.085 users) and a RobotUnion Marketplace was created. At a first stage it was tested within the *RobotUnion* Consortium and selected companies from the 1st Batch who were the only ones to have access to the group. The goal is that Marketplace could become a supportive tool for the selected startups who can use it to search for suppliers which could be used for the Technical Vouchers. Since July 2019 the Marketplace become public and special marketing campaign focused on attracting more users has been created.

3.2 WP2 Open Call Management and Beneficiaries Selection

RobotUnion launched two Open Calls (in 2018 and 2019) to select the 40 beneficiaries who entered Stage 1 of the program. The goal of the Open Calls was to receive a satisfactory number of applications and to ensure the quality of the beneficiaries selected to the program. As a result, in both Open Calls 1.138 applications were started and 424 of them were submitted and eligible for the program.

3.3 WP3 Research and Product Development

After a Welcome Camp Event for Stage 1, a first batch of companies had two months to create the final version of Feasibility Plans with the support of Technical and Business Mentors. The 10 most promising startups were selected to enter the Stage 2, Research & Product Development. With the assistance of assigned technical mentors the Individual Technical Mentoring Plans (ITMPs) were created, detailing technical development schedule and targets for each quarter of the 12 months stage as well as requested support from the Acceleration Program.

3.4 WP4 Live Due Diligence (Business Ignition)

The live due diligence consisted of an intensive mentoring and training program provided by key digital business ecosystem experts and entrepreneurs where teams were provided with the tools necessary to consolidate and thrive in their respective markets.

3.5 WP5 Pre-seed Round and Corporate Brokerage

The first strategy for the Startups investment mentoring was already issued. Introductions to the potential investors interested in *RobotUnion* Startups are executed continuously if the opportunity occurs.

3.6 WP6 Go-To-Market and Sustainability Plan

As a way to ensure the sustainability of the RobotUnion Acceleration Program and other products after the end of the project, the plan for exploitation and dissemination was developed in June 2018 and was updated in June 2019. The plan focuses on the

value propositions and business model canvases for all products created through the program.

Furthermore, RobotUnion has established a sustainability work group with partners whose task is to elaborate the elements of the future RobotUnion Business Plan and Toolkit.

4 Conclusion

The companies supported in the first call were TENDO (artificial tendon to grip, hold and release objects), ACCREA (Remote Medical Diagnostician), CYBERSURGERY (robot for spine surgery) and LEGEXO (most lightweight exoskeleton). In the 2nd call, the supported companies were AXILES BIONICS (bionic feet), AETHER MEDICAL (multi action bionic limb), CYBERSURGERY (returning startup) and LIFESCIENCE ROBOTICS (robot for efficient rehabilitation and early mobilization of patients).

RobotUnion has been conceived to be a sustainable pan-European Robotics Accelerator beyond the project, by providing a sustainable path for Scaleups (Path based on Private Funding support and Corporates agreements exposure to scale hand-in-hand with the corporations). *RobotUnion* has also a continuity strategy for the 'Acceleration Program' through the creation of a 'pan-European Continuity Fund', for the accelerator set up in the course of the project, and the standardisation of 'RobotUnion Accelerator', as an innovation instrument for European Regions, to foster the entrepreneurial discovery in the framework of their Research and Innovation Strategies for Smart Specialisation (RIS3) [2].

References

1. RobotUnion Project Website, https://robotunion.eu/. Accessed 20 July 2020
2. European Commission, *Smart Specialisation Platform: A Guide to RIS3*. https://s3platform.jrc.ec.europa.eu/s3-guide. Accessed 20 July 2020

Starting Up a Surgical Robotics Company: The Case of *Kirubotics*

Arantxa Renteria-Bilbao, Fernando Mateo, and Leire Martínez

Abstract This paper presents the steps followed by the Spanish start-up company Kirubotics, whose aim is to develop and market an innovative concept of surgical robot. It covers the phases of design, development of a functional protype, tests in laboratory, market research, analysis of regulatory requirements and contacts and agreements with future potential providers of components. In parallel, different types of funding sources have been achieved, while others are still being looked for. The process is still open. Preliminary results show that, as important as an innovative idea and a good technical team, it is to have enough economic backup at the right moment of the overall process.

1 Introduction

The Spanish operation robot BROCA (Brazo Robotico para Operaciones, (robotic arm for operations) Córdoba Andalucia), developed by Tecnalia together with the University Hospital Reina Sofía in Córdoba, not only features a modular construction but also offers intuitive operation and a universal scope of application. In comparison with other solutions in the market, the system is first and foremost affordable. The goal of its developers is to facilitate access for hospitals on a global scale to robotic surgery with the aid of BROCA—a purpose that, in view of frequently cited budget cuts accompanied by a shortage of personnel in the health care and nursing sector, could not be more relevant. In order to accomplish further development and commercialization phases, a start-up company, *Kirubotics*, was established in 2017.

A. Renteria-Bilbao (✉) · L. Martínez
Medical Robotics Group of Tecnalia, Basque Research Alliance, Derio, Spain
e-mail: arantxa.renteria@tecnalia.com

F. Mateo
Kirubotics, Córdoba, Spain

J. C. Moreno et al. (eds.), *Wearable Robotics: Challenges and Trends*,
Biosystems & Biorobotics 27, https://doi.org/10.1007/978-3-030-69547-7_107

2 Description of the Device

The robotic prototype is a 3 robot surgical system, tele-operated by a surgeon from a console with haptic joysticks and integrated 3D image of the abdominal area, to control the position and open/close movements of laparoscopic tools. Figure 1 shows the robotic system. The robot will be used for laparoscopic surgery, and it is based on a modular and wireless design. It consists of three independent arms which can be positioned wherever required in the operating room, depending on the type of intervention and needs of the surgeon. The robotic arms can also be removed quickly in case the operation needs to move to an open surgery.

Each robotic arm is provided with laparoscopic tools and endoscopy camera, so the surgeon is able to navigate in 3D and manipulate the end-effector thanks to the several degrees of freedom and sensors integrated in the tools (see Fig. 2). An easy to use person-robot interface allows the execution of robot movements, by actuating on two 7-degree of freedom joysticks, with haptic feedback (tactile information about the applied pressure), and the tele-operation of the robot in order to perform the trajectory inside the patient´s body. The software of the robot is open and the system itself is scalable, easy to set up, with no needs of special infrastructure in the operating room and can be used in several types of laparoscopic surgery.

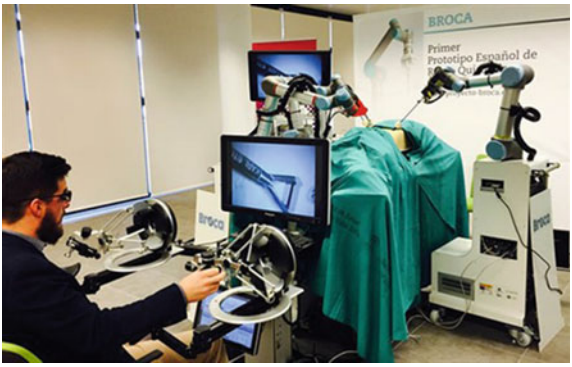

Fig. 1. The BROCA prototype

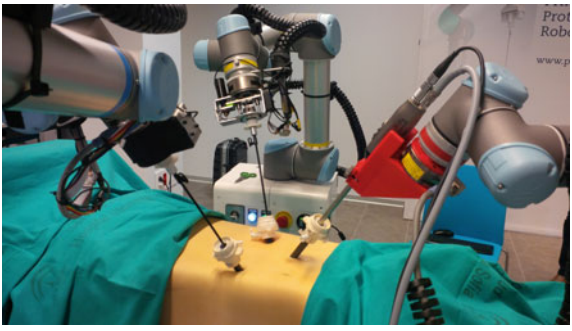

Fig. 2. Laparoscopic tools and endoscope manipulated by robotic arms

3 The Quest for Funding

Kirubotics faces several challenges. On one side there is the cost of manufacturing their own robots and on the other side the high cost of the final products. These two are usually related. For example, in surgical robotics the initial high investment makes it difficult for many hospitals to buy them and even when they had the money to buy them, through some particular funding, maintenance costs are usually high too, so many surgical robots are underused. The concept used in BROCA project provides a low-cost prototype of a surgical robot trying to overcome this barrier.

To avoid the high cost of developing robotic arms *Kirubotics* has developed its solution using commercial arms and haptic devices. This decision requires an investment when buying these commercial components, but it makes more sense for some of our clients, who look for already certified elements. Relying on commercial products has its own disadvantages too as you become dependent on someone else. Each project should at least think on how necessary it is to develop proprietary robots.

The aim of the company is to continue the development of the current prototype (TRL6) in order to achieve a certified commercial device, assessed through clinical trials (TRL9). *Kirubotics* follows the strategy to integrate commercial equipment. This strategy allows for:

- scale economies of the manufacturers (robotic arms, haptic joysticks, surgical tools).
- focus their effort on research and development.

The new company aims to change the business model around robotic surgery, by making revenues from:

- Selling systems.
- Maintenance services.

But the business around surgical tools, robots and vision system still belongs to the providers of these components.

3.1 National Funding (Public and Private)

During the period 2012–2015 the BROCA Project was carried out, with the aim to obtain a functional prototype. It was led by the Instituto Maimónides de Investigación Biomédica of Córdoba (institute for biomedical research). BROCA was the first project funded by the pre-commercial procurement programme in the field of bio-medicine in Spain, a new modality driven by the Minister of Economy and Competitiveness to foster the development of new technological products in private companies. The aim of this funding model was to reinforce the role of public administration as drivers of entrepreneurial innovation. The development of BROCA was granted to the University of Córdoba, and the public health system was also involved

with the partnership of surgeons from Hospital Reina Sofía, as consultants for the technical team. For the technical development, University of Córdoba subcontracted Tecnalia and University of Málaga.

Related to private funding, *Kirubotics* offers to private investors the possibility to share stocks of the company for the development phase and market launch. The company is currently working in updating its business plan, market positioning, target customers, selling strategies and analysis of the competency. A first round of private funding is under process, but the final confirmation depends on the availability of complementing national public grant.

3.2 Public European Funding

Additionally, *Kirubotics* have been involved in several proposal in H2020 programme related to surgical robotics in ICT related calls.

4 Market Analysis

The first claiming for patents and business plan is already made. The expected selling price is around 0.7 M€. Spanish public hospitals will be the main customers of the system, due to their impossibility to access to the expensive Da Vinci system. At first glance, the main differences between the BROCA robot and Da Vinci robot (apart from the price), are the different surgical procedures they are aimed to, the level of tool accessibility (better Da Vinci's), and the haptic feedback and quick set-up (better BROCA's) [1]. Each country has its own health system, different from each other and with different levels of coverage, which makes it more complex to put a health robot in the market successfully.

Some market forecasts, referred to European Union [2]:

- 35 million of surgery procedures per year.
- 31.25 million of non-laparoscopic procedures.
- 3.75 million of laparoscopic procedures.
- 3.65 million of non-robotized procedures.
- million of robotized laparoscopic procedures.

5 Conclusion

There are some critical points along the development of the entrepreneurial project. Among them, the delay or lack of availability of commercial components, faulty components, delay in the achievement of planned milestones which may pose a risk on the reliability of the project (and put some doubts on investors' side), problems

with technical developments or clinical trials, and difficulties during the certification process.

References

1. A. Brodie, N. Vasdev, The future of robotic surgery. Robot.: Ann. R. Coll. Surg. Engl. **100**, 4–13 (2018)
2. A. Kumar, *Medical Robotics and Computer Assisted Surgery* (The global market, BCC Research LLC, 2017).

Redesigning Tax Incentives for Inclusive and Green Robotics in the European Union Reconstruction

María Amparo Grau Ruiz

Abstract With a view to help with the urgent socio-economic recovery after the COVID-19 pandemic, the goal of this paper is to show a possible path to promote, through tax incentives for Responsible Research and Innovation, sound uses of robots in this context. Its scope is in line with the current priorities in the European Union, which are in turn aligned with the United Nations 2030 Agenda on global Sustainable Development. Some proposals are made to address the needs of social returns in the form of inclusive and green robotics, based upon the results of a jurisprudential critical review (focused in the Spanish experience as a tool for comparative Law analysis), bearing in mind relevant previous judgments of the European Union Court of Justice in the field and a recent tool presented by the OECD.

1 Introduction

Over the past two decades, many countries have increased the availability, simplicity of use and generosity of R&D (research and development) tax incentives. In 2018, 30 out of 36 OECD countries give preferential tax treatment for business R&D expenditures, up from 19 OECD countries in 2000. The EU Member States offering R&D tax relief increased from 12 in 2000 to 21 in 2018. Over the 2006–16 period, tax support for business R&D expenditure as a percentage of GDP increased in 26 out of 44 countries for which data are available [1, 2]. With few exceptions, a generalised shift towards this indirect type of support versus direct funding (through grants or public procurement) has been facilitated by the existence of international rules on trade and competition. Direct measures of support can be better targeted towards activities, firms and areas where higher additionality and spillovers could

Inbots project "Inclusive Robotics for a Better Society", European Union's Horizon 2020 research and innovation programme, Grant agreement No. 780073.

M. A. Grau Ruiz (✉)
Universidad Complutense de Madrid, Madrid, Spain
e-mail: grauruiz@ucm.es

Northwestern University, Chicago, IL, USA

J. C. Moreno et al. (eds.), *Wearable Robotics: Challenges and Trends*,
Biosystems & Biorobotics 27, https://doi.org/10.1007/978-3-030-69547-7_108

be generated. However, this entails higher costs of administration and also higher compliance costs for firms [1].

2 Materials and Methods

R&D tax incentives are complex objects of study. They may be subject to a combination of methods of evaluation from different perspectives. Here the legal method is used to highlight some critical aspects debated at various instances.

2.1 Results

2.2 The Court of Justice of the European Union

In the Judgment of 10 March 2005, Case C-39/04, ***Laboratoires Fournier SA v Direction des vérifications nationales et internationals*** ECLI:EU:C:2005:161, the Court declares that the Article 49 EC precludes legislation of a Member State which restricts the benefit of a tax credit for research only to research carried out in that Member State. The Court relies on the previous Case C-254/97, ***Société Baxter***, Judgment of 8 July 1999. Paragraph 23 reads "Such legislation is directly contrary to the objective of the Community policy on research and technological development which, according to Article 163(1) EC is, *inter alia*, 'strengthening the scientific and technological bases of Community industry and encouraging it to become more competitive at international level'. Paragraph 25 adds "national legislation which absolutely prevents the taxpayer from submitting evidence that expenditure relating to research carried out in other Member States has actually been incurred and satisfies the prescribed requirements cannot be justified in the name of effectiveness of fiscal supervision".

In its Judgment of 13 March 2008, Case C-248/06, ***Commission of the European Communities v Kingdom of Spain***, ECLI:EU:C:2008:161, the Court declares that, by maintaining in force rules for the deduction of costs relating to research and development and technological innovation which are less favorable in respect of costs incurred abroad than costs incurred in Spain (*ex* Article 35 of the Law on corporation tax, as amended by Royal Legislative Decree 4/2004 of 5 March 2004), Spain has failed to fulfil its obligations under Articles 43 EC and 49 EC on freedom of establishment and the freedom to provide services.

2.3 The Spanish Courts

Judgment 225/2015 of 28 April 2015, Madrid High Court of Justice, no. 152/2014. According to the ***Judgment of the Supreme Court of 20 May 2013***, No.6383/2011, R&D activity is an indeterminate legal concept that requires the assistance of technical/expert opinions/reports from experts in the field when determining its meaning and scope. The Advocate General points out that the technical reports of the certification bodies are mandatory but not binding, that the Ministry must ensure the general interest and correct use of public funds and that the technical reports of the Administration enjoy the presumption of impartiality and objectivity. However, the Court finds that the publication in the European Patent Register has an effect on the classification of the project for the purposes of the nature of the deductions for the corporation tax in respect of the financial year in which it has been carried out. The competent body at European level has assessed that the patented product or process meets the requirements of constituting a novelty that is not in the state of the art and may have industrial use. Based on the ***Judgment of the Supreme Court of 12 January 2014***, No. 843/2011, it concludes that, although there are as many technical reports from the Administration as from the appellant, the criterion of the inversion of the burden of proof can be applied to the Administration which, despite knowing the project was considered as an invention at a European level decided that it did not deserve the qualification of Research and Development. The appeal is upheld.

Judgment of 3 May 2013, National Audience, No. 161/2010 on a project for a palletizer with robot for pet drink bottles. It is noteworthy that the tax auditor clarified the question of the deduction without the technical assistance of experts. However, the expert reports provided by the appellant are limited to stating that the Centre for the Development of Industrial Technology approved its participation in the project, with insufficient accreditation of compliance with the requirements for applying the deduction. Nor can the report of the Patent and Trademark Office on the existence of any patent on the project support the claim because the technical characteristics of the project are missing from the proposal of the evidence. The non-exhaustive retrospective search in the database of Spanish Patents and Utility Models shows that numerous patent and utility model documents have been found. The action is dismissed.

3 Discussion

From the Governments' perspective, the European Commission adopted rules to facilitate the granting of aid measures by Member States in support of R&D+i (research, development and innovation). The specific state aid Framework sets out the conditions and the General Block Exemption Regulation clarifies the scope of measures that do not need to be notified to the Commission for prior approval [3]. After the COVID-19 crisis, the Commission Regulation (EU) 2020/972 of 2 July

2020 has amended Regulation (EU) No 1407/2013 as regards its prolongation and Regulation (EU) No 651/2014 as regards its prolongation and relevant adjustments.

Many Goverments are currently reviewing the tax incentives. In Spain, the "Autoridad Independiente de Responsabilidad Fiscal" [4] has recently suggested to frame any change of the fiscal benefits in the strategic planning of public policies to which they are related, assessing their *ex ante* effects and their *ex post* achievements. The National Institute of Statistics and the Tax Agency, following strict confidentiality criteria, have merged the Corporate Income Tax returns with the Survey on Business Innovation to evaluate the R&D+i tax benefit. Unfortunately, the evaluation was interrupted by the state of alarm and the expected publication was postponed. From the firms' perspective, binding rulings in Spain are issued by the Department with competencies in Science and Technology to provide certainty for taxpayers with regard to the qualification of activities that entitle fiscal incentives to innovation, as well to clarify the exclusive secondment of researchers to them. The interaction between different types of rulings (including advance agreements) and procedural aspects could be improved to avoid costs and delays [5]. In general, the R&D efforts in response to policy changes may vary depending whether these are perceived to be permanent or transitory by the firms. Ultimately, the public support may be adjusted in accordance to their behavior.

4 Conclusion

Fiscal policy has a key role in matter of trust and in the road to the Sustainable Development Goals. Policy makers should redefine the existing R&I incentives or introduce new ones to make them more efficient in terms of the social and environmental impact of robotics in the EU territory, respecting fundamental freedoms and the State aid rules. They should be drafted in a controllable way, by adjusting requirements (not only considering the input or output, but also the process) and procedures with other administrative Departments. Whether R&D+i tax incentives are good value for money should be assessed on a country-by-country basis. The finding of a partial crowding out effect does not necessarily mean that R&D tax relief measures are inefficient–their net benefit can still be positive if the combined private and social returns to R&D are sufficiently high [1].

Acknowledgements The author (INBOTS WP2 leader) acknowledges the invitation received by Dr. Conti (INBOTS WP1 leader) to show our cooperation. Prof. Grau leads the AudIT-S project on "Legal and financial significance of sustainability audit schemes through smart data management" (PID2019-105959RB-I00I).

References

1. S. Appelt, F. Galindo-Rueda, A. González Cabral, Measuring R&D tax support: findings from the new OECD R&D tax incentives database. In: OECD Science, Technology and Industry Working Papers, No. 2019/06, (OECD Publishing, Paris 2019). https://doi.org/10.1787/d16e6072-en. At 18, 20, 47
2. CPB Netherlands Bureau for Economic Policy Analysis, A Study on R&D tax incentives annex: country fiches FINAL REPORT TAXUD/2013/DE/315 FWC No. TAXUD/2010/CC/104, (The Hague, 2014). https://ec.europa.eu/taxation_customs/sites/taxation/files/resources/documents/taxation/gen_info/economic_analysis/tax_papers/country_fiches.pdf
3. https://ec.europa.eu/commission/presscorner/detail/en/MEMO_14_368, https://ec.europa.eu/competition/state_aid/modernisation/index_en.html#rdi, https://ec.europa.eu/competition/state_aid/legislation/block.html#gber
4. *Presentación segunda fase Spending review: la Airef resalta el coste de oportunidad que suponen los beneficios fiscales y la importancia de garantizar su eficacia*, Madrid, 22/07/2020. https://www.airef.es/wp-content/uploads/2020/07/BFISCALES/Nota-de-Prensa.pdf
5. M. Fabra Valls, Binding rulings as an instrument for the interpretation and application of fiscal incentives for innovation. RCyT. CEF, No. 412 (July 2017), pp. 47–82